

*Dartmouth College
Library*

*has purchased this book
from the income of the
Sanborn Library Fund*

established by

EDWIN WEBSTER SANBORN
of the Class of 1878

in memory of

EDWIN DAVID SANBORN
of the Class of 1832

DISCARDED BY
DARTMOUTH COLLEGE LIBRARY

*Ions and Ion Pairs
in Organic Reactions*

Contributors

ERNEST GRUNWALD, *Department of Chemistry, Brandeis University, Waltham, Massachusetts*

J. MILTON HARRIS, *Department of Chemistry, California State College, Fullerton, California*

STEPHAN HIGHSMITH, *Department of Chemistry, Brandeis University, Waltham, Massachusetts*

JOSEPH JAGUR GRODZINSKI, *Weitzmann Institute for Science, Rehovoth, Israel*

PATRIC C. MOWERY, *Department of Chemistry, University of California, Berkeley, California*

DOUGLAS J. RABER, *Department of Chemistry, University of South Florida, Tampa, Florida*

PAUL V. R. SCHLEYER, *Department of Chemistry, Princeton University, Princeton, New Jersey*

ANDREW STREITWIESER, *Department of Chemistry, University of California, Berkeley, California*

MICHAEL SZWARC, *Department of Chemistry, State University College of Environmental Science and Forestry, Syracuse, New York*

TING-PO I, *Department of Chemistry, Brandeis University, Waltham, Massachusetts*

Ions and Ion Pairs in Organic Reactions

VOLUME 2: Role of Ions and Ion Pairs in Chemical Reactions

MICHAEL SZWARC, F.R.S., Editor

*Chemistry Department
State University College of
Environmental Science and Forestry
Syracuse, New York*

A WILEY-INTERSCIENCE PUBLICATION

JOHN WILEY & SONS, New York • London • Sydney • Toronto

Copyright © 1974, by John Wiley & Sons, Inc.

All rights reserved. Published simultaneously in Canada.

No part of this book may be reproduced by any means, nor transmitted, nor translated into a machine language without the written permission of the publisher.

Library of Congress Cataloging in Publication Data:

Main entry under title:

Ions and ion pairs in organic reactions.

Includes bibliographies.

Vol. 2 has special title: Role of ions and ion pairs in chemical reactions.

1. Ions. 2. Chemistry, Organic. I. Szwarc, Michael, ed. II. Title: Role of ions and ion pairs in chemical reactions. [DNLM: QD561 S998i]

QD476.157 547'.1'372 71 170685

ISBN 0 471 84308 3

Printed in the United States of America

10 9 8 7 6 5 4 3 2 1

To the memory of Saul Winstein
who enlarged our vision and
our knowledge of ion pairs and
of their role in organic reactions

Preface

Free ions, a variety of ion pairs, and the still higher ionic aggregates are unquestionably distinct species, each endowed with its own physical properties. Their reality is demonstrated conclusively by the spectral evidence reviewed recently in Volume 1 of *Ions and Ion Pairs*, the most illuminating of these observations being those obtained by means of magnetic spectroscopy. In fact, the spectroscopic studies not only furnished the ways of differentiating between these species and determining their individual concentration but also provided much information about their lifetimes and therefore about rates of their interconversion.

The state of solvation or aggregation of ionic reagents frequently affects in a spectacular way their reactivities. Moreover, variation of solvent or counterion may lead to an abrupt change in the direction of an ionic process and result in entirely different products. Even the counterions not formally involved in a chemical process may affect its outcome. Therefore, synthetic organic chemists interested in directing a reaction toward a specific goal find ample opportunity to do so by investigating ionic processes.

How is the divergent behavior of ionic species influenced by their solvation and aggregation? A partial answer to this question will emerge from the discussions presented in this volume. Since the pertinent problems are complex, their systematic treatment could be facilitated by focusing attention on a few appropriately selected classes of elementary reactions. We have chosen for this review four kinds of elementary steps: electron-transfer, proton-transfer, electrophilic substitution, and propagation of ionic polymerization, all of these are strongly influenced by the nature of solvent, counterion, complexing agents, and so on.

The reactions chosen for our review are involved in many scientifically and industrially important processes, and their understanding ought to be valuable to any chemist. However, a fully comprehensive discussion of all

electron and proton transfers appears unfeasible in view of the size of this volume. It has been decided therefore to limit our review to those topics the studies of which have provided most information about the role of ions and ion pairs in elementary electron or proton transfers. Investigations of radical ions and of carbon acids provided exciting material, rich in the desired qualitative and quantitative observations. Discussion of these topics seems therefore to serve best our purpose.

Whenever possible, the solution reactions treated in this book have been compared with the analogous processes proceeding in the gas phase because such a comparison leads to a deeper understanding of the role of solvent in solution reactions. Moreover, only for gaseous reactions do the symbols used in the description of any elementary event, for example,



have a unique and well defined meaning. They denote simple entities such as free atoms or radicals, intact molecules, or charged species like ions. Even if they represent an aggregate its structure and stoichiometry is unique and well defined. In contrast, the nature of a reactant in a liquid phase is more complex, a point to be elaborated later.

Only in a rarified gas do the reagents possess truly intrinsic properties determined by their structure, charge if any, vibronic state, momentum, and so on. Each of the thus described species is far away from the other components of the system and it becomes aware of the existence of another particle only during the brief interlude when they collide. The colliding pair is still remote from all the other particles and therefore the immediate outcome of such a collision is not affected by their presence.

Any encounter affects the colliding species although most often in a minor way. For example, it alters their linear momentum or the state of their rotation. Collisions that modify the vibrational state of a reactant are more significant for chemists since the internal energy of the system is changed. The most important are the encounters that alter the nature of the reactant; these lead to conventional chemical reactions. For example, the colliding reactants may emerge from an encounter united—yielding either an intermediate aggregate or the final combination product of a reaction. They may be shattered, and the emerging fragments are then the products of decomposition. Alternatively, one of the reactants may become enriched at the expense of the other. Electron or proton transfer, or transfer of some larger moiety exemplifies such an elementary event. Finally, the structure of a reactant may change through a collision, an event referred to as an isomerization.

These events are not the only examples of conventional chemical reactions. A change may occur during the lonely journey of a reactant through space

as exemplified by spontaneous fluorescence, phosphorescence, or auto-ionization of an electronically excited species, or by the decomposition or isomerization of an energized entity. A reactant undergoing such a change is intrinsically transient. It is formed by some preceding event, such as a collision, interaction with radiation, or an exothermic decomposition of its precursor. If it survives its solitude, a subsequent encounter with another component of the system usually leads to its destruction or deprives it of its energy excess.

All the reactions discussed so far have one feature in common. While they occur, the reagent or the two colliding reagents are not perturbed by their neighbors since these are too far away. The outcome is determined *entirely* by the *intrinsic* properties of the reagents and is not influenced by the surroundings. However, in a liquid, and even in a dense gas, a radically different situation is created. The reactants are then ceaselessly interacting with their neighbors; consequently, their properties no longer are purely intrinsic but are affected, at least to some degree, by their surroundings. For example, solvents greatly influence the behavior of an ionic species because the latter powerfully interact with their environment. Even more powerful are the interactions between positively and negatively charged ions and indeed, it is often impossible to treat such a pair, even in the first approximation, as a transient association of two independent species. Therefore, ion pairs or higher aggregates have to be regarded as reactants in their own rights, participating as single entities in elementary steps of numerous reactions.

The last statement raises an important question: What is meant by a thermodynamically distinct species in a liquid phase? The simple treatment of elementary gaseous reactions avoids the distinction between those subspecies that differ from one another only by the magnitude of their linear momentum and by the state of their rotation and vibration. We refer to them as one kind of species and calculate their properties by the appropriate averaging procedure. A somewhat similar treatment is applicable to gaseous species immersed in a liquid; the averaging procedure takes cognizance of the various interactions of the dissolved entity with their surroundings. Such a treatment leads to the concepts of activities and activity coefficients, an approach useful and justified, especially when the species under consideration only weakly interact with their surroundings. Although this approach is still correct for strongly interacting systems, it might seem intellectually unsatisfactory. Indeed, the concept of activities hides all of the interesting details of the solute-solvent interactions responsible for a variety of structures that deserve thorough examination. Such structures become well defined and long lived in solutions of ions in polar liquids since there the intervening forces are strong.

The resulting molecular patterns involve the ion in question, or an ionic

aggregate, the neighboring solvent molecules, and often some other solutes present in the solution and referred to as the complexing agents. Due to the Brownian motion, the vigor of which depends on temperature, no pattern lasts long. Usually it persists for less than 10^{-10} sec although some of its basic features may be retained for a relatively long time. A set of patterns sharing such a common basic feature describes what shall be denoted as *a species* in liquid phase. The patterns composing such a set are easily interchanged, one being readily transformed into another. Nevertheless, the identity of such a defined species is preserved as long as the common basic features of the patterns are retained, but whenever the basic features are modified or destroyed, the respective species loses its original identity.

A solution is composed only of one type of ionic species if *all* the molecular patterns formed around the dissolved ionic aggregate belong to a single set, in other words, if all possess the same basic features. What constitutes such a species depends, however, on *our* definition of the basic features. A more rigorous and detailed specification may modify our statement and force us to treat the *same* solution, supposedly composed of one solute, as a mixture of two or more different kinds of ionic species.

This ambiguity makes one wonder whether the proposed description of ionic species is justified and useful. To clarify this point, let us consider a multicomponent solution, a system involving molecular patterns assigned to several sets each characterized by its own basic features. Such an assignment is useful *provided the respective sets are not overlapping*, because only then each molecular pattern is unambiguously attributed to one, and only one, set. The nonoverlap condition introduces an important restriction upon our choice of the basic features appropriate for defining a set. If these restrictions are met, the resulting nonoverlapping sets define a mixture of *thermodynamically distinct species* amenable to the conventional thermodynamic treatment.

Let us now consider a pattern developed in a solution around an ion or an ionic aggregate. Although it varies with time, its basic feature may be retained for a relatively long period thus permitting its identification with a kind of species. A sufficiently powerful fluctuation may suddenly transform it into a new pattern associated with another set. Such an event is interpreted as a reaction: species $i \rightarrow$ species j . In this context such concepts as the mole fraction, γ_i , of species i , their average lifetime, τ_i , and their rate constant, k_{ij} , of conversion into species j , become self-explanatory.

The sharp differentiation between the thermodynamically distinct species, say i and j , is the consequence of the nonoverlapping nature of the sets. However, the requirement of continuity implies that a transition from a pattern belonging to set i into a pattern associated with set j , proceeds through some "freak" patterns not included in any of the recognized sets.

These “freak” patterns, although excluded from our classification, appear in the solution under investigation. If their occurrence is rare, their contribution to the properties of the system is negligible and their omission is justified. Under such conditions the distinction between species i and j is not only permissible but also profitable.

This additional restriction of our definition of thermodynamically distinct species deserves further examination. The “freaks” represent the highly improbable patterns, the low probability of their occurrence caused often, although not always, by the high energy of their formation. As the thermodynamic conditions vary, for example, as the temperature rises, the proportion of the “freaks” may increase and reach a level when their omission is no longer justified. Our differentiation between these thermodynamically distinct species breaks down, and then they have to be treated as one kind only. The following two examples may clarify these ideas.

Two types of ion pairs may be present in a solution. Ions of one pair are virtually in contact with each other, and such a pair would be denoted as t . Alternatively, the two ions could be separated by one or two solvent molecules and kept apart at an average distance r . These looser pairs are referred to as l pairs. Since either pair may vibrate and the amplitude of the vibration increases with rising temperature, the distinction between the two kinds of pairs could be justified at low temperatures but it might be blurred at higher temperatures when the vibrations are strong and cause an overlap of the respective patterns. Thus the differentiation may fail even if the extrapolation from the low temperature data indicates that the concentrations of *both* kinds of pairs should be finite at high temperature. Hence the failure of differentiation between the two kinds of ion pairs is not caused by the disappearance of one type of pair from the solution. It arises from the breakdown of the concept of two types of pairs, a concept deprived of its justification in this temperature range.

Differentiation of free ions from ion pairs is unambiguous in a dilute salt solution. While the former are randomly distributed throughout the liquid and kept, on the whole, far away from one another, the latter represent two ions kept closely together. The ratio of free ions to ion pairs may be kept constant as the solution is concentrated, provided the temperature is varied judiciously. However, at a sufficiently high concentration of salt the average distance between the free ions becomes too small to justify the distinction between free ions and ion pairs and then it is no longer possible to maintain the concept of free ions and ion pairs as two distinct species. Surely, it is senseless to differentiate between free ions and ion pairs in a molten salt.

The two examples and the preceding discussion should clarify the meaning, as well as the limitations, of the concepts of ionic species. Discussion of ionic reactions becomes clearer when the reagents are described in these

terms. The treatment of the whole field becomes harmonious when the physical observations reviewed in Volume 1 are combined with the kinetic data discussed here. Moreover, much is gained by discussing the available observations in terms of the virtually invariant properties of different ionic species and the variable composition of the solution.

In solution reactions the omnipresent solvent molecules affect the behavior of unimolecular decompositions, which acquire the character of a cage reaction and modify bimolecular reactions by creating encounter complexes. In fact, in some systems, discussed in the second chapter of this volume, the encounter complexes are shown to behave as independent reactants directly involved in protonation. Omnipresence of solvent is responsible also for some specific character of solvolysis—a subject treated in the third chapter.

The last chapter deals with a most interesting and original treatment of dipolar properties of ion pairs which sheds much light on the details of their structure. Although this chapter should have been included in Volume 1, technical difficulties made this impossible. Its inclusion in this volume adds, however, much to the scope of this book, presenting a unique treatment of that subject.

In conclusion, it is hoped that these two volumes will raise further interest in ionic organic reactions and help to clarify the numerous phenomena encountered in their studies.

MICHAEL SZWARC

Syracuse, New York
August 1974

Contents

Chapter 1	Ions and Ion Pairs in Electron Transfer Reactions of Radical Anions, Carbanions, and Solvated Electrons	
	MICHAEL SZWARC AND JOSEPH JAGUR-GRODZINSKI	1
Chapter 2	Ions and Ion Pairs in Proton Transfer Reactions Involving Carbon Acids and Radical Anions	
	MICHAEL SZWARC, ANDREW STREITWIESER, AND PATRIC C. MOWERY	151
Chapter 3	Ions and Ion Pairs in Solvolysis Reactions	
	DOUGLAS J. RABER, J. MILTON HARRIS, AND PAUL V. R. SCHLEYER	247
Chapter 4	Ions and Ion Pairs in Ionic Polymerization	
	MICHAEL SZWARC	375
Chapter 5	Electric Permittivity, Dipole Moments, and Structure in Solutions of Ions and Ion Pairs	
	ERNEST GRUNWALD, STEFAN HIGHSMITH, AND TING-PO I.	447
Author Index		521
Subject Index		543
		xiii

*Ions and Ion Pairs
in Organic Reactions*

1

Ions and Ion Pairs In Electron Transfer Reactions of Radical Anions, Carbanions and Solvated Electrons

MICHAEL SZWARC

*Department of Chemistry
State University College of Environmental Science and Forestry
Syracuse, New York*

JOSEPH JAGUR-GRODZINSKI

*Weizmann Institute for Science
Rehovoth, Israel*

1. Introduction	2
2. Electron Ejection in the Gas Phase	4
3. Electron Capture in the Gas Phase	17
4. Determination of Electron Affinities	21
5. Dependence of Ionization Potentials and Electron Affinities on Molecular Structure	27
6. Solution Electron Affinities	31
7. Potentiometric Studies of Solution Electron Affinities	33
8. Polarographic Determination of Electron Affinities	38

2 Ions and Ion Pairs in Electron Transfer Reactions of Radical Anions

9. Correlation of Gaseous Electron Affinity with the Potentiometric and Polarographic Data	43
10. Electron Transfer Equilibria between Radical Anions and Aromatic Acceptors	45
11. Equilibrium between Aromatic Acceptors and Alkali Metals	51
12. Kinetics of Exchange Reactions	57
13. Intramolecular Electron Exchange	71
14. Electron Transfer $A + A^+ \rightarrow$ Exchange	85
15. Kinetics of Electron Transfer $A^- + B \rightleftharpoons A + B^-$	86
16. Disproportionation of Radical Anions	90
17. Reactions Initiated by the Disproportionation of Radical Anions	108
18. Electron Transfer to Organic Halides	111
19. Solvated Electrons	113
20. Optical and ESR Spectra of Solvated Electrons	123
21. Aggregation of Solvated Electrons	130
22. Electron Ejection in Liquids and Glasses	137
23. Concluding Remarks	139
References	139

1. INTRODUCTION

Many chemical reactions occurring in nature or studied in the laboratory are intrinsically associated with electron transfers. A chemical process in which a reagent gains an electron is known as its *reduction*, whereas deprivation of a reagent of one or more of its electrons represents its *oxidation*. Reductions and oxidations probably comprise the largest class of all chemical processes. They include numerous important inorganic, organic, and biological reactions; for example, respiration and photosynthesis, two of the most vital activities of living systems, are negotiated through electron transfer steps.

Although many oxidations and reductions are extremely complex, they can all be dissected into a series of simple elementary events among which are those resulting from a single electron transfer from some donor species, D, to another, A, which plays the role of acceptor. A variety of species may act as donors or acceptors; these include molecules and ions, as well as their aggregates or fragments. In an electrochemical reaction, the cathode is the donor while the anode acts as the acceptor. A solvent in which an electron ejection has taken place may be treated as the acceptor of an expelled electron, and in the same vein, empty space could be considered the acceptor of an electron ejected in a photoionization process involving a gaseous molecule or ion.

The subject of electron-transfer reactions is too vast to be encompassed in its entirety in a single chapter; we shall restrict our discussion to reactions proceeding in solution and involving organic reagents. Gaseous reactions will be mentioned occasionally; comparison of these with the analogous solution processes should clarify the role of solvents in electron-transfer

processes. A review of electron transfer in the gas phase is not available, although various aspects of that subject have been thoroughly discussed by many authors. For example, the problems of gaseous photoionization and autoionization were reviewed by Marr [1] and by Chupka [2]; those concerned with photoelectron spectroscopy by Turner [3]; electron impact phenomena were treated by Field and Franklin [4]; and electron-attachment reactions were surveyed by Page and Goode [5] and by Wentworth and Chen [6]. Interesting data on ion-molecule reactions in the gas phase are compiled in a book bearing this title and edited by Franklin [7]. Collisional phenomena observed in gaseous plasma are reviewed by McDaniel [9], and a general survey of problems pertaining to the interactions involving gaseous ions is provided in the classic monograph by Massey and Burhop [8].

Many of the interesting and important electron-transfer processes observed in solution involve ions of transition metals and their complexes with inorganic or organic ligands. These are conventionally classified as inorganic reagents and therefore their reactions will not be discussed here. The reader interested in that subject is referred to the excellent reviews and monographs by authoritative writers, including Taube, Halpern, Pearson, and Basolo [10].

Finally, intriguing electron-transfer processes occur in rigid media: in crystalline solids and in amorphous glasses. Some of them will be briefly reviewed in this chapter because their elucidation provides information clarifying several problems encountered in the course of studies of solution electron-transfer processes. However, other interesting electron-transfer phenomena occurring in rigid media belong to the field of solid state physics rather than chemistry, and these cannot be treated here. The reader who wishes to be introduced into the field of solid state physics may consult a concise book by Kittel [11].

By necessity, at least two of the reagents or products of any electron-transfer process are ions, that is, entities bearing a net positive or negative charge. Since the solution containing them has to be electrically neutral, the charges of the negative reagents have to be balanced by some positive ions while some negative ions balance the charges of the positive reagents. Formally, such counterions need not be engaged in the electron transfers under consideration, though, they often profoundly influence their rates and the position of the ultimate equilibria.

Ions interact strongly with their surroundings and with other ions present in solution. These interactions lead to the formation of a variety of thermodynamically distinct species. For example, an ion changes its identity and, to some extent, its chemical properties when the solvation shell surrounding it is modified; free ions have to be distinguished from ion pairs, triple ions, or still higher aggregates; and ion pairs composed of the same ions differently organized and solvated represent distinct thermodynamic entities. Each of

these species has its own characteristic physical properties that may permit its recognition and identification, a subject comprehensively discussed in Volume One of this book [12] and briefly elucidated in the preface to this Volume.

Since ionic species participate in every electron transfer, an understanding of the mechanisms of such reactions requires a detailed knowledge of the forms acquired by them as they react under the conditions prevailing in the process studied. The situation is often complex because two or more of such entities, each involving the pertinent reagent, may coexist in equilibrium and each may contribute then to the electron transfer, albeit to a different degree. Any variation of the thermodynamic parameters, such as concentration, temperature, or pressure, affects not only the rate constant and equilibrium constant of each elementary reaction, but it also modifies the proportions in which the various ionic entities are present in the system.

It is our main task to recognize these complex situations and to unravel the progress of such reactions by describing them in terms of elementary steps, each associated with a single type of ionic species. To achieve this goal, we need to know the chemical characteristics of the various ionic entities, as well as the thermodynamics and dynamics of their interconversion. Much of the data pertaining to the latter subject are provided in Volume One [12].

2. ELECTRON EJECTION IN THE GAS PHASE

Electron ejection and electron capture are the simplest electron-transfer processes. The former represents the transfer of an electron from a donor into its surroundings, which consists, in the case of gaseous reactions, of empty space. Ejection of an electron from a neutral molecule or an atom is referred to as its *ionization*,



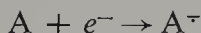
a term justified by the fact that an ion, or more correctly a radical cation, is produced in the reaction. The term "ionization process" is not entirely appropriate when applied to a step such as



because reaction (2), although a perfect analog of (1), destroys and does not produce an ion. Therefore the term "electron ejection" might be preferred to "ionization", since it applies equally well to both reactions.

The minimum amount of energy needed for the ejection of an electron from a gaseous species is referred to as its *ionization potential*, customarily denoted by symbols such as $I(D)$ or $I(A^-)$. The values of ionization potentials are generally given in units of electron volts (eV). The ionization potential of A^-

is, by definition, equal to the electron affinity of A, the maximum amount of energy *released* in the gaseous electron-capture process:



The electron affinity of A will be denoted by the symbol $EA(A)$ and its definition is expressed by the equation $EA(A) = I(A^-)$.

The conventional term "ionization potential" refers to the electron-ejection process that leaves the residue in its ground state. Paraphrasing this statement, we may say that the ejected electron comes from the highest occupied orbital of the species to be "ionized" while all the lower orbitals of the residue remain occupied. It is also possible to eject an electron from some lower orbital and leave the resulting residue in one of its excited states. The energy expended is then greater than that needed for the conventional process, its value being referred to as an *inner* ionization potential. Provided the approximation known as Koopmans theorem [13] is acceptable, the inner ionization potentials give the energy levels of the relevant atomic or molecular orbitals.

Several sources of energy may be used to induce an electron-ejection process.

1. *Thermal electron ejection.* For organic, electrically neutral molecules the ionization potentials are high, probably always higher than 6 eV, hence temperatures well above 10,000°C are required for thermal electron ejection. At these temperatures virtually all organic molecules are decomposed. However, the ionization potentials of radical anions are much lower, often less than 2 eV, and thermal ejection may then take place in an acceptable temperature range. Indeed, such a process is important under the experimental conditions used by Wentworth et al. [14] in their studies of electron affinities of aromatic molecules, see pp. 22–26.

2. *Photochemical electron ejection.* Two processes caused by photon absorption result in electron expulsion: direct ionization and autoionization. In the direct process, ejection occurs simultaneously with the photon absorption and no intermediate is produced. Autoionization, in contrast, results from spontaneous decay of an excited species formed by the primary absorption of a photon endowed with a sufficiently high energy. This intermediate, if produced by the irradiation of an atom, may decay either by the emission of radiation or by electron ejection. A third process, predissociation, is also possible when a molecule, but not an atom, absorbs the radiation. The emission of radiation occurs within times of the order of 10^{-8} sec while the relaxation times of electron ejection are usually much shorter. Consequently, autoionization is often more probable than fluorescence.

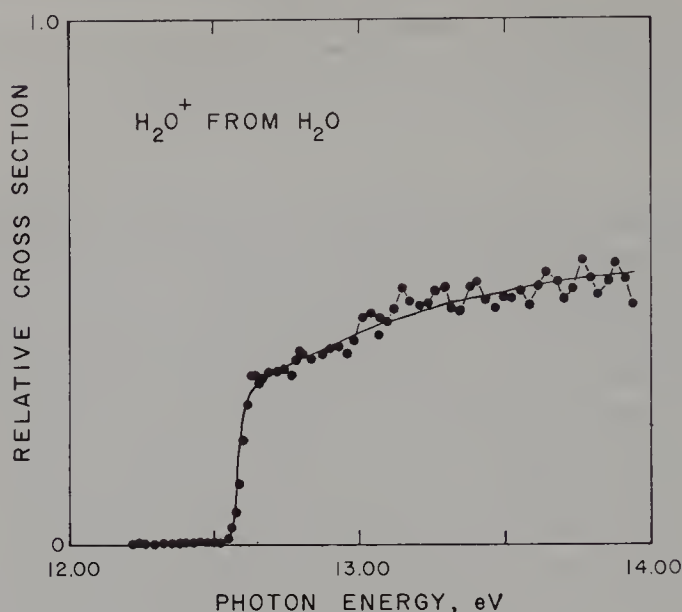


Figure 1. Probability of ionization of water vapor as a function of the frequency of the absorbed radiation. Note the steep rise of the ionization curve.

The probability of a direct photoelectron ejection is, in the first approximation, a step function of the frequency of the radiation. The onset of this process is abrupt, the electron ejection taking place when photon's energy reaches the critical threshold value. Thereafter, the probability of ionization varies only slightly with increasing frequency of the radiation as shown in Fig. 1 where the probability of the photoionization of water vapor is plotted as a function of radiation energy. However, closer examination of such curves reveals that the onset of ionization is not ideally abrupt; the probability of ionization rises steeply over a finite, although narrow, energy range.

The significance of this phenomenon becomes clearer on examination of the absorption spectra of molecules in the frequency range referred to as the vacuum UV. This high-energy radiation usually excites the least strongly bonded electron to a Rydberg state orbital, which spreads far away from the remaining electrons. The Rydberg electron therefore moves in a nearly spherically symmetric field of the ion core; its energy is given by the equation $E_n = I - \text{const}/(n - \delta)^2$, which resembles that describing the energy levels of a hydrogen atom. The Rydberg energy levels, like any energy levels, have a finite width. They converge to I as n tends to infinity; their spacing decreases gradually; and eventually, for sufficiently high values of n , the spacing becomes comparable to the line width and then the levels merge into a continuum *before* the ionization limit is reached. This accounts for the lack of sharpness in the onset of ionization, an effect amplified further by the unavoidable finite band width of the exciting radiation.

The well-established spectroscopic method of determining ionization potentials involves studies of spectral lines forming an appropriate Rydberg series. Extrapolation based on the equation $E_n = I - \text{const}/(n - \delta)^2$ provides the spectroscopic value of I . This approach, when applicable, gives the most accurate values of ionization potentials. Unfortunately, the usefulness of this method is limited to atoms and to some relatively simple molecules, because the spectra of larger molecules are often too complex to permit their unambiguous analyses.

Alternatively, ionization potentials may be determined by means of photoionization mass spectroscopy. This relatively new technique, developed by Watanabe and his co-workers [17, 18], is now successfully replacing the older and much less reliable electron-impact technique. In a photoionization mass spectrometer a monochromatic beam of photons impinges on a gaseous sample of the investigated material. The frequency of the incident light is gradually increased and the onset of the current, due to the investigated ions, signals the approach to the ionization threshold. The appearance of the desired ions is monitored by a conventional mass spectrometric analytic device.

The outcome of such experiments is recorded in the form of a plot of the photoionization current as a function of the energy of the impinging photons. Figure 1 illustrates such a curve. For some systems the shape of the photoionization curve also provides information about the vibrational energy levels of the residue. The direct excitation to higher vibrational states of the produced ion is manifested by the appearance of small steps superimposed

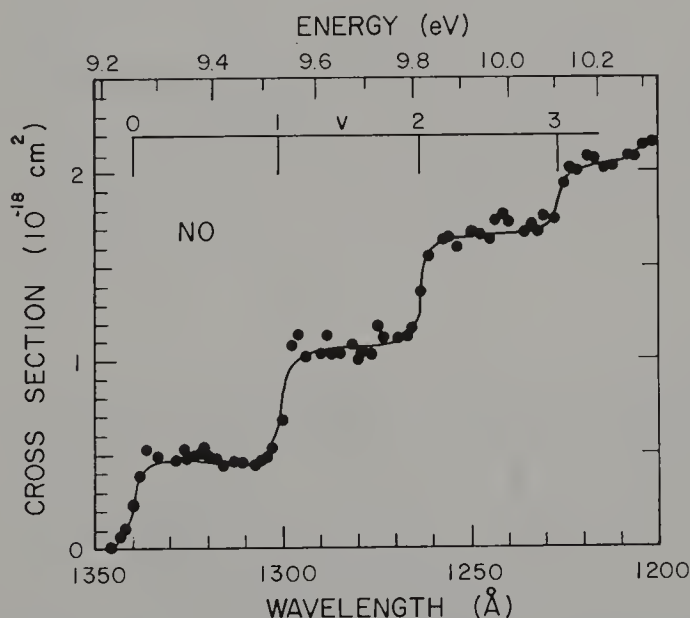


Figure 2. Photoionization curve of NO. Note the small steps revealing the formation of vibrationally excited NO⁺.

on the basically flat ionization curve. An example is provided by Fig. 2, which depicts the photoionization curve of NO.

An interesting example of an unusual ionization curve is presented in Fig. 3 where the photoionization cross section of methane is plotted as a function of the photon's energy. The hump revealed clearly by this figure implies a low probability of the transition to the vibrational ground state of the CH_4^+ ion. The equilibrium configuration of CH_4^+ is substantially distorted from the regular tetrahedral form of methane [15] by virtue of the Jahn-Teller effect; hence the Franck-Condon restrictions greatly reduce the probability of the transition from the regular tetrahedral CH_4 to the nonregular tetrahedral CH_4^+ ground state ion.

The photoionization mass spectroscopic technique provides us directly with the adiabatic ionization potential of the species investigated, that is, the energy of the $0 \rightarrow 0$ transition. Although there are few exceptions (e.g. the previously discussed photoionization of methane), this feature of photoionization mass spectroscopy is of great value. Let us recall that the electron-impact mass spectrometers furnish us with the *vertical* ionization potentials which involve ill-defined contributions of vibrational excitation energy. The reason for this difference calls for explanation. The quantum-mechanical wave packet describing an ionizing photon is relatively broad. Hence the time of interaction between such a photon and the irradiated molecule is

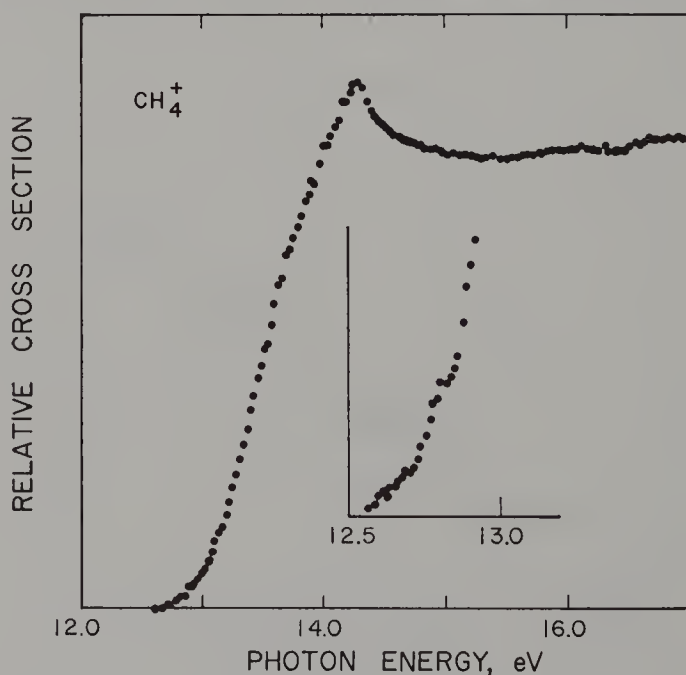


Figure 3. The photoionization cross section of CH_4 as a function of photon's energy. Note the hump in the ionization curve.

sufficiently long to provide a reasonable opportunity for the transition to the vibrational ground state of the product while an electron is ejected. This is not the case in electron-impact ionization, because the wave packet describing an electron is much narrower and the time of its interaction with the ionized molecule is much shorter than in the case of photoionization. The Franck-Condon restrictions are therefore more severe.

The application of photoionization mass spectroscopy to negative radical ions, say A^- , provides a precise means of determining their ionization potentials. By definition, these are identical with the electron affinities of the respective A molecules [19]. The technical details of this method were described by Smith and Branscomb [20] and by Branscomb [21]. Its successful application was reported in studies of the photoionization of some negative atomic ions such as H^- , O^- , and C^- . The onset of ionization is sharp and easily determined. The application of this method to diatomic species has been less satisfactory. For example, photoejection from O_2^- ions takes place at much too low a photon energy and the photodetachment cross section gradually increases with increasing frequency of light [22]. Therefore no reliable data for the electron affinity of O_2 could be derived from such studies. However, the investigations of electron photoejection from OH^- and OD^- [23], SH^- [24], and NO_2^- [25] did lead to reliable values for the electron affinities of these radicals.

3. *Photoelectron spectroscopy and ESCA.* Interaction of atoms or molecules with high-energy photons leads to the expulsion of electrons from inner orbitals of the irradiated species. In photoelectron spectroscopy the photoionization is achieved by means of UV light of $\lambda < 600 \text{ \AA}$, while in ESCA (Electron Spectroscopy for Chemical Analysis) soft X-rays serve as the ionizing agents. In both techniques a monochromatic beam of photons induces electron ejection, and the analysis is concerned not with the resulting ions but with the distribution of the kinetic energies of the ejected electrons. Denoting their kinetic energy by KE , we may write the basic relation of photoelectron spectroscopy,

$$KE = h\nu - I_k$$

where $h\nu$ gives the *constant* energy of the impinging photons and I_k is the energy of the k orbital. The spectrum of the kinetic energies of the ejected electrons is discrete, each peak being related to its I_k . The conventional adiabatic ionization potential is given by the peak corresponding to the highest kinetic energy of the expelled electrons.

The principles of photoelectron spectroscopy were described by Turner [26] in a popular and lucid paper published in 1968. Since then the technique has been greatly improved, both in its precision and in its resolution. Although lack of space prevents us from discussing this subject comprehensively,

some of the salient features of photoelectron spectra will be outlined briefly to illustrate the scope and breadth of this approach.

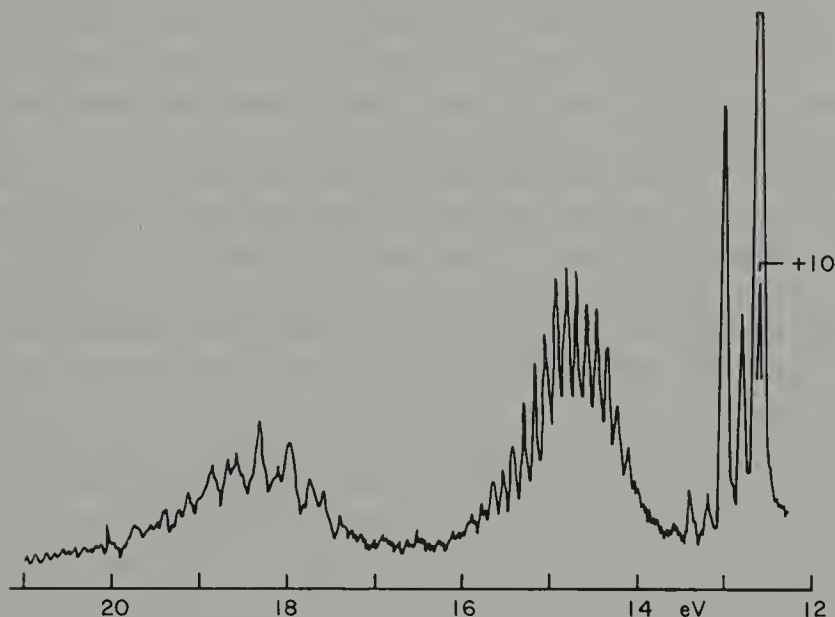
A photoelectron spectrum consists of a series of bands, each giving the energy of a molecular (or atomic) orbital (subject to the validity of Koopmans theorem [13]). In the first approximation, the intensity of each band is proportional to the number of electrons populating the pertinent orbital. This feature of the spectrum often facilitates the assignment of the bands to their orbitals. The sharpness of a band provides another hint useful in the characterization of the orbital from which the electron has been ejected. Expulsion of an electron from a nonbonding orbital does not affect the atomic framework; that is, the dimensions and the shape of the produced ion are virtually the same as those of the parent molecule. Consequently, such an ion is formed in its vibrational ground state; in other words, the process involves mainly the $0 \rightarrow 0$ transition. As a result, the corresponding peak of the photoelectron spectrum is sharp, and at higher resolution it shows very few vibrational lines. The binding energy of the atomic framework is greatly altered when an electron is ejected either from a strongly bonding or a strongly antibonding orbital, and thus the dimensions of the produced ions are substantially different from those of the parent molecule. For example, ejection of an electron from an orbital bonding two atoms of a parent molecule increases their separation in the ultimately formed ion. Hence, according to the Franck-Condon principle, such an ion is generated in a vibrationally excited state and the corresponding band of the photoelectron spectrum is broad and shows an extensive vibrational structure. The most intense vibrational line of such a band provides information about the position of the potential energy curve of the ion with respect to the potential energy curve of the parent molecule.

The assignment of the bands of a photoelectron spectrum to their appropriate orbitals is facilitated further by comparing the vibrational frequencies of the ion, reflected in the structure of a band, with the corresponding vibrational frequencies of the parent molecule. Both sets are virtually identical when the ejected electron originates from a nonbonding orbital. However, the vibrational frequencies of the ion are lower than the corresponding vibrational frequencies of the molecule when the electron is expelled from a bonding orbital, whereas they are higher if the ejection has taken place from an antibonding orbital.

The application of this criterion is unambiguous when adopted for the analysis of spectra of diatomic molecules, because each diatomic species is characterized by only one vibrational frequency. However, this criterion is even more useful when applied in the analysis of spectra of polyatomic molecules. Consider the ejection of an electron from an orbital involved in the bonding of two atoms of a polyatomic molecule. Such an ionization strongly

excites those vibrational modes of the ions which are associated with the two atoms in question. For example, the frequency of the respective stretching vibration is decreased on ionization if the depleted orbital is associated with the covalent bond linking these two atoms; alternatively, the bending frequency is reduced if the relevant orbital has maximum electron density between two atoms which formally are not bonded. The usefulness of such an analysis of vibrational structure is obvious.

To illustrate the application of these principles, let us consider the photoelectron spectrum of water vapor seen in Fig. 4. It consists of three bands



THE PHOTOELECTRON SPECTRUM OF H_2O USING THE HELIUM 584 Å LINE.

Figure 4. The photoelectron spectrum of water vapor.

corresponding to three molecular orbitals with energy levels 12.61, 13.7, and 17.22 eV. Molecular orbital calculations by Ellison and Schull [28] attributed the following ground state electronic configuration to H_2O :

$$(1a_1)^2(2a_1)^2(1b_2)^2(3a_1)^2(1b_1)^2 \cdots {}^1A_1$$

Inspection of the spectrum depicted in Fig. 4 shows that the first band ($I = 12.61$ eV) is sharp. The analysis of its vibrational structure yields a set of frequencies closely similar to those observed for H_2O . Hence this peak results from the expulsion of an electron residing in the nonbonding orbital ($1b_1$) representing the lone electron pairs of the oxygen.

The second band consists of a long series of approximately equally spaced vibrational lines. The calculated frequency is slightly lower than the bending frequency of H_2O . Both the length of the vibrational band and the decrease

of the vibrational frequency imply that the ejected electron is derived from the bonding orbital associated with the pseudo H—H bond of the H_2O molecule. Indeed, the $(3a_1)$ orbital has the highest electron density between the two H atoms and is associated with the restoring force partially responsible for the H—O—H bending vibration. These considerations permit the unambiguous identification of the second potential of 13.7 eV with the energy level of the $(3a_1)$ orbital.

A similar discussion, although more involved and less convincing, leads to the tentative identification of the third potential with the $(1b_2)$ orbital. A definite assignment of an orbital to that band is difficult for several reasons, the broadness of the individual vibrational lines being one of them.

The width of a line is a measure of the lifetime of the excited ion. This again provides useful information about the nature of the band and helps in its identification with a relevant orbital.

An interesting subtlety revealed by the photoelectron spectrum of chlorobenzene is worthy of mention. The band assigned to the lone electron pairs of the chlorine atom is split into two because the p_y atomic orbital of Cl, being perpendicular to the aromatic ring, is conjugated with the π system, whereas the p_x orbital, which lies in the plane of the ring, is not. The photoelectron spectra of other halogen-substituted aromatic and vinylic compounds show a similar feature.

The photoelectron spectrum of H_2O seen in Fig. 4 is induced by the H resonance radiation, $h\nu = 21.2168$ eV. Therefore no electrons could be ejected from orbitals deeper than 21 eV. Electrons residing in those orbitals can be expelled, however, by the soft X-rays used in the ESCA technique. Indeed, the ESCA spectra furnish information about energies of the deepest electronic levels classified as the atomic cores rather than the molecular orbitals. Although their energies are less affected by the molecular structure than the energies of the higher valence orbitals, they nevertheless show some "chemical shifts" [29] useful in chemical analysis. For example, the ESCA spectrum of ethyl trifluoroacetate contains four distinct lines corresponding to 1s orbitals of the four chemically different carbon atoms of this molecule.

One example illustrating subtleties of the spectra obtained by the ESCA technique may be discussed. The spectral band resulting from the ejection of an electron from the 1s orbitals of the O_2 molecule indicates the presence of two closely located energy levels in the product ion. This result is expected in molecules having nonzero electron angular momentum, J . When a core electron is ionized, the hole state is coupled to J in more than one way. This effect, termed the spin exchange splitting, should not be confused with the normal spin-orbit splitting. The simplest, as yet unobserved example of this phenomenon is expected in the ESCA spectrum of the Li atom. The ion resulting from expulsion of one of the 1s electrons may acquire either the 1s, $2s(^1S_0)$

or $1s, 2s(^3S_1)$ state. A related phenomenon has been observed in the ESCA spectrum of the NO molecule. In the resulting ion the residual $1s$ electron may be located around the N or O nucleus. However, since its coupling to the unpaired electron depends on its location, two peaks appear in the spectrum. Other interesting examples illustrating the complexities encountered in the ESCA spectra are given in a monograph by Siegbahn [30]. Unfortunately, the inherent width of the X-ray lines, amounting to about 0.8 eV, precludes studies of the vibrational structure of the ESCA bands.

4. *Autoionization phenomena.* Autoionization results from the excitation of an inner electron to some quasi-stable energy state located *above* the first ionization level of the investigated atom or molecule. Such an excited species may undergo spontaneous ionization—expulsion of an electron endowed with an appropriate kinetic energy—coupled with the virtual transition of the ionic core to a lower energy level. The autoionization phenomena are manifested by the appearance of absorption lines embedded in the continuum. In accordance with the uncertainty principle, such lines are broadened in inverse proportion to the lifetime of the autoionizing quasi-discrete state. In the simple case of one quasi-discrete state embedded in one continuum, the line shows a characteristic asymmetry due to the quantum mechanical interference between the two channels: the autoionization and the direct ionization. Detailed treatment of the theory of autoionization phenomena is outlined in a paper by Fano and Cooper [16].

A quasi-stable state also may be reached by simultaneous excitation of two electrons. For example, the $(2s, 2p), ^1P$ state of the helium atom is attained from its ground $(1s)^2, ^1S$ state on the excitation of both electrons. This state is relatively stable, although it lies 35 eV above the first ionization level of the atom. This is so because the ejection of one of the electrons is necessarily associated with the improbable transition of the other from the $2s$ to the $1s$ orbital. The perturbation responsible for this transition arises from the mutual repulsion between these two electrons.

Many of the electron-ejection processes to be discussed later arise from autoionization. Their discussion will clarify further the mechanistic details of this phenomenon.

5. *Electron ejection by electron impact.* This method of ionization is employed in the ordinary mass spectrometer. A beam of electrons, accelerated to the required potential, impinges on the investigated gas and the subsequent ionization is described by the equation $e^- + M \rightarrow M^+ + 2e^-$. This process leads to a vertical electron expulsion and yields vibrationally excited ions. Hence the onset of ionization is observed when the kinetic energy of the impinging electrons exceeds the value of the truly adiabatic ionization potential by 0.2–0.3 eV.

The cross section for the direct ionization of a molecule by electron impact

is zero at the threshold energy and varies approximately linearly with the excess of electron's kinetic energy, that is, its value σ is given approximately by

$$\sigma = \text{const}(E - E_0)^n$$

where E_0 denotes the threshold energy and n is close to unity. Therefore the curve representing the ionization current resulting from an electron impact process rises gradually from zero, and this greatly hinders the accurate determination of the energy threshold. Further difficulties are caused by the thermal distribution of the kinetic energies of the impinging electrons, since most electron-impact mass spectrometers do not operate with monochromatic electron beams.

A detailed discussion of electron-impact phenomena is given by Field and Franklin [4]. Here we wish only to reemphasize that ionization potentials determined by this technique are inferior to those obtained by the photoionization mass spectroscopy or by photoelectron spectroscopy. The following factors contribute to the uncertainty of the results:

- a. The ionization threshold has to be obtained through extrapolation, which depends on the nature of the investigated species.
- b. The result requires conversion of the vertical into the adiabatic ionization potential, the pertinent corrections being ill defined.
- c. The electron beams used in most electron impact mass spectrometers are not monochromatic and this requires still further corrections of the results.

6. *Electron ejection caused by ionizing radiation.* It is customary to refer to agents such as γ -rays, fast electrons ($E \sim 10^4$ – 10^6 eV), and other projectiles endowed with an extremely high kinetic energy as *ionizing* radiation. They hardly suffer any deflection as they move through the irradiated medium, and on encountering a molecule or an atom they transfer to it only a minute fraction of their energy. Nevertheless, the transferred energy is sufficiently large to cause ionization of the target species and ejection of very fast moving electrons. These so-called secondary electrons still have enough energy to ionize and excite the neighboring molecules and therefore virtually all of the observed effects of ionizing radiation result from their action. The direct contribution of the original projectiles to the overall process is almost negligible.

Let us consider in some detail the interaction of fast electrons with the briefly encountered molecules. A semiclassical treatment is sufficient to comprehend the salient features of this process. A molecule experiences an electric field generated by a swiftly moving electron during a time $\tau \approx b/v$, where b is the distance of the molecule from the electron's trajectory and v the velocity of the impinging electron. For a 100-V electron τ is usually less

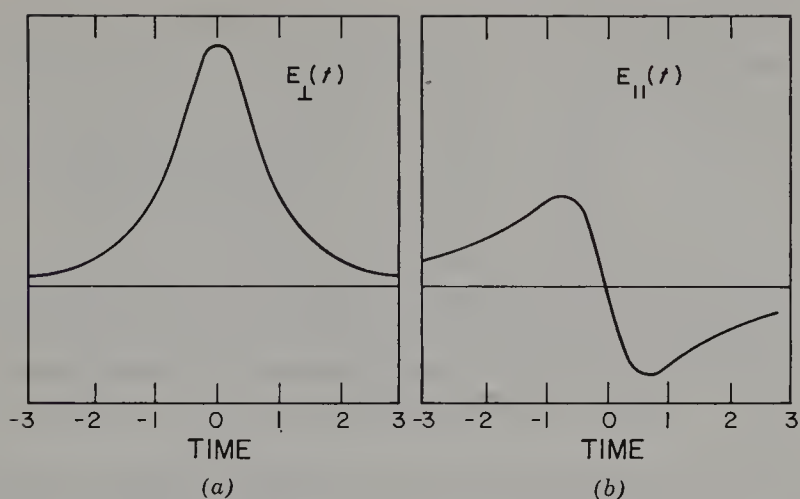


Figure 5. The time dependence of the electric field generated by a moving electron. (a) The field component perpendicular to the trajectory of the impinging electron. (b) The field component parallel to the trajectory of the impinging electron.

than 10^{-16} sec. The time dependence of the components of the field thus generated are shown in Fig. 5. Figure 5a refers to the component perpendicular to the electron's trajectory; the time dependence of the parallel component being shown in Fig. 5b. The moment when the impinging electron is at the shortest distance from the target is denoted as the zero time. Inspection of Figs. 5a and 5b clearly demonstrates that the electrons of the target experience a net force perpendicular to the trajectory of the impinging electron and therefore they are ejected in that direction. To calculate the amount of energy ΔE transferred in such an encounter let us assume that the target electron is at the distance b from the trajectory of the impinging electron. As is well known, the energy transferred, ΔE , is equal to the square of the momentum transferred divided by twice the electron's mass. The momentum transferred is given, in turn, by the product of the force, e^2/b^2 , and the time of the encounter, b/v . Thus one derives the relation

$$\Delta E = \frac{2e^4}{mv^2b^2} = \frac{e^4}{E_{\text{imp}}b^2}$$

where E_{imp} is the kinetic energy of the impinging electron. Hence the higher the velocity of the impinging electron, the less energy is transferred to a target, because the duration of the encounter becomes shorter. A 100-V electron passing a target electron at 1 Å distance transfers to it about 2% of its energy.

Alternatively, the outcome of an encounter between a fast-moving electron and a molecule may be deduced by treating the electron as equivalent to an appropriate beam of photons traversing the target. Thus the time-dependent electric field experienced by the target is represented by the sum (or integral)

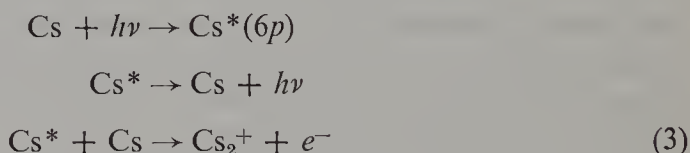
of its Fourier components. In this representation the spectrum of the “virtual photons” interacting with the target is given by the approximate relation $N_\nu = \text{const}/h\nu$, N_ν being the intensity of photons having frequency ν . The probability of an electronic transition involving an energy gain of $h\nu$ is proportional to N_ν for a constant oscillator strength. Hence this approach, in conjunction with conventional treatment of optical transitions, gives the value of the average energy transferred in a collision.

In conclusion, fast electrons induce molecular excitations and ionization leading to the formation of pairs e^- and M^+ . About 25 eV are dissipated in the creation of each pair when organic vapors are irradiated; however, this value is larger for gases like He (~ 40 eV), H_2 (~ 35 eV), N_2 (~ 35 eV), and CO_2 (~ 35 eV).

7. *Electron ejection induced by a chemical reaction.* Electron ejection may occur in a chemical reaction provided the energy liberated by the process is sufficiently high and is available for the ionization. The photosensitized ionization of alkali vapor provides an interesting example of such a process. Mohler and Boeckner [31] reported that ionization of cesium vapor has been induced by the absorption of light in the *discrete* range of the Cs spectrum; that is, electrons are ejected when $h\nu$ is still *smaller* than I . They showed that the rate of ionization is proportional to the first power of the intensity of the absorbed light while the pressure dependence of the quantum yield of ionization, ϕ , obeys the relation

$$\frac{1}{\phi} = A + \frac{B}{p}$$

These results are accounted for by the following mechanism:



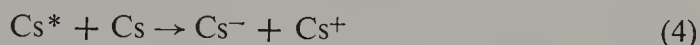
which implies that the bond dissociation energy of Cs_2^+ ($\text{Cs}_2^+ \rightarrow \text{Cs} + \text{Cs}^+$) is *greater* than that of Cs_2 ($\text{Cs}_2 \rightarrow 2\text{Cs}$). This unusual order of bond dissociation energies was in fact predicted by James' calculation [32] of the binding energies of Li_2 and Li_2^+ . The repulsion involving the electrons of inner shells is greater in Li_2 than in Li_2^+ ; however, since the integrals determining this repulsion involve exchanges between electrons of the inner and outer shells, no simple classic interpretation can be given to this phenomenon. The argument of James could be generalized. Indeed the spectroscopic studies of Barrow [33] confirm his prediction that $D(\text{Alk}-\text{Alk}) < D(\text{Alk}^+-\text{Alk})$, Alk denoting an alkali atom.

Table 1 Photoinduced Ionization of Alkali Vapor [34]

	K	Rb	Cs
Threshold of ionization (nm)	344.7	359.1	388.9
Threshold energy (eV)	3.59	3.45	3.19
Ionization potential of alkali atoms (V)	4.34	4.18	3.89
$\Delta E = \text{Threshold energy} - I$	0.75	0.73	0.70
Electron affinity ^a	0.47(?)	0.42(?)	0.39(?)

^a Electron affinities were estimated by Weiss [36]. The experimental values determined by the charge-transfer method are even lower, viz., 0.22, 0.16, and 0.13 eV, respectively (see [35]).

The photosensitized ionization was demonstrated by the onset of a photo-induced electric conductance of the vapor, and therefore an alternative explanation of the observed phenomenon could be suggested:



This reaction would be exothermic, and therefore possible, had the ionization potential of the *excited* cesium atom been *lower* than the electron affinity of the ground state atom. The threshold of excitation needed to induce the ionization is at 388.9 nm, corresponding to the energy threshold of 3.19 eV [31, 34]. The atomic ionization potential of Cs is 3.89 V; hence if the electron affinity of Cs atoms were higher than 0.7 eV reaction 4 could be feasible. The electron affinity of cesium atoms determined by the charge exchange method [35] is 0.13 eV, but even the higher value of 0.39 eV obtained through quantum mechanical calculations [36] is still not sufficient to allow the formation of a Cs^- and Cs^+ pair. It therefore seems that the observed photoconductance must result from reaction 3 and not 4.

The mobility of ions produced by the photolysis is too large to be accounted for by the formation of Cs^+ and Cs^- ions, and this furnishes further evidence for Eq. 3 [34]. These experiments were extended to the vapor of rubidium and potassium and the results showed that the diatomic ions, K_2^+ and Rb_2^+ , are formed in these systems.

Inspection of Table 1 summarizing the results of Lee and Mahen suggests that $D(\text{Alk}^+-\text{Alk})-D(\text{Alk}-\text{Alk})$ is about 0.7 eV for K_2 , Rb_2 , and Cs_2 . This increase in bond strength provides the additional energy needed for the ionization of the resulting dimer.

3. ELECTRON CAPTURE IN THE GAS PHASE

An interaction between a neutral atom or molecule and an electron could lead to its capture, resulting in a negative ion. To comprehend the origin

of the attractive force responsible for the electron attachment let us consider first the interaction of a neutral atom with an electron. A static atom does not attract an electron because its spherical symmetry prevents generation of an electric field at distances greater than its radius. However, an atom may be polarized by an electron, and then the electron-induced dipole generates an attractive field in the outside space the intensity of which falls off approximately with the fourth power of distance [37]. Due to the short range of such a field the negative ions resulting from electron capture have very few stationary states, if any. Moreover, the hindering effect of the Pauli exclusion principle makes the atoms with closed shells, or subshells, very poor electron acceptors.

The attachment of an electron to a molecule is, on the whole, more probable than its capture by an atom. The process may be especially facile with polar molecules which generate a strong attractive force for the passing electron. Electron capture by the nonpolar, but highly polarizable, aromatic hydrocarbons is also facile; the resulting radical ions will be discussed at length in later sections of this chapter.

Any electron capture produces an energized ion, provided the process is a nonradiative one. Under some conditions, radiative attachments of electrons are observed; for example, the attachment to atoms such as H, O, N, or halogens may proceed with light emission, although the probability of such an event is very low. The resulting radiation is continuous, its spectrum being referred to as the affinity spectrum [21]. For example, the visible continuum of solar radiation is due, to a great extent, to the radiative capture process $H + e \rightarrow H^-$.

The lifetimes of energized negative ions vary from as little as 10^{-15} sec to about 1 msec. The extremely short lived ions (10^{-15} – 10^{-13} sec) do not contribute to any chemical events, and their existence is manifested only by the resonance scatter experiments. The moderately short lived species (10^{-12} – 10^{-6} sec) can be stabilized by collisions, provided the pressure is sufficiently high, while many polyatomic and even some diatomic ions may live long enough ($>10^{-6}$ sec) to permit their mass spectroscopic observation.

The kinetic energy of a captured electron is an important factor determining the lifetime of the resulting negative ion. For example, the lifetime of *p*-benzoquinone radical anion decreases from 50 μ sec to about 10 μ sec as the kinetic energy of the captured electron increases from 1.6 to 3 eV [38]. A much larger span of lifetimes is found for the radical anions of 1,4-naphthoquinone; they last for about 350 μ sec when formed by the capture of thermal electrons, but their lifetime decreases to 10 μ sec as the kinetic energy of the electron rises to 1 eV. The relation between the lifetime of a negative ion and the kinetic energy of the captured electron often is given by the function depicted in Fig. 6.

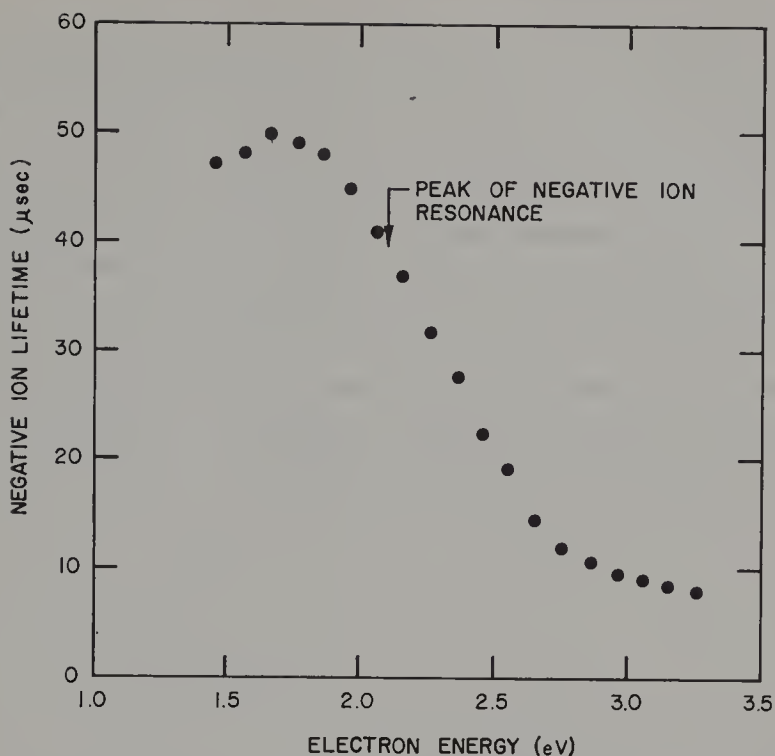


Figure 6. Lifetime of a negative ion as a function of kinetic energy of the captured electron.

The electron capture cross sections often show resonance effects; within a narrow range of electron kinetic energy their values become suddenly large. For example, an electronically excited Feshbach resonance is observed when the kinetic energy of the approaching electron matches the energy of some vibrational state of the electronically excited target molecule lying above the ionization level of the resulting negative ion. Similarly, a nuclear excited Feshbach resonance takes place when the kinetic energy of the electron matches some higher vibrational state of the eventually formed ion.

Not every atom or molecule ultimately forms a stable negative ion. The necessary condition for such a stability is expressed by the inequality

$$\epsilon_0^- > \sum_1^Z (\epsilon_i^0 - \epsilon_i^-)$$

where ϵ_0^- is the binding energy of the captured electron *in the negative ion*, and ϵ_i^0 and ϵ_i^- are the binding energies of the original Z electrons of the “captor” before and after the capture event [37]. Of course,

$$\epsilon_0^- - \sum_1^Z (\epsilon_i^0 - \epsilon_i^-) = \text{Electron affinity of the captor}$$

and

$$\sum_0^Z \epsilon_i^0 = \text{Total electronic binding energy of the captor.}$$

Electron capture by a neutral molecule may be regarded as a transition taking place between two electronic levels of the negative radical ion. In the initial state one of the electrons of the radical ion occupies an unbound orbital, the potential energy curve of such a system being that of the neutral molecule in its ground state. The final state is, of course, the electronic ground state of the resulting radical anion. An electron is captured if its kinetic energy is equal to the potential energy of the negative radical ion in its electronic ground state, having, however, a configuration of the neutral molecule in its lowest vibrational state (a consequence of the Frank-Condon principle). The transition then takes place and produces a vibrationally excited radical ion. The relevant relations are clarified by inspection of the potential energy curves of diatomic molecules shown in Fig. 7.

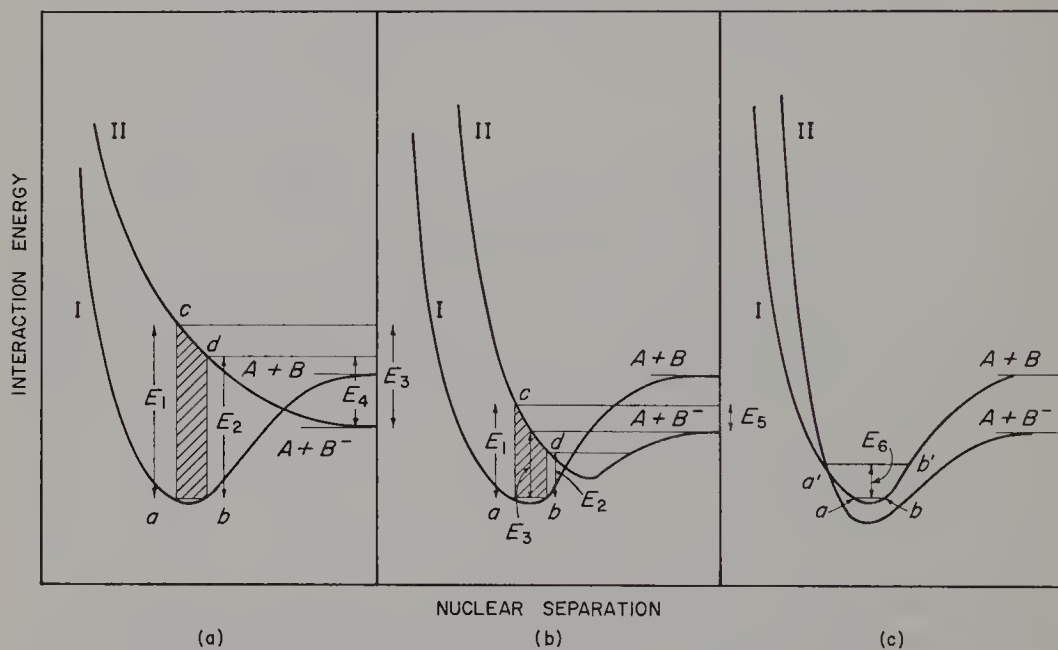


Figure 7. Potential energy curves showing the three possible ways in which diatomic negative ions AB^- may be formed by an electron-capture process.

In case *a* the potential energy of AB^- is repulsive and electron capture results in the dissociation of AB into $A \cdot + B^-$. The capture is efficient if the kinetic energy of the electron is greater than E_2 but smaller than E_1 ; electrons with energies higher than E_1 or lower than E_2 will be scattered instead of being captured.

In case *b* capture of an electron endowed with kinetic energy higher than E_2 but lower than E_3 leads to the formation of an AB^- radical ion which could be stabilized by subsequent collisions. Denoting by θ the relaxation time of spontaneous decomposition of a nonstabilized AB^- into $AB + e$, and by τ

the average time between collisions, one finds the probability for the formation of a stable radical ion by such a process to be $\omega = \theta/(\theta + \tau)$. Since $1/\tau$ is proportional to the gas pressure p , whereas θ is pressure independent, $\omega = p/(p + p')$ where p' denotes the pressure at which $\tau = \theta$.

Case *c* represents a most interesting situation when only a vibrationally excited molecule AB has a high probability of electron capture. Of course, left to itself the radical ion will lose its extra electron through a reverse process, but it may be stabilized, like the radical ion of case *b*, by collisions with gas molecules.

To recapitulate, diatomic molecules in the gas phase may capture electrons if their kinetic energies are within well-specified limits. Vibrationally excited negative radical ions are produced if the potential energy curves are favorably interrelated. These ions lose their extra electron in about 10^{-8} sec, but they become stable if a favorable collision with a gas molecule has taken place during this time. Hence at atmospheric pressure, when $\tau \sim 10^{-9}$ – 10^{-10} sec, stable radical ions may be formed through an electron-capture process involving suitable acceptor molecules.

Electron capture by polyatomic molecules resembles the process described for diatomic molecules. However, a polyatomic molecule has many degrees of freedom and a large number of available energy levels. Consequently, the restrictions imposed on the kinetic energy of the captured electron are greatly relaxed.

4. DETERMINATION OF ELECTRON AFFINITIES

The discussion of the problems associated with electron capture introduced us to the concept of the electron affinity of an acceptor. As was stated before, the electron affinity of a species A is equal to the amount of energy liberated in the formation of a negative A^- ion in its ground state in the course of attachment of a resting electron. Experimental determination of electron affinities is more difficult than determination of ionization potentials, and therefore our knowledge of electron affinities is still very meager. The methods available for the determination of this important quantity will now be surveyed.

The photoionization technique provides the most accurate and promising method for determining electron affinities. It has a great advantage over other methods in that the identity of the investigated ions is established by mass spectroscopic techniques as the photodetachment is studied.

Closely similar to photoionization is the technique of photoabsorption developed by Berry [39]. Both techniques were applied in the determination of electron affinities of halogen atoms and led to concordant results.

Much of the data now available were obtained by the surface ionization method originally developed by Mayer and his co-workers [40–43] and later utilized by other investigators [44]. Affinities are determined from studies of the equilibrium



established close to a hot wire emitting electrons. The experiment requires the determination of the ratio of concentrations of the free electrons and the X^- ions in the vapor surrounding the hot filament. This is achieved by measuring the current due to all the negative species, $e^- + A^-$, and remeasuring it when a suitable filter, preventing the electrons from reaching the anode, is employed. A coiled wire surrounding the hot filament may act as a filter. A current passing through the coil generates a magnetic field which drives the electrons into spiral paths and thus deflects them from the anode. This device, known as the magnetron, was recently improved by Page, who used it extensively in his studies of electron affinities of various acceptors [5]. Although some of the results obtained by the magnetron technique are reliable (e.g., those for O, OH, and halogen atoms [45, 46]), others are questionable. For example, the value of the electron affinity of CN determined by the magnetron technique [47] is lower by more than 0.6 eV than that determined by the photoionization method. The greatest drawback of the magnetron technique is its susceptibility to impurities that may vitiate the results.

The differences of electron affinities may be determined by a similar technique. This variant of the surface ionization method is more accurate than the direct approach, because the relative measurements are independent of several experimental parameters which are difficult to determine and to control, e.g. of the pressure of the surrounding gas and the work function of the filament. Studies of this nature were independently pursued by Bakulina and Ionov [49] and by Bailey [50]. A review of the details of the surface ionization technique was published recently by Zandberg and Ionov [51].

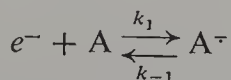
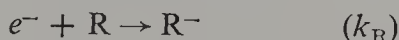
Attempts to determine the electron affinities of polyatomic molecules by the electron-impact method have been reported in the literature. The pertinent experiments were performed with benzene and some of its derivatives and with naphthalene [52]. However, the results provide only the lower limit for the actual electron affinity.

A most interesting method, uniquely applicable for the determination of electron affinities of polyatomic molecules, was developed recently by Becker, Wentworth, and their associates. Their design utilized an electron-capture detector developed by Lovelock [53] for gas chromatographic analyses. Such a detector operates at a low electric field and counts low-energy electrons. The vapor of the substance to be investigated is mixed with a very large excess of a suitable carrier gas that flows from a chromatographic

column into the device. A mixture of argon containing 10% methane is most conveniently used for this purpose. The ionization is achieved by irradiating the gas with β -rays from a tritium source. The primary fast electrons are rapidly slowed down, their kinetic energy being reduced to the thermal level through inelastic collisions with the molecules of the carrier, and in the course of this process secondary electrons and positive ions, as well as neutral radicals, are produced. The stationary concentrations of the latter two species remain constant if the operating conditions are standardized. In particular, they are not affected by the presence of the substance under investigation because its partial pressure is negligibly small when compared with that of argon and methane. On the other hand, only the molecules of the investigated vapor are capable of capturing thermal electrons; neither methane nor argon can undergo an electron-capture process. Accordingly, the presence of the substance under investigation reduces the concentration of thermal electrons in the plasma. The use of a chromatographic column ensures the purity of the investigated compound.

By applying a short-duration positive potential to the collecting electrode of such a device one can measure the concentration of thermal electrons. In the argon-methane mixture the current drawn from the electrode was found to be proportional to the electron density in the plasma, its value being independent of the pulse duration (0.5–5 μ sec) and of the applied voltage (10–80 V).

The following model [54] was proposed to account for the events occurring within the electron capture cell during the pulse sampling period: (1) the rate of formation of thermal electrons is assumed to be constant and not affected by the presence of the investigated vapor; (2) the pulse is assumed to remove most of the electrons leaving a large excess of positive ions, \oplus , and of radicals, R, in the plasma, that is $[\oplus] \gg [e^-]$ and $[R] \gg [e^-]$; (3) thermal electrons are supposed to be lost only by the following three reactions:



Hence in the absence of the investigated compound A,

$$\frac{d[e^-]}{dt} = k_p R_\beta - \{k_N[\oplus] + k_R[R]\}[e^-]$$

and in its presence,

$$\frac{d[e^-]}{dt} = k_p R_\beta - \{k_N[\oplus] + k_R[R]\}[e^-] - k_1[A][e^-] + k_{-1}[A^-]$$

Here $k_p R_\beta$ is the rate of formation of thermal electrons through the action of β -rays.

The stationary concentration of radical ions $[A^\cdot]$ is determined by four processes: their formation through electron capture, their destruction by the thermal electron ejection, and their loss in collisions with the positive ions and the radicals:

$$\frac{d[A^\cdot]}{dt} = k_1[A][e^-] - k_{-1}[A^\cdot] - \{k'_N[\oplus] + k'_R[R]\}[A^\cdot]$$

Denoting the sums $\{k_N[\oplus] + k_R[R]\}$ and $\{k'_N[\oplus] + k'_R[R]\}$ by k_D and k_L , respectively, we may rewrite the above equations as

$$\frac{d[e^-]}{dt} = k_p R_\beta - k_D[e^-] \quad (\text{in the absence of } A)$$

$$\frac{d[e^-]}{dt} = k_p R_\beta - k_D[e^-] - k_1[A][e^-] + k_{-1}[A^\cdot] \quad (\text{in the presence of } A)$$

and

$$\frac{d[A^\cdot]}{dt} = k_1[A][e^-] - k_{-1}[A^\cdot] - k_L[A^\cdot]$$

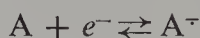
At a sufficiently long time ($t = \infty$), the simultaneous solution of these equations gives the stationary concentrations of electrons in the absence of A, denoted by $[e^-]_0$, and their stationary concentration in the presence of A, denoted by $[e^-]_A$. The electron capture coefficient K ,

$$K = \frac{[e^-]_0 - [e^-]_A}{[A][e^-]_A}$$

may therefore be calculated:

$$K = \frac{k_L k_1}{k_D(k_L + k_{-1})}$$

The pseudo first-order constants k_L and k_D refer to the diffusion-controlled reactions, and hence their ratio is essentially temperature independent, whereas k_{-1} increases exponentially with temperature. Thus at sufficiently high temperatures, $k_{-1} \gg k_L$ and then $K = (k_L/k_D)K_{eq}$, where K_{eq} is the equilibrium constant of the reaction



The plot of $\ln K/T^{3/2}$ versus $1/T$ is then linear and its slope gives the electron affinity of the compound studied provided that (1) the experiments have been performed within a sufficiently high temperature range, and (2) the ratio

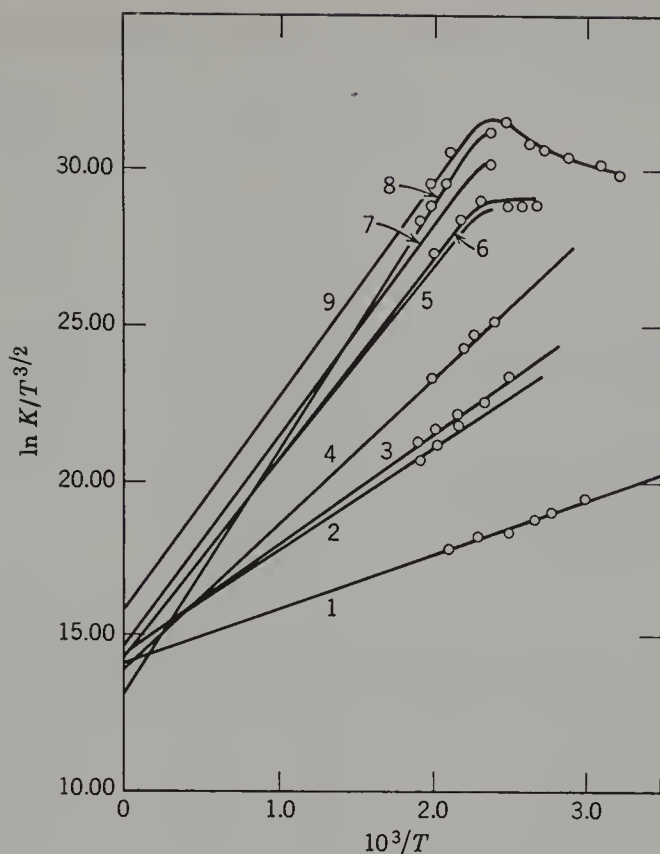


Figure 8. Electron affinities of aromatic hydrocarbons determined by the slope of lines giving $\ln (K/T^{3/2})$ versus $1/T$. K denotes the electron capture coefficient which, at sufficiently high temperatures, is proportional to K_{eq} , the equilibrium constant referring to the electron-capture reaction, $A + e^- \rightleftharpoons A^-$.

k_L/k_D as well as the ratio of partition functions of the radical anion and its parent molecule are temperature independent. In such cases all the lines should have a common intercept, but inspection of Fig. 8 and examination of the data collected in Table 2 indicate that this conclusion is only approximately correct [54, 56]. The accuracy of the electron affinity determination cannot be improved by assuming a constant value of the intercept, contrary to the feelings of the authors.

At low temperatures $k_{-1} \ll k_L$ and then $K = k_1/k_D$ becomes virtually temperature independent. The results obtained at lower temperatures, if included in the calculation, lead to values for the electron affinity which are too low. The pseudo-constant k_D may be estimated from the dependence of the current on the duration of the pulse. Thus an approximate evaluation of k_1 is possible and the values of k_1 , given in ref. 54, were found to range from 3.5 to 25×10^{12} liter mole $^{-1}$ sec $^{-1}$. This nearly tenfold variation of the rate

Table 2 Electron Affinities of Aromatic Hydrocarbons in the Gas Phase [54, 56]

Compound	Electron Affinity (eV)	Intercept
Naphthalene	0.152 ± 0.016	14.21
Triphenylene	0.284 ± 0.020	14.38
Phenanthrene	0.308 ± 0.024	14.33
Chrysene	0.419 ± 0.036	13.98
Benzo[<i>e</i>]pyrene	0.486 ± 0.155	
Picene	0.490 ± 0.110	
Benzo[<i>c</i>]phenanthrene	0.542 ± 0.040	14.44
Anthracene	$0.552 \pm 0.061(?)$	14.44
Pyrene	0.579 ± 0.064	14.66
Dibenz[<i>a,h</i>]anthracene	0.676 ± 0.122	
Dibenz[<i>a,j</i>]anthracene	0.686 ± 0.155	
Benz[<i>a</i>]anthracene	0.696 ± 0.045	
Benzo[<i>a</i>]pyrene	0.829 ± 0.121	12.94
Azulene	0.587 ± 0.065	16.06

Electron Affinities of Some Aromatic Aldehydes and Ketones [58]

Acetophenone	0.334 ± 0.004	14.70
Benzaldehyde	0.42 ± 0.010	15.89
Naphthaldehyde-2	0.62 ± 0.040	14.46
Naphthaldehyde-1	0.745 ± 0.070	12.61
Phenanthrene aldehyde-9	0.655 ± 0.14	14.92

constants of the diffusion-controlled processes again indicates that the assumption of a fixed intercept is questionable.

The results obtained for azulene deserve some comment. The rate constant k_1 of the electron-capture process for this hydrocarbon appears to involve an activation energy of about 0.15 eV, whereas no activation energy was anticipated or observed for other hydrocarbons. This might indicate that only vibrationally excited molecules of azulene may capture an electron; that is, the relevant process corresponds to case *c* of Fig. 7.

The method developed by Wentworth applies to nondissociative electron-capture processes—a point emphasized in one of his papers [57]. Although a similar approach led to successful treatment of the dissociative electron-capture processes [55], the results of such investigations do not yield values of the relevant electron affinities.

We conclude this section by briefly mentioning two more techniques utilized in the determination of electron affinities. Equilibrium between free electrons and acceptors is often established in flames, and such systems were first investigated by Rolla and Piccardi [59]. Injection of alkali metals into

flames provides a convenient source of thermal electrons. Their concentration may be determined by the degree of attenuation of microwaves traversing the flame. In the presence of a suitable electron acceptor, the following equilibria are established:



Knowing K_{alk} and the concentrations of Alk, e^- , and A in the flame, one can calculate K_{A} and, from its temperature dependence, the electron affinity of A. Alternatively, the electron affinity may be calculated from a value of K_{A} determined at one temperature by applying the third law of thermodynamics. In such calculations the reasonable assumption is made that the values of the translational, rotational, and vibrational partition functions are the same for A and A^- .

Recently the electron affinities of some gaseous radicals were estimated from the results obtained by studies of the thermal proton transfer reactions [61]. Thus the electron affinities of phenyl and benzyl radicals were estimated to be within the following ranges: more than 1.2 but less than 1.6 eV and more than 0.4 but less than 0.9 eV, respectively. The latter value seems to be rather low.

5. DEPENDENCE OF IONIZATION POTENTIALS AND ELECTRON AFFINITIES ON MOLECULAR STRUCTURE

The understanding of the effect of molecular structure on the ionization potential and electron affinity is of great importance. Therefore we shall discuss this subject briefly restricting, however, our review to organic molecules. The ionization potential of linear aliphatic hydrocarbons decreases with the length of the chain, approaching a value of about 10.1 eV for an infinite chain. The values for the first few members of that series are given in Table 3. Inspection shows that photoelectron spectroscopy, photoionization, and vacuum UV spectroscopy give concordant results with an accuracy better than ± 0.03 eV, whereas the electron-impact technique gives results too high by 0.2–0.3 eV.

Contrary to general belief, branching does not decrease the ionization potential of aliphatic hydrocarbons, or at most it affects it only very slightly. Probably the highest occupied molecular orbital of the $\text{C}_n\text{H}_{2n+2}^+$ ion involves mainly the C—C σ orbitals with little contribution of the $\pi\text{C—H}$ orbitals. Two examples of the effect of branching are given in Table 3.

Not surprisingly, the ionization potential of cyclopropane is substantially

Table 3 Ionization Potentials of Hydrocarbons

Hydrocarbon	Ionization Potential (eV)			
	Photoelectron Spectroscopy	Photoionization	Electron Impact	UV Spectroscopy
CH_4	12.98; 12.99	12.98	(13.22)	12.95
C_2H_6	11.51; 11.49	11.65	(11.86)	—
C_3H_8	11.06; 11.07	11.07	(11.52)	—
$n\text{-C}_4\text{H}_{10}$	10.67; 10.50	10.63	(10.90)	—
$n\text{-C}_5\text{H}_{12}$	10.37	10.35	(10.53)	—
$n\text{-C}_6\text{H}_{14}$	10.27	10.18	(10.43)	—
$n \rightarrow \infty$	extrap.	~ 10.1		
Effect of Branching				
$n\text{-C}_4\text{H}_{10}$	10.67; 10.50	10.63		
$iso\text{-C}_4\text{H}_{10}$	10.69; 10.78	10.57		
$n\text{-C}_5\text{H}_{12}$	10.37	10.35		
$neo\text{-Pentane}$	10.40	10.35		
Cyclic Aliphatic Hydrocarbons				
$\text{C-C}_3\text{H}_6$	10.06; 9.96	10.06	(10.53)	
$\text{C-C}_5\text{H}_{10}$	10.49	10.53	(10.92)	
$\text{C-C}_6\text{H}_{12}$	9.81; 9.79	9.88	(10.50)	
Olefins				
Ethylene	10.50; 10.48	10.51	(10.62)	10.51
Propene	9.69	9.73	(9.84)	9.70
1-Butene	9.59	9.58	(9.76)	—
<i>cis</i> -2-Butene	9.12	9.13	(9.29)	—
<i>trans</i> -2-Butene	9.12	9.13	(9.27)	—
Isobutene	9.17	9.23	(9.35)	—
Dienes				
Allene	9.83; 9.69	9.62	10.0	10.19(?)
1,3-Butadiene	9.07; 9.08	9.07	(9.24)	9.06
Cyclopentadiene	8.55	—	(8.7)	8.58
Acetylenes				
C_2H_2	11.36; 11.40	11.40; 11.41	11.39; 11.40	11.35
C_2D_2	11.40	11.42	—	—

lower than of *n*-propane (by about 1 eV). The ionization potential of cyclopentane seems to be slightly *higher* than of *n*-pentane, whereas that of cyclohexane is slightly *lower* than that of *n*-hexane. The electron-impact values are again too high by 0.4–0.6 eV.

The ionization potentials of olefins are substantially lower than those of paraffins, a well-known fact attributed to the weaker binding of π electrons. Again the agreement between the results obtained by photoelectron spectroscopy, photoionization, and vacuum UV spectroscopy is excellent. This may be seen from the data collected in Table 3.

The ionization potential of allene is higher than that of propene but lower than that of propane. The rigidity of cyclopentadiene, when compared with butadiene, accounts for the very low ionization potential of the former diene.

Finally, acetylene and its derivatives have substantially higher ionization potentials than the corresponding olefins. For example, the ionization potential of acetylene is higher than that of ethylene by nearly 1 eV.

Aromatic hydrocarbons and the related heterocyclics form a class of compounds which is especially important for our discussion of electron-transfer processes. Their ionization potentials are relatively low, and for the sake of illustration, the ionization potentials of some typical compounds of this class are listed in Table 4. The reliability of the data obtained by photoelectron spectroscopy or by photoionization is indicated by the striking agreement between these values. The recent data obtained from photoelectron studies of aromatic hydrocarbons are given in refs. 348–350.

The ionization of the aromatic hydrocarbons results from the ejection of the least strongly held π electron. Indeed, the experimental results agree well with those calculated by the various quantum mechanical approximations.

The effect of substituents on the ionization potential of benzene is exemplified by the data collected in the second part of Table 4. These ionization potentials are linearly correlated with σ^+ —an observation reported by Watanabe [62].

The situation is more complex for the heterocyclic analogs of aromatic hydrocarbons, because the least strongly held electron may be located either in a π orbital or in the *n*-orbital of the nitrogen atom. A systematic study of this problem was reported by Dewar and his associates [63], and their results are collected in the last part of Table 4. Comparison of the experimental data obtained by photoelectron spectroscopy with quantum mechanical calculation led to the conclusion that the lowest ionization potential of pyridine, 1,4-pyrazine, quinoline, isoquinoline, quinoxaline, and quinazoline corresponds to the ejection of a π electron, but in the first ionization of 1,3-pyrimidine, 1,2-pyridazine, cinnoline, and phthalazine an *n* electron is ejected.

Patterns reflecting the relation of structure to the electron affinity of acceptors are poorly established mainly due to the scarcity of electron

Table 4 Ionization Potentials of Aromatic Hydrocarbons, Their Derivatives, and Heterocyclic Analogs

Aromatic Compound	Ionization Potential (eV)		
	Photoelectron Spectroscopy	Photoionization	UV Spectroscopy
Condensed Aromatic Hydrocarbons			
Benzene	9.25	9.245	9.248
Naphthalene	8.12; 8.11	8.12	8.134
Anthracene	7.47	7.5; 7.38	7.41
Tetracene		6.88	
Biphenyl	8.23; 8.20	8.27	
Phenanthrene	7.69; 7.91; 7.86	7.75	7.69
Triphenylene			
Chrysene	7.60		
Pyrene		7.55	
Perylene	7.00	7.03	
Benzanthracene 1,2	7.47		
Benzipyrene 1,2	7.12		
Pentacene	6.74		
Benzipyrene, 3,4		7.2	
Azulene	7.43; 7.42	7.41	7.43
Fluoranthene	7.80		
Acenaphthylene	8.02		
Acenaphthene	7.73		
Fluorene	7.93		
Indene	8.14; 8.13		
Effect of Substitution			
Benzene	9.25	9.245	9.247
Toluene	8.82	8.82	
Fluorobenzene	9.19	9.195	
Chlorobenzene	9.06	9.07	
Bromobenzene	9.05	8.98	
Iodobenzene	8.67	8.73	
Benzotrifluoride	9.70	9.68	
Phenol	8.52	8.52	
Anisole	8.21	8.22	
Aniline	7.96	7.70	
Nitrobenzene	10.0	9.92	
Benzaldehyde	9.4	9.53	
Benzonitrile	9.68; 9.65	9.705	
Styrene	8.43	8.47	
Phenylacetylene		8.815	
Heterocyclic Analogs of Benzene and Naphthalene			
Benzene	9.24; 9.25	9.241	
Pyridine	9.31; 9.28	9.32	

Table 4 (Continued)

Aromatic Compound	Ionization Potential (eV)	
	Photoelectron Spectroscopy	UV Photoionization Spectroscopy
Heterocyclic Analogs of Benzene and Naphthalene		
Pyrazine	9.36; 9.27	9.29
Pyrimidine	9.42; 9.47	9.35
Pyridazine	8.90; 8.91	8.71
Naphthalene	8.11; 8.12	8.12
Quinoline	8.62; 8.67	8.62
Isoquinoline	8.54; 8.53	8.55
Quinoxaline	8.99	9.02
Quinazoline	9.02	
Cinnoline	8.51	8.95
Phthalazine	8.68	9.22
Acridine		7.78

affinity data. For aromatic hydrocarbons the Hückel approximation leads to the relation $I + EA = \text{const}$ [343] which is verified by the experimental data obtained for 8 aromatic hydrocarbons [56]. The pertinent *constant* was found to be 8.34 eV. Recalling that the $1/2(I + EA)$ is designated as a measure of electron negativity, we may conclude that the electron negativities of aromatic hydrocarbons are independent of their structure. Theoretical calculation of electron affinities are less reliable than the calculation of the respective ionization potentials. Apparently the addition of an electron more profoundly affects the energies of the original orbitals of the acceptor than the removal of its least bonded electron.

6. SOLUTION ELECTRON AFFINITIES

Combination of a gaseous acceptor, A, with a free electron, e^- , yielding the product A^- dissolved in a solvent is more exothermic than of the corresponding gaseous electron-capture process, the difference arising from the heat of solvation, $\Delta H_{\text{solv}}(A^-)$, of A^- . Thus the heat of the former reaction denoted by $-EA_{\text{solv}}(A)$, is

$$-EA_{\text{solv}}(A) = -EA(A) + \Delta H_{\text{solv}}(A^-)$$

where, in accord with the convention, the term $\Delta H_{\text{solv}}(A^-)$ is negative. The entity $EA_{\text{solv}}(A)$ will be referred to as the solution electron affinity of A.

The term $-\Delta H_{\text{solv}}(\text{A}^\cdot)$ is much greater than $-\Delta H_{\text{solv}}(\text{A})$, the exothermicity of solvation of a neutral molecule A; their difference may be calculated through the conventional approach due to Born:

$$-\Delta H_{\text{solv}}(\text{A}^\cdot) + \Delta H_{\text{solv}}(\text{A}) = \left(\frac{e^2}{2r}\right)\left(1 - \frac{1}{\mathcal{D}}\right)$$

provided A^\cdot is spherical and of radius r . Since the aromatic radical anions are flat, an "equivalent" radius r has to be attributed to each of them, but the choice of r is difficult and somewhat ambiguous. A more refined approach was suggested by Hush and Blackledge [139], who calculated the distribution of charge of the added electron over all the carbon atoms of the investigated radical anion, attributed an effective radius, r_j , to each center carrying the partial charge q_j , and finally summed up all the Born-type interaction terms. This approach gives

$$-\Delta H_{\text{solv}}(\text{A}^\cdot) + \Delta H_{\text{solv}}(\text{A}) = \sum_j \left(\frac{q_j}{2r_j}\right)\left(1 - \frac{1}{\mathcal{D}}\right)$$

The results of such computations are shown in Table 5 and, as expected, $-\Delta H_{\text{solv}}(\text{A}^\cdot) + \Delta H_{\text{solv}}(\text{A})$ decreases with increasing size of the radical anion. However, such calculations involve the arbitrary parameters r_j , and seem also to overestimate the effect of solvation by accepting the bulk dielectric constant \mathcal{D} of the solvent for its effective value.

Apparently the coordination of radical anions with the molecules of ethereal solvents is at least weak, if not negligible [140]. In contrast to small cations, such as Li^+ or Na^+ , these anions are not surrounded in ethers by tight and relatively long-lasting solvation shells. This is evident from the results of conductance studies [142, 149]; the diffusion constants of radical anions calculated from their electrical mobility are only slightly smaller than the diffusion constants of the parent hydrocarbons.

An interesting attempt to determine the solvation energies of aromatic radical anions was reported by Prock et al. [141]. They measured the threshold of electron photoejection from a cathode immersed in a solution of the investigated aromatic hydrocarbon relative to its vacuum value. The difference

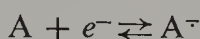
Table 5 Heat of Solvation of Aromatic Radical Anions in Tetrahydrofuran [139]

Parent Hydrocarbon	$\Delta H_{\text{solv}}(\text{A}^\cdot)$ (eV)
Benzene	1.8
Naphthalene	1.1
Phenanthrene	0.8
Anthracene	0.8

is attributed to the electron affinity of the solute and to the heat of solvation of its radical anion. Provided the former is known, the latter may be calculated from the experimental data. The method is promising, but it remains to be seen how reliable it will be. Some basic difficulties that may be anticipated include those associated with the polarization of the electrode.

7. POTENTIOMETRIC STUDIES OF SOLUTION ELECTRON AFFINITIES

An electrode immersed in a solution of an equimolar mixture of an acceptor A and its *free* radical anion $A^{\cdot -}$ acquires the standard potential of the reaction



This phenomenon is the basis of various potentiometric and polarographic techniques used in determining solution electron affinities.

The first reported potentiometric studies of electron affinities in solution were those of Bent and Keevil [143]. These workers determined the potential difference established between a sodium amalgam electrode and a bright platinum electrode immersed in a saturated solution of triphenylmethyl-sodium in diethylether. The measured potential obeyed the Nernst dilution law when the solution of sodium trityl was diluted, but the interpretation of such data is still far from being simple because of the lack of knowledge of the solvation energy and of the dissociation constant of Na^+ , $\bar{C}Ph_3$ ion pairs which form the bulk of the solute under these conditions. In fact, Keevil and Bent attempted to determine the dissociation constant of this salt in diethylether, but unfortunately their findings are unreliable because the investigated solutions were too concentrated. Subsequent and more refined studies by Swift [145] led to a more reasonable estimate of this constant, and on this basis he calculated the electron affinity of trityl radicals as 48 ± 5 kcal/mole. It would be desirable to verify this value, since it has been used by Matsen [169] in his extensive calculations of electron affinities of aromatic hydrocarbons.

The approach of Bent and Keevil was utilized in the investigation of other aromatic compounds in diethylether. However, the results have historical value only; the complexity of these solutions was not realized in those days.

A successful and reliable approach to potentiometric studies was developed by Hoijtink [146]. The potential difference between two platinum electrodes was measured; one of them was placed in a standard solution of a 50:50 mixture of biphenyl B and its radical anion $B^{\cdot -}$, while the other was immersed in a solution of the investigated aromatic hydrocarbon, A, of higher electron affinity than B. The procedure adopted in these studies resembles a

potentiometric titration of a redox system. The standard solution of $B + B^-$ was added gradually to a solution of A , thus converting it instantly into its radical anion, A^- ; i.e. $B^- + A \rightarrow B + A^-$. Therefore, the second electrode responded to the redox system $A - A^-$, its potential increasing as the titration proceeded. The potential difference measured in this setup becomes equal to the difference of electron affinities of A and B when one-half of A has been reduced to A^- .

The original apparatus of Hoijtink was improved in our laboratory [147] and its present design is shown in Fig. 9. A burette containing a standard

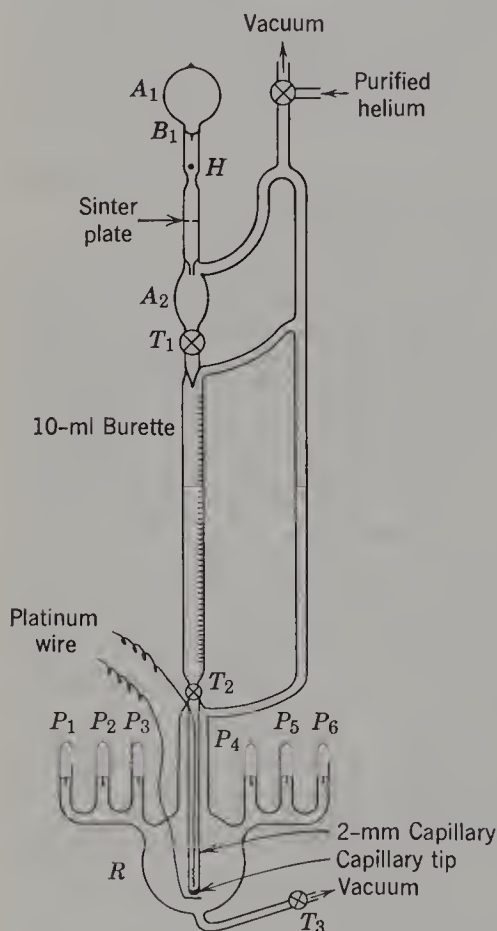


Figure 9. Apparatus used in the potentiometric titration of aromatic hydrocarbons with sodium biphenyl [147]: *R*, reactor; *P*₁–*P*₆, ampoules containing the hydrocarbon to be titrated; *T*₁, *T*₂, stopcocks; *A*₁, ampoule containing the $B + B^-$, Na solution; *B*₁, breakseal; *H*, magnetic hammer; *A*₂, storage ampoule. The two platinum wires form the electrodes.

solution of $B + B^-$ is terminated by a 2 mm bore capillary, its lower tip being sealed and then punched with a needle to form five to six tiny parallel capillaries. This arrangement slows considerably the diffusion of the solutes from the reactor *R* to the platinum electrode placed just above the sealed tip of the burette. The solutions of the investigated hydrocarbons are enclosed in evacuated and sealed ampoules *P*. Each of these solutions may be introduced into reactor *R* by crushing the appropriate breakseal. The titration is then

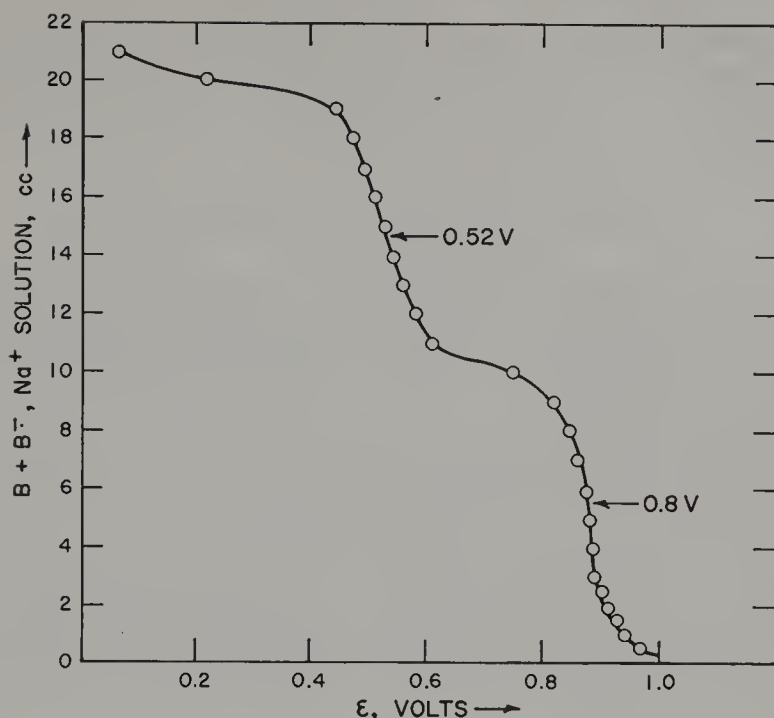


Figure 10. A typical potentiometric titration curve for perylene titrated with sodium biphenylide. The arrows denote the points corresponding to addition of $\frac{1}{2}$ and $\frac{3}{2}$ equivalents of sodium biphenylide, and the respective potentials are ϵ_1 and ϵ_2 .

performed, adequate mixing of the reagents being achieved by a magnetic stirrer. The potential is measured after the addition of each aliquot of the $B + B^-$ solution, and its value when plotted versus the volume of the added liquid results in a typical titration curve, illustrated by Fig. 10. After completion of the titration the contents of the reactor are sucked out by opening stopcock T_3 , a new solution stored in another ampoule P is introduced in turn into the reactor, and then the titration is repeated. This procedure prevents the exposure of the electrodes to the air.

All these operations are carried out under helium, the gas having been meticulously purified to free it of any traces of moisture or oxygen. The potential has to be measured with a voltmeter of virtually infinite impedance because the resistance of the redox circuit may be as high as 10 megohms.

The results of such titrations yield the proper difference of electron affinities of A and B , provided A^- and B^- are present entirely as *free* ions, that is, their pairing with counterions must be negligible. Apparently Hoijtink assumed that this condition was fulfilled in his experiments in which dimethoxyethane (DME) was used as a solvent. However, in dimethoxyethane, as well as in tetrahydrofuran, the radical anions are associated with counterions into ion pairs and the free ions represent only an extremely small fraction

of all the radical ions. The complications encountered in such systems were discussed by Jagur-Grodzinski et al. [147]. They showed that the measured potential difference, ϵ , is related to the difference of electron affinities, ϵ_0 , through the equation

$$\epsilon = \epsilon_0 + 0.03 \log \frac{K_{\text{diss}}(\text{B}^{\cdot-}, \text{Cat}^+)}{K_{\text{diss}}(\text{A}^{\cdot-}, \text{Cat}^+)} + 0.03 \log \frac{[\text{A}^{\cdot-}, \text{Cat}^+]}{[\text{B}^{\cdot-}, \text{Cat}^+]}$$

Here K_{diss} denotes the dissociation constant of the respective ion pair, $[\text{A}^{\cdot-}, \text{Cat}^+]$ denotes the total concentration of the $\text{A}^{\cdot-}$ salt in the reactor when one-half of A is reduced, and the total concentration of the $\text{B}^{\cdot-}$ salt in the burette is denoted by $[\text{B}^{\cdot-}, \text{Cat}^+]$.

The dissociation constants of salts of some radical anions in tetrahydrofuran and in dimethoxyethane have been determined [142, 149, 150], and the results obtained for sodium salts in tetrahydrofuran are presented in Fig. 11 in the form of plots of $\log K_{\text{diss}}$ versus $1/T$. At room temperature these dissociation constants vary by more than two powers of 10; nevertheless, the corrections needed for the calculation of ϵ_0 are small, usually less than 0.03 V. The less extensive data concerned with the dissociation of the sodium salts in

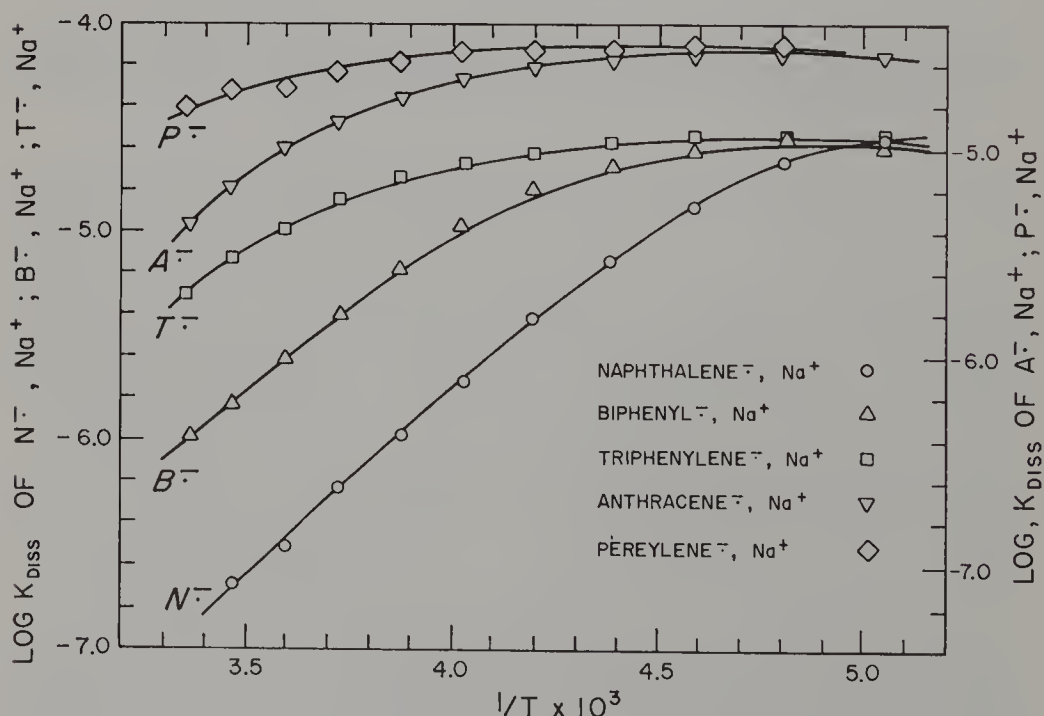


Figure 11. Dissociation constants K_{diss} of ion pairs of aromatic radical ions at different temperatures (range $+25$ down to -70°C). Solvent, tetrahydrofuran, sodium counterion. Note the striking difference between the heats of dissociation of naphthalene $^{\cdot-}, \text{Na}^+$ and perylene $^{\cdot-}, \text{Na}^+$. The lines marked $\text{A}^{\cdot-}$ and $\text{P}^{\cdot-}$ were shifted up by 0.2 units. Hence, all the lines nearly coincide at low temperature.

Table 6 Dissociation Constants, Heats, and Entropies of Dissociation of Sodium Salts of Aromatic Radical Anions

	Biphenyl ^{•-}	Triphenylene ^{•-}	Perylene ^{•-}
<hr/> In DME <hr/>			
$10^6 K_{\text{diss}}$ at 25°C (<i>M</i>)	4.6	5.6	6.0
$10^6 K_{\text{diss}}$ at -55°C (<i>M</i>)	17.0	14.8	18.8
ΔH_{diss} at 20°C (kcal/mole)	-2.1	-2.4	-2.5
ΔS_{diss} at 20°C (eu)	-31.5	-32.5	-32.5
ΔH_{diss} at -55°C (kcal/mole)	0	0	0
ΔS_{diss} at -55°C (eu)	-22.0	-22.0	-21.0
<hr/> In THF <hr/>			
$10^6 K_{\text{diss}}$ at 25°C (<i>M</i>)	1.0	5.2	15.5
$10^6 K_{\text{diss}}$ at -55°C (<i>M</i>)	24.5	28.8	28.5
ΔH_{diss} at 20°C (kcal/mole)	-7.3	-5.2	-2.2
ΔS_{diss} at 20°C (eu)	-52.0	-42.0	-29.0
ΔH_{diss} at -55°C (kcal/mole)	-1.6	-0.4	0
ΔS_{diss} at -55°C (eu)	-28.0	-23.0	-21.0

dimethoxyethane are collected in Table 6. They show that the extent of dissociation in this solvent is only slightly affected by the nature of radical anion. Hence the potentiometric data obtained with such solutions need no corrections, justifying Hoijtink's procedure.

Ion pairs seem to be completely dissociated in hexamethylphosphorictriamide (HMPA) [148] and therefore this solvent is admirably suited for potentiometric titrations. For the sake of comparison, electron affinities of a series of aromatic hydrocarbons determined potentiometrically in THF, DME, and HMPA are collected in Table 7.

The potentiometric titration fails when the resulting radical anions disproportionate or dimerize during the titration. Examples illustrating such complications are provided by tetraphenylethylene, whose radical anions extensively disproportionate in tetrahydrofuran (see p. 94), and by numerous *aza*-aromatics, such as quinoline or isoquinoline, whose radical anions are extensively dimerized in this solvent [151]. The use of hexamethylphosphorictriamide in such titrations is again beneficial, since the disproportionation or dimerization is then avoided [148].

In solutions where ion-pairing is virtually quantitative the potentiometric data give the equilibrium constant K of the reaction $B^{\cdot-}, \text{Cat}^+ + A \rightleftharpoons B + A^{\cdot-}, \text{Cat}^+$, i.e. the measured potential ϵ is given by $(RT/\mathcal{F}) \ln K$.

Table 7 The Relative Electron Affinities of Aromatic Hydrocarbons Determined Potentiometrically in Different Solvents

Aromatic Hydrocarbon	ϵ_0 in THF (eV) [142, 147]	ϵ in DME (eV) ^a [146, 160]	ϵ_0 in HMPA (eV) [152, 153]
Biphenyl	(0.0)	(0.0); (0.0)	(0.0)
Naphthalene	0.043 ± 0.02	0.09	—
Triphenylene	0.132 ± 0.01 ^b	0.19	—
Phenanthrene	0.142 ± 0.01	0.17	—
Chrysene	—	—	0.30; 0.29
Benzo[<i>a</i>]pyrene	0.484 ± 0.02	0.58	—
Pyrene	0.529 ± 0.01	0.60; 0.535	0.51; 0.48
Benzo[<i>a</i>]anthracene	0.590 ± 0.02	0.76	—
9,10-Dimethylantracene	0.616 ± 0.01	—	—
Anthracene	0.642 ± 0.01	0.78; 0.610	0.59
Benzo[<i>a</i>]pyrene	0.760 ± 0.02	0.90	—
Acenaphthylene	0.88 ± 0.03	1.12	—
Fluoranthrene	0.820 ± 0.02	0.94	—
Perylene	0.965 ± 0.01	1.09; 0.950	0.90
Tetracene	1.058 ± 0.02	1.28	—
Stilbene- <i>trans</i>	—	—	0.34
Diphenylacetylene	—	—	0.27
Tetraphenylethylene	—	—	0.465

^a These values refer to the equilibria between ion-pairs in DME. The first column gives the data reported by Hoiijtink [146], the following one lists the data reported in ref. [160].

^b The original value given in ref. 142 is 0.128; after rechecking it is found to be 0.132.

8. POLAROGRAPHIC DETERMINATION OF ELECTRON AFFINITIES

The polarographic technique of determining solution electron affinities is closely related to the potentiometric method. In a polarographic experiment current I passing through a cell is measured as the function of a variable potential V applied to a dropping mercury cathode. The surface of such an electrode is periodically renewed and therefore its polarization is prevented. The electrolyzed solution contains a supporting electrolyte, usually tetramethyl- or tetrabutylammonium iodide, and the compound A under investigation, the latter being reduced on the cathode. As the voltage reaches the value needed for the reduction of A, the current increases steeply because the electrode process, $A + e^- \rightleftharpoons A^-$, provides a sink for the cathodic charge. This event is reflected in the shape of the I versus V curve giving what is referred to as a polarographic wave, a steep S-shaped curve. The potential at the middle point of such a curve is denoted by $\epsilon_{1/2}$, and for a *reversible* reaction, $\epsilon_{1/2} = \epsilon_0(A) + \epsilon_{\text{ref}} - \chi(\text{Hg})$. Here ϵ_0 denotes the electron affinity of A

in solution, ϵ_{ref} is the potential of the reference electrode (corrected, if needed, for a potential drop on the liquid junction) and $\chi(\text{Hg}) = -4.54$ V is the work function of liquid mercury, that is, the potential required for ejection of an electron from a mercury surface under vacuum. It is common to use as a reference the calomel electrode; its absolute potential was calculated by Latimer, Pitzer, and Slansky to be -0.53 V [161]. However, some workers report their data with respect to the mercury pool, and then 0.53 V has to be added to the reported values to convert them into the conventional ones.

The stationary concentrations of A and of A^- are affected by the diffusion out of and into the layer surrounding the electrode. The diffusion processes may perturb the results and then the correction term $(RT/\mathcal{F})(D_{\text{A}^-}/D_{\text{A}})^{1/2}$ has to be introduced in the calculation of $\epsilon_0(\text{A})$, where D_{A^-} and D_{A} denote the diffusion constant of A^- and A, respectively, while the constant factor RT/\mathcal{F} has its conventional meaning. As has been pointed out previously, for aromatic hydrocarbons $D_{\text{A}} \approx D_{\text{A}^-}$ and therefore the correction mentioned above is negligible. Two additional reactions may affect the results—the association of A^- with the cations of the supporting electrolyte, and their protonation by any proton source which may be present in the solution. Both reactions tend to decrease the value of $\epsilon_{1/2}$. The pairing of A^- anions with the cations may be important when solvents of low dielectric constant, such as 95% aqueous dioxane, are used. To avoid rapid protonation the solvent employed has to be a nonprotonating, or at most a poorly protonating agent; 75 or 95% dioxane, 2-methoxy-1-ethanol (cellosolve) and dimethylformamide, for example, have been used successfully.

The absence of perturbing effects may be tested experimentally by the independence of polarographic waves from the drop time and the concentration of the reagents. Moreover, Hoijsink showed that identical results were obtained in 95 and 75% aqueous dioxane [162, 163], indicating therefore a slow rate of protonation in both solvents. Finally, the reliability of the results has been checked by comparing the data obtained by d.c. polarography in dimethylformamide [164] with those derived from the a.c. polarography employing the same solvent [165].

Some acceptors give two polarographic waves, the first due to the reduction $\text{A} + e^- \rightleftharpoons \text{A}^-$, while the second results from further reduction of radical anions to dianions, $\text{A}^- + e^- \rightleftharpoons \text{A}^{2-}$. The dianions are more extensively associated with the counterions than the radical anions and in addition they are more rapidly protonated (see p. 229). Indeed, the experimental tests mentioned previously confirm that the rapid protonation affects the $\epsilon_{1/2}$ of the second wave.

The interesting field of organic polarography was opened through the pioneering work of Laitinen and Wawzonek [166–168]. Their initial studies

of the polarographic reduction of styrene, α -methylstyrene, and 1,1-diphenylethylene were extended later to other aromatic hydrocarbons. Since the recorded potential was found to be independent of the pH of the solution, they assumed that the rate-determining step involves one electron transfer, $A + e^- \rightleftharpoons A^-$, a reversible and potential-determining reaction. The hypothetical step $A + e^- + \text{Cat}^+ = A^-$, $\text{Cat}^+(\text{Cat}^+ = \text{N}(\text{CH}_3)_4^+ \text{ or } \text{NBu}_4^+)$ is ruled out by the results of Hoijtink [162] noted earlier, i.e. by the virtual independence of $\epsilon_{1/2}$ of the amount of water added to dioxane solvent (5 or 25 %). Such an increase in the water content increases the dielectric constant of the solvent from 3.5 to 13 and this should affect greatly the degree of ion pairing.

Extensive polarographic studies of aromatic hydrocarbons were reported by Hoijtink and his associates [162–164] and by Bergman [156]. The latter determined the half-wave reduction potential of 78 aromatic hydrocarbons—a most comprehensive investigation of this subject. The results of various research groups are collected in Table 8 and compared with those obtained by potentiometric titrations. The agreement is indeed very good; the slightly more negative values obtained by potentiometric titration probably reflect the uncertainty in the potentiometric value of ϵ_0 of naphthalene, which might be higher by 0.05 V.

Table 8 Relative Polarographic Half-Wave Potentials of Aromatic Hydrocarbons (eV); Naphthalene Taken as the Reference, i.e. its $\epsilon_{1/2} = 0$.

Aromatic Hydrocarbon	Polarographic, $\epsilon_{1/2}$			Potentiometric, ϵ_0
	Laitinen and Wawzonek [166–168]	Bergman [156]	Hoijtink [162–164]	Szwarc [147, 152, 153]
Biphenyl	+0.20	+0.09	+0.20	+0.04
Naphthalene	(0.0)	(0.0)	(0.0)	(0.0)
Phenanthrene	−0.05	−0.05	−0.05	−0.08
Triphenylene	—	−0.01	−0.01	−0.10
Chrysene	—	−0.18	—	−0.25
Pyrene	−0.39	−0.37	−0.37	−0.48
Anthracene	−0.56	−0.52	−0.54	−0.60
Tetracene	—	−0.85	−0.92	−1.01
Perylene	—	−0.73	−0.83	−0.92
Stilbene	−0.16 ^a	—	−0.28; 0.23 ^a	−0.30
Tetraphenylethylene	−0.25	—	−0.34 ^a	−0.42
Diphenylacetylene	—	—	−0.25	−0.23

^a Recent polarographic studies of Dietz and Peover [172] give the following $\epsilon_{1/2}$ values referred to naphthalene as the standard: *trans*-stilbene, $\epsilon_{1/2} = 0.34$ eV, *cis*-stilbene, $\epsilon_{1/2} = 0.31$ eV, tetraphenylethylene, $\epsilon_{1/2} = 0.44$ eV, tetracene, $\epsilon_{1/2} = 1.09$ eV.

Table 9 Polarographic $\epsilon_{1/2}$ (in DMF) and Potentiometric ϵ_0 (determined in HMPA) for *aza*-Aromatics; Biphenyl Taken as the Reference Redox System

<i>Aza</i> -Aromatic	$-\epsilon_{1/2}$ (V) [159]	$-\epsilon_0$ (V) [153]
Biphenyl	(0.0)	(0.0)
Pyridine	-0.16	—
Pyrimidine	0.27; 0.22	—
Isoquinoline	0.40	0.33
7,8-Benzoquinoline	0.39	0.34
5,6-Benzoquinoline	0.42	0.37
Pyrazine	0.45	0.38
Quinoline	0.45	0.38
Phenanthridine	0.50	0.42
1,10-Phenanthroline	0.50	0.47
2,2'-Bipyridyl	0.43	—
4,4'-Bipyridyl	0.71	0.68
Phthalazine	0.60; 0.58	0.53
Cinnoline	0.81	0.80
Quinoxaline	0.82; 0.90	0.86
Naphthylidene	0.76; 0.73	—
Acridine	1.00	0.96
Benzo-(<i>e</i>)-cinnoline	1.07	1.00
Pyridopyrazine	—	1.11
Phenazine	1.42; 1.40	1.40 (in THF)

Polarographic studies have been extended to numerous classes of organic compounds. For example, in Table 9 the half-wave potentials of *aza*-aromatics are compared with those obtained by potentiometric titrations. Again the agreement is excellent. The polarographic half-wave potentials of various olefinic compounds are given in Table 10. Their radical anions dimerize rapidly and irreversibly, and this could affect the reported half-wave potentials. It was claimed, however, that the dimerization in aqueous dioxane is slow relative to the electrode process and that it presumably does not affect the half-wave potential. This is doubtful.

Table 10 Polarographic $\epsilon_{1/2}$ of substituted ethylenes in 75 % DOX [167]

Hydrocarbon	$\epsilon_{1/2}$ V (against saturated calomel electrode)
PhCH = CH ₂	2.35
PhCH = CH·CH ₃	2.54
Ph ₂ C = CH ₂	2.60
PhCH = CH — CH = CHPh	1.98
Ph ₂ C = CHPh	2.12

Polarographic techniques may be utilized in studies of kinetics of reactions following the primary electrode process. For example, Zuman et al. [170-171] discussed the effect of irreversible dimerization on the half-wave potential and subsequently applied their theory in studies of dimerization of tropylium radicals formed by polarographic reduction of tropylium cations. They deduced that the *measured* half-wave potential $\epsilon_{1/2}$ is related to its "true" value, $\epsilon_{0,1/2}$, by the equation

$$\epsilon_{1/2} = \epsilon_{0,1/2} + \left(\frac{RT}{n\mathcal{F}} \right) \left(\frac{1}{3} \ln ckt - 0.36 \right)$$

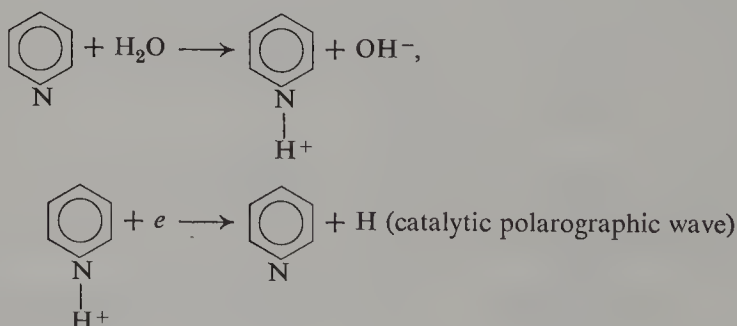
where k is the rate constant of dimerization, c the concentration of tropylium ions, and t the drop time.

Similarly, the treatment of irreversible protonation following polarographic reduction led Koutecky [173] to the relation between the potential $\epsilon_{1/2}$ observed at half-polarographic limiting current and the drop time t :

$$\epsilon_{1/2} = \epsilon_{0,1/2} + \frac{RT}{\alpha n\mathcal{F}} \ln \frac{kct^{1/2}}{0.76 D_A^{1/2}}$$

where c is the concentration of the protonating agent and k the rate constant of protonation. This relationship permits studies of the kinetics of protonation of radical anions (see also p. 221), a subject reviewed recently by Hoijtink [174].

Interesting side reactions are observed in polarographic studies of some aromatic bases such as pyridine in protic solvents. This subject has been reviewed by Kolthoff and Lingane [176], who pointed out that a catalytic hydrogen wave may be observed in addition to the normal type of reduction wave. The catalytic wave arises in aqueous solutions from the following reactions:



and finally



The net result is therefore



At $\text{pH} > 6$ the normal reduction wave is observed. The catalytic wave is avoided in aprotic solvents such as dimethylformamide, where the reduction of pyridine or quinoline proceeds normally [159, 165].

Much theoretical work has been inspired by the polarographic data. In a series of papers [162, 163, 180] Hoijsink correlated the half-wave potentials with the energy E of the lowest unoccupied orbitals of the respective hydrocarbons:

$$\varepsilon_{1/2} = \gamma E + \text{const.}$$

This relation applies to both alternant and nonalternant aromatics, and its significance has been reviewed recently by Hoijsink [174]. Various approaches were used in the calculation of E . For example, the original Hückel method gives $\gamma = -2.23$, Wheland's approximation [177] with the overlap integral of 0.24 gives $\gamma = -1.97$, Longuet-Higgins' method [178] leads to $\gamma = -1.81$. Correlation with the p bands of the absorption spectra of the respective hydrocarbons were reported by Bergman [156], with methyl affinities of aromatic hydrocarbons [179] by Matsen [169], and so on.

9. CORRELATION OF GASEOUS ELECTRON AFFINITY WITH THE POTENTIOMETRIC AND POLAROGRAPHIC DATA

Gaseous electron affinities listed in Table 2 are linearly correlated with the potentiometric electron affinities in THF [152]. The corresponding line in Fig. 12 has a slope of unity, implying that the heats of solvation of the investigated radical anions by THF are virtually constant and independent of their natures. However, this conclusion was challenged recently by Lyons et al. [175] and by Michl [344].

Interestingly, a similar conclusion may be drawn from the results obtained in HMPA. The potentiometric ϵ 's obtained in HMPA for anthracene or pyrene are identical with those deduced for the respective hydrocarbons in THF. Therefore the differences in the heat of solvation of biphenylide on the one hand and of anthracenide or pyrenide on the other are the same whether THF or HMPA are the solvating agents.

Both solvents, THF and HMPA, are aprotic. However, comparison of the potentiometric data in THF with the polarographic results in the protic solvent, 2-methoxyethanol, leads to a linear relation shown in Fig. 13 with a slope of 0.84. Apparently in this protic solvent the degree of solvation of large aromatic radical anions of higher electron affinity is *smaller* than that of biphenylide. Hydrogen bonding contributes appreciably to the energy of solvation of negative ions by protic solvents. This contribution seems to be affected more by the nature of radical anion than the less specific solvation resulting from the solvent polarity.

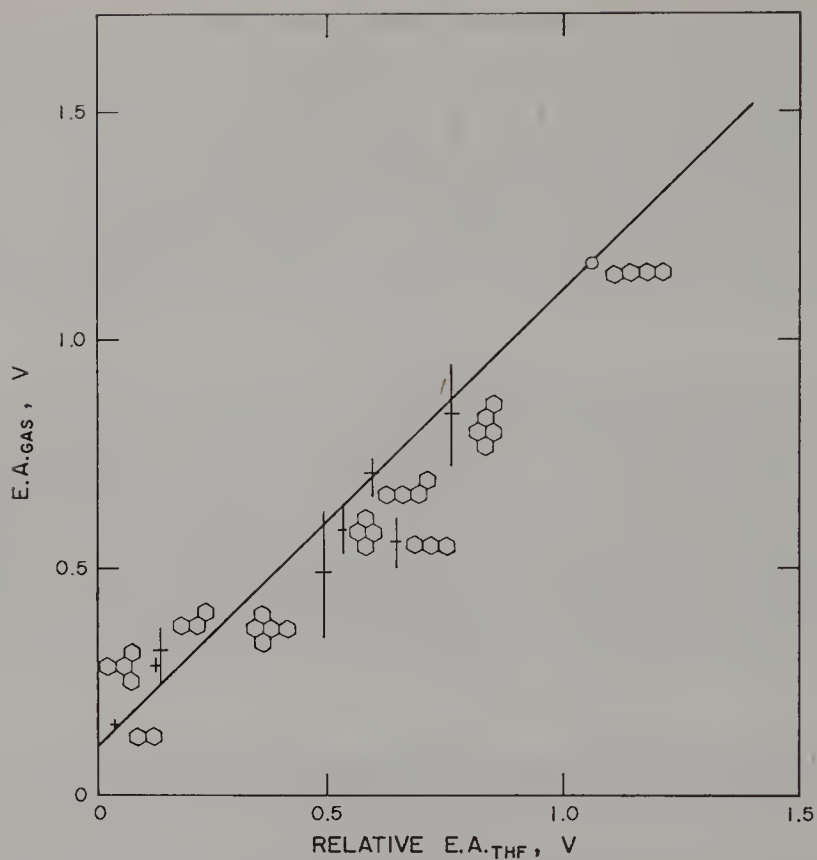


Figure 12. Linear relation between electron affinities of aromatic hydrocarbons determined in the gas phase and the potentiometric values determined in THF solution. Slope = 1.0.

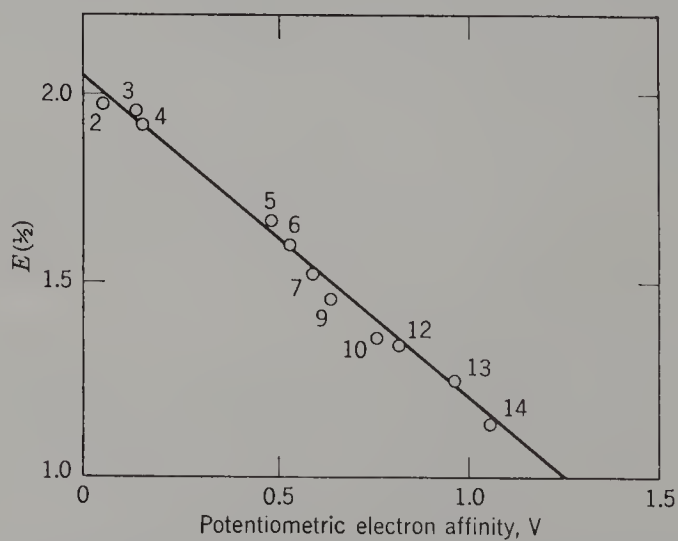


Figure 13. Linear relation between potentiometric ϵ 's in an aprotic solvent (THF) and polarographic $\epsilon_{1/2}$ in a protic solvent ($\text{CH}_3\text{O} \cdot \text{C}_2\text{H}_4\text{OH}$). Slope = 0.84.

10. ELECTRON TRANSFER EQUILIBRIA BETWEEN RADICAL ANIONS AND AROMATIC ACCEPTORS

Electron affinities govern the position of electron transfer equilibria such as



where A and B denote aromatic hydrocarbons and $A^{\cdot-}$ and $B^{\cdot-}$ their respective *free* radical anions. In fact, by determining K 's for numerous aromatic hydrocarbons one establishes the electrochemical series of these compounds; this procedure provides an alternative route leading to the relative values of electron affinities.

In the gas phase such reactions may be studied, at least qualitatively, by the mass spectrometric [345] or ion-cyclotron resonance [346] techniques. Under conditions prevailing in those experiments only exothermic reactions are observed, and hence, the appearance of $B^{\cdot-}$ ions in a system composed of $A^{\cdot-}$ and B demonstrates higher electron affinity of B than of A.

The position of equilibrium established in a solvent depends on the solution electron affinities of the reagents. Relative solution electron affinities may be determined, therefore, by studies of such equilibria. With this goal in mind, Paul, Lipkin, and Weissman [181] embarked on their pioneering spectrophotometric studies of the equilibria established in three systems: naphthalene-phenanthrene, naphthalene-anthracene, and anthracene-tetracene with the hydrocarbons partially reduced by sodium. Unfortunately, various technical difficulties encountered in such studies were not appreciated at that time. Moreover, some confusion arose because it was not realized that the reduction by alkali metals may produce the dianions as well as the radical anions. Consequently, the data obtained in this investigation were somewhat in error.

The studies of Weissman's group were repeated in our laboratory. The equilibria were established in THF at room temperature and the following criteria guided us in the selection of the systems to be investigated:

1. The difference in the reduction potentials of the investigated hydrocarbons should not exceed 0.15 V; that is, the equilibrium constants should not be larger than 250. Otherwise, a reliable determination of the concentration of one of the radical ions calls for an enormous excess of the other hydrocarbon. This, in turn, could lead to partial destruction of some radical ions and therefore to erroneous results. Indeed, such a difficulty vitiated Weissman's study of the system.



2. The spectra of the investigated radical ions should not overlap too greatly. A successful spectrophotometric study obviously requires such a condition. On this basis the systems tetracene-perylene, anthracene-pyrene, and naphthalene-triphenylene were selected. The results are summarized in Table 11.

Table 11 Equilibria $A^{\cdot-}, Na^+ + B \rightleftharpoons A + B^{\cdot-}, Na^+$ in THF at 25°C, [142, 147]

The Investigated Pair		$\Delta\epsilon_0$ (eV)			
		K_{\pm}	K_-	Calculated from	Observed
A	B			K_-	Potentiometric
Perylene	Tetracene	52	34	0.092	0.113
Pyrene	Anthracene	111	74.5	0.112	0.114
Pyrene	9,10-Dimethyl-anthracene	91	61	~ 0.107	0.097
Naphthalene	Triphenylene	3	3	0.029	0.089

The sodium salts of radical anions are associated in tetrahydrofuran; the association into ion pairs exceeds 90% at concentrations of about 10^{-4} M. Hence spectrophotometric studies of such solutions yield K_{\pm} , the equilibrium constant of the electron transfer,



which may differ considerably from K_- , the equilibrium constant referred to free ions. The following relation has to be obeyed:

$$\frac{K_{\pm}}{K_-} = \frac{K_{\text{diss},A}}{K_{\text{diss},B}}$$

where $K_{\text{diss},A}$ and $K_{\text{diss},B}$ denote the dissociation constants of the respective ion pairs. Since the latter are known [142, 149, 150] (see, e.g., Fig. 11 and Table 6), K_- may be calculated from the spectrophotometrically determined K_{\pm} .

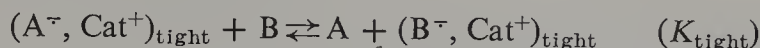
The standard potential $\Delta\epsilon_0$ of the reaction



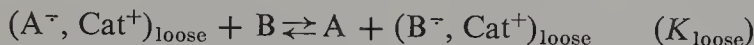
determined by potentiometric or polarographic techniques, is given by $0.06 \log K_-$. The calculated and observed $\Delta\epsilon_0$ are listed in the last two columns of Table 11 and its inspection shows a most satisfactory accord of the equilibrium approach with that based on the potentiometric studies.

Ion pairs exist in solution in a variety of forms [12], tight and loose ion pairs being the most common. Hence one should differentiate between

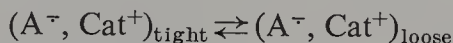
electron transfer equilibria such as



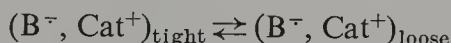
and



For a class of related solvents, for example, for various ethers, K_{tight} and K_{loose} appear to be nearly independent of the nature of the solvent, although the equilibria



and

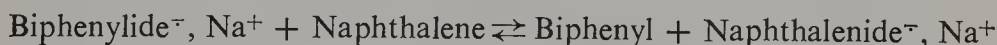


may be affected profoundly. This has been demonstrated by recent work of Karasawa, Levin, and Szwarc [182], who investigated the systems sodium biphenylide-naphthalene and sodium naphthalenide-triphenylene in tetrahydropyrene (THP), tetrahydrofuran (THF), and dimethoxyethane (DME).

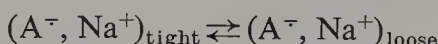
As noted by Karasawa et al. [182], spectrophotometric data give the *total* concentration of a salt, whatever the composition of the ion pairs. Therefore the results of spectrophotometric studies led to the *apparent* equilibrium constant of an electron-transfer process, this being defined as

$$K_{ap} = \frac{[A]\{(B^{\cdot-}, Cat^+)_{tight}\} + [(B^{\cdot-}, Cat^+)_{loose}]}{[B]\{(A^{\cdot-}, Cat^+)_{tight}\} + [(A^{\cdot-}, Cat^+)_{loose}]}$$

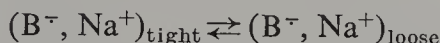
Consider now the specific example of the equilibrium



and denote biphenyl by A, naphthalene by B, and the equilibrium constants of the transformations



and



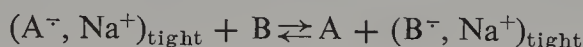
as K_A and K_B , respectively. Using this symbolism we recast the equation for K_{ap} into the form

$$K_{ap} = K_{tight} \frac{1 + K_B}{1 + K_A} = K_{loose} \frac{1 + K_B^{-1}}{1 + K_A^{-1}}$$

and find, as is easily demonstrated,

$$\frac{K_{tight}}{K_{loose}} = \frac{K_A}{K_B}$$

Here, as previously suggested, K_{tight} and K_{loose} refer to the respective electron transfer equilibria



and



each involving one kind of ion pair only.

Spectroscopic and ESR evidence suggests that sodium biphenylide and sodium naphthalenide form exclusively tight pairs in tetrahydropyran, but exclusively loose pairs in DME. Therefore the values of K_{tight} are derived from studies of THP solution, whereas the values of K_{loose} are obtained in dimethoxyethane. Both kinds of ion pairs coexist in tetrahydrofuran as implied by spectroscopic and ESR evidence and hence the spectrophotometric studies of the THF system lead to K_{ap} . The results presented in Fig. 14 support this conclusion. Nearly linear van't Hoff graphs are obtained on plotting the results pertaining to the THP or DME systems. However, a strange S-shaped curve having a maximum is obtained when the data derived from the THF system are plotted. Inspection of Fig. 14 suggests that tight pairs prevail in THF at higher temperatures, whereas the loose pairs dominate

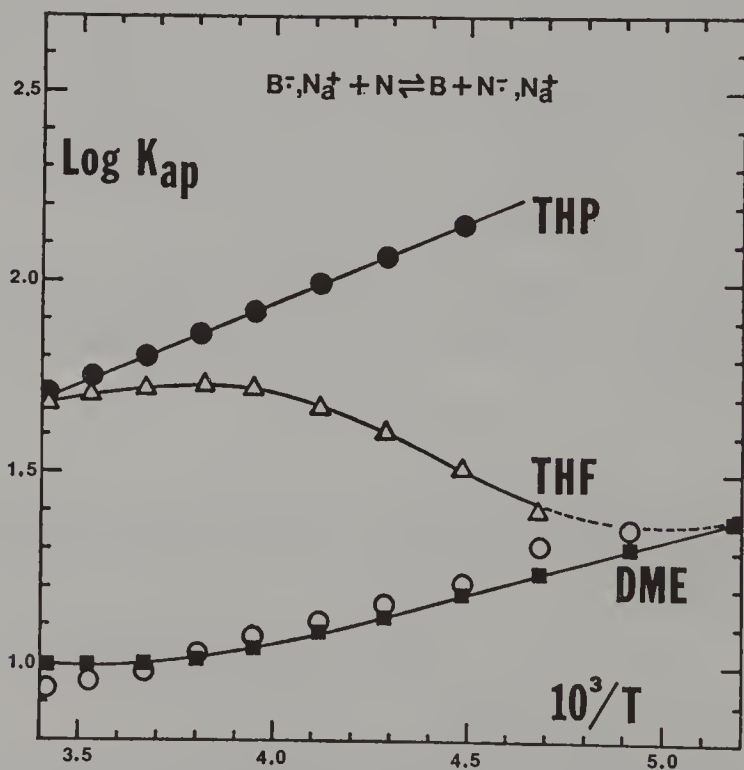


Figure 14. van't Hoff plots for the electron transfer equilibria, $B^{\cdot-}, Na^+ + N \rightleftharpoons B + N^{\cdot-}, Na^+$, K_{ap} , studied in THP, \bullet ; THF, \triangle , DME, \blacksquare ; and in THP + 10% of tetraglyme, \circ . The results obtained in THP + 10% tetraglyme are indistinguishable from those obtained in DME. The concentration of the ion pairs was $\approx 10^{-3} \text{ mol l}^{-1}$; hence the fraction of free ions is negligible even in DME. This was ascertained by repeating the experiments in the presence of Na^+, BPh_4^- ; the addition of the salt did not affect the results.

in the low-temperature range because K_{ap} determined in the THF system approaches K_{tight} at high temperatures and K_{loose} at the lowest temperatures.

Further evidence confirms this suggestion. Addition of small amounts of tetraglyme to a THP solution of the radical-anions converts the tight pairs into loose ones [183]. As shown again by Fig. 14, the electron-transfer equilibrium studied in THP in the presence of 10% tetraglyme is governed by equilibrium constants numerically indistinguishable from K_{loose} , that is, the equilibrium constant of this electron-transfer reaction is determined by the nature of ion pairs and not by the nature of the surrounding medium.

Accepting the proposition that K_{tight} and K_{loose} are independent of the nature of the ethereal solvent, Karasawa et al. [182] calculated K_A and K_B for the THF system using the experimentally observed values of K_{ap} in conjunction with the K_{tight} values derived from the THP system and the K_{loose} deduced from the DME system. The results, graphed in Fig. 15, may be

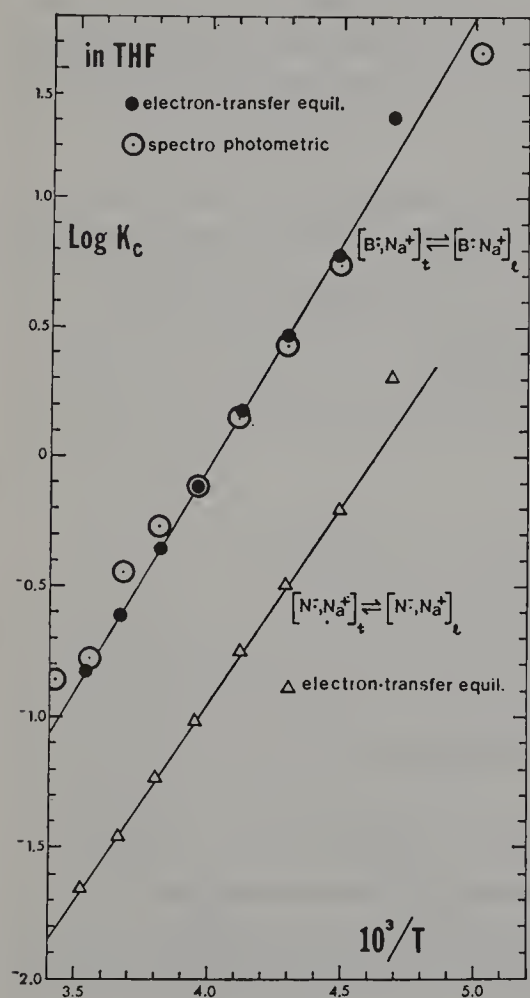
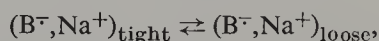
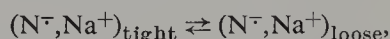


Figure 15. van't Hoff plots for the following equilibria:



and



in THF. ●, K_C from electron-transfer studies;

$$\Delta H = -7.9 \text{ kcal } (-32 \text{ kJ})/\text{mol};$$

$$\Delta S = -32 \text{ cal K}^{-1} \text{ mol}^{-1}$$

for biphenylide pairs,

$$\Delta H = -6.9 \text{ kcal } (-29 \text{ kJ})/\text{mol};$$

$$\Delta S = -32 \text{ cal K}^{-1} \text{ mol}^{-1}$$

for naphthalenide pairs.

compared with the independent findings derived from the direct spectroscopic or ESR studies. A most satisfactory agreement is reported.

The results discussed in the preceding paragraphs permit one to determine the temperature dependence of K_- , *free* biphenylide⁻ ion + naphthalene \rightleftharpoons biphenyl + *free* naphthalenide⁻ ion. The calculation requires knowledge, over a reasonable temperature range, of K_{ap} and of the dissociation constants of the relevant ion pairs; K_- may then be computed from the following relation:

$$K_- = \frac{K_{ap}K_{diss}(N^{\cdot-}, Na^+)}{K_{diss}(B^{\cdot-}, Na^+)}$$

Although the plots of $\log K_{ap}$ and of $\log K_{diss}$ versus $1/T$ are all strongly curved (see Figs. 14 and 11), the van't Hoff plot of K_- (Fig. 16) is linear. Interestingly, the entropy change of this electron-transfer reaction is small, $0.2 \text{ cal K}^{-1} \text{ mol}^{-1}$, further indicating only a slight dependence, if any, of the solvation of large radical anions on their structure (see p. 32).

Finally, the electron transfer between the *free* radical ions of biphenyl and naphthalene was studied in hexamethylphosphorotriamide [182], a solvent in which the association of radical ions with counterions is avoided [148]. The equilibrium constant determined at 20°C is 5.9 compared with the value of 7.2 found for K_- in THF.

Electron transfer equilibria involving two radical anions may also be investigated by employing the ESR technique, provided there are some

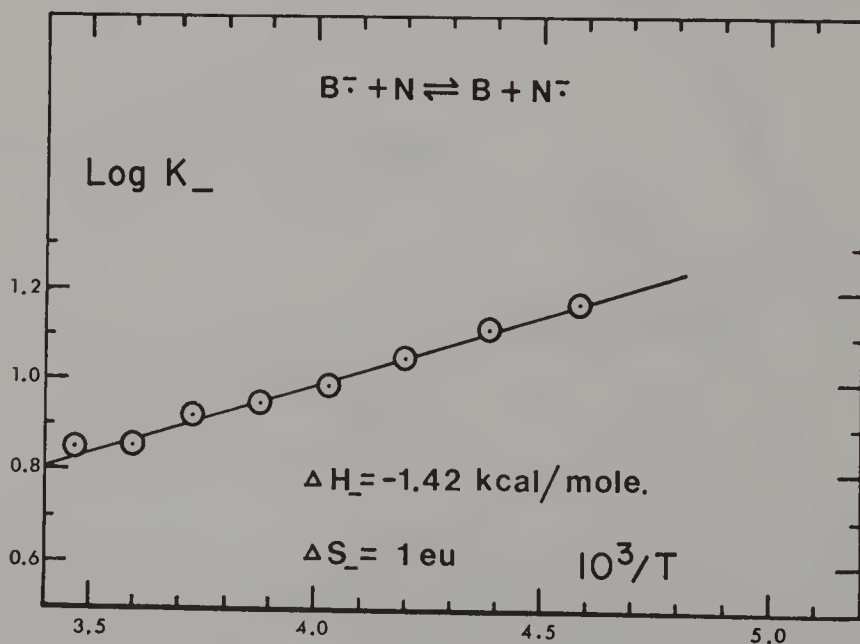
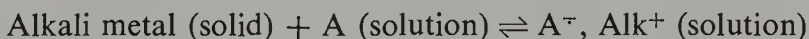


Figure 16. van't Hoff plot for the electron transfer equilibrium of free radical-anions, $B^{\cdot-} + N \rightleftharpoons B + N^{\cdot-}$, K_- in THF.

nonoverlapping lines. The reaction β -Et-naphthalenide $^-$, K^+ + α -Et-naphthalene \rightleftharpoons β -Et-naphthalene + α -Et-naphthalenide $^-$, K^+ , is such a case. This equilibrium was investigated in THF at temperatures ranging from 0 to -90°C [184]. The heat of the transfer was found to be -0.6 kcal/mole and $\Delta S = -0.4$ cal K^{-1} mol $^{-1}$. The electron affinity of α -ethylnaphthalene is therefore *higher* than that of the β isomer, although the inductive effect of the substituent should lead to the reverse order. This anomaly indicates the importance of the hyperconjugated effect of an alkyl group, which is greater for the α than for the β isomer. The same trend was reported previously by Streitwieser [190], who studied the polarographic reduction of substituted naphthalenes.

11. EQUILIBRIUM BETWEEN AROMATIC ACCEPTORS AND ALKALI METALS

As is well known, alkali metals reduce aromatic hydrocarbons to their corresponding radical anions. Basically this is an electron transfer process described by the equation



The heat of sublimation of alkali metals, ΔH_{sub} , and the ionization potential of their atoms, I^z , decrease in a series $\text{Li} > \text{Na} > \text{K} > \text{Rb} > \text{Cs}$. One therefore expects their reducing power to increase along this series. However, the heat of reaction yielding a dissolved reduction product is affected by an additional term, the heat of solvation of cations if free ions are formed in the solution, or the heat of solvation of the respective ion pairs if these form the bulk of the reduced product. In the latter case the exothermicity of the overall reduction is

$$-\Delta H = -\Delta H_{\text{sub}}(\text{metal}) - I^z(\text{Alk}) + EA(\text{A}) + \frac{e^2}{r} - \Delta H_{\text{solv}}(\text{A}^{\cdot-}, \text{Alk}^+)$$

In poorly solvating media the last term is small and the expected order of reducing power may be then observed, but in powerfully solvating media the exothermic solvation may be the dominant term and since the solvation of lithium pairs is stronger than that of cesium ion pairs, the order of reducing power may be reversed.

Since the extent of reduction of a chosen substrate by an alkali metal varies with the nature of solvent in which the reaction is performed, studies of such equilibria provide quantitative data concerning the strength of interactions of ion pairs with their surroundings. The concentration of free ions is minute in most of the systems studied, and hence the dissociation of ion pairs

into free ions may be neglected. Therefore the ratio $[A^{\cdot-}, Alk^+]/[A] = K$, which is independent of the initial concentration of the acceptor, serves as the equilibrium constant of the electron transfer reaction, $A + Alk \rightleftharpoons A^{\cdot-}, Alk^+$.

For many acceptors this equilibrium lies so far to the right that a reliable study of its thermodynamics is impractical. However, there are exceptions; for example, the reduction of biphenyl or naphthalene often converts only a small fraction of the hydrocarbon into its radical anion, the extent of the ultimate conversion being strongly influenced by solvent as well as by temperature. On the whole, the degree of reduction increases with decreasing temperature; that is, the overall reaction is exothermic.

Extensive work of Shatenshtein and his co-workers [185, 186] dealt with the system sodium metal + biphenyl. Their results are presented in Table 12,

Table 12 Equilibrium Constant for the Reaction
Metallic Sodium + Biphenyl (solution) $\rightleftharpoons Na^+$, Biphenyl $^{\cdot-}$ (solution)
 $K = [B^{\cdot-}, Na^+]/[B]$

Temperature (°K)	MEE	1,2-DMP _r	THF	MeTHF ^a	DEE	THP	1,3-DMP _r
318	0.07	0.07	0.08	—	—	—	—
313	0.12	0.09	0.10	—	—	—	—
303	0.28	0.20	0.20	—	—	—	—
293	0.75	0.49	0.36	0.02	0.07	—	—
283	2.55	1.40	0.66	0.036	0.11	—	—
273	7.0	5.0	1.50	0.055	0.19	0.06	—
263	—	—	2.90	0.11	0.39	0.10	0.12
258	—	—	—	0.14	0.61	—	0.20
253	—	—	—	0.20	1.25	0.17	0.34
248	—	—	—	0.29	2.25	—	0.61
243	—	—	—	0.45	8.7	0.29	1.20
238	—	—	—	0.64	—	—	2.75
233	—	—	—	1.18	—	0.48	—
228	—	—	—	—	—	0.75	—

Note: MEE = 1,2-methoxyethoxyethane; 1,2-DMP_r = 1,2-dimethoxypropane; THF = tetrahydrofuran; MeTHF = 2-methyltetrahydrofuran; DEE = 1,2-diethoxyethane;

^a Data of Slates and Szwarc [188].

which includes also some data of Slates and Szwarc. Plots of $\log K$ versus $1/T$ are seen in Fig. 17 and the heats and entropy terms are listed in Table 13. It is obvious that the solvation provides much of the driving force for the reaction and that the solvating power of the medium is strongly affected by steric factors. For example, at 25°C the equilibrium in 1,2-dimethoxyethane (DME) lies far to the right, but only 60% of biphenyl is reduced in 1-methoxy-2-ethoxyethane, and the conversion is even lower (15%) in 1,2-diethoxyethane. Interestingly, no conversion is observed in 1,1-dimethoxyethane. The

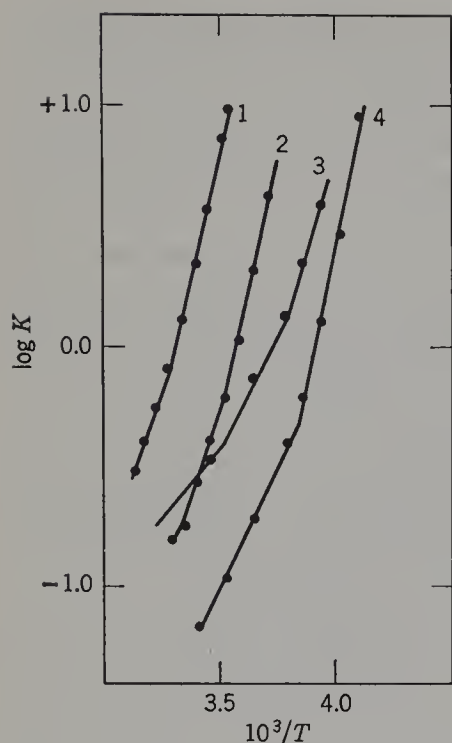
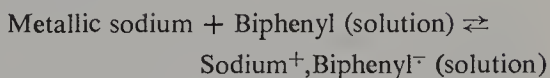


Figure 17. Equilibrium constants of the reaction



for various solvents as functions of temperature: (1) dimethoxyethane-heptane; (2) methoxyethoxyethane-heptane (MEE-Hp); (3) tetrahydrofuran-heptane; (4) diethoxyethane.

proper spacing of the OCH_3 groups appears to be crucial for high solvating power. As remarked previously, the conversion approaches 100% in 1,2-dimethoxyethane but only 6% in 1,3-dimethoxypropane. Significantly, 1,2-dimethoxypropane is a much better solvating agent for Na^+ ion pairs than 1,3-dimethoxypropane; in the former solvent the equilibrium constant $K = [\text{Na}^+, \text{B}^-]/[\text{B}]$ is about 5.0 at 0°C , but it decreases to 0.06 in the latter.

Table 13 Heat and Entropy Changes in the Reaction of Biphenyl with Metallic Sodium

Solvent ^a	K (273°K)	ΔH^b (kcal/mole)	ΔS (eu)
MEE	7.2 ± 0.8	-17.4 ± 0.5	-60 ± 2
1,2-DMP _r	4.6 ± 0.2	-16.5 ± 0.7	-58 ± 3
THF	1.4 ± 0.1	-11.2 ± 0.5	-40 ± 2
DEE	0.2 ± 0.05	-9.6 (at the lowest temp. $\Delta H = -22$)	-38 ± 2 (at the lowest temp. $\Delta S = -86$)
1,3-DMP _r	0.004	-15.5 ± 0.3	-63 ± 1
THP	0.06	-6.8 ± 0.2	-31 ± 1

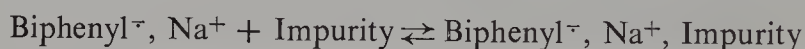
^a See Table 12 for explanation of abbreviations.

^b These values should be taken with some reservation because the van't Hoff lines are slightly curved. The exothermicity becomes larger at lower temperatures. A striking example is provided by DEE, for which $-\Delta H = +9.6$ kcal/mole at about 20°C and increases to $+22$ kcal/mole at -30°C . Note that small experimental errors in determination of K may lead to relatively large errors in ΔH .

Obviously, the cooperative coordination of both oxygens with the cation requires specific spatial configuration that is attained in the 1,2-dimethoxy compounds but not in their 1,1- or 1,3-derivatives.

Comparison of the equilibrium established between metallic lithium and biphenyl with that involving metallic sodium is instructive. In 1,2-diethoxyethane 45% of biphenyl is reduced by lithium but only 15% by sodium. This disparity is even larger in tetrahydropyrene; at -10°C lithium reduced 80% of biphenyl whereas sodium reduced only 10% [185]. The higher reducing power of lithium than of sodium demonstrates how much greater is the heat of solvation of the lithium than of sodium ion pairs. That such solvation effects are most specific has been shown by Shatenshtein, who found 4% of biphenyl to be reduced by sodium in dioxane but none by lithium. The specificity of interaction between solvent and cation is also evident when the reducing powers of sodium and potassium are compared. Sodium is a more powerful reducing agent than potassium in tetrahydrofuran or tetrahydropyrene, but the order is reversed in 1,3-dimethoxypropane [186].

A word of caution is needed. Radical anions become readily associated with other ion pairs in ethereal solvents. For example, small amounts of LiBr (less than $10^{-3} M$) shift the absorption maximum of the lithium diphenylketyl in tetrahydrofuran until a plateau is reached when the salt is in excess [187]. These findings were interpreted in terms of ion pair agglomerations. A new equilibrium is established whenever such an agglomeration occurs; for example, lithium or sodium alcoholates or hydroxides, often present as impurities in the alkali metal-acceptor solution, readily associate with the radical ions pairs and then an equilibrium such as



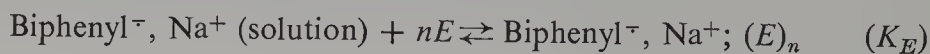
is established. Such an association shifts the overall equilibrium, to the right,



(whether associated or not)

and consequently the total concentration of sodium biphenyl increases in their presence. Indeed, such artifacts were observed in our laboratory. They lead to erroneous equilibrium constants and seriously distort the experimental ΔH of the reaction because even small but systematic temperature-dependent errors in the equilibrium constants profoundly affect the slope of the van't Hoff line.

The undesirable effect of impurities discussed in the preceding section may be advantageously exploited in studies of interesting equilibria of ion pairs with a variety of complexing agents (E), such as



The results of such studies were reported by Slates and Szwarc for the systems sodium metal-biphenyl in tetrahydropyran or in 2-methyltetrahydrofuran, using triglyme ($\text{CH}_3\text{O}\cdot\text{CH}_2\cdot\text{CH}_2\cdot\text{O}\cdot\text{CH}_2\cdot\text{CH}_2\cdot\text{OCH}_3$) or tetraglyme ($\text{CH}_3\text{O}\cdot\text{CH}_2\cdot\text{CH}_2\cdot\text{O}\cdot\text{CH}_2\cdot\text{CH}_2\cdot\text{O}\cdot\text{CH}_2\cdot\text{CH}_2\cdot\text{OCH}_3$) as the complexing agent [188]. As is easily verified,

$$K_E[E]^n = \frac{(K_{ap} - K)}{K}$$

where K_{ap} is the apparent equilibrium constant defined as the ratio

$$K_{ap} = \frac{\text{Total concentration of } B^- \text{ in the presence of complexing agent}}{\text{Concentration of the unconverted B}}$$

K_E is the previously defined equilibrium constant of the complex formation, and K denotes the ratio $[B^-, \text{Na}^+]/[B]$ in the absence of glyme.

The temperature dependence of K , as well as that of a series of K_{ap} , each referring to a different but constant concentration of glyme, is depicted by Fig. 18. The curves shown in this figure provide the data for the construction of isothermal plots of $\log (K_{ap} - K)/K$ versus $\log [\text{glyme}]$. Since the latter result in straight lines of unit slope, the complexation obeys 1:1 stoichiometry, that is, it is due to *chemical* coordination and not to a loose physical association.

As mentioned previously, we differentiate between tight, contact pairs and loose, solvent-separated pairs. The latter usually absorb at longer wavelength than the former (Chapter III of ref. 12). A shift in the absorption spectrum is noted when a small amount of a powerful solvating agent, such as tetraglyme, is added to the solution of tight biphenylide pairs [189], implying that a glyme molecule separates the ions. The spectrum of sodium biphenylide as well as that of its 1:1 complex with triglyme has its maximum of 400 nm at all the investigated temperatures, whereas the absorption maximum of the solution containing tetraglyme, although still at 400 nm at 25°C, is shifted to 407 nm at -40°C. In fact, for every concentration of tetraglyme it was possible to find a temperature at which two peaks of equal optical density were seen, one at 400 nm, the other at 407 nm. It could be concluded that one of them corresponds to a noncomplexed pair, the other to a pair separated by the glyme. However, the total concentration of the complexed ion pairs is greater than that of the species absorbing at 407 nm, and therefore two forms of complexes have to be present: one with a glyme molecule located on the periphery of an ion pair absorbs at 400 nm, like the complex with triglyme, while the other having a glyme molecule separating the ions absorbs at 407 nm. This is the first reported example of isomerism of ion pairs resulting from different locations of the complexing molecule in the solvated pair. Spectroscopic evidence demonstrating such an isomerism was

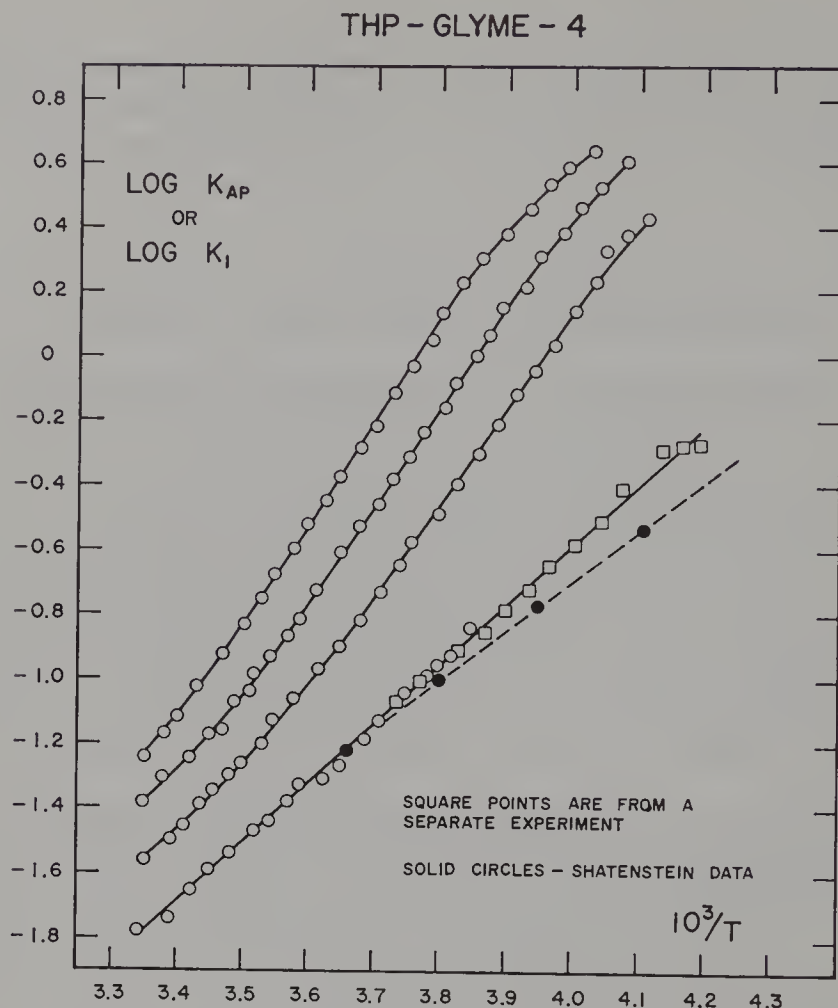
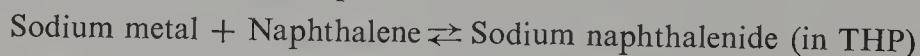


Figure 18. Equilibrium constant or the apparent equilibrium constant for the reaction
 Metallic sodium + Biphenyl (solution) \rightleftharpoons Sodium biphenylide ion pairs (solution)
 in the absence of glyme (lower line) and in the presence of increasing amounts of glyme
 (upper curves).

subsequently reported by Smid (see Chapter III of ref. 12) and by Lundgren et al. [230]. Three types of ion pair of lithium salt of 1,3-diphenylbutene in 2,5-dimethyltetrahydrofuran have been observed by Burley and Young [229].

Studies of Slates and Szwarc have been extended by Lee et al. [191], who investigated the systems naphthalene-sodium and naphthalene-potassium in tetrahydropyran (THP) and in diethylether (DEE) by spectrophotometric and ESR techniques. The equilibrium

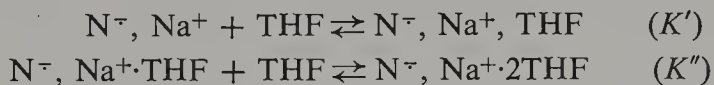


produces tight ion pairs. For this reaction, $\Delta H = -12.0$ kcal/mole, $\Delta S = -41$ cal. K^{-1} mol $^{-1}$.

The large negative ΔS indicates that even tight pairs are substantially solvated. On addition of dimethoxyethane, a new kind of ion pair, *externally* solvated by DME, is formed and this shifts the overall electron transfer equilibrium to the right. It was established that in the course of this complexation one of the THF molecules involved in the solvation of the original pair is replaced by one molecule of DME.

Sodium is hardly capable of reducing naphthalene in diethylether, and only minute concentrations of tight ion pairs are formed in this solvent. On addition of THF (0.05–0.5 *M*) a dietherate, sodium naphthalenide.2THF = $N^{\cdot-}Na^+.2THF$, is formed, with the THF molecules situated on the periphery of the ion pair. This solvation process is exothermic but it does not affect the entropy of the system, indicating that the two molecules of THF replaced two molecules of diethylether that were originally associated with the pair.

Why do we observe the formation of a dietherate and not a monoetherate? Does it mean that the second molecule of THF adds more easily than the first one? This need not be the case. Consider the equilibria



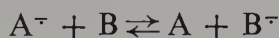
The concentration of THF in this system is larger than that of the complexes, and much larger than that of the uncomplexed $N^{\cdot-}, Na^+$. Hence if $K''[THF] \gg 1$, then the ratio $[N^{\cdot-}, Na^+.2THF]/[N^{\cdot-}, Na^+.THF]$ is also much greater than 1, even if $K' > K''$. Thus the monoetherate can hardly be observed in the large excess of dietherate. The product $K'''[THF]$ apparently is much smaller than 1, and therefore the concentration of trietherate is negligible.

Finally, the system potassium-naphthalene in DME calls for some comment. Only 13% of naphthalene is reduced by potassium when the reaction is performed in diethylether. The degree of reduction is independent of temperature, $\Delta H \approx 0$, and it is not affected by the addition of even 10% of THF.

The ionization potential of the atoms and the heat of sublimation of the metal are lower for potassium than for sodium. Nevertheless, the reducing power of potassium is relatively low in DEE + THF because of the lack of solvation. The solvent molecules merely surround potassium-naphthalenide ion pairs but do not form strongly attached solvation shells. In these terms the potassium ion pairs may be referred to as nonsolvated pairs.

12. KINETICS OF EXCHANGE REACTIONS

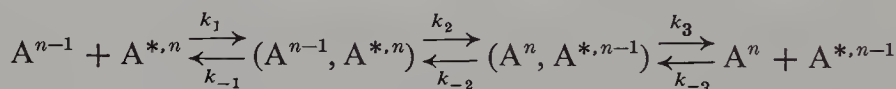
This section and the following one are devoted to the kinetics of electron transfers such as



Our discussion will cover the reactions involving free ions as well as those concerned with various ion pairs. The simplest examples of such transfers are the exchange reactions, and these will be discussed first. The exchanges involving ions of the transition metals cannot be treated here—a point made in the introduction. Nevertheless, a brief survey of such processes is appropriate because the salient features of the exchange reactions are similar for inorganic and organic systems.

Early studies of electron transfer exchanges [192, 207] revealed that small ions interact slowly but large, complex ions react rapidly. A qualitative explanation of this trend, offered by Libby [193], stressed the importance of solvent molecules which participate in the solvation of the interacting ions. Small ions are surrounded by tight solvation shells and therefore a substantial expenditure of energy is needed to modify them to meet the requirements of the reaction. This slows down the exchange. In contrast, the large ions are weakly solvated and hence the reorganization of solvent molecules is facile and the exchange fast.

These qualitative ideas were developed into a quantitative theory by Marcus [192b–192d]. The exchange, like any bimolecular reaction, involves three steps:



and therefore the forward rate constant of the overall exchange is

$$k_{\text{ex}} = \frac{k_1}{1 + k_{-1}/k_2 + k_{-1}k_{-2}/k_2k_3}$$

The rate constants k_2 and k_{-2} are optimized when the common pattern of solvent molecules surrounding either of the two encounter complexes, $A^{n-1}, A^{*,n}$ and $A^n, A^{*,n-1}$, equalizes their free energy. When such an organization of solvent molecules is attained by a favorable fluctuation, the electron tunnels freely from A^{n-1} to $A^{*,n}$, or vice versa, with a rate estimated by Marcus at about 10^{12} sec^{-1} . In an exchange process $k_2 = k_{-2}$ and $k_{-1} = k_3$; and since $k_{-1} \ll k_2$

$$k_{\text{ex}} = \frac{1}{2}k_1$$

In the terms of transition state theory, $k_1 = Z \exp(-\Delta G/kT)$, where Z is the diffusion-controlled collision frequency estimated at $10^{11} \text{ M}^{-1} \text{ sec}^{-1}$, and ΔG the free energy change of the process yielding the transition state from the encounter complex. A treatment of the thermodynamics of the non-equilibrium orientation of solvent molecules generally leads to

$$\Delta G = W + \frac{1}{2}\Delta\epsilon + \frac{(\Delta\epsilon)^2}{4\lambda} + \frac{\lambda}{4}$$

where W is the work needed to bring the two ions together, $\Delta\epsilon$ is the difference of the electron affinities of A^n and $A^{*,n}$, this being zero for any exchange, and finally λ , the so-called solvent's reorganization parameter, accounts for the relatively slow reorientation of dipoles when compared with the fast polarization of valence electrons. Thus

$$\lambda = \left(\frac{1}{2}r_{A^n} + \frac{1}{2}r_{A^{n-1}} - \frac{1}{r} \right) \left(\frac{1}{\mathcal{D}_{\text{opt}}} - \frac{1}{\mathcal{D}_{\text{st}}} \right) e^2$$

where r_{A^n} and $r_{A^{n-1}}$ are the radii of the respective ions, r the distance separating them in the encounter complex, and \mathcal{D}_{opt} and \mathcal{D}_{st} the "optical" and the static dielectric constants of the solvent, the former being given by the square of its refractive index. For an exchange reaction involving an ion and a *neutral* molecule $W = 0$ and

$$\Delta G^\ddagger = \frac{\lambda}{4}$$

The latter type of reaction is illustrated by an electron transfer from a *free* radical anion to its parent molecule, for example,



Their rates are conveniently studied by the ESR technique explored first by Weissman and his co-workers [194]. Two limiting approaches are commonly utilized. In the so-called slow exchange limit, the broadening of an individual ESR line—or the increase in the linewidth $\Delta\omega$ —is proportional to the concentration of the acceptor, C_{acp} , that is, $k_{\text{ex}} = \pi\sqrt{3} \times 2.83 \times 10^6 \cdot \Delta\omega/C_{\text{acp}}$, where $\Delta\omega$ is measured in gauss. This relation is valid provided the line is Lorentzian and its intensity small compared to the total intensity of the signal. For a high-intensity line a correction factor f has to be introduced [195]:

$$f = (1 - I_i/\Sigma I_j)^{-1}$$

I_i being the intensity of the line chosen for the study, ΣI_j the total intensity of the signal. This correction accounts for the fact that not every collision changes the energy of the system, and we should examine the underlying assumptions introduced in its derivation.

Does an electron transfer result in broadening of the line if the magnetic energy is not changed, that is, if the electron nuclear spin interaction is the same in the donor and acceptor? Broadening may still take place if the phase of the Ψ function describing the electron is altered [205] during its transition. However, to obtain a measurable effect, the time of transition has to be much longer than is feasible, and therefore those exchanges that leave the energy of the system unaltered do not contribute to broadening of the line [194].

The foregoing question is part of a more general problem: Does the probability of transfer depend on the nuclear spin state of the acceptor? Denote by N the total number of nuclear spin states and by g_k the number of those belonging to the energy E_k and therefore to the line k . The equation

$$\frac{1}{t_k} = \frac{1}{t} (N - g_k)/N$$

relates the characteristic time t_k determining the broadening of the line to the average time t spent by an electron on a molecule, provided the probability of transfer is independent of the nuclear state of the acceptor and that the transfer to any molecule of group E_k does not contribute to the broadening. The last point has been discussed and established in the preceding paragraph. The assumption of the independence of the transfer probability of the nuclear spin state of the acceptor can be tested experimentally by measuring the broadening of different lines. This has been done by Zandstra and Weissman [195], and their results confirmed the validity of this assumption.

One more point may be mentioned. The equation relating t_k with t shows that t_k is always larger than t . In a hypothetical case when all the molecules have the same spin energy $g_k = N$, and t_k becomes then infinitely long. Electron transfer does not contribute to broadening of the line in such a system.

The hyperfine lines of an ESR spectrum often overlap, and then their shape deviates from the simple Lorentzian or Gaussian form. Such a spectrum may be analyzed by computer simulation; the density-matrix approach of Kaplan and Alexander is helpful in such computations [196, 197]. Possible errors of such an analysis have been discussed [206].

In the other extreme—the “fast exchange limit”—the ESR spectrum collapses into one single line which narrows as the rate of exchange increases. Under these circumstances the rate constant of exchange, k_{ex} , is given by

$$k_{\text{ex}} = \frac{4}{\sqrt{3}} \pi \times 2.83 \times 10^6 \frac{\nabla}{C_{\text{acp}} \Delta \omega}$$

where ∇ is the second moment of the original spectrum and the other symbols have their previous meanings. The preceding equation applies again only to those broadened lines that acquire Lorentzian shape. The calculation of ∇ involves some problems that are discussed in the original literature [183, 198], to which the reader is referred.

An attempt to test whether Marcus' treatment applies to electron transfer between a radical anion and its parent molecule has been reported in the literature [183]. The reaction of *free* naphthalenide ions with naphthalene was investigated in three solvents: hexamethylphosphorictriamide (HMPA), THF-DME mixture, and pure THF [183, 199, 200]. In addition, its rate in

isopropyl alcohol could be deduced by extrapolating the data obtained by pulse radiolysis [201]. The results are collected in Table 14. The agreement with Marcus' theory is poor but at least a monotonic dependence of k_{ex} on λ is observed, a qualitative evidence supporting Marcus' approach.

Table 14 Electron-Transfer Exchange of *Free* Naphthalenide Ions with Naphthalene

Solvent	$k_{\text{ex}} \times 10^{-8}$ at 25°C ($M^{-1} \text{sec}^{-1}$)	λ (kcal/mole)	$k_{\text{ex}}/k_{\text{ex in HMPA}}$ (calculated from λ)	Ref.
Isopropyl alcohol	1 ^a	16.0	0.5	201
HMPA	5	14.5	1.0	183, 202
THF-DME (1:1)	12	12.5	2.3	199
THF	30	12.2	2.6	200

^a Extrapolated from data given in ref. 201. See ref. 183.

The temperature dependence of k_{ex} pertaining to *free* ions was investigated for the systems naphthalene [183], α - and β -ethylnaphthalene [202], and α -butylnaphthalene [203]. All these reactions were carried out in HMPA and proceed with virtually the same activation energy. The pertinent data are collected in Table 15, and it is interesting to note that within an experimental

Table 15 Electron-Transfer Exchange of Free Ions of Naphthalenide and Its Derivatives in HMPA

Hydrocarbon	k (15°C) $\times 10^{-8}$ ($M^{-1} \text{sec}^{-1}$)	E (kcal/mole)	$A \times 10^{-11}$ ($M^{-1} \text{sec}^{-1}$)
Naphthalene	4.0	4.1*	6.9*
α -Ethylnaphthalene	5.1	4.2	8.3
β -Ethylnaphthalene	4.8	4.1	5.9
α -Butylnaphthalene	4.9	4.3	7.8
Activation energy of HMPA viscosity		3.9	

* Remeasured values, see [202].

error of about ± 0.5 kcal/mole the activation energy of the transfer is the same as the viscosity of solvent. Apparently the transfer in HMPA proceeds with virtually zero activation energy, and temperature affects only the diffusion-controlled rate of collisions.

Association of radical anions with counterions affects the rate of exchange profoundly. The effect was observed first by Weissman [194], and his original work deserves a full review, even if our present interpretation of the results may differ somewhat from that which he then proposed. The study with Ward [194] revealed the influence of counterions and solvents on the rate of exchange between naphthalenide salts and naphthalene. The results, summarized in Table 16, were interpreted as an indication of transfers involving ion

Table 16 Effect of Counterion and Solvent on the Rate of Exchange of Naphthalenide Salts with Naphthalene

Counterion	Solvent	$10^{-7} \times k_{\text{ex}} (\text{M}^{-1} \text{sec}^{-1})$
K ⁺	DME	7.6 ± 3
K ⁺	THF	5.7 ± 1
Na ⁺	DME	~ 100
Na ⁺	THF	~ 1
Li ⁺	THF	46 ± 30

pairs and not the free ions. The striking hundredfold difference in the rate of exchange of the sodium salt in DME and THF was puzzling and unexplained at that time.

In a subsequent communication with Adam [208], Weissman furnished the first conclusive and positive proof for the existence of ion pairs, the splitting of the original ESR lines of a radical anion by the counterion. This criterion permitted the distinction between free ions and ion pairs. Single lines that appear in the ESR spectra are attributed to the former species, whereas multiplets such as the quadruplets seen in the ESR spectra of the sodium salts manifest the presence of the latter. Such multiplets result from the interaction of electron spin with different spin states of the counterion nucleus [see Chapters V and VIII of ref. 12]. Both single lines and multiplets were observed simultaneously in the ESR spectrum of sodium naphthalenide in THF, THP, and MeTHF, but only single lines were seen when the salt was dissolved in DME [209]. This observation led to the conclusion that only free naphthalenide ions are present in DME, and therefore the high rate of exchange of the sodium salt in DME, previously reported, was attributed to the fast reaction of the free ions. However, the conductance studies [149, 150] showed that the concentration of free ions in DME is low, and therefore the single lines observed in this solvent arise from the presence of loose ion pairs. Of course some free ions are also present in the solution, but provided their ESR spectrum closely coincides with that of the loose pairs, the distinction between them would be impossible with this technique. This interpretation was fully confirmed by Hirota [199, 210, 211], and hence the fast exchange of sodium naphthalenide in DME has to be attributed now to the reaction of loose pairs. Since the potassium salt forms tight ion pairs in THF as well as in DME the rate of exchange of this salt is similar in both solvents (see Table 16).

A digression is helpful here. Studies of the two types of ESR line seen in the spectra of sodium naphthalenide in THF permitted Atherton and Weissman [209] to calculate the dissociation constant of those ion pairs into free ions.

The results were, however, higher by a power of 10 than those derived from the conductance data [149]. A possible cause of this discrepancy has been suggested by Tuttle [212]. Sodium metal is often contaminated by potassium, and potassium ion pairs, even when tight, hardly split the proton hyperfine lines because the magnetic moment of ^{39}K is very low. The single lines observed by Atherton and Weissman probably resulted from a trace of potassium, and indeed when their work was repeated by Tuttle and his associates [212] with rigorously purified sodium, the results were concordant with those obtained by the conductance technique.

The temperature dependence of the rate of exchange of naphthalenide salts was studied meticulously by Zandstra and Weissman [204]. The broadening was determined for both types of line by a method described earlier [213]. The k_{ex} for contact ion pairs is very low in tetrahydropyran and in 2-methyltetrahydrofuran, 4.4 and $4.5 \times 10^6 \text{ M}^{-1} \text{ sec}^{-1}$, respectively, at 21°C ; nearly 10 times as high a value, $\sim 30 \times 10^6 \text{ M}^{-1} \text{ sec}^{-1}$, is found in THF. The values reported for free ions in THP and MeTHF are substantially higher; however, it seems to us that the reactions observed in these solvents are due to loose ion pairs and not to free ions.

A striking and initially puzzling observation was reported in that paper [204]. The rate constant of exchange of the sodium pairs in THF decreased with temperature, reached a minimum, and then increased as the temperature continued to decrease. This observation, although not fully understood in those days, indicates a change in the nature of ion pairs resulting from temperature variation. Indeed, this possibility was anticipated by Weissman.

The most comprehensive study of kinetics of exchange of naphthalenide salts was reported by Hirota and his students [199]. To gain further insight into the complexity of these processes they investigated the equilibria and kinetics of the interconversion of tight into loose ion pairs [199, 211] and utilized the results in unraveling the overall kinetics of electron transfer when both species participate simultaneously in the exchange. The fast exchange limit ESR technique was used in their work.

The directly observed rate constant of exchange, $k_{\text{obs,ex}}$, is given by $fk'_{\text{ex}} + (1 - f)k''_{\text{ex}}$, where k'_{ex} and k''_{ex} denote the constants of exchange of tight and loose pairs, respectively, and f is the fraction of tight ion pairs present in the equilibrium mixture. The observations of Zandstra and Weissman [204] were confirmed. The *overall*, directly observed constant of exchange, $k_{\text{obs,ex}}$, increases with decreasing temperature at the lower temperature range. However, they noted also that this strange behavior takes place in that temperature region where the experimental coupling constant to sodium decreases sharply; that is, when tight ion pairs become converted into loose pairs. Hence the rational explanation of the "negative activation energy" is obvious—the increase in the fraction of reactive loose pairs more than compensates

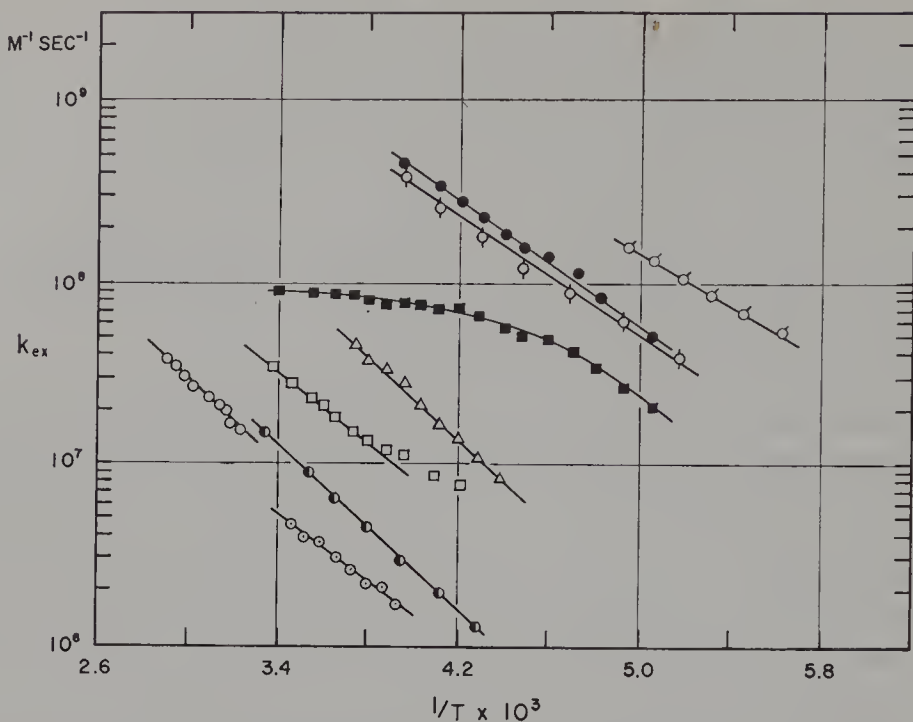


Figure 19. Temperature dependence of the rates of electron-transfer reactions of various naphthalenide salts: \circ , Na^+ , THF, tight ion pair; \bigcirc , Na^+ , THF, loose ion pair; \bullet , Na^+ , DME; \bigcirc , Na^+ , DEE; \bullet , Na^+ , DMTHF (0.50) + DEE; \bigcirc , Li^+ , DME; \blacksquare , K^+ , DME; \square , K^+ , THF; \triangle , Cs^+ , THF.

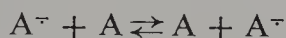
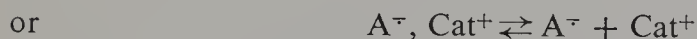
the retarding effect of decreasing temperature (see also Chapter IV where a similar phenomenon is discussed). However, the behavior of k'_{ex} and k''_{ex} is normal and does not show any anomalies.

The results of Hirota are summarized by Fig. 19 giving $\log k_{\text{ex}}$ for various species plotted versus $1/T$. The pertinent rate constants vary by more than two orders of magnitude. Interestingly, the rate of exchange of loose lithium ion pairs in THF is slightly slower than that of loose sodium pairs, and the latter is slightly higher than the rate of loose sodium pairs in DME. These results corroborate the conductance findings [149]. The sodium ions solvated by DME are "smaller" than those solvated by THF [214], and hence the former interact more strongly with the anion on forming loose pair than the latter. Therefore the corresponding exchange is slightly slower. A similar explanation accounts for the slight difference in the rate of exchange of loose Li^+ and Na^+ ion pairs.

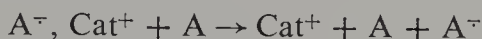
Tight ion pairs can be converted into loose ion pairs by adding a powerful solvating agent to their solution in a poorly solvating medium. A dramatic effect of such an addition on the ESR spectrum of sodium naphthalenide in tetrahydropyran has been reported by Höfelmann et al. [183]. The coupling to sodium decreased from 1.4 to 0.4 G on adding 0.01% of tetraglyme. The

loose, glyme-separated ion pairs exchange rapidly with naphthalene; however, the ESR spectrum observed at fast exchange limit reveals two maxima, implying the presence of two rapidly exchanging species. The computer simulation of such a spectrum gives the rate constants of exchange, 5×10^8 and $30 \times 10^8 M^{-1} \text{sec}^{-1}$. This observation resembles the findings of Chang and Johnson [198], who assumed that the free ions are responsible for the faster exchange. However, the results of conductance studies convinced Höfelmann et al. that in their system the concentration of free ions is too low to account for the observations, and hence the existence of two different loose pairs had to be postulated. A model of two distinct loose pairs has been proposed; it accounts for all the observed facts, although it is highly speculative.

Only an electron is transferred in exchange involving free ions. The reaction of ion pairs requires additionally the transfer of the counterion; therefore two mechanisms may be visualized:



The first requires the simultaneous transfer of electron and cation and hence it may be referred to as an atom transfer. The second represents the dissociation of ion pairs followed by electron transfer involving free ions. The reaction



is, of course, ruled out because it violates the principle of microscopic reversibility.

The results of Adam and Weissman [208] conclusively proved that the sodium ion is transferred with the electron. The ESR spectrum obtained in the fast exchange limit should have collapsed into one structureless line had the dissociation preceded the exchange. In such a process the electron interacts with a variety of acceptors and cations and therefore the specific features reflecting the properties of *both* species are lost in the spectrum. However, the simultaneous transfer of electron *and* cation leaves the electron interacting with a specific cation nucleus in spite of changing acceptors. Therefore the pattern characterizing the nuclear spin of the cation, for example, the quadruplet of the sodium nucleus, should be seen in the otherwise collapsed structureless spectrum. The ESR spectrum of sodium benzophenone observed in the presence of a large excess of the parent ketone showed the four characteristic lines of the sodium cation, proving that electron and cation are transferred simultaneously.

The ESR technique not only provides direct evidence of the existence of ion pairs but also demonstrates the existence of triple ions such as Na^+ , A^- , Na^+ . As shown by the studies of Gough [215], the ESR spectra of sodium salts of semiquinones observed in the presence of an excess of sodium tetraphenylboride reveal splitting of each proton hyperfine line into seven lines, as would be expected for an electron interacting with two identical sodium nuclei of total spin of 3. This implies a lasting association, on the ESR time scale, of Q^- , (Q denotes a quinone) with *two* sodium ions. The observation of Gough raises the question of what is the mechanism of electron transfer from a triple ion to the parent acceptor. The work of Adams et al. [216] furnished a conclusive answer. As seen in Fig. 20, in the fast exchange limit the ESR spectrum of the triple ions collapses into seven lines while the spectrum of the ion pairs collapses into four lines. Hence both cations are transferred simultaneously with the electron on the collision of a triple ion with the parent quinone.

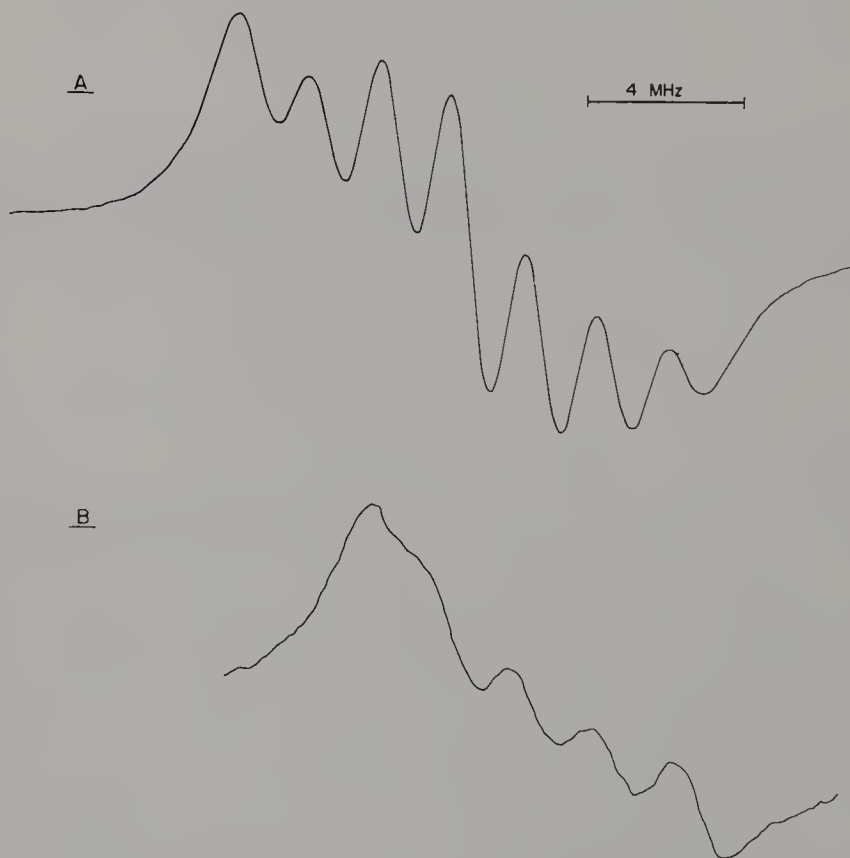


Figure 20. ESR spectra of the triple ions and of ion pairs of duroquinone radical anions in the presence of a large excess of duroquinone ($\sim 2 M$). Note the collapse of the spectrum of the triple ions into seven lines and the collapse of the spectrum of ion pairs into four lines.

Interesting results have been reported recently by Malinoski, Bruning, and Griffin [217] who studied the exchange of potassium salts of benzene, toluene, and xylene radical ions in THF and DME. The experimental k_{ex} in DME at 18°C were found to be 3.6×10^7 , 4.5×10^7 , and $4.3 \times 10^7 \text{ M}^{-1} \text{ sec}^{-1}$ for the benzene, toluene, and xylene radical anions, respectively, but the rate seems to be substantially higher in THF, $16.3 \times 10^7 \text{ M}^{-1} \text{ sec}^{-1}$ for benzene radical anion.

This reversal of the expected effect of solvent calls for a deeper examination of the mechanism of exchange involving ion pairs. It has been established that the counterion is transferred simultaneously with the electron. What model should be proposed for the transition state of such a reaction? Let us consider, to begin with, a transfer involving a loose pair. In such a species the cation is fully solvated, and therefore no major change in the structure of its solvation shell is needed in the transition state of an exchange in which the fully solvated cation becomes sandwiched between the acceptor and the donor. On the other hand, in a tight ion pair the cation is externally solvated, and a sandwich formed with the approaching acceptor has an asymmetric structure. The expected symmetric transition state could be formed in two ways. Either the initial tight pair has to be converted in the transition state into a loose pair, or the externally solvated tight pair has to be desolvated to permit a simultaneous tight contact with the donor and acceptor. In the former case the reaction is enhanced by facilitating the conversion of a tight pair into a loose pair, and then one expects the conversion process to be faster if DME rather than THF is the solvating agent. In the other case, the enhancement of the exchange requires facilitation of the desolvation process, which should be easier for the monodentate THF than for the di-dentate DME.

For ion pairs involving relatively large anions, the conversion of tight pairs into loose pairs should provide the preferred route for exchange. However, small ions like benzene⁻ in which the negative charge is more localized might be so strongly bonded to the cation that the alternative route of exchange would be preferred.

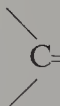
Let us summarize the results of all these ESR studies. Electron transfer from an aromatic radical anion to its parent molecule may involve free ions, tight or loose ion pairs, or triple ions. The transfer from free ions is essentially diffusion controlled and its bimolecular rate constant in ethereal solvents at ambient temperature is greater than $10^9 \text{ M}^{-1} \text{ sec}^{-1}$. Electron transfer from ion pairs proceeds simultaneously with the cation transfer [208], and in the reaction of triple ions both cations are simultaneously transferred with the electron [216]. The reactions of tight ion pairs are relatively slow, $k_{\text{ex}} \sim 10^6$ – $10^7 \text{ M}^{-1} \text{ sec}^{-1}$ at ambient temperatures, because a solvation or desolvation process has to accompany the transfer. On the other hand, loose ion pairs transfer an electron rapidly, sometimes even faster than the free ions, because

hardly any reorganization of solvent molecules surrounding the cations of loose pairs is needed to facilitate the reaction.

In many systems, tight and loose pairs coexist in dynamic equilibrium, the interconversion usually being so fast that only an average coupling to cation is observed in the ESR spectra. In such systems the observed k_{ex} is a weighted average of the slow rate of tight pairs and the fast rate of the loose pairs. Lowering the temperature shifts the equilibrium toward loose pairs, and this is manifested by a decrease in the cation coupling, since the coupling is much larger for tight pairs than for the loose pairs. By the same token, an apparent negative "activation energy" of exchange is often observed [195, 220], since the increase in the proportion of the highly reactive loose pairs more than compensates for the retarding effect of lower temperature [199]. As a rule, one frequently finds a correlation between cation coupling constant and rate of exchange: the smaller the coupling, the higher the rate.

The exchange of ketyls with parent ketones exemplifies another extensively studied electron-transfer process [218, 219]. Here again the nature of ion pairs greatly affects the rate of exchange. In contrast to the aromatic radical anions, in the ketyl series the more reactive species seems to be characterized by a *larger* coupling to cations than that of the more slowly exchanging ion pairs. This is clearly shown in a spectacular experiment described by Hirota and Weissman [219]. The ESR spectrum of sodium benzophenone in MeTHF is complex and difficult to unravel. However, in the presence of 1.2 *M* benzophenone it is readily subdivided into two sets of lines. One set consists of four intense and well-separated lines attributed to a fast exchanging species whose spectrum had collapsed, leaving only the quadruplet due to the coupling to ^{23}Na . The remaining slightly broadened lines were recognized as those of another sodium benzophenone ion pair, since its proton hyperfine lines are still split by sodium although the coupling constants of these quadruplets are much smaller than those of the fast exchanging species. The presence of the two species in this solution thus was revealed in the ESR spectrum by their greatly different rate of exchange.

Why is the correlation of reactivity with the cation coupling reversed in the ketyl series? Apparently two types of ketyl ion pairs coexist in equilibrium [310]. At higher temperatures and in solvents of lower solvating power the

cation preferentially hovers above the nodal plane of the  C=O group. Such

a structure leads to a relatively high coupling of the odd electrons to the alkali nucleus. Low temperatures and increasing solvation power of the solvent favors the structure in which the cation is located in the nodal plane of the molecule because, due to steric reasons, the solvation of the cation can be more extensive. The coupling of the electron to the cation nucleus is then low and sometimes even negative. Both types of ion pairs are classified as tight

ones, although the binding is weaker in the former type than in the latter. Therefore, the electron exchange, that proceeds with the simultaneous transfer of the cation, is faster for the form characterized by a larger a_{Alk} , in agreement with the observations.

The variations in the rate of exchange of ketyls caused by cation and solvent are seen in Table 17. The argument outlined in the previous discussion con-

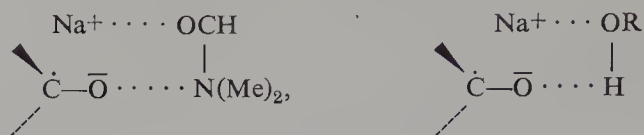
Table 17 Rate Constants k and Activation Energies E for the Electron Transfer Reaction; Ketyl + Ketone \rightarrow Exchange

Ketyl	Solvent ^a	Temperature (°C)	$k \times 10^{-8}$ (liter mole ⁻¹ sec ⁻¹)	E (kcal/mole)
Na ⁺ , xanthone ⁻	DME	37	4.6	5.1
	THF	25	4.5	4.3
	THP	7	4.7	—
	MeTHF	0	4.3	—
Rb ⁺ , xanthone ⁻	DME	25	2.5	—
Na ⁺ , benzophenone ⁻	DME	25	1.1	6.3
	THF	12	1.1	6
K ⁺ , benzophenone ⁻	THF	25	2.5	—
Rb ⁺ , benzophenone ⁻	DME	25	1.6	—
Mg ²⁺ (benzophenone ⁻) ₂	DME	24	<10 ⁻²	—
Ca ²⁺ (benzophenone ⁻) ₂	DME	24	<10 ⁻²	—
(Na ⁺ , benzophenone ⁻) ₂	MeTHF	24	<10 ⁻²	—
	Dioxane	24	<10 ⁻²	—
Free xanthone ⁻ ion	Acetonitrile	25	10	—

^a DME = dimethoxyethane; THF = tetrahydrofuran; THP = tetrahydropyrene; MeTHF = 2-methyltetrahydrofuran.

cerned with benzene radical anions may explain the effect of solvents upon the rate of exchange in ketyl system. Here one deals again with tight pairs externally solvated and a solvent molecule in the cation shell has to be removed and replaced by the acceptor (ketone) when the exchange takes place. Hence, the stronger the solvent-cation interaction, i.e., the higher the solvating power of the solvent, the slower the exchange. This gradation is revealed by the behavior of sodium salt of Xanthone Ketyls in MeTHF, THP, THF and DME (note the temperature of exchange in the data listed in Table 17 and see also p. 4423 of ref. 218). The same factor is responsible for the drastic *decrease* in the rate of exchange of sodium fluorenone ketyl in THF resulting from the addition of tetraglyme [218]. Since a_{Na} is only slightly affected by the addition of tetraglyme, this complexation process does not perturb much the location of the cation. In contrast, the addition of dimethylformamide (DMF) or iso-PrOH substantially increases a_{Na} although it still drastically reduces the rate of exchange. It seems that solvating agent shared

ion pairs are formed, e.g.,



Thus a_{Na} increases, due to the shift of the cation out of the nodal plane, while the necessity of transferring the solvating agent with the cation greatly reduces the rate of exchange. Not surprisingly, the effect of DMF is greater for Li^+ salt than for Na^+ , and more pronounced in MeTHF than in THF or DME. Isopropanol is also a solvating agent for the negative ketyl ion. This magnifies the effect caused by its addition since the exchange requires desolvation of the ketyl ion or solvation of the ketone by another iso-PrOH molecule, either requirement hindering the exchange. Extensive studies of the effect of the added alcohol upon the structure of ketyl salts have been reported recently [332].

In contrast with aromatic hydrocarbon radical anions, ketyls easily form paramagnetic dimers. As seen in Table 17, these are inert and exchange very slowly. Probably the approach of the acceptor to the cations of such dimers is sterically hindered.

Several workers studied exchanges of radical anions generated electrolytically in solvents of high polarity, such as dimethyl formamide (DMF). Adaptation of the electrolytic technique to ESR studies was first reported by Geske and Maki [221] and its utilization for studies of exchange was described by Adams and his co-workers [222, 223] and by Peover and his colleagues [224]. It could be argued that free ions are responsible for such reactions; however, the high concentration of supporting electrolyte may lead to at least some ion pairing. This is clearly demonstrated by the results of Peover [224]. The reported rate of exchange of *trans*-stilbene in DMF was $10.2 \times 10^8 \text{ M}^{-1} \text{ sec}^{-1}$ in the presence of $0.1 \text{ M NBU}_4\text{I}$, but it was only $7.5 \times 10^8 \text{ M}^{-1} \text{ sec}^{-1}$ when the concentration of the iodide was increased to 0.5 M .

The exchange of an electron between potassium 2,2'-bipyridyl radical anion and its parent molecule was investigated by Reynold [225]. His intention was to determine whether "complex" formation takes place during the electron transfer when the investigated species is a potent complexing agent. No peculiarity was observed in this system. The bimolecular rate constant of exchange was found to be $\sim 4 \times 10^6 \text{ liter mole}^{-1} \text{ sec}^{-1}$ at 20°C , the activation energy of transfer 10 kcal/mole , and the entropy of activation about $+5 \text{ eu}$.

The exchange between radicals and the corresponding carbanions was investigated by Jones and Weissman [369]:



Again, the broadening of the ESR lines of the neutral radical permitted the determination of the bimolecular rate constants. Their values are 4.4×10^8 and $6.0 \times 10^8 \text{ M}^{-1} \text{ sec}^{-1}$ for Na^+ and K^+ salts, respectively, in DME and 6.8×10^8 and $8.7 \times 10^8 \text{ M}^{-1} \text{ sec}^{-1}$ for these salts in pyridine, all determined at 25°C . The activation energies are low, being only of the order of 2 kcal/mole. The effects exerted by the nature of solvent and counterion indicate the involvement of ion pairs. This exchange is still faster in acetonitrile, its rate being $1.5 \times 10^9 \text{ M}^{-1} \text{ sec}^{-1}$ at 25°C , $E = 1 \text{ kcal/mole}$. Hence in this process the free ions appear to be only slightly more reactive than the ion pairs, indicating that these salts form loose ion pairs. This accounts for the similar rates of exchange in THF and DME; however, the fast exchange of potassium salt is surprising.

The rate of exchange between triphenylmethyl radicals and the corresponding carbonium ions was determined to be $1.3 \times 10^8 \text{ M}^{-1} \text{ sec}^{-1}$ in mixtures of trifluoroacetic-acetic acid at ambient temperature [271]. Unfortunately, the effect of anionic counterions on the rate of this exchange was not investigated.

It is not practical to discuss here all the exchanges studied by the ESR technique. However, for the convenience of the reader, the reported data are collected in Table 18, which includes the pertinent references.

13. INTRAMOLECULAR ELECTRON EXCHANGE

Molecules such as $\text{A}-(\text{CH}_2)_n\text{-A}$ may be reduced to the monoradical anion, $\text{A}-(\text{CH}_2)_n\text{-A}^\cdot$, where the moiety A denotes a suitable acceptor. In such systems an *intramolecular* electron transfer may be studied, provided the dilution is sufficiently high to make the *intermolecular* transfer insignificant.

Two somewhat different problems should be considered. The transfer may result from a quantum mechanical transition, which is easily visualized when the orbitals of the two A moieties overlap sufficiently. However, if direct overlap is negligible, the transition may still take place through the intermediacy of empty antibonding orbitals associated with CH_2 groups of the chain. Such a transfer may be referred to as an exchange through the chain; its quantum mechanical treatment was outlined by McConnell [227] and elaborated further by Harriman and Maki [234]. The frequency of the odd electron transfer in a rigid and symmetric molecule $\text{A}-(\text{CH}_2)_n\text{-A}^\cdot$ depends on the energy gap ϵ between the even and odd eigenfunctions of the symmetry operator, $\Psi_s = (1/\sqrt{2})(\Psi_{\text{A}'} + \Psi_{\text{A}''})$ and $\Psi_a = (1/\sqrt{2})(\Psi_{\text{A}'} - \Psi_{\text{A}''})$. Here $\Psi_{\text{A}'}$ and $\Psi_{\text{A}''}$ denote the degenerate orbitals corresponding to the localized states where the odd

Table 18 Electron-Exchange Reactions Involving Negative Radical-Ions

Parent Compound	Solvent/ Counter Ion	Ionic State	Tempera- ture (°C)	$k \times 10^{-7}$ ($M^{-1} \text{ sec}^{-1}$)	E (kcal/mole)	Ref.
Benzene	DME/K ⁺	IP	-50	<0.05	—	<i>a</i>
Benzene	DME/K ⁺	IP	18	3.6	6.4	<i>b</i>
Benzene	DME-THF/Na ⁺	IP	18	7.7	2.8	<i>c</i>
Benzene	THF/K ⁺	IP	18	16.3	5.3	<i>b</i>
Toluene	DME/K ⁺	IP	18	4.5	5.4	<i>b</i>
<i>p</i> -Xylene	DME/K ⁺	IP	18	4.3	5.9	<i>b</i>
Naphthalene	THP/Na ⁺	<i>t</i> -IP	25	0.2	—	<i>d</i>
Naphthalene	MTHF/Na ⁺	<i>t</i> -IP	21	0.5	—	<i>e</i>
Naphthalene	DMTHF/Na ⁺	<i>t</i> -IP	25	0.4	5.1	<i>f</i>
Naphthalene	THF/Li ⁺	<i>l</i> -IP	25	100	3.6	<i>f</i>
Naphthalene	THF/Li ⁺	<i>l</i> -IP	25	46	—	<i>h</i>
Naphthalene	THF/Na ⁺	<i>t</i> -IP	25	1.3	4.6	<i>f</i>
Naphthalene	THF/Na ⁺	<i>l</i> -IP	25	170	3.1	<i>f</i>
Naphthalene	THF/K ⁺	FI	23	300	—	<i>g, i</i>
Naphthalene	THF/K ⁺	<i>t</i> -IP	24	3.2	4.2	<i>f</i>
Naphthalene	THF/K ⁺	<i>t</i> -IP	24	6 ± 2	—	<i>g</i>
Naphthalene	THF/Cs ⁺	<i>t</i> -IP	25	8.4	5.1	<i>f</i>
Naphthalene	DME/Na ⁺	IP	23	<3.0	—	<i>g</i>
Naphthalene	DME/Na ⁺	<i>l</i> -IP	25	134	3.6	<i>f</i>
Naphthalene	DME/K ⁺	IP	23	10	—	<i>g</i>
Naphthalene	DME/K ⁺	IP	23	7.6	—	<i>h</i>
Naphthalene	DME/K ⁺	FI	23	220	—	<i>f</i>
Naphthalene	THF-DME/Na ⁺	<i>l</i> -IP	25	130	3.3	<i>f</i>
Naphthalene	THF-DME/Na ⁺	FI	24	120	—	<i>f</i>
Naphthalene	THP + G4/Na ⁺	<i>l</i> -IP	25	45	—	<i>d</i>
Naphthalene	THP + G4/Na ⁺	<i>vl</i> -IP	25	250	—	<i>d</i>
Naphthalene	DMF(electrol.)	FI(?)	20	65	—	<i>j</i>
Naphthalene	HMPA	FI	25	50	4.1	<i>k</i>
1-Naphthyl-1-phenyl ethane <i>d</i> -isomer	DME/K ⁺	IP	25	6.8	1.6	<i>l</i>
Racemic mix.	DME/K ⁺	IP	25	11.0	—	<i>l</i>
Hexahalocene <i>d</i> isomer	THF/K ⁺	IP	23	1200	—	<i>m</i>
Racemic mix.	THF/K ⁺	IP	23	300	—	<i>m</i>
Biphenyl	MTHF/Li ⁺	<i>l</i> -IP	~25	~30	—	<i>n</i>
<i>p</i> -Terphenyl	DMF(electrol.)	FI(?)	20	112	—	<i>j</i>
Anthracene	MTHF/Na ⁺	<i>t</i> -IP	~25	~1	—	<i>o</i>
Anthracene	DME/Na ⁺	<i>l</i> -IP	~25	~120	—	<i>o</i>
Anthracene	DMF(electrol.)	FI(?)	~25	48	—	<i>p</i>
<i>trans</i> -Stilbene	DME/Na ⁺	IP	16	180	2.5	<i>r</i>
<i>trans</i> -Stilbene	DME/K ⁺	IP	16	210	2.8	<i>r</i>
<i>trans</i> -Stilbene	THF/K ⁺	IP	16	250	2.6	<i>r</i>
<i>trans</i> -Stilbene	DMF(electrol.)	FI(?)	20	100	—	<i>j, s</i>
α -Methyl- <i>trans</i> -stilbene	DMF(electrol.)	FI(?)	20	14	—	<i>j</i>
2-Methyl- <i>trans</i> -stilbene	DMF(electrol.)	FI(?)	30	68	—	<i>t</i>
Hexamethyl- <i>trans</i> -stilbene	DMF(electrol.)	FI(?)	20	6	—	<i>j</i>
Tetraeyanoethylene	THF/Li ⁺	<i>l</i> -IP	~25	46	—	<i>u</i>
Tetraeyanoethylene	THF/Na ⁺ , K ⁺	<i>t</i> -IP	~25	5	—	<i>u</i>
Tetraeyanoethylene	DME/K ⁺	<i>l</i> -IP	15	410	—	<i>v</i>
Tetraeyanoethylene	DME + DBC/K ⁺	<i>l</i> -IP	15	150	—	<i>v</i>
Nitrobenzene ^v	DMF/K ⁺	FI	~25	3.0	—	<i>p, x</i>

Table 18 (continued)

Parent Compound	Solvent/ Counter Ion	Ionic State	Tempera- ture (°C)	$k \times 10^{-7}$ ($M^{-1} \text{ sec}^{-1}$)	E (kcal/mole)	\times Ref.
<i>p</i> -Dinitrobenzene	DMF(electrol.)	FI	21	60; 40	—	<i>w, x</i>
<i>p</i> -Dinitrobenzene	DMSO(electrol.)	FI	21	100	—	<i>w</i>
<i>p</i> -Dinitrobenzene	Acet. N(electrol.)	FI(?)	21	7	—	<i>w</i>
<i>m</i> -Dinitrobenzene	DMF(electrol.)	FI	~25	52	—	<i>p, x</i>
<i>p</i> -Chlorodinitro- benzene	DMF(electrol.)	FI	~25	7.9	—	<i>p, x</i>
<i>m</i> -Chlorodinitro- benzene	DMF(electrol.)	FI	~25	8.8	—	<i>p, x</i>
3,5-Dichlorodinitro- benzene	DMF(electrol.)	FI	~25	16	—	<i>p, x</i>
Fluorenone	THF/Na ⁺	IP	5	12	4.2	<i>i</i>
Fluorenone	THF + G4/Na ⁺	<i>l</i> -IP	5	~2	—	<i>i</i>
<i>p</i> -Benzoquinone	DMF(electrol.)	FI	~25	38	—	<i>p, x</i>
Duroquinone	DMF(electrol.)	FI	~25	6.2	—	<i>p, x</i>
<i>p</i> -Naphthaquinone	DMF(electrol.)	FI	~25	42	—	<i>p, x</i>
Benzonitrile	DMF(electrol.)	FI	~25	56	—	<i>s</i>
Benzonitrile	Acet. N(electrol.)	FI	~25	66	—	<i>s</i>
Benzonitrile	DMSO(electrol.)	FI	~25	39	—	<i>s</i>
Benzonitrile	(Pr) ₂ CO ₃	FI(?)	~25	26	—	<i>s</i>
Benzonitrile	Dioxane	?	~25	17	—	<i>s</i>

Note: The following symbols are used for the solvents: THP = tetrahydropyrane; THF = tetrahydrofuran; MeTHF = 2-Me-tetrahydrofuran; DMTHF = dimethyltetrahydrofuran; DME = dimethoxyethane; HMPA = hexamethylphosphorictriamide; DMF = dimethylformamide; DMSO = dimethylsulphoxide; G4 = tetraglyme; DBC = crown ether. Symbols for ionic state: IP = ion pair; *t*-IP = tight ion pair; *l*-IP = loose ion pair; FI = free ion.

^a T. R. Tuttle and S. I. Weissman, *J. Am. Chem. Soc.*, **80**, 5342 (1958).
^b G. L. Malinoski, W. H. Bruning, and R. G. Griffin, *J. Am. Chem. Soc.*, **92**, 2665 (1970).
^c G. L. Malinoski and W. H. Bruning, *J. Am. Chem. Soc.*, **89**, 5063 (1967).
^d K. Höffelman, J. Jagur-Grodzinski, and M. Szwarc, *J. Am. Chem. Soc.*, **91**, 4645 (1969).
^e P. J. Zandstra and S. I. Weissman, *J. Am. Chem. Soc.*, **84**, 4408 (1962).
N. Hirota, R. Carraway, and W. Schook, *J. Am. Chem. Soc.*, **90**, 3611 (1968).
^g R. Chang and C. S. Johnson, Jr., *J. Am. Chem. Soc.*, **88**, 2338 (1966).
^h R. L. Ward and S. I. Weissman, *J. Am. Chem. Soc.*, **79**, 2086 (1957).
ⁱ B. F. Wong and N. Hirota, *J. Am. Chem. Soc.*, **94**, 4419 (1972).
^j A. E. J. Forno, M. E. Peover, and R. Wilson, *Trans. Faraday Soc.*, **66**, 1322 (1970).
^k M. Szwarc and K. Shimada, *J. Polymer Sci.*, Symposium **44**, (1974).
^l W. Bruning and S. I. Weissman, *J. Am. Chem. Soc.*, **88**, 373 (1966).
^m R. Chang and S. I. Weissman, *J. Am. Chem. Soc.*, **89**, 5968 (1967).
ⁿ M. A. Komarynsky and S. I. Weissman, *Chem. Phys. Lett.*, **7**, 211 (1970).
^o N. Hirota, *J. Phys. Chem.*, **71**, 127 (1967).
^p T. Layloff, T. A. Miller, R. N. Adams, H. Fähs, A. Horsfield, and W. Procker, *Nature*, **205**, 382 (1965).
^r R. Chang and C. S. Johnson, Jr., *J. Chem. Phys.*, **46**, 2314 (1967).
^s B. A. Kowert, L. Marcoux, and A. J. Bard, *J. Am. Chem. Soc.*, **94**, 5538 (1972).
^t R. Dietz and M. E. Peover, *Disc. Faraday Soc.*, **45**, 154 (1968).
^u W. D. Phillips, J. C. Rowell, and S. I. Weissman, *J. Chem. Phys.*, **33**, 626 (1960).
M. T. Watts, Ming Liang Lu, and M. P. Eastman, *J. Phys. Chem.*, **77**, 625 (1973).
^w N. M. Katkova, V. S. Vainer, V. V. Brovko, S. M. Shein, and Yu. N. Molin, *Kinet. Kataliz.*, **11**, 64 (1970).
^x P. A. Malachewsky, T. A. Miller, T. Layloff, and R. N. Adams, *Proc. Symp. on Exchange Reactions*, Upton, N.Y., 1965, p. 157.
^y On the addition of increasing amounts of water the rate constant eventually decreased to 0.03 for 10% of water.

electron is associated with one or the other moiety A. The energy gap ϵ results from the different interaction of Ψ_s and Ψ_a with the virtual excited states of the CH_2 groups and this effect, which lifts their degeneracy, leads to their mixing. The natural resonance time between the two localized states is therefore given by $\tau_r = h/\epsilon$.

The foregoing treatment applies to diradicals where electron spins exchange without any transfer of charge [231]. However, in systems such as $\text{A}-(\text{CH}_2)_n-\text{A}^-$ the exchange involves electron transfer as well as spin transfer. It is clear, nevertheless, that both exchanges have to proceed simultaneously and their effect is reflected in the ESR spectrum, which, strictly speaking, measures only the spin transfer. The motion of an electron causes a new effect which is not encountered in diradical systems. Whenever an electron moves through a molecule, or through any dense medium, there is a tendency for nuclear motions to be correlated with the electronic motion. This correlation represents a breakdown of the Born-Oppenheimer approximation and it becomes important in degenerate systems. The nuclear motion tends then to "follow" the electron, and this leads to "self-trapping"—an effect that considerably slows down the exchange.

It should be stressed that even in the absence of the self-trapping effect the natural resonance time h/ϵ increases exponentially with the number of the CH_2 groups separating the A moieties. This relation is maintained in the self-trapping mechanism and numerical calculations suggest that the frequency of exchange decreases by an order of magnitude with each CH_2 group added to the chain. McConnell concluded therefore that the effect of exchange would be imperceptible in the ESR spectrum of radical anions in which the A moieties are separated by more than two CH_2 groups.

According to Harriman and Maki [234], the greatest contribution to electron self-trapping comes from the organization of polar solvent molecules around the moiety bearing the charge. On the whole, the perturbation affecting such a radical anion may be described in terms of a perturbing potential $V = S[rV_{A^{\cdot}} + (1 - r)V_{A^{\cdot -}}]$, where $V_{A^{\cdot}}$ and $V_{A^{\cdot -}}$ are the maximum stabilization energies provided by solvent organization around a center when the charge is localized on the one or the other A moiety. The parameters S and r vary from 0 to 1 and determine the depth and asymmetry of the two potential wells. The intervening barrier has to be overcome as the system is converted from one localized state to the other. The variation of V is caused by Brownian fluctuations of solvent's orientation.

It is convenient to define the matrix elements of V in terms of the localized state eigenfunctions $\Psi_{A^{\cdot}} = (1/\sqrt{2})(\Psi_s + \Psi_a)$ and $\Psi_{A^{\cdot -}} = (1/\sqrt{2})(\Psi_s - \Psi_a)$, and then to calculate the eigenenergies and eigenstates of V . The latter acquire the form $\Psi_i = m_i\Psi_s + n_i\Psi_a$ and eventually they can be given in terms of a single parameter $x = 2mn$. Finally, the equilibrium distribution function

of the various states of the radical anion is calculated in terms of the parameter x , the result being

$$W(x) = (32E_0kT)^{-1/2}\epsilon(1 - x^2)^{-3/2} \exp \{8E_0kT)^{-1}[\epsilon x(1 - x^2)^{-1/2} - 2E_0]^2\}$$

The parameter E_0 has an interesting meaning—it represents half of the difference between the energy of the most favorably solvated localized state and that of the state having the identical arrangement of solvent molecules but with the electron now localized on the other moiety A. Differentiation of $W(x)$ gives the most probable values of x , $\pm[1 - (\frac{1}{2}\epsilon/E_0)^2]$. For $\epsilon/E_0 \ll 1$ the values $x = \pm 1$, which correspond to the two localized states, are the most probable. A plot of $W(x)$ as a function of x shows that $W(x)$ peaks sharply for the value 1 or -1 . The exchange occurs as x changes from 1 to -1 or vice versa. This represents the most probable mechanism of exchange, at least in polar solvents, and shows that the fluctuation of orientation of solvent molecules determines its rate. In this respect, the result is similar to that anticipated from Marcus' theory.

Experimental evidence of intramolecular exchange was provided by the ESR studies of radical anions of 1,8- and 2,2-paracyclophanes [232]. Their spectra show nine evenly spaced lines with a binomial intensity distribution, implying that the rate of exchange is much faster than the reciprocal of the proton hyperfine splitting ($\gg 10^7 \text{ sec}^{-1}$). No exchange could be seen in the spectra of radical anions of 4,4-or 6,6-paracyclophane; these spectra consisted of five equally spaced lines, indicating that the electron is localized on one benzene ring only, the exchange being slower than 10^6 sec^{-1} . Radical anions of 3,4-paracyclophane show an intermediate behavior, the electron being transferred with a frequency greater than 10^6 sec^{-1} but smaller than 10^7 sec^{-1} .

Studies of the radical anion of 2,2-paracyclophane were retaken by Gerson and Martin [235], and their results were confirmed recently by Williams et al. [236]. The ESR spectrum of the potassium salt in THF at -90°C is interpreted as being generated by four sets of four equivalent protons; their hyperfine lines are split further by ^{39}K ($a = 0.12 \text{ G}$). This implies that an asymmetric ion pair is formed with the cation oscillating rather slowly from one side of the anion to the other, while the electron is delocalized over the entire molecule. However, the position of the cation biases the charge density, increasing it on one ring and decreasing it on the other. In contrast, the spectrum obtained from the DME solution indicates the presence of two sets of eight equivalent protons, implying that it results from free radical anions or rapidly interconverting loose ion pairs. In either case, the basic conclusion of Weissman is confirmed—the electron transfer between the rings is very fast even if the cation biases its residence time on one ring with respect to the other.

Investigation of 2,2-cyclophane radical anions was extended by Williams

[236] to the compounds containing naphthalene or anthracene moieties instead of benzene rings. Although the resolution of the relevant ESR spectra was not successful, these authors concluded that the electron is again completely delocalized over both aromatic moieties. This conclusion was confirmed by investigating the ESR spectrum of the anthracene derivative having deuterated aromatic rings. The spectrum revealed the presence of eight equivalent bridge protons; the intensities of the respective lines had the expected binomial ratios.

We therefore may conclude that in the radical anions of cyclophanes the *intramolecular* transfer is very fast, provided that at least one of the bridges linking the two rings contains not more than two CH_2 groups. Even the respective ion pairs of 2,2-cyclophanes exchange rapidly, although the asymmetric location of the cation affects the distribution of the electron densities. A *direct* overlap of the corresponding π orbitals, and not the McConnell mechanism, accounts for the exchange in these systems.

The McConnell approach may be pertinent in accounting for the behavior of odd electrons in the open systems $\text{A}-(\text{CH}_2)_n\text{-A}$. In the first reported study of the ESR spectrum of dibenzyl radical anions it was claimed that the odd electron is completely delocalized [233] because the relevant spectrum revealed nine evenly spaced lines. However, this claim is contradicted by a recent investigation of Gerson and Martin [235], who reported a spectrum generated by one set each of four and of three equivalent protons that is characteristic of an electron localized on one of the rings, provided that the two bridge protons and the aromatic *para* proton are magnetically equivalent as well as the *o* and *m* protons of the ring. Apparently the polarization of solvent around the benzene ring bearing the negative charge, amplified by the asymmetric location of the cation, impedes the exchange and decreases its frequency to below 10^6 sec^{-1} .

The effect of exchange is revealed in the ESR spectra of radical anions derived from $p,p'-(\text{O}_2\text{N}\cdot\text{C}_6\text{H}_4)\text{-X-(C}_6\text{H}_4\text{NO}_2)$, where $\text{X} = \text{CH}_2, \text{O}, \text{S}$ and $\text{CH}_2\cdot\text{CH}_2$ [234]. These radical anions were generated electrochemically at ambient temperature in acetonitrile and in dimethylsulfoxide (DMSO), with tetrapropylammonium perchlorate serving as the supporting electrolyte. The pairing of ions probably is eliminated under such conditions.

The ESR spectrum of p,p' -bis-(nitrophenyl)methane arises from two equivalent nitrogens, two sets of four equivalent protons, and one set of two equivalent protons—unmistakable evidence of a rapid exchange. Moreover, the coupling constant of the nitrogens is half as large as that observed in the spectrum of the radical anion derived from p -nitrotoluene, namely, 4.82 G compared to 10.79 G when the radical anions are dissolved in acetonitrile, and 4.36 G compared to 9.87 G when DMSO is used as the solvent. The rate of such exchange is higher than 10^8 sec^{-1} .

Table 19 Rate of Electron Transfer in $p,p'-(\text{O}_2\text{N}\cdot\text{C}_6\text{H}_4)_2\text{X}$

Compound	k (sec^{-1})	
	Acetonitrile	DMSO
$p,p'-(\text{O}_2\text{N}\cdot\text{C}_6\text{H}_4)_2\text{CH}_2$	$>10^8$	$>10^8$
$p,p'-(\text{O}_2\text{N}\cdot\text{C}_6\text{H}_4)_2\text{S}$	2×10^6	9×10^6
$p,p'-(\text{O}_2\text{N}\cdot\text{C}_6\text{H}_4)_2\text{O}$	1×10^6	3×10^6
$\text{O}_2\text{N}\cdot\text{C}_6\text{H}_4\cdot\text{CH}_2\text{CH}_2\cdot\text{C}_6\text{H}_4\cdot\text{NO}_2$	1×10^6	2×10^6

On the other hand, the spectra of radical anions of the remaining compounds show evidence of a slow exchange. Basically these spectra are accounted for in terms of coupling to one nitrogen and two sets of two equivalent protons, that is, the electron resides for a relatively long time on one benzene ring. However, the lines show alternating degrees of broadening—a characteristic feature indicating an exchange. Computer simulation of such spectra reveals that their shape is sensitive to the rate of exchange, and by matching the computed and the observed spectra the frequency of electron transfer has been determined. The results are collected in Table 19.

The ESR spectra of radical anions derived from $\text{A}-(\text{CH}_2)_2\text{-A}$, where $\text{A} =$ 1-naphthyl, 9-anthracyl, or 1-pyrenyl, were described by Williams et al. [236]. Unfortunately, the spectra were not resolved; however, it has been concluded from a qualitative inspection of their shapes that exchange does take place, its rate being faster for the anthracyl compound than for those with naphthyl or pyrenyl moieties. However, the argument accounting for this difference does not seem to be convincing.

Striking evidence for the effect of solvent upon the rate of intramolecular electron transfer was provided by studies of ESR spectra of 1,2-di(9-carbozyl)-ethane radical anion (only one of the carbozyl groups being reduced) in THF and DME [347]. The radical anions were prepared as potassium salt and the ESR spectra were recorded at -60°C . The spectrum of the THF solution resembled that of N-Ethylcarbazole radical anions, the exchange between the two carbazoles moieties being slow, $k_{\text{ex}} = 7.5 \times 10^5 \text{ sec}^{-1}$. However, a strikingly different spectrum was recorded when DME solution was investigated, implying a ten-fold increase in the rate of exchange, $k_{\text{ex}} \sim 1 \times 10^7 \text{ sec}^{-1}$. The computer simulated spectra (applying the method of Harriman and Maki [234] agreed fairly well with observed one.

It seems that tight ion pairs formed in THF are responsible for the slowness of the exchange, while the loose pairs, or perhaps the free ions, allow a rapid exchange in DME.

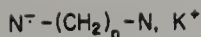
Let us summarize the experimental evidence provided so far. The exchange is very rapid in 1, n - and 2,2-cyclophanes ($>10^8 \text{ sec}^{-1}$) and a direct overlap of π orbitals seems to account for the transfer. The same mechanism may

operate in those $A \cdot X \cdot A^-$ compounds where the acceptors are separated by one atom only. The fast exchange observed in the radical anion of bis-(*p*-nitrophenyl)methane ($>10^8 \text{ sec}^{-1}$) contrasts with the relatively slow transfer ($\sim 10^6 \text{ sec}^{-1}$) in the analogous radical anions of the ether or sulfide. This is puzzling but regrettably, Harriman and Maki did not comment on this point. It may be that this phenomenon is caused, after all, by ion pairing with the cations of the supporting electrolyte. Undoubtedly, the cation is associated with one or the other nitro group, and since these are more negative in the ether or the sulfide, the dissociation that has to accompany the electron transfer could be impeded. McConnell's mechanism may account for the exchange in dibenzyl and its analogs, and probably it is the only mechanism capable of accounting for the exchange in 3,4-paracyclophane, if indeed there is any exchange at all.

Extensive study of *intramolecular* electron transfer in α -naphthyl- $(\text{CH}_2)_n$ - α -naphthyl $^-$ ($\text{N}-(\text{CH}_2)_n-\text{N}^-$) with $n = 3, 4, 5, 6, 8, 10, 12, 16$, and 20 was reported recently by Szwarc and his co-workers [237]. The exchange was studied over a 60°C temperature range in HMPA, a solvent in which the association of radical anions with cations is negligible, and the results were compared with those of the *intermolecular* exchange of *n*-butyl- α -naphthalenide with *n*-butyl- α -naphthalene in HMPA. The latter was proved to be diffusion controlled, its bimolecular rate constants being determined over the temperature range investigated. In addition, the ESR spectrum of *n*-butyl- α -naphthalenide was resolved and all the coupling constants were therefore obtained. It is reasonable to assume that these are also the coupling constants of $\text{N}-(\text{CH}_2)_n-\text{N}^-$.

Inspection of Figs. 21 and 22 shows clearly that the rate of *intramolecular* exchange in $\text{N}-(\text{CH}_2)_n-\text{N}^-$ increases at constant temperature (15°) with decreasing n , and for each constant n it increases with temperature. The contribution of the *intermolecular* exchange was virtually eliminated by dilution of the studied solutions. The frequency of *intramolecular* exchange was determined in the slow exchange limit by matching the ESR spectrum of the investigated dinaphthyl compound with that of *n*-butyl- α -naphthalenide broadened by the *intermolecular* transfer to *n*-butyl- α -naphthalene kept at a judiciously chosen concentration. For example, the bottom spectra shown in Figs. 22 and 23 have identical shapes; therefore the *rate* of electron transfer should be the same in both systems. The spectrum in Fig. 22 pertains to *intramolecular* exchange of $\text{N}-(\text{CH}_2)_{12}-\text{N}^-$; that shown in Fig. 23 is due to butylnaphthalenide exchanging with butyl naphthalene at concentration $2.5 \times 10^{-2} M$. Knowing the rate constant of the latter reaction and the concentration of the acceptor, one finds its rate. This is therefore the frequency of *intramolecular* collisions in $\text{N}-(\text{CH}_2)_{12}-\text{N}^-$.

The method of matching the ESR spectra fails in the intermediate and fast



15°C

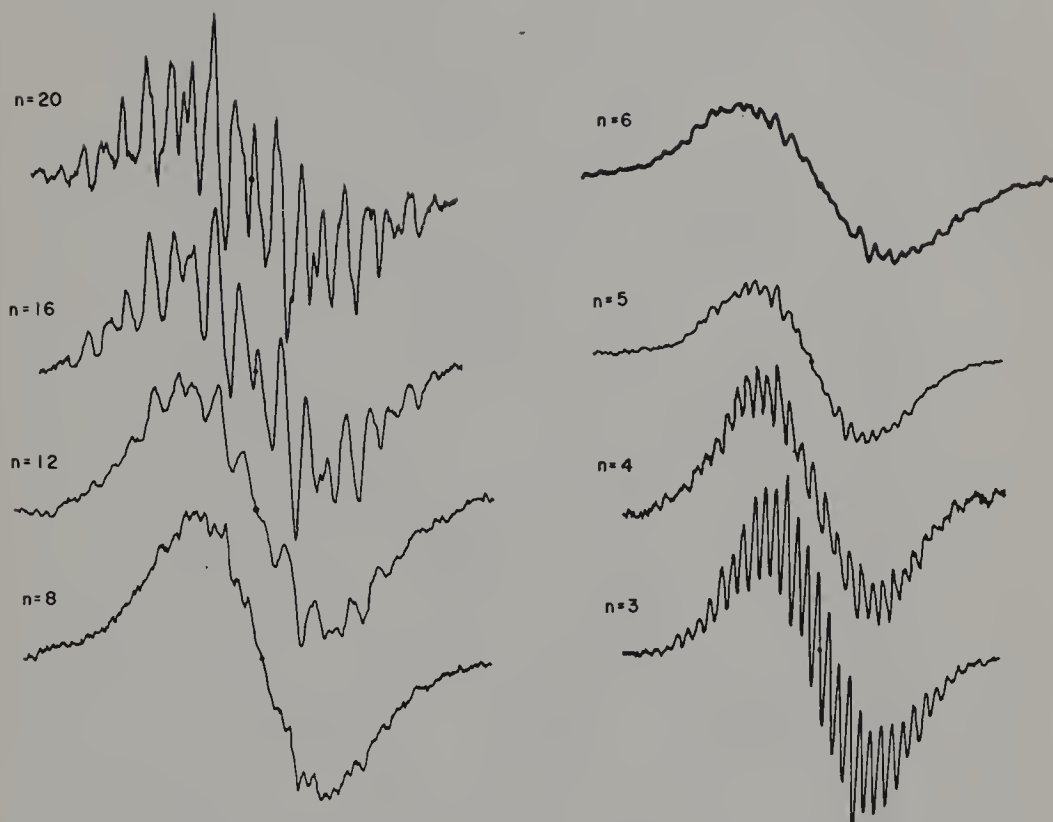


Figure 21. The ESR spectra of $\text{N}-(\text{CH}_2)_n-\text{N}^{\cdot-}$ radical ions recorded at constant temperature for various values of n . $T = 15^\circ\text{C}$.

exchange regions. In the fast exchange the ESR spectrum resulting from the *intermolecular* transfer collapses into the featureless line seen at the top of Fig. 23. However, in the *intramolecular* transfer the shape of the resulting spectrum approaches that of a hypothetical dimer $(-\text{CH}_2-\text{N})_2^{\cdot-}$. This new structure, although poorly resolved, is revealed in the upper spectrum of Fig. 22. It becomes better resolved as the rate of *intramolecular* exchange increases, for example, due to decrease of n . Indeed, the spectrum of $\text{N}-(\text{CH}_2)_3-\text{N}^{\cdot-}$, shown in the lower right corner of Fig. 21, seems to portray a reasonably well-resolved spectrum of the “dimer.”

The identification of the latter spectrum as that of the dimer was achieved by computer simulation [237, 239]. The upper spectrum seen in Fig. 24 is a computer-generated spectrum of a species possessing a number of protons double that of *n*-butyl naphthalenide, but having coupling constants half as

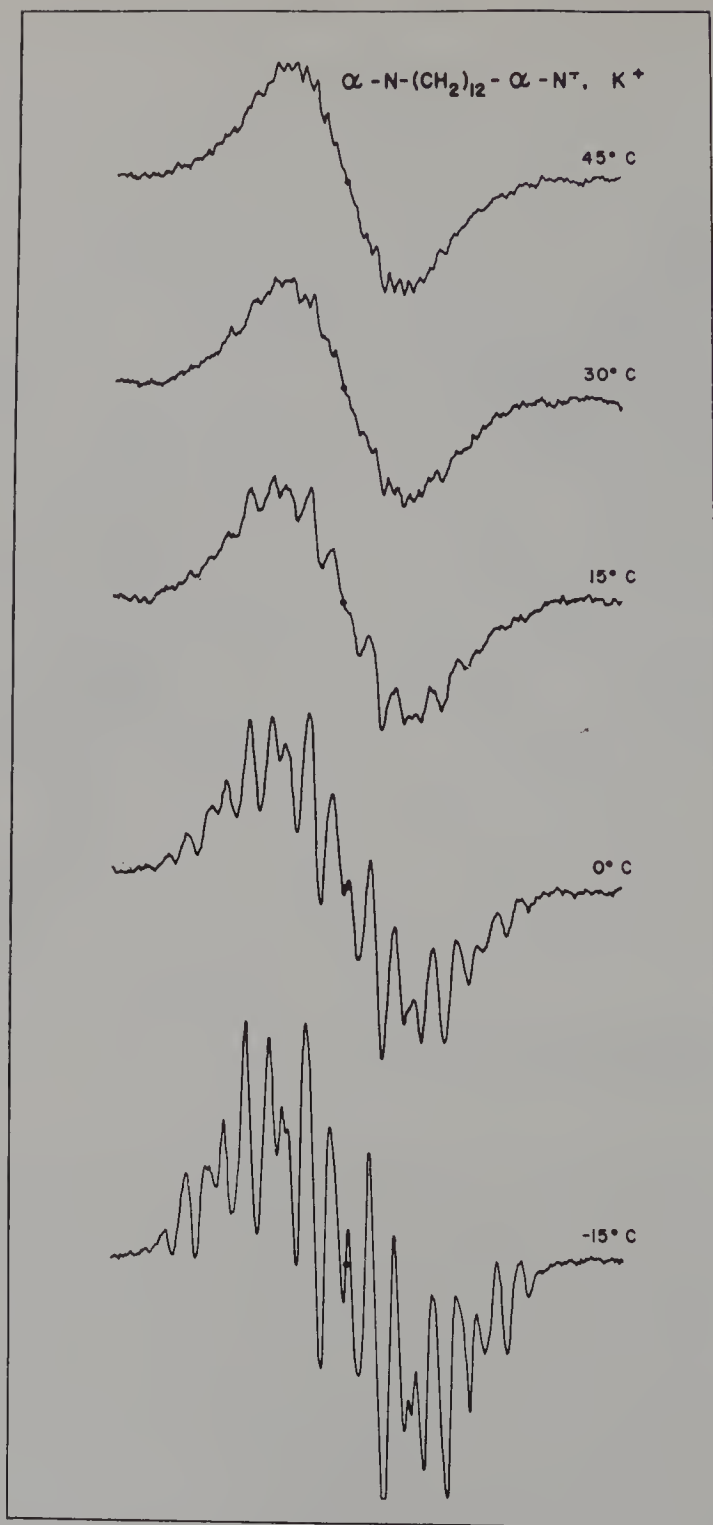


Figure 22. The ESR spectra of $\text{N-(CH}_2\text{)}_{12}\text{-N}^\cdot$ radical ions recorded at various temperatures.

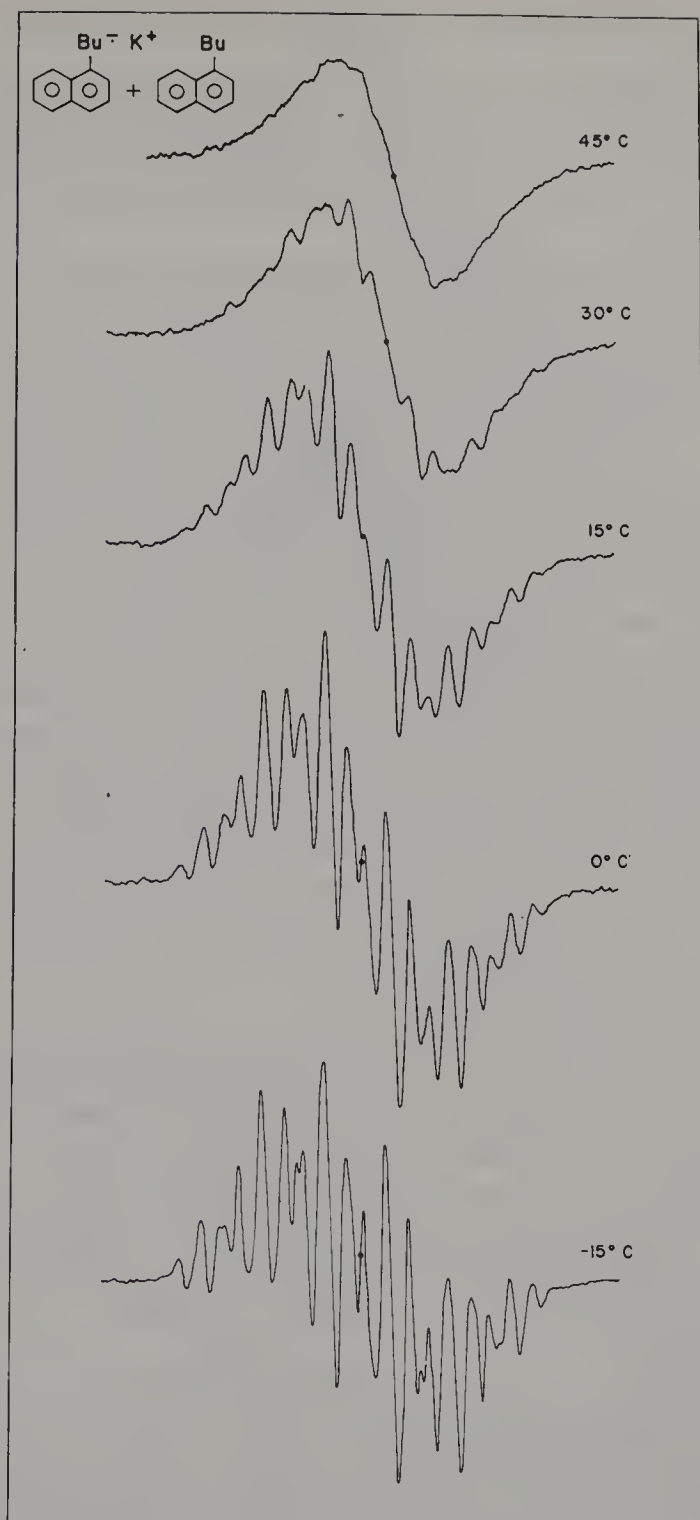


Figure 23. The ESR spectra of *n*-butyl- α -naphthalenide radical ions recorded at various temperatures in the presence of $2.5 \times 10^{-2} M$ of *n*-butyl- α -naphthalene.

large as the coupling constants of the corresponding protons of *n*-butyl-naphthalenide radical anion. This should be the spectrum of the hypothetical dimer and its shape is indeed indistinguishable from that of the ESR spectrum of $\text{N}-(\text{CH}_2)_3-\text{N}^\cdot$ taken at 45°C and shown in Fig. 24 below the computer-simulated spectrum.

The following approach was used to determine the rate of the *intramolecular* exchange under any conditions. In each $\text{N}-(\text{CH}_2)_n-\text{N}^\cdot$ radical anion, the electron interconverts p times per second between two naphthyl moieties having fixed configuration of proton spins. In each surroundings the electron contributes to a line in the ESR spectrum of a macroscopic sample. For every value of p the shape of the absorption spectrum of such a radical anion subspecies may be calculated with the aid of the equation derived by Gutowsky [240]. In a macroscopic sample there are k^2 of such subspecies present, where k is the number of different lines appearing in the spectrum. Therefore the absorption spectrum of a macroscopic sample, obtained at the frequency p of intramolecular exchange, is given by the sum of k^2 lines, each portraying the spectrum of one of the k^2 subspecies. Its derivative then gives the experimentally observed ESR spectrum. Since the frequencies of all the lines are known, being derived from the resolved spectrum of *n*-butyl- α -naphthalenide, the spectra to be anticipated can be computed for each value of p . The results of such computations are presented in Fig. 25, and matching the computed with the experimental spectrum gives the desired value of p [239]. For low rates of exchange the p values obtained by this general method agree with those derived by matching the ESR spectra of the *intramolecularly* and *intermolecularly* exchanging systems.

In conclusion, the study described gives the frequency of electron transfer p as a function of n and of temperature. The final results are shown in Fig. 26 in the form of isotherms giving $\log p$ (in gauss) as a function of $\log n$. The observed values of p vary from 10^6 sec^{-1} to more than 10^9 sec^{-1} .

What mechanism accounts for this *intramolecular* electron transfer? It seems that the transfer is caused by *intramolecular* collisions between the two naphthyl groups linked by a chain. Brownian motion that perpetually changes the conformation of the chain is responsible for this pseudo-bimolecular reaction.

It is interesting to compare the *intramolecular* collisions with the *intermolecular* process. Inspection of Figs. 22 and 23 shows that at -15°C the rate of *intramolecular* electron transfer for $\text{N}-(\text{CH}_2)_{12}-\text{N}^\cdot$ is equal to the rate of *intermolecular* transfer in the system *n*-butylnaphthalenide + *n*-butylnaphthalene with the concentration of the latter kept at $2.5 \times 10^{-2} M$. However, at $+15^\circ\text{C}$ the *intramolecular* transfer is faster than the *intermolecular* process, implying that the "activation energy" of the *intramolecular* exchange is greater than that of the *intermolecular* process.* The

* This has been more conclusively demonstrated in ref. 363.

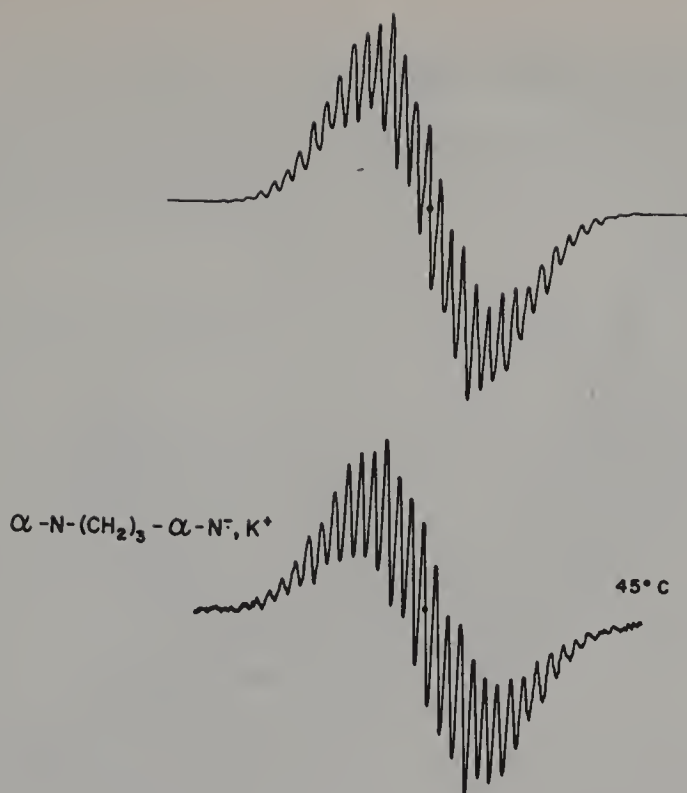


Figure 24. Computer-simulated ESR spectrum of the "dimer" $(-\text{CH}_2\cdot\text{N})_2^-$ (above) and the ESR spectrum of $\text{N}-(\text{CH}_2)_3-\text{N}^-$ radical ion at 45°C (below).

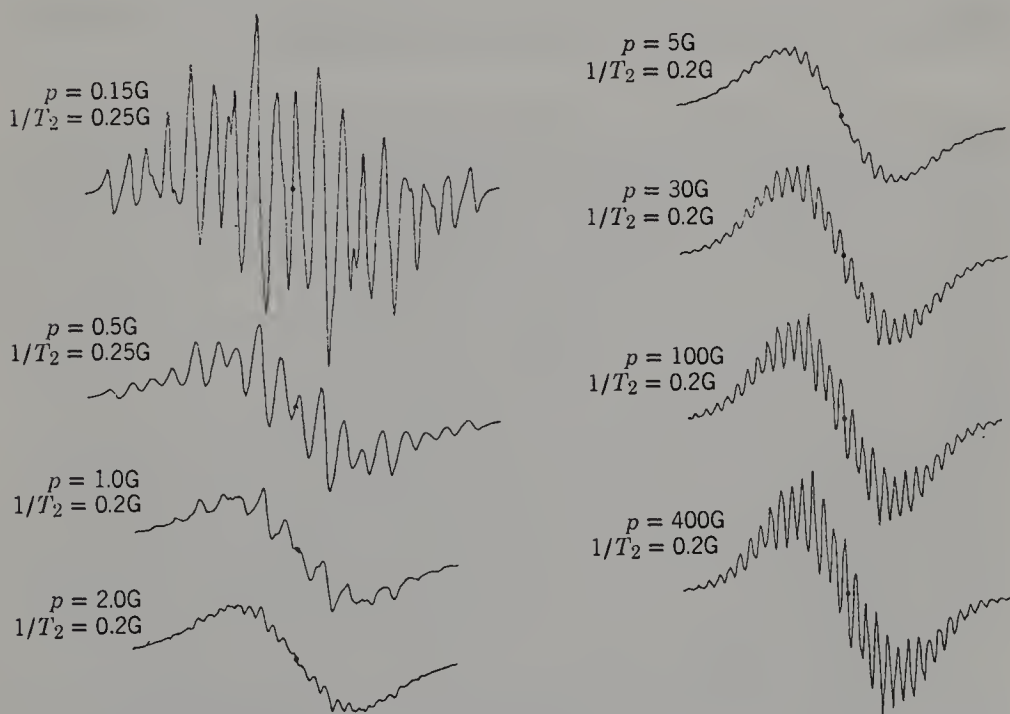


Figure 25. Computer-simulated ESR spectra of $\text{N}-(\text{CH}_2)_n-\text{N}^-$ for variable p = rate of exchange. p is given in Gauss.

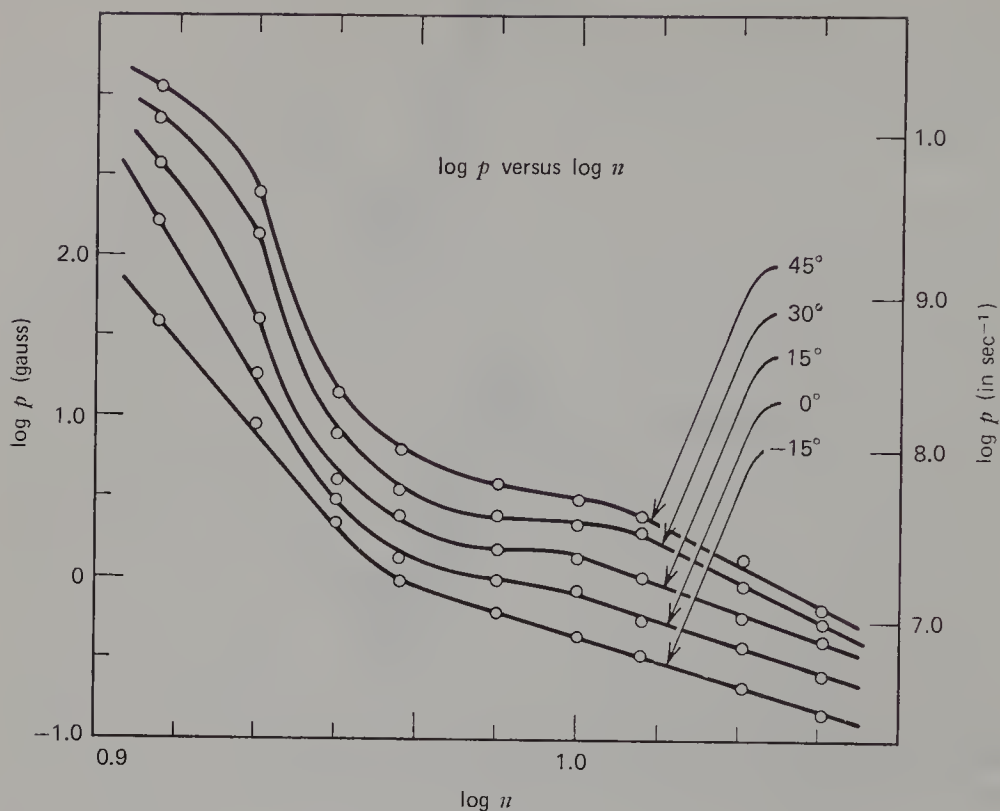


Figure 26. The rate of intramolecular electron-transfer process (p in Gauss) of $\text{N}-(\text{CH}_2)_n-\text{N}^\cdot$ as a function of n at various constant temperatures.

temperature dependence of that bimolecular reaction is determined by the “activation energy” of the viscosity of solvent, since the process is diffusion controlled. Of course, the diffusion of naphthyl units through the solvent still limits the rate of the intramolecular reaction, but in addition the configuration of the chain has to be adjusted to the motion of the end groups. Thus a term loosely named the “activation energy of chain viscosity” has to be added to the activation energy of diffusion, and this increases the temperature coefficient of the *intramolecular* compared with the *intermolecular* transfer.

The restrictions caused by the chain slow down the *intramolecular* process, as may be seen from the following reasoning. The *intramolecular* collisions may be treated as if they were *intermolecular* at a concentration of the acceptor corresponding to one molecule in a sphere having a radius equal to the length of the fully extended chain. Thus the equivalent concentration calculated for $\text{N}-(\text{CH}_2)_{12}-\text{N}^\cdot$ is $7 \times 10^{-2} M$, and this is the *minimum* value for the concentration of the acceptor, because the chain is rarely extended to its full length. However, as has been pointed out earlier, the spectra match each other when the concentration of *n*-butylnaphthalene is $2.5 \times 10^{-2} M$ only.

In this sense the *intermolecular* transfer is faster than the intramolecular, the rate-impeding restrictions imposed in the former by the chain are lifted when this interconnecting chain is broken.

14. ELECTRON TRANSFER $A + A^+ \rightarrow$ EXCHANGE

Although aromatic hydrocarbon radical cations are known [245] and their solutions are sufficiently stable to permit the investigation of their ESR spectra, no exchange studies involving these species are reported in the literature. The difficulties are caused by the facile association of radical cations A^+ with their parent molecules into paramagnetic dimers (A^+A) [246, 247]. Moreover, radical cations dimerize more easily than radical anions; for example, salts of radical cations of thianthrene readily dimerize into diamagnetic species in several solvents [248].

The exchange involving radical cations containing heteroatoms has been investigated. Early studies of exchange between the stable Wurster's Blue cation (tetramethyl-*p*-phenylenediamine) with the parent diamine revealed that the transfer from the *neutral* amine is much faster than from its protonated species [249–251]. Apparently the coulombic repulsion between two positively charged species, coupled with the necessity of proton transfer, slows down the exchange. The reported exchange between tetramethylhydrazine and its radical cation involves a peculiar ion pair, an associate of $N_2Me_4^+$ with I_2^- [252].

A most versatile electrochemical technique permitting a controlled oxidation of substrate and convenient studies of its exchange with the resulting radical cations was described recently by Bard et al. [253]. The oxidation *in situ* [254] was found to be superior to the more conventional oxidation performed outside the cavity since the former is less time consuming and permits studies of less stable radical cations. The rates were obtained in the "fast exchange limit," because the complexity of the investigated spectra is prohibitive. Acetonitrile, dimethylformamide, propylenecarbonate, DMSO, and dioxane were used as solvents. Some of the results are given in Table 20.

Electrolytic oxidation also was employed in studies of exchanges involving the dibenzo-*p*-dioxin cation system [255]. Both the slow and the fast exchange limits were utilized in deriving the kinetic data, and when the required corrections were introduced [206] both methods gave concordant results, which are included in Table 20. Since these studies were performed over a range of temperatures, the activation energy of exchange could be determined; it was 1.5 ± 0.3 and 2.3 ± 0.5 kcal/mole for the transfers in acetonitrile and in its mixture with chloroform (1:3), respectively.

It is commonly expected that the rate constant of ionic reactions should

Table 20 Rate of Exchange at Room Temperature of Radical Cations with Their Parent Compound

Compound	Solvent	$k_{\text{ex}} \times 10^{-9} (M^{-1} \text{sec}^{-1})$
Phenothiazine	ACN	6.7 ± 0.4
10-Methylphenothiazine	ACN	2.2 ± 0.3
Phenoxazine	ACN	4.5 ± 0.3
Phenoxathiin	ACN	3.6 ± 0.2
Wurster's Blue	ACN	1.0 ± 0.2
<i>N,N</i> -Dimethylphenylenediamine	ACN	0.75 ± 0.08
Dibenzo- <i>p</i> -dioxin	ACN	2.7 ± 0.4
Dibenzo- <i>p</i> -dioxin	ACN + CHCl_3 (1:3)	1.6 ± 0.25

increase, and its activation energy decrease, as the dielectric constant of the solvent decreases. The dielectric constant of acetonitrile (38.0) is much higher than that of chloroform (4.8) and therefore the data given at the end of Table 20 seem to contradict the rule. Apparently, free ions participate in the exchange occurring in acetonitrile, but the presence of some ion pairs (with ClO_4^-) retards the transfer in the acetonitrile-chloroform mixture.

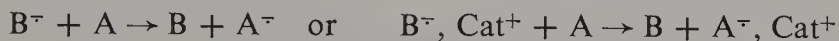
Zandstra and Weissman [195] demonstrated that the probability of electron transfer is independent of the initial and final nuclear spin state of the donor and acceptor (see Section 12 above). Their studies were concerned with radical anions where the odd electrons move from one half-filled antibonding orbital to an empty antibonding orbital. Hence the problem of spin pairing needs no consideration. However, in the transfer involving radical cations the electron moves into a half-filled bonding or nonbonding orbital and consequently the problem of spin pairing becomes significant. Sorensen and Bruning [255] therefore investigated this facet of the problem by measuring the increase of width of different lines of the dibenzo-*p*-dioxin cation. They concluded that even in this system the electron transfer is not sufficiently disturbed by the spin pairing or unpairing to invalidate the assumption of equal probabilities of exchange for all the spin states.

15. KINETICS OF ELECTRON TRANSFER $A^\cdot + B \rightleftharpoons A + B^\cdot$

The bimolecular reaction in which an electron is transferred from a radical anion to an acceptor of *higher* electron affinity than the donor is very fast and its study requires special techniques. As in the exchange reactions discussed previously, we have to distinguish between transfers involving free ions and those involving various ion pairs.

Consider a system $A^\cdot + B \rightleftharpoons A + B^\cdot$ or $A^\cdot, \text{Cat}^+ + B \rightleftharpoons A + B^\cdot, \text{Cat}^+$ in which the equilibrium lies far to the left, even if the concentration of B

exceeds the concentration of A by a large factor. By means of a flash of light, an electron may be ejected from A^- and captured by B. The equilibrium is therefore upset and after the flash the system relaxes into its original equilibrium state through the reaction



Since the absorption spectra of A^- and B^- are different, the progress of the transfer may be studied conveniently by following the disappearance of B^- or the reappearance of A^- .

The foregoing approach was adopted by Rämme, Fisher, Claesson, and Szwarc [226] in their studies of the system sodium pyrenide (π^- , Na^+) — biphenyl (B) investigated in tetrahydrofuran and tetrahydropyrene. A simple technique described in their paper permits reliable and reproducible preparation of $10^{-7} M$ solutions of the reagents, free of any damaging impurities. A flash of visible light ($\lambda > 400 \text{ nm}$) initiates the reaction leading to bleaching at 490 nm (λ_{max} of the pyrenide) and the appearance of a transient at 400 nm (λ_{max} of the biphenylide). The system returns precisely to its original state and even after 25 consecutive flashes the final spectrum is indistinguishable from the original one. By varying the concentration of radical anions, or by adding sodium tetraphenylboride, the proportion of free biphenylide ions and their sodium ion pairs could be varied at will. Thus the bimolecular rate constants of the reactions $B^- + \pi \rightarrow B + \pi^-$ and $B^-, \text{Na}^+ + \pi \rightarrow B + \pi^-, \text{Na}^+$ were determined.

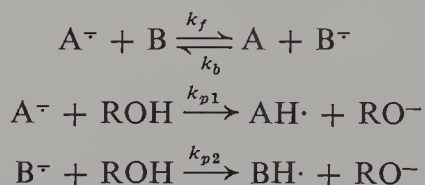
Alternatively, a nonequilibrated mixture of two radical ions and their parent compounds can be prepared by pulse radiolysis. A pulse of ionizing radiation generates solvated electrons and radical cations derived from the solvent molecules. If the pulsed solution contains an electron acceptor such as an aromatic hydrocarbon, the electron attachment yields the appropriate radical ion.

The electron attachment process is indiscriminate and very fast; under conventional experimental conditions of pulse radiolysis (concentration of the acceptor of about $10^{-3} M$), it is over in a few nanoseconds [242] yielding the products of electron capture. In a solution of two aromatic hydrocarbons in aliphatic alcohols the positive radical ions, ROH^+ , are converted extremely rapidly into ROH_2^+ ions and RO^\cdot radicals, while the aromatic hydrocarbons yield the relatively long lasting radical anions A^- and B^- . Their half-lifetimes depend on the nature of the alcohol and range from 0.4 to 175 μsec [243], being therefore sufficiently long to permit the observation of the reaction $A^- + B \rightarrow A + B^-$. The progress of such a reaction may be followed conveniently by the standard spectrophotometric technique.

This design was utilized by Dorfman and his associates [241, 244] to study the kinetics of electron transfer from aromatic hydrocarbon radical anions

to another aromatic hydrocarbon. Isopropanol was chosen as solvent, since the lifetime of the radical ions is sufficiently long in this liquid. The two aromatic hydrocarbons under investigation were dissolved in this alcohol, the resulting solution, about $10^{-3} M$, was pulsed, and the transients were recorded in the conventional way.

The kinetics of reversible electron transfer is complicated by the protonation of the radical ions. Thus the following reactions proceed simultaneously in the investigated system:



The reactions of $A^{\cdot-}$ and $B^{\cdot-}$ with ROH_2^+ or RO^{\cdot} were insignificant; their rates were extremely low because the concentrations of the latter reagents were exceedingly small relative to those of ROH, A, and B. The rate constants of protonation k_{p1} and k_{p2} were determined independently [243] and the solution of the set of differential equations pertaining to the kinetic scheme mentioned above led to the derived rate constants k_f and k_b . The results of these studies are collected in Table 21 together with the analogous result of Rämme et al. [226]. Since the cations ROH_2^+ were present at an exceedingly low concentration, and their interaction with aromatic radical

Table 21 Rate Constants of Electron Transfer Involving Free Radical Ions of Aromatic Hydrocarbons at 25°C

Radical Anion of	Acceptor	Solvent	$k_{\text{obs}} \times 10^{-9} (M^{-1} \text{ sec}^{-1})$
Biphenylide	Naphthalene	Isopropanol	0.26
Biphenylide	Naphthalene	Ethanol	0.20
Biphenylide	Naphthalene	Ethylenediamine	2.1
Biphenylide	Phenanthrene	Isopropanol	0.6 ± 0.3
Biphenylide	Phenanthrene	Ethyldiamine	4.2
Biphenylide	<i>p</i> -Terphenyl	Isopropanol	3.2 ± 0.7
Biphenylide	Pyrene	Isopropanol	5.0 ± 1.8
Biphenylide	Pyrene	THF	48 ± 5
Biphenylide	Anthracene	Isopropanol	6.4 ± 2.0
<i>p</i> -Terphenylide	Pyrene	Isopropanol	3.6 ± 1.1
<i>p</i> -Terphenylide	Anthracene	Isopropanol	5.5 ± 0.9
<i>m</i> -Terphenylide	Pyrene	Isopropanol	3.5 ± 1.2
<i>o</i> -Terphenylide	Pyrene	Isopropanol	4.0 ± 1.8
Pyrenide	9,10-di-Me-anthracene	Isopropanol	1.3
Pyrenide	9,10-di-Me-anthracene	Ethanol	2.0
Pyrenide	9,10-di-Me-anthracene	Ethylenediamine	4.4
Pyrenide	9,10-di-Me-anthracene	Diethylamine	22

anions cannot produce any stable ion pairs, the observed electron-transfer processes have to be attributed to the free ions.*

The k_{obs} values collected in Table 21 were used for testing Marcus' theory of electron transfer. The parameter λ (see Section 12 above) was calculated on the following assumptions:

$$r_{A^-} = r_B = 5\text{\AA} \quad \text{and} \quad r = r_{A^-} + r_B$$

Since the crucial process treated by Marcus is that of the actual electron transfer governed by the rate constant k_{tr} , and not the diffusion process determined by the rate constant k_{diff} , the former was calculated from the experimentally determined k_{obs} by using the relation

$$1/k_{\text{obs}} = 1/k_{\text{diff}} + 1/k_{\text{tr}}$$

It has been assumed that the largest k_{obs} values listed in Table 21 give the k_{diff} , and on this basis the latter was chosen, somewhat arbitrarily, to be $5 \times 10^9 M^{-1} \text{sec}^{-1}$. For the sake of testing the experimentally determined ratio $\{(k_{\text{tr}})_x \text{ for any pair}\} / \{(k_{\text{tr}})_0 \text{ for the biphenylide-naphthalene system}\}$ was compared with that calculated on the basis of Marcus' theory (again see Section 12). The results listed in Table 22 show a reasonable agreement between theory and experiment.

Alternatively, the k_{tr} values obtained for the system pyrenide-9,10-di-Me-anthracene in four solvents, ethanol, isopropanol, ethylenediamine, and diethylamine were plotted versus λ . As seen in Fig. 27, there is a reasonable linear relation between $\log k_{\text{tr}}$ and λ , although the experimental uncertainties are large. This plot provides an independent confirmation for Marcus' theory of electron-transfer processes.

Table 22 Correlation of Electron Transfer Rate Constants for Aromatic Anions in Isopropanol with the Theory

Donor-Acceptor Pair	k_{obs} ($M^{-1} \text{sec}^{-1}$)	$\Delta\epsilon_0$ (kcal/mole)	k_{tr} ($M^{-1} \text{sec}^{-1}$)	$(k_{\text{tr}})_x / (k_{\text{tr}})_0$	
				Exp.	Calc.
Anthracene ⁻ -pyrene	2.1×10^7	+2.61	2.1×10^7	0.081	0.041
9,10-Dimethyl-anthracene ⁻ -pyrene	3.7×10^7	+2.01	3.7×10^7	0.14	0.074
Biphenyl ⁻ -naphthalene	2.6×10^8	-0.99	2.7×10^8	(1.0)	(1.0)
Biphenyl ⁻ -phenanthrene	6×10^8	-3.28	6.7×10^8	2.6	5.3
Pyrene ⁻ -9,10-dimethylanthracene	1.3×10^9	-2.01	1.7×10^9	6.5	2.2
Pyrene ⁻ -anthracene	1.8×10^9	-2.61	2.6×10^9	10.1	3.4
Biphenyl ⁻ -pyrene	5.0×10^9	-12.2	—	—	—
Biphenyl ⁻ -anthracene	6.4×10^9	-14.8	—	—	—

* Pulse radiolysers studies may be extended to ion-pairs, see ref. 342.

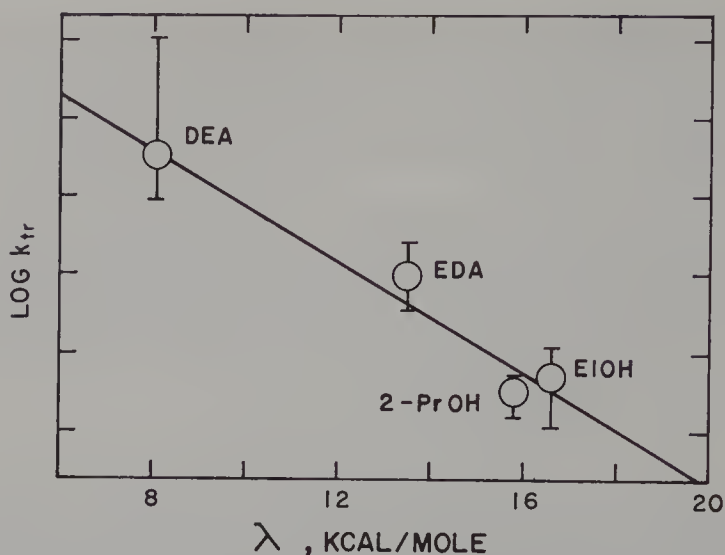


Figure 27. Plot of $\log k_{tr}$ versus λ for the pair pyrene⁻-9,10-dimethylantracene in four solvents. The straight line is calculated from Marcus' theory.

Pulse radiolysis of solutions of aromatic hydrocarbons, A, in chlorinated solvents yields the positive radical cations, A⁺ [351]. Kinetics of electron transfer $A^+ + B \xrightarrow{k_{AB}} A + B^+$ in 1,2-dichloroethane was investigated [354] using the approach previously developed for the anionic system. The cations A⁺ are formed by the reaction $(CH_2Cl \cdot CH_2Cl)^+ + A \rightarrow CH_2Cl \cdot CH_2Cl + A^+$, its rate constant is greater than $3 \times 10^{10} M^{-1} sec^{-1}$ for A = biphenyl at 25°C, and still greater than $1 \times 10^{10} M^{-1} sec^{-1}$ for A = *p*-terphenyl at -31°C. This remarkably high rate constant may result from the fast exchange $(CH_2ClCH_2Cl)^+ + CH_2Cl \cdot CH_2Cl \rightarrow CH_2Cl \cdot CH_2Cl + (CH_2Cl \cdot CH_2Cl)^+$ contributing to the "mobility" of the "hole" [355]. The rate constants k_{AB} were determined at 25°C for three pairs,

$$p\text{-terphenyl}^+, \text{anthracene} (k_{AB} = 8.1 \times 10^9)$$

$$\text{biphenyl}^+, p\text{-terphenyl}^+ (k_{AB} = 5.1 \times 10^9)$$

and

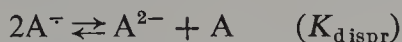
$$\text{biphenyl}^+, \text{pyrene} (k_{AB} = 9.9 \times 10^9)$$

all in $M^{-1} sec^{-1}$ units.

16. DISPROPORTIONATION OF RADICAL ANIONS

On acquisition of a second electron a radical anion A⁻ is reduced to the dianion A²⁻. Whenever such a reduction is possible, solutions of radical

anions eventually become equilibrated with their dianions through the reaction



The electron affinity of the parent molecule A is higher than that of $A^{\cdot -}$, because the coulombic repulsion hinders the addition of a second electron. In terms of the simple Hückel M.O. theory, the repulsion energy, ΔE_{rep} , is given by the integral

$$\Delta E_{\text{rep}} = \iint \bar{\phi}_{N+1}(1) \bar{\phi}_{N+1}(2) \left[\frac{e^2}{r_{1,2}} \right] \phi_{N+1}(1) \phi_{N+1}(2) d\tau_1 d\tau_2$$

where ϕ_{N+1} denotes the lowest antibonding orbital. For alternant aromatic hydrocarbons ΔE_{rep} is sufficiently large to make the disproportionation imperceptible in the gas phase [139]. However, the situation is different for solution disproportionation, especially in a polar and well-solvating medium. Accepting Born's approach and assuming that $A^{\cdot -}$ and A^{2-} may be represented by spheres of radius r , we find that the disproportionation decreases the free energy of solvation of the system by $\Delta_S = (e^2/r)(1 - 1/2)$, that is, the negative free energy of solvation of A^{2-} is four times as large as that of $A^{\cdot -}$. Hence in solution the free energy of disproportionation is

$$\Delta G_{\text{dispr}} = \Delta E_{\text{rep}} - \Delta_S$$

Thus calculated solvation energy is still too small to cause any significant degree of disproportionation, even in a solvent of high dielectric constant [139]. Nevertheless, this simple treatment accounts for the compensating effect leading to an approximately constant calculated value of ΔG_{dispr} ; as ΔE_{rep} decreases from 7.0 eV (benzene) to 5.1 eV (anthracene), ΔG_{dispr} varies randomly, within ± 0.2 eV of its mean value of -3.6 eV. The approximate constancy of ΔG_{dispr} was demonstrated by polarographic studies of aromatic hydrocarbons [146] and of polyphenyls [257].

The approach discussed here applies only to solutions of *free* radical ions. However, in most solvents the radical ions, and certainly the dianions, are paired with their counterions. In such systems the disproportionation is represented by the equation



where Cat^+ denotes the counterion. The free energy of disproportionation of ion pairs is given directly by the difference between the first and second reduction potentials determined by potentiometric titrations performed in those solvents in which the degree of ion pairing is high, e.g. in tetrahydrofuran.

Ion pairing is expected to favor the disproportionation, because the binding of two counterions by a dianion should be more than twice as powerful as that responsible for the pairing of $A^{\cdot -}$ with its counterion. However,

the problem is more complex than it appears. For example, strange temperature effects have been revealed in the spectra of salts of radical ions dissolved in methyltetrahydrofuran [258], the observation reported by de Boer [259] being the most spectacular. Lithium naphthalenide in 2-methyltetrahydrofuran exists at -120°C as the radical ion, the identity of this species being proved conclusively by its optical and ESR spectra. At -70°C the spectrum changes drastically and the paramagnetism disappears. Evidently the radical ions disproportionate, and indeed the spectrum of the resulting solution is identical to that reported for the naphthalene dianion [260]. Further increase of temperature reverses the trend and only the naphthalenide radical anions are detected at 25°C . These observations imply that this disproportionation is endothermic in the range -120° to -70°C and therefore the reaction is driven then by entropy increase and not by energy decrease. However, the disproportionation becomes exothermic at higher temperatures.

Why does the entropy of the system increase on disproportionation? Conversion of *free* $\text{A}^{\cdot-}$ ions into *free* dianions, A^{2-} , *decreases* the entropy of the solution because the immobilization of solvent molecules around A^{2-} is more extensive than around two $\text{A}^{\cdot-}$ ions. Hence, the disproportionation of *free* anions should be favored by *increasing* solvating power of the medium (implicitly a better solvent for anions). However, the situation is different for an ion pair system. At low temperature lithium naphthalenide ($\text{N}^{\cdot-}$, Li^+) in MeTHF probably forms loose ion pairs. The conversion of Li^+ , N^{2-} , Li^+ , which presumably forms tight aggregates, into loose $\text{N}^{\cdot-}$, Li^+ ion pairs is thus favored by the high energy of solvation of Li^+ but, by the same token, this process decreases the entropy of the solution by immobilizing solvent molecules around the loosely bonded Li^+ . Hence the equilibrium favors radical anions at very low temperatures (-120°C), since the term $-T\Delta S$ is then small, but at -70°C the reverse is true and the dianions become dominant. The radical anions and *not* dianions are again the main components of the solution at ambient temperature. This surprising effect results from the change of structure of the $\text{N}^{\cdot-}$, Li^+ ion pairs. The loose pairs prevail at -70°C but the tight $\text{N}^{\cdot-}$, Li^+ become dominant at $+25^{\circ}\text{C}$. The endothermicity of the disproportionation is therefore reduced and the equilibrium shifts back to the radical anions.

The role played by cations in the disproportionation process is further clarified by the recent studies of Rainis and Szwarc [160]. Using the potentiometric technique [146, 147] (see p. 34) they determined the disproportionation constant for the Li^+ , Na^+ , and K^+ anthracenide ($\text{A}^{\cdot-}$) and perylenide ($\text{Pe}^{\cdot-}$) in THF and DME:



The results collected in Table 23 show that the disproportionation is more

Table 23 Redox Potentials of Anthracene and Perylene as Functions of Solvent and Counterion and the Relevant Disproportionation Constant^a

Counterion and Solvent	Anthracene, A			Perylene, Pe		
	ϵ_1 mV	ϵ_2 mV	K_{dispr}	ϵ_1 mV	ϵ_2 mV	K_{dispr}
Li ⁺ /DME	605 ± 5	140 ± 10	1.8×10^{-8}	915 ± 5	350 ± 10	3.8×10^{-10}
Na ⁺ /DME	603 ± 5	150 ± 10	2.8×10^{-8}	923 ± 5	380 ± 10	8.9×10^{-10}
K ⁺ /DME	605 ± 5	190 ± 10	1.2×10^{-7}	903 ± 5	480 ± 10	8.9×10^{-8}
Li ⁺ /THF	612 ± 5	220 ± 10	2.9×10^{-7}	912 ± 5	390 ± 10	2.0×10^{-9}
Na ⁺ /THF	598 ± 5	310 ± 10	1.6×10^{-5}	906 ± 5	560 ± 10	1.7×10^{-6}
K ⁺ /THF	600 ± 5	230 ± 10	6.8×10^{-7}	890 ± 5	550 ± 10	2.2×10^{-6}

^a ϵ_1 refers to the reaction $\text{biphenyl}^\cdot, \text{Cat}^+ + \text{Ar} \rightleftharpoons \text{biphenyl} + \text{Ar}^\cdot, \text{Cat}^+$; ϵ_2 refers to the reaction $2 \text{biphenyl}^\cdot, \text{Cat}^+ + \text{Ar} \rightleftharpoons 2 \text{biphenyl} + \text{Ar}^{2-}, 2\text{Cat}^+$; K_{dispr} refers to the reaction $2\text{Ar}^\cdot, \text{Cat}^+ \rightleftharpoons \text{Ar} + \text{Ar}^{2-}, 2\text{Cat}^+$.

extensive in THF than in DME. The solvation of cations is more powerful in DME than in THF, but the degree of solvation decreases as loose 2Ar^\cdot , Cat^+ are converted into tight Ar^{2-} , 2Cat^+ , the decrease being larger in THF than in DME. This accounts for the observed solvent effect which is enhanced by the fact that the rupture of a $\text{Cat}^+ \text{—O}$ bond increases the entropy of the monodentate THF system, whereas in the bidentate DME system such a gain requires the rupture of two $\text{Cat}^+ \text{—O}$ bonds.

The gradation of K_{dispr} along the series Li^+ , Na^+ , and K^+ is interesting. Apparently Li^+ and Na^+ cations are strongly solvated in DME whether paired with a radical anion or dianion, whereas the larger K^+ ion is highly solvated when paired with a radical anion but becomes desolvated on its association with a dianion. The resulting entropy gain makes K_{dispr} of the potassium anthracenide or perylenide in DME substantially greater than the corresponding disproportionation constants for the lithium or sodium salts. In THF, Li^+ ions still seem to be substantially solvated even when associated with the dianions, while Na^+ ions, although solvated when paired with the radical anions, become largely desolvated on association with the dianions. Therefore, K_{dispr} sharply increases as Na^+ replaces Li^+ .

The behavior of the potassium salts in THF is intriguing. The disproportionation constant of potassium perylenide seems to indicate that this salt behaves in THF like the corresponding sodium salt, that is, the THF solvated K^+ ions are paired with perylenide anions but much of their solvation shell is lost on association with Pe^{2-} dianions. The extensive delocalization of the charge in the large perylenide anion is probably responsible for the substantial degree of K^+ solvation in Pe^\cdot , K^+ . However, the charge is more concentrated in the anthracenide ion, hence the K^+ ions appear to be poorly solvated whether associated with A^\cdot or A^{2-} . This may account for the

exceptionally low value of K_{dispr} of A^\cdot , K^+ in THF. As in the case of A^\cdot , Li^+ , the disproportionation does not provide any additional increase in the entropy of the system—the K^+ ion remains desolvated before and after disproportionation while the solvated Li^+ ion virtually does not lose its solvation shell in the disproportionation process.

Why is the disproportionation of anthracenide favored when compared with perylenide? The repulsion between the two electrons should be smaller in perylenide and therefore its degree of disproportionation would be expected to be greater than that of anthracenide, contrary to the observation. Such a relation should be valid for the free anions; however, in the cation paired system the gain in cation binding energy may be more important than the increase of repulsion energy. Since the former is greater for anthracenides, their disproportionation is favored in spite of greater repulsion energy.

The interplay of entropy gain and energy loss arising from cation solvation is reflected in disproportionation of other radical anions. For example, the degree of disproportionation of stilbenides increases with decreasing solvating power of the solvent, being larger in DOX and MeTHF than in THF [274]. In fact, the reported magnitude of the disproportionation constant in MeTHF ($>10^3$) is surprisingly large.

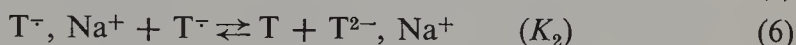
It should be stressed that the degree of disproportionation of the non-solvated cation-radical anion pairs in the gas phase is likely to *increase* with the decreasing radius of the cation, a reverse effect from that observed in ethereal solvents. In the gaseous systems the problems arising from the entropy of cation solvation are eliminated and the increase in the cation-anion Coulombic energy accompanying the disproportionation is then the dominant factor.

The most thoroughly investigated disproportionation is that of the radical ions of tetraphenylethylene denoted here by T^\cdot . Early studies of Schlenk [261] demonstrated the feasibility of the reduction of tetraphenylethylene (T) by metallic sodium in ether or dioxane, which results in the formation of its disodium salt, T^{2-} , 2Na^+ . Radical ions are not formed in these solvents even when a large excess of the parent hydrocarbon is available—a puzzling observation subsequently confirmed by the failure of the sensitive ESR technique to detect the radical ions [262]. However, later investigations proved that the ESR signal may be observed if the reduction is carried out in tetrahydrofuran or dimethoxyethane but *not* in dioxane [263, 264], a result stressing the important role of solvent. Further studies of this reduction showed that the intensity of the signal is affected not only by the nature of the solvent but also by the choice of the counterion and by temperature, increasing with the size of the cation and rising temperature [264–266]. Obviously, this is a more complex system than anticipated, and therefore further study of this disproportionation was required.

In ethereal solvents conducive to ion pairing, the above disproportionation should be represented by the equation



The degree of disproportionation represented by this equation should not be affected by dilution; however, spectrophotometric studies of this equilibrium in tetrahydrofuran revealed that the apparent equilibrium constant, K_{ap} , defined by the ratio $[T] \cdot [T^{2-} \text{ total}] / [T^{\cdot-} \text{ total}]^2$, decreases with dilution [266b, 267]. $[T^{2-} \text{ total}]$ denotes the concentration of *all* the dianions, whatever their form, while $[T^{\cdot-} \text{ total}]$ refers to the concentration of all the radical ions. The effect of dilution on K_{ap} may be accounted for if the system is governed by three equilibria:



in conjunction with the dissociative equilibria such as



and



Equilibrium 7 may, in fact, be disregarded because the concentration of the dianions, T^{2-} , is expected to be vanishingly small. Since the equilibrium constants K_1 and K_2 are correlated through the relation

$$\frac{K_1}{K_2} = \frac{K_{diss}, T^{\cdot-}, Na^+}}{K_{diss}, T^{2-}, 2Na^+}}$$

the apparent disproportionation constant, K_{ap} , is given by

$$K_{ap} = \frac{K_1(1 + K_{diss}, T^{2-}, 2Na^+ / [Na^+])}{(1 + K_{diss}, T^{\cdot-}, Na^+ / [Na^+])^2}$$

and, in accord with the experimental findings, its value decreases on dilution provided

$$K_{diss}, T^{2-}, 2Na^+ \ll K_{diss}, T^{\cdot-}, Na^+$$

The dissociation of both salts in THF was investigated [267] and the results, shown in Fig. 28, reveal two facts: (1) the dissociation constant of the $T^{\cdot-}, Na^+$ ion pairs is relatively high, although the exothermicity of the process is low—a behavior characteristic of loose ion pairs; and (2) the dissociation constant of $T^{2-}, 2Na^+$ is low, but this process is strongly exothermic, a characteristic behavior of tight ion pairs dissociating into anions and solvated

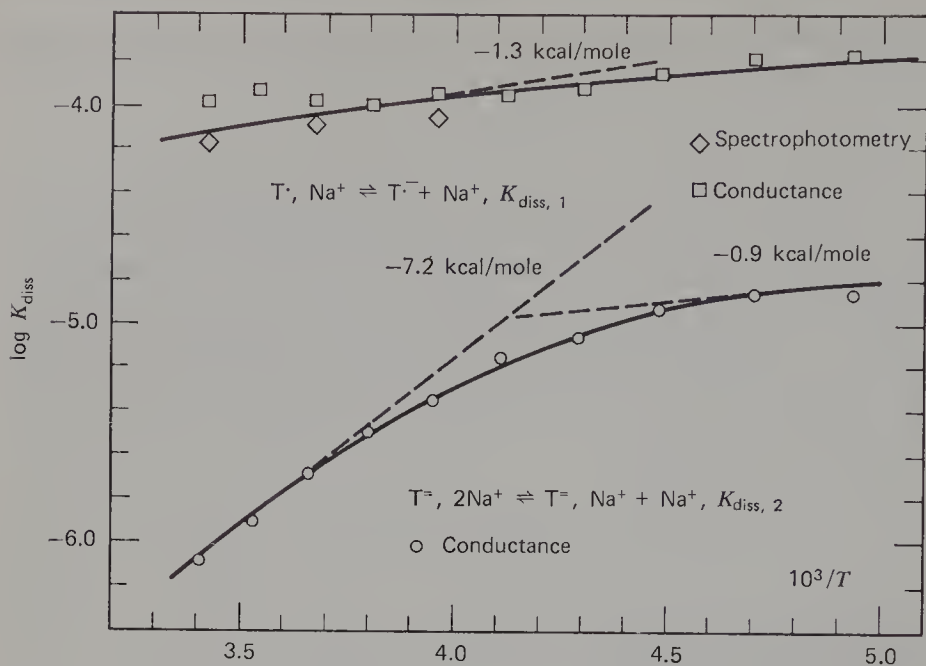


Figure 28. Dissociation constant of monosodium salt of radical anion ($T^{\bullet} Na^+$) derived from tetraphenylethylene (T) and of disodium salt of its dianion ($T^{2-} 2Na^+$). Both spectrophotometric and conductance studies were used in determining the dissociation constants of the respective ionic agglomerates: (\diamond) spectrophotometry (\square and \circ) conductance.

cations. Since under the usual conditions of the experiments the term $(K_{diss, T^{2-}, 2Na^+})[Na^+]^{-1}$ is much smaller than unity, the approximation

$$K_{ap} = \frac{K_1}{\{1 + (K_{diss, T^{\bullet}, Na^+})[Na^+]^{-1}\}^2}$$

is valid. The latter expression leads to the equation

$$\frac{1}{K_{ap}^{1/2}} = \frac{1}{K_1^{1/2}} + \left(\frac{K_{diss, T^{\bullet}, Na^+}^{1/2}}{K_1} \right)^{1/4} \{[T] \cdot [T^{2-} \text{ total}]\}^{-1/4}$$

Plots of $1/K_{ap}^{1/2}$ versus $\{[T][T^{2-} \text{ total}]\}^{-1/4}$ are shown in Fig. 29; and the values for K_1 and $K_{diss, T^{\bullet}, Na^+}$ are derived from their intercepts and slopes, respectively. The final results, giving K_1 and K_2 , determined over a range of temperatures, are displayed graphically in Fig. 30.

Let us assess the factors governing these reactions. Disproportionation of the loose T^{\bullet}, Na^+ ion pairs is favored by the entropy gain arising from the desolvation of sodium counterions as they become tightly bonded in the $T^{2-}, 2Na^+$ aggregates, as well as by the increase in the entropy of surroundings due to conversion of two T^{\bullet}, Na^+ dipoles into a $T^{2-}, 2Na^+$ quadrupole.

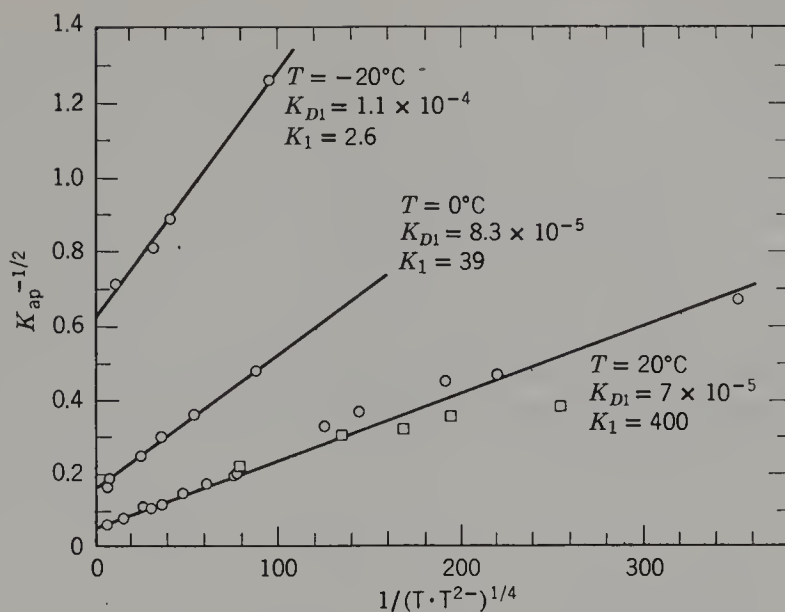


Figure 29. Linear plots of $1/K_{ap}^{1/2}$ versus $\{[T][T^{2-} \text{ total}]\}^{-1/4}$ for the system tetraphenyl ethylene and its radical ion and dianion: (O) Roberts and Szwarc [267]; (□) data of Garst [266b].

The entropy gain is more important than the opposing increase of ΔH caused by the desolvation of the cations, the latter being partially balanced by the greater binding energy of Na^+ ions to dianions than to radical ions. Hence the equilibrium constant, K_1 , is expected to be greater than the K_2 because the gain of entropy resulting from the desolvation of cations in the former reaction is twice as large as in the latter. This indeed is the case,

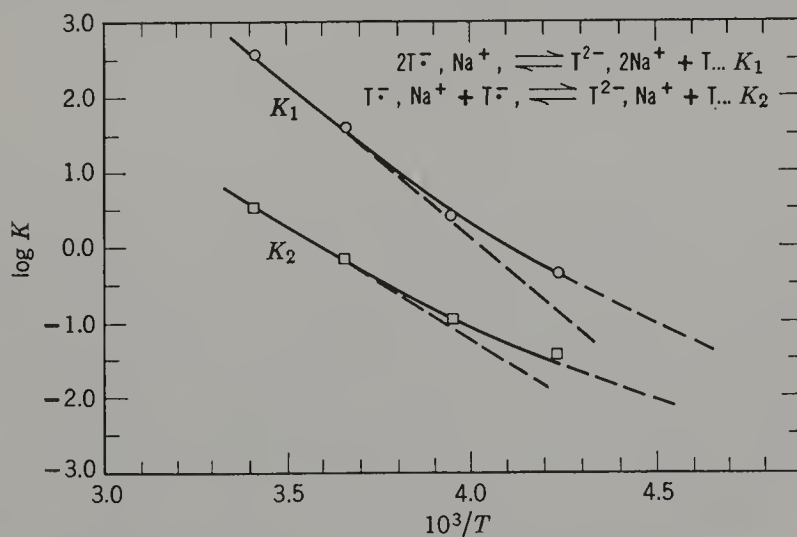


Figure 30. Plot of $\log K_1$ and $\log K_2$ versus $1/T$ for the disproportionation of radical ions of tetraphenylethylene.

$K_1 = 400$ whereas $K_2 = 3.3$ [267], although the endothermicity ΔH_1 is greater than ΔH_2 (see Fig. 30).

The importance of cations in determining the position of the equilibrium of disproportionation is clearly demonstrated by the study of the systems $2T^{\cdot-} \rightleftharpoons T^{2-} + T$ in HMPA. The mobility of the ions formed in this solvent proves that not only the $T^{\cdot-}$, Na^+ ion pairs but even all the T^{2-} , $2Na^+$ aggregates are completely dissociated in HMPA, the latter yielding T^{2-} dianions and sodium cations [154]. Ion pairing that favors the disproportionation is inoperative and consequently the concentration of the dianions is vanishingly small in this solvent, provided no excess of the alkali metal was used in the reduction. The respective equilibrium constant, $K_3 = 2 \times 10^{-4}$, was determined by potentiometric technique [154]. As implied by the

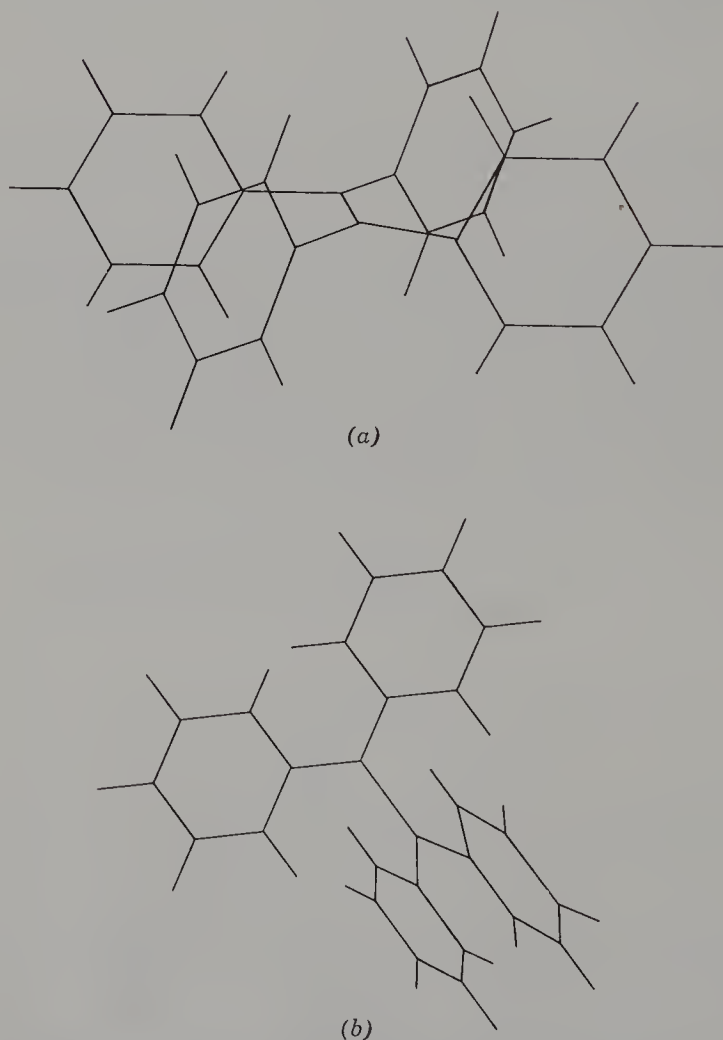


Figure 31. (a) Model of tetraphenylethylene. (b) Model of the dianion of tetraphenylethylene.

previous discussion, K_3 should *decrease* as the dielectric constant of the solvent decreases, a reverse trend from that observed for ion pairs. Indeed, approximate calculation leads to $K_3 < 10^{-8}$ in THF.

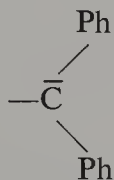
The formation of the loose T^\cdot , Cat^+ ion pairs is favored by strong solvation of cations, and therefore the degree of disproportionation at ambient temperature should be lower for the lithium salts than for the sodium pairs and very high for the salts of cesium. This conclusion is confirmed by experiment. [266].

Finally, let us ask why T^{2-} , $2Na^+$ tends to form tight ion pairs (at least at not too low temperatures) whereas T^\cdot , Na^+ forms loose ion pairs. The geometry of the T^{2-} ion is probably different from that of the T^\cdot radical ion. The latter is expected to have the shape of the parent hydrocarbon shown in Fig. 31*a*. Steric hindrance between the *cis*-placed phenyl groups prevents the $=CPh_2$ groups of this hydrocarbon from attaining a coplanar conformation [256] and the same factors should prevent the coplanarity of phenyl groups in the radical ion T^\cdot . Hence the bulkiness of this anion reduces its coulombic interaction with the cation and favors the formation of loose ion pairs.

The $C=C$ double bond is destroyed when the dianion, T^{2-} , is formed.

Consequently, rotation around the $C-C$ axis becomes possible and the di-

anion may then attain a skewed conformation shown in Fig. 31*b*. Such a conformation is favored for several reasons*; it reduces the repulsion between the extra electrons, releases the steric hindrance operating in the hydrocarbon, increases the resonance energy of the carbanions, and permits a close approach of the counterions to the planar negative centers of the carbanion,



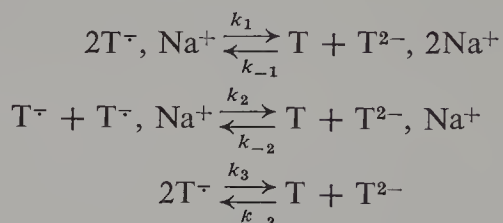
It is the last factor that favors the formation of tight ion pairs between the $-\bar{C}(Ph)_2$ carbanions and sodium cations.

The rate of disproportionation of radical anions of tetraphenylethylene was determined by Levin, Claesson, and Szwarc [272] by means of the flash photolysis technique. Irradiation of an equilibrated mixture of T , T^\cdot , Na^+ and T^{2-} , $2Na^+$ with a flash of visible light leads to the ejection of electrons from T^{2-} , $2Na^+$ and subsequently some of them are captured by T . Thus the concentrations of T and of T^{2-} , $2Na^+$ decrease after the flash, whereas the

* In a recent paper Eargle was arguing for planar configuration of T^{2-} [352]. His claims were subsequently refuted by Garst [353].

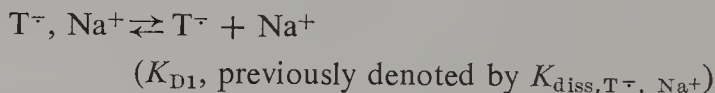
concentration of T^\cdot , Na^+ increases. The system returns to its state of equilibrium in the dark period after the flash—a process monitored by the conventional spectrophotometric technique.

Three reversible reactions contribute to this relaxation:

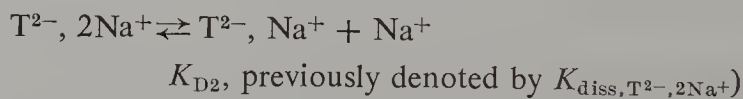


but, as will be shown later, the last reaction can be disregarded since its contribution to the overall process is negligible.

Under the conditions of these experiments, the equilibrium is reestablished in a few seconds and therefore the fast ionic association and dissociation reactions maintain at any time the equilibria



and



Denoting by x the deviation of the total concentration of T^\cdot , $Na^+ + T^\cdot$ from its equilibrium value, we find

$$-\frac{dx}{dt} = \left(k_{-1} + \frac{k_{-2}K_{D2}}{[Na^+]} \right) (ax + bx^2) = \left(k_1 + \frac{k_2K_{D1}}{[Na^+]} \right) K_1^{-1} (ax + bx)^2$$

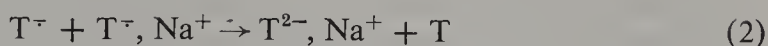
where a and b are constants determined by K_{D1} , K_{D2} , the equilibrium concentrations of the reagents (T , $T^\cdot + T^\cdot$, Na^+ , and T^{2-} , $Na^+ + T^{2-}$, $2Na^+$) and by that of Na^+ , all of them being known or determined from the final state of the system which, of course, is identical with its state before the flash. Thus each experiment provides the value of

$$k_{\text{obs}} = k_{-1} + \frac{k_{-2}K_{D2}}{[Na^+]}$$

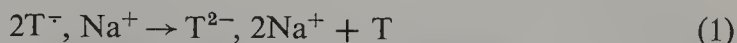
Since the concentration of Na^+ ions may be varied within large limits, for example, by the addition of Na^+ , BPh_4^- , a linear plot of k_{obs} versus $1/[Na^+]$ may be constructed. From its intercept and slope k_{-1} and k_{-2} can be determined. The previously discussed equilibrium study provided the values of $K_1 = k_1/k_{-1}$ and $K_2 = k_2/k_{-2}$, and therefore k_1 and k_2 could also be calculated.

The results led to $k_1 < 8 \times 10^6 M^{-1} \text{ sec}^{-1}$, $k_2 = 10 \times 10^6 M^{-1} \text{ sec}^{-1}$,

$k_{-1} < 4 \times 10^4 M^{-1} \text{ sec}^{-1}$, and $k_{-2} = 3 \times 10^6 M^{-1} \text{ sec}^{-1}$. Reaction 2



is therefore faster than reaction 1,



because in the latter Na^+ has to be transferred together with the electron thus slowing it relative to reaction 2. Moreover, the transition state of 2, $\text{T}^\cdot \cdots \text{Na}^+ \cdots \text{T}^\cdot$, results from the strong charge-dipole attraction, while the transition state of reaction 1, $\text{Na}^+, \text{T}^\cdot \cdots \text{Na}^+ \cdots \text{T}^\cdot$, involves the weaker dipole-dipole attraction.

The difference in rates is even larger when reactions -2 and -1 are compared. Again, no cation is transferred in -2 but a *tightly* bonded Na^+ ion has to be transferred in -1 , thus creating a greater hindrance for this process than that caused by the necessity of transfer of a *loosely* bounded Na^+ ion in reaction 1. Therefore, not surprisingly, k_{-1} is about 100 times smaller than k_{-2} , although k_1 is probably only 10 times smaller than k_2 .

The tentative assumption of negligible contributions to the overall process by reactions 3 and -3 may be now examined. Reaction 3 should be slow because the coulombic repulsion between the T^\cdot anions hinders it substantially. A recent example illustrating this effect is provided by the work of Abley and Halpern [273], who found the reaction $\text{BPh}_4^- + \text{IrCl}_6^{2-} \rightarrow \text{BPh}_4 + \text{IrCl}_6^{3-}$ to be much slower relative to $\text{BPh}_4 + \text{IrCl}_6^{2-} \rightarrow \text{BPh}_4^+ + \text{IrCl}_6^{3-}$, in spite of the much lower ionization potential of BPh_4^- than of BPh_4 . Hence the low concentration of T^\cdot combined with the low value of k_3 justifies the exclusion of reaction 3. Reaction -3 is undoubtedly very fast, being essentially diffusion controlled. But a reasonable estimate of the concentration of T^{2-} shows that the contribution of reaction -3 to the overall process is negligible, even for k_{-3} as large as $10^{11} M^{-1} \text{ sec}^{-1}$, due to the exceedingly low concentration of the unassociated dianions. The lack of deviation of the results from those predicted by the proposed kinetic scheme permits one to calculate the upper limits of k_3 and the contribution of reaction -3 . Again, this *a posteriori* calculation shows that reactions 3 and -3 may be disregarded when the disproportionation takes place under the conditions chosen in the flash-photolysis experiments.

The different behavior of tight and loose ion pairs accounts for the apparent anomaly reported by Zabolotny and Garst [274]. In tetrahydrofuran the degree of disproportionation of radical ions derived from stilbene *increases* with decreasing size of the cation; that is, the disproportionation equilibrium constant is greater for the lithium salt than that for the potassium. This reverse trend from that observed in tetraphenylethylene systems results apparently from the differences in structure of the ion pairs of these two

radical ions. The radical ions of stilbene seem to form contact pairs, even with Li^+ as the counterion; consequently, the gain in entropy which drives the disproportionation of tetraphenylethylene radical anions is not available for the disproportionation of stilbene radical anions. The latter reaction is driven, most probably, by the large binding energy of the anion-cation pair, the latter being evidently greater for the lithium than for the potassium salt. A study of the temperature dependence of this reaction is therefore desired.

The importance of steric strain in the disproportionation is again revealed by the strikingly different behavior of the radical anions of stilbene and α -methylstilbene [275]. The equilibrium constant of disproportionation of the sodium salt of the latter radical anion in MeTHF at 25°C exceeds 1000, while its value is 0.09 for the former system. The skewed geometry of the dianion releases the steric strain existing in the radical ion of α -methyl stilbene and favors its disproportionation.

The geometric factors also are important in the disproportionation of cyclooctatetraene radical anions. The parent hydrocarbon exists in a non-planar tub conformation (D_{2d} symmetry group) and has a pronounced olefinic character. In tetrahydrofuran solution it reacts readily with alkali metal, giving a dianion that yields cyclooctatriene on hydrolysis and the corresponding dicarboxylic acid on carboxylation [276]. Potentiometric and polarographic studies [277] showed that cyclooctatetraene is reversibly reduced in a two-electron process, i.e., the first reduction potential is higher than the second—a situation similar to that found for tetraphenylethylene [147]. The appearance of the ESR spectrum showed, nevertheless, that the radical ion exists [278]. Its ESR spectrum consists of nine evenly spaced lines (3.21 G) having the intensities predicted for an octuplet and the g value of 2.0036. A sharp spectrum is obtained when lithium is used as the reducing agent in THF, but it broadens when the reduction is performed with potassium. The degree of broadening increases with conversion, being insignificant for low K /hydrocarbon ratios, indicating that the broadening is due to a rapid electron exchange between the radical ion and the dianion, whereas the exchange with the parent hydrocarbon is slow. The absence of broadening in the lithium systems implies lack of exchange, the reason being unknown.

The value of 1.28 G for the ^{13}C splitting [279] demonstrates that the three valences radiating from each carbon atom of the eight-member ring are coplanar suggesting a planar form of a regular octagon for the radical ion. In view of its planar symmetry each carbon atom of cyclooctatetraene radical anion acquires $\frac{1}{8}$ of an electron's charge; however, this information is not sufficient to calculate the width of its ESR spectrum because Q depends on

the type of hybridization around the $\begin{array}{c} \text{C} \\ \diagup \quad \diagdown \\ \text{C} \end{array} \text{—H}$ centers. According to the

theory of π - σ interaction [280, 281], the value of Q should be -23.4 G for three equivalent sp_2 bonds (120° apart), as exemplified by the spectra of the benzene radical ion and the CH_3 free radical. The same treatment leads, however, to $Q = -10$ G for a regular octagon (bond angle of 135°) but the observed Q for cyclooctatetraene radical ion is -25.7 G. It has been proposed [282] that this contradiction may be resolved by invoking "bent" bonds [283] still having 120° bond angles. A similar conclusion would apply to the cycloheptatrienyl radical, for which Q was found to be in the range -25.6 to -27.6 G [284, 285].

The planar, regular octagonal conformation of the cyclooctatetraene radical anion calls for Jahn-Teller distortion, which should increase the g value over and above $g = 2.0023$ characteristic of a free electron. In addition, this effect should lead to a large line width and to a decrease in spin-lattice relaxation time [286]. This is not the case, and indeed on reexamination of the problem it has been concluded [287] that the Jahn-Teller effect may be insignificant in cyclooctatetraene radical ion, although it is large in benzene radical anion.

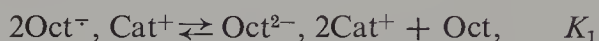
The preceding discussion leads to two conclusions: (1) the radical anion of cyclooctatetraene is planar whereas the parent hydrocarbon is puckered; and (2) the electron exchange between this radical anion and its parent hydrocarbon is slow but, significantly, the exchange with the corresponding dianion is relatively fast. The NMR evidence shows that the dianion is also planar, and hence we conclude that the need of geometric distortion considerably slows the electron exchange of the radical anion with the hydrocarbon, while the exchange with the dianion, which does not require any distortion of the reagents, is fast ($1 \times 10^9 \text{ M}^{-1} \text{ sec}^{-1}$) in spite of the negative charges residing on the interacting species which could hamper their approach [278a].

Conversion of the nonplanar cyclooctatetraene (Oct) into a hypothetical planar hydrocarbon requires compression energy E_c . However, the resulting structure is stabilized by delocalization of electrons, the delocalization energy E_d being 1.7β if Hückel approach is accepted. The first cathodic reduction potential ϵ_1 may therefore be smaller than ϵ_2 , provided that $E_c - E_d$ exceeds the electron repulsion energy arising in the reduction of Oct^- to Oct^{2-} . Polarographic data of Katz et al. [277] led to $\epsilon_1 - \epsilon_2 = -0.49$ V in 96% dioxane implying that the apparent disproportionation constant, K_{ap} ,

$$K_{\text{ap}} = [\text{Oct}_{\text{total}}^{2-}] \cdot [\text{Oct}] / [\text{Oct}_{\text{total}}^-]^2 = 10^8$$

This value is supported by the ESR data [282]. Determination of the concentration of Oct^- radicals by the ESR technique leads to K_{ap} of about 1×10^8 and 2.7×10^8 for the systems Li-THF and K-THF, respectively. The corresponding ΔH and ΔS values are $+1 \pm 0.5$ kcal/mole and 40 eu

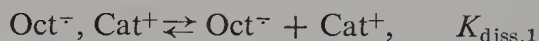
for the former and -5 ± 0.5 kcal/mole and 20 eu for the latter system. The ESR spectra reported in this study demonstrate that under the prevailing experimental conditions Oct^- anions were paired with the cations. Therefore, the reported K_{ap} refers to the equilibrium



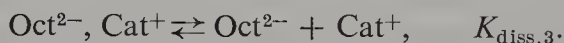
that is, the observed $K_{\text{ap}} \approx K_1 \approx 10^8$. The other two equilibrium constants K_2 and K_3 ,



may be calculated through the relations $K_2/K_1 = K_{\text{diss},2}/K_{\text{diss},1}$ and $K_3/K_2 = K_{\text{diss},3}/K_{\text{diss},2}$. The symbols $K_{\text{diss},i}$ refer to the dissociation processes:



and



The data given in ref. 282 permit us to calculate the approximate value of $K_{\text{diss},1}$ in THF as $10^{-6} M$. We estimate $K_{\text{diss},2}$ to be about 100 times smaller than $K_{\text{diss},1}$ and calculate $K_{\text{diss},3}$ from the approximate relation $|K_{\text{diss},3}| \approx |K_{\text{diss},2}|^2$. On this basis $K_2 \approx 10^6$ and $K_3 \approx 10^{-2}$, that is, for the *free ion* system the cathodic $\epsilon_1 - \epsilon_2 \approx +0.12$ V is positive.

This conclusion seems to be justified by the results of polarographic studies of Oct reduction in aprotic solvents DMF and DMSO [356]. Under conditions of those experiments the concentration of the cyclooctatetraene anions is small and their association with counterions is minor because of the relatively high dielectric of the medium and the bulkiness of cations. The following conclusions were reported:

1. The reduction to Oct^{2-} proceeds by *two* one-electron processes.
2. The cathodic $\epsilon_1 - \epsilon_2 = +0.24$ V, that is, $\epsilon_1 = 1.86$ V and $\epsilon_2 = 1.62$ V in respect to the mercury pool.
3. The electrode process, $\text{Oct} + e^- \rightleftharpoons$ is very slow, its activation energy presumably giving the compression energy of puckered cyclooctatetraene to its planar form.
4. The second electrode process, $\text{Oct}^- + e^- \rightleftharpoons \text{Oct}^{2-}$, is very fast.
5. Oct^- was formed since its ESR spectrum was observed.
6. Addition of even small amounts of K^+ ions greatly affects the potentials.

Therefore, $K_3 \approx 10^{-4}$ in DMF or DMSO, although this value seems to be

too small. The negative $\epsilon_1 - \epsilon_2$ reported for 96% dioxane [277] was attributed to a rapid protonation of Oct^{2-} .

The disproportionation equilibrium for the Oct^- system was investigated recently in liquid ammonia [357] and in HMPA [358]. In both systems the reduction was performed with alkali metal and the concentration of the reduced species was high (0.01–0.1 M according to the data reported in ref. 357). The pairing could therefore be appreciable in spite of the high dielectric constant and high solvating power of these solvents. K_{ap} was reported to be about 10^6 , 40 and 1 for K^+ , Na^+ , and Li^+ , respectively, in liquid ammonia (at 22°C), and in the range 10^3 – 10^4 for the HMPA system. Apparently Oct^{2-} , 2Cat^+ was the dominant dianion species while the majority of radical anions probably formed free Oct^- anions.

The authors of ref. 357 remarked that the effect of counterions on the Oct^- disproportionation equilibrium is much greater than their effect on the other properties of the radical anion such as their g -value and a_{H} . This statement, although correct, might be misleading since K_{ap} may be affected by a change of cation, even if virtually all of the Oct^- ions were *free*. For example, in a system in which only 1 to 10% of the radical anions are paired, a change of their degree of association kept within these limits cannot affect the *observed* g or a_{H} values. Moreover, hardly any coupling to the cation could be noted because the rapid exchange of cations broadens the weak lines of the ion pairs. The K_{ap} is given by

$$K_2(1 + K_{\text{diss},3}/[\text{Cat}^+] + [\text{Cat}^+]/K_{\text{diss},2})/(2 + K_{\text{diss},1}/[\text{Cat}^+] + [\text{Cat}^+]/K_{\text{diss},1})$$

and for $K_{\text{diss},1}/[\text{Cat}^+]$ varied from 0.01 to 0.1 this expression is reduced to $K_{\text{ap}} \approx K_2[\text{Cat}^+]^2/K_{\text{diss},1}K_{\text{diss},2}$ since $K_{\text{diss},2} \ll K_{\text{diss},1}$. The nature of cations affects K_2 , $K_{\text{diss},1}$, and $K_{\text{diss},2}$, and therefore it affects the value of K_{ap} . Two additional remarks are in place. (1) For a sufficiently large ratio $K_{\text{diss},1}/K_{\text{diss},2}$ the K_{ap} may be large even if the fraction of the Oct^- , Cat^+ pairs is small. (2) The presence of impurities sharing a common cation with the Oct^- , Cat^+ pairs may increase the observed K_{ap} by increasing the concentration of the free Cat^+ . The latter effect makes K_{ap} determined by the ESR technique susceptible to products of destruction of cyclooctatetraene anions.

The kinetics of disproportionation of cyclooctatetraene radical anions (Oct^-) has been studied by determining the rate of decay of the ESR signal resulting from the radical anions formed through irradiation of $\text{Oct}^{2-} + \text{Oct}$ mixtures in MeTHF [291]; the symbols denote the cyclooctatetraene dianion and the parent hydrocarbon. Such solutions were placed in the cavity of an ESR spectrometer and irradiated by steady, near UV light. This generates a photo signal whose intensity is greatly affected by the nature of the counterion. The solutions of lithium salts produce the most intense photosignal, about 1000 times stronger than the dark background, and give rise to a

nine-line spectrum, $h\nu = 3.17$ G, the peak-to-peak linewidth 0.06 G. No indication of Li $h\nu$ s was found within the investigated temperature range of 180° to 200°K. Hence these solutions involve either the free Oct^- ions or the loose Li^+ ion pairs. The spectra obtained with the sodium salt in the temperature range of 150 to 170°K definitely indicate the presence of Oct^- , Na^+ ion pairs and in addition the weak lines of the free Oct^- ions also are discerned in the recorded spectrum. The sodium $h\nu$ s, being 0.96 G, shows no temperature dependence. A weaker nine-peak photo signal was obtained with the potassium salt in the temperature range 140 to 160°K; the broadness of those lines indicates the unresolved K $h\nu$ s and therefore the spectrum is assigned to Oct^- , K^+ ion pairs. The rubidium salt produced an unresolved spectrum, and no photo signal was observed when the cesium salt was examined.

The photolysis leads to electron ejection from Oct^{2-} (or its salt) and to electron capture by Oct . Thus the photo stationary concentration of the radical anions, and therefore the intensity of the photo signal, is determined by the rates of two reactions. The photo oxidation,



followed by $\text{Oct} + e^-, \text{Cat}^+ \rightarrow \text{Oct}^-, \text{Cat}^+$, and the disproportionation,



The latter progressively decreases with decreasing temperature, whereas the rate of photooxidation is assumed to be independent of temperature and of the nature of the cation. On this basis the author concludes that the rate constant of the reaction $2\text{Oct}^- \rightarrow \text{Oct} + \text{Oct}^{2-}$ (presumably only the free ion species are present in the lithium system, although this seems to be a debatable point) is $3 \times 10^2 \text{ M}^{-1} \text{ sec}^{-1}$ at -100°C ($E = 13 \pm 1 \text{ kcal/mole}$); and that of the reaction $2\text{Oct}^-, \text{Na}^+ \rightarrow \text{Oct} + \text{Oct}^{2-}, 2\text{Na}^+$ is found to be 200 times faster, $6 \times 10^4 \text{ M}^{-1} \text{ sec}^{-1}$ at -100°C , decreasing to $2 \times 10^3 \text{ M}^{-1} \text{ sec}^{-1}$ at -126°C ($E = 9 \pm 1.5 \text{ kcal/mole}$). The potassium salt disproportionates even faster, $k_{\text{dispr}} = 5 \times 10^5 \text{ M}^{-1} \text{ sec}^{-1}$ at -124°C , $E = 3.6 \pm 0.5 \text{ kcal/mole}$, and presumably a still faster disproportionation takes place with the Rb^+ and Cs^+ salts. The enormous effect caused by change of counterion is indisputable; however, the discussion of the results may be questioned. The quantum yield of the photooxidation might be greatly affected by the nature of the counterion (see p. 138 where a similar problem is discussed), contradicting the basic assumption made in the paper [291]. Therefore, the decrease of the intensity of the ESR signal might reflect the decrease of the quantum yield on increasing the size of the cation and not the enhancement of the disproportionation.

The steric peculiarity of the cyclooctatetraene disproportionation and exchange is reflected in the system involving its dibenzo derivative. The parent

hydrocarbon is again nonplanar and olefinic in character, whereas the radical anion and the dianion are planar [288]. As in the cyclooctatetraene system the electron exchange between the radical ion and the parent hydrocarbon is much slower than the exchange with the dianion.

Another system resembling cyclooctatetraene has been investigated by Dauben and Rifi [289]. They showed that tropylmethylether reacts with potassium in tetrahydrofuran, giving a deep blue anion $C_7H_7^-$, K^+ , the existence of which had been questioned in the past. Simple Hückel molecular orbital treatment indicates that this conjugated system has two degenerate antibonding orbitals occupied by one electron in the $C_7H_7\cdot$ radical but by two in the anion. Hence, as predicted by the Jahn-Teller theorem, such a symmetric cyclic π system with a degenerate ground state should be stabilized by some perturbation which removes its degeneracy. Indeed, a stabilization by 6 kcal/mole is anticipated on distortion of the bond length.

This blue carbanion is diamagnetic; however, on further reduction a deep green radical anion is formed [290]. Its ESR spectrum has been recorded at -100°C ; it is an octet with hfs of 3.86 G split further by two magnetically equivalent Na^{23} ions into heptets with hfs of 1.74 G. The latter splitting provides an unequivocal evidence for its dianion character. This is an interesting example of a diamagnetic monoanion and a paramagnetic dianion. The dianion should be subject to Jahn-Teller stabilization, but no evidence is available yet on this point. It would be interesting to study the exchange and disproportionation in this system for a series of counterions.

We conclude this section with a brief discussion of a reaction involving electron transfer in tetrahydropyran from phenanthroquinone dianion (PQ^{2-}) to phenanthroquinone (PQ):



an inverse process of radical anion disproportionation, of which kinetics has been investigated [292]. The salts of radical anions of phenanthroquinone agglomerate into dimers, or still higher aggregates [292, 293], a phenomenon frequently observed for salts of radical anions of ketones and diketones [294].

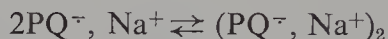
The dimers of $PQ^{\cdot-}$, Na^+ are diamagnetic and absorb at $\lambda_{\max} = 670$ nm. and their solutions are green, whereas the radical anions are paramagnetic, their solutions are red, and they have an absorption maximum at 499 nm. In fact, the dimers become associated further into tetramers [292]; however, this process does not change their absorption spectrum. The dimerization is undoubtedly affected by the counterions; the free ions, formed in HMPA, do not dimerize [292].

The question arises whether the reaction of PQ^{2-} , $2Na^+$ with PQ produces first the green dimer $(PQ^{\cdot-}, Na^+)_2$, which eventually dissociates partially into

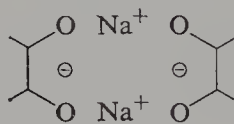
the red $PQ^{\cdot-}$, Na^+ radical anions, or whether the red $PQ^{\cdot-}$, Na^+ radical anions are formed first and these then associate into the green dimers. The results obtained by the stop-flow technique give a definite answer to this question. On mixing the reagents in a stop-flow apparatus a red solution appears first and this is subsequently converted into a green one. Hence the sequence is



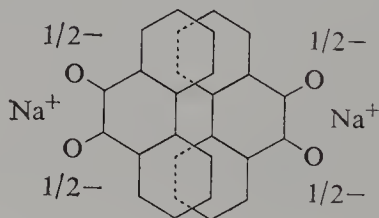
followed by



The bimolecular rate constant of the first reaction is $\sim 2 \times 10^6 M^{-1} \text{ sec}^{-1}$ while the forward rate constant of the second reaction is only $\sim 10^4 M^{-1} \text{ sec}^{-1}$. These results provide information about the structure of the dimer. It seems that structures such as



in which the $C=O$ groups are adjacent, are excluded because the "green" species would be formed prior to the "red" one. Hence the tentatively suggested structure is



The extension of these studies to other cations and solvents should be rewarding.

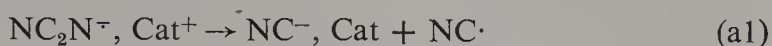
17. REACTIONS INITIATED BY THE DISPROPORTIONATION OF RADICAL ANIONS

In many systems disproportionation of radical anions is followed by some other process leading to the final products. Some of these reactions will be reviewed at this place.

Dinaphthylethane, $\alpha\text{-C}_{10}\text{H}_7\text{—CH}_2\text{·CH}_2\text{—}\alpha\text{-C}_{10}\text{H}_7$, denoted here by NC_2N , forms radical anions, $\text{NC}_2\text{N}^{\cdot-}$, having an absorption spectrum closely similar to that of the naphthalenide. Solutions of their salts decompose within a few minutes, the stoichiometry of the reaction being described by the equation



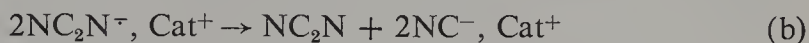
where NC^- denotes the $\alpha\text{-C}_{10}\text{H}_7\cdot\text{CH}_2^-$ carbanion. Three mechanisms may account for this result:



followed by



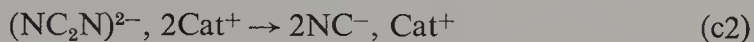
or, alternatively,



or



followed by the rate-determining step

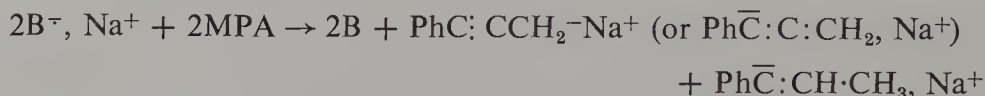


Kinetic studies of this reaction unequivocally determined its mechanism [295]. The rate of formation of $\text{CN}^-, \text{Cat}^+$ should be simply first order in $\text{NC}_2\text{N}^{\cdot-}, \text{Cat}^+$ if mechanism (a) is valid. It would be simply second order in $\text{NC}_2\text{N}^{\cdot-}, \text{Cat}^+$, provided the reaction is governed by mechanism (b), but the rate should be second order in $\text{NC}_2\text{N}^{\cdot-}, \text{Cat}^+$ and *retarded* by the presence of the unreduced NC_2N if mechanism (c) is the correct one. The last was proved to be the case; that is, a rapid disproportionation of radical anions $\text{NC}_2\text{N}^{\cdot-}, \text{Cat}^+$ produces a minute equilibrium concentration of the dianions which undergo a relatively slow unimolecular decomposition. The kinetic results therefore provide the product $2K_{c1}k_{c2}$; where K_{c1} is the equilibrium constant of the disproportionation and k_{c2} the unimolecular rate constant of decomposition of the dianion.

This reaction was investigated for the counterions Li^+ , Na^+ , K^+ , and Cs^+ in THF, and in addition for Na^+ in THP and in DME. The product, $2K_{c1}k_{c2}$, determined at 23°C , increases along the series Li^+ ($\sim 14 \times 10^{-3} \text{ sec}^{-1}$), Na^+ ($\sim 30 \times 10^{-3} \text{ sec}^{-1}$), K^+ ($\sim 40 \times 10^{-3} \text{ sec}^{-1}$), and Cs^+ ($\sim 70 \times 10^{-3} \text{ sec}^{-1}$); apparently due to the progressive increase in K_{c1} . For the sodium salt $2K_{c1}k_{c2}$ decreases with increasing solvating power of the solvent, the results being $47 \times 10^{-3} \text{ sec}^{-1}$ in THP, $30 \times 10^{-3} \text{ sec}^{-1}$ in THF, and 13×10^{-3} in DME, a trend similar to that found for the equilibrium disproportionation of tetraphenylethylene radical anions (see p. 94). Addition of small amounts of HMPA (up to $10^{-2} M$) to the THF solution of $\text{NC}_2\text{N}^{\cdot-}, \text{Na}^+$ gradually reduces the rate of decomposition; for example, when $[\text{HMPA}] = 1.2 \times 10^{-2} M$ the rate decreases by a factor of about 3. This result parallels the effect due to varying the solvating power of the medium.

Minute amounts of dianions maintained in equilibrium (or in stationary) concentration with the radical anions often are responsible for the reactions which might be formally attributed to the radical anions. For example,

electron transfer from sodium biphenylide ($B^{\cdot-}$, Na^+) to methylphenylacetylene (MPA) maintains a minute equilibrium concentration of the radical anions ($MPA^{\cdot-}$, Na^+) and the dianions (MPA^{2-} , $2Na^+$) of that hydrocarbon. The protonation of the *dianions* by MPA is the rate-determining step of the process [296] leading from



The rate of this reaction, $-d[B^{\cdot-}, Na^+]/dt$, is proportional to $[B^{\cdot-}, Na^+]^2 \cdot [MPA]^2/[B]^2$ (see also p. 230). Other examples of similar kinds of protonations are discussed in the following chapter (p. 229).

The electron transfer from sodium anthracenide ($A^{\cdot-}$, Na^+) to 1,1-diphenylethylene (D) leads eventually to the 1,1,4,4-tetraphenylbutane dianion (Na^+ , $Ph_2\bar{C}CH_2\cdot CH_2\cdot\bar{C}Ph_2$, $Na^+ = Na^+$, $^{-DD^-}$, Na^+):



One could presume that this process involves two steps:



followed by the rapid dimerization



or



followed by a rapid electron transfer from $A^{\cdot-}$, Na^+ to $\cdot DD^{\cdot-}$, Na^+ . However, the kinetic results [297] showed that $D^{\cdot-}$, Na^+ is formed by the reaction

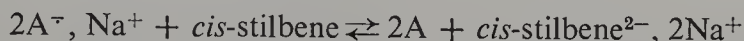


Again, the disproportionation of $A^{\cdot-}$, Na^+ and the transfer from A^{2-} , $2Na^+$ to D is faster than the direct electron transfer from $A^{\cdot-}$, Na^+ to D.

Similar results have been obtained in the course of study of the system sodium anthracenide ($A^{\cdot-}$, Na^+) + styrene. The reaction eventually leads to dimerization of styrene; however, it is not the radical anion but the dianion, A^{2-} , $2Na^+$ that starts the process [298]. This result is even more striking when one is reminded that the concentration of A^{2-} , $2Na^+$ is less than 1000 times smaller than that of $A^{\cdot-}$, Na^+ .

These types of reaction may change their course if different counterions or solvents are involved in the process. Such studies would therefore be interesting and should provide further examples illustrating the important role of ion pair structures in determining the reaction path of electron-transfer processes.

The isomerization of *cis*- into *trans*-stilbene induced by electron transfer process exemplifies another reaction involving dianions [359]. In THF the addition of sodium anthracenide ($A^{\cdot-}, Na^+$) to *cis*-stilbene leads to its isomerization by a pseudo-first order reaction without affecting the concentration of the anthracenide. However, the pseudo-first order constant is proportional to $\{[A^{\cdot-}, Na^+]/[A]\}^2$ —the nonreduced anthracene retarding the process. This kinetic relation implies that the *cis*-stilbene dianion isomerizes in a rate determining step, its minute stationary concentration being maintained by the overall equilibrium,

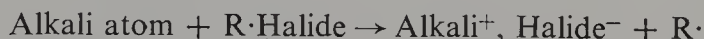


The resulting *trans* salt is converted into *trans*-stilbene by a rapid electron transfer to anthracene that regenerates the anthracenide.

The nature of the counterion affects the rate of isomerization of the dianion as well as the equilibrium of its formation. Interestingly, in HMPA, that is, in a solvent dissociating ion pairs, the analogous first order isomerization proceeds with a rate proportional to $[A^{\cdot-}]/[A]$; the free *cis*-stilbene radical anion is capable of isomerizing, while the isomerization of ion-pairs is too slow.

18. ELECTRON TRANSFER TO ORGANIC HALIDES

The gas phase reactions described by the equation



were extensively studied by Polanyi and his school [335]. The results of these investigations had a profound influence on the development of modern chemical kinetics, leading, for example, to the important relation between the heat of an elementary step and its activation energy.

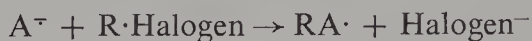
In the treatment of this dissociative process it is assumed that the alkali atom experiences no repulsion as it approaches the $R\cdot$ -halide electron acceptor. The activation energy of the displacement is then determined by the necessity of stretching the covalent R -halogen bond to the distance at which its stretching energy compensates the repulsive $R \cdots \text{halogen}^-$ energy of the equidistant $R\cdot\text{-halide}^-$ system. At this stage of expansion the spontaneous electron transfer from the alkali atom to the halogen completes the reaction. Closely similar is the treatment of the dissociative electron capture studied by Wentworth et al. [55].

Extension of these studies to the analogous reactions taking place in the liquid phase was initiated by the work of Warhurst and his students [336]. Radical anions ($A^{\cdot-}$) or dianions served as the electron donors in a process

assumed to be represented by the equation



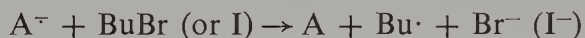
and the importance of solvent and counterion in determining its rate was revealed by the early work of Warhurst. Systematic studies of these factors are still lacking; however, the reaction is more complex than implied by the foregoing presentation. In addition to electron transfer, an S_N2 reaction,



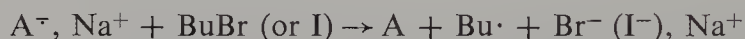
may lead to the annihilation of the radical anions. For example, alkyl chlorides yield with sodium naphthalenide the alkyl-substituted dihydronaphthalenes, although the reaction with benzyl chlorides produces dibenzyl resulting, presumably, from the dimerization of benzyl radicals.

Extensive studies of such systems, centered on the nature of the products, were reported by Lipkin (see, e.g., [337]), by Garst [338], and by Sargent and Lax [339]. This work has been thoroughly reviewed by Garst in his recent articles [340, 360].

Pulse radiolysis studies of the electron-transfer reactions



and



where A denotes naphthalene or biphenyl have been reported recently [342]. Secondary reactions, such as $A^- + \text{Bu} \cdot$, are prevented by the extremely low concentration of radical anions—a characteristic feature of pulse radiolysis. Spectral observations demonstrate that the S_N2 reaction does not take place in this system, since no intermediate absorbing in the visible region has been detected.* In each run the concentration of A^- (or A^-, Na^+) decayed in a first-order fashion and the pseudo-first-order rate constants were found proportional to the concentration of BuBr (or BuI). The bimolecular rate constants determined in THF at ambient temperatures are

	BuI ($M^{-1} \text{ sec}^{-1}$)	BuBr ($M^{-1} \text{ sec}^{-1}$)
Biphenyl $^-$	$(9.6 \pm 1.4) \times 10^9$	$(3.4 \pm 0.6) \times 10^7$
Biphenyl $^-$, Na $^+$	$(4.3 \pm 0.2) \times 10^8$	$(1.3 \pm 0.1) \times 10^6$
Naphthalene $^-$	$(7.4 \times 1.1) \times 10^9$	$(3.3 \pm 0.6) \times 10^7$
Naphthalene $^-$, Na $^+$	$(9.3 \pm 0.5) \times 10^7$	4×10^5

It is interesting to note that the free naphthalenide and biphenylide are equally reactive towards the halides, but the reaction with the iodide is more than 200 times faster than with the bromide. The respective ion pairs seem

* Some complicating features of the reactions were noted when biphenylide was the donor. However, the S_N2 reaction was ruled out even in that case.

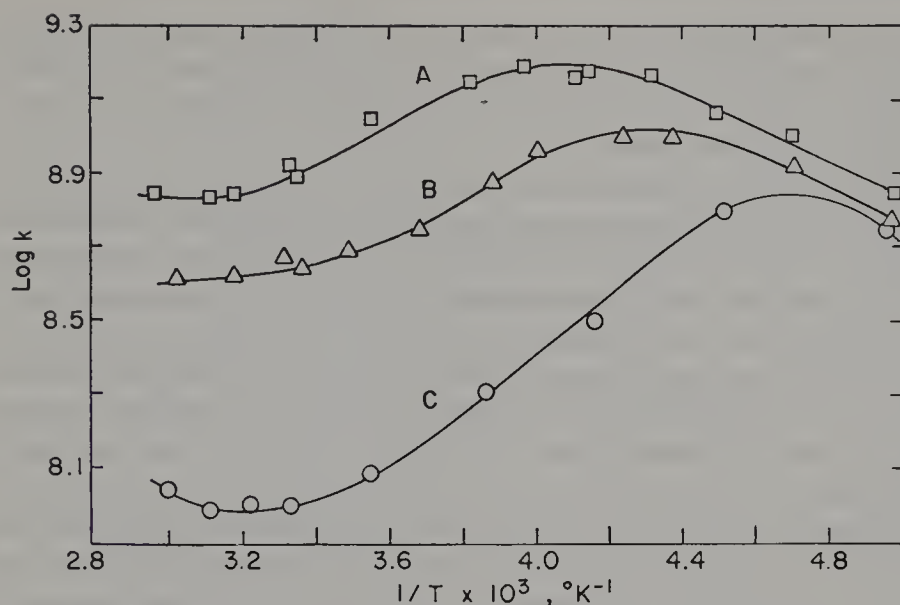
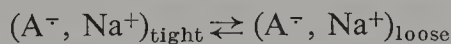


Figure 32. Temperature dependence of the rate constants of the reaction of sodium ion pairs of aryl radical ions with butyl bromide (or iodide) in tetrahydrofuran.

to be at least 20 times less reactive than the free radical anions; moreover, the biphenylide pair is more reactive than the naphthalenide. It is tempting to assume that Polanyi's model applies to the reactions of the free radical anions, although examples of donors of greatly different electron affinity are needed to confirm this suggestion. A more complex transition state, involving a counterion, should be invoked in discussing the reactions of ion pairs. Comparison of organic halide reactions with the protonation of radical ions discussed in Chapter 2 is most instructive. The free ions are more reactive toward halides than ion pairs, whereas the reverse is found in the protonation.

The importance of ion pair structure is well illustrated by the temperature dependence of the rate constants of the electron transfer from ion pairs, presented graphically in Fig. 32. The maxima seen in the Arrhenius plots resemble those observed in studies of anionic polymerization [341] discussed in the fourth chapter of this book. They indicate the higher reactivity of loose pairs than of tight ones and imply that the negative heat of conversion



is greater than the activation energy of the electron transfer (see also p. 48).

19. SOLVATED ELECTRONS

Ejection of electrons and their subsequent capture have been mentioned in several of the preceding sections. These processes proceed differently in the

liquid phase than in the gaseous, because the state of an electron is greatly different in solution than in a vacuum or in a low-density gas. It is desirable therefore to inquire about the properties of solvated electrons before reviewing their reactions in liquids.

Electrons in the gas phase are described by a planar wave function, their momentum being the only parameter needed in the description. Their motion carries them most of the time through a zero potential field which is only momentarily modified on encounter with a particle—an atom, molecule, or ion. This leads to a sudden change in the direction of their momentum, a phenomenon referred to as electron scattering. In a condensed phase, whether liquid, glassy, or crystalline, the electrons are always subjected to fields generated by their neighbors, and this radically changes their description and character.

In crystalline ionic solids and in metals the mobile electrons are influenced by a *periodic* long-range field generated by the orderly and repetitively arrayed ions. The field's periodicity is determined by a rigid lattice of a fixed geometry, and since its rigidity is high, injection of excess electrons does not modify its structure. A perfect translational symmetry of an ideal crystal demands a complete delocalization of those electrons, because any location within the lattice is indistinguished from all the other equivalent locations generated by translational transformations. This symmetry simplifies the structure of conduction bands formed by merging of sufficiently expanded molecular orbitals; their character and the degree of their occupancy by electrons accounts for much of the electric properties of a crystal and determines whether it behaves as an insulator, semiconductor, or conductor.

A more refined treatment of crystals has to take into account the thermal vibration of the lattice. The coupling of these vibrations with the motion of mobile electrons may then lead to the self-trapping of the latter. This suggestion has been put forward by Landau [64] in an attempt to explain the existence of *F* centers in ionic crystals. Although the formation of these centers has been traced to other causes, Landau's approach is, nevertheless, most valuable because it is applicable, as will be seen later, to other phenomena observed in condensed systems.

Any real crystal has some defects caused by impurities or structural imperfections and these act as fixed "electron traps." Such traps affect considerably the electrical behavior of solids; the most interesting and valuable properties of semiconductors result from their presence. Although this subject cannot be pursued further, because it is beyond the scope of this chapter, it should be stressed again that the electric phenomena encountered in crystalline solids basically result from the *periodicity* of the field and the presence of *localized* electron traps.

The concepts developed in the studies of crystals are also useful in

describing excess electrons in amorphous media, whether glasses or liquids, although extensive modifications are needed to make them applicable for treatment of problems associated with the disordered systems. The densities of liquids and glasses, like those of crystalline solids, are substantially higher than those of dilute gases. Consequently, the more expanded molecular orbitals may overlap, and such an overlap results again in the formation of conduction bands. However, the simplicity of the bands developed in crystals is lost because the translational symmetry is destroyed in amorphous or liquid materials. This lack of symmetry introduces also serious difficulties in other problems that must be solved to account for the properties of excess electrons in condensed media. Some of these difficulties have been partly alleviated by substituting an *average* potential field for the truly periodic potential characterizing the field in a crystal. This approximation neglects fluctuations and uses the ensemble average; moreover, it is applicable only to phenomena associated with times shorter than the periods of atomic or molecular motions.

The behavior of electrons injected into a condensed medium is determined by the forces acting on them. Two types of force are involved in the interaction of an electron with a nonpolar molecule or atom: the short-range repulsive forces and the long-range attractive forces, the latter resulting from the polarizability of the interacting atom or molecule. In addition, forces due to multipoles are operative when the interacting molecule is polar.

The repulsive forces are only slightly affected by the state of aggregation of the medium; this, in fact, is the consequence of their short range. On the other hand, the attractive long-range forces arising from the polarizability of the interacting particle are substantially affected by the aggregation, because the molecules placed outside the immediate vicinity of the electron are screened by those located between. Hence, for a molecule located at a large distance R from the electron, the effect of polarizability is lower in a condensed phase than in the gas phase. The same cause attenuates the coulombic forces acting on polar molecules not located in the immediate vicinity of an electron.

The electrons injected into a glass or liquid may be classified as quasi-free or localized. The behavior of quasi-free electrons has been reviewed recently by Jortner [65]. His theoretical treatment, accounting for their properties, is based on the concept of pseudo-potential, a device allowing one to circumvent the requirement of orthogonality for orbitals describing the excess electrons and those pertaining to atomic or molecular cores. The results apply to the rapidly moving electrons injected from a photo-cathode or from a field emission tip. Their velocities are much higher than those of the molecules surrounding them, although they are still lower than the velocities of valence electrons. Therefore the molecular pattern of the medium may be treated

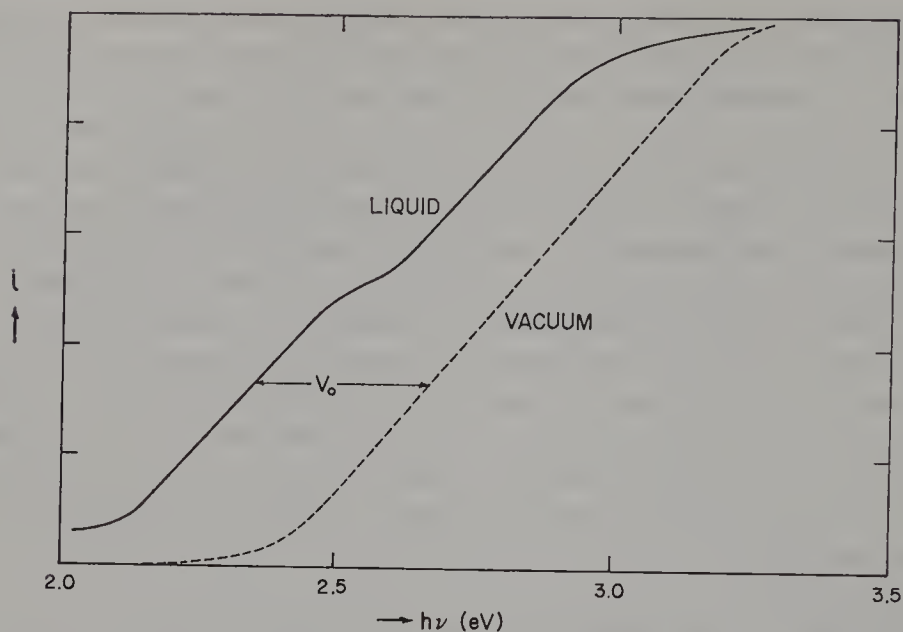


Figure 33. Experimental determination of the adiabatic barrier for the electron injections into a nonpolar liquid. Solid line refers to liquid; dashed line refers to a vacuum experiment. The difference V_0 gives the energy of the quasi-free electron.

as if it were rigid and independent of time, since no time for any rearrangement is available, while the highly mobile valence electrons become fully polarized by the injected electrons.

The ground state energy, V_0 , of the quasi-free electrons has been calculated for the simplest systems—the liquid rare gases. Its experimental value has been determined by measuring the work function of a photo-cathode immersed in the investigated liquid relative to its value in vacuum. The results of such experiments, reported by Rice and his co-workers [66], are presented schematically in Fig. 33. The agreement between the calculations and observations is fair, giving substance to this important entity that represents the energy difference of a quasi-free electron in the solvent and in vacuum. We may therefore interpret V_0 as a kind of solvation energy of a quasi-free electron.

For liquids composed of small and hardly polarizable atoms or molecules, such as liquid helium or hydrogen, V_0 was found to be *positive*. Hence the quasi-free electron is more stable in a vacuum than in those liquids because the short-range repulsive forces dominate in these systems. However, V_0 becomes negative in more polarizable liquids; even in liquid argon its value is -0.33 eV [66]; that is, the attractive, long-range electron-medium interactions are now decisive. This conclusion is confirmed by the independent studies of electron scatter by these gases.

The reality of quasi-free electrons is affirmed through investigations of their conductance in liquid argon, krypton, and xenon [70]. Their mobilities are exceptionally high—about five powers of 10 greater than the expected ionic mobility, and these startling results have been verified recently by Robinson and Freeman [111]. Moreover, electron mobilities in those liquified gases *decrease* with *increasing* temperature, a phenomenon characteristic of metallic conductance. Indeed, according to the theory, the mobility, μ , of freely moving electrons but scattered by atoms or molecules is given by

$$\mu \sim T^{-3/2}$$

and this relation has been fully confirmed by Miller et al. [70], who investigated the temperature dependence of mobility of excess electrons in liquid argon. In contrast, the mobilities of ions *increase* with *increasing* temperature, their values conforming, at least approximately, with Walden's rule.

The positive value of V_0 characterizing the quasi-free electrons in liquid helium or hydrogen points to their intrinsic instability; the action of short-range repulsion leads then to the formation of a "bubble" within which the electron becomes localized. Such an electron behaves somewhat like an ion—its mobility is determined by the mobility of a "bubble" and therefore is low. The dramatic decrease in the mobility of excess electrons in liquid helium or hydrogen when compared with liquid argon, krypton, and xenon are amply documented by the data collected in Table 24.

The formation of a "bubble" requires about 10^{-10} sec to allow for atomic motion. Hence even in liquid helium or hydrogen a fast electron injection process yields quasi-free electrons, in spite of their intrinsic instability. However, the conductance studies are associated with longer observation times and the localization then takes place.

The preceding remark should be emphasized. When considering quasi-free

Table 24 Mobilities of Electrons Injected into Non-polar Liquids

Liquid	Temperature (°K)	Mobility (cm ² V ⁻¹ sec ⁻¹)	Ref.
He ³	2.25	4.06×10^{-2}	68
He ⁴	4.2	2.16×10^{-2}	68
H ₂	20	5×10^{-2}	69
Ar	82	440	70, 111
Kr	117	1800	70, 111
Xe	163	2200	70, 111

electrons, one has to carefully specify the time scale of the experiment. The process of electron injection is associated with times of the order of 10^{-14} sec or less. Therefore the barrier determined for electron injection refers to the quasi-free electrons, whatever their energetic stability. The conductance studies associated with relatively long times of about 10^{-10} sec reveal only the stable state of excess electrons.

The modes of formation and the properties of localized electrons need further examination. Two types of localization should be distinguished. In the systems where the repulsive forces dominate, as in liquid hydrogen or helium, an added electron is trapped in a spherical cavity, the potential at its boundary being determined by the repulsive forces. This "bubble" model, proposed first by Careri [71], accounts successfully and quantitatively for the properties of electrons localized in liquid helium [65]. Although the short-range repulsion provides the driving force for the formation of a bubble and for the localization of an added electron, some energy has to be expended to form a void in the liquid. Therefore three terms—the surface energy of the "bubble," the pressure-volume term, and the kinetic energy of the electron in a spherical box—determine the radius of the cavity. Its value is then calculated by minimizing the sum of these three terms, and this calculated cavity radius may be compared with its experimental value deduced from the conductance data on the basis of Stokes' law. Both approaches lead to concordant results giving R of about 15–16 Å at zero pressure but decreasing to about 11 Å at 20 atm. This extremely high value of the radius is remarkable and it justifies the classic Stokes' treatment of the mobility of an electron localized in a "bubble."

An interesting phenomenon may be expected. Since the work needed for the formation of a cavity increases with increasing hydrostatic pressure, no bubble should be formed if the pressure is sufficiently high. This means that an electron localized in a bubble at low pressure should become quasi-free when the hydrostatic pressure rises above some critical limit value, providing this would not lead to solidification of the liquid.

The extent of stabilization of an electron on its localization is measured by its photoionization threshold. For example, the photoionization threshold for an electron in a bubble formed in liquid helium has been determined experimentally to be 0.9–1.0 eV. Nevertheless, the energy of such a localized electron is still slightly higher than that of an electron in vacuum, because V_0 , the negative "solvation" energy of a quasi-free electron in liquid helium, is about 1.05 eV [72].

In nonpolar but polarizable media the short-range repulsive forces are annulled by the long-range attractive forces caused by the polarization of the solvent; hence the gain resulting from a "bubble" formation is lost or at least greatly diminished. The excess electrons remain quasi-free, although they

are confined to the liquid by the attractive field of polarization surrounding them. As has been pointed out earlier, the high conductance of excess electrons in liquid argon, krypton, and xenon verifies this model. It might be that the quasi-free, and not the localized electron represents the lower energy state in liquid hydrocarbons. However, the early studies of electron's conductance in hydrocarbons led to very low values for their mobilities, often less than $10^{-2} \text{ cm}^2 \text{ V}^{-1} \text{ sec}^{-1}$ [73]. Higher mobilities, of the order of $1 \text{ cm}^2 \text{ V}^{-1} \text{ sec}^{-1}$, were reported by Freeman [74], and his results spurred Schmidt and Allen [75] to investigate electron mobilities in $\text{Si}(\text{CH}_3)_4$, a nonpolar liquid resembling hydrocarbons. A much higher value of μ of about $90 \text{ cm}^2 \text{ V}^{-1} \text{ sec}^{-1}$ was observed in this solvent, and therefore Schmidt and Allen concluded that the lower values of mobilities reported in the past could be caused by impurities such as traces of dissolved oxygen which trap the electrons. In fact, 1 ppm of oxygen in a liquid would be sufficient to trap all the electrons and yield erroneous results. A similar conclusion was drawn independently by Davis et al. [76].

However, the problem is far from being solved. Although Davis et al. observed a 50-fold increase in the mobility of electrons in liquid hexane after meticulous purification, the observed conductance was still relatively low. On the other hand, a very high electron mobility of about $200 \text{ cm}^2 \text{ V}^{-1} \text{ sec}^{-1}$ was reported recently for excess electrons in liquid methane [112] and only a slightly lower value of about $50 \text{ cm}^2 \text{ V}^{-1} \text{ sec}^{-1}$ in neopentane [110]. These results provide justification for the suggestion that the anisotropy of molecular polarizability is an important factor influencing the electron's behavior [109, 110] and that the mobility of electrons increases with increasing sphericity of the solvent molecules. Indeed, the mobilities in *n*-pentane and in neopentane, determined by Freeman's group [110, 113] and by Schmidt and Allen [112], differ by a factor as large as 300. Extension of these studies to olefines [113] revealed an unexpectedly large difference in the mobilities of electrons in *cis*- and *trans*-butene-2. Whereas the mobility in *cis*-butene-2 is reported to be $2.2 \text{ cm}^2 \text{ V}^{-1} \text{ sec}^{-1}$ at 293°K , its value decreases to $0.029 \text{ cm}^2 \text{ V}^{-1} \text{ sec}^{-1}$ in the *less* polar *trans*-butene-2. The structure of the hydrocarbon seems therefore to be another important factor determining the mobilities of injected electrons.

The behavior of excess electrons in polar liquids is basically different from that observed in nonpolar media. Those electrons, if endowed with a sufficiently large kinetic energy, may move in a conduction band of a polar liquid where they behave somewhat similarly to the quasi-free electrons in nonpolar solvents. However, an important new factor is introduced by the polarity of the solvent molecules which biases their *orientation* in the electric field of an added electron. The rate of orientation of dipoles is relatively slow and therefore the dipoles do not contribute to polarization of the medium at

high frequency of an external electric field. At lower frequencies this polarization lags behind the external electric vector \mathbf{E} , and thus a drag tending to trap the electron is introduced.

This effect of self-trapping, and hence localization of an added electron by the polarization field induced in the medium by its own presence, forms the basis of Landau's approach [64], known as the *polaron theory*. It should be stressed that the polarization arising from the effect of polarizability of valence electrons does not contribute to the trapping because it does not lag behind the electric field—the response is too fast. Nevertheless, such a polarization *does* contribute to the binding of the electron to the medium, although not to its localization.

The polaron theory of a localized electron will now be briefly outlined. The dielectric constant of the medium at high optical frequencies is due to the polarization of valence electrons. Its value, denoted by \mathcal{D}_{opt} , is given by the square of the refractive index of the solvent. Therefore the displacement of an electric vector, \mathbf{D} , at high frequencies is equal to $\mathcal{D}_{\text{opt}}\mathbf{E}$, and the polarization field, \mathbf{P}_{opt} , given by $(\mathbf{D} - \mathbf{E})/4\pi$, is $(1 - 1/\mathcal{D}_{\text{opt}})\mathbf{D}/4\pi$. At low frequencies the polarization field is due to both effects—the polarization of the valence electrons and the orientation of the dipoles. Under those conditions the displacement $\mathbf{D} = \mathcal{D}_{\text{st}}\mathbf{E}$, where \mathcal{D}_{st} denotes the static dielectric constant measured at low frequencies. Hence the total polarization field, \mathbf{P}_t , composed of the contributions due to the polarization of the valence electrons, \mathbf{P}_{opt} , and of those arising from the dipole orientation, \mathbf{P}_d , is given by

$$\mathbf{P}_t = \mathbf{P}_{\text{opt}} + \mathbf{P}_d = \frac{(\mathbf{D} - \mathbf{P})}{4\pi} = \frac{(1 - 1/\mathcal{D}_{\text{st}})\mathbf{D}}{4\pi}$$

Therefore the polarization field arising from the dipoles orientation only is given by

$$\mathbf{P}_d = \left(\frac{1}{4\pi}\right)\left(\frac{1}{\mathcal{D}_{\text{opt}}} - \frac{1}{\mathcal{D}_{\text{st}}}\right)\mathbf{D}$$

It is this field which imposes some new properties on excess electrons in a polar medium. Their description in the terms outlined above was proposed first by Davidov and Deigen [77], and this polaron model has been improved by Jortner [79], who substituted a self-consistent field for the adiabatic electronic polarization used in the Davidov and Deigen calculations. This seems to be essential because the binding energy of an electron injected into a polar solvent is quite substantial, amounting to about 30–40 kcal/mole for liquid ammonia or water [80].

The orientation of dipoles toward a common center produces a strong polarization field at that point. Such a center acts therefore as a trap localizing

an added electron, and its formation, favored by the presence of an electron, represents a process of electron self-trapping. However, a poorly organized trap may also be formed spontaneously due to the fluctuations in the liquid structure.

The model of a trap described here does not demand the existence of any cavity in the liquid, and indeed, the original approach of Davidov and Deigen refers to the limit of zero cavity radius. However, trapping of electrons in polar liquids seems to be associated with the formation of cavities. This has been clearly demonstrated by the substantial decrease in the density of alkali-metal solutions in liquid ammonia relative to those of the components. The volume expansion accompanying dissolution of sodium in liquid ammonia was reported first by Kraus and Lucasse [78] and the magnitude of the dilation is conveniently measured by

$$\Delta V = \frac{V_{\text{solution}} - (V_{\text{NH}_3} + V_{\text{metal}})}{\text{Gram-atoms of metal}}$$

ΔV being a function of metal concentration. The largest expansion was observed for the lithium solutions; in fact, a saturated solution of lithium in ammonia is the lightest liquid known at room temperature, having a density of only 0.477 g cm^{-3} . The dilution data permitted calculation of the size of the cavities formed in liquid ammonia; it seems that they correspond to spheres of a radius of about 4.5 \AA , having a volume of about 100 \AA^3 . Such a volume corresponds to that occupied by three ammonia molecules.

The reasons for the cavity formation are not obvious. The short-range repulsions are probably responsible for this phenomenon, although the effects of long-range polarization would make such cavities smaller than those formed in nonpolarizable solvents. Indeed, the radius of a "bubble" formed in liquid helium is claimed to be about four times greater than that of the cavity created in liquid ammonia, and apparently a still smaller cavity accommodates the hydrated electron in water.

Further improvement of polaron theory called therefore for the consideration of the role of a cavity in the model [79]. The radius of the cavity was introduced as a semiempirical parameter. However, it has been obvious that its value should be influenced by the surface energy term, which in turn is related to the surface tension of the solvent. Hence, it is justified to expect a smaller radius for the hydrated electron in water than for the electron in liquid ammonia. The size of the cavity need not be equivalent to the "volume" of the orbital of the added electron; in fact, it has been concluded that about 30–40% of electron's charge "leaks out" of the cavity formed in liquid ammonia.

The energy of an injected electron localized in a polar liquid is given

therefore by two terms: (1) the energy needed to create a center of localization; and (2) the energy of an electron in the potential field of the center. The first term involves the unfavorable interactions between the molecular dipoles oriented toward the center, the energy associated with the polarization of valence electrons, and the energy needed for creation of a void in the liquid. The second term corresponds to the energy of a stationary electron moving in the spherical field of the center and calculated from the appropriate Hamiltonian. Obviously, the stationary orbitals of localized electrons calculated from this model are not formed by the combination of molecular orbitals of the individual solvent molecules but result from the existence of an electric field of polarization governing the motion of the added electron.

Since a localized electron moves in a field of spherical symmetry, its angular momentum is preserved and therefore its orbitals could be classified according to the quantum numbers of the angular momentum as *s* or *p* orbital. The first absorption band of such an electron would result from its excitation from the ground $1s$ state to the $2p$ excited state, the associated energy being $\{E_{2p}$ (in the configuration of solvent molecules corresponding to the $1s$ state) $- E_{1s}\}$. In the same terms, the photoelectric threshold for electron emission from the solution to the gas phase is equal to E_{1s} , while the heat of solution of an electron in a polar solvent is given by $-E_{1s}$ + energy required for the formation of the center. Hence no relation is expected between the heat of solution and the energy of the first absorption band. Further discussion of the spectra of solvated electrons in polar liquids will be continued in the next section.

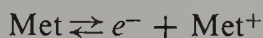
Finally, a few words should be devoted to the mobility of solvated electrons in polar media. The limiting value of the equivalent conductance of sodium solutions in liquid ammonia at -33°C was determined by Kraus [81] at the beginning of this century. Its value, $\Lambda_0 = 1022 \text{ cm}^2/\text{ohm equiv}$, is substantially greater than the contribution of Na^+ ions, which amount to $130 \text{ cm}^2/\text{ohm equiv}$. This observation provided the first indication that some unusual species is formed in this system, a species subsequently identified as the solvated electron.

The mobilities of solvated electrons in polar liquids, although lower by about three or four orders of magnitude than the mobilities of quasi-free electrons, are substantially greater than the mobilities of small negative ions such as Cl^- . For example, the mobility of solvated electrons is $1.08 \times 10^{-2} \text{ cm}^2 \text{ V}^{-1} \text{ sec}^{-1}$ in liquid ammonia at 200°K [82] and $2.5 \times 10^{-3} \text{ cm}^2 \text{ V}^{-1} \text{ sec}^{-1}$ [83] in water at 300°K . These values are five to seven times greater than the mobilities of chloride ions. The discrepancy between the observed mobilities of solvated electrons and those expected on the basis of Stokes' law have been discussed by some workers. For example, Kaplan and Kittel [84] argued that the slippage of solvent molecules may be different for a solvated electron and

for a solvated ion, or that Stokes' law should be modified when applied to particles having sizes comparable to solvent molecules. Although these assertions are valid, the higher mobility of solvated electrons calls for some additional justification. Apparently this phenomenon may result from tunnelling of an electron from its trap to a not too distant cavity developed, perhaps not perfectly, by spontaneous density fluctuations of the solvent molecules.

20. OPTICAL AND ESR SPECTRA OF SOLVATED ELECTRONS

Our knowledge of solvated electrons has been greatly enriched by the spectroscopic and ESR studies reviewed in this section. The blue solutions of alkali metals in liquid ammonia, known since 1864 [85], have been the subject of intense investigations summarized by several authors [86, 317, 318]. Their results led to the belief that solvated electrons are formed in these systems through the dissociation of alkali atoms:



Subsequent extension of these investigations to alkali metals dissolved in amines, and later to their ether solutions, demonstrated that the blue species are also formed in those solvents, implying a basic similarity between the ammonia, ether, and amine systems.

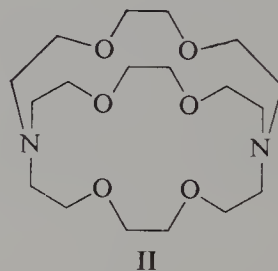
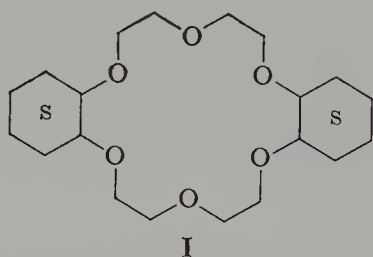
Is the blue color due to solvated electrons? This has been a tempting suggestion, but the answer is rather complex. Ammonia solutions of alkali metals show only one broad and structureless absorption band extending to the infrared [118, 119]. Early investigators claimed that this absorption obeys Beer's law [119a], suggesting that the light-absorbing species is not involved in any dissociative or associative equilibria. However, later studies demonstrated that this law applies only approximately, in a relatively narrow concentration range (see, e.g., [120]); furthermore, the shape and the intensity of the absorption is markedly temperature dependent [118]. Thus it became apparent that the absorption spectrum recorded in liquid ammonia results from the overlap of two absorption bands [120], and its tentative resolution has been achieved recently by studies of its concentration dependence [121].

The electronic spectra of alkali metals in amines or ethers have two clearly distinct bands, referred to as R and IR.* The position of the maximum of

* Earlier studies of these spectra were confused by the observation of a band at 660 nm which appeared in the spectra of all alkali metal solutions. It has been shown recently that this band is due to sodium leached out from the glass of the vessels used in the preparation of the solutions investigated [122].

the R bands depends on the nature of the dissolved metal, implying that it results from the absorption of some aggregate, whereas the shape and the position of the IR band is independent of the metal's nature. For this reason, the IR band was attributed to the solvated electrons [95, 307]—a conclusion firmly established by Dye et al. [308].

Spectral studies of solvated electrons formed by dissolving alkali metals in amines or ethers have been greatly hindered by the low solubility of the metals. A recent observation of Dye and his co-workers [115] greatly facilitated such investigations. The solubility of alkali metals in amines and ethers is substantially enhanced by the presence of small amounts of crown ethers or cryptates. Crown ethers such as **I**, synthesized originally by Pedersen [116], are powerful complexing agents for alkali ions [305]. Even more powerful



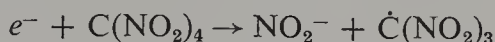
agents, referred to as cryptates, **II**, have been described recently by Lehn et al. [117, 361]. Their addition to ethers and amines increases not only the solubility of alkali metals but also the stability of the resulting solutions.* For example, by adding 5×10^{-3} mole of crown **I** per liter of the solvent one can easily prepare 10^{-4} M solutions of potassium or cesium in THF, stable for days if kept at -78°C . These complexing agents permit one to dissolve an alkali metal even in diethylether cooled to -78°C . Such solutions are stable for a few hours at -78°C and last 5–10 minutes at ambient temperatures.

With the aid of these complexing agents, solutions of sodium and potassium have been prepared in a great variety of solvents [304]. A broad infrared band attributed to the solvated electron is clearly discerned in all these solvents; however, its shape as well as its λ_{max} is greatly affected by their nature. For example, the λ_{max} in ethylamine and diethylether solutions are found to be virtually identical, but the spectrum is substantially broader in the latter than in the former solvent. The position of λ_{max} and the width of the spectrum are strongly influenced by temperature; λ_{max} shifts to *higher* energies and the spectrum broadens as the temperature decreases.

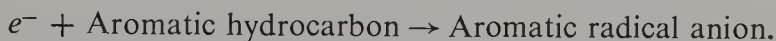
Studies of the optical spectra of solvated electrons gained enormously from the development of pulse radiolysis and flash photolysis techniques. Although pulse radiolysis is a relatively new technique, it has provided, in less

* The lack of stability of alkali metals solution formed in the absence of complexing agents was the source of many difficulties and confusion in the past investigations.

than two decades, the absorption spectra of solvated electrons in a great variety of liquids. While the presence of various aggregates of solvated electrons with cations complicates and often confuses the investigation of e^- absorption in alkali metal solutions, these difficulties are eliminated in pulse radiolysis studies. The shapes of such spectra are those of the genuine solvated electrons. Accurate values for the extinction coefficients are obtained by adding efficient electron-trapping agents to the pulsed liquid and determining the products spectrophotometrically; for example,



or



The most extensive studies have been those of the hydrated electrons, the results being summarized in a recent paper by Hart [123]. The spectrum of hydrated electrons is independent of pH [124] as well as of the mode of their formation. For example, solutions prepared by pulse radiolysis and by the reaction $\text{H} + \text{OH}^- \rightarrow \text{H}_2\text{O} + e^-$ [127], have identical spectra. On the whole, the spectrum of hydrated electrons resembles closely that of ammoniated electrons, but it is displaced toward shorter wavelength, λ_{max} being about 670 nm at 25°C. A bathochromic shift of the absorption is observed as the temperature rises [126], and interestingly the spectrum is still observed at, and even above, the critical temperature of water [125].

Pulse radiolysis and flash photolysis studies of the absorption spectra of electrons solvated by other liquids have been reported by several workers [128, 130, 300, 301]. These spectra resemble those of the hydrated and ammoniated electrons by being intense and broad, showing marked asymmetry at shorter wavelengths and lack of structure even at -78°C . The oscillator strength varies from 0.6 to 0.9, which implies that no intense band exists at energies higher than 4 eV. For the sake of illustration, the spectra of solvated electrons in a series of aliphatic alcohols are shown in Fig. 34.

The agreement between λ_{max} of solvated electrons determined by pulse radiolysis and by the study of alkali metal solutions is fair. A plot of the former versus the latter gives a reasonably good straight line of unit slope [304]; however, the spectra obtained by pulse radiolysis are on the whole sharper than those obtained in alkali metal solutions. Apparently the presence of other species* and the higher concentration broadens the latter spectra. Most of the available data are collected in Table 25.

The characteristic broadness of the spectra of solvated electrons may arise from some unresolved transitions to higher energy levels; alternatively it may

* This point will be thoroughly discussed in the section dealing with the equilibria between solvated electrons and the aggregates.

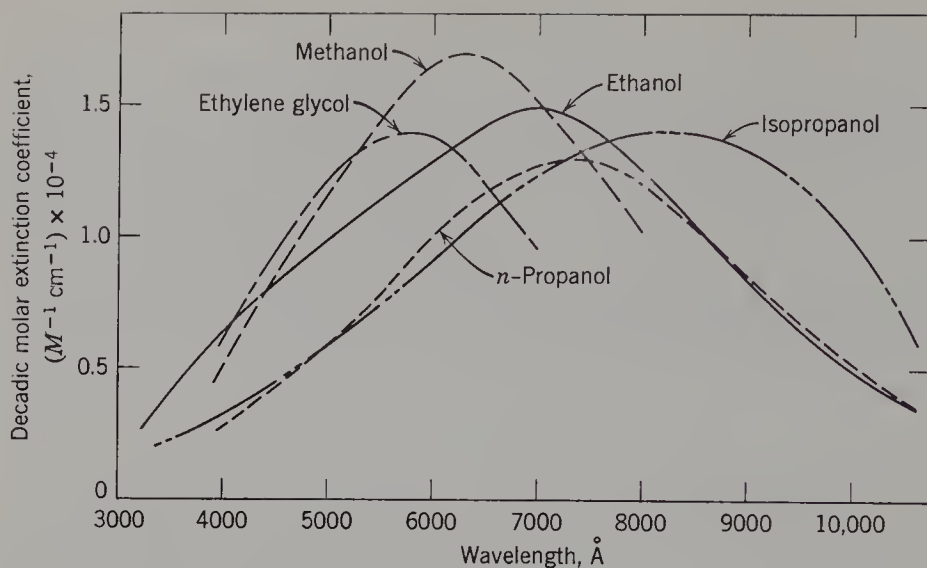


Figure 34. Spectra of solvated electrons in a series of aliphatic alcohols.

Table 25 Spectra of Solvated Electrons in Polar Liquids

Solvent	λ_{\max}^a (nm)	$10^{-4} \epsilon$ (dec) at λ_{\max} ($M^{-1} \text{ cm}^{-1}$)	Oscillator Strength	Ref.
Water	630	1.6	0.65	126
Liquid ammonia	1480 (200 K)	4.9 (200 K)	0.77	302
Ethylenediamine	1315	—	—	
Ethylamine	1805 ^b	—	—	304
Ethyleneglycol	580	1.4	0.68	300
Methanol	630	1.7	0.78	300
Ethanol	700	1.5	0.87	300
1-Propanol	740	1.3	0.59	300
2-Propanol	820	1.4	0.67	300
Diethylether	2300; 1930 ^b	3.5	~1	301, 304
2-Methyltetrahydrofuran	2015	3.9	~1	301
Tetrahydrofuran	2020; 2050 ^b	4.0	~1	301, 304
Dimethoxyethane	2050; 1740 ^b	3.4	~1	301, 304
Diglyme	1915; 1610 ^b	—	—	301, 304
Triglyme	1838	—	—	301
Tetraglyme	1792	—	—	301
Hexamethylphosphorictriamide	2250	—	—	303

Note: The broadness of the spectra makes the determination of λ_{\max} uncertain within ± 15 nm. The extinction coefficients are uncertain to ± 0.2 .

^a When two values are given they are listed in the same sequence as the references.

^b Obtained in the presence of crown ethers or cryptates, see ref. 304.

be attributed to a distribution of cavity sizes [132]. In this connection an interesting observation of Linschitz et al. [134] should be recalled. Photoejection of electrons from lithium carbazole dissolved in methylamine glass at 70°K leads to the formation of trapped, solvated electrons. Their spectrum shifts to shorter wavelengths when the temperature of the glass is slightly raised and then lowered again. This phenomenon implies that the ejected electrons are trapped initially by some poorly developed cavities existing in the glass prior to its irradiation. The low mobility of solvent molecules, caused by the rigidity of the glass, prevents them from attaining the thermodynamically most favorable orientation around a trapped electron. At slightly higher temperatures the mobility of solvent molecules increases sufficiently to permit their reorientation resulting in the formation of "proper" traps. These retain their structure as the temperature is lowered.

This interpretation implies that the preexisting cavities in a liquid or a glass act as primary traps for the injected electrons, their reorientation requiring time. This conclusion is verified by the results reported by Richards and Thomas [135], who observed the spectra of electrons formed at the end of a 12 nsec pulse and trapped in ethanol, or in 3-methylhexane, or 2-methyltetrahydrofuran glass at 77°K. These spectra are changed within 4 μ sec after the flash, indicating a rearrangement of solvent molecules around the trapped electrons. For example, in frozen ethanol a significant growth of the absorbance is observed at 750 nm, whereas the absorbance at longer wavelengths decays. The growth and the decay are synchronous, implying that both result from the same process. Similarly, the absorption maximum observed in 3-methylhexane glass shifts in 4 μ sec from about 1600 nm, observed at the end of the pulse, to about 1400 nm.*

An alternative explanation of these spectral changes should be mentioned. A variety of electron traps is randomly formed in a glass—some are shallow, others deep. It has been suggested by Hammill [136] that the injected electrons are indiscriminately trapped by any imperfection, whatever its well's depth. However, a tunneling process eventually leads to their movement from the shallow to the deep traps. This reallocation process is thus responsible for the observed spectral changes.

The results deduced from the optical spectra have been supplemented by those obtained through ESR spectroscopy. The ESR spectra of alkali metal solutions in liquid ammonia were first reported by Hutchinson and Pastor [87], who extended their investigation down to concentrations as low as 10^{-3} *M*. The line observed at high dilutions is remarkably sharp; for example, its width is only 0.05 G for a 4×10^{-3} *M* solution of potassium in liquid ammonia at -33°C. The equivalent intensity of the signal increases with dilution: the molar magnetic susceptibility approaches a value corresponding to one electron per metal atom at concentrations lower than 10^{-3} *M*.

* Similar results were reported by other investigators [367, 368].

No hyperfine splitting due to protons, ^{14}N , or cations was ever observed in the ESR spectra of liquid ammonia solutions of alkali metals. However, studies of spin relaxation [98–100] provided some information about the interaction of the solvated electron with its surroundings. Such studies are affected, however, by the presence of other paramagnetic species such as e^- , Met^+ ion pairs, which exist even in relatively dilute solutions. At high dilution T_2 becomes concentration independent, but it increases with rising temperature. The results of Pollak [99] indicate that the ^{14}N contact is the limiting factor of T_2 and its contribution to the line width is large. The rate of exchange of NH_3 between the solvation shell of the e^- and the neighboring solvent increases with rising temperature, and this leads to the observed sharpening of the ESR line at higher temperatures because the exchange process takes place in the fast exchange region.

The interaction of solvated electrons with ammonia molecules is manifested by the shift, Δ_K , of nuclear paramagnetic resonance, an effect often referred to as the Knight shift (see ref. 12, p. 254). McConnell and Holm [101] were the first to observe this phenomenon in solutions of sodium in liquid ammonia. A large *positive* shift of the ^{14}N resonance has been observed while the resonance of the ^{23}Na is shifted to a lesser degree. Although no proton resonance shift was observed by McConnell and Holm [101], subsequent work of Hughes [103] revealed a small *negative* proton Knight shift. The proton resonance line appears as a singlet in the spectrum of solution in which the ratio of NH_3/Na exceeds 100, indicating a rapid exchange of protons.

Both the ^{14}N and the ^{23}Na Knight shifts are temperature dependent [105]. The temperature dependence has been accounted for by a model postulating the presence of two paramagnetic species in the liquid ammonia solution [120], namely, a free electron detached from sodium and embedded in a cavity formed in liquid ammonia [102], and an e^- , Na^+ ion pair. Only the latter species contributes to the Knight shift of ^{23}Na , and therefore

$$R \Delta_K(^{23}\text{Na}) \sim \frac{y(1 - \alpha)}{T}$$

where R denotes the ratio NH_3/Na , $y = \chi(T)/\chi(T_0)$ with $\chi(T)$ being the spin susceptibility at T° , and α is the degree of dissociation of e^- , Na^+ ion pairs. For dilute solutions the plot of the reported $R\Delta_K(^{23}\text{Na})$ versus the calculated values of $y(1 - \alpha)/T$ results in a good straight line [120], thus providing evidence for the existence of e^- , Na^+ ion pairs and for the virtual absence of any type of sodium atoms in dilute solutions of sodium in liquid ammonia. A similar treatment calls for a linear relation of $R\Delta_K(^{14}\text{N})$ with y/T ; however, this dependence is poorly obeyed although the expected trend is clearly seen [120]. It seems that the solvated electrons move in a polaron orbital to which the $3s$ atomic orbitals of the neighboring nitrogens contribute—a reminiscence

of a model proposed by Pitzer [104]. The *negative* proton Knight shift may be then explained in a similar way as the negative coupling to protons in radical anions of aromatic hydrocarbons.

The behavior of the blue solutions of alkali metals in amines and in ethers is much more complex because various aggregates of electrons with cations become important, a subject to be discussed in the next section. The blue solutions of alkali metals in amines mostly contain diamagnetic species [95]. Exceptions have been reported; for example, lithium solutions in methylamine give a strong single ESR line [106]. Solutions of sodium in methylamine or ethylenediamine show only a singlet [315]. In contrast, a sharp singlet superimposed on a complex multiplet appears in the ESR spectra of solutions of lithium in several higher amines and their mixtures [107] and a similar ESR spectrum is obtained from solutions of potassium, rubidium, and cesium in aliphatic amines [316a].

Solutions of potassium and cesium in tetrahydrofuran and in dimethoxyethane, originally described by Wilkinson and his associates [94], are also blue and resemble the amine solutions. The first published reports [88, 89] described them as diamagnetic but subsequent investigations of Grob and Ostermayer [114] showed the appearance of ESR spectra of highly dilute solutions of potassium in DME consisting of a sharp single line superimposed on a multiplet. The appearance of such a line has been confirmed by the recent work of Glarum and Marshall [108].

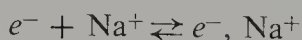
The intensity of the ESR spectrum of alkali metal solutions in amines or in ethereal solvents is greatly enhanced by the addition of crown ethers or cryptates [115]. As has been pointed out earlier, these complexing agents increase the solubility of alkali metals in those solvents, but, significantly, the increase of the signal intensity is greater than the increase in solubility. As in other solutions, a multiplet, arising from the coupling to the nuclear spin of the alkali, is often discerned in those ESR spectra in addition to a sharp single line. A single, extremely sharp ESR line is also obtained from solutions of alkali metals in hexamethylphosphorictriamide [93]. In fact, under favorable conditions, the line observed in the sodium solutions is narrower than 0.05 G. Hexamethylphosphorictriamide is a remarkable solvent for alkali and even for alkaline earth metals [90–92]. The solutions are again blue and extremely reactive; although they burst into flame on contact with air, they are stable at room temperature for at least a day under vacuum. Eventually they decompose forming red, diamagnetic solutions of unknown composition.

The appearance of the sharp line demonstrates the presence of detached, solvated electrons (or perhaps loose e^- , Met^+ pairs) in the pertinent solutions. It is significant that only those solutions that reveal the IR band in their optical spectrum display a sharp single line in their ESR spectrum [307].

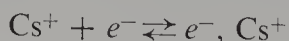
This correlation further strengthens the assignment of the IR band to the solvated electrons. Indeed, as the intensity of the IR band increases, the sharp ESR signal becomes stronger; for example, an increase in the proportion of ammonia in ethylamine-ammonia mixtures enhances both the IR band and the ESR signal [308]. The solvated electrons seem to coexist in equilibrium with aggregates involving cations, and apparently some of these aggregates contribute to absorbance in the IR band, because the concentration of the species giving rise to the sharp ESR line is usually smaller than that calculated from the intensity of the IR band (see p. 136). The nature of these aggregates and their properties will be reviewed in the following section, but we wish to emphasize at this point that the evidence for the presence of solvated electrons in, at least, some alkali metal solutions is undeniable.

21. AGGREGATION OF SOLVATED ELECTRONS

The evidence demonstrating the existence of solvated electrons was reviewed in the preceding section, where the possibility of their association with cations into a variety of aggregates was alluded to. Our knowledge of such aggregates is mainly derived from studies of solutions of alkali metals; for example, concentration dependence of the conductance of solutions of sodium in liquid ammonia [86, 137] provided the first indication of the aggregation tentatively described by equations such as



The symbol e^-, Na^+ denotes some unspecified associate involving an electron and a cation; its nature has been the subject of much speculation (e.g., [313]) which suffered, in the past, from lack of a broad experimental support. The above equilibrium accounts reasonably well for the decrease of equivalent conductance with increasing concentration of the dissolved metal and the corresponding equilibrium constants have values similar to those found for typical ionophores. An instructive example of such a system is provided by dilute solutions of cesium in ethylenediamine [309]. Their optical spectra reveal only the IR band, their limiting conductance obeys Walden's rule, and the equilibrium constant for association

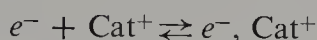


has a value of about $10^4 M^{-1}$ [326], like that of ion pairs of similar salts dissolved in this solvent.

At higher concentrations of the dissolved metal the system changes dramatically. The equivalent conductance reaches a minimum value and

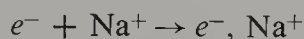
thereafter it *increases* with increasing concentration of the metal [306]. Apparently a transition to the metallic state takes place; the overlap of the atomic orbitals of the cations, which become crowded under such conditions, leads to a conduction band and the valence electrons move then independently of the liquid.

The association of solvated electrons with cations may be observed spectrophotometrically. Photoejection of electrons from suitable salts dissolved in ethereal solvents leads to solvated electrons absorbing at λ_{\max} of about 1300 nm* [311, 312]. This transient decays, giving rise to a new transient whose λ_{\max} depends on the cation; 850 nm for sodium and 1100 nm for potassium. The experimental data indicate a second-order decay attributed to the process



and confirm the expected 1:1 stoichiometry of association. The formation of e^- , Na^+ has also been observed in the flash photolysis of extremely dilute solutions of sodium pyrenide in THF [299], and from the kinetic data reported in that work the equilibrium constant of the dissociation $e^-, \text{Na}^+ \rightleftharpoons e^- + \text{Na}^+$ (in THF) was calculated to be $5 \times 10^{-7} M$, a value typical of ion pairs of comparable salts.

The most convincing evidence demonstrating the combination of solvated electrons with sodium cations has been obtained by the pulse radiolysis technique [314]. Pulses as short as 20 nsec produce solvated electrons [301], $\lambda_{\max} = 2120$ nm in tetrahydrofuran. In the presence of an excess of sodium tetraphenylboride, the solvated electrons are converted into a new transient having an absorption maximum at 890 nm. The kinetics of its formation then rigorously obeys the first-order law, and the pseudo-first-order rate constant is strictly proportional to the concentration of the free Na^+ ions and not to the concentration of the salt.† Hence the reaction represents the association



its bimolecular rate constant being determined as $(7.9 \pm 0.7) \times 10^{11} M^{-1} \text{sec}^{-1}$, a value similar to that previously obtained from the photolysis study of sodium pyrenide, $\sim 4 \times 10^{11} M^{-1} \text{sec}^{-1}$ [299]. Interestingly, this rate constant is *higher* than that calculated by the Debye approach for diffusion-controlled association, implying that the collision cross-section of electron capture is greater than the cross-section determining its diffusion. Sodium cation is therefore one of the most efficient scavengers of electrons.

* Observed in MeTHF at -150°C .

† Apparently the reaction $e^- + \text{Na}^+$, $\text{BPh}_4^- \rightarrow e^-, \text{Na}^+ + \text{BPh}_4^-$ is much slower than $e^- + \text{Na}^+ \rightarrow e^-, \text{Na}^+$.

The association reaction has an activation energy of 1.4 kcal/mole; the corresponding enthalpy and entropy of activation are 0.8 kcal/mole and $-1 \text{ cal K}^{-1} \text{ mol}^{-1}$, respectively, both values being consistent with the virtual diffusion character of the process.

Comparison of the spectrum of e^- , Na^+ with that of e^- shows that the latter exhibits a large shift toward shorter wavelength amounting to 0.8 eV—a substantial perturbation of the transition energy of e^- by the sodium cation. The width at half-height of the 890-nm band is 7000 cm^{-1} compared with 3500 cm^{-1} found for e^- in THF; that is, the association of a solvated electron with sodium considerably broadens its absorption. The decimal extinction coefficient of e^- , Na^+ at λ_{max} is 2.40×10^4 , it was determined by the conversion of e^- , Na^+ to sodium biphenylide. The oscillator strength is calculated to be about 1. The 890-nm band shifts toward the blue with decreasing temperature, λ_{max} being 840 nm at -59°C . Hence the interaction of the electron-sodium pair with the solvent is strong.

It is only reasonable to anticipate that free atoms, Met, also should be among the products of dissolution of alkali metals. These in turn may ionize into e^- , Met^+ ion pairs, which could eventually dissociate into free solvated electrons, e^- , and cations, Met^+ . Two questions arise: What are the proportions of free atoms in various systems? and what is the nature of a free atom in a solution and how does it differ from a gaseous atom?

ESR studies shed much light on the problems of the existence and the nature of free alkali atoms in amines or ethers. Let us first review the reported facts and then try to arrive at a plausible conclusion.

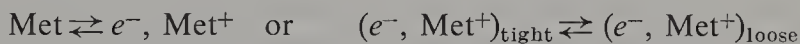
Metal hyperfine splittings in solutions of alkali metals (Rb and Cs) in methylamine were reported in 1963 [315] and these findings were soon confirmed and the observations extended to other systems by several research groups [107, 308, 316, 319]. A very extensive study of Bar-Eli and Tuttle [107] showed well-resolved quadruplets in solutions of potassium in ethylamine without revealing any singlet. Obviously, free potassium atoms or e^- , K^+ pairs, and not solvated electrons, have to be present in such a solution. The potassium coupling constant increases with rising temperature and decreases on the addition of a better solvating agent; for example, on addition of methylamine to a solution of potassium in ethylamine the lines broaden, their spacing decreases, and eventually they merge into a single, broad line that becomes sharper as the proportion of methylamine increases. These observations seem to have a general validity—they apply to solutions of other alkali metals, including Na [316a], Rb, and Cs [319], and to other solvents, such as THF [316b]. It is not uncommon to observe a collapse of the multiplet into a broad line at a sufficiently low temperature and subsequent sharpening of that line as the temperature decreases further. It is also significant that, at least in some systems, the external lines of a multiplet—those corresponding

to higher m_s values—are broader than the internal ones [316b, 319], a fair evidence of some exchange process.*

In some systems, as mentioned previously, a singlet line is superimposed on a multiplet, as exemplified by solutions of sodium in ethylamine-ammonia mixtures [316a] or of cesium or rubidium in ethylamine [319]. Dilution then increases the intensity of the singlet and, in fact, the relation $[\text{singlet}]^2/[\text{multiplet}] = \text{constant}$ has been claimed for the sodium-ethylamine-ammonia system [316a].

Several models may account for the observations presented above. The discovery of the metal hyperfine splitting proves unequivocally the 1:1 stoichiometry of the “monomers,” and it is important to note that the coupling may reach or even surpass 50% of its atomic value under suitable conditions. This implies the presence of free Met atoms which are in a rapidly established equilibrium with e^- , Met^+ ion pairs. Significantly, the largest metal hyperfine coupling constants are not affected by further increase of temperature,† again evidence indicating the existence of free metal atoms.

The reported temperature dependences of the metal hyperfine multiplets may be rationalized in terms of the rapid equilibria



The coupling constants are expected to decrease along the series $\text{Met} > (e^-, \text{Met}^+)_{\text{tight}} > (e^-, \text{Met}^+)_{\text{loose}}$, and it is plausible to anticipate a shift to the right of the above equilibria at lower temperatures. The proposed transformations also account for the m_z dependence of the multiplet components and for their broadening at lower temperatures. Since the recorded lines result from fast exchanges, cooling leads to line broadening.

Line broadening is observed when the solvating power of the medium is increased by the addition of a better solvating agent. In a mixture of two or more solvents species having solvation shells of different composition are present and then exchange processes are more complex than in a pure solvent. This accounts for the increased width of the lines. Furthermore, the exchange in a more powerful solvating liquid is slower than in a poorer solvent, and this factor also leads to broader lines.

Other processes that contribute to the line width include exchange of solvent molecules between the solvation shells and the bulk of the liquid, and exchange with the cations. The latter exchange,



* See, however, ref. 319, where anisotropy is invoked to explain the line width dependence as well as the trend in the line spacing in the multiplet.

† Extrapolation of the metal hyperfine coupling, a_{Me} , to infinite temperature, e.g., by plotting a_{Me} versus $1/T$, leads to a value close for those of the gaseous atoms.

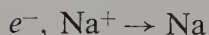
was clearly demonstrated by the effect of added potassium iodide on the ESR spectrum of potassium metal solution in a methylamine-ethylamine mixture [107]. Thereupon the quadruplet collapsed into a single sharp line.

The rapid exchange of solvent molecules between the solvation shells and the bulk of the liquid smears out the hyperfine structure due to the solvent nuclei. One striking exception has been reported; the ESR spectra of lithium dissolved in aliphatic amines show a multiplet of nine lines resulting from coupling to four equivalent nitrogens, but surprisingly no coupling to Li is seen [107, 316c]. Apparently four molecules of amine are tightly bound to some paramagnetic species. It is not the solvated electron that binds the amines, because the nature of the counterion should be then of no importance, contrary to the experimental evidence. It is improbable that lithium atoms are capable of bonding the amines so strongly, and hence the binding to Li^+ cation of an e^- , Li^+ pair remains as the only plausible explanation of this phenomenon. The equivalence of the four N nuclei could result from a rapid rotation of the Li^+ (amine)₄ complex.

An interesting observation of Fisher, Rämme, Claesson, and Szwarc [299] should be mentioned. An equilibrium such as $e^-, \text{Na}^+ \rightleftharpoons \text{Na}$ could be upset by a sudden increase of the concentration of the pairs, but not of the monomer. For example, electron photoejection from sodium pyrenide, π^- , Na^+ , suddenly increases the concentration of e^- , Na^+ if induced by a flash of light. The electron return



may be delayed, for example, by high dilution of the reagents, and then the collapse of the pair



may compete successfully with the reformation of the pyrenide. Of course, the sodium atoms react with pyrene, π , and hence all the photolyzed π^- , Na^+ is reformed eventually. The collapse of the pair is manifested by the rapid decay of the transient absorption due to e^- , Na^+ compared to the slower reappearance of π^- , Na^+ . The kinetic results demonstrate the first-order character of the collapse, its unimolecular rate constant being determined as about 10^4 sec^{-1} . Since the reaction $e^-, \text{Na}^+ + \pi \rightarrow \pi^-, \text{Na}^+$ proceeds with a bimolecular rate constant of the order of $10^{10} M^{-1} \text{ sec}^{-1}$, the collapse can be observed only if the concentration of pyrene is $10^{-7} M$ or less. Such high dilutions were attained in the work of Fisher et al. [299] by a relatively simple approach (see ref. 226).

The conclusions of Fisher et al. have been questioned recently by Gilling and Kloosterboer [365] who claimed that the disappearance of e^- , Na^+ pairs

is due to their capture by benzene,



followed by the reaction



However, the addition of large amounts of benzene (up to $10^{-2} M$) to the photolyzed solution did not affect the rate of e^- , Na^+ disappearance.

The models of the "monomer" postulating the presence of several distinct species, such as Met, $(e^-, \text{Met}^+)_{\text{tight}}$, $(e^-, \text{Met}^+)_{\text{loose}}$, should be contrasted with the model of the expanded atom proposed by Becker, Lindquist, and Alder [313] and elaborated by Bar-Eli and Tuttle [107]. The highest s electron of a dissolved alkali atom is supposed to move in an expanded orbital that overlaps one or more layers of solvent molecules. At lower temperatures an increasing number of solvent layers become involved in the expanded orbital, reducing therefore the odd electron density on the metal nucleus. In spite of its appeal, this model does not seem realistic, although it cannot be decisively ruled out.

Finally, some thoughts should be devoted to the diamagnetic species formed in alkali metal solutions in liquid ammonia, amines, and ethers. In fact, these species represent the bulk of the metal dissolved in some amines and ethers. Various interpretations of their nature led to much confusion in the past, but it seems that the correct structure has been deduced recently by Golden, Guttman, and Tuttle [320]. These workers described the diamagnetic species as negative alkali ions, Met^- . The existence of the negative alkali ions in the gas phase was recognized some years ago [321–323], and in solution their stability should be substantially increased by solvation. Recent isolation of the crystalline salt $(\text{Na cryptate})^+$, Na^- and its characterization by chemical analysis and by its chemical behavior, as well as by single crystal X-ray studies, provides undeniable proof for the reality of Na^- ions [362]. The salt is stable in vacuo for days at room temperature. It has a shiny metallic appearance but the conductance of the solid indicates its semiconductor structure.

Negative alkali ions are responsible for the R band absorption of alkali metal solutions in amines and ethers. This absorption is interpreted as a charge transfer-to-solvent transition [324] similar to that characterizing the spectrum of I^- anion. It shows all the features of such a transition: pronounced dependence of λ_{max} on the solvent, shift of the maximum to higher energies on lowering the temperature of the solution, correlation of λ_{max} with the size of the anion, and so on [304]. For example, the λ_{max} of Na^- at ambient temperature shifts from 763 nm in hexamethylphosphorotriamide to 658 nm in ethylene diamine, whereas in those two solvents K^- absorbs at

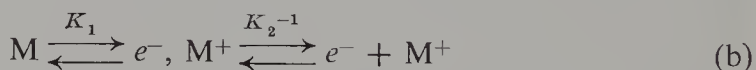
935 and 847 nm, respectively. The R band becomes narrower at lower temperatures, behavior contrasting that of the IR absorption of e^- , which broadens under these conditions.

The stoichiometry of Met^- (two e^- for one Met^+) is established by determining the oscillator strength of Na^- in ethylene diamine [325]. The extinction coefficient of Na^- in that solvent was determined by converting e^- into Na^- . Mixing in a stop-flow apparatus a dilute solution of cesium in ethylene diamine* with a known amount of NaBr or NaI in the same solvent leads to the desired conversion. The extinction coefficient of Na^- at its λ_{max} is found to be $(8.2 \pm 0.3) \times 10^4$, leading to the oscillator strength of 1.9 ± 0.2 . A value of 2 is expected for an absorber with two equivalent electrons participating in the transition.

Studies of the conductance of Na^+ , Na^- in methylamine [326] led to Λ_0 of 158. Walden's rule gives Λ_0^+ of 64 for Na^+ , and hence $\Lambda_0^- = 94$ for Na^- ; the negative ion is more mobile than the positive Na^+ because of its lesser solvation.

The negative sodium ion, Na^- , seems to behave differently from the solvated electron. The rate constant of the dissociation, $\text{Na}^- \rightarrow \text{Na} + e^-$ (or $\text{Na}^+ + 2e^-$?) is apparently smaller than 10^3 sec^{-1} [325]; hence Na^- may react before being dissociated. Indeed, it is claimed that Na^- forms a charge transfer complex with anthracene while e^- is rapidly captured yielding anthracene radical anion.

Let us examine the relations between the equilibria established in alkali metal solutions. The following scheme represents most conveniently the alkali metal systems:



The neutral M is probably the minor component of the system. In a powerfully solvating medium such as liquid ammonia and at high dilution the complete dissociation to $e^- + \text{M}^+$ is favored. Lowering the solvating power of the medium favors the association (c) and the formation of M^- . The addition of cation complexing agents, crowns or cryptates, affects equilibria (b) and (d) and increases the concentration of e^- by removing M^+ : $\text{M}^+ + \text{crown (cryptate)} \rightarrow \{\text{M}^+, \text{crown (cryptate)}\}$. The concentration of all the solvated

* Cesium in dilute ethylene diamine solution is virtually quantitatively dissociated into e^- and Cs^+ .

electron pairs also increases, because $\{e^-, \text{crown (cryptate), } M^+\}$, as well as e^-, M^+ , is now present in the solution; although, the concentration of the latter pairs is *not* affected by the addition of the complexing agent. The increase in the concentration of e^- leads to increase in the concentration of M^- through equilibrium (c). For a saturated solution in the absence of the complexing agent, the ratio

$$\frac{[M^-] + [M^-, M^+]}{[e^-] + [e^-, M^+]} = \text{const} \frac{1 + K_4[M^+]}{1 + K_2[M^+]}$$

where $\text{const} = K_1[M]$ depends only on the nature of solvent and on its temperature. The addition of complexing agent has a twofold effect: it produces the complexed ion pairs of e^-, M^+ and of M^-, M^+ (the respective complexing constants being K_{e^-, M^+} and K_{M^-, M^+}) and *decreases* the concentration of M^+ because its complexing increases the concentration of the free e^- and M^- ions. Therefore, in a saturated solution, the ratio

$$\frac{[M^-] + [M^-, M^+] + [M^-, X, M^+]}{[e^-] + [e^-, M^+] + [e^-, X, M^+]} = \text{const} \frac{1 + K_4(1 + K_{M^-, M^+})[M^+]}{1 + K_2(1 + K_{e^-, M^+})[M^+]}$$

varies only slightly as the concentration of the complexing agent increases. For most systems one expects $K_2 > K_4$ but $K_{e^-, M^+} < K_{M^-, M^+}$.

In conclusion, the addition of increasing amounts of a cation complexing agent increases the concentration of e^- , M^- , and of their *complexed* ion pairs, but the concentration of the neutral atoms M and of the uncomplexed pairs e^-, M^+ and M^-, M^+ remains unaffected. Therefore in a solution produced with the aid of such complexing agents only a negligible proportion of the dissolved metal is present in the form of neutral atoms, M , in agreement with the observations.

22. ELECTRON EJECTION IN LIQUIDS AND GLASSES

Ejection of electrons in a liquid or glass may be achieved either photochemically or by radiolysis. In a conventional photolysis the electron is ejected from solute molecules which absorb the actinic light; the solvent is usually transparent. In contrast, radiolysis leads to ejection of electrons from the solvent.

Lewis and his co-workers [328] were the first to recognize fully the significance of photoionization taking place in a glass. UV irradiation of frozen solutions of phenols, amines, and some dyes led to the formation of radical cations which were identified spectrophotometrically; however, solvated electrons were not detected in the course of that study. Their detection was accomplished later, during photolytic investigations of frozen solutions of

metallic lithium or lithium carbazole in methylamine [134]. Photoejection of electrons from frozen solutions of aromatic radical-anion salts in 2-MeTHF was observed by Zandstra and Hoijtink [329]. Subsequently, van Voorst and Hoijtink [330] reported the appearance of a broad absorption at $\nu_{\max} = 7.7$ kK, which was attributed to solvated electrons because it was unaffected by the nature of the generator (whether perylene $^{\cdot-}$, Li $^+$ or tetracene $^{2-}$, 2Li $^+$). Similar results, obtained by flash photolysis of aqueous solutions of other negative ions, were reported by other investigators (e.g., [331, 127]).

Flash photolytic studies of electron photoejection from aromatic radical anions and dianions have been reported recently by several groups [226, 272, 299, 311, 312]. These investigations not only demonstrate the occurrence of electron photoejection but also show that solvated electrons are formed first and thereafter they become associated with cations into pairs.

Is the solvated electron the first product of photoejection, or does the process initially produce a quasi-free electron? The answer to this question was provided by recent studies of Rentzepis et al. [333], who utilized the ultrafast picosecond spectroscopy [334]. The results demonstrate that a quasi-free electron is formed first and it becomes localized about 2 psec later. Furthermore, the IR spectrum of the hydrated electrons “evolves in time.” It shifts toward longer wavelengths and the “normal” absorption spectrum of hydrated electrons develops after 4 psec.* These findings, which refer to aqueous solution of ferrocyanide, need not be valid for other systems. One may visualize transitions in which an electron tunnels directly from the excited species to a neighboring cavity formed in the irradiated liquid by random fluctuations of its density. Such a process most likely occurs in an indirect photoionization proceeding through an autoionizing state.

This brings us to the next question: Is the electron photoejection process of a free ion different from that of its ion pairs? The results reported by our group [226, 272, 299] shed light on this problem. Under identical irradiation conditions the quantum yield of electron ejection from sodium pyrenide is about 15 times greater in tetrahydrofuran than in tetrahydropyrane [226]. The quantum yield in tetrahydrofuran is not affected by the addition of Na $^+$, BPh $_4^-$, which converts the free pyrenide ions into ion pairs. Hence the effect has to be attributed to the different structures of the ion pairs—tight pairs are present in tetrahydropyrane but loose pairs are dominant in tetrahydrofuran.**

An even more striking observation was reported by Levin et al. [272]. Flash photolysis leads to electron photoejection from the sodium salt of tetraphenylethylene dianion in tetrahydrofuran, but no ejection is observed

* A detailed discussion of these problems is outlined in ref. 364.

** Alternative interpretation of these observations is reported in ref. 365. The rebuttal is pending.

in dioxane solution, even for flashes of higher power. In both systems the dianions are paired with two sodium cations, but apparently their structures are different.

The effect of ion pairing and of the nature of ion pairs on the probability of electron photoejection deserves further study. Apparently the auto-ionizing excited state is capable of transferring the electron to the associated cation, and the resulting new pairs undergo electron transfer in a cage process before the partners have time to separate. Some new informations pertaining to these problems have been obtained recently by means of picosecond spectroscopy [366].

23. CONCLUDING REMARKS

We surveyed in this chapter some simple elementary reactions involving electron-transfer steps. The complex redox processes, although of great interest to organic chemists, were not discussed. It has been our intention to show the reader the physical aspects of electron-transfer steps and to focus his attention on the role played in these reactions by the solvent, counterions, complexing agents, and so on. This intention has largely determined the choice of examples for the discussion, and although some of them are esoteric, they serve well in revealing the principles operating in electron-transfer steps. For the same reason much space has been devoted to the discussion of gas phase reactions and to detailed considerations of models of the solvated electrons and of their aggregates with counterions.

In conclusion, we wish to acknowledge the support of our studies by the National Science Foundation.

REFERENCES

1. G. V. Marr, *Photoionization Processes in Gases*, Academic Press, New York, 1967.
2. W. A. Chupka, in *Ion-Molecule Reactions*, J. L. Franklin (Ed.), Plenum Press, New York, 1972, pp. 33-76.
3. D. W. Turner et al., *Molecular Photoelectron Spectroscopy*, Interscience, New York, 1970.
4. F. H. Field and J. L. Franklin, *Electron Impact Phenomena*, Academic Press, New York, 1957.
5. F. M. Page and G. C. Goode, *Negative Ions and Magnetron*, Interscience, New York, 1969.
6. W. E. Wentworth and E. Chen, to be published.
7. J. L. Franklin (Ed.), *Ion-Molecule Reactions*, Plenum Press, New York, 1972.
8. H. S. W. Massey and E. H. S. Burhop, *Electronic and Ionic Impact Phenomena*, Clarendon Press, New York, 1952.
9. E. N. McDaniell, *Collision Phenomena in Ionized Gases*, Wiley, New York, 1964.

10. (a) J. Halpern, *Q. Rev.*, **15**, 207 (1961); (b) R. A. Marcus, *Ann. Rev. Phys. Chem.*, **15**, 155 (1964); (c) F. Basolo and R. G. Pearson, *Mechanisms of Inorganic Reactions*, 2nd ed., Wiley, New York, 1967; (d) I. Ruff, *Q. Rev.*, **22**, 199 (1968); (e) H. Taube, *Electron Transfer Reactions of Complex Ions in Solution*, Academic Press, New York, 1970.
11. C. Kittel, *Elementary Solid State Physics*, Wiley, New York, 1962.
12. M. Szwarc (Ed.), *Ions and Ion Pairs in Organic Reactions*, Interscience, New York, 1972.
13. T. Koopmans, *Physics*, **1**, 104 (1934).
14. W. E. Wentworth, E. Chen, and J. E. Lovelock, *J. Phys. Chem.*, **70**, 445 (1966); see also ref. 6.
15. C. A. Coulson and H. A. Strauss, *Proc. Roy. Soc. (London) A*, **269**, 443 (1962).
16. U. Fano and J. W. Cooper, *Rev. Modern Phys.*, **40**, 441 (1968).
17. K. Watanabe, *J. Chem. Phys.*, **22**, 1564 (1954); **26**, 542 (1957).
18. K. Watanabe, F. F. Marmo, and E. C. Y. Inu, *Phys. Rev.*, **91**, 1155 (1953).
19. L. M. Branscomb, in *Advances in Electronics and Electron Physics*, L. Marton (Ed.), Vol. IX, Academic Press, New York, 1957.
20. S. J. Smith and L. M. Branscomb, *Rev. Sci. Instrum.*, **31**, 733 (1960).
21. L. M. Branscomb, in *Atomic and Molecular Processes*, D. R. Bates (Ed), Academic Press, New York, 1962.
22. D. S. Burch, S. J. Smith, and L. M. Branscomb, *Phys. Rev.*, **112**, 171 (1958); see also Erratum, *Phys. Rev.*, **114**, 1652 (1969).
23. L. M. Branscomb, *Phys. Rev.*, **148**, 11 (1966).
24. B. Steiner, *J. Chem. Phys.*, **49**, 5097 (1968).
25. P. Warneck, *Chem. Phys. Lett.*, **3**, 532 (1969).
26. D. W. Turner, *Chem. Brit.*, **4**, 435 (1968).
27. Chapter II of ref. 3.
28. F. O. Ellison and H. Schull, *J. Chem. Phys.*, **23**, 2348 (1955).
29. (a) R. Nordbeg, K. Siegbahn, and B. J. Lindberg et al., *Ark. Kemi*, **28**, 257 (1967); (b) B. J. Lindberg, *23rd International IUPAC Congress*, Boston, 1971, (c) I. D. Thomas, *J. Chem. Phys.*, **52**, 1373 (1970); *J. Am. Chem. Soc.*, **92**, 4184 (1970).
30. K. Siegbahn et al., *ESCA—Electron Spectroscopy for Chemical Analysis*, Uppsala University, Uppsala, Sweden, 1971.
31. F. Mohler and C. Boeckner, *J. Res. Nat. Bur. Std.*, **5**, 51, 399 (1930).
32. H. M. James, *J. Chem. Phys.*, **3**, 9 (1935).
33. (a) R. F. Barrow, N. Travis, and C. V. Wright, *Nature*, **187**, 141 (1960); (b) E. W. Robertson and R. F. Barrow, *Proc. Chem. Soc.*, **1961**, 329.
34. Y. Lee and B. H. Mahan, *J. Chem. Phys.*, **42**, 2893 (1965).
35. Yu. F. Bydin, *Soviet Phys.—JETP*, **19**, 1091 (1964).
36. A. W. Weiss, *Phys. Rev.*, **166**, 70 (1968).
37. H. S. W. Massey, *Negative Ions*, Cambridge University Press, Cambridge, 1950.
38. P. M. Collins, L. G. Christophorou, E. L. Chaney, and J. G. Carter, *Chem. Phys. Lett.*, **4**, 646 (1970).
39. (a) R. S. Berry, C. W. Reimann and G. N. Spokes *J. Chem. Phys.*, **37**, 2278 (1962); (b) R. S. Berry and C. W. Reimann, *J. Chem. Phys.*, **38**, 1540 (1963); (c) R. S. Berry,

- J. C. Mackie, R. L. Taylor, and R. Lynch, *J. Chem. Phys.*, **43**, 3067 (1965); (d) R. S. Berry, C. W. David, and J. C. Mackie, *J. Chem. Phys.*, **42**, 1541 (1965).
40. P. P. Sutton and J. E. Mayer, *J. Chem. Phys.*, **2**, 145 (1934).
 41. J. J. Mitchell and J. E. Mayer, *J. Chem. Phys.*, **8**, 282 (1940).
 42. D. T. Vier and J. E. Mayer, *J. Chem. Phys.*, **12**, 28 (1944).
 43. P. M. Doty and J. E. Mayer, *J. Chem. Phys.*, **12**, 323 (1944).
 44. G. Glockler and M. Calvin, *J. Chem. Phys.*, **3**, 771 (1935); **4**, 492 (1936).
 45. F. M. Page, *Trans. Faraday Soc.*, **56**, 1742 (1960); **57**, 359 (1961).
 46. (a) J. Kay and F. M. Page, *Trans. Faraday Soc.*, **62**, 3081 (1966); (b) A. L. Farragher and F. M. Page, *Trans. Faraday Soc.*, **62**, 3072 (1966); **63**, 2369 (1967).
 47. F. M. Page, *J. Chem. Phys.*, **49**, 2466 (1968).
 48. J. Berkowitz, W. A. Chupka, and T. A. Walter, *J. Chem. Phys.*, **50**, 1497 (1969).
 49. I. N. Bakulina and N. I. Ionov, *Dokl. Akad. Nauk. SSSR*, **105**, 680 (1955); *Soviet Phys. Doklady*, **2**, 243 (1957).
 50. T. L. Bailey, *J. Chem. Phys.*, **28**, 792 (1958).
 51. E. Ya Zandberg and N. I. Ionov, *Soviet Phys. Uspekki*, **67**, 255 (1959).
 52. R. N. Compton, R. H. Huebner, P. W. Reinhardt, and L. G. Christophorou, *J. Chem. Phys.*, **48**, 901 (1968).
 53. (a) J. E. Lovelock, *Nature*, **189**, 729 (1961); *Anal. Chem.*, **33**, 162 (1961); **35**, 474 (1963); (b) J. E. Lovelock, P. G. Simmonds, and W. J. A. Vandenheuvel, *Nature*, **197**, 249 (1963).
 54. W. E. Wentworth, E. Chen, and J. E. Lovelock, *J. Phys. Chem.*, **70**, 445 (1966).
 55. W. E. Wentworth, R. S. Becker, and R. Tung, *J. Phys. Chem.*, **71**, 1652 (1967).
 56. R. S. Becker and E. Chen, *J. Chem. Phys.*, **45**, 2403 (1966).
 57. W. E. Wentworth and R. S. Becker, *J. Am. Chem. Soc.*, **84**, 4263 (1962).
 58. W. E. Wentworth and E. Chen, *J. Phys. Chem.*, **71**, 1929 (1967).
 59. (a) L. Rolla and G. Piccardi, *Atti. Acad. Nazl. Lincei*, **2**, 29, 128, 173 (1925); (b) G. Piccardi, *Atti. Acad. Nazl. Lincei*, **3**, 413, 566 (1926); (c) G. Piccardi, *Z. Physik*, **43**, 899 (1927); (d) L. Rolla and G. Piccardi, *Atti. Acad. Nazl. Lincei*, **5**, 546 (1927).
 60. H. Smith and T. M. Sudgen, *Proc. Roy. Soc. A*, **211**, 31, 58 (1952).
 61. D. K. Bohme and L. B. Young, *Can. J. Chem.*, **49**, 2918 (1971).
 62. K. Watanabe, T. Nakayama, and J. Mottl, *Rept. to the Dept. of Army*, No. 5B-99-01-004 ORD TB2-001-00R (1959).
 63. M. J. S. Dewar and S. D. Worley, *J. Chem. Phys.*, **51**, 263 (1969).
 64. L. Landau, *Physik. Z. Sowjetunion*, **3**, 664 (1933).
 65. J. Jortner, in *The Chemical and Biological Action of Radiation*, **14**, pp. 7-72, Masson et Cie, Paris (1970).
 66. B. Halpern, J. Lekner, S. A. Rice, and R. Gomer, *Phys. Rev.*, **156**, 351 (1967).
 67. T. F. O'Malley, *Phys. Rev.*, **130**, 1020 (1963).
 68. L. Meyer, H. T. Davis, S. A. Rice, and R. J. Connelly, *Phys. Rev.*, **126**, 1927 (1962).
 69. B. Halpern and R. Gomer, *J. Chem. Phys.*, **43**, 1069 (1965).
 70. L. S. Miller, S. Howe, and W. E. Spear, *Phys. Rev.*, **166**, 861 (1968).
 71. G. Careri, F. Scarmuzi, and J. O. Thompson, *Nuovo Cimento*, **13**, 186 (1959).
 72. B. E. Springett, M. H. Cohen, and J. Jortner, *J. Chem. Phys.*, **48**, 2720 (1968).

73. O. H. LeBlanc, *J. Chem. Phys.*, **30**, 1443 (1959).
74. P. H. Tewari and G. R. Freeman, *J. Chem. Phys.*, **49**, 4394 (1968).
75. W. F. Schmidt and A. O. Allen, *J. Chem. Phys.*, **50**, 5037 (1969).
76. R. M. Minday, L. D. Schmidt, and H. T. Davis, *J. Chem. Phys.*, **50**, 1473 (1969).
77. A. S. Davidov and M. F. Deigen, *Zh. Expt. Theoret. Phys. USSR*, **26**, 300 (1954).
78. C. A. Kraus and W. W. Lucasse, *J. Am. Chem. Soc.*, **43**, 2529 (1921).
79. J. Jortner, *Molec. Phys.*, **5**, 257 (1962); *J. Chem. Phys.*, **30**, 839 (1959).
80. J. H. Baxendale, *Radiation Res., Suppl.* **4**, 139 (1964).
81. C. A. Kraus, *J. Am. Chem. Soc.*, **30**, 1323 (1908).
82. C. A. Kraus, *J. Am. Chem. Soc.*, **43**, 749 (1921).
83. K. H. Schmidt and W. L. Buck, *Science*, **151**, 70 (1966).
84. J. Kaplan and C. Kittel, *J. Chem. Phys.*, **21**, 1429 (1953).
85. W. Weyl, *Pogg. Ann.*, **121**, 601 (1864).
86. C. A. Kraus, *J. Chem. Educ.*, **30**, 83 (1953).
87. C. A. Hutchison and R. C. Pastor, *J. Chem. Phys.*, **21**, 1959 (1953).
88. F. Cafasso and B. R. Sundheim, *J. Chem. Phys.*, **31**, 809 (1959).
89. F. S. Dainton, D. M. Wiles, and A. N. Wright, *J. Polymer Sci.*, **45**, 111 (1960); *J. Chem. Soc. (London)*, **1960**, 4283.
90. H. Normant and M. Larchevegue, *Compt. rend.*, **260**, 5062 (1965).
91. H. Normant, T. Guvigny, J. Normant, and B. Angelo, *Bull. Soc. Chim. (France)*, **1965**, 1561.
92. H. Normant, *Bull. Soc. Chim. (France)*, **1966**, 3362.
93. G. Frenkel, S. H. Ellis, and D. T. Dix, *J. Am. Chem. Soc.*, **87**, 1406 (1965).
94. J. L. Down, J. Lewis, B. Moore, and G. Wilkinson, *Proc. Chem. Soc.*, **1957**, 209; *J. Chem. Soc.*, **1959**, 3767.
95. G. W. A. Fowles, W. R. McGregor, and M. C. R. Symons, *J. Chem. Soc.*, **1957**, 3329.
96. S. Windwer and B. R. Sundheim, *J. Phys. Chem.*, **66**, 1254 (1962).
97. R. R. Dewald and J. L. Dye, *J. Phys. Chem.*, **68**, 121 (1964).
98. C. A. Hutchison and D. E. O'Reilly, *J. Chem. Phys.*, **34**, 1279 (1961).
99. V. L. Pollak, *J. Chem. Phys.*, **34**, 864 (1961).
100. R. J. Blume, *Phys. Rev.*, **102**, 31 (1956).
101. H. M. McConnell and C. H. Holm, *J. Chem. Phys.*, **26**, 1517 (1957).
102. R. A. Ogg, *Phys. Rev.*, **69**, 668 (1946).
103. T. R. Hughes, *J. Chem. Phys.*, **38**, 202 (1963).
104. K. S. Pitzer, *J. Chem. Phys.*, **29**, 453 (1958).
105. J. V. Acrivos and K. S. Pitzer, *J. Phys. Chem.*, **66**, 1693 (1962).
106. E. C. Levinthal, E. H. Rogers, and R. A. Ogg, *Phys. Rev.*, **82**, 182 (1951).
107. K. Bar-Eli and T. R. Tuttle, *J. Chem. Phys.*, **40**, 2508 (1964).
108. S. H. Glarum and J. H. Marshall, *J. Chem. Phys.*, **52**, 5555 (1970).
109. P. H. Tewari and G. R. Freeman, *J. Chem. Phys.*, **51**, 1276 (1969).
110. J. P. Dodelet and G. R. Freeman, *Can. J. Chem.*, **50**, 2667 (1972).
111. M. G. Robinson and G. R. Freeman, *Can. J. Chem.*, **51**, 641 (1973).

112. W. F. Schmidt and A. O. Allen, *J. Chem. Phys.*, **52**, 4788 (1970).
113. J. P. Dodelet, K. Shiusaka, and G. R. Freeman, *J. Chem. Phys.* **59**, 1293 (1973).
114. C. R. Grob and F. Ostermayer, *Helv. Acta*, **45**, 1119 (1962).
115. J. L. Dye, M. G. DeBacker, and V. A. Nicely, *J. Am. Chem. Soc.*, **92**, 5226 (1970).
116. C. J. Pedersen, *J. Am. Chem. Soc.*, **89**, 7017 (1967); **92**, 386, 391 (1970).
117. J. M. Lehn, J. P. Sauvage, and B. Dietrich, *Tetrahedron Lett.*, **34**, 2885 (1969); *J. Am. Chem. Soc.*, **92**, 2916 (1970).
118. H. Blades and J. W. Hodgins, *Can. J. Chem.*, **33**, 411 (1955).
119. (a) M. Gold and W. L. Jolly, *Inorg. Chem.*, **1**, 818 (1962); (b) R. K. Quinn and J. J. Lagowski, *J. Phys. Chem.*, **72**, 1374 (1968).
120. S. Golden, C. Guttman, and T. R. Tuttle, *J. Chem. Phys.*, **44**, 3791 (1966).
121. T. R. Tuttle, G. Rubenstein, and S. Golden, *J. Phys. Chem.*, **75**, 3635 (1971).
122. I. Hurley, T. R. Tuttle, and S. Golden, *J. Chem. Phys.*, **48**, 2818 (1968).
123. E. J. Hart, in *Metal-Ammonia Solution* (Suppl. to Int. J. Pure Appl. Chem.) **1970**, 413.
124. M. J. Bronskill, R. K. Wolff, and J. W. Hunt, *J. Phys. Chem.*, **73**, 1175 (1969).
125. B. D. Michael, E. J. Hart, and K. H. Schmidt, *J. Phys. Chem.*
126. W. C. Gottschall and E. J. Hart, *J. Phys. Chem.*, **71**, 2102 (1967).
127. M. S. Matheson, W. A. Mulac, and J. Rabani, *J. Phys. Chem.*, **67**, 2613 (1963).
128. (a) J. H. Baxendale, E. M. Fielden, and J. P. Keene, *Science*, **148**, 637 (1965); (b) G. E. Adams, J. H. Baxendale, and J. W. Boag, *Proc. Roy. Soc. (London) A*, **277**, 549 (1964).
129. J. M. Anbar and E. J. Hart, *J. Phys. Chem.*, **69**, 1244 (1965).
130. L. M. Dorfman, in *Solvated Electrons*, Adv. Chem. Ser., **50**, 36 (1965).
131. L. R. Dalton, J. L. Dye, E. M. Fielden, and E. J. Hart, *J. Phys. Chem.*, **70**, 3358 (1966).
132. M. J. Blandamer, L. Shields, and M. C. R. Symons, *J. Chem. Soc. (London)*, **1965**, 3759.
134. H. Linschitz, M. G. Berry, and D. Schweitzer, *J. Am. Chem. Soc.*, **76**, 5833 (1954).
135. J. T. Richards and J. K. Thomas, *J. Chem. Phys.*, **53**, 218 (1970).
136. W. H. Hamill, *J. Chem. Phys.*, **53**, 473 (1970).
137. C. A. Kraus, *J. Am. Chem. Soc.*, **36**, 864 (1914).
138. E. Arnold and A. Patterson, *J. Chem. Phys.*, **41**, 3098 (1964).
139. N. S. Hush and J. Blackledge, *J. Chem. Phys.*, **23**, 514 (1955).
140. See, e.g., M. Szwarc, *Carbanions, Living Polymers and Electron Transfer Processes*, Interscience, New York, 1968, Chap. V.
141. A. Prock, M. Djibelian, and S. Sullivan, *J. Phys. Chem.*, **71**, 3378 (1967).
142. R. V. Slates and M. Szwarc, *J. Phys. Chem.*, **69**, 4124 (1965).
143. (a) H. E. Bent and N. B. Keevil, *J. Am. Chem. Soc.*, **58**, 1228, 1367 (1936); (b) N. B. Keevil, *J. Am. Chem. Soc.*, **59**, 2104 (1937).
144. N. B. Keevil and H. E. Bent, *J. Am. Chem. Soc.*, **60**, 193 (1938).
145. E. Swift, *J. Am. Chem. Soc.*, **60**, 1403 (1938).
146. G. J. Hoijsink, E. de Boer, P. H. Van der Meij, and W. P. Weijland, *Rec. Trav. chim.*, **75**, 487 (1956).

144 Ions and Ion Pairs in Electron Transfer Reactions of Radical Anions

147. J. Jagur-Grodzinski, M. Feld, S. L. Yang, and M. Szwarc, *J. Phys. Chem.*, **69**, 628 (1965).
148. A. Cserhegyi, J. Chaudhuri, E. Franta, J. Jagur-Grodzinski, and M. Szwarc, *J. Am. Chem. Soc.*, **89**, 7129 (1967).
149. P. Chang, R. V. Slates, and M. Szwarc, *J. Phys. Chem.*, **70**, 3180 (1966).
150. D. Nicholls, C. Sutphen, and M. Szwarc, *J. Phys. Chem.*, **72**, 1021 (1968).
151. J. Chaudhuri, S. Kume, J. Jagur-Grodzinski, and M. Szwarc, *J. Am. Chem. Soc.*, **90**, 6421 (1968).
152. J. Chaudhuri, J. Jagur-Grodzinski, and M. Szwarc, *J. Phys. Chem.*, **71**, 3063 (1967).
153. J. Chaudhuri, J. Jagur-Grodzinski, and M. Szwarc, unpublished results.
154. A. Cserhegyi, J. Jagur-Grodzinski, and M. Szwarc, *J. Am. Chem. Soc.*, **91**, 1892 (1969).
155. G. Levin, J. Jagur-Grodzinski, and M. Szwarc, *J. Am. Chem. Soc.*, **92**, 2268 (1970).
156. I. Bergman, *Trans. Faraday Soc.*, **50**, 829 (1954); **52**, 690 (1956).
157. C. Parkanyi and R. Zahradnik, *Bull. Soc. Chim. Belg.*, **73**, 57 (1964).
158. D. van der Meer and D. Feit, *Rec. Trav. chim.*, **87**, 746 (1968).
159. B. J. Tabner and J. R. Yandle, *J. Chem. Soc. (A)*, **1968**, 381.
160. A. Rainis and M. Szwarc, *J. Amer. Chem. Soc.*, **96**, 3008 (1974).
161. W. M. Latimer, K. S. Pitzer, and C. M. Slansky, *J. Chem. Phys.*, **7**, 108 (1939).
162. G. J. Hoijtink, J. van Schooten, E. de Boer, and W. I. Aalbersberg, *Rec. Trav. chim.*, **73**, 355 (1954).
163. G. J. Hoijtink and J. van Schooten, *Rec. Trav. chim.*, **71**, 1089 (1952); **72**, 691, 903 (1953).
164. A. C. Aten, C. Büthker, and G. J. Hoijtink, *Trans. Faraday Soc.*, **55**, 324 (1959).
165. T. H. Given, *J. Chem. Soc.*, **1958**, 2684.
166. H. A. Laitinen and H. Wawzonek, *J. Am. Chem. Soc.*, **64**, 1765 (1942).
167. H. Wawzonek and H. A. Laitinen, *J. Am. Chem. Soc.*, **64**, 2365 (1942).
168. S. Wawzonek and J. W. Fan, *J. Am. Chem. Soc.*, **68**, 2541 (1946).
169. F. A. Matsen, *J. Chem. Phys.*, **24**, 602 (1956).
170. P. Zuman and O. Manousek, *Coll. Czech. Commun.*, **26**, 2134 (1961).
171. P. Zuman, Polarography and Reaction Kinetics, in *Advances in Physical-Organic Chemistry*, V. Gold (Ed.), Academic Press, New York, 1967.
172. R. Dietz and M. E. Peover, *Disc. Faraday Soc.*, **45**, 154 (1968).
173. J. Koutecky, *Coll. Czech. Commun.*, **18**, 311 (1953).
174. G. J. Hoijtink, in *Advances in Electrochemistry*, P. Delahay and C. Tobias (Eds.), Wiley, New York, 1970, pp. 221-280.
175. L. E. Lyons, G. C. Morris, and L. J. Warren, *J. Phys. Chem.*, **72**, 3677 (1968).
176. I. M. Kolthoff and J. L. Lingane, *Polarography*, 2nd ed, Vol. II, Interscience, New York, 1952, p. 809.
177. G. W. Wheland, *J. Am. Chem. Soc.*, **63**, 2025 (1941).
178. H. C. Longuet-Higgins, *J. Chem. Phys.*, **18**, 265 (1950).
179. J. H. Binks and M. Szwarc, *J. Chem. Phys.*, **30**, 1494 (1959); *Theoretic Organic Chemistry*, Chem. Soc. Spec. Publ., 1959, p. 262.
180. G. J. Hoijtink, *Rec. Trav. Chim.*, **73**, 895 (1954).
181. D. E. Paul, D. Lipkin, and S. I. Weissman, *J. Am. Chem. Soc.* **78**, 116 (1956).

182. Y. Karasawa, G. Levin, and M. Szwarc, *Proc. Roy. Soc. London A*, **326**, 53 (1971).
183. K. Höfelmann, J. Jagur-Grodzinski, and M. Szwarc, *J. Am. Chem. Soc.*, **91**, 4645 (1969).
184. G. Moshuk, H. D. Connor, and M. Szwarc, *J. Phys. Chem.*, **76**, 1734 (1972).
185. A. I. Shatenshtein, E. S. Petrov, and M. I. Belousova, *Organic Reactivity*, Vol. 1, Tartu State University, Estonia, U.S.S.R., 1964, p. 191.
186. A. I. Shatenshtein, E. S. Petrov, and E. A. Yakovleva, *International Symposium on Macromolecular Chemistry*, Prague, 1965; *J. Polymer Sci. C*, **16**, Part 3, 1729 (1967).
187. D. G. Powell and E. Warhurst, *Trans. Faraday Soc.*, **58**, 953 (1962).
188. R. V. Slates and M. Szwarc, *J. Am. Chem. Soc.*, **89**, 6043 (1967).
189. L. L. Chan and J. Smid, *J. Am. Chem. Soc.*, **89**, 4547 (1967).
190. A. Streitwieser and I. Schwager, *J. Phys. Chem.*, **66**, 2316 (1962).
191. L. Lee, R. Adams, J. Jagur-Grodzinski, and M. Szwarc, *J. Am. Chem. Soc.*, **93**, 4149 (1971).
192. (a) B. J. Zwolinski, R. J. Marcus, and H. Eyring, *Chem. Revs.*, **55**, 157 (1955); (b) R. A. Marcus, *J. Chem. Phys.*, **24**, 966 (1956); (c) R. A. Marcus, *Disc. Faraday Soc.*, **29**, 21 (1960); (d) R. A. Marcus, *J. Chem. Phys.*, **43**, 679 (1965).
193. W. F. Libby, *J. Phys. Chem.*, **56**, 863 (1952).
194. R. L. Ward and S. I. Weissman, *J. Am. Chem. Soc.*, **79**, 2086 (1957).
195. P. J. Zandstra and S. I. Weissman, *J. Chem. Phys.*, **35**, 757 (1961).
196. R. F. Adams and N. M. Atherton, *Chem. Phys. Lett.*, **1**, 351 (1967).
197. J. R. Norris, *Chem. Phys. Lett.*, **1**, 333 (1967).
198. R. Chang and C. S. Johnson, *J. Chem. Phys.*, **46**, 2314 (1967); *J. Am. Chem. Soc.*, **88**, 2338 (1966).
199. N. Hirota, R. Carraway, and W. Schook, *J. Am. Chem. Soc.*, **90**, 3611 (1968).
200. R. Chang and C. S. Johnson, *J. Am. Chem. Soc.*, **88**, 2338 (1966).
201. S. Arai and L. M. Dorfman, *Adv. Chem. Ser.* **82**, 1968, 378.
202. M. Szwarc and K. Shimada, *J. Polymer Sci. Symposium* **44**, (1974).
203. H. D. Connor, K. Shimada, and M. Szwarc, *Chem. Phys. Lett.*, **14**, 402 (1972).
204. P. J. Zandstra and S. I. Weissman, *J. Am. Chem. Soc.*, **84**, 4408 (1962).
205. H. E. McConnell and H. E. Weaver, *J. Chem. Phys.*, **25**, 307 (1956).
206. C. S. Johnson and J. B. Holz, *J. Chem. Phys.*, **50**, 4420 (1969).
207. C. B. Amphlett, *Quart. Revs.*, **8**, 219 (1954).
208. F. C. Adam and S. I. Weissman, *J. Am. Chem. Soc.*, **80**, 1518 (1958).
209. N. M. Atherton and S. I. Weissman, *J. Am. Chem. Soc.*, **83**, 1330 (1961).
210. N. Hirota and R. Kreilick, *J. Am. Chem. Soc.*, **88**, 614 (1966).
211. N. Hirota, *J. Am. Chem. Soc.*, **90**, 3603 (1968).
212. P. Graceffa and T. R. Tuttle, *J. Phys. Chem.*, **77**, 1566 (1973).
213. S. I. Weissman, *Z. Elektrochem.*, **64**, 47 (1960).
214. C. Carvajal, K. J. Tölle, J. Smid, and M. Szwarc, *J. Am. Chem. Soc.*, **87**, 5548 (1965).
215. T. E. Gough and P. R. Hindle, *Can. J. Chem.*, **47**, 1998, 3393 (1969).
216. R. F. Adams, T. L. Staples, and M. Szwarc, *Chem. Phys. Lett.*, **5**, 474 (1970).
217. G. L. Malinoski, W. H. Bruning, and R. G. Griffin, *J. Am. Chem. Soc.*, **92**, 2665 (1970).

218. B. F. Wong and N. Hirota, *J. Am. Chem. Soc.*, **94**, 4419 (1972).
219. N. Hirota and S. I. Weissman, *J. Am. Chem. Soc.*, **86**, 2537 (1964).
220. N. Hirota, *J. Phys. Chem.*, **71**, 127 (1967).
221. D. H. Geske and A. H. Maki, *J. Am. Chem. Soc.*, **82**, 2671 (1960).
222. P. Ludwig and R. N. Adams, *J. Chem. Phys.*, **37**, 828 (1962).
223. T. A. Miller, R. N. Adams, and P. M. Richards, *J. Chem. Phys.*, **44**, 4022 (1966).
224. A. E. Forno, M. E. Peover, and R. Wilson, *Trans. Faraday Soc.*, **66**, 1322 (1970).
225. W. L. Reynold, *J. Phys. Chem.*, **67**, 2866 (1963).
226. G. Rämme, M. Fisher, S. Claesson, and M. Szwarc, *Chem. Phys. Lett.*, **9**, 306 (1971); *Proc. Roy. Soc. (London) A*, **327**, 467 (1972).
227. H. M. McConnell, *J. Chem. Phys.*, **35**, 508 (1961).
228. S. I. Weissman, *J. Am. Chem. Soc.*, **80**, 6462 (1958).
229. J. W. Burley and R. N. Young, *J. Chem. Soc., Part 2*, **1972**, 835.
230. B. Lundgren, S. Claesson, and M. Szwarc, *Chem. Scripta.*, **5**, 60 (1974).
231. H. M. McConnell, *J. Chem. Phys.*, **33**, 115 (1960).
232. S. I. Weissman, *J. Am. Chem. Soc.*, **80**, 6462 (1958).
233. V. V. Voyerodskii, S. S. Solodovnikov, and V. M. Chibrikov, *Doklady Akad. Nauk. SSSR*, **129**, 1082 (1959).
234. J. E. Harriman and A. H. Maki, *J. Chem. Phys.*, **39**, 778 (1963).
235. F. Gerson and W. B. Martin, *J. Am. Chem. Soc.*, **91**, 1883 (1969).
236. D. J. Williams, J. M. Pearson, and M. Levy, *J. Am. Chem. Soc.*, **93**, 5483 (1971).
237. (a) H. D. Conner, K. Shimada, and M. Szwarc, *Macromolec.*, **5**, 801 (1972); (b) M. Szwarc, in *Nobel Symposium*, Vol. 22, Almquist and Wiksell, Stockholm, 1973, pp. 291-306.
238. M. Szwarc and K. Shimada, *J. Polymer Sci.*, in press.
239. K. Shimada, G. Moshuk, H. D. Connor, P. Caluwe, and M. Szwarc, *Chem. Phys. Lett.*, **14**, 396 (1972).
240. H. S. Gutowsky, D. W. McCall, and C. P. Slichter, *J. Chem. Phys.*, **21**, 279 (1953).
241. S. Arai, D. A. Grev, and L. M. Dorfman, *J. Chem. Phys.*, **46**, 2572 (1967).
242. I. A. Taub, D. A. Harter, M. C. Sauer, and L. M. Dorfman, *J. Chem. Phys.*, **41**, 979 (1964).
243. S. Arai and L. M. Dorfman, *J. Chem. Phys.*, **41**, 2190 (1964).
244. J. R. Brandon and L. M. Dorfman, *J. Chem. Phys.*, **53**, 3849 (1970).
245. G. Vincow, in *Radical Ions*, E. T. Kaiser and L. Kevan (Eds.), Interscience, New York, 1968, p. 202.
246. I. C. Lewis and L. S. Singer, *J. Chem. Phys.*, **43**, 2712 (1965).
247. O. W. Howorth and G. K. Fraenkel, *J. Am. Chem. Soc.*, **88**, 4514 (1966).
248. M. de Sorgo, B. Wasserman, and M. Szwarc, *J. Phys. Chem.*, **76**, 3468 (1972).
249. C. R. Bruce, R. E. Norberg, and S. I. Weissman, *J. Chem. Phys.*, **24**, 473 (1956).
250. C. S. Johnson, *J. Chem. Phys.*, **39**, 211 (1963).
251. A. D. Britt, *J. Chem. Phys.*, **41**, 3069 (1964).
252. D. Romans, W. H. Bruning, and C. J. Michejda, *J. Am. Chem. Soc.*, **91**, 3859 (1969).
253. B. A. Kowert, L. Marcoux, and A. J. Bard, *J. Am. Chem. Soc.*, **94**, 5538 (1972).

254. L. H. Piette, P. Ludwig, and R. N. Adams, *Anal. Chem.* **34**, 916 (1962).
255. S. P. Sorensen and W. H. Bruning, *J. Am. Chem. Soc.*, **94**, 6352 (1972).
256. G. Favini and M. Simonetta, *Theoret. Chim. Acta*, **1**, 294 (1963).
257. G. H. Hoijtink and P. H. van der Meij, *Z. Phys. Chemie. (Frankfurt)*, **20**, 1 (1959).
258. J. Dieleman, Thesis, Univeristy of Amsterdam (1962).
259. E. de Boer, unpublished results.
260. K. H. J. Buschow and G. J. Hoijtink, *J. Chem. Phys.*, **40**, 2501 (1964).
261. W. Schlenk, J. Appenrodt, A. Michael, and A. Thal, *Chem. Ber.*, **47**, 473 (1914).
262. D. W. Ovenall and D. H. Whiffin, *Chem. Soc. (London) Spec. Pub.*, **12**, 139 (1958).
263. A. G. Evans, J. C. Evans, E. D. Owen, and B. J. Tabner, *Proc. Chem. Soc.*, **1962**, 226.
264. J. F. Garst and R. S. Cole, *J. Am. Chem. Soc.*, **84**, 4352 (1962).
265. (a) J. E. Bennett, A. G. Evans, J. C. Evans, E. D. Owen, and B. J. Tabner, *J. Chem. Soc.* **1963**, 3954; (b) A. G. Evans and B. J. Tabner, *J. Chem. Soc.*, **1963**, 4613.
266. (a) J. F. Garst, E. R. Zabolotny, and R. S. Cole, *J. Am. Chem. Soc.*, **86**, 2257 (1964); (b) J. F. Garst and E. R. Zabolotny, *J. Am. Chem. Soc.*, **87**, 495 (1965).
267. R. C. Roberts and M. Szwarc, *J. Am. Chem. Soc.*, **87**, 5542 (1965).
268. E. J. Hart, S. Gordon, and J. K. Thomas, *J. Phys. Chem.*, **68**, 1271 (1964).
269. A. G. Sykes, *Adv. Inorg. Chem.*, **10**, 153 (1967).
270. P. A. Malachewsky, T. A. Miller, T. Layloff, and R. N. Adams, *Proceedings of the Symposium on Exchange Reactions*, Upton, N.Y., 1965, p. 157.
271. J. W. Lown, *Proc. Chem. Soc. (London)*, **1963**, 283.
272. G. Levin, S. Claesson, and M. Szwarc, *J. Am. Chem. Soc.*, **94**, 8672 (1972).
273. P. Abley and J. Halpern, *Chem. Commun.*, **1971**, 1238.
274. E. R. Zabolotny and J. F. Garst, *J. Am. Chem. Soc.*, **86**, 1645 (1964).
275. J. F. Garst, J. G. Pacifici, and E. R. Zabolotny, *J. Am. Chem. Soc.*, **88**, 3872 (1966).
276. W. Reppe, O. Schlichting, K. Klager, and T. Toepel, *Ann.*, **560**, 1 (1948).
277. T. J. Katz, W. H. Reinmuth, and D. E. Smith, *J. Am. Chem. Soc.*, **84**, 802 (1962).
This paper contains references to the previous polarographic studies of cyclooctatetraene.
278. T. J. Katz and H. L. Strauss, *J. Chem. Phys.*, **32**, 1873 (1960).
- 278a. T. J. Katz, *J. Amer. Chem. Soc.*, **82**, 3785 (1960).
279. H. L. Strauss and G. K. Fraenkel, *J. Chem. Phys.*, **35**, 1738 (1961).
280. H. M. McConnell, *J. Chem. Phys.*, **24**, 632, 764 (1956).
281. I. Bernal, P. H. Rieger, and G. K. Fraenkel, *J. Chem. Phys.*, **37**, 1489 (1962).
282. H. L. Strauss, T. J. Katz, and G. K. Fraenkel, *J. Am. Chem. Soc.*, **85**, 2360 (1963).
283. C. A. Coulson and W. E. Moffitt, *Phil. Mag.*, **40**, 1 (1949).
284. D. E. Wood and H. M. McConnell, *J. Chem. Phys.*, **37**, 1150 (1962).
285. J. dos Santos-Veiga, *Mol. Phys.*, **5**, 639 (1962).
286. H. M. McConnell and A. D. McLachlan, *J. Chem. Phys.*, **34**, 1 (1961).
287. L. C. Snyder and A. D. McLachlan, *J. Chem. Phys.*, **36**, 1159 (1962).
288. T. J. Katz, M. Yoshida, and L. C. Siew, *J. Am. Chem. Soc.*, **87**, 4516 (1965).
289. H. J. Dauben and M. R. Rifi, *J. Am. Chem. Soc.*, **85**, 3041 (1963).

148 Ions and Ion Pairs in Electron Transfer Reactions of Radical Anions

290. N. L. Bauld and M. S. Brown, *J. Am. Chem. Soc.*, **87**, 4390 (1965).
291. H. van Willigen, *J. Am. Chem. Soc.*, **94**, 7966 (1972).
292. T. L. Staples and M. Szwarc, *J. Am. Chem. Soc.*, **92**, 5022 (1970).
293. K. Maruyama, *Bull. Chem. Soc. Jap.*, **37**, 553 (1964).
294. N. Hirota, in *Radical Ions*, E. T. Kaiser and L. Kevan (Eds.), Interscience, New York, 1968, p. 35.
295. A. Lagendijk and M. Szwarc, *J. Am. Chem. Soc.*, **93**, 5359 (1971).
296. G. Levin and M. Szwarc, *Chem. Comm.*, **1971**, 1029.
297. J. Jagur-Grodzinski and M. Szwarc, *Proc. Roy. Soc. London A*, **288**, 224 (1965).
298. S. C. Chadha, J. Jagur-Grodzinski, and M. Szwarc, *Trans. Faraday Soc.*, **63**, 2994 (1967).
299. M. Fisher, G. Rämme, S. Claesson, and M. Szwarc, *Proc. Roy. Soc. A*, **327**, 481 (1972).
300. M. C. Sauer, S. Arai, and L. M. Dorfman, *J. Chem. Phys.*, **42**, 708 (1965).
301. F. J. You and L. M. Dorfman, *J. Chem. Phys.*, **58**, 4715 (1973).
302. D. F. Burow and J. J. Lagowski, in *Solvated Electron*, *Adv. Chem. Ser.*, **50**, 125 (1965).
303. J. M. Brooks and R. R. Dewald, *J. Phys. Chem.*, **72**, 2655 (1968).
304. M. T. Lok, F. J. Tehan, and J. L. Dye, *J. Phys. Chem.*, **76**, 2975 (1972).
305. (a) J. J. Christensen, J. O. Hill, and R. M. Izatt, *Science*, **174**, 459 (1971); (b) C. J. Pedersen and H. K. Frensdorff, *Angew. Chem. Int. Ed. (English)*, **11**, 16 (1972).
306. D. S. Berns, in *Solvated Electron*, *Adv. Chem. Ser.*, **50**, 82 (1965).
307. M. C. R. Symons, *J. Chem. Phys.*, **30**, 1628 (1959).
308. L. R. Dalton, J. D. Rynbrandt, E. M. Hansen, and J. L. Dye, *J. Chem. Phys.*, **44**, 3969 (1966).
309. R. R. Dewald and J. L. Dye, *J. Phys. Chem.*, **68**, 128 (1964).
310. K. S. Chen, S. W. Mao, K. Nakamura, and N. Hirota, *J. Amer. Chem. Soc.*, **93**, 6004 (1971).
311. L. J. Gilling, J. G. Kloosterboer, R. P. H. Rettschnick, and J. D. W. van Voorst, *Chem. Phys. Lett.*, **8**, 457 (1971).
312. J. G. Kloosterboer, L. J. Gilling, R. P. H. Rettschnick, and J. D. W. van Voorst, *Chem. Phys. Lett.*, **8**, 462 (1971).
313. E. Becker, R. H. Lindquist, and B. J. Alder, *J. Chem. Phys.*, **25**, 971 (1956).
314. B. Bockrath and L. M. Dorfman, *J. Phys. Chem.*, **77**, 1002 (1973).
315. K. D. Vos and J. L. Dye, *J. Chem. Phys.*, **38**, 2033 (1963).
316. (a) R. Catterall, M. C. R. Symons, and J. W. Tipping, *J. Chem. Soc. A*, **1967**, 1234; (b) R. Catterall, J. Slater, and M. C. R. Symons, *J. Chem. Phys.*, **52**, 1003 (1970); (c) R. Catterall, I. Hurley, and M. C. R. Symons, *J. Chem. Soc. (Dalton)*, **1972**, 139.
317. M. C. R. Symons, *Q. Rev.*, **13**, 99 (1959).
318. J. L. Dye, *Accounts Chem. Res.*, **1**, 306 (1968).
319. K. Bar-Eli and T. R. Tuttle, *J. Chem. Phys.*, **44**, 114 (1966).
320. S. Golden, C. Guttman, and T. R. Tuttle, *J. Am. Chem. Soc.*, **87**, 135 (1965).
321. V. M. Dukelskii, E. Ya Zandberg, and N. I. Ionov, *Dokl Akad. Nauk SSSR*, **62**, 232 (1948); **68**, 31 (1949); Ya M. Fogel, *Soviet Phys.-Usp.*, **3**, 390 (1960).

322. Ya M. Fogel, V. F. Koslov, and G. N. Polykova, *Zh. Eksperim. i Teor. Fiz.*, **39**, 1186 (1960).
323. H. Ebinghaus, *Z. Naturforsch.* **19a**, 727 (1964).
324. S. Matalon, S. Golden, and M. Ottolenghi, *J. Phys. Chem.*, **73**, 3098 (1969).
325. J. L. Dye, M. G. DeBacker, J. A. Eyre, and L. M. Dorfman, *J. Phys. Chem.*, **76**, 839 (1972).
326. R. R. Dewald and K. W. Browall, *J. Phys. Chem.*, **74**, 129 (1970).
327. M. G. DeBacker and J. L. Dye, *J. Phys. Chem.*, **77**, 215 (1973).
328. (a) G. N. Lewis and D. Lipkin, *J. Am. Chem. Soc.*, **64**, 2801 (1942); (b) G. N. Lewis and J. Bigeleisen, *J. Am. Chem. Soc.*, **65**, 520 (1943).
329. P. J. Zandstra and G. J. Hoijtink, *Molec. Phys.*, **3**, 371 (1960).
330. J. D. W. van Voorst and G. J. Hoijtink, *J. Chem. Phys.*, **42**, 3995 (1965).
331. G. Dobson and L. I. Grossweiner, *Trans. Faraday Soc.*, **61**, 708 (1965).
332. K. Nakamura, B. F. Wong, and N. Hirota, *J. Amer. Chem. Soc.*, **95**, 6919 (1973).
333. P. M. Rentzepis, R. P. Jones, and J. Jortner, *Chem. Phys. Lett.*, **15**, 480 (1972).
334. P. M. Rentzepis, *Chem. Phys. Lett.*, **2**, 117 (1968); *Science*, **169**, 239 (1970).
335. M. Polanyi, *Atomic Reactions*, Williams and Norfolk, Baltimore, Ma. (1932).
336. (a) D. J. Morantz and E. Warhurst, *Trans. Faraday Soc.*, **51**, 1375 (1955); (b) E. Warhurst and R. Whittaker, *Trans. Faraday Soc.*, **62**, 707 (1966).
337. (a) D. Lipkin, F. R. Galiano, and R. W. Jordan, *Chem. Ind. (London)*, **1963**, 1657; (b) D. Lipkin, G. J. Davis, R. W. Jordan, *Preprints of the Division of Petroleum Chemistry*, San Francisco, April 1968, p. D60.
338. J. F. Garst, J. T. Barabas, and F. E. Barton, *J. Am. Chem. Soc.*, **90**, 7159 (1968).
339. G. D. Sargent and G. A. Lux, *J. Am. Chem. Soc.*, **90**, 7160 (1968).
340. (a) J. F. Garst, in *Solute-Solvent Interactions*, J. F. Coetzee and C. D. Ritchie (Eds.), Marcel Dekker, New York, 1969; (b) J. F. Garst, *Accounts of Chem. Res.*, **4**, 400 (1971).
341. T. Shimomura, K. J. Tölle, J. Smid, and M. Szwarc, *J. Am. Chem. Soc.*, **89**, 796 (1967).
342. B. Bockrath and L. M. Dorfman, *J. Phys. Chem.* **77**, 2618 (1973).
343. N. S. Hush and J. A. Pople, *Trans. Faraday Soc.*, **51**, 600 (1955).
344. J. Michl, *J. Mol. Spectr.*, **20**, 66 (1969).
345. Principles of mass-spectrometric technique involving chemical ionization are outlined by M. S. B. Munson and F. H. Field, *J. Am. Chem. Soc.*, **88**, 2621 (1966), and by F. H. Field in Chapter 6 of ref. [7].
346. J. L. Beauchamp, *Ann. Rev. Phys. Chem.*, **22**, 527 (1971).
347. D. J. Williams, A. O. Goedde, and J. M. Pearson, *J. Am. Chem. Soc.*, **94**, 7580 (1972).
348. R. Boschi, J. N. Murrell, and W. Schmidt, *Disc. Faraday Soc.*, **54**, 116 (1972).
349. R. Boschi and W. Schmidt, *Tetrahedron Lett.*, 2577 (1972).
350. F. Brogli and E. Heilbronner, *Ang. Chem.*, **84**, 551 (1972).
351. S. Arai, H. Ueda, R. F. Firestone, and L. M. Dorfman, *J. Chem. Phys.*, **50**, 1072 (1969).
352. D. H. Eargle, *J. Am. Chem. Soc.*, **93**, 3859 (1971).
353. J. F. Garst, *J. Am. Chem. Soc.*, **93**, 6312 (1971).

354. N. E. Shank and L. M. Dorfman, *J. Chem. Phys.*, **52**, 4441 (1970).
355. (a) T. Shida and W. H. Hamill, *J. Chem. Phys.*, **44**, 2369 (1966).
(b) H. Ueda, *Bull. Chem. Soc. Japan*, **41**, 2578 (1968).
356. R. D. Allendoerfer and P. H. Rieger, *J. Am. Chem. Soc.*, **87**, 2336 (1965).
357. F. J. Smentowski and G. R. Stevenson, *J. Phys. Chem.*, **73**, 340 (1969).
358. G. R. Stevenson and J. G. Conception, *J. Phys. Chem.*, **76**, 2176 (1972).
359. G. Levin, T. A. Ward, and M. Szwarc, *J. Am. Chem. Soc.*, **96**, 270 (1974).
360. J. F. Garst, in *Free Radicals*, Vol. I, J. K. Kochi, Ed., Wiley, 1973, pp. 503-546.
361. J. M. Lehn, *Struct. Bonding*, **16**, 1 (1973).
362. J. L. Dye, J. M. Ceraso, M. T. Lok, B. L. Barnett, and F. J. Tehan, *J. Am. Chem. Soc.*, **96**, 608 (1974).
363. K. Shimada and M. Szwarc, *J. Am. Chem. Soc.*, in press (1974).
364. P. M. Rentzepis, R. P. Jones, and J. Jortner, *J. Chem. Phys.*, **59**, 766 (1973).
365. L. J. Gilling and J. G. Kloosterboer, *Chem. Phys. Lett.*, **21**, 127, (1973).
366. W. S. Struve, T. L. Netzel, P. Rentzepis, G. Levin, and M. Szwarc, to be published.
367. J. H. Baxendale and P. Wardman, *Nature*, **230**, 449 (1971); *Chem. Com.* 429 (1971).
368. M. J. Bromskill, R. K. Wolf, and J. W. Hunt, *J. Chem. Phys.*, **53**, 4201 (1970).
369. M. T. Jones and S. I. Weissman, *J. Am. Chem. Soc.*, **84**, 4269 (1962).

2

Ions and Ion Pairs in Proton Transfer Reactions Involving Carbon Acids or Radical Anions

MICHAEL SZWARC

*Department of Chemistry
State University College of
Environmental Science and Forestry
Syracuse, New York*

ANDREW STREITWIESER

*Department of Chemistry
University of California
Berkeley*

PATRICK C. MOWERY

*Department of Chemistry
University of California
Berkeley*

1. Introduction	152
2. Thermodynamics of Proton Transfer Reactions	153
2.1. Acidities of Carbon Acids	153
2.2. The Effect of Hydrogen Bonding on the Acidity of RH	156

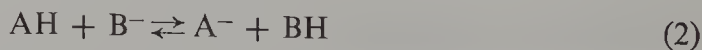
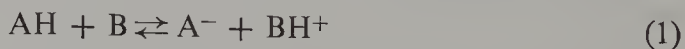
2.3. Ion-Pair Acidity and Ion-Pair Dissociation	158
2.4. Acid-Base Equilibria in Systems $R_1H + R_2^- \rightleftharpoons R_1^- + R_2H$	162
2.5. Acidity Scales	167
2.6. Structural Factors Affecting pK	172
3. Kinetics of Proton Transfer	180
3.1. Brønsted Relation	180
3.2. Isotope Effects in Proton Transfer Involving Free Ions	195
3.3. Kinetics of Proton Transfer Involving Ion Pairs and Higher Aggregates	201
3.4. Stereochemistry of Proton Transfer	207
3.5. Protonation of Radical Anions and Dianions	221
References	240

1. INTRODUCTION

The subject of proton-transfer reactions covers a vast field of chemistry, the significance and importance of which is clearly outlined in the classic monograph by Bell [1]. The proton holds a unique place among singly charged cations since its nucleus is not screened by electrons. This property it shares with a few multiply charged ions, like He^{2+} or Li^{3+} , but none of these is important in chemical processes taking place under conventional conditions.

It is not our intention to survey the whole field of proton chemistry. Our review is limited to proton-transfer reactions involving carbon acids, carbanions, and organic radical ions as reagents or products. Moreover, we shall be concerned only with reactions proceeding in nonaqueous solvents. Although a large part of this subject was covered in the excellent book by Cram [2] published in 1965, a wealth of new information about carbanions and carbon acids that has become available in recent years warrants a new examination of the reported data.

In every proton-transfer reaction a *charged* particle, H^+ , is transferred from an acid AH to a base B . Such reactions exemplified by Eq. 1 or 2,



must involve, by necessity, at least two ions as the reagents or products. Various factors affect the structure of ionic species in solution; these include their concentration, the concentration and type of the counterions balancing their charge, the nature of the solvent, and thermodynamic parameters like temperature or hydrostatic pressure. As has been shown in Volume One of this book [3], these factors modify the solvation shells of ionic reagents, vary the degree of their association into ion pairs or higher aggregates, alter the structure of the resulting pairs or aggregates, and so on. For example, lowering the temperature of a solution or increasing the hydrostatic pressure

often leads to conversion of dissolved ion pairs from “tight” forms into “loose” ones [4, 5]. The contributors to the first volume unequivocally demonstrated that such modifications could and should be interpreted as evidence for the existence of thermodynamically distinct species, each characterized by its own specific physical properties, and therefore each exhibiting its own distinct chemical reactivity. It will be our task to show the role of these species in proton-transfer reactions, to demonstrate how a proton transfer involving free ions differs from that arising from a reaction of ion pairs or in what respect the reactions of tight ion pairs diverge from those of loose pairs. Moreover, we will attempt to uncover the reasons for observed differences and to interpret them in physical terms.

The role and significance of solvent and counterions in proton-transfer reactions are better appreciated when the reactions taking place in solution are compared with the same processes proceeding in the gaseous phase. Such comparisons will be attempted whenever the required information is available. A brief discussion of gaseous proton-transfer reactions is presented by Kebarle in Volume One [6].

2. THERMODYNAMICS OF PROTON-TRANSFER REACTIONS

2.1. Acidities of Carbon Acids

We begin our discussion of proton-transfer reactions by considering the dissociation of electrically neutral carbon acids, RH, infinitely diluted by solvent S. Such reactions yield *free* ions and proceed according to Eq. 3,



where R^- and SH^+ denote the resulting carbanion and a protonated solvent molecule, respectively. The heat of these reactions is affected by two kinds of structural factor: those related to the nature of the acid RH and its conjugate base R^- , and the other determined by the nature of the solvent. A comprehensive discussion of the effect of the structure of the acid on its relative acidity is beyond the scope of this chapter, although some aspects of this problem will be examined later. At present we shall focus our attention on the role played in these processes by the solvent.

The heat of reaction 3 in the gas phase, $\Delta H^\circ(3)_g$, is given by

$$\Delta H^\circ(3)_g = \Delta H_f^\circ(\text{R}^-) - \Delta H_f^\circ(\text{RH}) + \Delta H_f^\circ(\text{SH}^+) - \Delta H_f^\circ(\text{S})$$

where the terms appearing on the right-hand side of the equation denote the heats of formation of the respective gaseous species. For a specific acid, RH, and a series of solvents, S_i , the variations of $\Delta H^\circ(3)_g$ arise from changes of

the values of $\Delta H_f^0(\text{SH}^+) - \Delta H_f^0(\text{S})$. By definition, $\Delta H_f^0(\text{SH}^+) - \Delta H_f^0(\text{S})$ is related to the gaseous proton affinity of molecule S:

$$\text{PA}(\text{S}) = -\{\Delta H_f^0(\text{SH}^+) - \Delta H_f^0(\text{S})\} + \Delta H_f^0(\text{H}^+)$$

the last term being a constant. Hence the higher the proton affinity of S, the more negative is $\Delta H^0(3)_g$ and the greater the gaseous acidity of RH with respect to S. Proton affinities of molecules of some common solvents are listed in Table 1. Inspection shows that the gradation deduced from the data

Table 1 Gaseous Proton Affinities of Molecules of Common Solvents

Solvent	Proton Affinity (kcal/mole)	Ref.
H ₂ O	166 ± 2	a, b, c
HCN	170 ± 2	a
C ₆ H ₆	178 ± 2	h
HCOOH	179 ± 2	a
PA(CH ₃ COOH) > PA(HCOOH)		d
CH ₃ OH	182 ± 3	a, e
PA(C ₂ H ₅ OH) > PA(CH ₃ OH)		
CH ₃ CHO	185	g
CH ₃ CN	186 ± 1	a
C ₆ H ₅ ·CH ₃	187 ± 1	h
<i>p</i> -C ₆ H ₄ (CH ₃) ₂	188 ± 1	h
<i>m</i> -C ₆ H ₄ (CH ₃) ₂	188 ± 1	h
<i>o</i> -C ₆ H ₄ (CH ₃) ₂	188 ± 1	h
CH ₃ COCH ₃	188 ± 2	a
Aniline	215.9 ^j	i
Pyridine	223.6 ^j	i
Cyclohexylamine	227 ^j	i
NH ₃	207 ± 3	a, b
CH ₃ NH ₂	217.8 ^j	i
(CH ₃) ₂ NH	222.3 ^j	i
(CH ₃) ₃ N	240.3 ^j	i

^a M. A. Haney and J. L. Franklin, *J. Phys. Chem.*, **73**, 4328 (1969).

^b M. A. Haney and J. L. Franklin, *J. Chem. Phys.*, **50**, 2028 (1969).

^c S. T. Vetchinkin, I. I. Pshenichnov, and N. B. Sokolov, *J. Phys. Chem., Moscow*, **33**, 1269 (1959).

^d E. W. Godbole and P. Kebarle, *Trans. Faraday Soc.*, **58**, 1897 (1962).

^e M. S. B. Munson, *J. Am. Chem. Soc.*, **87**, 2332 (1965).

P. Kebarle, R. N. Hayness, and J. G. Collins, *J. Am. Chem. Soc.*, **89**, 5753 (1967).

^g K. M. A. Rafacy and W. A. Chupka, *J. Chem. Phys.*, **48**, 5205 (1967).

^h S. L. Chong and J. L. Franklin, *J. Am. Chem. Soc.*, **94**, 6630 (1972).

ⁱ J. P. Briggs, R. Yamdagni, and P. Kebarle, *J. Am. Chem. Soc.*, **94**, 5128 (1972).

Calculated from the directly determined difference of PA(NH₃) and PA(X), taken from ref. i on the assumption that $\Delta S = 0$, and accepting the value of 207 for PA(NH₃).

collected in this table *does not* conform to that anticipated on the basis of general experience gained from studies of solution reactions. Moreover, studies of gaseous proton affinities call for reexamination of some generally accepted principles. For example, solution studies lead to the conclusion that aniline and pyridine are weaker bases than ammonia. The explanation offered in every textbook invokes resonance and the electron-withdrawing effect of phenyl groups as the causes of such trends. Since these are intrinsic molecular factors, they should be revealed in the gaseous proton affinities. However, recent qualitative studies by Dzidic [36] and quantitative studies by Kebarle and his students [37] demonstrate that in the gas phase pyridine and aniline are stronger bases than ammonia. It is obvious therefore that other factors substantially contribute to the basicities of *liquid* solvents. The thermodynamic dissection of the solution basicities of amines into gas phase and solvation contributions has recently been discussed by Arnett et al. [163] and by Aue et al. [170].

In solution the SH^+ ions, as well as R^- ions and the electrically neutral RH molecules, are solvated. The simplest model of ionic solvation, developed by Born [7] and known as the *sphere in continuum* approximation, gives the free energy of solvation of an ion in terms of its radius, charge, and the macroscopic dielectric constant of the solvent. According to this model $\Delta H^\circ(3)_{\text{sol}}$ should decrease as the dielectric constant of the solvent increases, provided that the "size" of the SH^+ ions remains constant.

The sphere in continuum model greatly oversimplifies the situation encountered in real systems. Here the dimensions of solvent molecules are comparable to the size of ions and it becomes highly questionable whether the medium can be treated as a continuum. While ignoring the possible effect of hydrogen bonding, which will be considered later, it becomes obvious that the solvating power of a solvent is a complex function of a variety of factors. It does depend on polarity and polarizability of solvent molecules—these two properties are reflected, at least partially, in the value of the solvent dielectric constant. However, the solvating power depends also on the geometry of solvent molecules and on their mode of packing in the liquid and around the ions. For example, it does not suffice to know the value of the overall dipole or quadrupole moment of solvent molecules to assess their solvating capacity, but the detailed knowledge of the spatial distribution of charges within those molecules is also needed. Indeed, many solvents often show a greatly different solvating capacity toward two ions of identical size and geometry but bearing charges of opposite sign—a clear demonstration of the shortcomings of the Born model. The dielectric saturation of solvent shells neighboring the ions may substantially reduce their microscopic dielectric constant, making the effective value of the dielectric constant considerably lower than its nominal magnitude.

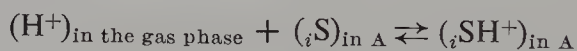
We will not pursue this subject further; a thorough discussion has been presented elsewhere [8]. It is useful, however, to combine the solvating capacity of a solvent for SH^+ cations with the proton affinity of S molecules and derive a concept of a solvent's basicity. The latter is defined as the *free* energy change resulting from proton-transfer from the gaseous phase (at zero pressure) into an infinitely large volume of the studied solvent. The solvent basicity defined in this manner includes all of the entropy contributions to the solvation of SH^+ ions. These are quite substantial, whereas the entropy change associated with the gaseous process



is usually negligible [37].

An alternative approach to the basicity of solvents was described by Ritchie [9], who utilized in his presentation the concept of activity coefficients. A similar treatment was outlined by Bates [17], and Strehlow [18] presented a most inspiring discussion of this and related problems.

The basicities of a series of solvents ${}_i\text{S}$ should be distinguished from the acidities of the respective ${}_i\text{SH}^+$ ions in some common solvent, say A. The latter are associated with the reactions



and depend on the solvation of ${}_i\text{SH}^+$ ions, and of ${}_i\text{S}$ molecules, by A. The difference between free energies of solvation of ${}_i\text{SH}^+$ ions by two solvents, say A and A', need not be independent of i ; however, the magnitude of this difference is often small. An appropriate example is provided by the acidities of pyridinium ion in DMF [11] and methanol [13]. Arnett reported the pK_a 's of protonated DMF and methanol in water to be -0.01 and -2.2 , respectively [14]. Clearly, in water solution DMF is a better proton acceptor than methanol by about two powers of 10, and in view of this difference one would estimate the pK_a 's of acids to be by about two units lower in DMF than in methanol [12]. Indeed, the pK 's of picolinium ions decrease by 1.2 units as methanol is replaced by DMF, the respective values being 6.1 and 4.9 [11].

Finally, let us not forget that the solvation of R^- ions, and to a lesser extent of RH molecules, also contribute to the acidity of RH. Since the degree of solvation of R^- ions by various solvents is affected by the nature of R^- , the relative acidities of RH in different solvents need not be constant. This point will be discussed more thoroughly in Section 2.5.

2.2. The Effect of Hydrogen Bonding on the Acidity of RH

The influence of hydrogen bonding on the relative acidities determined in various solvents may be illustrated by comparing the acidities of hydroxy

acids in methanol and DMF [10–12]. The dielectric constants of both solvents are similar, 32.6 and 36.7, respectively. Therefore the pertinent magnitude of the electrostatic interactions should be comparable in both media. However, as shown in the preceding section, the basicity of DMF is greater than that of methanol and hence the pK 's of acids should be lower in the former solvent than in the latter. Nevertheless, the pK of *p*-nitrophenol is greater in DMF (12.3, [9]) than in methanol (11.15, [11]) by more than one unit. Likewise, acetic acid is less acidic in DMF than in methanol, the respective pK 's being 12.5 and 9.7 [9, 10]. These differences have been ascribed to the greater degree of solvation of the conjugate base in methanol than in DMF. In methanol, the conjugate base is stabilized by hydrogen bonding to CH_3OH molecules, whereas a similar interaction does not operate in DMF. The effect is further magnified because the stabilization of the acid by hydrogen bonding to solvent is greater in DMF than in methanol.

A comprehensive discussion of the effect of hydrogen bonding on solvation and acid-base equilibria is unnecessary here, since Ritchie has treated this topic thoroughly in a recent review [9]. However, we wish to comment on two interesting points.

The capacity of a solvent to act as an acceptor in hydrogen bonding interactions often has been compared with its basicity. Indeed, Gordy and Stanford [22] reported long ago a good correlation between the ability of a solvent to abstract a proton from aqueous acids and its capacity to act as an acceptor in hydrogen bonding as measured by the shift in the O-D stretching frequency of CH_3OD . This led many workers to believe that the strength of hydrogen bonding and the ease of proton transfer could be used, almost interchangeably, as a measure of the same property, the substrate basicity. In a recent paper Arnett [23] reported a large discrepancy in responses of different bases to these two processes. In view of his findings the correlations between hydrogen bonding and solvent basicity should be treated with some reservation.

The effect of dispersion forces on acid-base equilibria has been discussed thoroughly by Grunwald and Price [16]. Usually such interactions affect chemical equilibria negligibly because their influence on the initial and the final state of the system is virtually identical. However, the effect of dispersion forces can be perceived if molecules with high excited states (colorless) are converted into those possessing low excited states (highly colored), because the latter interact more strongly with the environment than the former. Such a situation is encountered in conversion of the so-called one-color indicators from their colorless acidic form into a highly colored basic form. Since the effect of dispersion forces increases as the surrounding region becomes more polarizable, the acidity of such indicators should increase as the solvent is varied from H_2O to CH_3OH , C_2H_5OH , and C_4H_9OH . The expected change in

the acidity is observed when equilibria such as picric acid (one-color indicator)-acetate are determined in this series of solvents, but no effect is found for the system trichloroacetic acid-acetate. A similar behavior is observed in methanol and DMF. Picric acid is more acidic in the DMF more polarizable than in the less polarizable methanol, the relevant pK 's being 1.2 and 3.8 [15]. This large ΔpK of 2.6 contrasts with the smaller ΔpK found for most phenols studied in these two solvents [11], and hence this finding may be quoted as an additional evidence confirming Grunwald's approach.

The foregoing interpretation may be questioned because *p*-nitrophenol, also a one-color indicator, behaves normally. Table 2 shows the pK of acetic

Table 2 pK of Oxygen Acids in Different Solvents [10]

Acid	$pK(H_2O)$	$pK(CH_3OH)$	$pK(DMF)$	$pK(DMSO)$
Picric	0.71	3.8	1.2	-1.9
2,4-Dinitrophenol	4.10	7.9	6.0	5.2
4-Nitrophenol	7.15	11.15 ^a	12.34 ^a	10.4 ^b
Acetic	4.76	9.6	12.5	11.6

^a Ref. 9.

^b C. D. Ritchie, personal communication.

acid, *p*-nitrophenol, and picric acid in water, DMF, methanol, and DMSO. The variations in pK of nitrophenol and acetic acid are readily rationalized in terms of the decreasing ability of the solvent to stabilize a conjugate base through hydrogen bonding. Such stabilization appears to be less important for picrate ions due to the extensive charge delocalization, which reduces the effect of hydrogen bonding. Differences in solvent basicity then become dominant and thus the more basic DMF induces greater dissociation of picric acid than the less basic methanol. In this respect the behavior of 2,4-dinitrophenol is intermediate between those of *p*-nitrophenol and picric acid.

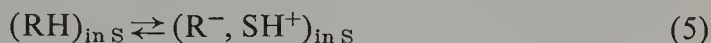
The contribution of dispersion forces to heats of protonation was discussed recently by Arnett and Carter [24]. However, the problem they posed is radically different from that discussed by Grunwald [16]. Arnett has shown that the effect of dispersion forces increases the heat of protonation by increasing the heat of solution of the acid, but this need not increase its acidity as defined by Eq. 3.

2.3. Ion-Pair Acidity and Ion-Pair Dissociation

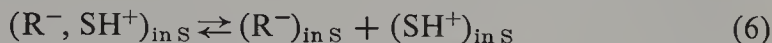
A solution reaction



resulting in the formation of free ions should be contrasted with reaction 5,



The latter produces an ion pair—a species capable of dissociation into free ions:



The degree of dissociation (Eq. 6) strongly depends on the value, \mathcal{D} , of the macroscopic dielectric constant of the medium, because in the first approximation the free energy of charge separation is given by

$$\Delta F_0(6) = \frac{e^2}{d\mathcal{D}}$$

where e is the ionic charge and d is the distance separating the ions in a pair. The above equation neglects the effect of the dielectric saturation of the solvent, which is significant when the two ions are in close proximity. The magnitude of the resulting error is discussed in ref. 8, (pp. 238–240).

Reaction 5 may be designated as the ion pair acidity of RH in S; reaction 4 represents its ionization coupled with the dissociation of the ion pair. The conventional thermodynamic definition of pK refers to the latter, being derived from the equilibrium constant of Eq. 4:

$$K(4) = \left\{ \frac{[\text{R}^-][\text{SH}^+]}{[\text{RH}]} \right\} \left\{ \frac{\gamma_{\text{R}^-} \gamma_{\text{SH}^+}}{\gamma_{\text{RH}}} \right\}$$

whereas the equilibrium constant of Eq. 5 is determined by

$$K(5) = \left\{ \frac{[\text{R}^-, \text{SH}^+]}{[\text{RH}]} \right\} \left\{ \frac{\gamma_{\text{R}^-, \text{SH}^+}}{\gamma_{\text{RH}}} \right\}$$

Furthermore, although the ratio $[\text{SH}^+]/[\text{RH}]$ increases on dilution, the ratio $[\text{R}^-, \text{SH}^+]/[\text{RH}]$ remains virtually constant.

Examples of ion pair acidities of RH in protophilic solvents are furnished by the recent studies of some relatively strong hydrocarbon acids in cyclohexylamine [52]. The equilibria described by Eq. 5a

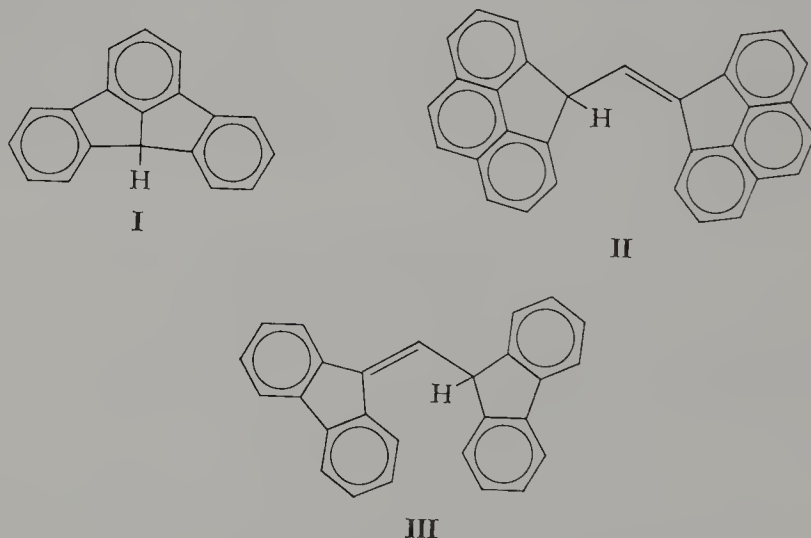


were investigated for the four hydrocarbons listed in Table 3. The relevant equilibrium constants, $K(5a)$, defined by

$$K(5a) = \frac{[\text{R}^-, \text{C}_6\text{H}_{11}\text{NH}_3^+]}{[\text{RH}]}$$

Table 3 $pK_{\text{ion pair}}$ of Strongly Acidic Hydrocarbons in Cyclohexylamine (CHA)

Hydrocarbon	(A) ^a	(B) ^b	(C) ^c	(D) ^d	$\Delta(\text{AB})$	$\Delta(\text{AC})$	$\Delta(\text{AD})$
	in CHA	DMSO/ <i>t</i> -BuOK	DMSO/ Pr_3N	Cs salt in CHA			
1,1,3,3-bis(4,5-Phenanthrylene)- Propene (II)	* 1.38	13.43	13.43	13.26	12.05	12.05	11.88
1,1,3,3-bis(Biphenylene)- Propene (III)	2.05	14.09	14.17	13.79	12.04	12.12	11.74
Fluoradene (I)	0.44	13.80	13.77	—	13.36	13.33	—
1,3-Diphenylindene	2.21	15.40	—	13.92	13.19	—	11.71

^a Ref. 52.^b Ref. 54.^c Ref. 56.^d Derived from ΔpK and standardized on the pK value of 9-phenylfluorene (see ref. 52). The K values in Columns B, C, and D are given in m/l units; those in Column A are unitless.

were shown to be independent of the concentration of RH , provided that the solutions were sufficiently dilute. The values of $K(5a)$ may be recast into the corresponding ion pair pK 's:

$$pK_{\text{ion pair}} = -\log K(5a)$$

given in Table 3. These may be used to establish an ion pair pK scale of hydrocarbon acids in cyclohexylamine.

The carbanions derived from the acids listed in Table 3 are relatively large, and the anionic charge is highly delocalized. Hence the dissociation constants of the corresponding ion pairs should be approximately independent of the nature of R^- , implying the relation $\Delta pK_{\text{ion pair}} \approx \Delta pK_{\text{ionic}}$. This conclusion seems to be verified by the data listed in columns B and C of Table 3. The

latter give the conventional ionic pK obtained in DMSO and, as shown in the last three columns of Table 3, the differences $pK_{\text{CHA}} - pK_{\text{DMSO}}$ are approximately constant. However, some significant deviations may be noted which could be attributed to the differences in the structure of ion-pairs.

Ionic species in solution form a mixture of subspecies; for example, the convenient symbol $(\text{SH}^+)_{\text{in S}}$ represents *all* of the subspecies formally denoted by $(\text{SH}^+)\text{S}_n$, each referring to a particular value of n and to a specific configuration of solvent molecules surrounding the ion. In fact, the description of the subspecies may be even more complex; for example, the symbol H_3O^+ , so often used in texts, poorly describes a hydrated proton. A more realistic notation may be H_9O_4^+ , which represents a proton tetrahedrally surrounded by four molecules of water. Hence such a proton does not belong to a particular molecule of water but instead is associated with a cluster of water molecules.

The following two questions may be posed at this stage: Is the differentiation between the various subspecies justified and feasible? Should they be treated as individual, thermodynamically meaningful entities or should they be lumped together and the behavior of the system discussed in terms of activities and activity coefficients? These questions have been discussed elsewhere* ([19]; see also pp. 222–225 and again pp. 262–264 of ref. 8). It has been concluded that two aspects of the problem need consideration. One aspect is conceptual: When does a series of fluctuating molecular patterns deserve the designation as a thermodynamic species? The other aspect is operational: What kinds of observation permit the differentiation between the subspecies? Numerous examples reported and discussed in Volume One [3] demonstrate conclusively the feasibility of the differentiation between various subspecies in many systems pertinent to our discussion, and for such systems their separate thermodynamic treatment is justified. Indeed, this has been stated previously in the introduction to this chapter.

All that was said above applies to the $(\text{R}^-, \text{SH}^+)_{\text{in S}}$ ion pairs as well as to $(\text{SH}^+)_{\text{in S}}$ ions. Ion pair species undoubtedly represent the bulk of the ionized acid in protophilic solvents of low dielectric constant. Their presence contributes to the spectral absorbance of R^- but not to the conductivity of the solution. In fact, studies of conductivity provide the only reliable method of differentiation between free ions and the various kinds of ion pair.

Some problems associated with the presence of ion pairs call for further elaboration. The differentiation between various types of ion pair, such as tight and loose ion pairs, is often possible through spectroscopic studies of their UV, visible, or IR spectra [20]. These techniques should also be applicable to different types of $(\text{R}^-, \text{SH}^+)$ ion pair in a solvent S . Studies of the temperature dependence of acidities in protophilic, low dielectric constant

* See the preface to this volume.

solvents might well be interesting and profitable in this regard. Such studies might also provide useful data for differentiation between the (R^- , SH^+) ion pairs and R^- free ions, especially by corroboration with relevant conductance data.

The problems of acidity are even more complex in mixed solvents. Not only may two or more distinct bases become available for protonation, but the pertinent S_1H^+ , S_2H^+ , . . . , ions, or R^- , S_1H^+ , R^- , S_2H^+ , . . . , ion pairs, may be surrounded by solvation shells of different composition. As is well known, the microscopic composition of a mixed solvent surrounding ions or ion pairs may diverge substantially from its nominal macroscopic composition [69].

2.4. Acid-Base Equilibria in Systems $R_1H + R_2^- \rightleftharpoons R_1^- + R_2H$

Systems composed of only two types of ion, R^- and SH^+ , were discussed in the preceding section. The presence of any other ion in such systems was not demanded by any compelling reasons. In contradistinction, the presence of some cations, Cat^+ , is mandatory in the systems $R_1H + R_2^- \rightleftharpoons R_1^- + R_2H$, in order to maintain the overall electric neutrality. Two equilibria govern the composition of such solutions:



and



The equilibrium constants of Eqs. 7 and 8, denoted as $K_{1,2}^-$ and $K_{1,2}^\pm$, respectively, are related through the equation $K_{1,2}^-/K_{1,2}^\pm = K_{diss,1}/K_{diss,2}$, where the symbols on the right-hand side represent the dissociation constants of the relevant ion pairs, R_1 , Cat^+ and R_2^- , Cat^+ .

In low dielectric constant solvents the concentration of free ions may be exceedingly low and experiment then provides the value of $K_{1,2}^\pm$, whereas the conventionally defined acidities of the two acids, R_1H and R_2H , are related to $K_{1,2}^-$; that is, $-\log K_{1,2}^- = pK_1 - pK_2$. It follows, however, from the previously mentioned relation that

$$-\log K_{1,2}^\pm = pK_1 - pK_2 - \log \left(\frac{K_{diss,1}}{K_{diss,2}} \right)$$

thus $pK_1 - pK_2$ may be calculated from $K_{1,2}^\pm$ provided that $K_{diss,1}$ and $K_{diss,2}$, or at least their ratio, are known.

The dissociation constants of ion pairs composed of large R^- carbanions with delocalized charge, such as those derived from conjugated aromatic hydrocarbons, are relatively insensitive to the nature of R^- . Thus the relation

$K_{1,2}^- \approx K_{1,2}^\pm$ should be valid for the corresponding RH acids, and the determination of $K_{1,2}^\pm$ then provides an acceptable value for the difference, $\text{p}K_1 - \text{p}K_2$. The reliability of such results may be judged by inspection of the data collected in Table 4, which appears in a later section of this chapter (p. 170).

The small variations of $K_{1,2}^\pm$ derived from studies of equilibria involving salts of different cations may be rationalized in the foregoing terms. For example, $K_{i,j}^\pm$ values have been determined spectrophotometrically for lithium and cesium salts of a series of conjugated aromatic hydrocarbon acids in cyclohexylamine [26, 27]. The results were eventually presented in the form of individual $\text{p}K$'s relative to 9-phenylfluorene as the reference point ($\text{p}K = 18.49$). Conductometric studies [25] showed that the dissociation constant of lithium fluorenyl in cyclohexylamine is about $10^{-10} M$, and a still lower value is expected for the cesium salts. Therefore free ions represent less than 1% of ion pairs even in solutions as dilute as $10^{-5} M$, and hence their presence in the system can be safely disregarded.

The temperature variation of the spectra of these salts in cyclohexylamine or in cyclohexylamine-diethylamine mixtures [28] conclusively prove that the lithium salts form loose "solvent-separated" ion pairs in these solvents, whereas the cesium salts are present as tight ion pairs. Hence the closeness of the gegenion to the carbanion stabilizes the latter pairs more than the former—an effect recognized from qualitative comparison of the trends noted for the relevant $\text{p}K$'s [26].

This observation has recently been put on a quantitative footing [28] for several carbanions expected to be planar. The charge distribution was calculated using a standard Pariser-Parr-Pople SCF- π method. The resulting distributions were treated as a collection of point charges not perturbed by the cation. Coulomb's law was used then to calculate the electrostatic energies U of the ion pairs, where

$$U = q \sum_{i=1}^n \frac{q_i^-}{r_i}$$

q_i^- denotes the charge on atom i , and r_i is its distance from the cation of charge q . The cation was assumed to be located above the plane of the anion. U was minimized with respect to the coordinates of the cation, subject to the constraint that its distance d from the plane of the anion is constant. The location of the cation was found to be nearly independent of d when d was varied between 3.1 and 4.1 Å. Since the lithium salts are present in this system as loose pairs, they are less affected by the electrostatic interaction than are the tight cesium pairs, which under these conditions account for the bulk of the cesium salts. Therefore one expects a correlation between U and the equilibrium constant of reaction 9,



in cyclohexylamine where R_0^- denotes 9-phenylfluorenyl anion. In our notation

$$-\log K(9) = (pK_{R_iH} - pK_0)_{\text{for Cs}^+ \text{ pairs}} - (pK_{R_iH} - pK_0)_{\text{for Li}^+ \text{ pairs}}$$

Figure 1 is a plot of $-\log K(9)$ versus the electrostatic energies calculated for $d = 3.1 \text{ \AA}$, and the excellent linear correlation confirms the soundness of this simple electrostatic treatment.

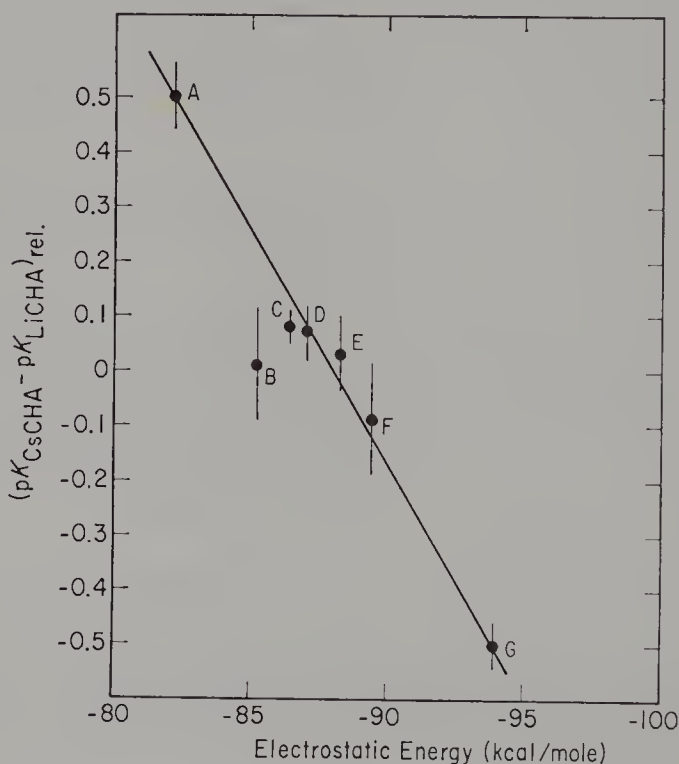


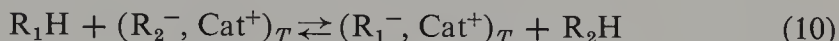
Figure 1. Differences between pK 's calculated from the equilibria involving cesium and lithium salts, respectively, in cyclohexylamine versus electrostatic energy u . Letters represent: A, benzanthrene; B, 2,3-benzofluorene; C, 1,2-benzofluorene; D, 3,4-benzofluorene; E, 4,5-methylenephenanthrene; F, fluorene; G, indene. Reproduced from ref. 28.

Electrostatic interaction is indeed low for lithium salts of carbanions having highly delocalized charge and dissolved in well-solvating media, because solvation of the small lithium cation produces loose solvent-separated ion pairs. The equilibrium involving such loose pairs leads to K^\pm closely similar to K^- . An example is provided by lithium salts of 1,3-diphenylindene and 1,1,3,3-bis(4,5-phenanthrylene)propene (**II**) dissolved in cyclohexylamine. The study of such an equilibrium led to $\Delta pK = 1.71$ [52] as compared with a more ionic $\Delta pK = 1.97$ in DMSO.

Even for such systems which involve large carbanions one can detect the effect of ion pairing on ΔpK when cesium salts are employed. The relatively

large cesium cation is poorly solvated by the solvent and tends to form “tight” or “contact” ion pairs. In the case of 1,3-diphenylindene and **II**, for example, the cesium ion pair ΔpK is only 0.62 [52]. The effect of ion pairing becomes smaller when the equilibrium between still larger anions is considered. An example is provided by 1,1,3,3-bis-4,5-phenanthrylenepropene (**II**) and 1,1,3,3-bis-biphenylenepropene (**III**), whose ΔpK is roughly the same under all conditions studied (Table 3).

Let us pursue this subject still further. The ion pairs R_1^- , Cat^+ and R_2^- , Cat^+ may in principle form a mixture of tight and loose ion pairs. For such a case the following two equilibria are important:



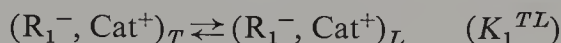
and



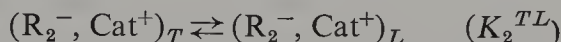
The subscripts T and L refer to tight and loose ion pairs, respectively. The equilibrium constants of Eqs. 10 and 11, denoted as $K_{1,2}^T$ and $K_{1,2}^L$, are related through the equation

$$\frac{K_{1,2}^L}{K_{1,2}^T} = \frac{K_1^{TL}}{K_2^{TL}}$$

where K_1^{TL} and K_2^{TL} are the equilibrium constants of the conversions



and



Spectrophotometric studies often provide us only with the total concentration of ion pairs; that is, the experimental data lead to $[(R_1^-, Cat^+)_T] + [(R_1^-, Cat^+)_L] = [(R_1^-, Cat^+)_{total}]$ and to the analogously defined value of $[(R_2^-, Cat^+)_{total}]$. These data yield the *apparent* equilibrium constants, $K_{1,2}^*$, defined as

$$K_{1,2}^* = \frac{[(R_1^-, Cat^+)_{total}][R_2H]}{[(R_2^-, Cat^+)_{total}][R_1H]}$$

that is

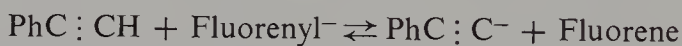
$$K_{1,2}^* = \frac{\{[(R_1^-, Cat^+)_T] + [(R_1^-, Cat^+)_L]\}[R_2H]}{\{[(R_2^-, Cat^+)_T] + [(R_2^-, Cat^+)_L]\}[R_1H]}$$

A rearrangement leads then to the relations

$$K_{1,2}^* = K_{1,2}^T \frac{1 + K_2^{TL}}{1 + K_1^{TL}} = K_{1,2}^L \frac{1 + 1/K_2^{TL}}{1 + 1/K_1^{TL}}$$

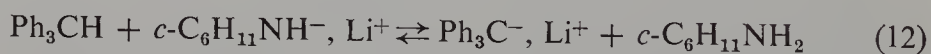
The temperature dependence of $K_{1,2}^*$ may therefore be rather complex. To our knowledge such a treatment of acid-base equilibria has not yet been reported in the literature, although similar studies of electron-transfer equilibria have been disclosed [29, 57] see p. 48.

In a system in which one hydrocarbon yields tight ion pairs while the other gives rise to loose pairs the equilibrium approach may lead to an erroneous value of ΔpK . An example is provided by the studies of equilibria established in cyclohexylamine between lithium salts of fluorenyl derivatives on the one hand and phenylacetylene or *t*-butylacetylene on the other [35]. The fluorenyl-lithium and its derivatives form loose pairs in this solvent while lithium phenylacetylenide or *t*-butylacetylenide are present as tight pairs. The degree of dissociation into free ions is substantially higher for the fluorenyl salts than for those of acetylenides. Hence the "correct" equilibrium constant K^- referring to the conventional reaction of free ions.

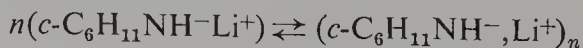


is substantially smaller than the directly determined value of K^\pm . The ΔpK^\pm calculated directly from the equilibrium involving the above salts requires a large correction to give the proper value of the conventional ΔpK^- and, on the whole, any experimental ΔpK obtained for such "mixed" ion pairs must be used with caution.

The equilibria involving different kinds of ion pair are associated with relatively large entropy and enthalpy changes. The conversion of loose to tight pairs releases solvent molecules and thus increases the entropy of the system, but at the price of a higher enthalpy. This results in a marked temperature effect. A dramatic illustration is afforded by the equilibrium of triphenylmethane with lithium cyclohexylamide [28]:



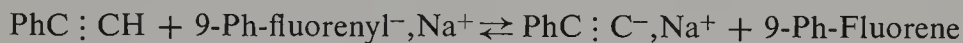
When a mixture of these compounds in cyclohexylamine is heated in a sealed optical cell, the original red solution becomes colorless above 100°. However, the color is regenerated on cooling to room temperature and the cycle can be repeated indefinitely. The equilibrium constant has a value of about 50 at room temperature with $\Delta H = -12$ kcal/mole and $\Delta S = -32$ eu. The reaction is exothermic due to the increased solvation of Li^+ in the loose $\text{Ph}_3\text{C}^-, \text{Li}^+$ ion pairs but at the expense of entropy lost in localizing additional solvent molecules. As a result, increased temperature shifts the equilibrium to the left until the highly colored $\text{Ph}_3\text{C}^-, \text{Li}^+$ species becomes undetectable. This system does not seem to be complicated by the aggregation of the lithium cyclohexylamide pairs,



which shifts the equilibrium even further to the left; however, since ΔH of this aggregation is about zero [31a], it has no effect on the thermochromism discussed above.

In many systems association of ion pairs into higher aggregates is endothermic [32] because the solvation energy even of tight ion pairs is greater than the aggregation energy into the still less solvated clusters. Such an effect, if operative in the previously discussed example, would enhance the thermochromism.

Ion pairing and the aggregation of ion pairs is extensive in diethyl ether, and even more in benzene. The pioneers [33, 34] who studied the equilibria between the salts of carbon acids in these solvents were not aware of these complications which affected their results. Hence the values of pK determined in those days have only qualitative significance and some are substantially in error. Nevertheless, these studies served admirably to focus our attention on the important problem of hydrocarbon acidities and their variation with molecular structure. An example of an erroneous result is provided by the system phenylacetylene and 9-phenylfluorene. On the McEwen scale, phenylacetylene and 9-phenylfluorene are equally acidic. This result was derived from studies of the equilibrium

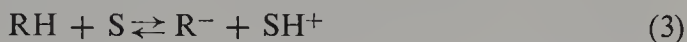


established in diethyl ether. It is probable that the sodium salt of phenylacetylene is extensively aggregated in diethyl ether, and the equilibrium is thereby shifted far to the right. Consequently, the calculated ΔpK is too low and the apparent acidity of phenylacetylene is too high. Studies of the corresponding equilibrium involving the respective lithium salts in cyclohexylamine [35] have led to ΔpK of about 5, implying that phenylacetylene is five powers of 10 less acidic than 9-phenylfluorene. As our previous discussion suggests (see p. 159) even this large ΔpK applies to a mixed ion pairs system and the ΔpK for free ions is undoubtedly larger yet.

Most likely, similar complications affect the results of Shatenstein et al. [70], who studied the acidities of carboranes. These workers interpreted their findings in terms of "solvent-differentiating" effects; it would seem, however, that cation solvation and aggregation are responsible for the peculiarities of their observations.

2.5. Acidity Scales

In principle, an acidity scale may be established in every solvent S by investigating the equilibrium



According to the accepted convention, $pK_{RH \text{ in } S}$ is identified with $-\log K(3)$; the activity of the pure solvent is taken as unity and infinitely dilute solutions of RH , R^- , and SH^+ are their reference states. Such a definition leads to different acidity scales for various solvents, the difference, $\Delta pK = pK_{RH \text{ in } S_1} - pK_{RH \text{ in } S_2}$ being determined by the free energies of the following transfer reactions [21]:

- a. Transfer of a proton from its infinitely dilute solution in S_1 to an infinitely large volume of S_2 .
- b. A similar transfer of an R^- ion.
- c. A similar transfer of the RH acid.

The term arising from transfer *a* is constant for all acids RH , since its value depends only on the nature of the two investigated solvents, S_1 and S_2 . By contrast, the terms arising from transfers *b* and *c* depend on the individual properties of R^- ions and RH molecules, as well as on the nature of the investigated solvents. Hence, although the first term leads only to a shift in the pK values, leaving the difference $\Delta = pK_{R_iH} - pK_{R_jH}$ independent of the solvent, the variations of the other two terms affect the relative pK values as well as the absolute values of the individual pK 's. This makes it impossible to set up a universal pK scale for all of the hydrocarbon acids [35].

The dependence of the free energies of transfers *b* and *c* on the nature of R^- and RH is a fundamental reason preventing the creation of universal pK scale, whereas the phenomenon of ion pairing introduces only technical difficulties in establishing such a scale. Ion pairing affects the concentrations of the *free* R^- and SH^+ ions but it does not influence the value of $K(3)$, provided that the concentrations of *free* ions are used in the computation. Similarly, ion pairing may lead to erroneous values of $\Delta pK_{i,j}$ if the determinations are based on the approximate relation $\Delta pK_{i,j} = -\log K_{i,j}^\pm$. However, the correct values of $-\log K_{i,j}^-$ may always be deduced, provided that the relevant dissociation constants, or at least their ratio, are known. Only experimental difficulties may prevent us from obtaining these data; in principle, they are measurable.

Several techniques may be used in practical determinations of pK 's of hydrocarbon acids:

1. The direct determination of $K(3)$ is limited to strongly protophilic solvents of high dielectric constant. Such severe limitations make this method of little importance.
2. Application of the H_- method is more common. The foundations of this technique as well as its limitations and drawbacks have been extensively examined in recent reviews by Boyd [38] and by Rochester [39]. As is now well recognized, various indicators lead to different values for H_- for the same

solvent-base combination. Moreover, since many of the hydrocarbons studied are structurally greatly different from the indicators used in setting up the H_- scales, it is questionable whether the underlying assumption calling for equal ratios of activity coefficients can be justified even approximately. In particular, hydrogen bonding between anions of indicators possessing negative charge on oxygen or nitrogen is generally different from and more important than that operating with highly delocalized carbanions. Consequently, the ratios of the corresponding activity coefficients are expected to be markedly different. In view of this effect it should be stressed that the value of 18.5 assigned to the pK of 9-phenylfluorene in dilute aqueous solution is only approximate. Nevertheless, it is useful and convenient to retain such a reference point until a better and more reliable estimate becomes available. The value of 18.49 advocated for the pK of 9-phenylfluorene has been derived from several determinations performed in a variety of aqueous solvents [40].

3. The glass electrode technique has been successfully applied by Ritchie and Uschold [41, 42] in their determination of pK 's of many hydrocarbon acids in DMSO. Ion pairing is avoided in dilute DMSO solution because the dielectric constant of that medium is high. Therefore the potentiometric results provide directly the conventional pK 's referred to infinitely dilute DMSO solutions as the standard states.

4. Studies of the equilibria $R_1^-, Cat^+ + R_2H \rightleftharpoons R_1H + R_2^-, Cat^+$ have led to the most extensive set of data for numerous carbon acids. To date, pK values for several dozen hydrocarbons have been obtained by Streitwieser and his co-workers, and work along this line still continues. Although the primary results of such studies provide ΔpK 's, the absolute values referred to dilute aqueous solution as the standard state could be calculated by accepting, somewhat arbitrarily, the value of 18.49 for the pK of 9-phenylfluorene in that reference state.

The conceptual dilemmas encountered in such studies have been discussed in the previous sections of this chapter, hence they need not be considered again. However, some experimental problems affecting the measurements deserve some comments. The position of the equilibria investigated was determined spectrophotometrically, taking advantage of the strong and distinct absorptions in the near UV and visible spectrum range of the ion pairs R_1^-, Cat^+ and R_2^-, Cat^+ [27, 28]. The appearance of an isosbestic point may then serve to check the reliability of the primary data. The spectrophotometric approach has recently been expanded. Pairs of carbon acids were investigated even when only one of the resulting carbanions absorbs in the useful range of the spectrum [35, 43, 55]. This imposes a high demand on the purity of the reagents and solvents and requires meticulous exclusion of moisture and oxygen during the manipulations. All of the experimental

Table 4 Acidities of Hydrocarbons

Compound	Water Standard State				Absolute pK DMSO ^e	Ion Pair pK in CHA ^{f,k}
	MSAD ^a	LiCHA ^{b,k}	CsCHA ^{c,k}	DMSO (H ₁) ^d		
Fluoradene	11				10.5	1.38
1,3-Diphenylindene			13.94	15.40		3.15
Cyclopentadiene	15					
1,12-(<i>o</i> -Phenylene)-7,12-dihydropleiadene			15.39		14.4	4.60
4-Cyano-9-phenylfluorene				15.40		
9-Phenyl-3,4-benzfluorene				16.60		4.89
9-(<i>m</i> -Chlorophenyl)fluorene				17.66		
9-(<i>m</i> -Trifluoromethyl-phenyl)fluorene				17.69		
9-(<i>p</i> -Chlorophenyl)fluorene				18.10		
9-(<i>m</i> -Anisyl)fluorene				18.47		
9-(<i>m</i> -Tolyl)fluorene				18.84		
9-(<i>p</i> -Tolyl)fluorene				18.96		
9-(<i>p</i> -Anisyl)fluorene				19.01		
9-(<i>p</i> - <i>N,N</i> -Dimethylamino-phenyl)fluorene				19.61		
9-Phenyl-3,4-benzfluorene			15.68			4.89
9-Phenylfluorene	(18.5)	(18.49)	(18.49)	(18.59) ⁱ	16.4	7.70
3,4-Benzfluorene		19.68	19.75	19.62		8.96
Indene	18.5	20.24	19.93		18.5	9.14
1,2-Benzfluorene		20.27	20.35			9.56
9-Benzylfluorene			21.27 ^h	21.20		10.48
9-Methylfluorene		22.6 ^h	22.44 ^h	21.80	19.7	11.65
9-Ethylfluorene		22.96 ^h	22.58 ^h	22.22		11.79
4,5-Methylenephenanthrene		22.60	22.93	21.79	20.0	12.14
Fluorene	22.9	23.09	23.04	22.10	20.5	12.25

Phenylacetylene	18.5	23.2 ^g			12.4
9- <i>i</i> -Propylfluorene		23.75	23.25 ^h	22.70	12.46
2,3-Benzfluorene		23.47	23.47		12.68
9- <i>t</i> -Butylfluorene		24.82 ^h	24.25 ^h	23.41	13.46
Acetylene	25				
<i>t</i> -Butylacetylene		25.5 ^g			14.7
1,1,3-Triphenylpropene	26.5		26.59		15.80
10-Biphenyl-9,9-dimethyl-9,10-dihydroanthracene			27.7		17.65
10-Phenyl-9,9-dimethyl-9,10-dihydroanthracene			28.04		17.25
<i>p</i> -Biphenyldiphenylmethane			30.20	25.3	19.41
bis(<i>p</i> -Biphenyl)methane			30.86		20.07
Triphenylmethane	32.5		31.48	27.2	20.69
Diphenylmethane			33.45	28.6	22.66
4-Phenyltoluene			38.7		27.9
Toluene (α position)	35		41 ⁱ		30
Benzene	37		43 ^j		32
Cumene (α position)	37				

^a Ref. 2.

^b Ref. 27.

^c Ref. 26, 101.

^d Ref. 51, 65.

^e Ref. 42.

^f Ref. 52.

^g Ref. 35.

^h Ref. 53, 54.

ⁱ Ref. 54.

^j Ref. 55.

^k pK per hydrogen; CHA ≡ cyclohexylamine or cyclohexylamide.

^l pK measurement for CH₃OH-DMSO taken as reference standard for H₂O-DMSO.

difficulties were eventually surmounted and reproducible results have been obtained [35].

5. Equilibrium studies were extended to alkanes by Applequist and O'Brien [44], who investigated systems involving organolithium reagents and alkyl iodides in ether or ether-pentane mixtures:



Although equilibrium 14 was found to be relatively insensitive to dilution, the interpretation of the results is questionable because organolithium reagents are aggregated into tetramers or hexamers [45]. Moreover, the binding in these compounds is only partially ionic and such compounds can be treated to only a limited extent as ion pairs. Similar objections cloud the interpretation of the results of Dessy and his co-workers [46, 47], who studied the equilibria



Dialkylmercury compounds should be classified as covalently bonded and not as ionic. Even dialkylmagnesiums can hardly be treated as ion pairs, although the latter do have more ionic character than the former.

Because the ionic character of carbon-metal bonds is greatly changed in these reactions, the reactivity scale derived from such equilibria is expected to be compressed when compared to that based on the related equilibria of ion pairs.

2.6. Structural Factors Affecting pK

The experimental data available in 1965 were combined by Cram [2] into the so-called MSAD scale of pK's presented in Table 4. In spite of the difficulties arising from the heterogeneous nature of these values, some of which may be questioned, this scale provided the best and most thorough compendium of equilibrium acidities of hydrocarbon acids. Although updated by Kosower [48], the MASD scale suffers, nevertheless, from some minor limitations which should not be disregarded.

Table 4 also includes the more recent pK values derived from the studies of equilibria involving lithium and cesium salts in cyclohexylamine (the LiCHA and CsCHA columns, respectively) and the data obtained by the H_- technique in DMSO. All of these data are given in the form of pK's referred to a water standard. The last two columns of Table 4 list the original data of Ritchie [41] referred to DMSO as the standard, and the ion pair pK values in cyclohexylamine.

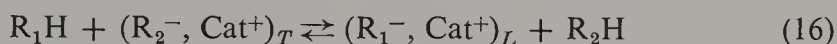
It is worth stressing that differences between the pK's referred to water as the standard and those referred to DMSO are approximately constant and

amount to about 2 pK units. This confirms the basic self-consistency of all of the collected values, albeit a closer examination of the data reveals a greater compression for the pK values determined in DMSO than for those obtained from experiments involving cyclohexylamine as the solvent. The anions of the stronger acids probably exist in DMSO as free ions, but those derived from weaker acids might be partially paired with the cation. On the other hand, in cyclohexylamine all of the anions are present as ion pairs.

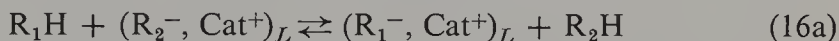
Our discussion of the data listed in Table 4 will be limited to some structural problems clarified by the recent studies. A general discussion of this subject has been reported elsewhere [102].

Despite the overall harmony and simplicity shown by these data, some interesting differences are noted between the relative pK's referred to lithium cyclohexylamide and those pertaining to the cesium salt. The underlying causes of these discrepancies were amply discussed in the previous sections of this chapter. We wish, however, to stress a point that could be easily overlooked.

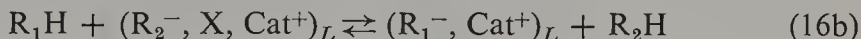
Consider an acid-base equilibrium,



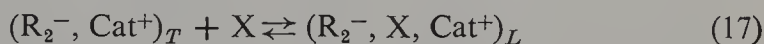
where virtually all the R_2^- , Cat^+ pairs are tight while R_1^- , Cat^+ are loose. Let us assume that $K(16)$ is about unity, although the hypothetical equilibrium,



is displaced far to the right. The addition of a powerful solvating agent X in an amount small but sufficient to convert nearly all of the $(R_2^-, Cat^+)_T$ tight pairs into the loose, separated by X $(R_2^-, X, Cat^+)_L$, would shift then the equilibrium far to the left; thus for



$K(16b)$ is much smaller than $K(16)$, although $K(16a)$ is much larger than $K(16)$. In fact, denoting by $K_2(17)$ the equilibrium constant of



we find $K(16b) = K(16)K_2(17)[X]$.

In the most general case, X may be coordinated with R_1^- , Cat^+ and R_2^- , Cat^+ . The system involves then four types of ion pair,* $(R_1^-, Cat^+)_L$,

* The equilibrium concentrations of $(R_1^-, Cat^+)_T$ and $(R_2^-, Cat^+)_L$ are assumed to be negligible.

Table 5 Temperature Dependence Studies

Fluorene-9-X X =	DMSO [51]		CsCHA [53]		LiCHA [53]	
	ΔpK		ΔpK	ΔH° (cal/mole)	ΔH° (cal/mole)	ΔS° (eu)
H	0	0	0	0	-290 \pm 60	1.8 \pm 0.2
Methyl	-0.3	-0.41	-0.41	-740 \pm 40	-780 \pm 50	0.0 \pm 0.2
Ethyl	0.12	-0.14	-0.14	-650 \pm 50	-770 \pm 40	-1.8 \pm 0.2
<i>i</i> -Propyl	0.60	0.46	0.46	400 \pm 40	180 \pm 40	-2.1 \pm 0.2
<i>t</i> -Butyl	1.31	1.49	1.49	1320 \pm 40	1100 \pm 200	-3.8 \pm 0.2
Benzyl	-0.90	-1.47	-1.47	—	—	—

^a The reported ΔH_0 and ΔS_0 refer to the reaction 9-X-fluorene + 2,3-Benzofluorenyl⁻, Li⁺ \rightleftharpoons 9-X-fluorenyl⁻, Li⁺ + 2,3-Benzofluorene.

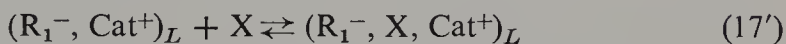
$(R_1^-, X, Cat^+)_L$, $(R_2^-, Cat^+)_T$, and $(R_2^-, X, Cat^+)_L$. The apparent equilibrium constant, K_{ap} , defined as

$$K_{ap} = \frac{\{[(R_1^-, Cat^+)_L] + [(R_1^-, X, Cat^+)_L]\}[R_2H]}{\{[(R_2^-, Cat^+)_T] + [R_2^-, X, Cat^+)_L]\}[R_1H]}$$

is therefore given by the equation

$$K_{ap} = \frac{K(16)(1 + K'_1(17)[X])}{1 + K(17)[X]}$$

where $K'_1(17)$ denotes the equilibrium constant of the association



In conclusion, the hydrocarbon giving rise to ion pairs that become more extensively associated with X appears to be more acidic on the addition of such a solvating agent.

Let us return to the discussion of the effect of substituents on the acidity of hydrocarbon acids. The determination of the acidities of 9-alkylfluorenes is of considerable interest and the results should help to establish the nature of the electronic effects of alkyl groups at an sp_2 hybridized carbon center. Studies of Bowden et al. [51] and of Ritchie and Uschold [58] have shown that 9-methylfluorene is *more* acidic than fluorene. The relevant pK's referred to free ions were determined in DMSO-H₂O mixtures and in DMSO. Similar results have been obtained from studies of equilibria involving the respective cesium or lithium salts in cyclohexylamine [53]. All of the pertinent results, as well as those concerned with other 9-alkylfluorenes, are collected in Table 5.

The acidity decreases along the series Me, Et, *iso*-Pr, and *t*-Bu but sharply increases for the benzyl substituent. This gradation combined with the inequality $pK(\text{fluorene}) > pK(9\text{-methylfluorene})$ might appear strange. Nevertheless, an excellent linear relation, shown in Fig. 2, is obtained on plotting the pK's of benzyl, methyl, ethyl, and *iso*-propyl fluorenes versus Taft's σ^* ; a slight deviation observed for the *t*-butyl substituent seems to result from steric effects. The steric strain, revealed also by the spectrum of the 9-*t*-butylfluorenyl salt [53], could distort that carbanion from the planar configuration characterizing the other related carbanions.

The fact that fluorene itself does not fit the correlation is not surprising. It is well known that the parent compounds often deviate from correlations

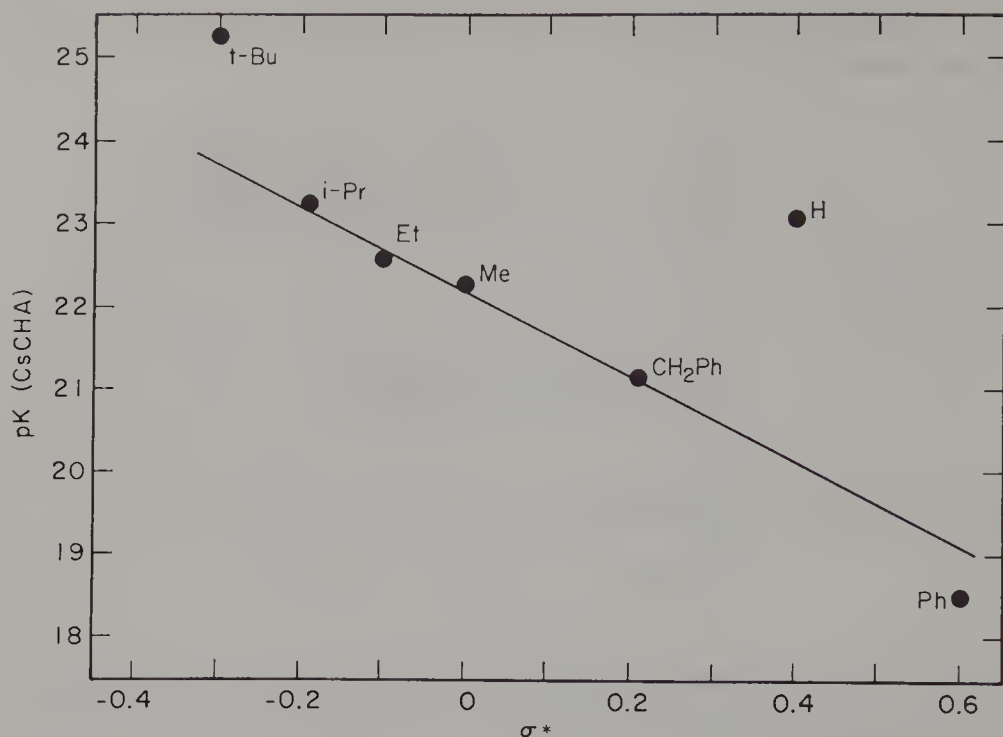


Figure 2. pK's of substituted 9-R-fluorenyls versus Taft's σ^* . Reproduced from ref. 53.

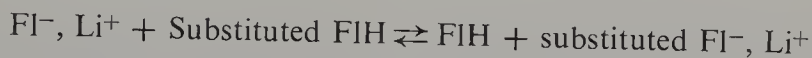
shown by their derivatives because secondary hydrogens may behave differently from tertiary.

Correlations with σ^* are generally attributed to the operation of the relative inductive effect. Alkyl substituents seem therefore to be electron donating with respect to a trigonal carbon, and the observed gradation of pK's is due to the higher electronegativity of sp_2 orbitals when compared with sp_3 . It is particularly gratifying to observe how well the benzyl substituent fits into this correlation. Indeed, all of the available criteria point to a lower electron-donating power of benzyl than of the other alkyls, and the position of the point representing this substituent on Fig. 2 is fully justified. Thus it would seem that even in this system the alkyl groups act as electron-donating substituents.

Why, therefore, is 9-methylfluorene *more* acidic than the unsubstituted fluorene? Apparently the stabilization of fluorenyl anions by alkyl groups results from the change in the σ bond strength as the $C_{sp_3}-C_{sp_3}$ bond is converted into a $C_{sp_3}-C_{sp_2}$ bond. In the unsubstituted fluorene the comparable bond change involves the transformation of $C_{sp_3}-H$ into $C_{sp_2}-H$ and there is abundant evidence that an increase in the s character leads to a greater stabilization of the C—C bond than of the C—H bond [59, 60]. In the fluorenyl anion the delocalization of the negative charge diminishes the polar

effect of the methyl, as well as of other alkyl substituents. Thus the destabilizing polar effect of the methyl group is more than compensated by the relative increase in the C—C bond strength when compared with the increase in the strength of the C—H bond, and hence the substitution of a methyl group for hydrogen leads to a net stabilizing effect on the carbanion. In less delocalized systems the relation could be reversed and methyl substitution should cause a net destabilization. The results collected in Table 5 may be rationalized in these terms; moreover, such reasoning leads to the prediction that toluene should be a stronger acid than ethylbenzene (statistical factors being taken into account).

The observed temperature dependence of equilibria involving salts of substituted fluorenes deserves some comment. The data collected in Table 5 indicate a decrease in the entropy of the reaction

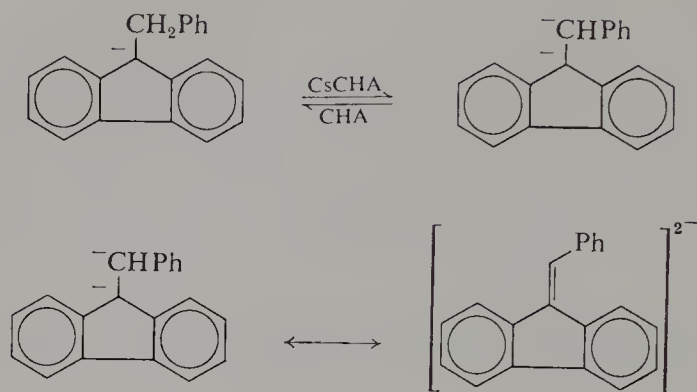


particularly for the *t*-butyl substituent, whereas in the analogous reaction involving cesium salts ΔS is small and constant. Apparently the lithium ion enlarged by its solvation shell, but not the smaller nonsolvated Cs^+ ion [63], hinders the free rotation of the alkyl substituent. Although this explanation is plausible, technical difficulties encountered in these studies [53] make this conclusion tentative.

We may digress at this juncture and discuss briefly the nature of lithium ion pairs derived from the 9-substituted fluorenes. Chan and Smid [61] concluded that the higher proportion of loose ion pairs in solutions of 9-hexylfluorenyl lithium as compared with the unsubstituted salt, as well as the substantially higher heat of conversion of the tight into loose pairs in the former than in the latter system, are due to steric hindrance preventing a close approach of the lithium ion to the carbanion. It seems, however, that these observations may be better accounted for by considering the interference of the substituent with the *external* solvation of the Li^+ cation in a *tight* pair [62]. Indeed, only this explanation accounts for the pressure effects observed in these systems [62]. A similar conclusion has been deduced from the studies of substituted fluorenes [53].

Finally, it is interesting to note the drastic changes in the spectrum of 9-benzylfluorenyl $^-$, Cs^+ in cyclohexylamine as the base concentration increases [53]. At low base concentration the spectrum closely resembles those of the other alkyl-substituted lithium fluorenyls, but an entirely new spectrum appears at high concentration of the base. The original spectrum reappears as the concentration of the base decreases. These reversible spectral changes

indicate the formation of a dilithium salt:



Steric hindrance affects the relative acidities of toluene, diphenylmethane, and triphenylmethane. The difference of 7.5 units between the pK of toluene and diphenylmethane clearly contrasts with the difference of only two units when pK's of diphenylmethane and triphenylmethane are compared. Undoubtedly, this peculiarity reflects the noncoplanarity of the triphenylmethyl anion. In this crowded ion the phenyl groups are tilted out of the plane of the central trigonal carbon atom, which diminishes their degree of conjugation. Interestingly, the substitution of a phenyl group for one *p*-hydrogen in triphenylmethane or diphenylmethane results in a nearly identical decrease of pK by 1.3 and 1.2 units, respectively. Apparently the biphenyl group of biphenyldiphenylmethane acquires a nearly coplanar configuration with the trigonal carbon atom leaving the other two phenyl groups tilted, because such a configuration makes the most efficient use of the π -system conjugation. Therefore the effect of this substitution is as pronounced in the triphenylmethyl system as it is in the planar diphenylmethyl.

The foregoing principle is underscored by the contrary observations in the dihydroanthracene series. The replacement of the 10-phenyl group by biphenyl in 9,9-dimethyl-10-phenyldihydroanthracene leads to an increase in the acidity by only 0.4 units. The two benzo groups of dihydroanthracene are firmly locked into a nearly coplanar configuration, whereas the 10-phenyl group has to be tilted out of plane. The stability of the relevant ion is therefore only slightly increased on replacing that phenyl group by biphenyl. Even in 9-phenylfluorene the enhanced acidity compared to fluorene itself results largely from the inductive effect of the phenyl substituent; there is only a slight enhancement of conjugation since it is hindered by the steric strain. Indeed, as may be seen from Fig. 2, the 9-phenyl group affects the acidity only slightly more than expected on the basis of its σ^* value.

The noncoplanarity of the benzene ring in the 9-phenylfluorene anion was further demonstrated by Cockerill and Lamper [65]. The pK_a 's of nine 9-arylfluorenes were measured in aqueous DMSO-tetramethylammonium hydroxide and were fitted to an extended Hammet-type correlation,

$$\log \left(\frac{K}{K_0} \right) = \rho(\sigma_1 + n\sigma_R)$$

Although the value for n of 0.6 indicates some phenyl conjugation, a 4-cyano substituent exerts a greater effect on the fluorenyl system than do substituents in the phenyl ring.

Finally, let us consider the acidities of aryl hydrogens. The acidities of some fluorinated benzenes were determined by investigating the equilibria involving the respective cesium salts in cyclohexylamine with 9-*t*-butylfluorene, di-*p*-biphenylmethane, triphenylmethane, and tri-*p*-tolylmethane as the indicators [55]. The results are summarized in Table 6, the pK 's being

Table 6 Acidities of Fluorinated Benzenes

Compound	pK^a
	Toward CsCHA in Cyclohexylamine (CHA)
<i>o</i> -C ₆ H ₄ F ₂	35.0 ^b
1,2,3,4-C ₆ H ₂ F ₄	31.5
C ₆ HF ₅	25.8

^a Per hydrogen.

^b Only 3- and 6-hydrogens assumed active.

referred, as previously, to $pK = 18.49$ assigned to 9-phenylfluorene.

The effectiveness of the fluorosubstituents in stabilizing the substituted phenyl anion depends on their position. These effects agree with those calculated on the basis of the Kirkwood-Westheimer model invoking the electrostatic interaction of the substituent dipole with a localized phenyl anion in a dielectric cavity [71].

The results given in Table 6 may be converted into partial ΔpK factors, that is, the ΔpK of stabilization of the phenyl anion for each fluorine atom. Such partial ΔpK 's are listed in Table 7 and are found to be almost identical with the analogous partial rate factors computed from the rates of hydrogen isotope exchange of fluorobenzenes catalyzed by lithium cyclohexylamide.

Table 7 Carbanion Stabilization Factors for Fluorobenzenes

	ΔpK Ar^-, Cs^+ in CHA [55]	$\Delta \log k$ (40°) for t Exchange with NaOMe [66]	$\log k_{rel}$ ($C_6H_6 = 1$) 25° for t Exchange with LiCHA [55, 71]
<i>ortho</i>	5.7	5.25	5.43
<i>meta</i>	2.3	2.07	1.95
<i>para</i>	1.1	1.13	1.03

The results presented in Tables 6 and 7 may be extrapolated to furnish the pK value for benzene. A plot of the predicted rates of exchange in NaOH—MeOH using the data of Table 7 versus pK 's given in Table 6 is linear and extrapolates to pK of benzene of 42.93. The alternative linear extrapolation utilizing the rates of exchange catalyzed by lithium cyclohexylamide leads also to $pK = 42.90$ for benzene. Thus the value $pK = 43$ provides the best presently available estimate of the acidity of benzene based on the reaction



3. KINETICS OF PROTON TRANSFER

3.1. Brønsted Relation

Reactions such as



have been the subject of numerous investigations. Insight into their mechanism is facilitated by studies of Brønsted relations and by the determination of isotope effects.

A linear free energy relation between rates of proton transfer and the respective ΔpK was revealed by Brønsted studies in 1923 [72], and the underlying ideas justifying this functional dependence were fully expanded a few years later [73]. According to Brønsted, for a series of chemically similar acids, A_iH , derived by introducing substituents into A_oH , the rate constants k_i of their reaction with a common base B obey the relation

$$\log \left(\frac{k_i}{k_o} \right) = \alpha \log \left(\frac{K_i}{K_o} \right) = \alpha \Delta pK_{i,o}$$

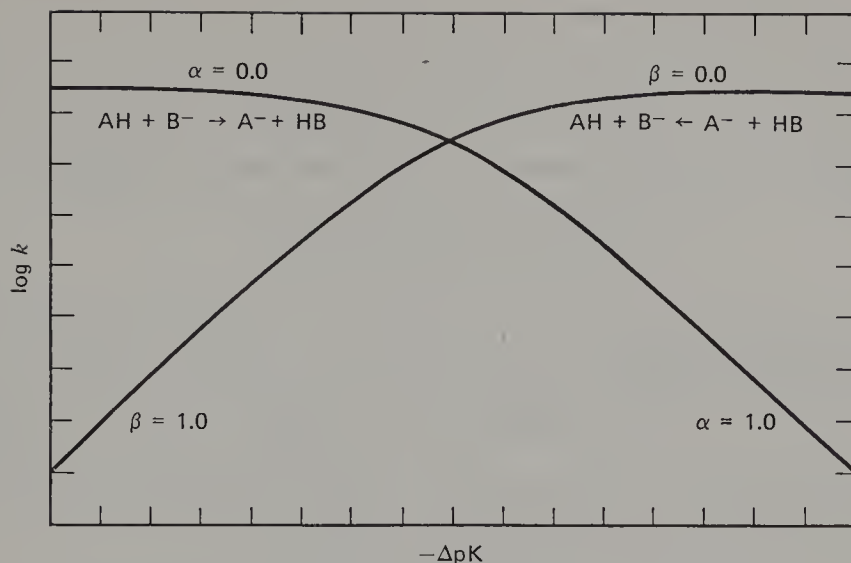


Figure 3. Eigen's plot showing the anticipated variations of Brønsted α and β with ΔpK

Thermodynamics then demands for the reverse reactions proceeding with the rate constants k_{-i} that

$$\log \left(\frac{k_{-i}}{k_{-o}} \right) = -(1 - \alpha) \log \left(\frac{K_i}{K_o} \right) = -(1 - \alpha) \Delta pK_{i,o} = -\beta \Delta pK_{i,o}$$

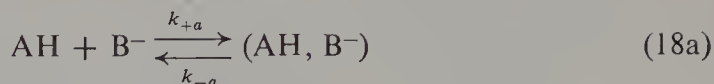
In the following years the value of α has often been used as the criterion of the extent of proton transfer in the transition state [1, 67, 68].

Following Eigen [68], one expects a smooth variation of α from 1 to 0 as the differences in the acidities of A_iH and B^- increase. Indeed, for a series of very strong acids α should be 0, because the reaction then becomes diffusion controlled and therefore its rate is independent of the nature of A_iH . On the other hand, α should be unity for a series of extremely weak acids since the reverse reaction, $A_i^- + BH$, becomes diffusion controlled under those conditions. Moreover, it would be plausible to expect α values of about 0.5 for $\Delta pK_{i,BH} \approx 0$. Verification of these relations as depicted schematically in Fig. 3 have been provided by Eigen's work. Consequently, it is frequently assumed that $\alpha \approx 0.5$ is indicative of a symmetric proton-transfer transition state, whereas $\alpha \approx 0$ and $\alpha \approx 1$ imply highly unsymmetric transition states.

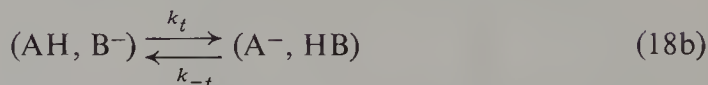
A discussion of some general features of bimolecular solution processes yielding two species as the products is in place here. Such reactions involve three steps [2, 9]:

1. The diffusion-controlled approach of the reagents to the distance at

which they form an "encounter" complex:



2. The actual transfer of proton within the "encounter" complex:



3. The diffusion of the products out of the "caged" encounter complex into the bulk of the liquid:



On the assumption of stationary state for both encounter complexes the overall forward reaction rate constant k_i is given by

$$k_i = \frac{k_{+a}k_t k_{+b}}{k_{-a}k_{+b} + k_t k_b + k_{-a}k_{-t}}$$

For many processes the actual proton-transfer steps are rate controlling; that is, k_t and k_{-t} are much smaller than k_{+a} , k_{+b} , k_{-a} , and k_{-b} . Provided that the concentrations of the encounter complexes are very small and stationary, the overall rate of the forward reaction is then given by

$$k_i = K_a \cdot k_t$$

where $K_a = k_{+a}/k_{-a}$. However, for k_t much greater than k_{-a} and k_{-t} , the rate of the encounters becomes rate determining and thus $k_i = k_{+a}$.

In most systems the rate of formation of the encounter complex is indeed determined by the rate of diffusion since the two reagents brought into proximity of each other remain together for a sufficiently long time to acquire the configuration needed for the proton transfer. This is not always the case. If one or both reagents are strongly solvated, a partial desolvation is needed before they come into a proper "encounter," and then k_{+a} may become smaller than the diffusion-controlled rate constant. Alternatively, the proton involved in the transfer may participate in an *intramolecular* hydrogen bond which has to be dissolved before the proper configuration of the reagents is attained. This may also decrease the value of k_{+a} . Both situations have been observed and discussed fully by Eigen [68].

A reverse situation has also been described. In hydrogen-bonded solvents such as water, the proton transfer may occur through intervening solvent molecules, that is, in an enlarged "encounter complex." This leads to an abnormally large collision cross section [87] and therefore to k_{+a} values greater than expected for a diffusion-controlled reaction. Proton transfer from

benzoic acid to benzoate ion in methanol solution [80] illustrates such a process. Further examples of these phenomena are provided by recent studies of Grunwald and Ku [81] and Grunwald and Ralph [82].

In some processes k_{-t} is greater than k_b and k_t . This inequality leads to an extensive "internal return" and slows the observed overall proton transfer. In the extreme case, the experimentally determined rate constant is given by

$$k_i = K_a K_t k_{+b} = K_a K_t K_b \cdot k_{-b} = k_{-b} K_{\text{overall}},$$

provided that $k_{-a} \gg k_{+b}$.

The reactions of the acids A_iH with a solvent S acting as a base exemplify an important case of pseudo-first-order proton transfers, its pseudo-first-order rate constants, k_i^I , being

$$k_i^I = \frac{k_t k_{+b}}{k_{-t} + k_{+b}}$$

This equation is reduced to $k_i^I = k_t$ provided $k_{+b} \gg k_{-t}$, that is, the products have a much higher chance to diffuse out of the "cage" than to react and reform the initial reaction encounter pair.

The classic approach to the Brønsted relation identifies the observed rate constant of proton transfer with k_t . As shown in the preceding discussion such an identification is not always permissible. Moreover, the conventional ΔpK is given by $-\log K_a K_t K_b$ while the reasoning implicit in Brønsted relation should refer to $-\log K_t$. The identification of the conventional ΔpK with $-\log K_t$ is strictly justified only when $K_a K_b = 1$.

Our attention has been focused on proton-transfer reactions involving either neutral bases or bases present as free anions. Proton transfer to an ion pair, B^- , Cat^+ , may be more complex. A "proper" encounter is attained when the reagents acquire a configuration in which the acidic proton is placed in the vicinity of that site of the base which eventually will accommodate the new H-base bond. The counterion may be left then in an unfavorable position, its transfer to the ultimate anion being hindered. In such systems some substituents may affect the rate of the reaction by facilitating or further hindering the cation transfer, whereas their effect on the intrinsic proton transfer may be negligible or even contrary to the effect exerted on the transfer of the cation.

Before further pursuing the problems arising from the Brønsted relation, let us survey some of the available experimental data. A classic example of the Brønsted relation applied to carbon acids was reported by Pearson and Dillon [74]. These workers studied a series of carbon acids in which the developing carbanion becomes conjugated to nitro, carbonyl, cyano, or sulfonyl groups. A plot of each relevant k_i versus the corresponding pK_i

referred to aqueous solution is presented in Fig. 4. In spite of a substantial scatter, the experimental points, covering a large range of pK 's amounting to 14 units, comply reasonably well with a straight line having a slope $\alpha = 0.6$. The absence of any curvature is particularly remarkable when these results are compared with those derived from Eigen's studies of hydroxy acids and nitrogen bases. There, the values of α often vary from 0 to 1 within a relatively narrow range of 7 units of the relevant pK 's [68].

The relative ability of the acid to form in the encounter complex a hydrogen bond with the attacking base may account for the differences just noted. Indeed, the stronger the hydrogen bond, the more facile the proton transfer should be. Therefore the Brønsted α could be anticipated to decrease with increasing strength of hydrogen bond and, furthermore, the range of ΔpK within which α varies from 1 to 0 should become narrower. These conclusions seem to be verified by studies of Ahrens and Maass [75].

The strength of a hydrogen bond decreases along the series of oxygen, nitrogen, and sulfur acid bases. The value of $\alpha = 0.6$ in the Pearson-Dillon linear plot is therefore consistent with this effect, because the conjugated carbon acids form, at best, only weak hydrogen bonds with the bases.

The enhancing effect of hydrogen bonding discussed in the preceding section should be distinguished from the effect arising from hydrogen bonding by the solvent. Ritchie and Uschold [76] showed that nitromethane, water, phenol, and *p*-toluenesulfonic acid all react at approximately the same rate with trityl anion or with 9-fluorenyl anion in DMSO, although the acids used include a carbon acid as well as oxygen acids. This result contrasts sharply with the pattern observed in aqueous solution; there, carbon acids react by orders of magnitude more slowly than oxygen acids. Ritchie and Uschold therefore postulated that the lack of hydrogen bonding of water to carbon acids is responsible for their relatively slow proton transfer in aqueous media; a large degree of solvent reorganization is then needed in the transition state to stabilize the incipient anion. On the other hand, hydroxy acids are already extensively hydrogen bonded to water in the way that stabilizes the incipient anion, and this allows for a fast proton transfer to the investigated base. In polar aprotic solvents, such as DMSO, neither type of acid forms hydrogen bonds with the solvent. Under these conditions carbon acids and hydroxy acids may be treated on a more comparable basis because the latter's reactivity is not enhanced by the solvent. Therefore the large difference in their reaction rates is greatly reduced. These qualitative conclusions have recently been placed on a more rigorous basis by Kurz and Kurz [162].

Alternatively, hydrogen bonding of solvent to the base or the acid may prevent the occurrence of proton transfer. For example, a carbon acid must compete with methanol molecules for a methoxide base if the reaction is carried out in methanol. This means that a hydrogen bond,

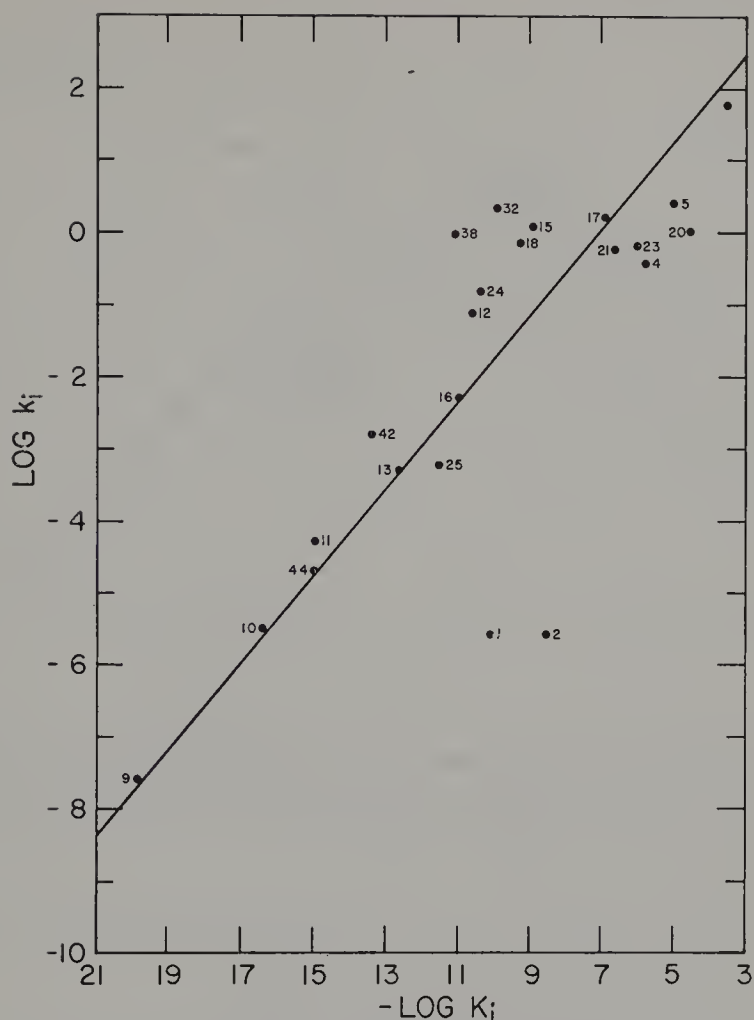


Figure 4. Brønsted plot giving the rates of ionization k_i of carbon acids as a function of the respective ionization equilibrium constants K_i . ΔpK 's refer to aqueous solutions. The numbers refer to: 1-MeNO₂, 2-EtNO₂, 4-C₂H₅OCO.CH₂NO₂, 5-CH₃COCH₂NO₂, 9-CH₃COCH₃, 10-CH₃CO.CH₂Cl, 11-CH₃CO.CHCl₂, 12-CH₃COCH₂COOEt, 13-CH₃-COCH(C₂H₅)COOEt, 15-CH₃COCH₂COCH₃, 16-CH₃COCH(CH₃)CO.CH₃, 17-CH₃-COCHBrCOCH₃, 18-CH₃COCH₂COPh, 20-CH₃CO.CH₃COCF₃, 21-PhCOCH₂COCF₃, 23- α -(COCH₂COCF₃)thiophene, 24- α -(COOEt)-pentanone, 32-CH₃COCH₂COOMe, 38-CH₂(CN)₂, 42-CH₂(COOEt)₂, 44-CH(Et)(COOEt)₂. Reproduced with permission from ref. 74.

CH₃OH \cdots ⁻OCH₃, must be broken to allow for the reaction and therefore a greater reorganization of the solvent is taking place in such a transition state. Consequently, the proton transfer may be hindered in these systems, and the same reaction performed in an aprotic solvent such as in DMSO should proceed faster. Examples of this situation have been provided by Ritchie and

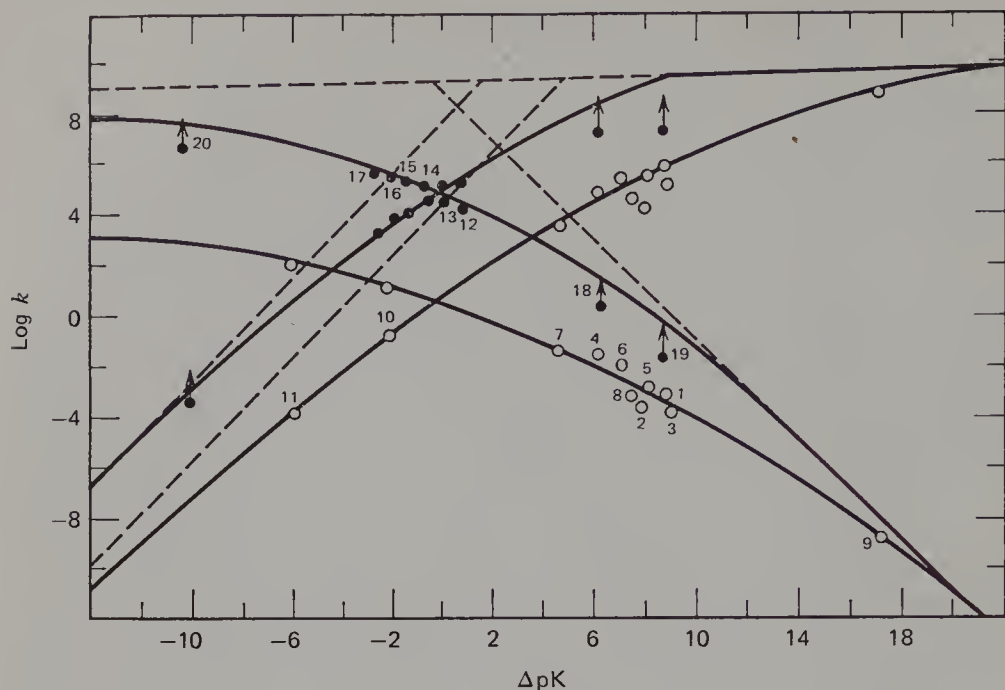


Figure 5. Brønsted plot of forward and backward rates of reactions of hydrocarbon acid with anionic oxygen bases in methanol (open circles) and in DMSO (closed circles). The numbers refer to: 1–10, substituted fluorenes and Ph_3CH with CH_3O^- ; 12–17, substituted fluoradenes and 9-carbomethoxy fluorene with fluoradene and 9-carbomethoxy fluorene carbanion. Reproduced with permission from ref. 77.

Uschold [77], who studied proton transfer between benzoic acid and carbanions in DMSO and methoxide ion in methanol.

These factors also account for another interesting observation derived from the work of Ritchie and Uschold [77]. The Brønsted plot of their rate constants (Fig. 5) indicates that for the reaction proceeding in methanol the Brønsted α varies from 1 to 0 as ΔpK increases by 18 units, whereas a much smaller ΔpK range leads to the same effect in DMSO. The interpretation of these results in terms of the foregoing discussion is obvious. A more rigorous treatment of all of these problems was presented recently by Murdoch [161], who showed that the changes of α are affected not only by ΔpK but also by the height of the potential barrier for proton transfer at $\Delta\text{pK} = 0$ and by differences in the limiting proton transfer rates at $\alpha = 0$ for the forward and $\beta = 0$ for the reverse reaction, $\beta = 1 - \alpha$.

A closer inspection of the Pearson-Dillon plot in Fig. 4 reveals that the slope of the line drawn by them was determined by the points referring to the carbonyl compounds. However, a line determined by the nitro compounds (points 1, 2, 4, 5, and 6 of their graph) has $\alpha > 1$. Brønsted relations with $\alpha > 1$ might appear strange. Nevertheless, the recently reported experimental

evidence leaves no doubt about their reality. Bordwell et al. [78, 79] showed that the rates of deprotonation of 12 derivatives of $\text{ArCH}(\text{Me})\text{NO}_2$ in 50% aqueous methanol conform to the Brønsted relation with a slope $\alpha = 1.31$; the correlation coefficient for these experimental points has the high value of 0.992. The results obtained for 13 compounds of the type $\text{ArCH}_2\text{—CH}(\text{Me})\text{NO}_2$ again conform to the Brønsted relation with an even higher α of 1.61, the correlation coefficient being 0.977. These findings imply, of course, that the reverse reactions, the general base-catalyzed deprotonation of solvent by the corresponding nitromethyl carbanions, display the opposite behavior, thus the Brønsted $\beta (= 1 - \alpha)$ is then negative.

Further difficulties encountered in the conventional interpretation of the Brønsted relation emerge from the following facts. The reactions of weak acids such as 1-phenylnitroethane ($\text{pK} = -8.6$) and 1-phenyl-2-nitropropane ($\text{pK} = -8.9$) with aqueous OH^- are expected to proceed through a reactant-like transition state because their $-\Delta\text{pK}$'s are so large. Therefore the anticipated values of α should be close to 1. However, the experimentally determined α 's for 1-arylnitroethanes and 1-arylnitromethanes were found to be 1.14 and 1.5, respectively, when the reaction was carried out in water at 25°C [83]. Moreover, according to the usual interpretation, the transition state of proton transfer should become more symmetric when OH^- is replaced by a weaker base. However, recent results of Bordwell and Boyle [83] refute this idea. These workers studied the deprotonation of *meta*-substituted 1-arylnitroethanes and aryl nitromethanes in water caused by hydroxide ion, pyridine, diethylamine, piperazine, and morpholine. Their findings, illustrated by the data collected in Table 8, show *no* increase in α in spite of large

Table 8 Brønsted α Values for Deprotonation of *meta*-Substituted 1-Arylethanes in Water at 25°C [83]

Base	ΔpK	α
Hydroxide	-8.6	1.14
Piperidine	-4.1	0.99
Diethylamine	-4.0	0.96
Piperazine	-2.5	0.90
Morpholine	-1.6	0.93

changes in ΔpK . In fact, α remains approximately constant while ΔpK changes by 7 units.

To clarify the problems of α variation we have to examine the factors responsible for changes of pK and of the rate constant. It has been said repeatedly that α may measure the extent to which the proton is transferred in

the transition state, its transfer being complete in the final state. The transfer of a proton is associated with the development of negative charge on the acid residue, R_i , the charge being developed partially in the transition state but fully in the final state. Consider now a series of acids R_iH derived from R_oH by introducing dipolar substituents. Such substituents interact with the charge developed in the transition state or acquired in the final state. The interaction energy depends on the charge distribution as well as on the degree of its transfer to R_i . For a series of R_i 's in which the charge distribution in the transition state is virtually the same as in the eventually formed carbanion R_i^- , the interaction of the dipolar substituent with the charge would be stronger in the final state than in the transition state. This would make $\alpha < 1$ and its numerical value could then provide a valid measure of the degree of charge development and hence of the degree of proton transfer. However, this simple relation does not follow when the distribution of charge in the transition state is substantially different from that attained in the final state.

Let us realize, to begin with, that the strange behavior of α is observed for a series of compounds for which ΔpK and the respective rates vary only slightly. The developing charge may be located mainly on a side chain in the transition state; for example, in aryl nitromethanes the central carbon atom appears to be highly pyramidal in the transition state and the anionic charge is only partially delocalized into the aromatic ring. However, this central carbon acquires a trigonal hybridization in the final stage and the charge is then greatly delocalized into the nitro group. Consequently, the dipolar *meta* substituent may interact more strongly with the partially developed charge formed in its vicinity than with the fully developed but delocalized charge of the final anion [78]. In such a situation the α is greater than 1, and of course its value does not provide any guidance about the degree of proton transfer in the transition state. A similar although somewhat differently worded argument was presented recently by Kresge [84].

Large changes in acidity of carbon acids are caused by the increased delocalization of the negative charge in the resulting carbanion. This factor makes toluene, for example, a much weaker acid than diphenylmethane. For such systems the Brønsted α should provide a valid measure of the degree of proton transfer in the transition state. Naively, one might anticipate one-half of the charge being delocalized into the incipient carbanion provided that the transition state is symmetric; α should then have a value of about 0.5. In fact, the situation is more complex, as we shall see later. However, let us first consider some other examples of the Brønsted relation before we continue with this discussion.

An example of a Brønsted relation not affected by changes in charge distribution was provided by Cram and Kollmeyer [85], who studied base-catalyzed deuterium exchange of polyarylmethanes and fluorene in methanolic

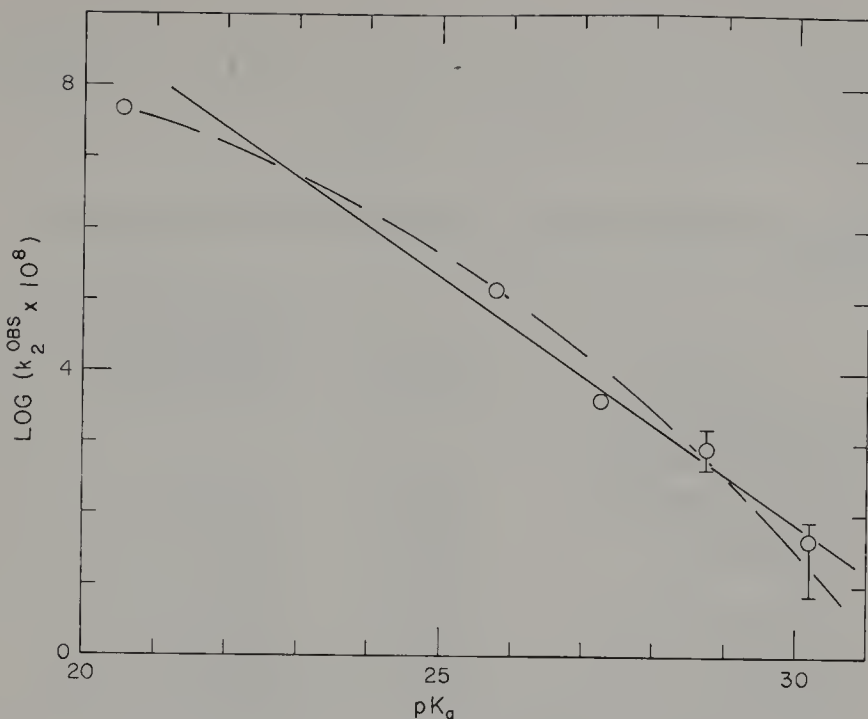


Figure 6. Brønsted plot for base-catalyzed ($\text{CH}_3\text{O}^-\text{K}^+$) deuterium exchange of polyaryl-methanes and fluorene in methanolic DMSO. Reproduced with permission from ref. 85.

DMSO containing potassium methoxide. Their results are graphed in Fig. 6. Although a single line corresponding to $\alpha = 0.7$ has been drawn through all five points in Fig. 6, it would appear that a curve should fit the data better to give α of about 0.5 for fluorene and about 1 in the pK region of triphenyl-methane.

A related reaction, tritium exchange between similar hydrocarbons and methanolic sodium methoxide, has been studied extensively by Streitwieser et al. [49, 50]. The relative rates were determined at 45°C for 14 hydrocarbons and the results, summarized in Table 9, show the reactivities of the investigated hydrocarbons to vary within 10 powers of 10. The choice of the pK values needed for the construction of a proper Brønsted plot presents some problems. Few data are available for the equilibrium pK's of hydrocarbons in methanol, although many data for these hydrocarbon pK's are available in other solvents, for example, in aqueous solutions by way of H_L methods, in DMSO by the glass electrode method, and in cyclohexylamine through studies of equilibria involving cesium salts. The latter pK's are also listed in Table 9, and Fig. 7 gives the corresponding Brønsted plot. It is apparent that the data may be divided into two sets: those pertaining to fluorene-type compounds and the other to polyarylmethanes. Both sets give

excellent linear Brønsted plots. For the 9-fluorene-type compounds the Brønsted α is 0.37 and for the 5-polyarylmethane points it has a value of 0.58. Neither set can be correlated better by a curve; moreover, no reasonable curve can accommodate the entire set of 14 points.

Table 9 Equilibrium and Kinetic Acidities of Some Hydrocarbons [49, 50]

Hydrocarbon	pK (CsCHA) (per H)	k_2 ($M^{-1} \text{ sec}^{-1}$), 45°, Tritium Exchange in MeOH-MeONa
1,12- <i>o</i> -Phenylene-7,12-dihydropleiadene (1)	15.39	5.63×10^{-1}
9-Phenyl-3,4-benzfluorene	15.68	1.03×10^{-1}
9-Phenylfluorene	18.49	1.73×10^{-2}
3,4-Benzfluorene	19.75	9.03×10^{-3}
Indene	19.93	5.00×10^{-3}
1,2-Benzfluorene	20.35	3.19×10^{-3}
4,5-Methylenephenanthrene	22.93	6.85×10^{-4}
Fluorene	23.04	3.95×10^{-4}
2,3-Benzfluorene	23.47	2.15×10^{-4}
10-Phenyl-9,9-dimethylhydroanthracene	28.04	6.98×10^{-8}
<i>p</i> -Biphenyldiphenylmethane	30.20	4.39×10^{-9}
bis(<i>p</i> -Biphenyl)methane	30.86	2.28×10^{-9}
Triphenylmethane	31.48	6.41×10^{-10}
Diphenylmethane	33.45	5.43×10^{-11}

These results imply that the fluorenes and arylmethanes form two distinct Brønsted "families." Hence the respective points in Brønsted plot should be treated separately and not lumped together. Only then do the relevant α 's have the proper physical meaning.

A similar example was published recently by Jencks and co-workers [163]. The aminolyses of acetylimidazole or *p*-tolyl-*N,N*-dimethylacetimidate led to different values of the Brønsted α , depending on whether oxygen or amine base was the catalyst. This signals a change in the nature of Brønsted "family" resulting from a change in the nature of the base.

It seems probable that the Cram and Kollmeyer results presented in Fig. 6 manifest the same phenomenon. The points representing the four polyarylmethanes lie on an excellent straight line while the "best fit" curve drawn in their figure is dominated by the point representing fluorene. Unfortunately, Cram and Kollmeyer investigated only one fluorene-type hydrocarbon; therefore a dissection of their data into two different straight lines cannot yet be achieved.

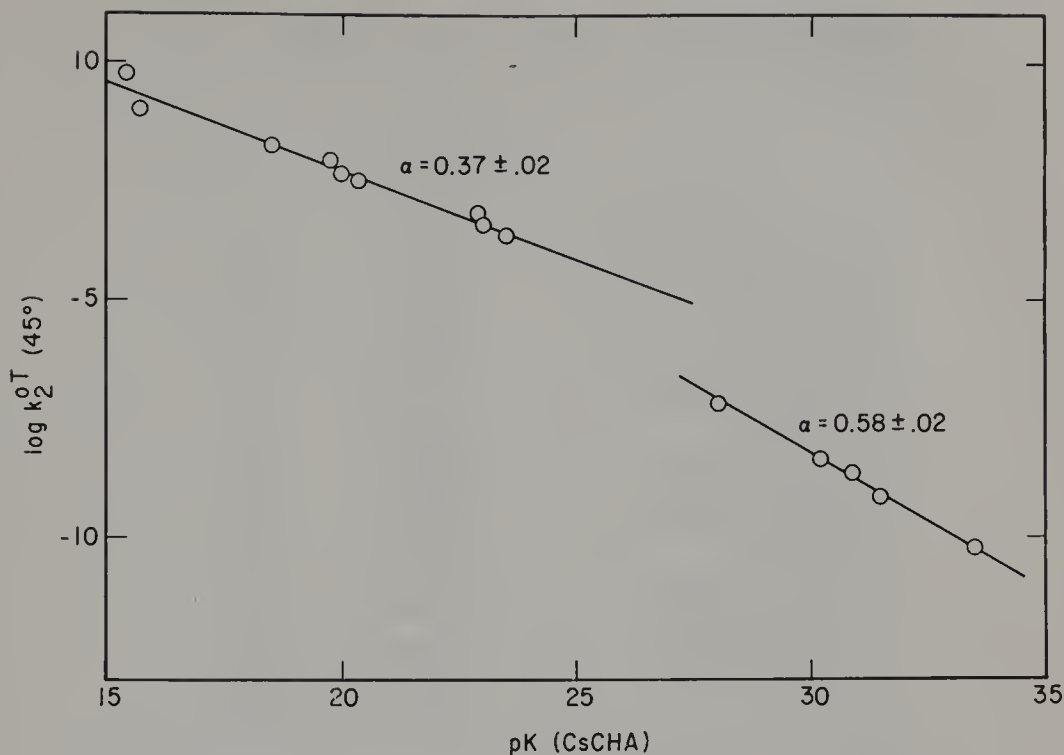


Figure 7. Brønsted plots for tritium exchange between sodium methoxide and substituted fluorenes (left) and triarylmethanes (right) in methanol. Note that the fluorenes and triarylmethanes represent two distinct Brønsted “families” and are related by different α ’s. Reproduced from ref. 50.

The reason for the different α values for these two series of hydrocarbons has not yet been established. Probably it is associated with the special aromaticity of the central cyclopentadienyl ring of the fluorenyl systems. In such systems the anionic charge associated with a given degree of proton transfer may be delocalized more effectively than in the arylmethyl systems.

The rates of tritium exchange in cyclohexylamine with lithium cyclohexylamide as a base were investigated for *p*-biphenyldiphenylmethane, bis-*p*-biphenylmethane, triphenylmethane, diphenylmethane, and 4-phenyltoluene [54, 55]. Their pK’s were determined by studying the equilibria established with cesium cyclohexylamide [101]. The results, collected in Table 10, were used to construct a Brønsted plot shown in Fig. 8. The experimental points yield an excellent straight line with $\alpha = 0.264$.*

* Some of the results collected in Tables 9 and 10 pertain to the same acids but participating in *different* reactions, namely the exchange in MeOH–MeONa and the exchange in cyclohexylamine lithium cyclohexylamide. These are then two distinct Brønsted families and, not surprisingly, their α ’s are different.

Table 10 The Brønsted Relation for Arylmethanes in Cyclohexylamine Systems

Compound	log <i>k</i> rel (DPM = 1)	
	LiCHA, 50°	pK (CsCHA)
<i>p</i> -Biphenylyldiphenylmethane	0.83 ^c	30.20 ^a
bis(<i>p</i> -Biphenylyl)methane	0.56 ^c	30.86 ^a
Triphenylmethane	0.47 ^c	31.48 ^a
Diphenylmethane (DPM)	0.00 ^c	33.45 ^a
4-Phenyltoluene	−1.45 ^c	38.7 ^a
3-Methylfluoranthene	0.280	32.2 ^b
1-Methylpyrene	0.266	32.3 ^b
4-Methylantracene	−0.442	34.9 ^b
2-Methylantracene	−0.552	35.3 ^b
9-Methylphenanthrene	−0.764	36.05 ^b
2-Methylpyrene	−0.867	36.4 ^b
3-Methylnaphthalene	−0.897	36.6 ^b
8-Methylfluoranthene	−0.892	36.6 ^b
1-Methylnaphthalene	−1.040	37.1 ^b
2-Methylnaphthalene	−1.175	38.1 ^b
Toluene	−2.04	40.9 ^b

^a Table 4.^b Estimated from Brønsted correlation (rates from Ref. 128).^c Ref. 101.

The rate constants of the exchange of a number of polycyclic arylmethanes with lithium cyclohexylamide in cyclohexylamine were determined by Streitwieser and Longworthy [128]. By using their data in conjunction with the Brønsted plot shown in Fig. 8, the pK values of these hydrocarbons may be calculated. These pK's are included in Table 10 and are strictly comparable with all the others determined by the equilibrium technique involving cesium salts in cyclohexylamine.

Although the Brønsted plot in Fig. 8 appears to be highly reliable, it would be even better had the rates and equilibria been determined for the same types of ion pair. Unfortunately this could not be done because the rates of exchange with cesium cyclohexylamide are about 10,000 times faster than with lithium cyclohexylamide [129] and could not be measured conveniently. On the other hand, lithium cyclohexylamide is too weak a base to allow the equilibrium studies for hydrocarbon acids weaker than triphenylmethane [28].

The Brønsted α derived from the plot in Fig. 8 would appear to be low, although, according to all indications, it should provide a valid measure of the degree of charge delocalization in the transition state. The primary

isotope effect (see Section 3.2) implies that the above transition state is symmetric: the proton is half transferred and, at that stage of the reaction, the carbanion should have about one-half of the negative charge. These results can be reconciled by assuming a substantially pyramidal structure of the

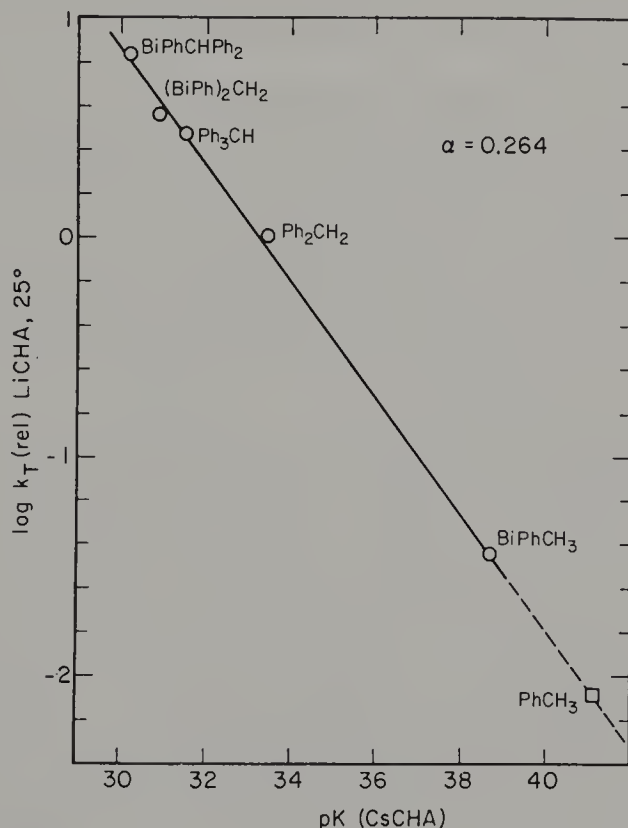


Figure 8. Brønsted plot for tritium exchange between polyarylmethanes and cyclohexylamine catalyzed by lithium cyclohexylamide. The pK's were determined from the equilibria established between the hydrocarbons and their cesium salts in cyclohexylamine. Reproduced from ref. 54.

central C atom in the transition state. Only a small portion of the total charge donated by the attacking base is then delocalized into the π system; most of it still remains on the pyramidal central carbon atom.

Unfortunately, there is no other strong evidence yet to discriminate between a planar and a pyramidal configuration in such a transition state. The secondary α -deuterium isotope effect obtained from studies of exchange involving toluene- α -d₃ ($k_H/k_D = 1.15$ per deuterium at 50°) [130] lacks suitable analogies at this time for a proper structural interpretation. The

$\sigma - \rho$ correlation with $\rho = 4.0$ [96b] is approximately what one would expect for a pyramidal benzyl carbanion with restricted conjugation with the benzene ring. A correlation with σ^- would be more definitive but few substituents suitable for such a test are stable under the conditions of the exchange. The available examples indicate definite conjugation of the central carbon with the benzene ring, for example, with such substituents as *p*-F [96b] and *p*-SiMe₃ [131] but even slight conjugation would explain the observations.

In conclusion, all of the results are consistent with the hypothesis of a relatively pyramidal benzyl transition state involving some conjugation with the benzene rings but substantially lesser than that expected for a planar carbanion.

The foregoing results corresponding to a relatively low value of α contrast with those derived from studies of the hydrogen isotope exchange in the *ortho*, *meta*, and *para* positions of fluorobenzene with LiCHA. The respective Brønsted plot led in this system to $\alpha \approx 1$. Apparently when the proton transfer gives a highly localized carbanion, the transition state for proton transfer to the hydrocarbon is virtually identical with the final state.

It is important to recognize that fluorenyl and polyarylmethyl hydrocarbons belong to different Brønsted "families" since this has wide repercussions. For example, the "curved" Brønsted correlation of Ritchie and Uschold [77] displayed in Fig. 5 is strongly biased by the point referring to triphenylmethane at one extreme and by the set of points associated with several fluorene-type hydrocarbons at the other end of the scale. Their correlation also included compounds having dipolar substituents, 9-trifluoromethylfluorene being an outstanding example. Hence the resulting correlation spans regions characterized by different interaction mechanisms determining reactivities and stabilities, and therefore its significance in revealing deeper features of the Brønsted relation is blurred.

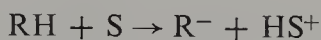
An example of an erroneous Brønsted relation is found in a paper by Zatzepina et al. [86], who tried to obtain the pK values of a variety of heterocyclic compounds by determining their rates of exchange with methanol catalyzed by methoxide ions. The rates of this reaction were determined for only three hydrocarbons, fluorene, diphenylmethane, and triphenylmethane, and the results were used for the construction of a Brønsted plot. This plot was then utilized for extrapolation to give the desired pK's of the heterocyclics.* Thus the derived pK values have only qualitative significance; the assumed Brønsted correlation is based on hydrocarbons belonging to different Brønsted sets and therefore extrapolation is questionable. This uncertainty is further magnified by the fact that heterocyclic compounds contain dipolar

* pK of methylpyridines have been determined recently by Zoltewieg and Helmick [169].

substituents (the heteroatom) and therefore belong to a greatly different Brønsted family than the hydrocarbons used in that investigation.

3.2. Isotope Effects in Proton Transfer Involving Free Ions

The degree of dissociation in a solvent S is significantly different for a labeled and unlabeled acid, say RH and RD . The main effect arises from the difference in the zero point energies of their bonds. For the reaction



the energy gained in forming the bond $S^+—H$ but breaking $R—H$ is given by $D(S^+—H) - D(R—H)$. The corresponding energy gain in the dissociation of the isotopic acid is $D(S^+—D) - D(R—D)$. Thus the net change in energy differentiating these two processes is given by

$$\{D(S^+—H) - D(R—H)\} - \{D(S^+—D) - D(R—D)\} \\ \approx \frac{1}{2}h(\nu_{R-H} - \nu_{S^+-H})(1 - 2^{-1/2})$$

For $\nu_{R-H} > \nu_{S^+-H}$ this expression is positive, implying that the degree of dissociation of RH is higher than that of RD . A more comprehensive treatment of this problem is found in ref. 1.

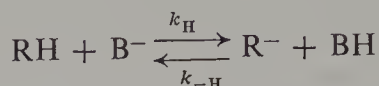
In the specific case of a carbon acid dissociating in a protophilic solvent the relation $\nu_{R-H} > \nu_{S^+-H}$ is undoubtedly correct. However, an additional factor needs to be considered. The carbon acid is poorly solvated whereas the interaction of S^+H with the molecules of the protophilic solvents is strong. This interaction results in vibrations involving the acidic hydrogen and the respective zero point energies facilitate the dissociation of RD and oppose the original gain in energy favoring RH .

For oxygen acids dissociating in H_2O or D_2O the available data [90] indicate that the process $RH + H_2O \rightarrow R^- + H_3O^+(K_H)$ is favored over $RD + D_2O \rightarrow R^- + D_3O^+(K_D)$, although in these systems both the acid and the cation are solvated. However, these dissociations differ from those discussed previously since not only the isotopic composition of the acid but also that of the solvent has been changed.

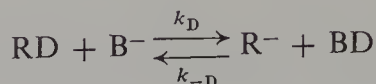
The Brønsted relation appears to apply to some isotope effects [90]. A plot of $\log K_H/K_D$ for 15 oxygen acids versus pK is roughly linear, giving the approximate relation $d \log (K_H/K_D) = -0.02 d(pK_H)$.

In mixed solvents, such as mixtures of H_2O , HDO , and D_2O , the problem becomes more complex and it is necessary to distinguish between k_H and k_D (rate constants in H_2O and D_2O , respectively) and $\kappa_H/\kappa_D = (H/D)_{\text{product}}/(H/D)_{\text{solvent}}$. A detailed discussion of this problem is reported by Kreevoy [91].

In a proton transfer from an acid to a base the isotope effect refers to reactions such as



and

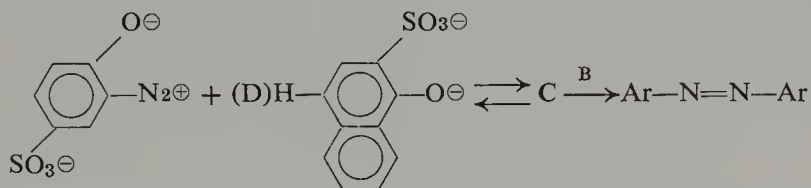


As was first suggested by Westheimer [88], for a series of similar proton-transfer reactions, the isotope effect, measured by $k_{\text{H}}/k_{\text{D}}$, should have a maximum value when the transition state is symmetric in the sense that the two force constants pertaining to the hydrogen being transferred (between base and carbanion) are equal. This conclusion is compatible with the model of the transition state suggested by Biegeleisen [92]. Although it is difficult to give a quantitative measure of the departure of the transition state from the symmetrical state, it is reasonable to relate it, as was pointed out earlier, to the ΔpK referring to the pair of acids RH and BH . The first experimental verification of this conclusion was reported by Bell and Goodall [89], who studied the kinetic isotope effects in reactions of nitro compounds with OH^- , pyridine, 2,6-lutidine, and acetate ions as the bases. The plot of $\log k_{\text{H}}/k_{\text{D}}$ versus pK given in their paper clearly reveals a maximum at $\Delta\text{pK} \approx 0$; the data cover a large range of ΔpK , from -8 to $+14$, causing a variation of $k_{\text{H}}/k_{\text{D}}$ from about 4 to 10. The reaction involving 2,6-lutidine appears to be unusual, resulting in an exceptionally high isotope effect of about 20. A similar result was reported previously by Lewis et al. [93]. Apparently quantum mechanical tunneling contributes substantially to this process and accounts for the abnormal $k_{\text{H}}/k_{\text{D}}$ ratio.

The findings of Bell and Goodall have been augmented recently by Bordwell and Boyle [94], who investigated many more nitro compounds. Their results, corrected for the secondary isotope effect, allowed them to fill the gap in the original Bell-Goodall plot where no points were presented for ΔpK close to zero (the 2,6-lutidine being the only exception). Though the maximum appears to be real, it is rather flat. Hence one may conclude that either $k_{\text{H}}/k_{\text{D}}$ is relatively insensitive to the symmetry of the transition state, or else that its symmetry does not change over a wide range of ΔpK . Not surprisingly, Bordwell and Boyle derive a rather pessimistic conclusion: "The hope for a simple correlation of Brønsted coefficients, kinetic isotope effects, and solvent effects with the extent of proton transfer in the transition state has proved vain."

Alternatively, the validity of the relation associating isotope effects with the symmetry of the transition state of proton transfer may be tested by comparing it with the β coefficient of Brønsted. This approach, suggested by

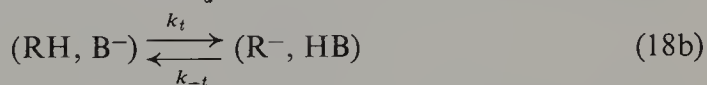
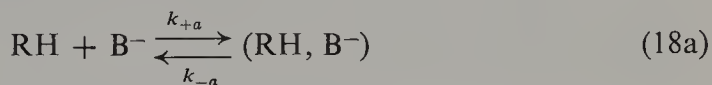
Bell and Goodall, was explored by Zollinger et al. [95]. Their studies of the general base-catalyzed diazo coupling, where **C** denotes the aggregate of the



two reagents, provided evidence for the expected variation of $k_{\text{H}}/k_{\text{D}}$ with pK at a constant β .

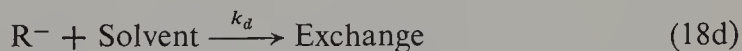
Small variations observed in isotope effects are subject to considerable experimental uncertainty and their interpretation is therefore ambiguous. The vibrations which are not associated with the stretching of the C—H bond ruptured in the process may contribute significantly to the observed effect. Such contributions may annul the expected trends, although unambiguous examples demonstrating these deviations are not yet available. However, the greatest difficulties preventing valid evaluation of “true” isotope effects are caused by the internal return step of the overall reaction.

Let us consider again the complete scheme of the bimolecular reaction outlined in Section 3.1:



Our interest is focused on reaction 18b. Here we deal with the transition state associated with proton transfer and this process contributes basically to the studied isotope effect. The rates of the diffusion steps, such as k_{+c} and k_{-c} , are affected little, if at all, by the isotopic composition of the reagents.

The exchange that measures the isotope effect may result from reaction 18d,

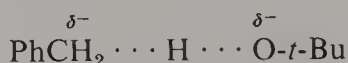


following step 18c. Thus the observed rate of exchange is determined entirely by k_t if and only if $k_{-t} \ll k_{+c}$; in this case the experimental isotope effect sheds light on the structure of the transition state of proton transfer. Generally the observed rate of exchange, k_{ex} , is given by

$$k_{\text{ex}} = \frac{k_t k_{+c}}{k_{-t} + k_{+c}}$$

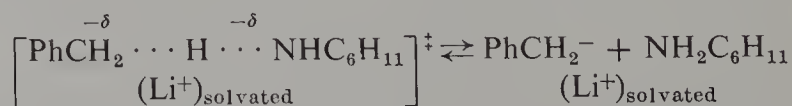
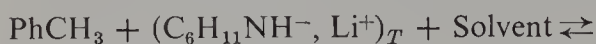
and therefore k_{ex} always is somewhat smaller than k_t . In the extreme case when $k_{+c} \ll k_{-t}$, the observed k_{ex} is equal to $(k_t/k_{-t})k_{+c} = K_t k_{+c}$, where K_t denotes the equilibrium constant of reaction 18b. Although this equilibrium constant depends on isotopic composition of the reagents, the dependence is small because the isotope effect of the backward reaction partially cancels that of the forward process. Consequently, in such a limiting case the observed isotope effect may be insignificant, though the "true" isotope effect could be large. The experimental findings then are misleading, since they do not pertain to the proper proton-transfer process [98].

To illustrate the problems arising from internal return, let us consider a few examples reported in the literature. Studies of the isotope effect in the hydrogen-deuterium exchange taking place between toluene and cyclohexylamine under the influence of lithium cyclohexylamide led to the ratio $k_{\text{H}}/k_{\text{D}} > 10$ [96]. However, in DMSO the exchange between toluene and toluene- α - d_3 catalyzed by potassium *t*-butoxide corresponds to the ratio $k_{\text{H}}/k_{\text{D}}$ of 0.6 [97]. The former ratio undoubtedly reflects the "true" isotope effect arising from the proton transfer, implying that under conditions of those experiments $k_{+c} \gg k_{-t}$. In contrast, the results derived from studies of the DMSO system indicate a rapid internal return, $k_{+c} \ll k_{-t}$ for the reaction proceeding in that solvent. We may only speculate about the factors responsible for the different behavior of these two systems. The reaction in DMSO may involve a purely ionic encounter complex,



which does not involve a counterion and lasts relatively long. Moreover, it is plausible that the barrier separating the two minima representing the initial and final stages of the transfer is low in respect to *both* minima. In such a case the equilibrium may be attained before the separation takes place.

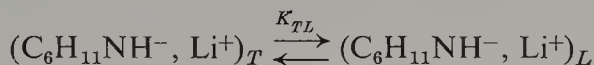
The analogous process occurring in cyclohexylamine involves a tight pair, $(\text{C}_6\text{H}_{11}\text{NH}^-, \text{Li}^+)_T$, but it results in a loose $(\text{PhCH}_2^-, \text{Li}^+)_L$ pair:



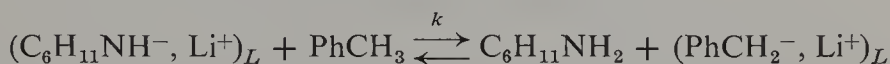
The shift of the proton between the two minima is coupled therefore with a substantial shift of the counterion and with its solvation; hence it cannot be fast. In fact, the need of desolvation of the cation in the transition state adds considerably to the slowness of the return. The high degree of solvation is indicated by the experimentally obtained values of ΔH^\ddagger and ΔS^\ddagger for the exchange in cyclohexylamine. The entropy of activation is -39 eu, implying

a considerable increase in the solvation of the transition state—undoubtedly associated with that of the Li^+ cation [31a].

The large negative entropy of activation of that exchange could be accounted for by an alternative mechanism: by postulating a high reactivity of loose $\text{C}_6\text{H}_{11}\text{NH}^-$, Li^+ ion pairs and an extremely low reactivity for the tight pairs. Thus the exchange would involve two steps, a rapid transformation of the tight amide pairs into loose ones:



and the actual exchange involving only the loose pairs:



The observed rate constant would then be equal to kK_{TL} and the negative entropy of the transformation, common for the conversions of tight into loose ion pairs, could explain the result.

In this example the reported observations are accounted for by the different behavior of various types of ion pair. Such differences in the behavior of ionic species will be discussed more thoroughly in a later section.

Internal return is especially pronounced when the geometry of the acid remains essentially unaltered in the proton transfer. Two examples illustrate this generalization. The isotope effect of the exchange of polyfluorobenzenes with methanol catalyzed by sodium methoxide show $k_{\text{H}}/k_{\text{D}} \approx 1.0$ [66]. The loss of tritium from the hydrocarbon is fast, as is its rate of incorporation from tritiated methanol; that is, the equilibrium is not affected by the isotopic composition of the reagents. The lack of any appreciable isotope effect on the rate is attributed to the extensive return facilitated by the identical geometry of PhH and Ph^- . Nevertheless, an isotope effect is observed in the reaction catalyzed by $\text{C}_6\text{H}_{11}\text{NH}^-$, Li^+ in cyclohexylamine [71]. Again, the participation of the counterion accounts for the slowness of the return in the latter system.

The bridgehead 1-*H*-undecafluorobicyclo(2.2.1)heptane provides another example of a molecule whose structure must remain essentially unaltered in the transition state of proton transfer. The exchange reaction was investigated [99] and, indeed, no isotope effect was observed.

Internal return is expected to be slow whenever the geometry of the transition state substantially differs from that of the initial state, even if the reaction involves free ions. Examples are provided by the exchange of 2-(*N,N*-dimethylcarboxamido)-9-methylfluorene proceeding in methanolic DMSO-potassium methoxide [85] and of a variety of nitroalkanes exchanging in aqueous solution [94]. In these systems an extensive reorganization has to

take place in the transition state and therefore the isotope effects are indeed large.

An interesting method allowing one to determine the extent of internal return from isotope effects data has been developed recently [50]. Studies of isotopic exchange between fluorene labeled by tritium in carbon 9 and deuterated methanol (CH_3OD) permits the loss of tritium and the loss of protons to be followed simultaneously. The former is determined by the loss of radioactivity and it gives $k_{\text{ex},\text{T}}$. The latter is measured by the rate of deuterium incorporation into the hydrocarbon. Thus from the experimental results one finds directly

$$\frac{k_{\text{ex},\text{T}}}{k_{\text{ex},\text{H}}} = \frac{k_t^{\text{T}} k_{+c}^{\text{T}} (k_{-t}^{\text{H}} + k_{+c}^{\text{H}})}{t_t^{\text{H}} k_{+c}^{\text{H}} (k_{-t}^{\text{T}} + k_{+c}^{\text{T}})}$$

where the symbols have the usual meaning defined by Eqs. 18a, 18b, and 18c applied to the reactions involving tritium (T) or protons (H), respectively. It is reasonable to assume that $k_{+c}^{\text{H}} = k_{+c}^{\text{D}} = k_{+c}^{\text{T}}$; that is, the diffusion step is not affected by the isotopic composition of the product. On this basis, the preceding equation may be recast into the following form:

$$\frac{k_t^{\text{T}}}{k_t^{\text{H}}} = \frac{k_{\text{ex},\text{T}}}{k_{\text{ex},\text{H}}} + a_{\text{T}} \left(\frac{k_{\text{ex},\text{T}}}{k_{\text{ex},\text{H}}} - \frac{K_{\text{T}}}{K_{\text{H}}} \right)$$

where

$$a_{\text{T}} = \frac{k_{-t}^{\text{T}}}{k_{+c}^{\text{T}}}, \quad K_{\text{T}} = \frac{k_t^{\text{T}}}{k_{-t}^{\text{T}}}, \quad \text{and} \quad K_{\text{H}} = \frac{k_t^{\text{H}}}{k_{-t}^{\text{H}}}$$

Similar experiments performed in ordinary methanol (CH_3OH) with deuterated fluorene labeled with tritium give the ratio

$$\frac{k_t^{\text{T}}}{k_t^{\text{D}}} = \frac{k_{\text{ex},\text{T}}}{k_{\text{ex},\text{D}}} + a_{\text{T}} \left(\frac{k_{\text{ex},\text{T}}}{k_{\text{ex},\text{D}}} - \frac{K_{\text{T}}}{K_{\text{D}}} \right)$$

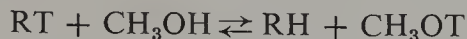
It should be stressed that the $k_t^{\text{T}}/k_t^{\text{H}}$ ratio determined in CH_3OD is slightly different from that which would be obtained were the reaction followed in ordinary methanol (CH_3OH). However, it is assumed that this difference is negligible and thus $k_t^{\text{T}}/k_t^{\text{H}}$ determined in CH_3OD and $k_t^{\text{T}}/k_t^{\text{D}}$ obtained in CH_3OH were treated as equal.

According to the Swain-Schaad treatment [100] the isotope effects of the primary proton-transfer step are related:*

$$\frac{k_t^{\text{T}}}{k_t^{\text{H}}} = \left(\frac{k_t^{\text{T}}}{k_t^{\text{D}}} \right)^y \quad (y = 3.26)$$

* A slightly different treatment outlined in ref. 49 gives a value of 3.344 for the exponent y .

The assumed independence on k_{+c} of the isotopic composition of the product implies that $K_T/K_H = K'_T$, where K'_T denotes the equilibrium constant of the reaction



K'_T is expected to be virtually the same for all of the hydrocarbons.

Having determined K'_T for 9-phenylfluorene ($K'_T = 1.3$) and substituting into the Swain-Schaad relation the derived values of k_t^T/k_t^H and k_t^T/k_t^D , one gets the equation

$$A + (A - B)a_T = \{1 - (B^{1/y} - 1)a_T\}^y$$

where A and B are experimentally determined quantities defined as

$$A = \frac{(k_{ex,D}/k_{ex,T})^y}{(k_{ex,H}/k_{ex,T})}$$

and

$$B = \left(\frac{k_{ex,D}}{k_{ex,T}} \right)^y K'_T$$

By using this approach, the values of a_T were evaluated for several hydrocarbons [50].

Insignificant internal return was found for the exchange of 9-methylfluorene and 9-phenylfluorene with sodium methoxide in methanol. However, the studies of the exchange with triphenylmethane performed under the same conditions led to a low value for the isotope effect, $k_D/k_T = 1.34$ at 100°C , and internal return was calculated to amount to about 66%. After correcting for the internal return, k_t^T/k_t^D was found to be 1.85 at 100°C , being only slightly smaller than the isotope effect of 9-methylfluorene and 9-phenylfluorene (2.08 at 100°C).

3.3. Kinetics of Proton Transfers Involving Ion Pairs and Higher Aggregates

In many ionic reactions a small fraction of the ionic substrate is present in the form of a highly reactive species. These may then be the main contributors to the observed process. For example, in $10^{-3} M$ solution of sodium polystyryl in tetrahydrofuran, about 1% of the salt is present as free polystyryl ions; however, that 1% of the reagent is responsible for more than 90% of polymerization [103]. A similar situation is encountered in some proton-transfer reactions as shown by the recent studies of Chan and Smid [104], who investigated the proton transfer from triphenylmethane to polystyryl base in a variety of solvents. Sodium or potassium constituted the counterions

balancing the negative charge of the carbanions. The initial rate of the reaction, $(dR^-/dt)_0$, determined the apparent bimolecular rate constants, k_{ap} :

$$\left(\frac{dR^-}{dt}\right)_0 = k_{ap}[\text{Ph}_3\text{CH}]_0[\text{polystyryl}^-, \text{Cat}^+]_0$$

and, although k_{ap} was independent of $[\text{Ph}_3\text{CH}]_0$, its value was proportional to the reciprocal of $[\text{polystyryl}^-, \text{Cat}^+]_0^{1/2}$. Such a relation, illustrated by Fig. 9, indicates that although the bulk of the base is in the form of ion pairs, a small fraction, present as free ions which are in equilibrium with ion pairs,

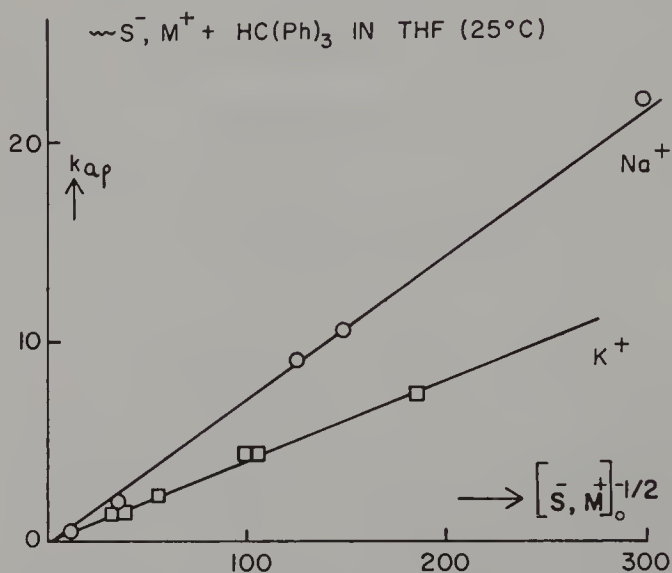
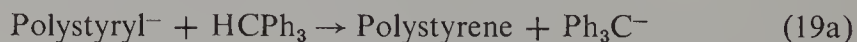


Figure 9. Plot of the apparent bimolecular rate constants k_{ap} of the proton transfer reaction from triphenylmethane to sodium (\circ) or potassium (\square) salt of polystyryl carbanions as a function of the reciprocal of the square root of the salt concentration. Reproduced from ref. 104.

is responsible for the deprotonation of triphenylmethane. The slopes of the lines in Fig. 9, in conjunction with the known dissociation constants of polystyryl ion pairs into free ions [103, 105], lead to the bimolecular rate constants of the reaction of free carbanions:



The contribution of reaction 19a could be depressed by adding an inert but highly dissociated salt sharing a common counterion with the polystyryl salt. By this technique, the bimolecular rate constant of ion pairs deprotonation (Eq. 19b) has been determined:



Table 11 Proton Transfer from Triphenylmethane to Polystyryl Base at 25°C

Cation	Solvent	Rate Constant of Proton Transfer ($M^{-1} \text{sec}^{-1}$)	
		For Free Ions	For Ion Pairs
		k^-	k^\pm
Na^+	THF	178	0.15
Na^+	DME	138	11
K^+	THF	142	<0.2

The results, collected in Table 11, demonstrate the considerably higher reactivity of free polystyryl ions compared to its ion pairs. The reactivity of the free polystyryl ions appears to be the same in tetrahydrofuran (THF) and in dimethoxyethane (DME), whereas the reactivity of sodium ion pairs increases substantially when DME is substituted for THF as the solvent. It seems that the sodium ion pairs are present in two forms—the unreactive tight pairs and the reactive loose pairs. The proportion of the more reactive loose pairs is higher in DME than in THF [103, 105], and this accounts for the differences in the rates of the deprotonation as well as for the similar differences in the rates of anionic polymerization [103, 105]. In fact, it was suggested that the observed rate constants k^\pm reflect the reactivity of the loose pairs [107]:

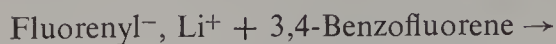
$$k^\pm = f k_{\text{loose pairs}}$$

where f denotes the fraction of the loose pairs present in each of these two solvents. The reactivity of the tight pairs apparently is too low to be observed. Provided that this suggestion applies to both systems—polymerization and proton transfer—the ratios $k^\pm(\text{DME})/k^\pm(\text{THF})$ should be the same for both reactions and, indeed, they differ only slightly.

A complete study of the foregoing proton transfer was not attempted. The kinetics is complicated by the higher degree of dissociation of Ph_3C^- , Cat^+ ion pairs than polystyryl $^-$, Cat^+ pairs. Thus the concentration of free Cat^+ increases as the reaction proceeds; the dissociation of polystyryl ion pairs is therefore depressed and the protonation is retarded. Qualitative examination of the conversion curves confirms this conclusion.

Proton transfer from 3,4-benzofluorene or 1,2-benzofluorene to various fluorenyl salts acting as bases was investigated by Hogen-Esch and Smid [106]. The reaction was performed in dioxane, THF, and DME. Although this study was qualitative rather than quantitative, it nevertheless revealed that the bimolecular rate constant of the proton transfer to lithium fluorenyl increases steeply with dilution of the salt. In fact, the increase is much steeper than would be expected for a reaction arising from free ions. For example,

the bimolecular rate constant of the reaction



proceeding in THF increased by a factor of 60 on 260-fold dilution of the salt, although the free ion mechanism predicts at most an increase by a factor of only 16. For the reaction with 1,2-benzofluorenyl, the rate constant increased by a factor of 30 as the concentration of sodium polystyryl decreased by factor of ~ 60 from 4×10^{-4} to $6 \times 10^{-6} M$. Similar results were reported for the reaction in DME.

The authors suggest that the pronounced decrease of the rate constant with increasing concentration of the lithium salt is caused by further association of ion pairs into higher aggregates. This suggestion does not seem correct; one does not expect much aggregation of such ion pairs in the range 10^{-4} – $10^{-6} M$. Moreover, the conductance data of the same workers [4] demonstrate that within this concentration range fluorenyllithium ion pairs are not associated in THF. Further evidence against aggregation of ion pairs comes from conductance studies of lithium anthracenide [108], the results of which led to the same value for the mobility of fluorenyl and anthracenide ions whether the Li^+ or Na^+ salts were used in the investigation. Aggregation of the lithium fluorenyl pairs would call for modification of the calculation and would destroy this plausible result.

The kinetics of the above deprotonation seems to be simple when sodium, cesium, or tetrabutylammonium salts of fluorenyl are used as the bases. The relevant bimolecular rate constants appear to be independent of dilution whether the reaction proceeds in THF or DME, indicating that these reactions involve only ion pairs. The concentration of free ions is apparently too low and their reactivity not sufficiently high to reveal their participation in the reaction.* The enormous increase in the rate of sodium fluorenyl reaction as THF solvent is replaced by DME ($\sim 4000 M^{-1} \text{ sec}^{-1}$ in THF but $80,000 M^{-1} \text{ sec}^{-1}$ in DME) is significant. Apparently the loose pairs in this system also are much more reactive than the tight pairs.

In the gas phase the deprotonation by free ions is extremely fast, provided that the reaction is exothermic. For example, the gaseous reaction



proceeds on every collision [108]. In solution the desolvation of the original ion and the solvation of the newly formed ion considerably slow down the process. The role of the counterion depends on the structure of the transition

* However, unpublished studies of Smid and Wong of protonation of fluorenyl salts by 9-methylfluorene again demonstrated higher reactivities of free ions than ion pairs.

state, and a comprehensive discussion of this aspect of protonation will be outlined in Section 3.5.

The substantially higher reactivity of free ions than of ion pairs is revealed also by the work of Shatenstein [110], who studied the deuteration of various hydrocarbons catalyzed by potassium deuteroamide in deuterated liquid ammonia. The apparent bimolecular rate constants again increase with dilution of the salt, indicating higher reactivity of free ND_2^- ions than of ion pairs.*

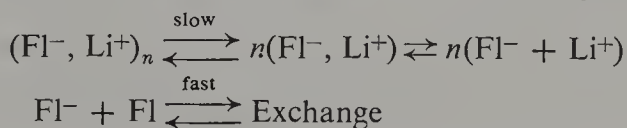
A striking example of the effect of association on the rate of proton transfer is provided by the work of Brauman et al. [133] and of Ritchie and Uschold [134]. Both groups investigated the transfer of protons from the fluorene-type hydrocarbons to their lithium salts in DMSO. Brauman utilized an elegant NMR double resonance technique and by necessity had to investigate the reaction in a relatively concentrated salt solution ($\sim 0.5 M$). From the exchange data



he determined the bimolecular rate constant to be about $0.5 M^{-1} \text{ sec}^{-1}$. Ritchie applied a stop-flow technique in his study of proton transfer between two fluorenyl-type hydrocarbons of similar acidity and found a bimolecular rate constant of $1.4 \times 10^3 M^{-1} \text{ sec}^{-1}$, about 1000 times greater than that reported by Brauman. The flow technique utilizes a dilute salt solution; in fact, its concentration in Ritchie's experiments was $5 \times 10^{-4} M$.

It is plausible to assume that the lithium salts are present in some aggregated and unreactive form in concentrated solutions but dissociate into much more reactive, less associated species on dilution. According to this hypothesis the nominal rate constant, k_{ap} , derived from experiments performed in dilute solution should be higher than that calculated from the results obtained in more concentrated systems. Unfortunately, this simple device cannot account for the *numerical* results reported by Brauman and by Ritchie. The increase of the total concentration of the salt *cannot* decrease the absolute concentration of the less associated species. Therefore the product $k_{\text{ap}} \times (\text{total concentration of the salt})$ cannot *decrease* with concentration. However, this product is 0.25 based on Brauman results and 0.7 on the basis of Ritchie's findings.

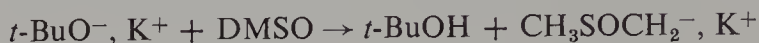
Closer examination of the NMR technique reveals that the results may pertain to the rate of dissociation of aggregates into less associated species. We suggest therefore that the results of Ritchie reflect the reactivity of free ions, whereas the results of Brauman are accounted for by the scheme



* Not always are the free ions more reactive; see e.g. pp. 234–235.

in which the dissociation of the unreactive aggregate into ion pairs is the rate-determining step maintaining the minute concentration of ion pairs. Not surprisingly, the addition of another salt sharing the common ion with lithium fluorenyl did not affect the results of Brauman (a footnote in ref. 133).

The rate constant of the reaction



also dramatically increases on dilution of the reagents. The rate constant measured by the broadening of Raman lines in 0.57 *M* concentration of *t*-BuO[−], K⁺ in DMSO [136, 137] is about 100 times lower than that estimated in dilute solution by Ritchie [42]. Again, the aggregation of ions is responsible for the different findings of these groups.

The aggregation of dimsyl ions in DMSO is reflected not only in the kinetic data but also in the equilibrium. For example, Corey and Chaykovsky [138] determined the equilibrium constant for the proton transfer between Ph₃C[−] anions and DMSO as 200. They studied this system at about 0.3 *M* concentration of dimsyl ions. At higher dilution, in the concentration range 10^{−2}–10^{−3} *M*, the equilibrium constant was found to be 1.3 × 10⁴ by Steiner and Gilbert [139] and 1.4 × 10⁴ by Ritchie and Uschold [76].

The aggregates of ion pairs usually are less reactive than ion pairs. For example, the hydrogen isotope exchange in cyclohexylamine depends on the first power of lithium cyclohexylamide concentration at high dilution of the catalyst, but at high amide concentration the reaction becomes independent of amide concentration [31a, 111]. The monomeric pair, but not its aggregate, obviously acts as the base in this proton transfer, and for a high degree of aggregation the concentration of monomeric pairs becomes an insensitive function of the concentration of the aggregates.

Finally, the kinetic studies by Waack and his co-workers [112], who investigated the metalation of triphenylmethane by lithium alkyls [112], revealed not only the large effect of the alkyl structure on the rate of proton transfer but also the importance of aggregation. Their results are collected in Table 12. The most stable, resonance-stabilized, lithium alkyls—benzyl and allyl—are the most reactive, contrary to the expectation based on their “basicity.”

The degree of association seems to be the most essential factor determining the reactivity of lithium alkyls. The kinetic data demonstrate that benzyl-, allyl-, and phenyllithium are monomeric, and the rates of proton transfer depend on the first power of their concentration. On the other hand, the rates of protonation by the remaining lithium compounds depend on low fractional power of their concentration: the higher aggregates of these compounds are unreactive, but they are in equilibrium with a small fraction of

Table 12 Relative Reactivities of Lithium Alkyls Toward Triphenylmethane in THF

RLi	Reaction with Ph ₃ H		Addition to Ph ₂ C=CH ₂
	[RLi] = 0.1	[RLi] = 0.01	[RLi] = 0.01
Methyl	1.0	1.0	1.0
Phenyl	6.3	2.8	0.34
Vinyl	4.2	4.3	0.72
Allyl	90	14	33
<i>n</i> -Butyl	23	20	1900
Benzyl	450	150	650

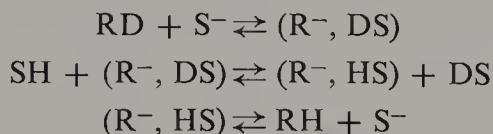
less aggregated but more reactive species formed by dissociation of the higher aggregates. The less aggregated species are then responsible for metalation.

The kinetic results of Waack et al. differ fundamentally from those reported previously by Gilman and McNinch [113]. In the kinetic work, the rate of formation of Ph₃C⁻, Li⁺ was followed spectrophotometrically. The investigation of Gilman and McNinch was based on product analysis. Apparently in Gilman's work the composition of the products was determined by thermodynamic and not just by the kinetic conditions.

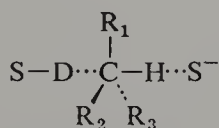
The results of metalation of triphenylmethane were compared with kinetic studies of the addition of lithium alkyls to 1,1-diphenylethylene in THF [114]. As shown in the last column of Table 12, the general trend is similar in both reactions, although the actual relative rates differ somewhat.

3.4. Stereochemistry of Proton Transfer

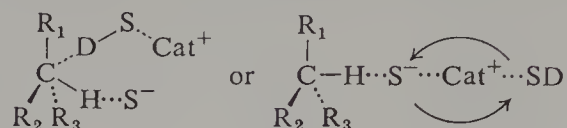
An isotope exchange reaction involving free ions and a solvent proton donor may proceed as follows:



For steric reasons the proton should be transferred from a neighboring solvent molecule located on the other side of the acid than the base, provided that the exchange is induced by a *free* anion base. Such an exchange, depicted below, leads to inversion of configuration. However, if the exchange involves



an ion pair, the proton added should come from a solvent molecule located on the same side as the base, because the separation of charges is energetically unfavorable. The relevant arrangement, as shown here, then leads to an exchange with retention of configuration. The above route becomes even



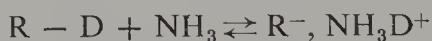
more favorable by the virtue of cation-solvent interaction, which enhances the acidity of the coordinated solvent.

Alternatively, when the newly formed carbanion is sufficiently stable it may diffuse out of the encounter "cage" and react later with the solvent. On the whole, conjugated carbanions have a planar trigonal C^- center and hence the subsequent protonation may take place on either side of the carbanion. In such a case the exchange is associated with racemization. This alternative is probable when a relatively stable free anion base induces the exchange. A similar reaction induced by ion pairs has to proceed by two steps:



It is also possible to visualize systems in which the newly formed carbanion rotates, retaining, nevertheless, its association with the molecule of the acid formed from the base catalyzing the exchange. In such a case racemization, but no exchange, occurs. Such an event is most probable when the association of the cation with the anion base is perpetuated *after* the base had been converted into an acid. This molecule of acid would participate preferentially in the subsequent protonation of the newly formed carbanion, because its acidity is enhanced by the association with the cation.

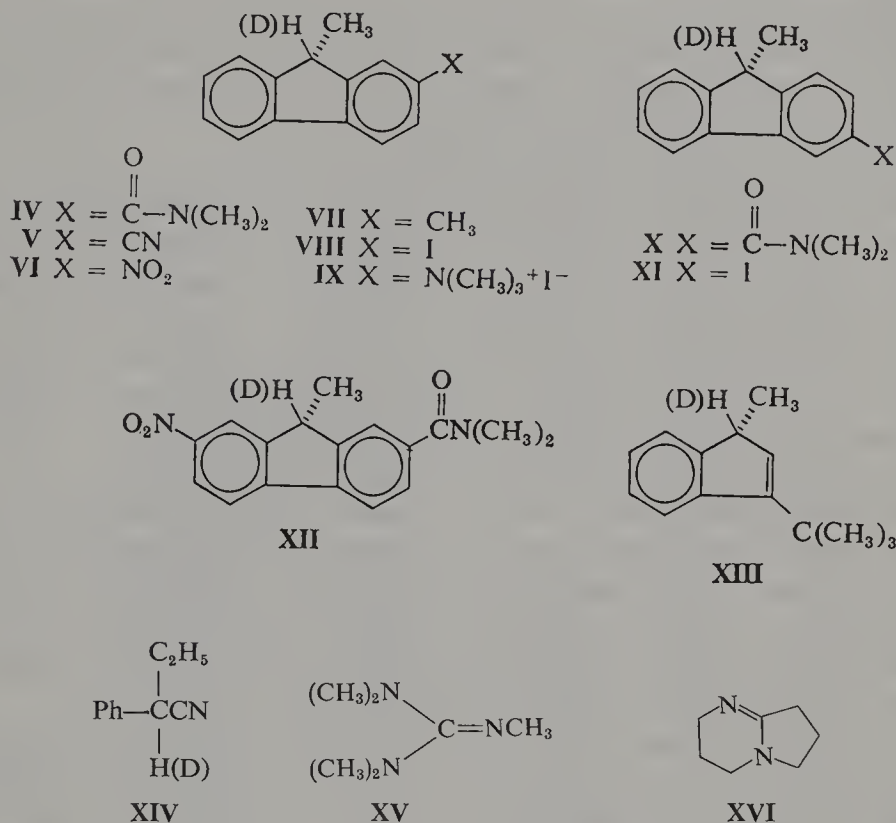
Exchange catalyzed by neutral base leads to the formation of ion pairs. For example,



The reverse reaction leads to an exchange with retention of configuration, provided the ammonium ion had a chance to rotate. In "good" solvents the ion pair may dissociate into free ions and then, for symmetric carbanions, the exchange becomes associated with racemization.

The stereochemical consequences of proton transfer involving ion pairs have been subjects of many recent and brilliant investigations, especially by Cram and his co-workers [98, 115–126, 165]. They synthesized a series of optically active compounds such as **IV–XIV**, studied their rate of exchange k_{ex} and of racemization k_α , using a 1-point kinetic technique. The ratio k_{ex}/k_α provides a measure of the stereochemical fate of the intermediate ion pair

formed in the course of proton transfer. A large value of k_{ex}/k_{α} is indicative of a retention mechanism in which the exchange of the hydrogen isotope by a solvent hydrogen occurs at the original side of the compound; that is, the



intermediate ion pair maintains its stereochemistry through the course of the reaction. An alternative although highly improbable mechanism would require an even number of inversions of configuration during the net replacement of one hydrogen isotope by another. The participation in the exchange of a symmetric intermediate or of a rapidly racemized ion pair is indicated by a value of k_{ex}/k_{α} of unity. The replacement of the original hydrogen isotope by another located on the opposite side of the compound results in a k_{ex}/k_{α} ratio of 0.5. Low values of k_{ex}/k_{α} indicate an internal return with the intermediate ion pair being racemized in the time needed for the original isotope to return. Cram refers to this last mechanism as an "isoinversion" or "isoracemization."

Cram and his co-workers have shown that proton transfers within ion pairs generally involve a complex set of simultaneous processes with participation, to different degrees, of retention, isoinversion, inversion, and racemization mechanisms. The degree of participation of each mechanism in the

overall exchange depends on the reactivity of the intermediate carbanion, the character of the proton pool in solvent, the nature of the cation, and the substituents present on the anion.

In solvents of low polarity conducive to ion pairing the exchange with retention of configuration is the most common. This kind of exchange is even more pronounced when the base contains exchangeable protons. For example, in tetrahydrofuran (THF) with 0.3 *M* ammonia or 0.5 *M* *n*-propylamine (*n*-PrNH₂) as the catalyst, the optically active 2-(*N,N*-dimethylcarboxamido)-9-methylfluorene-9-*d* (**IV-d**) undergoes to a large extent exchange with retention of configuration, the k_{ex}/k_{α} 's being 148 and >56, respectively [115]. As the availability of protons in the base decreases, so does the ratio k_{ex}/k_{α} ; for example, its value is reduced to 9 when di-*n*-propylamine replaces *n*-propylamine as the catalyst. The increase in proton availability of the solvent, coupled with a further decrease of proton availability in the base, reduces the k_{ex}/k_{α} ratio even more. As THF is replaced by *t*-butanol and *n*-propylamine by tripropylamine, the value of k_{ex}/k_{α} falls to 6.

The value of k_{ex}/k_{α} is very sensitive to some apparently minor changes in the structure of the carbon acid. For example, whereas **IV** shows a large degree of retention of configuration for exchange in THF with *d*-PrNH₂, its nitro derivative, 2-(*N,N*-dimethylcarboxamido)-7-nitro-9-methylfluorene-9-*d* (**XII**) undergoes complete racemization under the same conditions, $k_{\text{ex}}/k_{\alpha} = 1$. The higher stability of the **XII** anion imparted by the nitro-substituent implies a longer lifetime with more opportunities for racemization.

The polarity of the solvent also plays an important role in determining the value of k_{ex}/k_{α} . For example, the exchange of 3-(*N,N*-dimethylcarboxamido)-9-methylfluorene-9-*d* (**X**) was studied in benzene, THF, and pyridine, with *n*-propylamine as the catalyst. The dielectric constant increases in this series of solvents, being 2.27, 7.4, and 12.3 for benzene, THF, and pyridine, respectively. The ease of racemization follows the same trend, k_{ex}/k_{α} decreasing from 4 to 1. Racemization is accelerated by the partial separation of ions in a pair, which facilitates the rotation of the anion with respect to the cation, or by the hopping of the cation from one side of the anion to another (see, e.g., ref. 3, pp. 226–240). Although the bulk dielectric constant is not the best measure for the tightness of an ion pair, a high dielectric constant reduces the electrostatic interaction and should favor relatively loose pairs with more facile partial separation.

Racemization decreases with decreasing basicity of the base and increasing acidity of its conjugate acid. For example, although **XII** is entirely racemized by *n*-propylamine in THF ($k_{\text{ex}}/k_{\alpha} = 1$), retention is substantial when *p*-methylaniline is used as a base. The latter is a much weaker base than the former, and anilinium ion is a much stronger acid than *n*-PrNH₃⁺. Hence the proton is transferred more readily to the carbanion from *p*-methylanilinium

in the intermediate and the rotation process, which gives rise to racemization, has less time to occur. Various examples illustrating these simple principles are collected in Table 13.

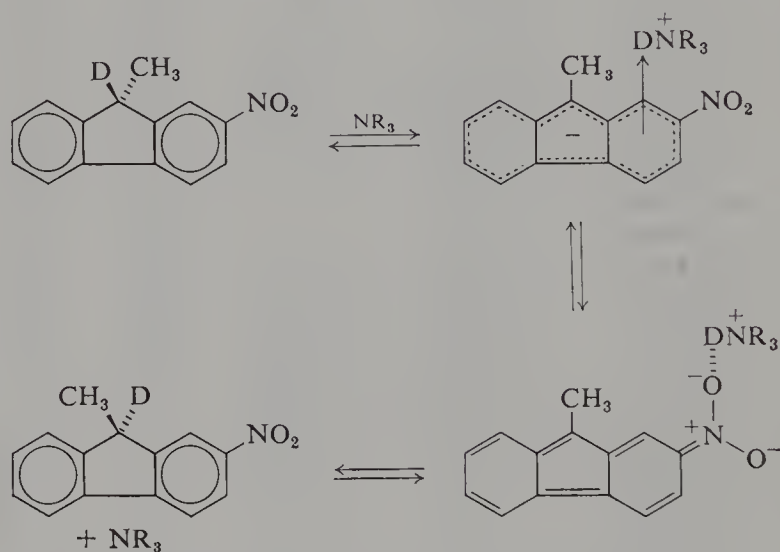
Table 13 Retention and Racemization for Amine-Catalyzed Isotope-Exchange Reactions

Compound	Solvent	Base		Temperature (°C)	k_{ex}/k_{α}	Ref.
		Nature	Conc. (M)			
IV	THF	NH ₃	0.3	145	148	115
IV	THF	<i>n</i> -PrNH ₂	0.5	145	>56	115
IV	THF	Pr ₂ NH	0.6	145	>8.5	115
IV	<i>t</i> -BuOH	Pr ₃ N	1.1	200	5.7	115
XII	THF	<i>n</i> -PrNH ₂	0.10	-22	1	116
XII	THF	<i>p</i> -MeC ₆ H ₄ NH ₂	0.50	131	6	116
XII	THF- <i>t</i> -BuOH	(<i>n</i> -Pr) ₃ N	0.60	75	<0.1	116
XII	THF	None		140	0.3	116
XII	THF- <i>t</i> -BuOH	None		140	1.0	116
V	<i>t</i> -BuOH	(<i>n</i> -Pr) ₃ N	1.1	100	0.1	116
VI	<i>t</i> -BuOH	(<i>n</i> -Pr) ₃ N	1.1	50	≤0.1	116
X	<i>t</i> -BuOH	(<i>n</i> -Pr) ₃ N	0.6	130	0.14	116
X	C ₆ H ₆	<i>n</i> -PrNH ₂	0.69	75	4.4	116
X	THF	<i>n</i> -PrNH ₂	0.4-1.2	25-75	1.4-2.5	116
X	C ₅ H ₅ N	<i>n</i> -PrNH ₂	0.69	25	1.0	116
IV- <i>d</i>	<i>t</i> -BuOH	XV	0.098	25	0.3	159
IV- <i>d</i>	<i>t</i> -BuOH	XVI	0.10	25	0.42	159
X- <i>d</i>	<i>t</i> -BuOH	XV	0.037	25	0.21	159
VII	<i>t</i> -BuOD	XV	0.59	50	0.41	159
VIII- <i>d</i>	<i>t</i> -BuOH	XV	0.11	25	0.33	159
IV- <i>d</i>	<i>t</i> -BuOH	Pr ₃ N ^a	0.37	175	≥10	159
VIII- <i>d</i>	<i>t</i> -BuOH	Pr ₃ N	0.68	175	1.9	159
VIII- <i>d</i>	<i>t</i> -BuOH	Pr ₃ N ^a	0.21	175	24	159
XI- <i>h</i>	<i>t</i> -BuOD	DABCO	0.42	175	1	159
IX- <i>d</i>	<i>t</i> -BuOH-DMSO	Pr ₃ N	0.44	25	1	159

^a Contains <10⁻³ M Pr₃N·HI.

A low concentration of protons in the solvent, coupled with a strong base devoid of exchangeable protons, favors isoinversion. For example, 7-nitro-2-(*N,N*-dimethylcarboxamido)-9-methylfluorene-9-*d* (XII) undergoes a rapid racemization with tri-*n*-propylamine in THF-*t*-butanol mixture, with only little exchange, $k_{\text{ex}}/k_{\alpha} < 0.1$. The ion pair may racemize by rotation of the anion within the intermediate ion pair, but eventually it decomposes through internal return without exchange.

The isoinversion process is strikingly facile with some compounds but not with others. For example, 2-cyano-9-methylfluorene (V), 2-nitro-9-methylfluorene (VI), and even 3-(*N,N*-dimethylcarboxamido)-9-methylfluorene (X) readily isoinvert, whereas 2-(*N,N*-dimethylcarboxamido)-9-methylfluorene (IV) does not. The difference in the behavior of the last two compounds is striking in view of their great structural similarity. To account for this peculiarity Cram suggested a "conducted tour" mechanism in which the protic acid of the contact ion pair travels along the π system of the carbanion, reaches a negative freely rotating substituent, and, after being attached to it, the acid is transferred by rotation of the substituent to the other side of the anion.



Cram's conducted tour mechanism for the fluorene system.

Ford and Cram [117, 127] have studied the stereochemistry of some fluorene exchanges and their results are summarized in Table 14. Compound X, although only 1.4 times as acidic as IV, racemizes 75 times faster than IV. The relative influence of the 2-carboxamido, 2-cyano, and 2-nitro substituents on the k_{ex}/k_{α} ratio parallels their ability to stabilize a carbanion via conjugation. The carboxamido group placed in the 2 position does not sufficiently stabilize the anion to allow isoracemization through a conducted tour mechanism, although nitro and cyano groups, even in the 2 position, stabilize the carbanion sufficiently to permit its operation.

It has been repeatedly pointed out that ion pairs may exist in the same solvent in two or more different forms coexisting in equilibrium with each

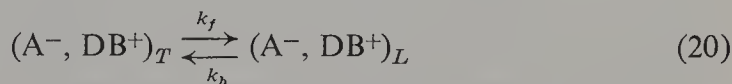
Table 14 Kinetic Data for Isotope Exchange of Methylfluorenes in the *n*-PrNH₂-THF System

Compound	$k_{\text{rel}}(\text{exch})^a$ at 25°	$k_{\text{rel}}\alpha^b$ 25°	$\Delta H_{\text{exch}}^+{}^b$	$\Delta S_{\text{exch}}^+{}^b$	$\Delta H_{\text{rac}}^+{}^b$	$\Delta S_{\text{rac}}^+{}^b$
IV ^c	1.0	1.0	10 ± 3	-45 ± 5	4.6 ± 0.5	-69 ± 2
X ^c	1.4	75	9 ± 6	-47 ± 11	5.1 ± 1	-59 ± 4
V ^d	375					
VI ^d	905					
XII ^{d,e}	5500		7.1 ± 0.9	-54 ± 4	10.5 ± 0.5	-39 ± 2

^a $k_{d(\text{rel})}$ from third-order rate constants.^b From $k_h(t)$ racemization.^c Ref. 117.^d Ref. 116.^e Activation parameters for $k_d(-)$ in THF-*t*-BuOH-(*n*-Pr)₃N [127].

See p. 209 for the structure of the protonated compounds.

other. Let us consider a system composed of two types of A⁻, DB⁺ ion pairs:



Each of these pairs may collapse and yield a nonexchanged AD acid; each may racemize, or react with the solvent, and produce the exchanged AH acid. The rate constants of these reactions are denoted, respectively, by $k_{c,T}$ and $k_{c,L}$ for the collapse of either pair, $k_{\text{ex},T}$ and $k_{\text{ex},L}$ for their exchange with solvent, and $k_{\alpha,T}$ and $k_{\alpha,L}$ for their racemization resulting from the rotation of the anion with respect to the cation or from the operation of the conducted tour mechanism. The final result of all of these reactions gives the observed k_{ex}/k_{α} ratio.

It is obvious that this result is a complex function of all of the rate constants of the participating steps. For example, internal return—the collapse of a pair—is more probable for a tight than for a loose pair, whereas racemization by rotation, but not by the conducted tour mechanism, is more likely to occur in the loose than in the tight pair. To appreciate the complexity of the problem let us consider a few simple cases.

Case a.

$$k_{c,T} \neq 0, \quad k_{c,L} = 0, \quad k_{\alpha,T} = 0, \quad k_{\alpha,L} \neq 0, \\ k_{\text{ex},T} = 0, \quad \text{and} \quad k_{\text{ex},L} \neq 0$$

The tight pairs contribute neither to exchange nor to racemization and the observed k_{ex}/k_{α} ratio equals $k_{\text{ex},L}/k_{\alpha,L}$, being independent of $k_{c,T}$. Moreover,

this result is also independent of the rate and equilibrium constant of reactions 20. However, the *absolute* values of the observed k_{ex} and k_{α} depend on the rates of Eq. 20; for example, for k_f and k_b much greater than $k_{c,T}$, $k_{\alpha,L}$, and $k_{\text{ex},L}$, respectively, the observed k_{ex} and k_{α} are given by

$$\{K(20)/[1 + K(20)]\} k_{\text{ex},L} \quad \text{and} \quad \{K(20)/[1 + K(20)]\} k_{\alpha,L},$$

where $K(20) = k_f/k_b$. Note that these rates are given with respect to the total concentration of the ion pairs and not with respect to the concentration of the exchanged acid. On the other hand, for the improbable case in which k_f and k_b are much smaller than $k_{c,T}$, $k_{\alpha,L}$, and $k_{\text{ex},L}$, the observed k_{ex} and k_{α} are equal to $k_f k_{\text{ex},L}$ and $k_f k_{\alpha,L}$, provided the pairs are originally formed as tight pairs and the proportion of loose pairs is very small.

Case b. In a system in which the racemization occurs by the conducted tour mechanism involving tight pairs only and the exchange results entirely from the reaction of loose pairs, the respective rate constants are

$$k_{c,T} \neq 0, \quad k_{c,L} = 0, \quad k_{\alpha,T} \neq 0, \quad k_{\alpha,L} = 0, \\ k_{\text{ex},T} = 0, \quad \text{and} \quad k_{\text{ex},L} \neq 0$$

Now the final observed k_{ex}/k_{α} ratio *does* depend on the rates of reaction 20. For example, for k_f and k_b , both much greater than $k_{c,T}$, $k_{\alpha,T}$, and $k_{\text{ex},L}$, the relative concentrations of the tight and loose pairs are in proportion 1:K(20); this ratio is not affected by the exchange or racemization. The observed k_{ex}/k_{α} ratio is then equal to $k_{\alpha,T}/k_{\text{ex},L}K(20)$ and again it is *independent* of $k_{c,T}$. However, the observed k_{ex}/k_{α} ratio does depend on $k_{c,T}$ if $k_{c,T}$ is not much smaller than k_f .

We shall not pursue this subject further. The preceding examples give the reader a glimpse into the intricate relations encountered in practice. It may be useful, however, to survey some of the reported data.

The kinetics of exchange of compounds **IV** and **X** in THF-*n*-PrNH₂ system has been carefully investigated [117]. The exchange was found to be first order in the acid but of a mixed first and second order in the amine catalyst. The second-order component of this relation indicates that the amine is present in this system in monomeric and dimeric forms, the latter being apparently a stronger base than the former. The pseudo-first-order rate constant for the exchange of compound **X** was dissected into the contributions of isoinversion, exchange with retention, and exchange proceeding with the inversion of configuration. The exchange with retention component was found to be five times as large as the other two components, the latter two being of comparable magnitude. The Arrhenius parameters indicate that all of these reactions involve tight ion pairs.

Although conjectural at this stage of our knowledge, it is reasonable to postulate that the exchange with retention results from the rotation of the amine, exposing an ordinary hydrogen of the ammonium ion to the anion, followed thereafter by the collapse of the tight pair. The isoinversion is probably caused by the concerted tour mechanism with a nonrotating cation, whereas the simultaneous combination of both mechanisms leads to the exchange with inversion. The exchange with inversion may also result from a reaction with another proton-donating species present in the system, for example, with an amine and not with the ammonium ion associated with the anion, but such a mechanism would lead to the separation of charges by the acid produced, and it is unlikely in solvents of low dielectric constant.

The kinetics of isoinversion of compound **XII** accompanying the hydrogen isotope exchange catalyzed by Pr_3N in THF-*t*-BuOH (80:20 by volume) was also extensively studied. The reaction was first order with respect to both reagents, the hydrocarbon and the base [127]. The concerted tour mechanism could again provide a most attractive explanation of the observed stereochemistry, but the Arrhenius parameters found for this system differ markedly from those obtained from studies of the exchange of compounds **IV** and **X** in the *n*-PrNH₂-THF system. As may be seen from Table 14, in the reactions of **IV** and **X** differences of the activation energy and entropy of activation of the exchange and racemization, $\Delta\Delta H^\ddagger$ were 5.4 and 3.9 kcal/mole, and $\Delta\Delta S^\ddagger$ 24 eu for **IV** and **X**, respectively. In contrast, the $\Delta\Delta H^\ddagger$ and $\Delta\Delta S^\ddagger$ for the reaction involving compound **XII** were found to be *negative*, -3.4 kcal/mole and -15 eu, respectively. Hence for this reaction the entropy of the transition state of the exchange is lower than for racemization.

The relations observed in reactions of compound **IV** and **X** may be rationalized easily. The exchange and the racemization involve a tight pair, but in the concerted tour mechanism the ion pair dipole increases in the transition state and hence the degree for solvation of this transition state becomes greater than that in the transition state of racemization, $\Delta S_{\text{rac}}^\ddagger < \Delta S_{\text{ex}}^\ddagger$. The reversed relation observed in the reaction of compound **XII** may indicate that here the exchange occurs in the loose pair coexisting with the tight pair, although the tight pair is still involved in racemization. Since the entropy of conversion of tight to loose pairs is substantially negative [4, 20], $\Delta S_{\text{ex}}^\ddagger < \Delta S_{\text{rac}}^\ddagger$. The high relative value of k_{ex} found for compound **XII**, compared with the low values for compounds **IV** and **X**, provides further support for this suggestion.

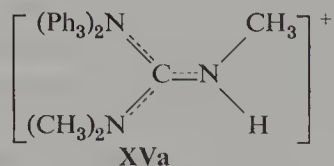
Further evidence for the participation of loose pairs in the reaction of **XII** comes from the data collected in Table 15. The proportion of loose pairs increases on lowering the temperature of the solvent or on increasing its polarity (e.g., through addition of the more polar Pr_3N). These conclusions are confirmed, however, the trends are small and therefore not too convincing.

A recent study of the 9-methylfluorenyl system by Chu and Cram [165] has been most revealing. When 0.001 *M* tri-*n*-propylammonium hydriodide is added to the tripropylamine alcohol system, trace amounts of dipropylamine are formed. This finding is sufficient to imply a change of the mechanism from net isoinversion to net exchange with retention. Apparently the exchange catalyzed by dipropylamine is many times faster than that catalyzed by tripropylamine.

Table 15 Temperature and Medium Effects on Isoracemization of 7-Nitro-2-(*N,N*-dimethylcarbox-amido)-9-methylfluorene XII [127]

Temperature (°C)	Pr ₃ N (mole %)	<i>t</i> -BuOH (mole %)	k_{ex}/k_{α}
25	0.6	17.6	0.22
25	2.3	17.3	0.21
25	10.0	16.0	0.10
50	0.4	17.7	0.15

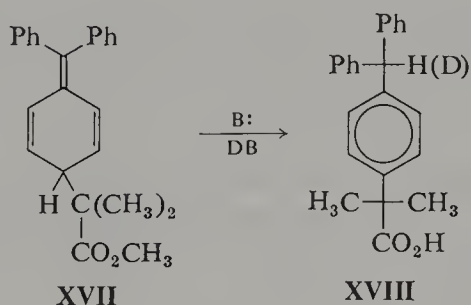
Cram and Chu also demonstrated that charge-delocalizing bases could catalyze isoinversion despite the lack of a carbanion which could facilitate a concerted tour mechanism. Tripropylamine in *t*-BuOH–DMSO and 1,4-diazabicyclo[2.2.2]octane (DABCO) in *t*-BuOH catalyze the complete exchange with racemization of 2-(*N,N,N*-trimethylammonium)-9-methylfluorene-9-*d* (IX-*d*) and 3-iodo-9-methylfluorene-9-*d* (XI-*d*), respectively. However, pentamethylguanidine (XV) and 1,5-diazabicyclo[4.3.0]non-5-ene (XVI) catalyze exchange with isoinversion (Table 8). In this “nonstructured” isoinversion mechanism, the delocalized conjugate acid of the basic catalyst (e.g., XVa) results in an ion pair intermediate possessing a sufficient lifetime



to allow the carbanion to pass into an achiral environment. Arrhenius parameters obtained from detailed kinetic studies imply a tight ion pair intermediate in the isoinversion component. Hence when “charge-localizing” amines (e.g., Pr₃N) are catalysts, delocalized carbanions need a concerted tour pathway for isoinversion, whereas “charge-delocalizing” amines obviate the need of such a pathway for delocalized carbanions.

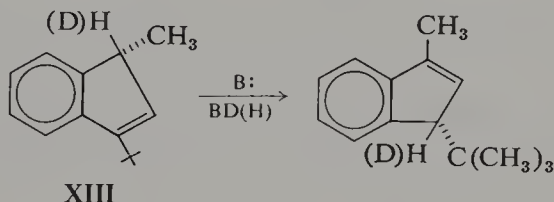
The conducted tour mechanism appears to be encountered commonly in many reactions of the above type. Its operation is favored by the planar structure of the π carbanionic system and by low polarity of solvents conducive to the formation of tight ion pairs. For example, the extremely low value of $k_{\text{ex}}/k_{\alpha} = 0.05$, observed in the exchange reaction of α -phenyl- α -*d*-butyronitrile (XIV) performed in THF containing 1.5 *M* *t*-butanol with Pr_3N as a catalyst, has to be interpreted as another manifestation of that mechanism [118].

Interesting examples directly demonstrating the operation of the conducted tour mechanism are provided by some rearrangements studied recently by Cram's group [119, 120]. The rearrangement



was found to be over 95% intramolecular. The reaction took place in 50:50 mixture of THF and *t*-BuOH using 1,4-diazabicyclo[2.2.2]octane (DABCO) as a catalyst, or in triethylcarbinol with Pr_3N as the base.

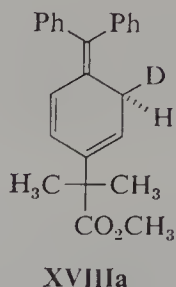
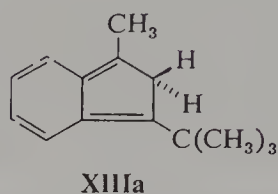
A similar rearrangement was observed for 1-methyl-1-*d*-3-*t*-butylindene (XIII) when allowed to react with Pr_3N in THF at 50°C [121, 122]:



This reaction proceeds virtually intramolecularly on one face of the π system only. The simple exchange takes place with little isomerization, $k_{\text{ex}}/k_{\alpha} > 7.5$.

Both of these rearrangements proceed in a fashion demanded by the conducted tour mechanism. No σ intermediate such as **XIIIa** or **XVIIIa** has been found, although evidence of their appearance has been sought. The high degree of their intramolecular character and the clean kinetics, first order in

the substrate and the base, rule out any possibility of a chain process.



Amines are not unique in their ability to preserve carbanionic asymmetry in ion pair systems. Retention of carbanionic asymmetry can occur even with potassium ion as a ligand. Examples are summarized in Table 16. For example,

Table 16 Effects of Cations on Carbanion Stereochemistry

Compound	Solvent	Base	Concentration (M)	Temperature (°C)	k_{ex}/k_a
IV	90% C ₆ H ₅ - 10% ϕ OH	ϕ OK	0.1	75	18
IV	Same	ϕ ONMe ₄	0.05	75	1.0
IV	<i>t</i> -BuOH	<i>t</i> -BuOK	0.024	25	1.0
XIII	<i>t</i> -BuOH	<i>t</i> -BuOK	—	—	2–5
XIV	<i>t</i> -BuOD	<i>t</i> -BuOK	0.233	115.8	>46
IX- <i>d</i>	C ₆ H ₆ - ϕ OH ^c	ϕ OK	0.057	100	7.9 ^d
IX- <i>d</i>	Same ^a	Same ^a	0.058	110	2.3 ^d
IX	THF	<i>n</i> -PrND ₂	0.19	37.5	>30 ^d
IX	Same	<i>n</i> -PrND ₂ ^b	0.19	37.5	0.62 ^d

^a 0.1 M crown ether.

^b 1.5 M crown ether.

^c 75% C₆H₆, 25% ϕ OH by volume.

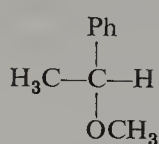
^d Starting material.

^e Ref. 2, p. 88.

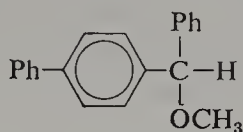
Structures of IV, IX, XIII, and XIV are given on p. 209.

compound IV undergoes exchange with predominant retention of configuration in a benzene-phenol mixture with potassium phenoxide as the base [115]; see p. 208 for diagrammatic representation of the mechanism. Predominant retention in this reaction also occurs with 1-phenyl-1-methoxyethane XIX [98] and *p*-biphenylphenylmethoxymethane XX [123]. These

results can be interpreted on the basis of simple electrostatic interaction between cation and anion. Proton transfer to the opposite side of the car-



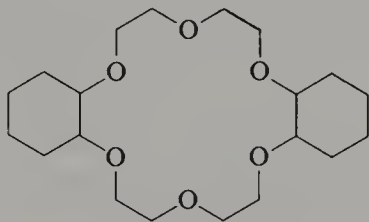
XIX



XX

banion would result in the separation of the ions; the potassium ion and the anion would be placed on the opposite sides of the substrate—an unfavorable process in nonpolar solvents. Even racemization of the potassium-carbanion pair through relative rotation of anion in respect to cation, requires some separation of the ions. Hydrogen exchange with compound **IV** in benzene-phenol mixture catalyzed by tetramethylammonium phenoxide occurs with racemization [2]. The large tetramethylammonium ion is now constrained to a larger distance from the negative charge of the carbanion and the weaker electrostatic interaction facilitates racemization by anion rotation.

The racemization is greatly enhanced by the use of crown ethers [132].



A crown ether

As shown by Almy, Garwood, and Cram [124] compound **XIII** undergoes in benzene-phenol mixture an exchange predominantly with retention of configuration when potassium phenoxide is used as a catalyst. Addition of the crown ether considerably enhances racemization. Crown ethers convert tight ion pairs into loose pairs [20] and thus the rotation leading to isomerization is facilitated.

The effect of the crown ether on amine catalysis in the indene rearrangement is also dramatic. The k_{ex}/k_{α} for the reaction of compound **XIII** decreases from 30 to 0.62 in THF-PrND₂ on the addition of the crown ether; yet the rates of isomerization and exchange are lowered only slightly [124]. Obviously, the crown ether does not affect the neutral amine which acts as a base; that is, the rate of formation of ion pairs is not affected by the addition of the ether, although the structure of ion pairs is profoundly changed.

It is perhaps surprising to find an ion pair mechanism still operating in solvents as polar as methanol and DMSO because the degree of ion pair dissociation should be substantial in those media. Hence the racemization would be expected to prevail over exchange. Nevertheless, the examples collected in Table 17 show the ratios k_{ex}/k_{α} to be low, their values often being substantially smaller than 1.

Table 17 Stereochemical Fate of Ion Pairs in Dissociating Solvents

Compound	Solvent	Base	Temperature (°C)	k_{ex}/k_{α}	Ref.
IV	CH ₃ OH	(<i>n</i> -Pr) ₃ N	75	0.65	115
IV	CH ₃ OH	CH ₃ OK	25	0.69	115
IV	(CH ₂ OH) ₂	Et ₃ N	50	0.94	115
IV	DMSO	NH ₃	25	1.0	115
X	CH ₃ OH	(<i>n</i> -Pr) ₃ N	50	0.84	125
X	(CH ₂ OH) ₂	KHCO ₃	25	0.87	125
X	CH ₃ OD	CH ₃ OK	25	0.92 ^a	122
X	DMSO	DABCO	25	1 ^a	122

^a Starting material. Structures of IV and X are given on p. 209.

The operation of the conducted tour mechanisms in those solvents is not less surprising. Its participation in the overall reaction is indicated by studies of intramolecular proton transfer in indenenes, for example, in compound XIII. Such a reaction involves transfer of a proton across the ring [122, 124]. Even more convincing evidence for the conducted tour mechanism is provided by the intramolecular 1-5 migration of proton in the hexatriene XVII to yield

Table 18 Extent of Intramolecular Rearrangement in Polar Solvents

Substrate ^a	Solvent	Base	Time (hr)	Tempera- ture (°C)	Percentage of Intramolecular Reactions to Product	Ref.
XIII	MeOD	KOMe	7.7	25	13	122
VIII- <i>d</i>	MeOH	KOMe	46.2	25	0	122
XIII	<i>t</i> -BuOH	DABCO	16	50	100	122
XVII	Et ₃ COH	Et ₃ N	89	75	98	120
XVII	MeOD	MeONa	3	22	47	120
XVII	10% MeOD- DMSO- <i>d</i> ₆	MeOK	2	22	40	120
XVII	(CH ₂ OD) ₂	DOCH ₂ - CH ₂ OK	24	55	17	120

^a For structures of XIII and XVII, see pps. 209 and 217.

a substituted benzene XVIII [120]. These reactions performed in THF-*t*-BuOH mixture have been discussed previously. It seems that the acid reacting with a base produces first a tight pair, even in strongly polar solvents. Such pairs may rearrange or exchange before being converted into loose pairs or free ions. The extent of intramolecular rearrangement taking place in different solvents is shown in Table 18.

3.5. Protonation of Radical Ions and Dianions

Kinetic studies of protonation of radical anions have special value to those interested in the role of ions and ion pairs in proton-transfer reactions because our current knowledge of structure and dynamics of radical anion-cation pairs is more advanced than is our knowledge of any other type of ion pair (see, e.g., Chapter 5 of ref. 3). The protonation of radical anions or dianions is complicated by the occurrence of some consecutive reactions. To clarify this point, consider the protonation of radical anions of naphthalene, denoted by $N^{\cdot-}$, proceeding according to Eq. 21,



The product of that reaction is a radical, NH^{\cdot} , formed among numerous, not yet protonated $N^{\cdot-}$ radical anions. Electron transfer is usually much faster than protonation, and hence reaction 21 should be followed by the rapid reaction 22,



yielding a delocalized carbanion NH^- . The latter is, on the whole, a stronger base than the original radical anion and hence its protonation is faster than Eq. 21. Thus dihydronaphthalene, NH_2 , and the regenerated naphthalene, N , are the final products of the reaction, their formation being coupled with the destruction of two $N^{\cdot-}$ radical anions.

This consecutive mechanism of protonation was proposed first by Paul, Lipkin, and Weissman [140] and recently tested experimentally by Bank and Bockrath [141]. Using a stop-flow technique, these workers searched for the transient formation of NH^{\cdot} radicals or NH^- carbanions in the reacting mixture of $N^{\cdot-}$ and water dissolved in THF. None was found. A similar test, again leading to a negative result, was reported by Dye and his students [142]. The protonation of anthracenide salts by ethanol was investigated in THF and in DME. A stop-flow technique combined with a fast-scanning spectral analysis demonstrated that all the features of the absorption spectrum of the anthracenide remained unaltered through the course of the reaction, although its intensity decreased rapidly. Eventually the solution was bleached, but at no stage of the process could a transient be detected.

Indeed, quantitative studies [143] demonstrate that the exothermic electron-transfer processes proceed with bimolecular rate constants higher than $10^7 M^{-1} \text{ sec}^{-1}$, and frequently their rates are limited only by the rate of diffusion. The bimolecular rate constants of radical anion protonation are much lower, rarely reaching values as high as $10^6 M^{-1} \text{ sec}^{-1}$. The most convincing evidence showing the greater rapidity of electron transfer than of radical anion protonation is provided by the pulse radiolysis studies of Dorfman [144]. The kinetics of electron transfer such as $A^\cdot + B \rightarrow A + B^\cdot$ (A and B denote aromatic hydrocarbons) could be followed in alcoholic solvents such as isopropanol. Although the concentrations of the aromatic hydrocarbons were only about $10^{-3} M$ or less, they competed effectively for the anion with the alcohol which formed the bulk of the solution.

Kinetics of protonation of free radical anions by methanol, ethanol, *n*-propanol, isopropanol, and *t*-butanol was investigated by Arai and Dorfman [145]. The radical anions were generated in these alcohols by pulse radiolysis. Two species are formed initially in such a system: solvated electrons, e^- , and positive holes. The former are captured rapidly by the aromatic hydrocarbon dissolved in the alcohol. The bimolecular rate constant of electron capture is higher than $10^{10} M^{-1} \text{ sec}^{-1}$ [143]; hence for a typical concentration of the aromatic hydrocarbon of about $10^{-3} M$, the half-lifetime of e^- is less than 10^{-7} sec . Therefore at about $1 \mu\text{sec}$ after the pulse, when the kinetic measurements start, virtually all of the solvated electrons are converted into the corresponding radical anions. The positive holes, ROH^+ , react extremely fast with the surrounding alcohol; the reaction $\text{ROH}^+ + \text{ROH} \rightarrow \text{RO}^\cdot + \text{ROH}_2^+$ is completed in a time shorter than 10^{-9} sec . Thus at the onset of the kinetic studies radical anions, Ar^\cdot , and the protonated molecules of the alcohol are present in the solution, their typical concentrations being about $10^{-6} M$.

Two reactions occur during the kinetic observation, the pseudo-first-order reaction:



and the second-order reaction:



The decay of Ar^\cdot radical anions was followed spectrophotometrically; the resulting reaction was strictly first order, provided the initial Ar^\cdot concentration was not higher than $10^{-6} M$. It seems therefore that under these experimental conditions the pseudo-first-order protonation is much faster than the recombination of ions. This conclusion was verified by separate experiments. Studies of pulse radiolysis of alcoholic solutions of aromatic hydrocarbons slightly acidified with HCl allowed Arai and Dorfman to

determine the bimolecular rate constant of Eq. 24. Its value was found to be $2\text{--}3 \times 10^{10} \text{ M}^{-1} \text{ sec}^{-1}$, whereas the half-lifetime of the pseudo-first-order protonation was typically $10^{-5}\text{--}10^{-6} \text{ sec}$. At the concentration of ROH_2^+ of about 10^{-6} M or less, the recombination could hardly compete with the protonation.

From their studies, Arai and Dorfman [145] deduced the rates of protonation of biphenylide, anthracenide, and triphenylide in bulk methanol, ethanol, *n*-propanol, and isopropanol. Their findings are summarized in Table 19. They demonstrate that the rate of protonation is affected only

Table 19 The Pseudo-First-Order and the Bimolecular Rate Constants^a of Protonation of Free Radical Anions by Alcohols in the Pure Alcohol at $T \approx 25^\circ\text{C}$ [145]

Alcohol	Biphenylide		Anthracenide		<i>p</i> -Triphenylide	
	$k_I \text{ sec}^{-1}$	$k_{23} \text{ sec}^{-1} \text{ M}^{-1}$	$k_I \text{ sec}^{-1}$	$k_{23} \text{ sec}^{-1} \text{ M}^{-1}$	$k_I \text{ sec}^{-1}$	$k_{23} \text{ M}^{-1} \text{ sec}^{-1}$
MeOH	17×10^5	6.9×10^4	20×10^5	8.1×10^4	9×10^5	4×10^4
EtOH	4.4×10^5	2.6×10^4	4×10^5	2.3×10^4	4×10^5	2×10^4
<i>n</i> -PrOH	4.3×10^5	3.2×10^4	3.2×10^5	2.4×10^4		
<i>iso</i> -PrOH	0.7×10^5	0.55×10^4	0.47×10^5	0.36×10^4		
<i>t</i> -BuOH	Too slow to be determined					

^a The bimolecular rate constant is calculated from the pseudo-first-order rate constant, k_I , by dividing its value by the molarity of alcohol in the bulk solvent.

slightly by the nature of the aromatic moiety, but strongly by the nature of the alcohol. In fact, these results correlate well with the relative acidities of these alcohols determined with the aid of nitrophenyl indicator is isopropanol [146]:

	Methanol	Ethanol	<i>n</i> -Propanol	Isopropanol
Relative rates of protonation	10	3.3	3.8	0.6
Relative acidities	10	2.4	~ 1.3	0.2

It should be stressed that these data are not strictly comparable. The acidities were determined in a constant milieu of isopropanol, whereas the milieu was variable in the protonation study, each rate constant referring to another alcohol environment.

Later studies [147] extended the work described here. The investigation of a wider range of aromatic acceptors showed that the rate of protonation is affected, after all, by the nature of the aromatic hydrocarbon. The following

bimolecular rate constants of protonation k_{23} were determined in isopropanol (units $M^{-1} \text{ sec}^{-1}$):

Anthracenide:	0.36×10^4
Biphenylide:	0.55×10^4
<i>m</i> -Triphenylide:	1.1×10^4
Phenanthrenide:	2.6×10^4
Naphthalenide:	4.4×10^4

while the protonation of *p*-triphenylide and pyrenide were too slow to be studied by this technique. These results, although interesting, are puzzling because no correlation with any obvious property of these aromatic hydrocarbons seems possible.

The temperature dependence of protonation was determined for three aromatic radical anions, anthracenide, biphenylide, and naphthalenide; the pertinent results [147] are summarized in Table 20. The activation energies

Table 20 Temperature Dependence^a of Radical Anion Protonation in Bulk Alcohol [147]

Alcohol	Biphenylide		Anthracenide		Naphthalenide	
	<i>E</i> (kcal/mole)	<i>A</i> ($M^{-1} \text{ sec}^{-1}$)	<i>E</i> (kcal/mole)	<i>A</i> ($M^{-1} \text{ sec}^{-1}$)	<i>E</i> (kcal/mole)	<i>V</i> ($M^{-1} \text{ sec}^{-1}$)
MeOH	2.7	6.2×10^6	2.1	3.7×10^6	—	—
EtOH	3.1	3.9×10^6	2.4	1.2×10^6	—	—
Iso- propanol	5.8	150×10^6	6.7	320×10^6	3.4	1.3×10^6

^a Temperature ranged from about -30 to 25°C .

were found to be approximately independent of the nature of the protonated radical anions when methanol or ethanol was the protonating agent. However, a substantially higher activation energy, coupled with a higher entropy of activation, was observed when the radical anions were protonated by isopropanol, although even in this medium the activation energy of protonation of naphthalenide was reported to be similar to those observed in the protonation of anthracenide and biphenylide in methanol and ethanol. These reviewers believe therefore that the high activation energies reported for the protonation of biphenylide and anthracenide in isopropanol might require verification.

The large effect of environment on the rate of protonation was revealed by the studies of Brandon and Dorfman [148]. The protonation of biphenylide, again formed by pulse radiolysis, was studied in mixtures of ethanol or glycol and triethyl- or diethylamine. In the absence of ethanol, protonation in the

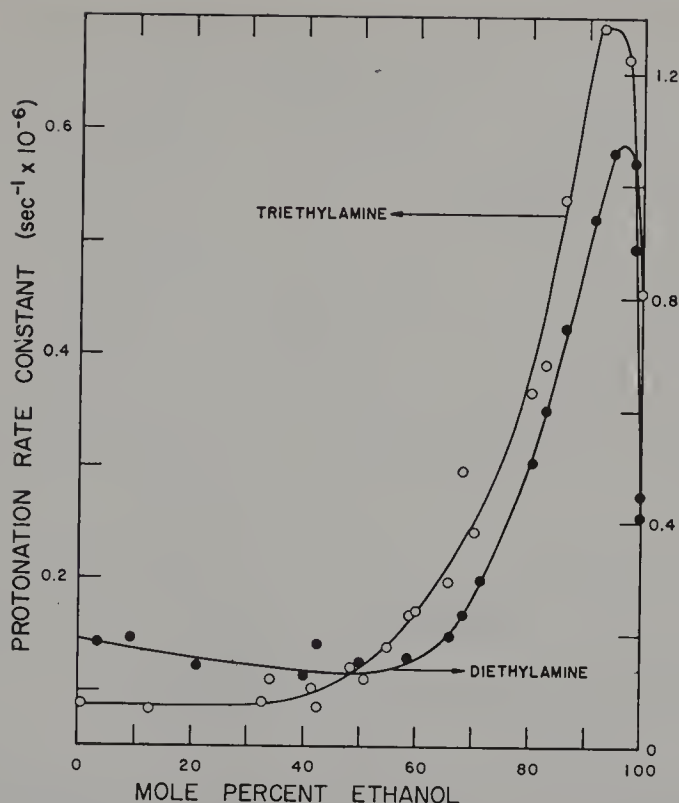


Figure 10. The effect of the addition of diethylamine or triethylamine on the rate of protonation of biphenylide by ethanol. (Open circles = the addition of triethylamine; solid circles = the addition of diethylamine.) Reproduced from ref. 148.

amines is five or six times slower than in the pure ethanol, and the authors suggested that even this relatively slow protonation could result from some impurities present in the amines. Nevertheless, the rate of protonation sharply increased by about 50% on the addition of small amounts of the amines to the alcohol (5–10 mole %). Further addition of the amine caused a catastrophic drop in the rate of protonation as seen in Fig. 10. It is highly improbable that the amines affect the reactivity of biphenylide, and most likely they affect the acidity of the alcohols. Some complexes formed through hydrogen bonding between alcohol and the amine seem to be more reactive than the pure alcohol; apparently these are converted into less reactive species on further addition of amine.

The behavior of the amines contrasts with that of cyclohexane. Figure 11 shows that the addition of the hydrocarbon affects only slightly the rate of protonation by ethanol. Apparently the reaction is intrinsically accelerated by the addition of cyclohexane, perhaps due to the conversion of some ethanol polymers (or cyclic oligomers) into more acidic lower aggregates. This effect

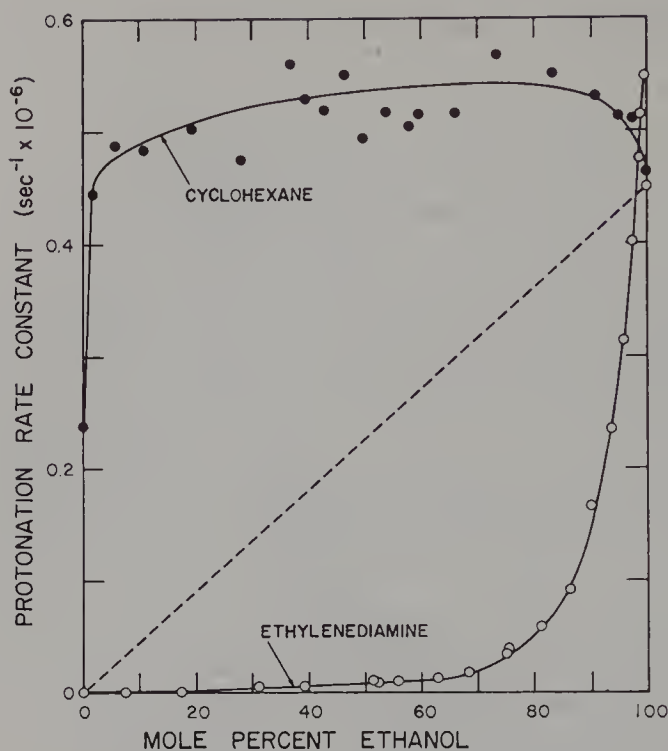


Figure 11. The contrasting effects of the addition of cyclohexane and of ethylenediamine on the rate of protonation of biphenylide by ethanol. (Open circles = ethanol-ethylenediamine system; closed circles = ethanol-cyclohexane system.) Reproduced from ref. 148.

is then compensated by dilution. The amines, when present at higher concentration, may react preferentially with the lower aggregates and reduce, or even destroy, their acidity by becoming hydrogen bonded to them.

Under the experimental conditions of pulse radiolysis, the rate of disappearance of the free radical anions determines directly the bimolecular rate constant of the protonation. The loss of radical anions through an electron transfer to $\text{ArH}\cdot$ radicals is insignificant because the concentration of those radicals is extremely low.

Protonation of the radical anion pairs has been studied by the conventional stop-flow technique. A solution of the investigated radical anions in a desired solvent is mixed with a solution of the protonating agent in the same medium and the progress of the ensuing reaction is followed by the spectrophotometric technique. Such studies are more difficult than those concerned with the protonation of *free* radical anions by bulk alcohols since the following complexities of the system need to be investigated: (a) the nature of the protonated species; and (b) the forms in which the protonating agents reacts in the reaction medium.

In most of the investigated systems the radical anions are present in the form of ion pairs, their structure being determined by the nature of the cation and of the solvent as well as by the thermodynamic variables. The free ions may also be present, and their proportion could be not insignificant if the solutions are highly dilute. In addition, the presence of another species needs to be considered. Radical anions coexist in equilibrium with their dianions. Such equilibria, resulting from electron-transfer reactions, have been discussed extensively in the preceding chapter. Since the dianions are much stronger bases than the radical anions, their presence, even at exceedingly low proportion, may profoundly affect the course of protonation. The equilibrium constants of the disproportionation of radical anions into dianions are greatly affected by the structure of the relevant ion pairs (again see Chapter 1, p. 92). Therefore the contribution of dianions to the protonation is influenced by the nature of the investigated system.

Protonating agents such as alcohols and water associate easily through hydrogen bonds into larger aggregates. In basic solvents such as ethers they are expected to be in a monomeric form, although a small fraction of dimers, and perhaps even higher aggregates, may coexist with the monomers. The former may then affect the protonation if their acidity is substantially higher than that of the monomeric agents, and indeed extensive studies of protonation of some radical anions in ethereal solvents by various alcohols and by water revealed the importance of dimers in the overall reaction.

Protonation of lithium anthracenide ($A^{\cdot-}$, Li^+) in dimethoxyethane (DME) or tetrahydrofuran (THF) is strictly first order in $A^{\cdot-}$, Li^+ and in alcohol, whether MeOH or *t*-BuOH are the protonating agents [156]. We deal here with the simplest reaction,



However, as revealed by the extensive study of Rainis, Tung, and Szwarc [153] the protonation of sodium anthracenide in DME by MeOH, EtOH, *iso*-PrOH or water is more complex although still first order in $A^{\cdot-}$, Na^+ . Apparently monomeric and dimeric alcohols contribute to the reaction because the pseudo first-order protonation constant (in respect to $A^{\cdot-}$, Na^+), denoted by k_I , has a mixed first- and second-order dependence on the alcohol concentration:

$$k_I = 2k_M[ROH] + 2k_DK_D[ROH]^2$$

This dependence is clearly demonstrated by Figure 12 in which $k_I/[ROH]$ is plotted versus $[ROH]$; the excellent linear relations lead then to the values of k_M and k_DK_D presented in Table 21. A similar result was obtained in THF [156].

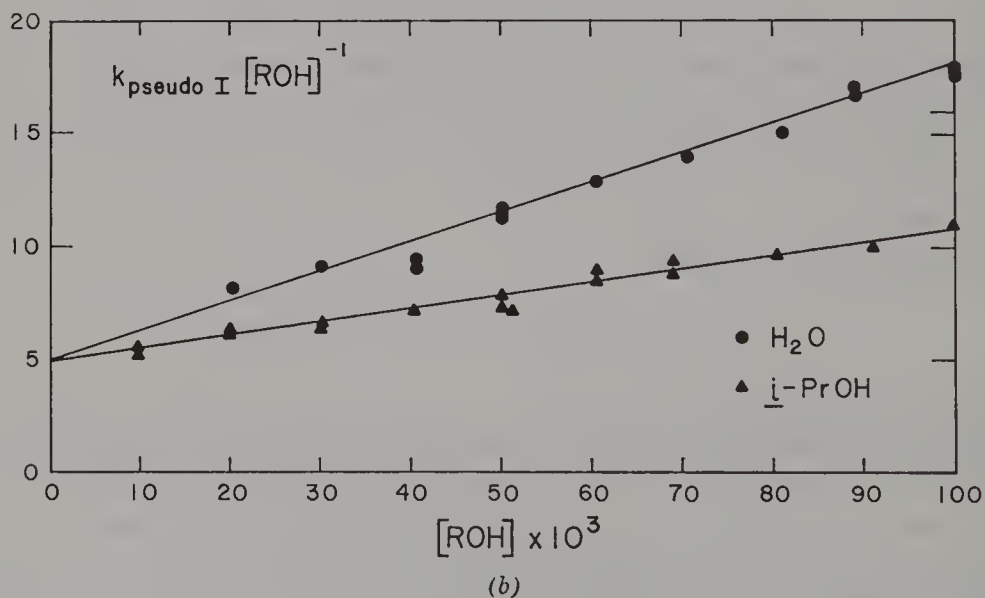
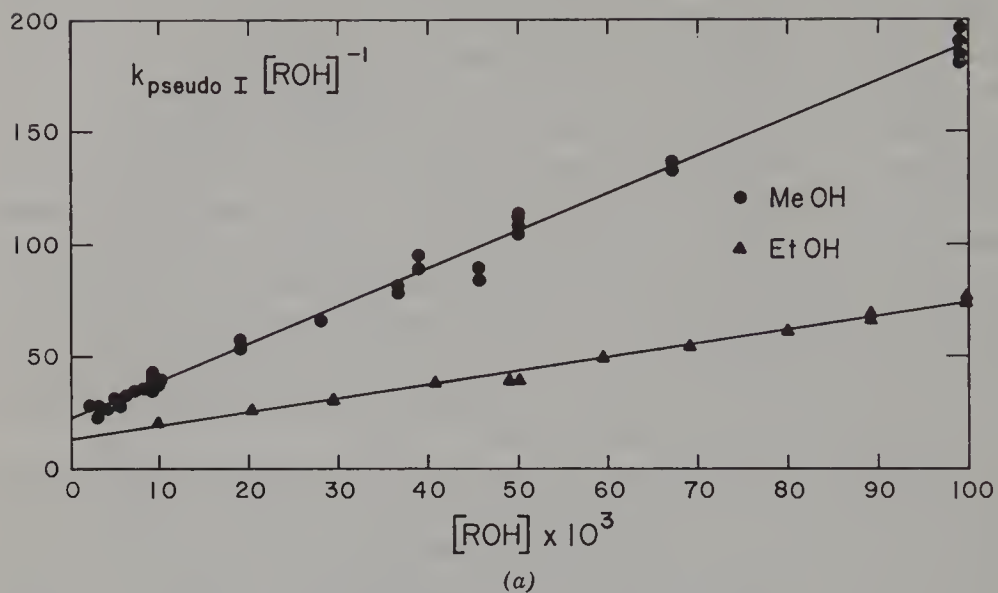


Figure 12. The effect of the protonating agent concentration on the apparent, first order with respect to A^- , Na^+ , rate constants of protonation of sodium anthracenide (A^- , Na^+) by methanol, ethanol, isopropanol, and water in DME. Reproduced from ref. 153.

Table 21 The Bimolecular Rate Constants of Protonation of Sodium Anthracenide in DME by the Monomer, ROH, and the Dimer, (ROH)₂

Alcohol	$k_M (M^{-1} \text{ sec}^{-1})$	$k_D K_D (M^{-2} \text{ sec}^{-1})$
MeOH	10.5	875
EtOH	6.5	310
<i>iso</i> -PrOH	2.4	31
<i>t</i> -BuOH	0.57	0
H ₂ O	2.2	69

According to the proposed interpretation k_M denotes the bimolecular rate constant of the reaction, $\text{ROH} + \text{A}^\cdot, \text{Na}^+ \rightarrow \text{RO}^-, \text{Na}^+ + \text{AH}^\cdot$, while k_D refers to the step, $(\text{ROH})_2 + \text{A}^\cdot, \text{Na}^+ \rightarrow (\text{RO}^-, \text{Na}^+, \text{ROH}) + \text{AH}^\cdot$. K_D is therefore the equilibrium constant of dimerization $2\text{ROH} \rightleftharpoons (\text{ROH})_2$, and its value decreases apparently with the bulkiness of R, that is, K_D decreases along the series $\text{CH}_3 > \text{C}_2\text{H}_5 > \text{iso-C}_3\text{H}_7 > \text{t-C}_4\text{H}_9$. This probably accounts for the steeper decrease in the values of $k_D K_D$ than of k_M . Implicit in the treatment outlined above is the assumption that, under conditions of those experiments, the alcohol dimers form only a negligible fraction of the monomeric alcohol.

In contrast, protonation of sodium perylenide ($\text{Pe}^\cdot, \text{Na}^+$) in THF is second order in the radical anions, particularly when *t*-BuOH is the protonating agent [149]. To repress the presence of any free perylenide ions, an excess of sodium tetraphenylboride has been added to the solution of the perylenide salt, since, as is well known, the tetraphenylboride salts are substantially dissociated in this ether. The apparent bimolecular rate constants are then proportional to the concentration of the protonating agent, the latter being varied from about $10^{-3} M$ to less than $10^{-1} M$; furthermore, the rates have been inversely proportional to the concentration of the added perylene. These findings prove conclusively that sodium perylenide is too weak a base to contribute appreciably to the protonation under those experimental conditions. The observed protonation involves, therefore, the sodium salt of perylene dianions, $\text{Pe}^{2-}, 2\text{Na}^+$, formed and maintained at their equilibrium concentration by the disproportionation of radical anions:



The equilibrium constant of this disproportionation is known to be 1.2×10^{-6} [150]; hence the absolute rate constants of the truly bimolecular reactions



could be calculated. These data are listed in Table 22.

Table 22 The Bimolecular Rate Constants of the Reaction Pe^{2-} , $2\text{Na}^+ + \text{ROH} \rightarrow \text{PeH}^-$, $\text{Na}^+ + \text{RO}^-$, Na^+ in THF at 25°C [149]^a

ROH	$k_{24} \times 10^{-6} (M^{-1}\text{sec}^{-1})$	$\log k_{\text{relative}}$	pK in DMSO
MeOH	1.2	2.00	27.0
MeOD	0.17	—	—
EtOH	0.76	1.80	27.4
<i>iso</i> -PrOH	0.52	1.65	(27.7)
<i>t</i> -BuOH	0.11	0.91	29.1
H ₂ O	0.08	0.52	(30.1)
D ₂ O	~0.01	—	—

^a The pK values given in parentheses are interpolated from the Brønsted plot shown in Fig. 13.

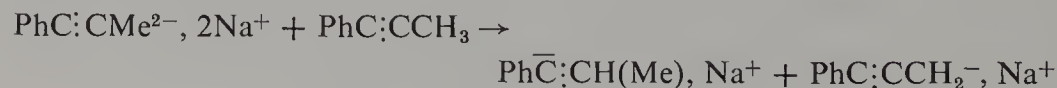
Protonation rate constants of Pe^{2-} , 2Na^+ are about 100 times greater than those determined by Dorfman for the free radical anions. This is not surprising; after all, the dianions are much more basic than monoanions. The rate constants of the dianion protonation have been plotted against the pK of the alcohols determined in DMSO [151]. An excellent Brønsted straight line with a slope of 0.4 has been obtained as shown in Fig. 13. Using this relation, the pK's of isopropanol and water have been calculated, the pertinent results being included in Table 22.

The low reactivity of water may appear strange; however, the unpublished results of Steiner quoted in Ref. 151 indicate that water in DMSO is a weaker acid than *t*-butanol. Apparently the same is true for THF solution. The alcohols and water are present in THF mainly as monomeric species hydrogen bonded to this basic cyclic ether. This undoubtedly reduces their acidity compared to that characterizing the respective alcohol in bulk.

The data collected in Table 22 show a large isotope effect for these proton transfers. According to the usual interpretation, this implies a high degree of O—H rupture in the transition state of this protonation—a surprising result in view of the high basicity of the dianions.

The foregoing studies show the importance of dianions in a reaction formally attributed to radical anions. Moreover, they demonstrate that in this system the disproportionation is capable of maintaining their equilibrium concentration. In fact, the reported data [149] yield the lower limit of the bimolecular rate constant of that disproportionation.

Dianions are also the dominant protonated species in an interesting reaction involving the methylphenylacetylene and sodium biphenylide, B^\cdot , Na^+ . Kinetic studies and the analysis of the products [152] showed that the step



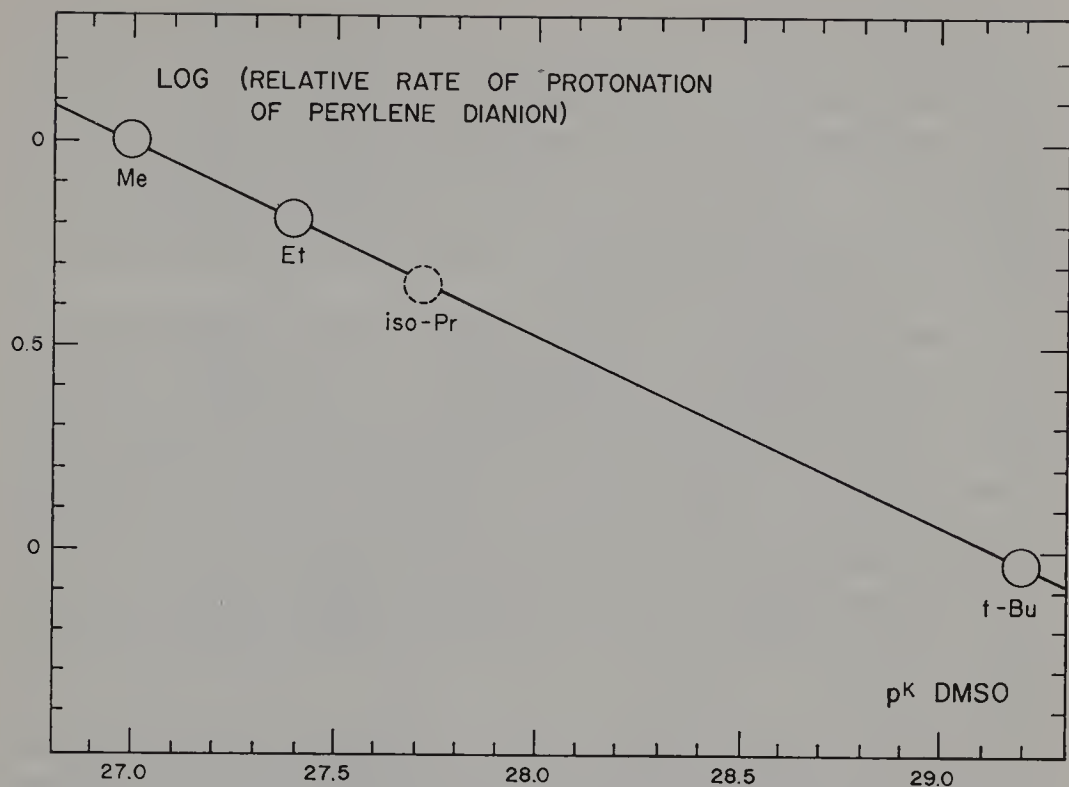
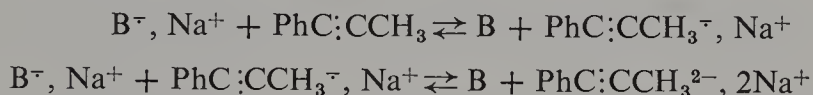


Figure 13. A pseudo-Brønsted plot of the rate constants of protonation of the sodium salt of perylene-dianion in THF by methanol, ethanol, and *t*-butanol versus the pK's of these alcohols determined in DMSO. Reproduced from ref. 149.

is the rate determining in the overall process in which a minute equilibrium concentration of the $\text{PhC}:\text{CMe}^{2-}, 2\text{Na}^+$ dianions is maintained by two electron-transfer reactions:



Sodium biphenylide, $\text{B}^{\cdot-}, \text{Na}^+$, is the electron donor reducing the acetylene, but this base is not protonated by $\text{PhC}:\text{CMe}$. In accordance with this mechanism, the reaction is retarded by biphenyl, B, its rate being proportional to the square of the ratio $[\text{B}^{\cdot-}, \text{Na}^+]/[\text{B}]$ and to the square of the concentration of the acetylene.

This example reveals again that a dianion, although in lower concentration than radical anion, may be the sole object of protonation. Methylphenylacetylene is too weak an acid to protonate the $\text{PhC}:\text{CMe}^{\cdot-}, \text{Na}^+$ radical anions, or for that matter sodium biphenylide; a stronger base, namely a dianion, has to be formed to allow the reaction to proceed.

The addition of dihydroanthracene to this system substantially speeds up the reaction, preserving, however, its second-order character with respect to B^- , Na^+ and the inverse proportionality of its rate with respect to $[B]^2$. Dihydroanthracene has proved to be a much stronger acid than methylphenylacetylene, although still too weak to protonate biphenylide or the $PhC:CMe^-$, Na^+ radical anions. In fact, the kinetic data show that the rate constant of protonation of $PhC:CCH_3^{2-}$, $2Na^+$ by dihydroanthracene is seven times greater than that by $PhC:CCH_3$.

The observation of Shen, Levin and Szwarc [167] may be mentioned here. Phenylacetylene acts as a proton donating acid converting sodium anthracenide in DME or THF into 9,10-dihydroanthracene. With sodium naphthalenide it acts as electron acceptor being eventually reduced to styrene. The ionization potential of naphthalenide is lower than that of anthracenide and this accounts for the reverse behavior of the former compared with the latter. We deal here with an unusual case, an encounter between two species which may lead either to a proton transfer from the first to the second or an electron transfer from the second to the first. The nature of solvent or counterion may modify the degree of participation of each of these reactions to the overall process.

The examples discussed so far deal with the relatively simple situations when either the radical anion or the dianion is the only protonated species that contributes perceptibly to the rate of the reaction. However, in many systems both species contribute to the process and then the rate of protonation is given by a sum of two terms:

$$\frac{-d[Ar^-, Cat^+]}{dt} = k_I[Ar^-, Cat^+] + k_{II}[Ar^-, Cat^+]^2$$

Kinetics of such reactions, studied over a sufficiently large range of radical anions concentration, leads then to the values of the pseudo-rate constants k_I and k_{II} .

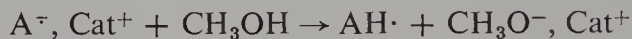
Protonation of sodium anthracenide in DME by *t*-butanol provided the first example of such a system [153]. The first-order process is still dominant in this reaction and the initial contribution of the second-order protonation amounts to only 25–50% of the former. The second-order process becomes dominant in systems such as potassium anthracenide in DME or THF, or sodium anthracenide in THF if protonated by methanol [166], and the reaction becomes purely second order in radical anions when the less reactive *t*-butanol replaces methanol as the protonating agent. The available constants, showing the relative contributions of the first- and second-order reactions to the protonation of anthracenide salts in DME and THF, are collected in Table 23. The mathematical treatment of the primary data yielding the

Table 23 Contribution of the First-Order, k_I , and Second-Order, k_{II} , Reactions to the Protonation of Anthracene Salts in DME and THF. (Initial Concentration of Anthracene $5 \times 10^{-4} M$; Concentration of Anthracene $1 \times 10^{-2} M$)

Alcohol and Counterion	k_I (sec $^{-1}$)	[ROH] $\sim 10^{-2} M$ k_{II} (M^{-1} sec $^{-1}$)	Relative Contribution $k_I/k_{II}[A^-, Cat^+]_0$	k_I (sec $^{-1}$)	[ROH] $\sim 10^{-1} M$ k_{II} (M^{-1} sec $^{-1}$)	Relative Contribution $k_I/k_{II}[A^-, Cat^+]_0$
Solvent DME						
CH ₃ OH/Li ⁺	10 ³	0.0	∞		Too fast	∞
<i>t</i> -BuOH/Li ⁺	7	0.0	∞	70	0.0	∞
CH ₃ OH/Na ⁺	0.4	0.0	∞	20	0.0	∞
<i>t</i> -BuOH/Na ⁺	0.1	20	5	0.1	10 ²	10
CH ₃ OH/K ⁺	0.04	$\sim 10^3$	0.8	~ 5.0	8×10^3	1.2
<i>t</i> -BuOH/K ⁺	0.0	8×10^2	0	0.0	5×10^3	0
Solvent THF						
CH ₃ OH/Li ⁺	15	Too fast	—	150	Too fast	—
<i>t</i> -BuOH/Li ⁺	4	0.0	∞	200	0.0	∞
CH ₃ OH/Na ⁺	0.0	10 ⁵	0.08	0.0	$\sim 3 \times 10^5$	1.3
<i>t</i> -BuOH/Na ⁺	0.1	4×10^4	0	10	$\sim 3 \times 10^5$	0
CH ₃ OH/K ⁺	0	1×10^4	0.02	0	6×10^4	0.3
<i>t</i> -BuOH/K ⁺		4×10^4	0		1×10^4	0

reliable values for k_I and k_{II} has been outlined in the original papers [153, 166].

Some qualitative conclusions transpiring from the data presented in Table 23 deserve to be mentioned. It is clearly demonstrated that for a given solvent and for a specific protonating agent the apparent bimolecular rate constant of protonation of *radical anions*, $k_I/2[\text{ROH}]$, decreases drastically in the series $\text{Li}^+ > \text{Na}^+ > \text{K}^+$. For example, the bimolecular rate constants of the reactions involving *monomeric* methanol in DME



are about $5 \times 10^4 \text{ M}^{-1} \text{ sec}^{-1}$ for the lithium salt, $10 \text{ M}^{-1} \text{ sec}^{-1}$ for the sodium, and probably much less than $1 \text{ M}^{-1} \text{ sec}^{-1}$ for the potassium.* On the other hand, these rate constants increase as THF replaces DME as the solvent; thus the protonation of sodium anthracenide by *monomeric* methanol is about ten times faster in THF than in DME.

Apparently two opposing factors affect the rate of protonation of anthracenide salts: the nature of the counterion and, for a fixed counterion, the tightness of the pair. In spite of the increasing tightness of the ion pairs with increasing size of the cation [3], the rate of their protonation decreases along the series $\text{Li}^+, \text{Na}^+, \text{K}^+$. Such a gradation calls for explanation.

The acidity of an alcohol is expected to increase on complexation with a cation and the smaller the cation's radius the greater should be the enhancement. Since such a cation-alcohol complex is visualized in the transition state of all the protonations discussed here, the rate of these reactions should decrease, in accord with the observations, as Li^+ is replaced by Na^+ or K^+ .

The closer the acidic proton to the anion, the more facile should be the transfer. Hence the protonation should be faster when the alcohol is coordinated with the cation of a tight pair than when it is associated with a cation of a loose pair. This expectation is borne out by the data presented in Table 23—the pairs are tighter in THF than in DME [3] and the protonation is enhanced accordingly. Apparently the first factor dominates over the second and thus the trends with the cation size revealed by the table are rationalized.

The most convincing evidence revealing the decrease in the ion pair reactivity with its increasing "looseness" is provided by the recent observations of Dye et al. [142]. It was found that the addition of dicyclohexyl-18-crown-6-ether [132] to the solution of potassium anthracenide in tetrahydrofuran greatly retards the protonation. The striking results are shown in Fig.

* Protonation of $\text{A}^\cdot, \text{K}^+$ in THF by MeOH seems to involve $(\text{MeOH})_2$, that is, k_I —the contribution of radical anions, and not dianions, to the protonation—is strictly proportional to $[\text{MeOH}]^2$.

14. In the absence of the crown ether the protonation was completed in less than 0.1 sec (curve *C* of Fig. 14), whereas in the presence of an excess of the crown ether but otherwise under identical conditions, the reaction was still incomplete after 2 sec (curve *A* of Fig. 14). The "crown" forms a 1:1 complex with the cation of an ion pair [20] and converts it into a looser and obviously less reactive pair. The addition of the crown ether in a concentration lower than that of the anthracenide led to a fast reaction followed by a slow pro-

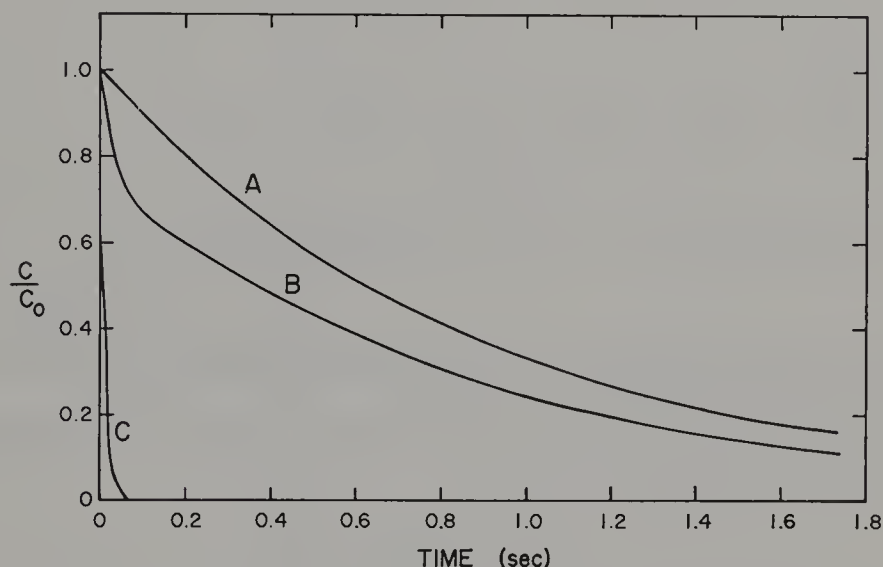


Figure 14. The decay of potassium anthracenide (A^- , K^+) in THF during its protonation by ethanol. Curve *A* = in the presence of an excess of crown-ether; Curve *B* = crown-ether concentration lower than of A^- , K^+ ; Curve *C* = in the absence of crown ether. Reproduced from ref. 142.

tonation (curve *B* of Fig. 14). This result demonstrates the simultaneous presence of two types of ion pairs—those coordinated with the crown ether are less reactive, whereas uncoordinated pairs being more reactive. Moreover, this observation implies that the crown ether remains strongly coordinated to the radical anion pair and is not transferred to the salt of the alkoxide formed by the protonation.

In the protonation of radical anions by alcohols the *free* radical anions are even less reactive than the loose ion pairs. This is shown by the results depicted in Fig. 15. The protonation of lithium anthracenide in DME by *t*-butanol follows perfectly a first-order kinetics when lithium tetraphenylboride is added to the solution. However, in its absence the otherwise linear log plot is concave [156], since then the proportion of free A^- ions increases as the reaction proceeds and their lower reactivity leads to a progressive retardation of protonation. Lithium ion pairs are the most dissociated among

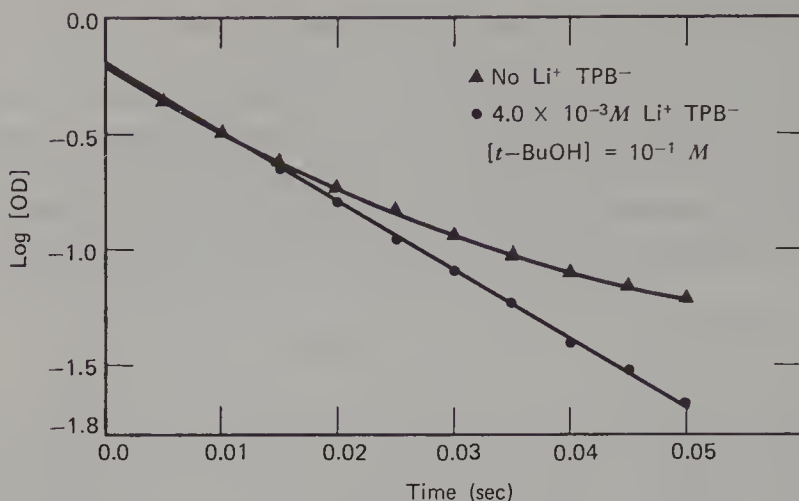
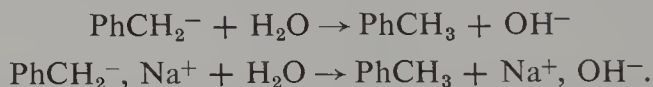


Figure 15. Plot of $\log[\text{OD}]$ versus t for the protonation of A^- , Li^+ by $t\text{-BuOH}$ in DME. Initial concentration of A^- , $\text{Li}^+ \sim 3 \times 10^{-4} \text{ M}$. Reproduced from ref. 156,

the alkali pairs and therefore the phenomenon described here is spectacular in this system, but not unique. The same behavior, although less pronounced, has been observed in other systems [153, 156].

Protonation of free benzyl carbanions by H_2O in THF was compared with the reaction of PhCH_2^- , Na^+ [168],



Benzyl carbanions were formed by pulse radiolysis of mercury dibenzyl in THF, $(\text{PhCH}_2)_2\text{Hg} + e^- \rightarrow \text{PhCH}_2^- + \text{PhCH}_2\text{Hg}^\cdot$. In the presence of Na^+ , BPh_4^- the electron capture leads to $\text{PhCH}_2^-, \text{Na}^+$. The presence of water leads then to protonation and the kinetics demonstrated that the rate constant is 100 times greater for the protonation of $\text{PhCH}_2^-, \text{Na}^+$ than for the protonation of the free PhCH_2^- anions. These studies were extended to a series of alcohols and the final results are collected in Table 24.

Table 24 Bimolecular Rate Constants of Protonation of $\text{PhCH}_2^- (k_-)$ and $\text{PhCH}_2^-, \text{Na}^+ (k_\pm)$ in THF at $24^\circ\text{C} (M^{-1} \text{ sec}^{-1})$

Proton Donor	$k_- \times 10^{-8}$	$k_\pm \times 10^{-8}$
MeOH	2.3 ± 0.3	58 ± 8
EtOH	1.4 ± 0.2	37 ± 5
EtOD	1.2 ± 0.2	21 ± 3
$t\text{-BuOH}$	0.16 ± 0.02	13 ± 2
H_2O	0.53 ± 0.2	55 ± 7

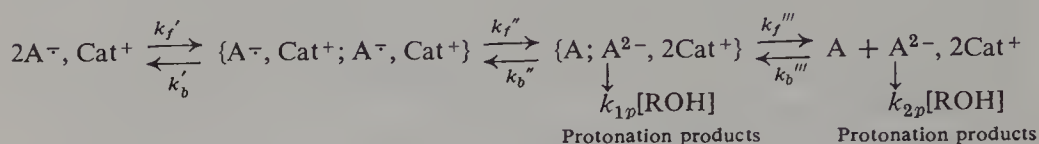
The gradation of reactivities reported in other studies is seen again. Interestingly, water is less reactive than MeOH or EtOH when the free ion is protonated but its relative reactivity is much higher in the protonation of ion pair. The isotope effect found in this study is small, being comparable to that observed by Bank and Bockrath [141, 158]. It seems that the large isotope effect reported for the protonation of perylene dianions [148] is associated with the nature of dianion.

This trend in reactivities of ions and ion pairs is the reverse of that observed in anionic polymerization [157] or in the protonation of living polystyrene by triphenylmethane [104]. When the interaction of an acid with the cation of a pair is strong a cation acts beneficially increasing the acidity of the protonating agent. This effect operates for alcohols but not for carbon acids. In the absence of such an interaction, the reaction is enhanced by polarization of the acid due to the electric field of the anion, and such a field is stronger when generated by a free anion than by an ion pair. A similar explanation accounts for the behavior of ionic polymerization of nonpolar monomers [157].

Another aspect of protonation of *radical anions* deserves a comment. The fast protonation of lithium anthracenide by methanol in DME is first order in the alcohol [156], but the protonation of the sodium salt shows a mixed, first- and second-order behavior with respect to methanol [153], whereas the protonation of the potassium salt is strictly second order in that alcohol [156]. It seems that the acidity of the monomeric alcohol "activated" by its coordination with a small cation is sufficiently great to make the relative contribution of the dimer to the overall protonation insignificant. Such an "activation" becomes insufficient when the cation is large and then the dimer becomes the dominant protonating agent. Alternatively, these observations may be rationalized in terms of a termolecular reaction as outlined in the original paper [156].

The kinetics of the anthracene dianions protonation is much more complex than that of the previously discussed perylene dianions. The absolute rate constants of their protonation are by several orders of magnitude greater than those of radical anions—an obvious consequence of their high basicity. The high basicity of the dianions alleviates the difference in their reactivities toward monomeric and dimeric alcohols; consequently only the abundant monomeric alcohols contribute significantly to the protonation [153, 156]. The same trend applies to the reactivities of different alcohols. The reactivity of *t*-butanol is much lower than of MeOH when the protonation involves radical anions (see, e.g., Table 21), but their reactivities are comparable, as will be seen later, when they protonate the highly basic dianions. This accounts for the greater relative contribution of k_{II} to the protonation by *t*-butanol than to the protonation by MeOH (see Table 23).

Protonation of dianions formed from radical anions is described by the following mechanism which takes into account the protonation of the second encounter complex:*



The value of k_{II} reflects therefore the combined rates of protonation of the encounter complex $\{A; A^{2-}, 2Cat^+\}$ and of the genuine dianion $A^{2-}, 2Cat^+$. The concentration of the first encounter complex, $\{A^{\cdot-}, Cat^+; A^{\cdot-}, Cat^+\}$, is undoubtedly maintained by the respective equilibrium because k''_f is much smaller than k'_b . Also, the equilibrium concentration of the second encounter complex is maintained, because k''_b —the unimolecular rate constant of the strongly exothermic electron transfer—is greater than 10^{11} sec^{-1} and therefore $k''_b > k_{1p}[ROH] + k'''_f$. On this assumption,

$$\frac{1}{2}k_{II} = K'K''k_{p1}[ROH] + K'K''k'''_f / \left\{ 1 + \left(\frac{k'''_b}{k_{p2}} \right) \left(\frac{[A]}{[ROH]} \right) \right\}$$

where $K' = k'_f/k'_b$ and $K'' = k''_f/k''_b$.

Detailed study of the kinetics of these reactions, that is, the dependence of the rate on $[ROH]$ and $[A]$, permitted the determination of the constants $K'K''k_{p1}$, $K'K''k'''_f$, and k'''_b/k_{p2} . These, in conjunction with the disproportionation constants, $K'K''K'''$, determined potentiometrically for the various counterions and solvents [166], led to the values of $K'K''k'''_f$, $K'K''k_{p1}$, k_{p2} , and k'''_b listed in Table 25 [156], which includes also the data reported by Dye et al. [142] for the system $A^{\cdot-}K^+$, THF, EtOH. The remarkable agreement between the data obtained by the two independent groups is gratifying.

Some conclusions drawn from these data should be stressed. The absolute rate constants of protonation of the salts of anthracene dianions, k_{p2} , are nearly diffusion controlled and therefore not much affected by the nature of alcohol—a point made previously. They are substantially higher than those of protonation of the sodium salt perylene dianions—a reasonable finding. The bimolecular rate constants of the highly exothermic electron-transfer $A + A^{2-}, 2Cat^+ \rightarrow 2A^{\cdot-}, Cat^+$ are virtually diffusion controlled and, as required by the mechanism, independent of the nature of the alcohol although they are slightly affected by the nature of the solvent and cation.

* Basically the same mechanism was proposed by Dye and his students. The idea proposed in their preliminary communication [154] was fully developed in the subsequent paper [142].

Table 25 The Characteristic Rate Constants of Protonation of the Sodium and Potassium Salts of Anthracene Dianions in DME and THF by MeOH and *t*-BuOH

System	$10^7 K'K''K'''$	$K'K''\bar{k}_{p1}$ ($M^{-2} \text{ sec}^{-1}$)	$K'K''k_f'''$ ($M^{-1} \text{ sec}^{-1}$)	$10^{-9} k_{p2}$ ($M^{-1} \text{ sec}^{-1}$)	$10^{-10} k_b'''$ ($M^{-1} \text{ sec}^{-1}$)
Na ⁺ , MeOH, DME	0.3	Not observed, the first-order protonation too fast			
Na ⁺ , <i>t</i> -BuOH, DME	0.3	$2.1 \cdot 10^2$	$2.4 \cdot 10(?)$	0.14(?)	0.08(?)
K ⁺ , MeOH, DME	1.3	$2.7 \cdot 10^4$	$1.9 \cdot 10^3$	6.4	1.4
K ⁺ , <i>t</i> -BuOH, DME	1.3	$1.1 \cdot 10^4$	$1.8 \cdot 10^3$	3.3	1.3
Na ⁺ , MeOH, THF	130	$1.3 \cdot 10^5(?)$	$1.3 \cdot 10^5$	5.5	0.95
Na ⁺ , <i>t</i> -BuOH, THF	130	$3.5 \cdot 10^5$	$1.3 \cdot 10^5$	1.7	1.3
K ⁺ , MeOH, THF	7.4	$1.8 \cdot 10^5$	$1.5 \cdot 10^4$	9.3	2.0
K ⁺ , <i>t</i> -BuOH, THF	7.4	$1.0 \cdot 10^5$	$1.3 \cdot 10^4$	7.5	1.8
K ⁺ , EtOH, THF ^a	7.4	$1.2 \cdot 10^5$	$0.5 \cdot 10^4$	2.0	0.7

^a These values were obtained by Dye et al. [142]; the remaining are from the paper by Rainis, Tung, and Szwarc [156].

These changes in the character of protonation arise from variations of the disproportionation constant which is much lower in DME than in THF and decreases with the increasing size of the cation (see Chapter 1, p. 93). The effect of solvent and counterion on the disproportionation reflects the changes in the structure of ion pairs; the pairs are tighter in THF than in DME and their "tightness" decreases with the decreasing size of the cation.

The relatively high equilibrium constant of disproportionation of sodium perylenide in THF (16×10^{-7}) in conjunction with the relatively low protonation constants of the sodium salt of its dianions (10^5 – $10^6 M^{-1} \text{ sec}^{-1}$) permits the maintenance of an equilibrium concentration of Pe^{2-} , 2Na^+ . This concentration is substantially higher than that of its encounter complex. These factors account for the relatively simple character of the protonation in the perylene system.

In view of the complexity of these reactions some minor contradictory claims reported by three research groups, Bank and Bockrath [141, 158], Dye et al. [142, 154], and Rainis, Tung, and Szwarc [153, 156], are not surprising. Let us stress, however, the degree of agreement between their findings and conclusions, before discussing the disagreements.

All three groups have concluded that the protonation is faster in THF than in DME; that is, for a specific cation the tight pairs seem to be more reactive than the loose pairs. The kinetic orders of the reactions deduced from the data of Dye et al. and Szwarc et al. are similar and even the numerical values of the pertinent rate constants are close (see Table 24). However, neither Dye et al. nor Bank and Bockrath added to their solutions salts sharing a common cation with the protonated radical-anions in order to repress the dissociation of ion

pairs. This omission distorted somewhat the conversion curves and affected the results. Such distortions were likely to be considerable in studies of Bank and Bockrath, because the construction of their equipment forced them to work at an exceedingly low concentration of radical anions of about $10^{-5} M$ —approximately a 100 times lower than the concentrations maintained in the study of Dye et al. or Szwarc et al. Moreover, minor impurities may also affect the results—a difficulty mentioned in the paper of Dye et al. [142]. The latter difficulties were greatly amplified in the work of Bank and Bockrath, and they probably account for the high degree of non-reproducibility of their results (a scatter often within a factor of 3) and for some of their disputable findings. For example, the protonation of sodium naphthalenide by water is claimed to be first order in water over a concentration range of $4 \times 10^{-4} M$ to $4 M$ [141]. This seems to be unlikely; the bimolecular rate constant is expected to increase with water concentration. In fact, Fujihara, Suzuki, and Hayano [159], who protonated with water the electrochemically produced radical anions in dimethylformamide, reported an exponential increase of the apparent first-order rate constant with increasing water concentration.

The problems we have dealt with in the preceding paragraph are rather technical; nevertheless, their discussion is desired, since it gives the reader an opportunity to critically evaluate the reported results. The protonation processes are often complex, but much of this complexity has been unraveled during the past years. Many of the elementary steps composing the overall reaction have been defined and characterized, the structural and other factors influencing their rates have been recognized, and their effect is now understood.

This work was supported by the National Science Foundation (M. Szwarc) and in part by U.S. Public Health grant no. GM-12855 (A. Streitwieser).

REFERENCES

1. R. P. Bell, *The Proton in Chemistry*, Cornell University Press, Ithaca N.Y., 1963. A second edition has appeared in 1973.
2. D. J. Cram, *Fundamentals of Carbanion Chemistry*, Academic Press, New York, 1965.
3. M. Szwarc, Ed., *Ions and Ion Pairs in Organic Reactions*, Interscience, New York, 1972.
4. T. E. Hogen-Esch and J. Smid, *J. Am. Chem. Soc.*, **87**, 669 (1965); **88**, 307, 318 (1966).
5. S. Claesson, B. Lundgren, and M. Szwarc, *Trans. Faraday Soc.*, **66**, 3053 (1970).
6. Ref. 3, pp. 43–47.
7. M. Born, *Z. Physik*, **1**, 45 (1920).
8. M. Szwarc, *Carbanions, Living Polymers, and Electron-Transfer Processes*, Interscience, New York, 1968, Chap. V.
9. C. D. Ritchie, in "Interactions in Dipolar Aprotic Solvents," in *Solute-Solvent Interactions*, J. F. Coetzee and C. D. Ritchie (Eds), Marcel Dekker, New York, 1969.

10. B. W. Clare, D. Cook, E. C. F. Ko, Y. C. Mac, and A. J. Parker, *J. Am. Chem. Soc.*, **88**, 1911 (1966).
11. C. D. Ritchie and G. H. Megerle, *J. Am. Chem. Soc.*, **89**, 1447 (1967).
12. C. D. Ritchie, G. A. Skinner, and V. G. Badding, *J. Am. Chem. Soc.*, **89**, 2063 (1967).
13. C. D. Ritchie and P. D. Heffley, *J. Am. Chem. Soc.*, **87**, 5402 (1965).
14. E. M. Arnett, *Prog. Phys. Org. Chem.*, **1**, 223 (1963).
15. P. G. Sears, R. K. Wolford, and L. R. Dawson, *J. Electrochem. Soc.*, **103**, 633 (1956).
16. E. Grunwald and E. Price, *J. Am. Chem. Soc.*, **86**, 4517 (1964).
17. R. G. Bates, in *Interactions in Dipolar Aprotic Solvents*, J. F. Coetzee and C. D. Ritchie (Eds.), Marcel Dekker, New York, 1969.
18. H. Strehlow, in *The Chemistry on Non-aqueous Solvents*, Vol. I, J. J. Lagowski (Ed.), Academic Press, New York, 1966.
19. M. Szwarc, *Accts. Chem. Res.*, **2**, 87 (1969); *Science*, **170**, 23 (1970).
20. J. Smid ref. 3, Chap. 3, and W. F. Edgell, ref. 3, Chap. 4.
21. R. G. Bates in *Solute-Solvent Interactions*, J. F. Coetzee and C. D. Ritchie (Eds.), Marcel Dekker, New York, 1969.
22. W. Gordy and S. C. Stanford, *J. Chem. Phys.*, **9**, 204 (1941).
23. E. M. Arnett and E. J. Mitchell, *J. Am. Chem. Soc.*, **93**, 4052 (1971).
24. E. M. Arnett and J. V. Carter, *J. Am. Chem. Soc.*, **93**, 1516 (1971).
25. A. Streitwieser, W. M. Padgett, and I. Schwager, *J. Phys. Chem.*, **68**, 2922 (1964).
26. A. Streitwieser, E. Ciuffarin, and J. H. Hammons, *J. Am. Chem. Soc.*, **89**, 63 (1967).
27. A. Streitwieser, J. H. Hammons, E. Ciuffarin, and J. I. Brauman, *J. Am. Chem. Soc.*, **89**, 59 (1967).
28. A. Streitwieser, C. J. Chang, W. B. Hollyhead, and J. R. Murdoch, *J. Am. Chem. Soc.*, **94**, 5288 (1972).
29. Y. Karasawa, G. Levin, and M. Szwarc, *Proc. Roy. Soc. (London) A*, **326**, 53 (1971).
30. A. Streitwieser and J. I. Brauman, *J. Am. Chem. Soc.*, **85**, 2633 (1963).
31. (a) A. Streitwieser, R. A. Caldwell, M. R. Granger, and P. M. Laughton, *J. Phys. Chem.*, **68**, 2916 (1964); (b) A. Streitwieser and W. Padgett, *J. Phys. Chem.*, **68**, 2919, 2922 (1964).
32. (a) M. DeSorgo, B. Wasserman, and M. Szwarc, *J. Phys. Chem.*, **76**, 3468 (1972); (b) T. L. Staples and M. Szwarc, *J. Am. Chem. Soc.*, **90**, 5022 (1970).
33. J. B. Conant and G. W. Wheland, *J. Am. Chem. Soc.*, **54**, 1212 (1932).
34. W. K. McEwen, *J. Am. Chem. Soc.*, **58**, 1124 (1936).
35. A. Streitwieser and D. M. E. Reuben, *J. Am. Chem. Soc.*, **93**, 1794 (1971).
36. I. Dzidic, *J. Am. Chem. Soc.*, **94**, 8333 (1972).
37. J. P. Briggs, R. Yamdagni, and P. Kebarle, *J. Am. Chem. Soc.*, **94**, 5128 (1972).
38. For reviews, see R. H. Boyd, "Acidity Functions," in *Solute-Solvent Interactions*, J. F. Coetzee and C. D. Ritchie (Eds.), Marcel Dekker, New York, 1969.
39. C. H. Rochester, *Acidity Functions*, Academic Press, New York, 1970, Chap. VII.
40. C. H. Langford and R. L. Burwell, *J. Am. Chem. Soc.* **82**, 1503 (1960); K. Bowden and R. Stewart, *Tetrahedron* **21**, 261 (1965).
41. C. D. Ritchie, *J. Am. Chem. Soc.*, **91**, 6749 (1969).

42. C. D. Ritchie and R. E. Uschold, *J. Am. Chem. Soc.*, **90**, 2821 (1968); **89**, 2960 (1967).
43. A. Streitwieser, L. Nebenzah, and S. Ewing, unpublished results.
44. D. E. Applequist and D. F. O'Brien, *J. Am. Chem. Soc.*, **85**, 743 (1963).
45. See, e.g., L. D. McKeever, ref. 3, Chap. 6.
46. R. E. Dessy, W. Kitching, T. Psarras, R. M. Salinger, A. Chen, and T. Chivers, *J. Am. Chem. Soc.*, **88**, 453, 460 (1966).
47. R. M. Salinger and R. E. Dessy, *Tetrahedron Lett.*, **1963**, 729.
48. E. M. Kosower, *An Introduction to Physical Organic Chemistry*, Wiley, New York, 1968, p. 27.
49. A. Streitwieser, W. B. Hollyhead, A. H. Pudjaatmaka, P. H. Owens, T. L. Kruger, P. A. Rubenstein, R. A. MacQuarrie, M. L. Brokaw, W. K. C. Chu, and H. M. Niemeyer, *J. Am. Chem. Soc.*, **93**, 5088 (1971).
50. A. Streitwieser, W. B. Hollyhead, G. Sonnichsen, A. H. Pudjaatmaka, C. J. Chang, and T. L. Kruger, *J. Am. Chem. Soc.*, **93**, 5096 (1971).
51. K. Bowden and A. F. Cockerill, *J. Chem. Soc. B*, **1970**, 173.
52. A. Streitwieser, C. J. Chang, and W. B. Hollyhead, *J. Am. Chem. Soc.*, **94**, 5292 (1972).
53. A. Streitwieser, C. J. Chang, and D. M. E. Reuben, *J. Am. Chem. Soc.*, **94**, 5730 (1972).
54. A. Streitwieser, M. R. Granger, F. Mares, and R. A. Wolf, *J. Am. Chem. Soc.*, **95**, 4257 (1973).
55. A. Streitwieser, P. J. Scannon, and H. N. Niemeyer, *J. Am. Chem. Soc.*, **94**, 7936 (1972).
56. R. Kuhn and D. Rewicki, *Ann.*, **706**, 250 (1967).
57. M. Szwarc, *Int. J. Pure Appl. Chem.*, **4**, 511 (1971).
58. C. D. Ritchie and R. E. Uschold, *J. Am. Chem. Soc.*, **89**, 1721 (1967).
59. G. B. Kistiakowsky, J. R. Ruhoff, H. A. Smith, and W. E. Vaughan, *J. Am. Chem. Soc.*, **57**, 876 (1935).
60. A. Streitwieser and J. H. Hammons, *Prog. Phys. Org. Chem.*, **3**, 41 (1965).
61. L. L. Chan and J. Smid, *J. Am. Chem. Soc.*, **90**, 4654 (1968).
62. B. Lundgren, S. Claesson, and M. Szwarc, *Chem. Scripta*, **3**, 53 (1933).
63. C. Carvajal, K. J. Toelle, J. Smid, and M. Szwarc, *J. Am. Chem. Soc.*, **87**, 5548 (1965).
64. A. Streitwieser and J. R. Murdoch, unpublished results.
65. A. F. Cockerill and J. E. Lamper, *J. Chem. Soc. B*, **1971**, 503.
66. A. Streitwieser, J. A. Hudson, and F. Mares, *J. Am. Chem. Soc.*, **90**, 648 (1968).
67. J. E. Leffler and E. Grunwald, *Rates and Equilibria of Organic Reactions*, Wiley, New York, 1963, pp. 156–168, 238–242.
68. M. Eigen, *Angew. Chem. Int. Ed. Engl.*, **3**, 1 (1964).
69. H. Schneider, in *Solute-Solvent Interactions*, J. R. Coetzee and C. D. Ritchie (Eds.), Marcel Dekker, New York, 1969, Chap. V.
70. A. I. Shatenstein, L. I. Zakharkin, E. S. Petrov, E. A. Yakovleva, F. S. Yakushin, Z. Vukm-rovich, G. G. Isaeva, and V. N. Kalinin, *J. Organomet. Chem.*, **23**, 313 (1970).
71. A. Streitwieser and F. Mares, *J. Am. Chem. Soc.*, **90**, 644 (1968).
72. J. N. Brønsted and K. J. Pedersen, *Z. Physik. Chem.*, **108**, 185 (1923)...
73. J. N. Brønsted, *Chem. Rev.*, **5**, 322 (1928).

74. R. G. Pearson and R. L. Dillon, *J. Am. Chem. Soc.*, **75**, 2439 (1953).
75. M. L. Ahrens and G. Maass, *Angew. Chem. Int. Ed. Engl.*, **7**, 818 (1968).
76. C. D. Ritchie and R. E. Uschold, *J. Am. Chem. Soc.*, **86**, 4488 (1964).
77. C. D. Ritchie and R. E. Uschold, *J. Am. Chem. Soc.*, **90**, 3415 (1968).
78. F. G. Bordwell, W. J. Boyle, Jr., and K. C. Yee, *J. Am. Chem. Soc.*, **92**, 5926 (1970).
79. F. G. Bordwell, W. J. Boyle, J. A. Hautala, and K. C. Yee, *J. Am. Chem. Soc.*, **91**, 4002 (1969).
80. E. Grunwald, C. F. Jumper, and S. Meiboom, *J. Am. Chem. Soc.*, **85**, 522 (1963).
81. E. Grunwald and A. Y. Ku, *J. Am. Chem. Soc.*, **90**, 29 (1968).
82. E. K. Ralph and E. Grunwald, *J. Am. Chem. Soc.*, **90**, 517 (1968).
83. F. G. Bordwell and W. J. Boyle, *J. Am. Chem. Soc.*, **93**, 511 (1971).
84. A. J. Kresge, *J. Am. Chem. Soc.*, **92**, 3210 (1970).
85. D. J. Cram and W. D. Kollmeyer, *J. Am. Chem. Soc.*, **90**, 1791 (1968).
86. N. N. Zatzepina, A. W. Kirova, and J. F. Tupizin, *Organic Reactivity* (Tartu State University, Estonia), **5**, 70 (1968).
87. M. Eigen and L. DeMaeyer, *Proc. Roy. Soc. A*, **247**, 505 (1958).
88. F. H. Westheimer, *Chem. Rev.*, **61**, 265 (1961).
89. R. P. Bell and D. M. Goodall, *Proc. Roy. Soc. (London) A*, **294**, 273 (1966).
90. See ref. 1, p. 188.
91. (a) M. M. Kreevoy, R. Eliason, R. A. Landholm, T. S. Straub, and J. L. Melquist, *J. Phys. Chem.*, **76**, 2951 (1972); (b) J. M. Williams and M. M. Kreevoy, *Adv. Phys. Org. Chem.*, **6**, 63 (1968).
92. J. Bigeleisen, *J. Pure Appl. Chem.*, **8**, 217 (1964).
93. (a) E. S. Lewis and J. D. Allen, *J. Am. Chem. Soc.*, **86**, 2022 (1964); (b) E. S. Lewis and L. Funderburk, *J. Am. Chem. Soc.*, **86**, 2531 (1964).
94. F. G. Bordwell and W. J. Boyle, *J. Am. Chem. Soc.*, **93**, 512 (1971).
95. S. B. Hanna, C. Jermini, and H. Zollinger, *Tetrahedron Lett.*, **1969**, 4415.
96. (a) A. Streitwieser, W. C. Langworthy, and D. E. Van Sickle, *J. Am. Chem. Soc.*, **84**, 251 (1962); (b) A. Streitwieser and H. F. Koch, *J. Am. Chem. Soc.*, **86**, 404 (1964).
97. J. E. Hofmann, A. Schriesheim, and R. E. Nickols, *Tetrahedron Lett.*, **1965**, 1745.
98. D. J. Cram, C. A. Kingsbury, and B. Rickborn, *J. Am. Chem. Soc.*, **83**, 3688 (1961).
99. A. Streitwieser and D. Holtz, *J. Am. Chem. Soc.*, **89**, 692 (1967).
100. C. G. Swain, E. C. Stivers, J. F. Reuer, and L. J. Schaad, *J. Am. Chem. Soc.*, **80**, 5885 (1958).
101. A. Streitwieser, J. R. Murdoch, G. Häfeling, and C. J. Chang, *J. Am. Chem. Soc.*, **95**, 4248 (1973).
102. A. Streitwieser and J. H. Hammons, in *Progress in Physical Organic Chemistry*, Vol. 3, Interscience, New York, 1965, pp. 41–80.
103. D. N. Bhattacharyya, C. L. Lee, J. Smid, and M. Szwarc, *J. Phys. Chem.*, **69**, 612 (1965).
104. L. L. Chan and J. Smid, *J. Phys. Chem.*, **76**, 695 (1972).
105. T. Shimomura, J. Smid, and M. Szwarc, *J. Am. Chem. Soc.*, **89**, 5743 (1967).
106. T. E. Hogen-Esch and J. Smid, *J. Am. Chem. Soc.*, **89**, 2764 (1967).

107. T. Shimomura, K. J. Tölle, J. Smid, and M. Szwarc, *J. Am. Chem. Soc.*, **89**, 796 (1967).
108. D. Nicholls, C. A. Sutphen, and M. Szwarc, *J. Phys. Chem.*, **72**, 1021 (1968).
109. K. R. Ryan and J. H. Futrell, *J. Chem. Phys.*, **42**, 824 (1965).
110. (a) A. I. Shatenstein, *Tetrahedron*, **18**, 95 (1962); (b) A. I. Shatenstein, in *Advances in Physical Organic Chemistry*, Vol. 1 V. Gold (Ed.), Academic Press, New York, 1963, p. 162.
111. A. Streitwieser, D. E. Van Sickle, and W. C. Langworthy, *J. Am. Chem. Soc.*, **84**, 244 (1962).
112. (a) R. Waack and P. West, *J. Am. Chem. Soc.*, **86**, 4494 (1964); (b) P. West, R. Waack, and J. I. Purmort, *J. Am. Chem. Soc.*, **92**, 840 (1970).
113. H. Gilman and H. A. McNinch, *J. Org. Chem.*, **27**, 1889 (1962).
114. R. Waack and M. A. Doran, *J. Am. Chem. Soc.*, **91**, 2456 (1969).
115. (a) D. J. Cram and L. Gosser, *J. Am. Chem. Soc.*, **85**, 3890 (1963); (b) D. J. Cram and L. Gosser, *J. Am. Chem. Soc.*, **86**, 5445 (1964).
116. D. J. Cram, W. T. Ford, and L. Gosser, *J. Am. Chem. Soc.*, **90**, 2598 (1968).
117. W. T. Ford and D. J. Cram, *J. Am. Chem. Soc.*, **90**, 2612 (1968).
118. D. J. Cram and L. Gosser, *J. Am. Chem. Soc.*, **86**, 2950 (1964).
119. D. J. Cram, F. Willey, H. P. Fischer, and D. A. Scott, *J. Am. Chem. Soc.*, **86**, 5370 (1964).
120. D. J. Cram, F. Willey, H. P. Fischer, H. M. Relles, and D. A. Scott, *J. Am. Chem. Soc.*, **88**, 2759 (1966).
121. J. Almy, R. T. Uyeda, and D. J. Cram, *J. Am. Chem. Soc.*, **89**, 6768 (1968).
122. J. Almy and D. J. Cram, *J. Am. Chem. Soc.*, **91**, 4459 (1969).
123. W. D. Kollmeyer and D. J. Cram, *J. Am. Chem. Soc.*, **90**, 1779 (1968).
124. J. Almy, D. C. Garwood, and D. J. Cram, *J. Am. Chem. Soc.*, **92**, 4321 (1970).
125. D. J. Cram and L. Gosser, *J. Am. Chem. Soc.*, **86**, 5457 (1964).
126. W. T. Ford, E. W. Graham, and D. J. Cram, *J. Am. Chem. Soc.*, **89**, 691, 4661 (1967).
127. W. T. Ford and D. J. Cram, *J. Am. Chem. Soc.*, **90**, 2606 (1968).
128. A. Streitwieser and W. C. Langworthy, *J. Am. Chem. Soc.*, **85**, 1757 (1963).
129. A. Streitwieser, R. A. Caldwell, R. G. Lawler, and G. R. Ziegler, *J. Am. Chem. Soc.*, **87**, 5399 (1965).
130. A. Streitwieser and D. E. Van Sickle, *J. Am. Chem. Soc.*, **84**, 254 (1962).
131. F. Mares and A. Streitwieser, *J. Am. Chem. Soc.*, **89**, 3770 (1967).
132. C. J. Pedersen, *J. Am. Chem. Soc.*, **89**, 7017 (1967).
133. J. I. Brauman, D. F. McMillen, and Y. Kanazawa, *J. Am. Chem. Soc.*, **89**, 1728 (1967).
134. C. D. Ritchie and R. E. Uschold, *J. Am. Chem. Soc.*, **89**, 1730 (1967).
136. J. I. Brauman, N. J. Nelson, and D. C. Kahl, *J. Am. Chem. Soc.*, **90**, 490 (1968); J. I. Brauman and N. J. Nelson, *J. Am. Chem. Soc.*, **90**, 491 (1968).
137. J. I. Brauman, J. A. Bryson, D. C. Kahl, and N. J. Nelson, *J. Am. Chem. Soc.*, **92**, 6679 (1970).
138. E. J. Corey and M. Chaykovsky, *J. Am. Chem. Soc.*, **87**, 1345 (1965).
139. E. C. Steiner and J. M. Gilbert, *J. Am. Chem. Soc.*, **85**, 3054 (1963).
140. D. E. Paul, P. Lipkin, and S. I. Weissman, *J. Am. Chem. Soc.*, **78**, 116 (1956).

141. S. Bank and B. Bockrath, *J. Am. Chem. Soc.*, **93**, 430 (1971).
142. E. R. Minnich, L. D. Long, J. M. Ceraso, and J. L. Dye, *J. Am. Chem. Soc.*, **95**, 1061 (1973).
143. M. Szwarc and J. Jagur-Grodzinski, Chap. 1 of this book.
144. S. Arai, D. A. Grev, and L. M. Dorfman, *J. Chem. Phys.*, **46**, 2572 (1967).
145. S. Arai and L. M. Dorfman, *J. Chem. Phys.*, **41**, 2190 (1964).
146. J. Hine and M. Hine, *J. Am. Chem. Soc.*, **74**, 5266 (1952).
147. S. Arai, E. L. Tremba, J. R. Brandon, and L. M. Dorfman, *Can. J. Chem.*, **45**, 1119 (1967).
148. J. R. Brandon and L. M. Dorfman, *J. Chem. Phys.*, **53**, 3849 (1970).
149. G. Levin, C. Sutphen, and M. Szwarc, *J. Am. Chem. Soc.*, **94**, 2652 (1972).
150. J. Jagur-Grodzinski, M. Feld, S. L. Yang, and M. Szwarc, *J. Phys. Chem.*, **69**, 628 (1965).
151. Ref. 9, p. 229.
152. G. Levin and M. Szwarc, *Chem. Comm., London*, **1971**, 1029.
153. A. Rainis, R. Tung, and M. Szwarc, *J. Am. Chem. Soc.*, **95**, 659 (1973).
154. E. R. Minnich and J. L. Dye, Abstract, 161st National Meeting of the American Chemical Society, Los Angeles, Calif., March (1967).
155. N. Hirota, *J. Phys. Chem.*, **71**, 127 (1967); *J. Am. Chem. Soc.*, **90**, 3603 (1968).
156. A. Rainis, R. Tung, and M. Szwarc, *Proc. Roy. Soc.* in press.
157. M. Szwarc, ref. 8, Chap. VII.
158. S. Bank and B. Bockrath, *J. Am. Chem. Soc.*, **94**, 6076 (1972).
159. M. Fujihara, H. Suzuki, and S. Hayano, *J. Electroanal. Chem.*, **33**, 393 (1971).
160. P. Kebarle, ref. 3, Chap. II.
161. J. R. Murdoch, *J. Am. Chem. Soc.*, **94**, 4410 (1972).
162. J. L. Kurz and L. C. Kurz, *J. Am. Chem. Soc.*, **94**, 4451 (1972).
163. J. P. Fox, M. I. Page, A. Satterthwait, and W. P. Jencks, *J. Am. Chem. Soc.*, **94**, 4729 (1972).
164. A. G. Evans, M. A. Hamiel, and N. H. Rees, *J. Chem. Soc. B*, **1971**, 2164.
165. K. C. Chu and D. J. Cram, *J. Am. Chem. Soc.*, **94**, 3521 (1972).
166. A. Rainis and M. Szwarc, *J. Amer. Chem. Soc.*, **96**, 3008 (1974).
167. E. Shen, G. Levin, and M. Szwarc, to be published.
168. B. Bockrath and L. M. Dorfman, *J. Amer. Chem. Soc.*, **96**, in press (1974).
169. J. A. Zoltewicz and L. S. Helmiak, *J. Org. Chem.* **38**, 658 (1973).
170. D. M. Aue, H. M. Webb, and M. T. Bowers, *J. Am. Chem. Soc.* **94**, 4726 (1972).

3

Ions and Ion Pairs in Solvolysis Reactions

DOUGLAS J. RABER

*Department of Chemistry,
University of South Florida,
Tampa, Florida*

J. MILTON HARRIS

*Department of Chemistry,
The University of Alabama in Huntsville,
Huntsville, Alabama*

PAUL v. R. SCHLEYER

*Department of Chemistry,
Princeton University,
Princeton, New Jersey*

1. Introduction	248
2. Salt Effects	249
2.1. Common Ion Rate Depression	249
2.2. Common Ion Exchange	252
2.3. Normal Salt Effects	257
2.4. Special Salt Effects	271
	247

3. Equilibration of Labeled Oxygen in <i>p</i> -Nitrobenzoate and <i>p</i> -Toluenesulfonate Esters	279
3.1. Allylic Systems	279
3.2. Nonrearranging Systems	284
3.3. Wagner-Meerwein Rearrangements	290
4. Miscellaneous Methods for the Detection of Ion Pairing	297
4.1. Secondary Deuterium Isotope Effects	297
4.2. Interconversion of Substrates Through a Common, Ion-Paired Intermediate	305
4.3. Polydentate Leaving Groups	311
5. Ion Pairs in the Solvolysis of Primary and Secondary Derivatives	322
5.1. Competitive S_N1 and S_N2 Reactions	326
5.2. The Ion Pair Mechanism	328
5.3. Implications of the Ion Pair Mechanism	345
6. Miscellaneous Methods for the Generation of Ion Pairs	350
6.1. Thermal Decomposition of Alkyl Formates, Sulfinates, and Related Compounds	350
6.2. Diazonium Ions	356
6.3. Acid Addition to Olefins	361
7. Some Observations on the Detailed Mechanism of Solvolysis	363
References	366

1. INTRODUCTION

Despite the compelling evidence for the existence of carbonium ions first gathered around 1900, it took many decades before the intermediacy of such charged species gained general acceptance [1]. The pendulum then swung too far to the other extreme, and *free* carbonium ions tended to be postulated indiscriminately. Although many examples where the nature of the counterion or leaving group influenced the detailed course of carbonium ion reactions were known, an appreciation of the role of ion pairs has developed only recently [1]. Hammett clearly recognized the importance of ion association and differentiated between *ionization* and *dissociation* [2]. However, the now classical work of Winstein (from the early 1950s) explicitly delineated the importance of ion pairing in the solvolytic generation of cationoid species [3]. The separation of the charged species during heterolytic bond cleavage was shown not to be a continuous process but to proceed through discrete ion pair stages.

While S_N2 processes have traditionally been regarded as proceeding smoothly, without the intervention of intermediates, it has been stressed recently that ion pairs may intervene here as well [4]. In fact, S_N1 and S_N2 reactions may involve a continuous mechanistic spectrum depending on the relative timing of nucleophilic attack and leaving-group departure. However, whether or not the pendulum has now swung too far to the ion pair extreme remains to be established with certainty.

Nevertheless, the more stable the cationoid component, the more compelling is the evidence for the intermediacy of ion pairs. This is exemplified by the recent suggestion that S_N2' reactions may proceed not by nucleophilic attack on covalent substrate but rather on preformed ion pairs [5].

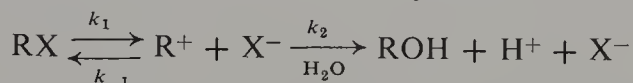
Evidence for the intervention of ion pairs during solvolysis reactions are considered in this review.

2. SALT EFFECTS

2.1. Common Ion Rate Depression (Mass Law Effect)

In the classic work of Hughes and Ingold and their co-workers on the mechanism of solvolysis, a variety of criteria were used to distinguish between the "unimolecular" (S_N1) and "bimolecular" (S_N2) mechanisms [6]. Since the nucleophile (solvent) is always in large excess with regard to substrate, *both* of these mechanisms are anticipated to follow first-order kinetics in a solvolysis reaction. Consequently, to a first approximation, the kinetic behavior of a solvolysis will afford no information regarding the mechanism. However, Ingold and his co-workers [6, 7] pointed out that the formation of ions as reaction products might be expected to alter the kinetic behavior during the course of a reaction.

These workers treated S_N1 reactions according to the mechanism illustrated in Scheme I for the hydrolysis of an alkyl halide, RX. According to this



Scheme I

scheme, the intermediate carbonium ion R^+ can undergo reaction either with solvent (to give ROH) or with halide ion (to regenerate the alkyl halide). The rate of the latter reaction depends on the concentration of X^- , and a qualitative analysis suggests that an increase in halide ion concentration will result in a greater proportion of return to alkyl halide (k_{-1}) at the expense of the product-forming step (k_2). Consequently, as the solvolysis reaction proceeds and the concentration of X^- increases, a decrease might be expected in the observed titrimetric constant; an example of this behavior is illustrated in Table 1.

Table 1 Integrated First-Order Rate Constants for the Solvolysis of 0.0463 M *p,p'*-Dimethylbenzhydryl Chloride in 90 % Aqueous Acetone at 0°^a

% Reaction	8.0	16.2	27.6	37.5	48.9	57.0	69.2	74.9	79.7
$k \times 10^5$ (sec ⁻¹)	8.68	8.30	7.83	7.53	7.33	7.05	6.87	6.77	6.70

^a Data from Ref. 8.

Table 2 Effects of Added Salts on the Initial Rate Constants for Solvolysis of Benzhydryl Halides in 80 % Aqueous Acetone at 25° ^a

Added Salt, 0.1 M	Benzhydryl Chloride		Benzhydryl Bromide	
	$k \text{ (sec}^{-1}) \times 10^5$	Change (%)	$k \text{ (sec}^{-1}) \times 10^3$	Change (%)
None	7.00	—	1.53	—
LiBr	8.16	+17	1.33	-13
LiCl	6.09	-13	1.94	+27

^a Data from Ref. 9.

Subsequent work by Benfey, Hughes, and Ingold [9] clearly demonstrated that such rate depressions were not a result of changes in the ionizing power of the solvolysis medium but were definitely a consequence of a common ion effect. Table 2 summarizes a series of experiments in which these workers studied the solvolysis of benzhydryl halides in the presence of both common and noncommon ion salts.

If rate depression of the alkyl chloride solvolysis in the presence of chloride ion were a consequence of altering the character the solvolysis medium [6] by the addition of an ionic species, then similar rate depressions would be expected for each of the four cases in Table 2 in which the solvolysis was carried out in the presence of added salt. In contrast, only those cases in which the added halide ion is the same as the leaving group show depressed rate constants; the presence of a noncommon ion salt actually leads to rate enhancement. The latter effect (which is discussed in Section 2.3) is a consequence of an increase in the ionic strength of the solvolysis medium. The ionic strength effect is superimposed on the common ion effect, and consequently the common ion rate depressions must be even larger than the percentages given in Table 2 (which are based on the rate constants in the absence of salts).

If the effects of ionic strength are disregarded, the use of the steady state approximation permits the observed solvolysis rate constant to be expressed in terms of Eq. 1:

$$k_{\text{obs}} = \frac{k_1 k_2}{k_2 + k_{-1}[\text{X}^-]} \quad (1)$$

Rearrangement of Eq. 1 leads to Eq. 2:

$$k_{\text{obs}} = \frac{k_1}{1 + \alpha[\text{X}^-]} \quad (2)$$

where $\alpha = k_{-1}/k_2$. Equations 1 and 2 indicate that as the concentration of X^- increases the observed rate constant will decrease and the rate depression

(k_1/k_{obs}) should be a linear function of $[X^-]$. The limiting value of k_{obs} as $[X^-]$ approaches zero will be k_1 , the rate constant for ionization.

Kohnstam and co-workers [10, 11] studied the solvolysis of dichlorodiphenylmethane in several mixtures of aqueous acetone. When the common ion effect was studied at a constant total salt concentration to minimize ionic strength effects) the kinetics were found to follow Eq. 2. Their results for 75% aqueous acetone are presented in Table 3; these data lead to $k_1 =$

Table 3^a Initial Rate Constants for the Solvolysis of Diphenyldichloromethane^b in 75 % Aqueous Acetone at 0° with a Total Salt Concentration of 0.0507 M^c

$[\text{Cl}]_0 \times 10^3 \text{ M}^d$	0.80	5.88	10.95	16.02	21.10	26.20
$10^4 k_{\text{obs}}$	4.71	3.91	3.44	3.04	2.71	2.45
$10^4 k_{\text{calc}}^e$	4.68	3.96	3.43	3.03	2.71	2.45

^a Data from Ref. 10.

^b 0.005 M.

^c Both common ion (KCl) and noncommon ion (KBr) salts were present; $[\text{KCl}] + [\text{KBr}] = 0.0507$.

^d $[\text{Cl}]_0 = [\text{KCl}] + 0.8 \times 10^{-3} \text{ M}$ since $0.8 \times 10^{-3} \text{ M}$ chloride ion was formed by hydrolysis before the first reading.

^e Calculated from Eq. 2 using $k_1 = 4.82 \times 10^{-4} \text{ sec}^{-1}$ and $\alpha = 36.9 \text{ M}^{-1}$

$4.82 \times 10^{-4} \text{ sec}^{-1}$ and $\alpha = 36.9 \text{ M}^{-1} \text{ mol}$ (for the specific total salt concentration under consideration).

Ingold and his co-workers reasoned [7] that the magnitude of the common ion effect should increase with the stability of the corresponding carbonium ion R^+ . This conclusion was apparently based on stability-selectivity arguments: As the stability of R^+ increases, its selectivity with regard to reaction with halide ion ($k_{-1}[\text{X}^-]$) relative to reaction with solvent (k_2) should also increase. Thus the mass law constant α (the ratio k_{-1}/k_2), which measures the magnitude of the common ion effect, was expected to increase with the stability of the carbonium ion. Such stability-selectivity relationships are often found in organic chemistry.

Table 4 indicates that this conclusion appears to be valid: As the stability of the carbonium ion (as measured by the solvolysis rate of the corresponding chloride) increases, the magnitude of the common ion effect as measured by α^0 increases in the same order. (Here α^0 is the mass law constant α extrapolated to zero ionic strength. The extrapolation process [7] is complex and will not be considered here.)

The common ion or mass law effect is a direct consequence of the recombination of the ionic intermediates formed by ionization of RX . If the recombination rate is increased by the addition of a salt, MX , it is apparent

Table 4 Comparison of Values of the Mass Law Constant α^0 with Rate Constants for Solvolysis in 80% Aqueous Acetone, 0° ^a

Alkyl Chloride	α^0	k (sec ⁻¹)
<i>t</i> -Butyl	(Small)	$5.90 \times 10^{-8}{}^b$
Benzhydryl	10	2.82×10^{-6}
<i>p-t</i> -Butylbenzhydryl	20	3.59×10^{-5}
<i>p</i> -Methylbenzhydryl	35	8.35×10^{-5}
<i>p,p'</i> -Dimethylbenzhydryl	69	1.60×10^{-3}

^a Data from Ref. 7.

^b Ref. 12.

that the X⁻ anions formed by ionization of RX to R⁺ + X⁻ and those corresponding to the added MX are chemically indistinguishable. Thus ionization of RX in such cases must afford R⁺ and X⁻ as *dissociated ions* with little or no interaction between R⁺ and X⁻. Consequently, the observation of a common ion effect in a solvolysis reaction provides strong evidence for the intermediacy of dissociated or "free" carbonium ions.

2.2. Common Ion Exchange

If a substance RX undergoes solvolysis by the mechanism depicted in Scheme I, in which the dissociated ions R⁺ and X⁻ are *reversibly* formed, it follows that in addition to a kinetic (i.e., common ion) effect, an exchange process also could be observed. Since the intermediate carbonium ion R⁺ is no longer associated with the particular X⁻ to which it was originally bonded, collapse to RX can take place with other X⁻ ions in solution as well. The mass law effect is presumably a direct consequence of this exchange process.

Ordinarily such exchange is degenerate and is thus not detected. However, if the reaction medium contains added salt MX*, where X* is isotopically labeled but otherwise chemically identical to X, then the exchange process will lead to the formation of isotopically labeled RX*. Whenever a common ion effect has been observed it has invariably also been possible to demonstrate exchange [13, 14].

Winstein and co-workers [13] studied the acetolysis of a series of alkyl arenesulfonates with regard to the phenomena of common ion rate depression and exchange and their results are summarized in Table 5. The occurrence of common ion rate depression was indicated either by a downward drift of the integrated first-order titrimetric rate constants (cf. Table 1) or by a depressed rate on the addition of the appropriate lithium arenesulfonate.

Table 5 Occurrence of Common Ion Rate Depression and Exchange in the Acetolysis of Several Alkyl Arenesulfonates^a

Arenesulfonate ^b	Common Ion	
	Rate Depression	Exchange
<i>exo</i> -2-Norbornyl OBs	No	No
1- <i>p</i> -Anisyl-2-propyl OTs	No	—
<i>d,l</i> -threo-3- <i>p</i> -Anisyl-2-butyl OBs	No	Yes
<i>d,l</i> -threo-3- <i>p</i> -Anisyl-2-butyl OTs	No	—
Cholesteryl OBs	Yes	Yes
Cholesteryl OTs	Yes	Yes
2-(2,4-Dimethoxyphenyl)-ethyl OBs	Yes	Yes

^a Ref. 13.^b OBs = *p*-bromobenzenesulfonate; OTs = *p*-toluenesulfonate.

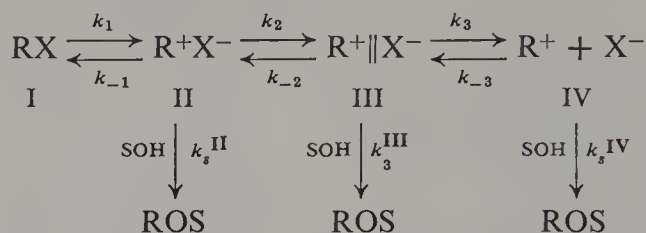
The presence or absence of anion exchange was investigated by the use of the closely similar tosylate (*p*-toluenesulfonate) and brosylate (*p*-bromobenzenesulfonate) anions. It was reasoned that the presence of a *p*-methyl rather than a *p*-bromo substituent on the aromatic ring should have relatively little effect on the exchange reaction. For example, when cholesteryl brosylate was solvolyzed in the presence of lithium tosylate, the instantaneous first-order solvolysis rate constant decreased steadily until it reached the value expected for solvolysis of cholesteryl tosylate under the same conditions. Thus efficient exchange of tosylate for brosylate took place. Similarly, when cholesteryl tosylate was solvolyzed in the presence of lithium brosylate, the rate constant drifted upward, indicating that exchange had resulted in formation of the more reactive cholesteryl brosylate.

The key entry in Table 5 is that for *d,l*-threo-3-*p*-anisyl-2-butyl brosylate; for this compound exchange of the anion took place, yet there was no common ion rate depression. This is clearly inconsistent with the solvolysis mechanism depicted in Scheme I. According to this scheme, as discussed earlier, common ion rate depression and exchange are both manifestations of the same mechanistic feature: collapse of the dissociated carbonium ion R⁺ with free halide ion X⁻.

Winstein and co-workers [13] pointed out, however, that there should be certain conditions under which solvolytic reactions of the carbonium ion type might fail to exhibit the phenomena of common rate depression and exchange. In particular they were concerned with the problem of ion pair intermediates, which appeared likely on the basis of other evidence [15, 16]. These situations can be most conveniently discussed in terms of Winstein's solvolysis scheme [17] (Scheme II), which takes into consideration the role of ion pairs.

According to Winstein's interpretation [18, 19] the ionization of an alkyl halide or arenesulfonate (I) proceeds through a series of progressively more

dissociated intermediates: **II** (an “intimate” or “internal” ion pair [15, 16, 20], **III** (a “solvent-separated” or “external” ion pair [18, 21]), and **IV** (the dissociated carbonium ion and gegenion).



Scheme II. Winstein's solvolysis scheme.

In relation to Scheme II, Winstein defined several terms regarding the reverse reactions which regenerate covalent RX under the general classification of “return” [13]:

1. Internal return—Collapse of intimate (or internal) ion pair (**II** → **I**).
2. External ion pair return—Collapse of the solvent-separated (or external) ion pair (**III** → **I**).
3. External ion return—Combination of dissociated carbonium ion R^+ and X^- (**IV** → **I**).
4. Ion pair return—A broader category which includes both 1 and 2 above.
5. External return—A broader category which includes both 2 and 3 above.

According to this general scheme attack by solvent can take place on any or all of the “three varieties of carbonium ion, **II**, **III**, and **IV**”* [22]. The intermediate or intermediates involved would depend on the nature of RX and on the choice of solvent. Winstein and co-workers implied [13] that as the relative stability of R^+ increases, the site of solvent attack would shift to the right in Scheme II (i.e., further ionization of an ion pair would become more favorable relative to attack by solvent).

Winstein also proposed that the close association of the anion X^- in the intimate ion pair **II** should effectively block solvent attack from that side [22]. Consequently solvent attack on an intimate ion pair (i.e., k_s^{II}) would be expected to afford product of inverted configuration. However, in the case of a bridged nonclassical ion the backside of the intimate ion pair would be shielded against solvent attack also, and solvent attack on **II** would not be important. Thus Winstein proposed that derivatives solvolyzing via anchimerically assisted ionization should react only at the stages of solvent-separated ion pair **III** and dissociated carbonium ion **IV** [19]. For such systems the

* Reference to the species **II**, **III**, and **IV** as carbonium ions is misleading, since the term is generally taken to indicate **IV** only. Reactions involving **II** and **III** (but not **IV**) are better classified as cationoid (see Ref. 23, footnote 8).

number of intermediates giving rise to products is reduced to only two, and treatment of kinetic data is accordingly simplified.

When the steady state approximation is applied to intermediates **II**, **III**, and **IV**, and k_s^{II} is assumed to be negligibly small, the observed titrimetric rate constant, k_t (for the formation of ROH + HX), can be expressed by Eq. 3 [13]:

$$k_t = k_1 / 1 + \frac{k_{-1}/k_2}{\left[k_s^{\text{III}} + \frac{k_3 k_s^{\text{IV}}}{k_{-3}[\text{X}^-] + k_s^{\text{IV}}} \right] / \left[k_{-2} + k_s^{\text{III}} + \frac{k_3 k_s^{\text{IV}}}{k_{-3}[\text{X}^-] + k_s^{\text{V}}} \right]} \quad (3)$$

Analysis of Eq. 3 shows that there are several conditions for which common ion rate depression will not be observed [13]:

1. $k_3 \ll k_s^{\text{III}}$. The free carbonium ion **IV** is not formed to a significant extent.
2. $k_s^{\text{IV}} \ll k_{-3}[\text{X}^-]$. The free carbonium ion **IV** undergoes virtually complete return to **III**.
3. $k_{-3}[\text{X}^-] \ll k_s^{\text{IV}}$. The free carbonium ion **IV** does not undergo return.
4. $k_{-2} \ll k_s^{\text{III}}$. The solvent-separated ion pair **III** does not undergo return.

In each of these cases Eq. 3 reduces to a less complex equation which is independent of the concentration of X^- . In effect, each of the conditions 1 to 4 above serves to remove the "equilibrium" between RX and $\text{R}^+ + \text{X}^-$, which is the basis for the mass law effect. Clearly, common ion rate depression should be associated not just with the formation but with the *reversible formation* of dissociated carbonium ions from covalent starting material.*

The "anomalous" behavior of *d,l*-threo-3-anisyl-2-butyl brosylate in Table 5 was discussed by Winstein and co-workers [13] with regard to conditions 1 to 4.† On the basis of the trends observed in Table 5 (which is arranged in

* One additional situation (5) exists for which no rate depression will be observed for a carbonium ion reaction: The rate enhancing effect of increased ionic strength (see Section 2.3) is equal to or greater than the rate-depressing effect of common ions. This can be detected relatively easily by a plot of the solvolysis rate constant against the concentration of added common ion salt. Only in the absence of common ion rate depression will the resulting line have an extrapolated value at zero salt concentration (no ionic strength effect) which is equal to the actual rate constant in the absence of added salt (cf. Ref. 13).

† The possibility of condition 5 was not discussed explicitly by Winstein. Although a plot of k_t versus common ion salt concentration might permit this situation to be ruled out or confirmed, the solvolysis of the 3-anisyl-2-butyl brosylate was investigated [13] at only a single concentration of added lithium brosylate. However, the similarity of the rate effects produced by addition of either lithium brosylate or lithium tosylate [13] suggests that the possibility of compensating rate-depressing (common ion) and rate-enhancing (ionic strength) effects can be discounted.

the order of increasing stability of the corresponding carbonium ions), it was concluded that the absence of a common ion rate depression and the presence of exchange for 3-anisyl-2-butyl brosylate was a consequence of condition 1: the dissociated carbonium ion was not formed. This reasoning led to the further conclusion that, for substrates giving less stable carbonium ions than 3-anisyl-2-butyl, dissociated carbonium ions would not be formed under the conditions of acetolysis. Since the intimate ion pairs of bridged nonclassical ions were presumed to be relatively inert to solvent attack [22], this reasoning leads to the further restriction that for nonclassical ions corresponding to carbonium ions less stable than that from 3-anisyl-2-butyl brosylate solvent, capture in acetolysis will take place only at the stage of a solvent-separated ion pair (III).

Winstein's results (Table 5) are not consistent with simple ionization to free carbonium ions (Scheme I), and they provide strong support for the intervention of ion pairs as intermediates in acetolysis reactions (Scheme II). Furthermore, it appears that efficient anion exchange can occur at either the solvent-separated ion pair (III) or the dissociated carbonium ion (IV) stage (i.e., it may arise from either type of external return).*

The combination of common ion rate depression and exchange appears to offer considerable value for the determination of the nature of the intermediates in solvolysis reactions. The intermediacy of dissociated carbonium ions generally will result in both a mass law effect and exchange. When exchange takes place in the absence of a mass law effect, it is likely that free carbonium ions (IV) are not involved (although other explanations are

* A highly significant experiment on exchange processes was reported by Grunwald, Heller, and Klein [24], who investigated the acid-catalyzed racemization and oxygen exchange reactions of 1-phenylethanol in water. They discovered that the rate of racemization exceeded that for oxygen exchange by 25%. Since both processes appeared to take place via an ionization process, it appears that the ionic intermediates can racemize without undergoing exchange. Although the ionization of a protonated alcohol does not yield an ion pair of the same type that has been discussed previously (the leaving group corresponding to X^- is now a neutral water molecule), the fates of the two fragments with regard to configuration and to exchange must be governed by the same processes as for ion pairs with a negatively charged leaving group, X^- . The disparity between exchange and racemization rates indicates that in the ionic intermediate there must be some bonding character between the central carbon atom and the leaving water molecule; otherwise the two processes would be expected to occur at the same rate. In the present case it is difficult to rationalize the results as the effect of a solvent cage, since the leaving group and the solvent are identical. Extension of this reasoning to solvolysis of alkyl halides or arenesulfonates leads to the conclusion that there is still some bonding character between the central carbon atom of R^+ and the leaving group X^- at the ion pair stage (see ref. 23, footnote 8). Whether this statement is applicable to both intimate and solvent-separated ion pairs is not entirely clear, but evidence [19, 25] implicating the latter species (III) as the intermediate responsible for racemization in other instances suggests that this may be the case.

possible, as discussed previously) and that solvolysis is taking place via attack on the solvent-separated ion pair III.*

2.3. Normal Salt Effects

In their analysis of solvolysis reactions proceedings by the "unimolecular mechanism," Hughes, Ingold, and their co-workers interpreted the influence of added salts on solvolysis rates in terms of a combination of ionic strength effects and mass law (common ion) effects. They found [8, 30-32] that addition of a noncommon ion salt to a solvolysis medium resulted in an increase in the initial rate constant, and this result was qualitatively explained [7] on the basis of an increase in polarity of the medium. As in the case of an actual change of solvent composition [33], it was suggested [7] that stabilization of the ionic transition state would be greater than stabilization of the neutral ground with a resulting increase in the rate constant for ionization.

The theoretical treatment of such S_N1 reactions by Bateman, Church, Hughes, Ingold, and Taher [7] afforded the relationship between ionic strength and initial rate constant (k_1) given by Eq. 4:

$$\log \frac{k_1}{k_1^0} = \frac{0.912 \times 10^{16} \sigma \mu}{\epsilon^2 T^2} \quad (4)$$

Equation 4 is based on the ionization mechanism shown in Scheme I, and the initial rate constant for solvolysis and the ionization rate constant k_1 were thus assumed to be identical (since initially there is no common ion X^- , the reverse reaction should be minimized). According to Eq. 4 the initial rate constant k_1 is a function of the parameters σ (a measure of charge separation in the transition state), μ (the ionic strength, *which for a univalent electrolyte is equal to the molarity*), ϵ (the dielectric constant of the pure solvent), T (the absolute temperature), and k_1^0 (the initial rate constant in the absence of added salt).

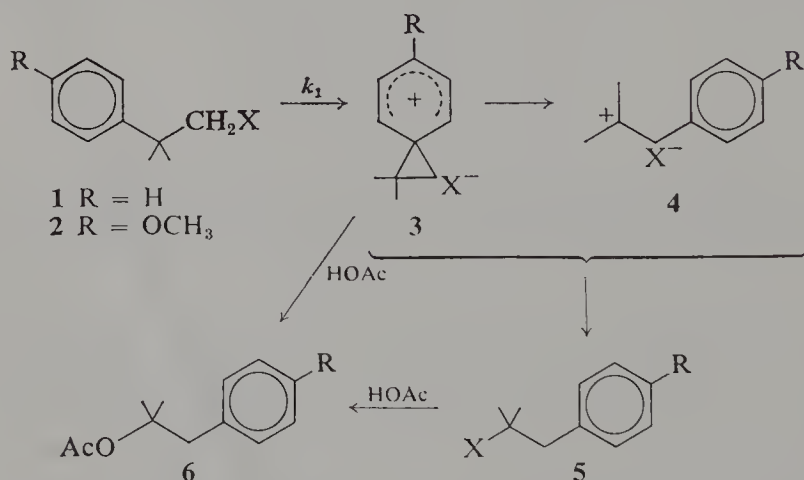
For a series of experiments in which the salt concentration or solvent composition was varied, Bateman and co-workers [7] found that the initial rate constant for solvolysis varied in the manner predicted by Eq. 4. The

* It is of course necessary to be certain that anion exchange is not occurring by way of a direct displacement. Such a process could result in the observation of exchange when the reaction did not involve dissociated carbonium ions or solvent-separated ion pairs. For example, Winstein, Ledwith, and Hojo [26] provided evidence that radiochloride exchange of *p*-chlorobenzhydryl chloride in anhydrous acetone takes place predominantly by S_N2 attack on an intimate ion pair. Such complicating factors will be a function of both substrate and solvent characteristics. When the substrate has a propensity for reaction via a carbonium ion mechanism (e.g., a high m value [27-29]) and the solvent has a high ionizing power (Y value [27-29]) such direct displacement should be minimized.

transition state parameter σ was calculated from Eq. 4 using the rate ratio k_1/k_1^0 for one set of conditions; values of k_1/k_1^0 were then calculated with Eq. 4 for other conditions. These experiments are summarized in Table 6.

The close agreement between calculated and observed values of k_1/k_1^0 indicates that Eq. 4 can indicate the direction and magnitude of the effects of changes in the solvolysis medium. However, as later emphasized by Winstein [34], the limited number of experiments in Table 6 does not permit a valid assessment of the accuracy or generality of Eq. 4.

Winstein and his co-workers subsequently investigated the acetolysis of a variety of substrates in the presence of added salts. To avoid problems associated with ion pair return, their initial work [34] was concerned with the acetolysis of neophyl (1) and *p*-methoxyneophyl (2) halides and arenesulfonates. Fainberg and Winstein [34] argued that these derivatives solvolyzed with anchimeric assistance (via 3) and that any ion pair return would yield the extremely reactive tertiary derivative 5. Consequently they felt that the observed titrimetric rate constant k_t would be equal to the rate constant for ionization k_1 .



When the neophyl derivatives were solvolyzed in acetic acid in the presence of varying amounts of lithium perchlorate, Fainberg and Winstein observed [34] that the solvolysis rate increased with the concentration of added salt. The titrimetric rate constants were found to be a linear function of the salt concentration as given by Eq. 5:

$$k = k^0(1 + b[\text{salt}]) \quad (5)$$

where b represents the magnitude of the normal salt effect. The effect of added lithium perchlorate on the rate constant for acetolysis of neophyl tosylate (Fig. 1) illustrates the behavior observed by Fainberg and Winstein [34].

Winstein and his co-workers criticized the logarithmic relationship of Eq. 4 as having been inadequately tested [34], but even the linear relationship of

Table 6 Medium Effects on the Initial Rate Constants for Solvolysis of Alkyl Halides in Aqueous Acetone^a

Alkyl Halide	Conditions for Determining σ				Conditions for Testing Eq. 4			
	% Acetone ^b	Temperature (°C)	Salt Conc. (mol l ⁻¹) ^c	k_1/k_1^0 (obs)	% Acetone ^b	Temperature (°C)	Salt Conc. (mol l ⁻¹) ^c	k_1/k_1^0 (obs) k_1/k_1^0 (calc) ^d
Benzhydryl chloride	90	50	0.1009	2.13	70	25	0.0999	1.31 1.33
<i>p,p'</i> -Dimethylbenzhydryl chloride	90	0	0.0512	1.71	85	0	0.0512	1.50 1.53
<i>p,p'</i> -Dimethylbenzhydryl chloride	90	0	0.0512	1.71	80	0	0.0540	1.40 1.40
<i>p-t</i> -Butylbenzhydryl chloride	90	50	0.0501	1.70	90	50	0.1000	2.88 2.88

^a Ref. 7.

^b Percent by volume; the number refers to acetone.

^c Sodium azide.

^d Calculated with Eq. 4.

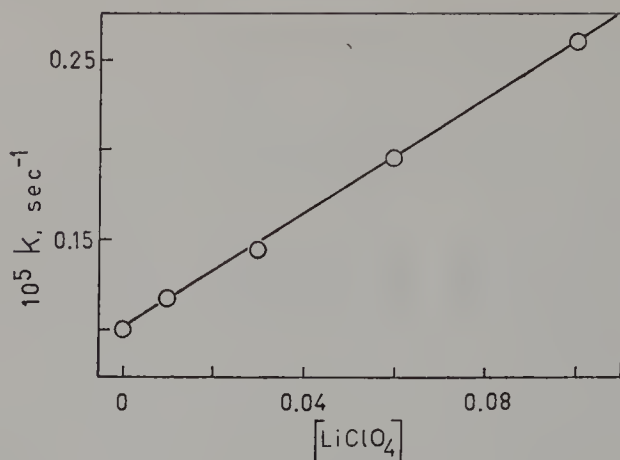
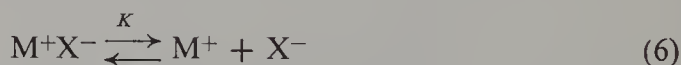


Figure 1. A plot of k_1 versus $[\text{LiClO}_4]$ for the acetolysis of neophyl tosylate at 50° [34].

Eq. 5 does not always predict normal salt effects more accurately than the logarithmic relationship [7, 35]. In the case of acetolysis, a linear relationship between $\log k$ and $[\text{salt}]$ might not be expected as a consequence of formation of ion pairs of the added salt. Winstein, Klinedienst, and Robinson [36] noted that inorganic salts tend to be largely undissociated in glacial acetic acid; that is, the free ions are in equilibrium with ion pairs:



$$K = \frac{[\text{M}^+][\text{X}^-]}{[\text{M}^+\text{X}^-]} \quad (7)$$

$$[\text{M}^+] = [\text{X}^-] = ([\text{M}^+\text{X}^-]K)^{1/2} \quad (8)$$

Consequently, the concentration of free ions M^+ and X^- would be proportional to the *square root* of the concentration of added salt, and the use of the molarity of added salt for the ionic strength μ in Eq. 4 might not be valid. In any event, the empirical relationship of Eq. 5 appears to be general for acetolysis and for many other solvolysis reactions as well.

A second criticism of the theoretical treatment of Bateman, Church, Hughes, Ingold, and Taher [7] does appear to be quite valid. Equation 4 predicts that normal salt effects should depend only on ionic strength and should be independent of the nature of the ionic species. However, considerable specificity of salt effects with regard to the nature of the added salt has been found [34, 35, 37]. The effects of a variety of salts on the acetolyses of neophyl halides and arenesulfonates (**1**) are summarized in Table 7. Clearly the magnitude of the normal salt effect is highly affected by the nature of the salt.

Table 7 Normal Salt Effects for the Acetolysis of Neophyl Halides and Arenesulfonates (1)^a

Salt	<i>b</i> Values, Eq. 5					
	1, X = Cl(100°)	1, X = Br(75°)	1, X = OTs		1, X = OBs	
			50°	75°	50°	75°
HOTs ^b	—	—	1.4	1.0	—	—
LiOTs ^b	—	—	3.9	3.2	3.3	2.9
LiOAc	0.6	0.6	—	—	2.0 ^b	1.1 ^b
LiClO ₄	7.6	6.4 ^b	15	12.5	11.6	10.0
DPGHOAc ^c	3.9	3.2	—	—	—	—
DPGHClO ₄ ^{b,d}	7.2	9.8	—	—	—	—

^a Ref. 34.^b Only a single concentration of salt was studied;^c Diphenylguanidinium acetate.^d Diphenylguanidinium perchlorate.

In addition to the specificity of normal salt effects with regard to the identity of the added salt, Table 7 shows that there is also considerable dependency on the nature of the leaving group and on the temperature. Both of these effects are in agreement with the theory of Bateman, Church, Hughes, Ingold, and Taher [7]. As the leaving group is changed, so should the degree of charge separation in the transition state; according to Eq. 4 such changes are reflected in the rate enhancement. Similarly, the rate enhancement is found to vary inversely with the temperature, although the magnitude of the change appears to be somewhat smaller than predicted by Eq. 4.

Changes in the magnitude of the salt effect with variations in the dielectric constant of the solvent also follow Eq. 4, at least qualitatively. Table 8 summarizes the lithium perchlorate salt effects on the solvolysis rates of *p*-methoxyneophyl tosylate (2) for a series of solvents ranging from highly polar to relatively nonpolar. In accord with the theory [7], the magnitude of the salt effect is found to decrease when the solvent polarity is increased, although a linear relationship between $\log k/k_0$ and $1/\epsilon^2$ is not observed. Inspection of Table 8 indicates that the acidic solvents do not fall in line with the aprotic solvents. This suggests that the influence of the solvent on salt effects is related (in addition to the dielectric constant) to other factors such as the ability to form hydrogen bonds to the leaving group.

A second unusual characteristic of the salt effects in Table 8 is the extremely large value for *b* in diethyl ether. Winstein, Friedrich, and Smith [39] subsequently observed that salt effects in very nonpolar solvents such as acetone were highly dependent on the nature of the cation of the salt (Table 9). The salt effect on the ionization of *p*-methoxyneophyl tosylate (2-OTs) is much lower for tetra-*n*-butylammonium perchlorate than for lithium perchlorate;

Table 8 Salt Effect of Lithium Perchlorate on the Ionization of *p*-Methoxyneophyl Tosylate in a Variety of Solvents at 75°^a

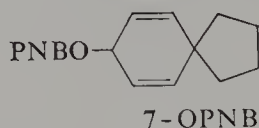
Solvent	ϵ	b (Eq. 5)
Dimethylsulfoxide	49	0
Dimethylformamide	37	1
Acetic acid ^b	6	12
50% Acetic acid-acetic anhydride ^b		13
Acetone	21	47
Acetic anhydride	22	47
<i>n</i> -Octanoic acid ^c		461
12.5% Acetic acid-dioxane		462
Tetrahydrofuran		482
Ethyl acetate	6	553
Diethyl ether ^{b, c}	4	3×10^5

^a Ref. 38.

^b 50°.

^c The plot of k versus [salt] was not linear.

the change for the spirodienyl paranitrobenzoate (7-OPNB) is even more dramatic. Winstein and his co-workers considered the large salt effects of lithium perchlorate in these cases to be a consequence of salt-promoted ionization [37–39], a process which presumably involves coordination of the



metal ion with the leaving group. A similar large salt effect produced by mercuric chloride on the rates of racemization and radiochloride exchange of *p*-chlorobenzhydryl chloride in acetone [40] appears to involve a salt-promoted ionization to the complex ion pair $R^+HgCl_3^-$.

Winstein and co-workers [34] initially selected neophyl derivatives for the study of normal salt effects since for these systems the solvolysis rate is equal

Table 9 Cation Specificity of Salt Effects in Anhydrous Acetone^a

Substrate	b (LiClO ₄)	b (NaClO ₄)	b (Bu ₄ NClO ₄) ^b
2-OTs	47	17	3
7-OPNB	2×10^4	2×10^3	12

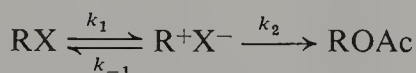
^a Ref. 39.

^b Tetra-*n*-butylammonium perchlorate.

to the ionization rate. If the salt effect on an individual rate constant takes the form of Eq. 5, then the salt effect on the observed titrimetric rate constant for a solvolysis involving ion pair return might be expected to be a complex function of the different salt effects on the individual rate constants. In contrast, however, a relatively large number of investigated systems, both in acetolysis and in other solvolyses, show normal salt effects of the form predicted by Eq. 5. Much of the available literature data on normal salt effects are presented in Tables 10 and 11.

The influence of ion pair return on the magnitude of the normal salt effect has been studied in the cases of *threo*-2-phenyl and *threo*-2-*p*-anisyl-3-butyl arenesulfonates [22, 37]. For the optically active derivatives the polarimetric rate constant k_a can be taken as equal to the ionization rate constant k_1 ; consequently, both k_1 and k_t can be measured independently. The acetolyses of these derivatives take place with considerable ion pair return as indicated by the k_a/k_t ratio of about 4 for both the phenyl [20] and anisyl [22] derivatives. As shown in Table 12, the b values for k_a and for k_t are of the same order of magnitude. The much larger lithium perchlorate salt effects (which are presumably more accurate) for the acetolyses of *threo*-3-*p*-anisyl-2-butyl arenesulfonates suggest that the salt effect is even larger for the titrimetric rate constant than for the ionization rate constant.

Although it might initially appear surprising that the salt effect for the ionization step (to an intimate ion pair) is less than the salt effect for the overall solvolysis reaction, this observation is consistent with theoretical expectations. On the basis of a simple reaction sequence for acetolysis involving reversible ionization to an intimate ion pair which in turn leads to the product in Scheme III, the rate of ionization is given by Eq. 9, and the solvolysis rate



Scheme III

is given by Eq. 10:

$$\frac{d[\text{R}^+\text{X}^-]}{dt} = k_1[\text{RX}] \quad (9)$$

$$\frac{d[\text{ROAc}]}{dt} = k_2[\text{R}^+\text{X}^-] \quad (10)$$

The use of the steady state approximation leads to Eq. 11 and 12:

$$[\text{R}^+\text{X}^-] = \frac{k_1}{k_{-1} + k_2} [\text{RX}] \quad (11)$$

$$\frac{d[\text{ROAc}]}{dt} = \frac{k_2 k_1}{k_{-1} + k_2} [\text{RX}] \quad (12)$$

Table 10 Normal Salt Effects in the Acetolysis of a Variety of Alkyl Derivatives, $RX^{a,b}$

Alkyl Group, R	Salt	Temperature (°C)	Leaving Group	<i>b</i>	Ref.
<i>p</i> -Methoxyneophyl	LiClO ₄	25	OTs	16	18
<i>exo</i> -2-Norbornyl	LiClO ₄	25	OBs	37	18
<i>threo</i> -3- <i>p</i> -Anisyl-2-butyl	LiClO ₄	25	OBs	22	18
<i>erythro</i> -3- <i>p</i> -Anisyl-2-butyl	LiClO ₄	25	OBs	19	18
2- <i>p</i> -Anisyl-1-propyl	LiClO ₄	50	OTs	24	18
<i>p</i> -Methoxyneophyl	NaOAc	50	OBs	0.5	34
<i>p</i> -Methoxyneophyl	LiClO ₄	25	OBs	15.4	34
<i>p</i> -Methoxyneophyl	LiClO ₄	50	OBs	12.2	34
<i>p</i> -Methoxyneophyl	LiOTs	25	OBs	3.6	34
<i>p</i> -Methoxyneophyl	LiOTs	50	OBs	2.6	34
<i>p</i> -Methoxyneophyl	HOTs	25	OBs	1.1	34
<i>p</i> -Methoxyneophyl	HOTs	50	OBs	1.1	34
2-Phenylethyl	LiClO ₄	99.9	OTs	14	41
2- <i>o</i> -Anisylethyl	LiClO ₄	50	OTs	13.1	41
2- <i>o</i> -Anisylethyl	LiClO ₄	75	OTs	11.1	41
2- <i>p</i> -Anisylethyl	LiClO ₄	50	OTs	11	41
2- <i>p</i> -Anisylethyl	LiClO ₄	75	OTs	10	41
2- <i>p</i> -Anisylethyl	KOAc	75	OTs	2 ± 2	41
<i>trans</i> -2- <i>p</i> -Anisylcyclopentyl	LiClO ₄	25	OBs	26.5	42
<i>trans</i> -2- <i>p</i> -Anisylcyclopentyl	LiClO ₄	50	OBs	23.3	42
<i>trans</i> -2- <i>p</i> -Anisylcyclohexyl	LiClO ₄	50	OBs	29	42
<i>trans</i> -2- <i>p</i> -Anisylcyclohexyl	LiClO ₄	75	OBs	26	42
1- <i>p</i> -Anisyl-2-propyl	LiClO ₄	50	OBs	27.4	42
1- <i>p</i> -Anisyl-2-propyl	LiClO ₄	75	OBs	26.5	42
Pinacolyl	LiClO ₄	50	OTs	33.7	37
Pinacolyl	LiClO ₄	75	OTs	30.5	37
Pinacolyl	LiOAc	50	OTs	2.4	37
Pinacolyl	LiOAc	75	OTs	2.4	37
Pinacolyl	HOTs	50	OTs	3.0	37
Pinacolyl	HOTs	75	OTs	3.4	37
Pinacolyl	LiClO ₄	50	OBs	24	37
Pinacolyl	LiClO ₄	75	OBs	17	37
Pinacolyl	LiOAc	50	OBs	1.8	37
Pinacolyl	LiOAc	75	OBs	2.3	37
Pinacolyl	KOAc	70	OBs	1.0	37
Cyclohexyl	LiClO ₄	50	OTs	37.2	37
Cyclohexyl	LiClO ₄	75	OTs	29	37
Cyclohexyl	DPGHOAc ^c	75	OTs	4.6	37
Cyclohexyl	DPGHOAc ^c	100	OTs	3.6	37
Cyclohexyl	KOAc	75	OTs	4.5	37
1-Phenyl-1- <i>p</i> -anisyl-2-propyl	LiClO ₄	25	OBs	16.5	37
1-Phenyl-1- <i>p</i> -anisyl-2-propyl	LiClO ₄	50	OBs	12.8	37
1-Phenyl-1- <i>p</i> -anisyl-2-propyl	LiOAc	25	OBs	1.8	37

Table 10 (continued)

Alkyl Group, R	Salt	Temperature (°C)	Leaving Group	<i>b</i>	Ref.
1-Phenyl-1- <i>p</i> -anisyl-2-propyl	LiOAc	50	OBs	1.2	37
1-Phenyl-1- <i>p</i> -anisyl-2-propyl	LiOTs	25	OBs	4.1	37
1-Phenyl-1- <i>p</i> -anisyl-2-propyl	LiOTs	50	OBs	3.4	37
1-Phenyl-1- <i>p</i> -anisyl-2-propyl	HOTs	25	OBs	1.6	37
1-Phenyl-1- <i>p</i> -anisyl-2-propyl	HOTs	50	OBs	1.4	37
<i>cis</i> -5-Methyl-2-cyclohexenyl	LiClO ₄ ^d	30	Cl	28.3	37
Cholesteryl	LiClO ₄	50	OTs	28	43
Cholesteryl	HClO ₄	50	OTs	~28	43
Cholesteryl	DPGHClO ₄ ^e	50	OTs	12	43
Cholesteryl	DPGHOAc ^c	50	OTs	6	43
Cholesteryl	LiOAc	50	OTs	2	43
Cholesteryl	LiClO ₄	50	OBs	30	43
2-(2,4-Dimethoxyphenyl)-ethyl	LiClO ₄	50	OBs	12	43
2-(2,4-Dimethoxyphenyl)-ethyl	DPGHOAc ^c	50	OBs	2	43
<i>t</i> -Butyl	LiClO ₄ ^f	50	Br	13	44
1- <i>p</i> -Anisyl-2-propyl	Bu ₄ NOTs ^g	50	OTs	4.3	36

^a Salt effects were calculated with Eq. 5.

^b When special salt effects are present also (see below), the value of *b* is that for the normal salt effect only; i.e., it is calculated from the linear portion of the plot of *k* versus [salt].

^c Diphenylguanidinium acetate.

^d Buffered with sodium acetate.

^e Diphenylguanidinium perchlorate.

^f Buffered with lithium acetate.

^g Tetra-*n*-butylammonium tosylate.

Thus the observed rate constants for ionization (Eq. 9) and solvolysis (Eq. 12) respectively would be k_1 and $k_1\{k_2/(k_{-1} + k_2)\}$, and the two rate constants differ by the factor $k_2/(k_{-1} + k_2)$. Consequently the salt effect for ionization would be greater than that for solvolysis only if the latter factor decreased in the presence of added salt, that is, only if the salt effect on k_{-1} were greater than that on k_2 . Such a situation would be opposite to the view [6, 7] that creation of charge is aided by an increase in the polarity of the medium. The rate constant for collapse of the ion pair to neutral substrate (k_{-1}) is not expected to increase in the presence of added salt, in conformity with the data for *threo*-3-*p*-anisyl-2-butyl brosylate.

Additional information about the salt effects on individual rate constants is available from the acetolysis of systems which undergo ion pair return to detectable isomeric substrates (Scheme IV).^{*} At early stages in the solvolysis

^{*} Both Schemes III and IV are simplified versions of Winstein's general scheme for solvolysis (Scheme II). That this simplification (i.e., the absence of external return) is justified in the presence of added lithium perchlorate will be shown in Section 2.4.

Table 11 Normal Salt Effects in the Solvolyses of a Variety of Alkyl Derivatives, $RX^{a,b}$

Alkyl Group, R	Salt	Temperature (°C)	Leaving Group	<i>b</i>	Ref.
90% Acetone					
Benzhydryl	NaN_3	50	Cl	11^e	7
Benzyhydryl	LiBr	50	Cl	8^e	7
Benzyhydryl	NaN_3	50	Br	11^e	7
<i>p</i> - <i>t</i> -Butylbenzhydryl	LiBr	50	Cl	9^e	7
<i>p</i> - <i>t</i> -Butylbenzhydryl	NaN_3	50	Cl	16	7
<i>p,p'</i> -Dimethylbenzhydryl	NaN_3	0	Cl	14^e	7
<i>t</i> -Butyl	LiBr	50	Br	4	7, 44
<i>t</i> -Butyl	NaN_3	50	Br	4^e	7
<i>t</i> -Butyl	LiCl	50	Br	4-6	7, 44
<i>t</i> -Butyl	$LiClO_4$	50	Br	3	44
85% Acetone					
<i>p,p'</i> -Dimethylbenzhydryl	LiBr	0	Cl	9^e	7
<i>p,p'</i> -Dimethylbenzhydryl	NaN_3	0	Cl	10^e	7
<i>p,p'</i> -Dimethylbenzhydryl	$NMe_4NO_3^k$	0	Cl	10^e	7
80% Acetone					
<i>p</i> -Chlorobenzhydryl	$Bu_4NClO_4^c$	25	Cl	0.5	45
<i>p</i> -Chlorobenzhydryl	Bu_4NBr^d	25	Cl	1	45
<i>p</i> -Chlorobenzhydryl	$LiClO_4$	25	Cl	4	45
<i>p</i> -Chlorobenzhydryl	NaN_3	100	OPNB	16^e	25
<i>p,p'</i> -Dimethylbenzhydryl	NaN_3	0	Cl	7^3	7
Benzhydryl	LiBr	25	Cl	2^e	9
Benzhydryl	LiCl	25	Br	3^e	9
70% Acetone					
Benzhydryl	NaN_3	25	Cl	3^e	7
75% Dioxane					
2-Adamantyl	NaN_3	75	OTs	3.5	46
70% Dioxane					
1-Phenylethyl	$LiClO_4$	40	Cl	4	14
60% Dioxane					
1-Phenylethyl	$LiClO_4$	40	Cl	2	14
1-Phenylethyl	$Et_4NClO_4^l$	40	Cl	1	14
1-Phenylethyl	LiBr	40	Cl	2	14

^a Salt effects were calculated with Eq. 5.

^b When special salt effects are present also (see below), the value of *b* is that for the normal salt effect only; i.e., it is calculated from the linear portion of the plot of *k* versus [salt].

^c Tetra-*n*-butylammonium perchlorate.

^d Tetra-*n*-butylammonium bromide.

^e Only one concentration of salt was investigated.

^f 50 weight percent.

Table 11 (continued)

Alkyl Group, R	Salt	Temperature (°C)	Leaving Group	<i>b</i>	Ref.
<u>48% Dioxane^f</u>					
Neophyl	NaOH	50	OTs	−1	35
Neophyl	NaCl	50	OTs	−0.3	35
Neophyl	NaBr	50	OTs	0.4	35
Neophyl	NaNO ₃	50	OTs	0.5	35
Neophyl	NaI	50	OTs	0.6	35
Neophyl	NaClO ₄	50	OTs	2	35
Neophyl	2-C ₁₀ H ₇ SO ₃ Na	50	OTs	0.4	35
<i>threo</i> -3-Phenyl-2-butyl	NaOH	25	OTs	−1 ^g	35
<i>threo</i> -3-Phenyl-2-butyl	NaCl	25	OTs	−0.3 ^g	35
<u>48% Dioxane^b</u>					
<i>threo</i> -3-Phenyl-2-butyl	NaBr	25	OTs	0.7 ^g	35
<i>threo</i> -3-Phenyl-2-butyl	NaNO ₃	25	OTs	0.4 ^g	35
<i>threo</i> -3-Phenyl-2-butyl	NaI	25	OTs	2 ^g	35
<i>threo</i> -3-Phenyl-2-butyl	NaClO ₄	25	OTs	0.9 ^g	35
<i>threo</i> -3-Phenyl-2-butyl	2-C ₁₀ H ₇ SO ₃ Na	25	OTs	0.2 ^g	35
<i>threo</i> -3-Phenyl-2-butyl	Me ₄ NCl ⁱ	25	OTs	0.1 ^g	35
<i>threo</i> -3-Phenyl-2-butyl	(C ₆ H ₅) ₄ PCl ^j	25	OTs	−0.4 ^g	35
<u>30% Dioxane</u>					
2-Octyl	LiClO ₄	36	OMs	1.0	47
2-Octyl	NaNO ₃	36	OMs	0.7	47
2-Octyl	NaBr	36	OMs	0.7	47
<u>25% Dioxane</u>					
2-Octyl	LiClO ₄	36	OMs	1.2	47
<u>Ethanol</u>					
2-Phenylethyl	LiClO ₄	75	OTs	3.0	41
2- <i>p</i> -Anisylethyl	LiClO ₄	50	OTs	2.6	41
2- <i>p</i> -Anisylethyl	LiClO ₄	75	OTs	3.6	41
<u>80% Ethanol</u>					
2-Adamantyl	NaN ₃	75	OTs	3	46
1-Adamantyl	NaN ₃	75	Br	2	46
1-Phenyl-2-propyl	NaN ₃	100	OTs	2 ^h	48
1- <i>p</i> -Tolyl-2-propyl	NaN ₃	75	OTs	3 ^h	48
1- <i>p</i> -Anisyl-2-propyl	NaN ₃	50	OTs	−0.6 ^h	48
2-Phenyl-1-propyl	NaN ₃	100	OTs	2 ^h	48

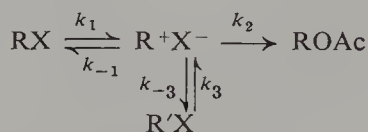
^g Polarimetric rates.^h Based on the phenonium ion pathway only (i.e., k_{Δ} was used in Eq. 5) [48].ⁱ Tetramethylammonium chloride.^j Tetraphenylphosphonium chloride.^k Tetramethylammonium nitrate.^l Tetraethylammonium perchlorate.

Table 12 Salt Effects on b derived from Polarimetric and Titrimetric Rate Constants for Acetolysis

Substrate	Salt	b	
		k_a	k_t
<i>threo</i> -3-Phenyl-2-butyl tosylate ^a	LiClO ₄	—	31
	LiClO ₄	—	37 ^b
	NaOAc	4 ^c	3 ^c
	NaOTs	1 ^c	0.1 ^c
<i>threo</i> -3- <i>p</i> -Anisyl-2-butyl brosylate	LiClO ₄	16	22
<i>threo</i> -3- <i>p</i> -Anisyl-2-butyl tosylate	LiClO ₄	17	28

^a Ref. 47; 75°.^b 50°.^c Determined from a single concentration of salt.

(i.e., for initial rate constants) the reaction will not be complicated by the solvolysis of R'X (i.e., $k_3[\text{R}'\text{X}]$ is small) and the analysis discussed for the



Scheme IV

3-anisyl-2-butyl arenesulfonates will apply to the rate constants for solvolysis and for ionization. In addition, the initial rates of solvolysis (Eq. 13) and rearrangement (Eq. 14) may be compared directly, since both rearrangement

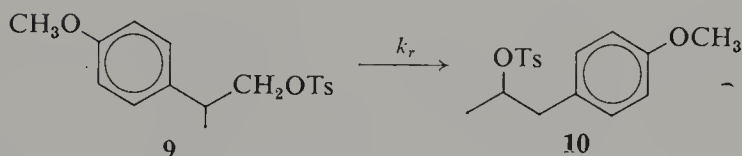
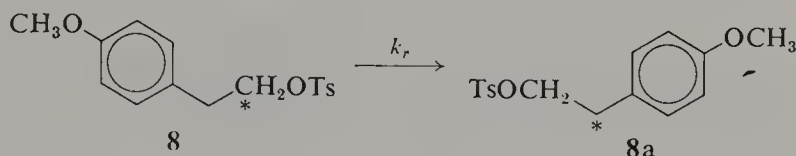
$$\frac{d[\text{HX}]}{dt} = k_t[\text{RX}] = k_2[\text{R}^+\text{X}^-] \quad (13)$$

$$\frac{d[\text{R}'\text{X}]}{dt} = k_r[\text{RX}] = k_{-3}[\text{R}^+\text{X}^-] \quad (14)$$

and solvolysis involve reaction of the same species (R^+X^-). Thus the difference in salt effects on solvolysis and rearrangement will reflect the differences in the individual salt effects on k_2 and k_{-3} only.

Two such systems were studied by Winstein and his co-workers [49, 50]: 2-*p*-anisylethyl tosylate (8) and 2-*p*-anisyl-1-propyl tosylate (9). In each case ion pair return can lead either to the original tosylate or to an isomeric tosylate (note the tosylates 8 and 8a are isomeric only by virtue of an isotopic label). For the acetolysis of each compound, lithium perchlorate salt effects were determined for the initial titrimetric rate constant k_t , for the ionization rate constant k_1 , and for the rate constant for rearrangement k_r . The b values for these salt effects are presented in Table 13.

Table 13 again shows that the salt effects on the rate constants for ionization are somewhat less than those on the rate constants for solvolysis. The salt effect on the rate constants for rearrangement are not only considerably smaller—they are *actually negative*. Thus the rate constants for rearrangement via ion pair return are decreased in the presence of lithium perchlorate. In terms of Eq. 13 and 14 this means that the salt effect on k_{-3} is much



smaller than the salt effect on k_2 , and it suggests that the former may well be negative* (as would be expected on the basis of effects of the polarity of the medium [6, 7]).

Although all of the discussion to this point has been concerned with salt effects on reactions proceeding via cationoid mechanisms, the effects of added salts on direct displacement reactions should be considered also. For an S_N2 reaction of either neutral substrate or intimate ion pair the displacement step by solvent would result in the generation of increased charge

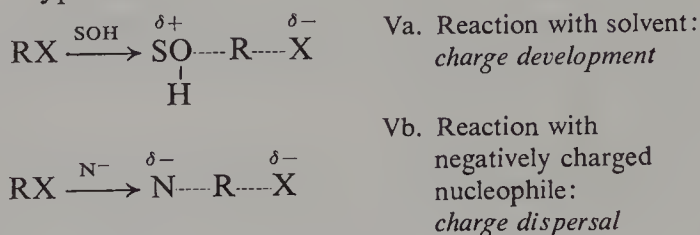
Table 13 Lithium Perchlorate Salt Effects on the Rate Constants for Ionization, Solvolysis, and Rearrangement of β -Arylalkyl Tosylates in Acetic Acid

Substrate	<i>b</i> Values		
	k_1	k_t	k_r
1- ¹⁴ C-2- <i>p</i> -Anisylethyl tosylate (8) ^a	11	12	-5
2- <i>p</i> -Anisyl-1-propyl tosylate (9) ^b	12	23	-8

^a Data for ref. 49, 75°.

^b Data for ref. 50; 50°.

* Alternatively, it is possible that a very large salt effect for the dissociation of R^+X^- (i.e., on k_2) is responsible for the decrease in k_r . In other words, a large increase in k_2 in the presence of added lithium perchlorate could cause a decrease in the steady state concentration of R^+X^- with a consequent decrease in the observed rate constant for rearrangement.



The effect of added salts on direct displacement reactions by solvent, however, is complicated by the fact that the anions of most salts can also behave as nucleophiles. In contrast to the solvolysis reaction, the S_N2 reaction with a negatively charged nucleophile (Scheme Vb) would result in charge dispersal, and the rate should be decreased by an increase in solvent polarity [6, 33]. Such S_N2 reactions of alkyl halides and arenesulfonates would be expected to show a negative salt effect. This negative salt effect would not be detected easily, however, since there is an opposing rate-enhancing effect caused by an increase in the concentration of the nucleophile N^- .

For a substrate RX disposed to reaction by direct displacement reactions, the addition of nucleophile N^- to a solvolysis medium could result in both processes of Scheme V occurring simultaneously. In the absence of salt effects, the observed titrimetric rate constant k_{obs} would be the sum of the pseudo-first-order rate constants for solvolysis (k_s , Scheme Va) and for attack by nucleophile ($k_N[N^-]$, Scheme Vb) as given by Eq. 15:

Taking into account the salt effects just discussed, the observed rate constant would be given by Eq. 16:

$$k_{\text{obs}} = k_s^0(1 + b_s[\text{N}^-]) + k_N[\text{N}^-](1 + b_N[\text{N}^-]) \quad (16)$$

where k_s^0 denotes the rate constant in the absence of salts, and the expected magnitudes of the salt effects on the displacements by solvent b_s and by added nucleophile b_N are given by Eq. 17:

$$b_N \leq 0 \leq b_s \quad (17)$$

Clearly, in the presence of these opposing effects, it is difficult to predict *a priori* the influence of added salts on direct displacement reactions.*

* Attempts to use the effects of added salts of differing nucleophilic character to gain information on the mechanism of solvolysis reactions is discussed later in Section 5.

Therefore, the presence or absence of a change in the titrimetric rate constant for a solvolysis reaction resulting from the addition of a salt to the medium does not appear to provide sufficient information for the assignment of a mechanism.

2.4. Special Salt Effects

In 1954 Winstein, Clippinger, Fainberg, and Robinson [18] reported that several alkyl arenesulfonates exhibit highly unusual salt effects. When these compounds were solvolyzed in acetic acid in the presence of varying amounts of lithium perchlorate, the titrimetric rate constants were greatly increased by very small concentrations of added salt. Further increases in salt concentration, however, resulted only in the more modest rate enhancements associated with normal salt effects. Thus the lithium perchlorate salt effect on the acetolysis of 3-anisyl-2-butyl brosylate (Fig. 2) was described [18] as a two-stage effect with a large initial increase in the solvolytic rate constant followed (at higher concentrations of added salt) by the more typical salt effect described by Eq. 5. Such a large initial rate increase was designated [41] a special salt effect.

Since the compounds which exhibit the special salt effect also show normal salt effects, the linear portion of a plot (cf. Fig. 2) of the titrimetric rate constant versus salt concentration can be treated in terms of Eq. 5a [18]:

$$k_t = k_{\text{ext}}^0(1 + b[\text{salt}]) \quad (5a)$$

In addition, the special salt effect can be described by k_{ext}^0/k_t^0 and $[\text{salt}]_{1/2}$, where k_t^0 is the actual titrimetric rate constant in the absence of added salt, k_{ext}^0 is the extrapolated value of the linear portion of the curve to zero salt concentration, and $[\text{salt}]_{1/2}$ is the concentration of salt which corresponds to a titrimetric rate constant halfway between k_t^0 and k_{ext}^0 (see Fig. 2). Consequently the salt effects (of noncommon ion salts) on the titrimetric rate constants for all solvolysis reactions* can be described by three parameters: b , k_t^0/k_{ext}^0 , and $[\text{salt}]_{1/2}$.

Subsequent papers by Winstein, Clippinger, Fainberg, and Robinson [22, 41–43, 50] reported the observation of the special salt effect for a number of other systems, and the appropriate data are presented in Tables 14 and 15. Several of the compounds in Tables 14 and 15 had previously been shown [15, 16, 20] to undergo ion pair return during acetolysis. On the other hand, *p*-methoxyneophyl tosylate (which solvolyzes without ion pair return [34])

* For those systems that do not show a special salt effect k_{ext}^0/k_t^0 is equal to unity, $[\text{salt}]_{1/2}$ becomes meaningless, and Eq. 5a is equivalent to Eq. 5.

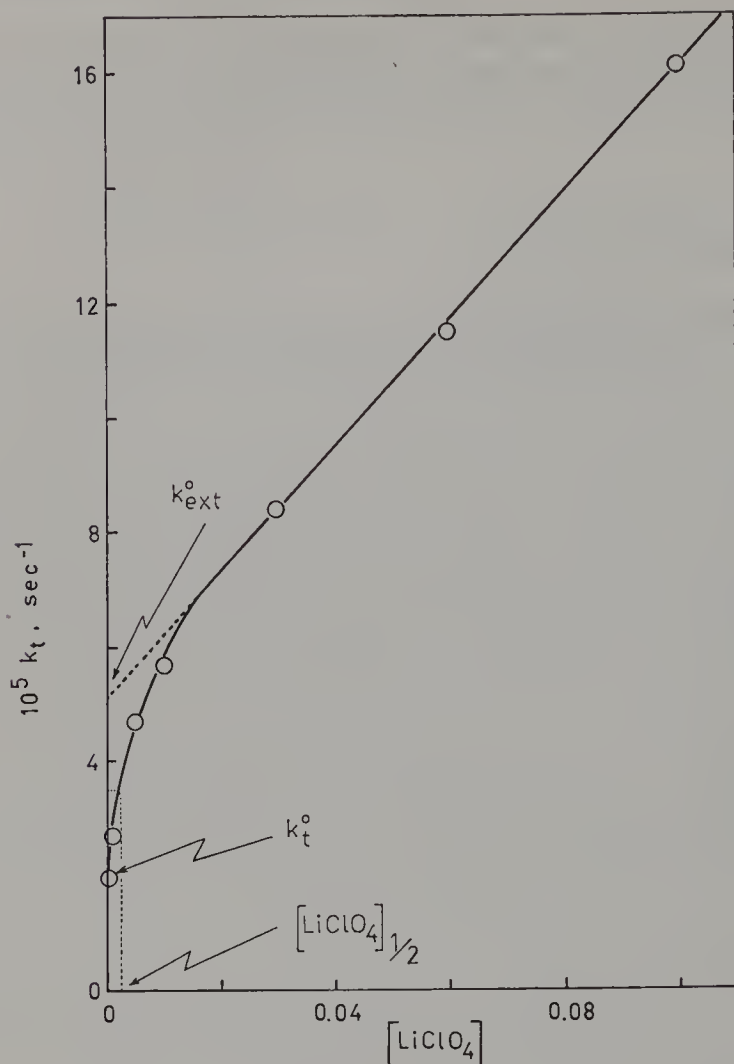


Figure 2. An example of the special salt effect: The acetolysis of *threo*-3-*p*-anisyl-2-butyl brosylate in the presence of added lithium perchlorate [22].

was found [18] not to show a special salt effect, despite its similarity to 3-anisyl-2-butyl brosylate. These observations led Winstein and his co-workers to suggest [18] that the rate increase of the special salt effect resulted from a decrease in ion pair return in the presence of the added salt. Thus for a system which did not undergo ion pair return, no special salt effect would be anticipated.

Yet ion pair return was shown not to be a sufficient criterion for the special salt effect, since only normal salt effects were observed for 2-*exo*-norbornyl brosylate and 3-phenyl-2-butyl tosylate [18]. Furthermore, just as the addition of lithium perchlorate did not remove the ion pair return associated with the acetolysis of norbornyl brosylate or 3-phenyl-2-butyl brosylate, neither did

Table 14 Lithium Perchlorate Salt Effects for the Acetolysis of Compounds Which Show the Special Salt Effect

Compound	Temperature (°C)	k_{ext}^0/k_t^0	$[\text{LiClO}_4]_{1/2}$	<i>b</i>	Ref.
<i>threo</i> -3- <i>p</i> -Anisyl-2-butyl OBs ^a	25	2.6 ^a	2.3×10^{-3}	22	18, 22
<i>erythro</i> -3- <i>p</i> -Anisyl-2-butyl OBs	25	3.1	4×10^{-3}	18	18, 42
2- <i>p</i> -Anisyl-1-propyl OTs	50	2.5	4×10^{-5}	24	18, 50
2-(2,4-Dimethoxyphenyl)-ethyl OBs	50	2.2	8×10^{-5}	12	18, 43
2- <i>o</i> -Anisylethyl OTs	50	3.2	2×10^{-4}	13	41
2- <i>o</i> -Anisylethyl OTs	75	2.9	2×10^{-4}	11	41
2- <i>p</i> -Anisylethyl OTs	50	3.3	3.4×10^{-4}	11	41
2- <i>p</i> -Anisylethyl OTs	75	2.9	3.4×10^{-4}	12	41
<i>trans</i> -2- <i>p</i> -Anisylcyclopentyl OBs	25	2.1	5×10^{-3}	27	42
<i>trans</i> -2- <i>p</i> -Anisylcyclopentyl OBs	50	1.9	4×10^{-3}	23	42
<i>trans</i> -2- <i>p</i> -Anisylcyclohexyl OBs	50	1.7	3×10^{-3}	29	42
<i>trans</i> -2- <i>p</i> -Anisylcyclohexyl OBs	75	1.5	3×10^{-3}	26	42
1- <i>p</i> -Anisyl-2-propyl OTs	50	2.4	3×10^{-3}	27	42
1- <i>p</i> -Anisyl-2-propyl OTs	75	2.1	3×10^{-3}	26	42
Cholesteryl OTs	50	2.3	4×10^{-5}	28	18, 43
Cholesteryl OBs	50	2.1	6×10^{-5}	30	18, 43
<i>threo</i> -3- <i>p</i> -Anisyl-2-butyl OTs	25	2.9	—	28	22
<i>cis</i> -3-Bicyclo[3.1.0.]hexyl OTs	50	3.2	4×10^{-3}	23	52
<i>trans</i> -3-Bicyclo[3.1.0.]hexyl OTs	75	1.4 ± 0.2	—	18	52
Trichloromethylpentamethylbenzene ^b	25	38	4×10^{-3}	22	53

^a Values for k_{ext}^0/k_t^0 of 1.6 and 1.5 were found for 50% acetic-acetic anhydride and acetic anhydride, respectively [51].

^b 85% aqueous dioxane; LiNO_3 .

it completely eliminate ion pair return for *threo*-3-*p*-anisyl-2-butyl brosylate. If ion pair return were completely eliminated by the special salt effect, extrapolation of the linear portion of the plot in Fig. 2 would have given a value of k_{ext}^0 equal to the rate constant for ionization. However, the latter had been determined polarimetrically [26] and was found to be greater than k_{ext}^0 by about a factor of 2.

Although intimate and solvent-separated ion pairs were discussed earlier in connection with the process of anion exchange, it was the two-stage character of the special salt effect that led Winstein and his co-workers [18] to postulate the intermediacy of two different kinds of ion pair. Since the special salt effect only eliminated a certain portion of ion pair return (i.e., the special salt effect was operative only at low salt concentrations; at higher concentrations just the normal salt effect was observed), the data suggested that return from two different intermediates was involved. Yet the experiments on common ion rate depression indicated that return from dissociated carbonium

Table 15 Effects of Various Salts on the Acetolysis of Compounds Which Show the Special Salt Effect^a

Compound	Salt	k_{ext}^0/k_t^0	$[\text{Salt}]_{1/2}$	b
2- <i>p</i> -Anisylethyl OTs ^b	LiClO ₄	2.9	3.4×10^{-4}	10
2- <i>p</i> -Anisylethyl OTs ^b	KOAc	2.5 ± 0.4	—	2 ± 2
Cholesteryl OTs	LiClO ₄	2.3	4×10^{-5}	28
Cholesteryl OTs	HClO ₄	2.4	6×10^{-5}	28
Cholesteryl OTs	DPGHClO ₄ ^c	2.3	4×10^{-4}	12
Cholesteryl OTs	DPGHOAc ^d	2.3	$<2 \times 10^{-3}$	6
Cholesteryl OTs	LiOAc	2.3	$<2 \times 10^{-3}$	2
2-(2,4-Dimethoxyphenyl)-ethyl OBs	LiClO ₄	2.1	6×10^{-5}	30
2-(2,4-Dimethoxyphenyl)-ethyl OBs	DPGHOAc ^d	2.2	8×10^{-5}	12
2-(2,4-Dimethoxyphenyl)-ethyl OBs	LiOAc	2.3	3×10^{-3}	2
1- <i>p</i> -Anisyl-2-propyl OTs ^e	Bu ₄ NBr ^f	1.52 ^g	—	—
1- <i>p</i> -Anisyl-2-propyl OTs ^e	LiBr	1.52 ^g	—	—
1- <i>p</i> -Anisyl-2-propyl OTs ^e	LiClO ₄	1.49	—	—
3- <i>p</i> -Anisyl-2-butyl OBs ^h	LiBr	2.56 ^g	—	—
3- <i>p</i> -Anisyl-2-butyl OBs ^h	LiClO ₄	2.58	—	—

^a Ref. 43; 50°.^b Ref. 41; 75°.^c Diphenylguanidinium perchlorate.^d Diphenylguanidinium acetate.^e Ref. 54; 50°.^f Tetra-*n*-butylammonium bromide.^g From the extrapolated rate constant for bromide exchange.^h Ref. 54; 25°.

ions did not occur for substrates such as *threo*-3-*p*-anisyl-2-butyl brosylate [13]. Clearly if return from two different intermediates were involved in the acetolysis of the latter compound, it was highly likely that both intermediates were involved in the acetolysis of the latter compound, it was highly likely that both intermediates were ion pairs.

Strong supporting evidence for the interpretation that the special salt effect is a consequence of preventing a certain proportion of ion pair return is available from studies of salt effects on rate constants for ionization [22, 50]. Even in systems in which the titrimetric rate constants show a special salt effect, the *rate constants for ionization show only the normal salt effect*. Figure 3 illustrates this behavior for the acetolysis of 2-*p*-anisyl-1-propyl tosylate [50].

Although the special salt effect substantially decreases the gap between k_t and k_1 , the latter continues to be greater. Winstein and his co-workers [18]

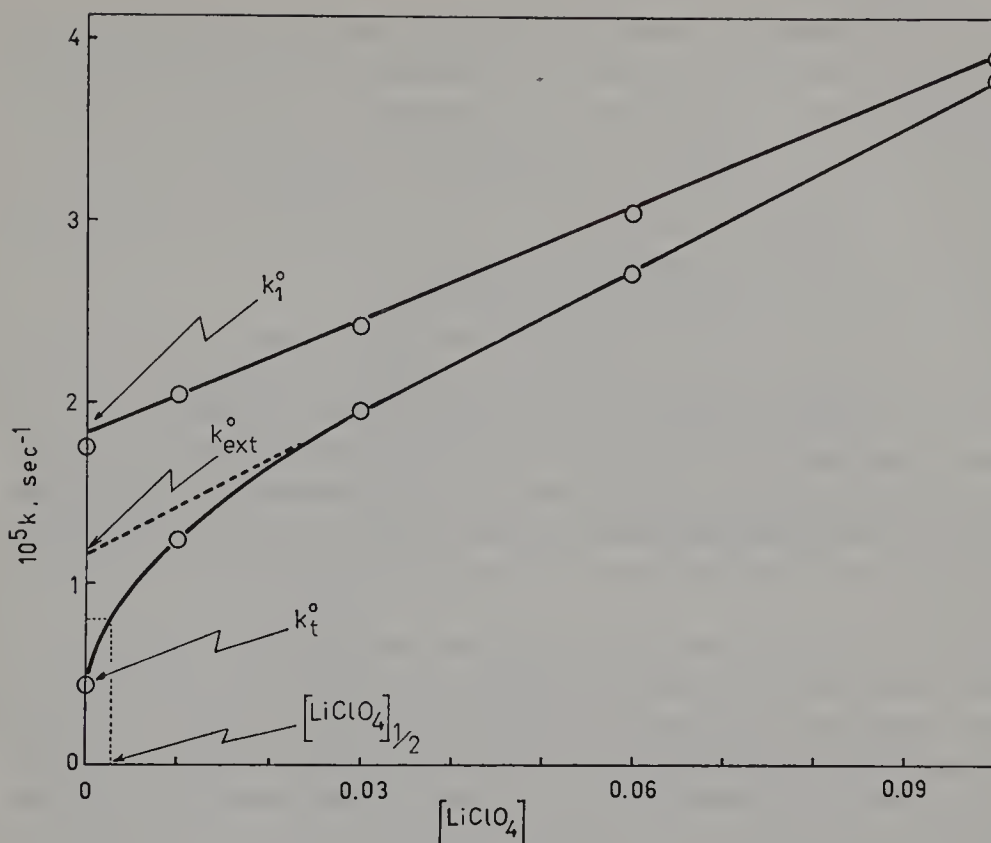


Figure 3. Salt effects of lithium perchlorate in the acetolysis of 2-*p*-anisyl-1-propyl tosylate [9]. The rate constants are those for reaction of the primary derivative only, and have been corrected for contributions from the rearranged secondary isomer 10 (see ref. 50).

interpreted this behavior in the following way: The special salt effect is a consequence of interference with return from solvent-separated ion pairs. Thus for substrates that undergo only internal return (return from intimate ion pairs) only normal salt effects are observed. However, for substrates that undergo both internal return and external ion pair return (return from both intimate and solvent-separated ion pairs) added salts interfere with external ion pair return, with a consequent increase in the titrimetric rate constant (but with no influence on the ionization rate constant other than the normal salt effect). Above a certain concentration of added salt, the prevention of return from solvent-separated ion pairs is essentially complete and only the normal salt effect is observed.

In terms of Fig. 3, the linear portion of the curve for k_t then represents the rate constant for solvolysis in the absence of external return. The upper line (k_1) gives the rate constant for ionization (to an intimate ion pair), the lower line (k_{ext}) gives the rate constant for formation of solvent-separated ion pairs, and the experimental curve (k_t) gives the rate of formation of

product. The special salt effect results in the equality of the latter two rate constants (i.e., all solvent-separated ion pairs give rise to product). On this basis the intercept k_{ext}^0 should give the rate constant for formation of solvent-separated ion pairs in the absence of added salt. If the foregoing analysis of the special salt effect is correct, then the value of k_{ext}^0 should be independent of the nature of the salt. Inspection of Table 15 reveals this to be the case: although the parameters b and $[\text{salt}]_{1/2}$ vary considerably as the salt is changed, the values of k_{ext}^0/k_t^0 remain essentially constant.

Relatively little information is available which can serve to differentiate between intimate and solvent-separated ion pairs. However, in the earlier discussion on anion exchange it was argued that such exchange could take place at either the solvent-separated ion pair or the free carbonium ion stage but not at the stage of an intimate ion pair. If this argument is correct, then a correlation should exist between anion exchange and the special salt effect. Table 16 demonstrates that there is an exact correspondence between the two phenomena.

Winstein and his co-workers initially postulated [17] that elimination of external return was associated with the special salt effect and that salts such as lithium perchlorate acted as relatively efficient traps for the solvent-separated ion pair. The close correspondence between exchange and the special salt effect eventually permitted them to suggest a more detailed mechanism. Winstein, Klinedienst, and Robinson [36] proposed that the special salt

Table 16 Correspondence of the Special Salt Effect and Anion Exchange in Acetolysis^a

Compound	Exchange	Special Salt Effect ^b
2- <i>exo</i> -Norbornyl OBs	No	No
<i>threo</i> -3- <i>p</i> -Anisyl-2-butyl OBs	Yes	Yes ^c
Cholesteryl OTs	Yes	Yes
Cholesteryl OBs	Yes ^d	Yes
2-(2,4-Dimethoxyphenyl)-ethyl OBs	Yes	Yes
<i>p</i> -Chlorobenzhydryl chloride ^e	Yes ^e	<i>e, f</i>
1- <i>p</i> -Anisyl-2-propyl OTs	Yes ^g	Yes ^h

^a Data from ref. 43.

^b Lithium perchlorate.

^c Ref. 22.

^d Ref. 13.

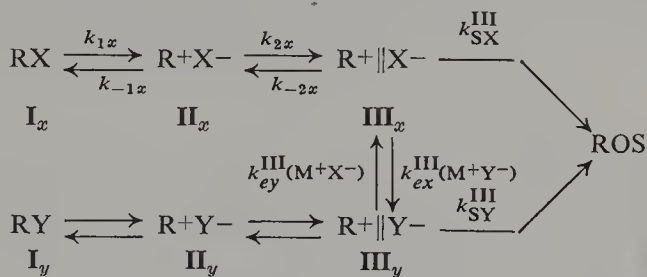
^e Ref. 45; 80% acetone.

^f Only two concentrations of added salt were studied; nevertheless, extrapolation gives a ratio of 1.06 for k_{ext}^0/k_t^0 .

^g Ref. 54.

^h Ref. 50.

effect was a consequence of an exchange process taking place at the solvent-separated ion pair stage as illustrated in Scheme VI.

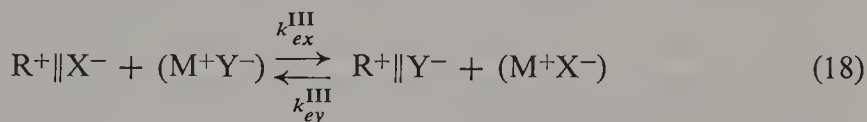


Scheme VI. A possible mechanism for the special salt effect [54].

Scheme VI is a modified version of Scheme II, which takes into account the possibility of anion exchange at the stage of the solvent-separated ion pair **III**. The dissociated carbonium ions (**IV**) have been omitted for simplicity, and appropriate subscripts indicate the identity of the gegenion for each of the intermediates and rate constants.

A key piece of evidence which supports this interpretation of the special salt effect is provided by the effects of various salts. Although a variety of salts can produce the special salt effect (cf. Table 15), "the common ion salt is able to exercise a normal salt effect on ionization rate, but is peculiarly incapable of exercising a special salt effect" [22]. This observation (which is illustrated in Fig. 4 for 1-*p*-anisyl-2-propyl tosylate) provides a compelling argument for a mechanism of the special salt effect which involves a specific interaction between a solvolytically generated ion pair (e.g., **III**_x) and the ions (or ion pairs) of the added salt MY. The correspondence between the special salt effect and the phenomenon of anion exchange (Table 16) combined with the failure of common ion salts to produce a special salt effect is most simply explained by an exchange process like that illustrated in Scheme VI.

According to Scheme VI the specific reaction that results in the special salt effect is the exchange reaction summarized by Eq. 18:



If the exchange mechanism for the special salt effect (Scheme VI) is correct, then the equilibrium reaction of Eq. 18 should be dependent on the concentration of MY (i.e., the equilibrium should be subject to a common ion effect). Thus even for a compound which ordinarily shows no common ion effect, the addition of a noncommon salt is expected to inhibit the special salt effect by "preventing" the overall exchange reaction of Eq. 18. Winstein, Klinedienst, and Robinson [36] studied the influence of common ion salts in the presence of noncommon ion salts and found that the common salt did in fact

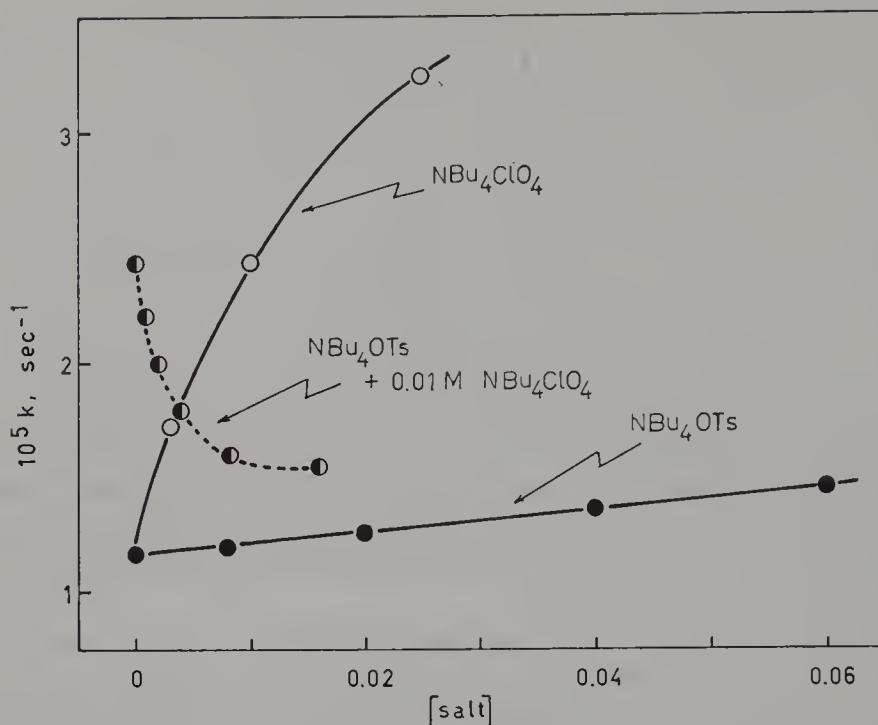


Figure 4. Special salt effect and induced common ion rate depression in the acetolysis of 1-*p*-anisyl-2-propyl tosylate. The open circles show the special salt effect produced by tetra-*n*-butylammonium perchlorate, and the filled circles show the influence of tetra-*n*-butylammonium tosylate which produces normal salt effects only. The half-filled circles show the inhibition of the special salt effect when the acetolysis is conducted in the presence of 0.01 *M* tetra-*n*-butylammonium perchlorate with varying concentrations of tetra-*n*-butylammonium tosylate. (Data from Ref. 36.)

decrease the magnitude of the special salt effect. Such inhibition of the special salt effect was classified as induced common ion rate depression [36], and these authors commented that "the phenomenon of induced common ion rate depression has been observed in these laboratories in the acetolysis of every system which displays the special salt effect" [36]. The phenomenon of induced common ion rate depression (illustrated in Fig. 4 for 1-*p*-anisyl-2-propyl tosylate) provides additional strong evidence for the exchange mechanism of the special salt effect.

Further work by Winstein, Klinedienst, and Clippinger [54] demonstrated that the correspondence between anion exchange and the special salt effect was not merely a coincidence. They studied the exchange reactions of 1-*p*-anisyl-2-propyl tosylate and 3-*p*-anisyl-2-butyl brosylate with bromide salts; for these reactions ion pair return from $R^+ \parallel Y^-$ yields a stable product RY ($Y = Br$). When the pseudo-first-order rate constants (k_{RBr}) for exchange were extrapolated to zero bromide concentrations, the values of k_{RBr}^0 were found to be identical with k_{ext}^0 obtained with lithium perchlorate (see Table

15). Thus both the special salt effect and anion exchange appear to provide a measure of the rate constant for formation of solvent-separated ion pairs, and all of the available data support the exchange process shown in Scheme VI as the mechanism of the special salt effect.

3. EQUILIBRATION OF LABELED OXYGEN IN *p*-NITROBENZOATE AND *p*-TOLUENESULFONATE ESTERS

The determination of the extent and rate of ^{18}O scrambling in *p*-nitrobenzoate and *p*-toluenesulfonate esters is probably the single most powerful tool for the detection of ion pairs in solvolysis reactions. The study of rates of racemization requires systems which rearrange to give enantiomeric or symmetrical cations [55]; in contrast to substrates exhibiting the special salt effect, ^{18}O scrambling can be utilized for the study of species which give internal return only (e.g., simple alkyl derivatives) [56].

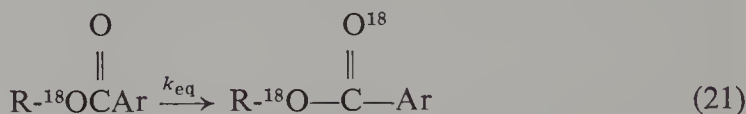
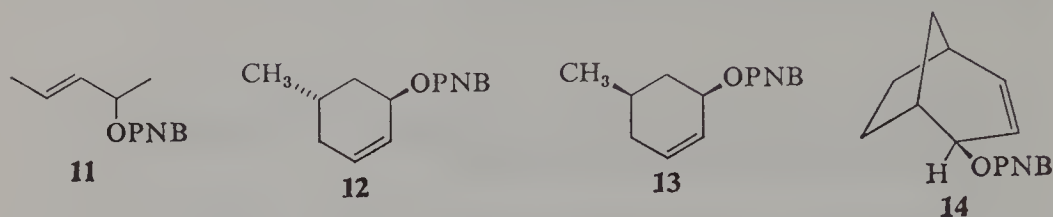
Most of the ^{18}O -scrambling work has utilized *p*-nitrobenzoate esters, and the use of this relatively unreactive leaving group introduces the possibility of acyl-oxygen instead of the desired alkyl-oxygen cleavage. Goering and Silversmith [57] have shown that acyl-oxygen cleavage in aqueous solvents is not important for esters which are significantly more reactive than 2-pentyl *p*-nitrobenzoate. This secondary ester is hardly affected by 10-week exposure to 90% aqueous acetone at 100°. However, if powerful nucleophiles such as azide ion are present, acyl-oxygen cleavage can become important even for such reactive compounds as allylic esters [58]. This problem can essentially be eliminated by the use of tosylates instead of *p*-nitrobenzoates.

Denney and Denney [59] pioneered the use of the ^{18}O scrambling technique for solvolysis reactions. Goering and his co-workers subsequently utilized this tool extensively, and the following discussion is largely an account of these investigations.

3.1. Allylic Systems

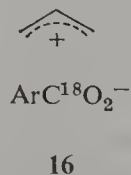
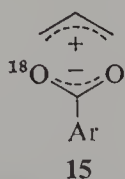
Particular attention has been focused on ^{18}O equilibration in allylic systems since rearrangements or racemization in symmetrical cases affords an independent means of studying ion pair return. Consequently, Goering and his associates examined compounds **11** [60], **12** [61], **13** [62], and **14** [55a], all of which can give symmetrical ion pairs. For all four systems, racemization, k_{α} (Eq. 19), was found to be greater than k_t (Eq. 22). By demonstrating that external return is not involved, the excess racemization was shown to be the result of internal return (Eq. 20). For **11** (in 60 and 90% acetone) [60]

and **13** (in 80% acetone), k_{eq} (Eq. 21) was found to equal k_{rac} ($k_{rac} = k_{\alpha} - k_t$). Thus it appears that internal return in allylic systems results in racemization and complete oxygen equilibration; otherwise one would have

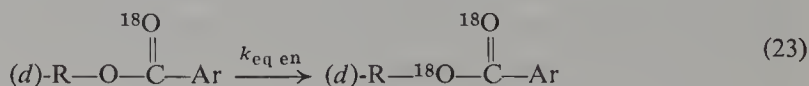


to postulate fortuitous agreement between k_{rac} and k_{eq} for two substrates in three solvents.

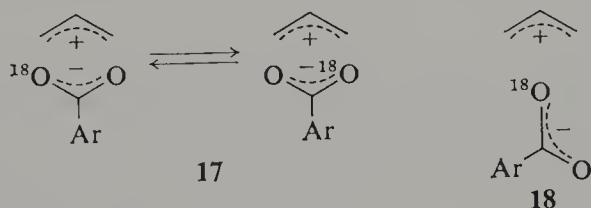
However, this conclusion does not establish whether return without rearrangement results in equilibration of oxygens. In other words, although the data demand a symmetrical ion pair, either **15**- or **16**-type species could be involved. For example, if the solvolysis of either labeled **11** or **13** proceeded through **15**, return to the carbon to which the leaving group was attached would give all ether ^{18}O , while return to the other carbon would give all carbonyl ^{18}O . The end result, if carbons were not distinguished, would be complete equilibration. On the other hand, ion pair **16** would give complete ^{18}O equilibration at both carbons. It is possible to distinguish between **15** and **16**



by partial solvolysis of optically active ester followed by recovery and resolution of unsolvolyzed ester. This procedure allows the following distinction to be made between the two oxygens and between the two carbons:



It is also necessary to consider the two equivalent ion pairs **17** as possibilities. If the barrier is low enough for interconversion to compete with internal return, partial equilibration of oxygens will be observed in each enantiomer. Complete equilibration would be the eventual result, but it would occur at a rate slower than racemization. An ion pair such as **18**, in which there is no oxygen scrambling, is, of course, ruled out in these cases.



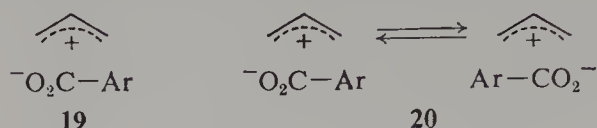
The process of oxygen equilibration within an enantiomer (Eq. 23) is designated $k_{\text{eq en}}$. Goering used the term k_s for this process; however, we prefer to reserve k_s to indicate nucleophilic assistance by solvent [63].

Goering and his co-workers determined the ^{18}O distributions of both recovered enantiomers for **11** [60] and **13** [62]. For **13**, $k_{\text{eq en}} = k_{\text{eq}} = k_{\text{rac}}$. Therefore the ion pair involved in the solvolysis of this compound is **16**. However, k_{eq} and k_{rac} for **11** were found to be 2.9 times larger than $k_{\text{eq en}}$; **15** must be involved. Appreciable equilibration of oxygens for each enantiomer shows that the actual process involved is represented by **17** and that the barrier to interconversion is slightly greater than that for $k_{\text{internal return}}$.

Compound **11** was studied in both 60 [60b] and 90% [60a] acetone; first to determine k_{eq} , k_{rac} , and $k_{\text{eq en}}$ and to measure internal return from polar intermediates, second to compare effects of solvent polarity on tightness of the ion pair as measured by $k_{\text{eq en}}/k_{\text{rac}}$, and third to see if the two independent methods of studying ion pair return (k_{rac} and k_{eq}) would show agreement in two solvents. All four rate constants, k_{rac} , k_{eq} , $k_{\text{eq en}}$, and k_t were found to increase with increase in solvent polarity, strongly implying that all the processes involved are the result of ionization and that the agreement between k_{rac} and k_{eq} in 90% acetone [60a] was not fortuitous. The ratio k_{rac}/k_t decreased from 4.4 in 90% acetone to 1.2 in the more polar 60% acetone, thus confirming that dissociation becomes more important as the ionizing power of the solvent increases [19]. Interestingly the ratio of $k_{\text{eq en}}/k_{\text{rac}}$ increases from 0.34 in 90% acetone to 0.42 in 60% acetone. This result is consistent with a decrease in the tightness of the ion pair in the more polar solvent and a consequent lowering of the barrier to interconversion (**17**).

The rates of equilibration and racemization have also been determined for **12** [61] and **14** [55a]. Somewhat surprisingly, $k_{\text{eq}} > k_{\text{rac}}$ for both compounds [55a]. Since each can give a symmetrical cation, anion positions must maintain the asymmetry of the starting ester. The simplest possibility for

such an ion pair is **19**. Racemization in these cases must involve either process **20** or another symmetric ion pair (either **15** or **16**). The possibility that two ion pairs (**19** and its enantiomer) are involved is indeed intriguing



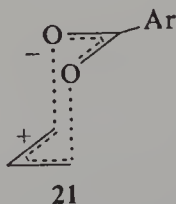
since evidence based on other techniques has led to similar conclusions [64–66]. These results emphasize the need for consideration of the anion when discussing solvolysis reactions; although some cations have the potential to be symmetric, structures of lower symmetry may be more stable.

Three types of ion pairs in allylic systems have now been discussed, **15** from **11**, **16** from **13**, and **19** from **12** and **14**, but the factors which determine the relative stabilities of these different types are not readily apparent (Table 17).

Table 17 Racemization and ^{18}O -Label Scrambling in Allylic *p*-Nitrobenzoates at 100° in Aqueous Acetone [**55a**, **60–62**]

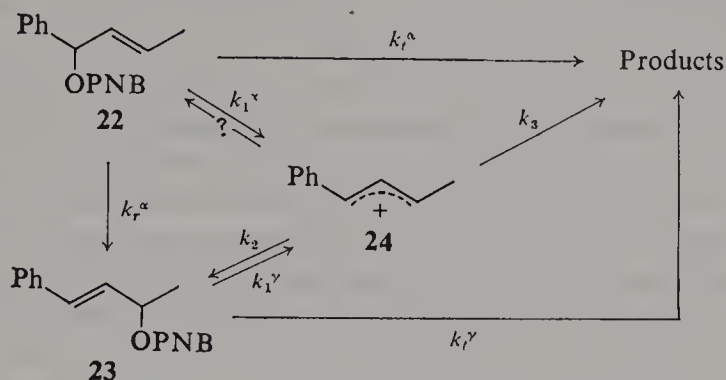
Compound (Solvent)	k_a/k_t	$k_{\text{eq}}/k_{\text{rac}}$	$k_{\text{rac}}/k_{\text{eq en}}$
11 (90 % Acetone)	5.4	1.0	2.9
12 (80 % Acetone)	1.5	1.7	—
13 (80 % Acetone)	1.8	1.0	1.0
14	>1	>1	—

Goering, Doi, and McMichael [62] suggest that solvolysis of an allylic *p*-nitrobenzoate will proceed through **21** (a chairlike, [67] three-dimensional representation of **15**) if this arrangement does not involve unfavorable steric interactions. Therefore acyclic **11** will give **21** but the cyclohexenyl and bicyclic derivatives, **12–14**, will not. However, this reasoning does not explain why *cis*- and *trans*-5-methyl-2-cyclohexenyl derivatives (**13** and **12**) behave differently from each other.



Goering and Linsay [68] have also compared the oxygen equilibration and rate of racemization methods with a third independent measure of the extent of ion pair return devised by Sneen and Rosenberg [58] (Scheme VII). These

workers observed that **22** is approximately 300 times more reactive than **23** in aqueous dioxane; thus when **22** is solvolized, return from **24** results in **23**,



Scheme VII

stable under the reaction conditions. The amount of return is measured simply by the difference between theoretical and experimental infinity titers (formation of **23** produces no acid) using Eq. 24. A comparison of $k_{eq}^{\gamma}/k_t^{\gamma}$ for ^{18}O -labeled **23** with $k_r^{\alpha}/k_t^{\alpha}$ for **22** provides a test of the amount of equili-

$$\frac{\text{23}}{[\text{Alcohol products}]} = \frac{k_r^{\alpha}}{k_t^{\alpha}} = \frac{k_2}{k_3} \quad (24)$$

bration resulting from return.

The requisite experiments were performed in 70, 80, and 90% acetone. The results are presented in Table 18; in addition to $k_{eq}^{\gamma}/k_t^{\gamma}$ and $k_r^{\alpha}/k_t^{\alpha}$, the percent rearrangement of **22** to **23** is also given. As can be seen from the ratio of $k_{eq}^{\gamma}/k_t^{\gamma}$ to $k_r^{\alpha}/k_t^{\alpha}$, oxygen equilibration does not measure all internal return. This result indicates that the oxygen equilibration method is a very good but not an absolute measure of the amount of internal return.

Of all the cases discussed in this section, the oxygen scrambling method is known to fail only for the solvolyses of **22** and **23**, and even there it measures

Table 18 Oxygen-18 Equilibration to Solvolysis Ratio ($k_{eq}^{\gamma}/k_t^{\gamma}$) and k_{rac}/k_{eq} for **23**, Rearrangement to Solvolysis Ratio ($k_r^{\alpha}/k_t^{\alpha}$) for **22**, and ^{18}O Equilibration for the **22** to **23** Rearrangement [68]

Solvent (% Acetone)	Temp- erature (°C)	$k_{eq}^{\gamma}/k_t^{\gamma}$	$k_r^{\alpha}/k_t^{\alpha}$	k_{rac}/k_{eq}	$\frac{100(k_{eq}^{\gamma}/k_t^{\gamma})}{(k_r^{\alpha}/k_t^{\alpha})}$	^{18}O Equilibration % for 22 to 23
90	99.41	2.10 ± 0.12	2.50 ± 0.05	0.65 ± 0.04	84 ± 7	90
80	78.47	1.03 ± 0.03	1.10 ± 0.05	0.49 ± 0.05	94 ± 6	97
70	49.04	0.66 ± 0.02	0.73 ± 0.01	0.16 ± 0.07	90 ± 5	100

approximately 90% of all return. However, for cases in which $k_{\text{eq}} > k_{\text{rac}}$ (such as the solvolysis of **12** and **14**) it is not possible on the basis of the available data to decide whether oxygen scrambling is an absolute measure of all of the return.

Goering, Koerner, and Linsay [69] also studied the behavior of optically active **22** and **23**. Since these substrates are not symmetrical, racemization can occur only by attack of the anion on the enantiomeric face of cation **24**. In 90% acetone, 65% loss of optical configuration was observed from either **22** or **23**. In the cyclic systems **12** and **13** geometrical purity was preserved during solvolysis (i.e., **12** and **13** did not interconvert), evidently due to conformational factors [67], but this was not the case with **14** and its *endo*-isomer [55a].

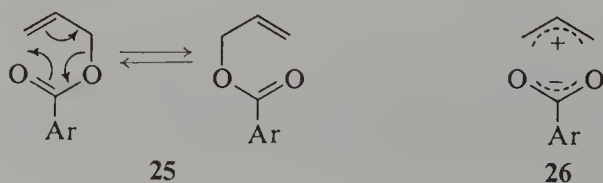
The decrease in $k_{\text{eq}}^{\gamma}/k_t^{\gamma}$ (Table 18) with increasing solvent water content is indicative of increasing dissociation with increasing solvent ionizing power. The corresponding decrease in $k_{\text{rac}}/k_{\text{eq}}$ is interpreted as evidence for the operation of two ion pairs with different degrees of "capturability" in the solvolysis of **23** [67]. If ionization gave only one ion pair, an increase in dissociation should have approximately equal effects on racemization and on oxygen equilibration. If two ion pairs were involved, an increase in dissociation would preferably remove the more dissociated of the two, which in all likelihood returns with greater racemization.

3.2. Nonrearranging Systems

The results obtained with allylic compounds show that internal return in these relatively reactive esters is accompanied by substantial scrambling of ester oxygens, even when return is to the carbon to which the ester function was originally attached. It is reasonable to expect that substrates which are more reactive than allylic esters involve longer lived intermediates and give complete scrambling of oxygens upon return. In addition, concerted rearrangements of the type shown in **25**, or structures such as **26**, cannot occur in nonrearranging systems. Thus for such nonrearranging, reactive systems, Eq. 25 should give a very good estimate of the rate of ionization:

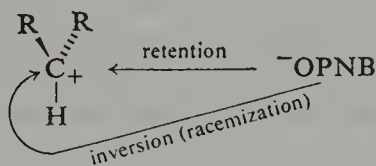
$$k_{\text{ionization}} = k_{\text{eq}} + k_t \quad (25)$$

There is a possibility of course that all internal return will not be measured even if equilibration is complete (see above). Nevertheless, Eq. 25 provides in



practice an excellent measure of the rate of ionization for the systems in question.

Winstein and his associates have studied extensively the rates of racemization and radioactive chloride exchange in *p*-chlorobenzhydryl chloride [19]. Since the rate of racemization, when corrected for external return (by means of radio chloride exchange), is greater than the rate of solvolysis, internal return is implicated. These results, accompanied by the expectation that oxygen equilibration would be complete upon return in these systems, led Goering and his group to determine the rate of oxygen equilibration for benzhydryl [70] and *p*-chlorobenzhydryl [72] *p*-nitrobenzoates. A technique other than racemization rates is needed for these compounds since k_{rac} cannot detect return occurring with retention of configuration. In substrates such as benzhydryl, return without racemization should be a favored process since the counterion must migrate to the opposite face of the cation in order to give the enantiomer (27) [17].



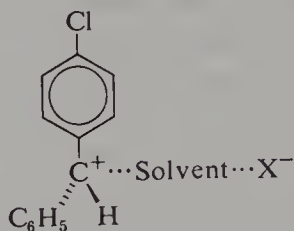
27 R = alkyl, aryl

Solvolysis of ^{18}O -labeled benzhydryl *p*-nitrobenzoate in 90% aqueous acetone [70] gave k_{eq}/k_t of approximately 3, thus confirming Winstein's evidence [45, 71] that internal return is important in these systems and providing a new method for the study of nonrearranging systems. The comparatively slow intermolecular exchange reaction of these derivatives with ^{14}C -labeled *p*-nitrobenzoic acid showed that oxygen equilibration is an intramolecular process.

Goering, Briody, and Levy [72] have determined k_t , k_{eq} , and k_{rac} for *p*-chlorobenzhydryl *p*-nitrobenzoate in 80 and 90% acetone. In 80% acetone 60% of the ion pairs returned to starting substrate (i.e., $k_t = 4.41 \times 10^{-3} \text{ hr}^{-1}$ and $k_{\text{eq}} = 6.5 \times 10^{-3} \text{ hr}^{-1}$); of the ion pairs returning, 57% gave retained stereochemistry (i.e., $k_{\text{rac}} = 2.8 \times 10^{-3} \text{ hr}^{-1}$). In 90% acetone these figures changed to 72 and 62%, respectively. As in the allylic cases, the ion pair is less tight and return is less important in a more ionizing solvent.

Goering and Levy [73] performed an important experiment with *p*-chlorobenzhydryl *p*-nitrobenzoate which provided evidence that two ion pairs are involved in its solvolysis. As noted above, $k_{\text{eq}} = 6.5 \times 10^{-3} \text{ hr}^{-1}$ and $k_{\text{rac}} = 2.8 \times 10^{-3} \text{ hr}^{-1}$; however, in the presence of 0.1411 *M* NaN_3 , k_{rac} dropped to zero while k_{eq} was essentially unchanged ($k_{\text{eq}} = 5.9 \times 10^{-3} \text{ hr}^{-1}$). Two ion pairs are postulated [73]: first, a tight or intimate ion pair which allows

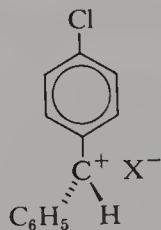
equilibration of ^{18}O but no racemization upon return, and is not trapped by azide ion; and second, a solvent-separated ion pair which gives racemization upon return and is trapped by azide ion. These experiments have been duplicated by Winstein [19] with chloride as leaving group. In this case, k_{rac} was reduced by the addition of NaN_3 but was still measurable. This result suggests differences in behavior of the chloride (**28a**) and *p*-nitrobenzoate (**28b**) solvent-



28a $\text{X} = \text{Cl}$

28b $\text{X} = \text{OPNB}$

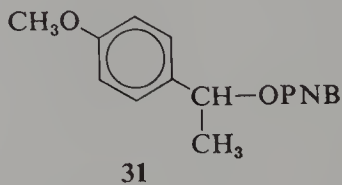
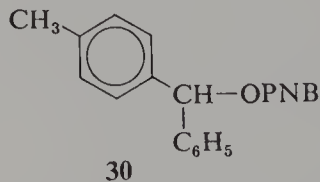
separated ion pairs. Since k_{rac} is not reduced to zero for the chloride, there may be some return to starting substrate from **28a** in the presence of NaN_3 ; yet there is none from **28b**. This may be the result of differing nucleophilicities of the gegenions. Alternatively, tight ion pair **29a** may be able to racemize, whereas **29b** cannot.



29a $\text{X} = \text{Cl}$

29b $\text{X} = \text{OPNB}$

Goering and his co-workers also studied the effects of added NaN_3 on the reactions of the *p*-methylbenzhydryl (**30**) [74] and α -anisylethyl (**31**) [75] esters. The results obtained were in sharp contrast to those for *p*-chlorobenzhydryl (Table 19). Instead of eliminating racemization completely, the addition of NaN_3 to the reactions of **30** and **31** resulted in only slight decreases in

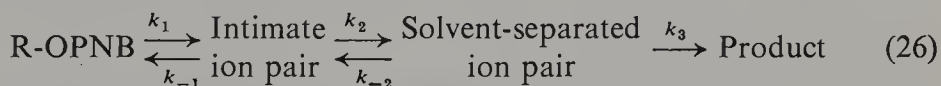


$k_{\text{rac}}/k_{\text{eq}}$. In addition, a special salt effect (Section 2.4) was observed for the reactions of **30** and **31**. However, oxygen equilibration was not eliminated,

Table 19 Oxygen Equilibration and Racemization with Added NaN_3 for *p*-Chlorobenzhydryl, *p*-Methylbenzhydryl, and α -Anisylethyl *p*-Nitrobenzoate [74, 75]

R-OPNB, R =	$[\text{NaN}_3]$	Solvent	Temperature (°C)	k_{eq}/k_t	$k_{\text{rac}}/k_{\text{eq}}$
<i>p</i> -Chlorobenzhydryl	0	80% Acetone	99.38	1.44	0.41
	0.141			0.28	0.0
<i>p</i> -Methylbenzhydryl (30)	0	90% Acetone	99.5	2.90	0.59
	0.1155			0.55	0.52
<i>p</i> -Anisylethyl (31)	0	90% Acetone	78.6	2.21	0.54
	0.120			0.42	0.43

even at high salt concentrations. These results were interpreted in terms of Eq. 26:



where the process with the rate constant k_{-1} occurs with oxygen equilibration and racemization and is not prevented by the added N_3^- . The step represented by k_{-2} also gives oxygen equilibration and racemization but is eliminated by N_3^- , and the special salt effect and a decrease in k_{eq}/k_t result. The comparable reduction of both oxygen equilibration and racemization by added N_3^- is responsible for the essentially constant $k_{\text{rac}}/k_{\text{eq}}$ ratio for **30** and **31** (Table 19). Thus the intimate ion pairs derived from **30** and **31** return with racemization, whereas that from *p*-chlorobenzhydryl *p*-nitrobenzoate does not. These differences apparently are due to variations in stability of the ion pairs.

N_3^- does not appear to attack the intimate ion pair. Furthermore, attack on the solvent-separated ion pair from **30** yields *retained* alcohol and *inverted* azide products [74]; this result is consistent with the prediction made by Schleyer and co-workers [48] for attack on a solvent-separated ion pair.

Goering and Hopf [74] have determined k_{eq} and k_t in 90% acetone for a series of benzhydryl *p*-nitrobenzoates with *para* substituents ranging from chloro to methoxy (Table 20). Whereas the range of reactivities k_t varied by more than 10^3 , k_{eq}/k_t remained essentially constant (2.4–3.0). Since oxygen equilibration is expected to become more important as the stability of the ion pair increases, such equilibration should be minimized with the *p*-chloro compound. Therefore, if equilibration were not complete in the *p*-chloro derivative, k_{eq}/k_t would have increased as k_t increased. However, since k_{eq}/k_t remains constant, equilibration of oxygens upon internal return must be complete for the *p*-chloro and for all the other benzhydryl *p*-nitrobenzoates. The slight increase in $k_{\text{rac}}/k_{\text{eq}}$ with increasing reactivity is consistent with a

Table 20 Oxygen Scrambling and Racemization Results for *Para*-Substituted Benzhydryl *p*-Nitrobenzoates [74]

Substituent	Temperature (°C)	rel k_t	k_{eq}/k_t	k_{rac}/k_{eq}
<i>p</i> -Cl	99.6	1	2.4	0.35
<i>p</i> -H	99.5	2	2.9	—
<i>p</i> -CH ₃	99.5	22	2.9	0.60
	48.8		3.0 ^a	0.17 ^a
<i>p</i> -OCH ₃	99.5	2,500	—	—
	48.8		2.4	0.28

^a Extrapolated value.

weakening of the attractive forces in the ion pair. Similar results were obtained from a comparison of k_{eq}/k_t and k_{rac}/k_{eq} for α -anisylethyl and α -phenylethyl *p*-nitrobenzoates [75].

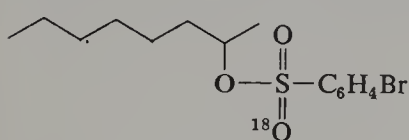
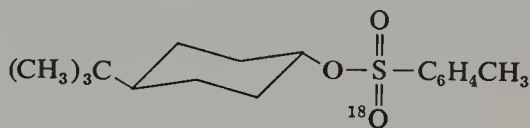
The constancy of k_{eq}/k_t with changes in reactivity of up to 3×10^4 (α -anisylethyl (31) versus α -phenylethyl *p*-nitrobenzoates) [75] seems to confirm that return during solvolysis of systems as reactive as allyl and benzhydryl *p*-nitrobenzoates is accompanied by complete oxygen equilibration. These results should be contrasted with those of White and Elliger [76], who generated the benzhydryl benzoate ion pair by the decomposition of an *N*-nitrosoamide and found that 20% of the return occurs without oxygen equilibration. However, benzhydryl benzoate solvolyzes [77] with $k_{eq}/k_t = 0.9$, a value much lower than those in Table 20.

Goering and Rubenstein [78] have determined that $k_{rac}/k_{eq} = 0.7$ for cyclopropylmethylcarbonyl *p*-nitrobenzoate in 80% acetone, the largest value measured for a nonrearranging system. The smallest value of k_{rac}/k_{eq} is 0.04 observed by Goering and Sandrock [79] for α -phenylethyl *p*-nitrobenzoate in 70% acetone. These results clearly illustrate that oxygen scrambling is a better method than racemization of starting material for measuring ion pair return in nonrearranging substrates.

Goering and Chang [80] have studied ¹⁸O equilibration and racemization of 2-phenyl-2-butyl *p*-nitrobenzoate, the first nonrearranging tertiary substrate to be examined. Interestingly, k_{eq}/k_t was only 0.60 (in 90% acetone), in contrast to values of 2.2–3.2 for resonance stabilized secondary derivatives [74]. Since this tertiary ester is relatively reactive, return probably occurs with complete or nearly complete oxygen equilibration. The low value of k_{eq}/k_t indicates that dissociation or reaction with solvent is more important for the tertiary derivative. The reason for this is not obvious. For example, some of the secondary benzhydryl derivatives studied by Goering and Hopf [74] are more reactive than 2-phenyl-2-butyl *p*-nitrobenzoate, whereas

others are less reactive; thus no simple relationship with reactivity exists. As expected for steric reasons (see 27), there is much less racemization of substrate upon return for the tertiary derivative (8%) than for the secondary derivatives (38–53%) [72–74, 81]. It is possible that the increased dissociation of the tertiary derivative also has a steric origin.

We turn now from reactive, nonrearranging derivatives in which return is probably associated with complete equilibration of ester oxygens to a discussion of the behavior of unreactive, nonrearranging derivatives. Diaz, Lazdins, and Winstein [56] investigated ^{18}O -labeled 2-octyl brosylate (**32**) and *trans*-4-*t*-butylcyclohexyl tosylate (**33**), the only ^{18}O study performed to date on simple secondary alkyl derivatives.

**32****33**

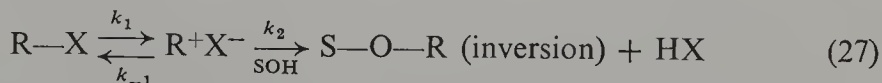
Both k_{eq} and k_t were determined in methanol, acetic acid, formic acid, and trifluoroacetic acid for **32** and **33**. A selection of the results are presented in Table 21; k_{eq} comprises from 1.1 to 19.9% of the total ionization rate con-

Table 21 Summary of ^{18}O Equilibration Data for Alkyl Arenesulfonates

Solvent	32	F_{eq}^a	33
CH_3OH	1.1		—
$\text{CH}_3\text{CO}_2\text{H}$	6.2		3.9
HCO_2H	8.1		2.9
$\text{CF}_3\text{CO}_2\text{H}-\text{CF}_3\text{CO}_2\text{Na}$	19.9		7.6

$$^a F_{\text{eq}} = 100k_{\text{eq}}/(k_{\text{eq}} + k_t).$$

stant ($k_{\text{eq}} + k_t$). These values are lower limits of the amount of return since return of such relatively high-energy ion pairs is not expected to occur with complete equilibration (i.e., $k_{-1} > k_{\text{eq}}$). The inversion of stereochemistry upon solvolysis of **32** [82] and **33** [83, 84] indicates that any ion pair involved is an intimate ion pair which would yield product as shown in Eq. 27:

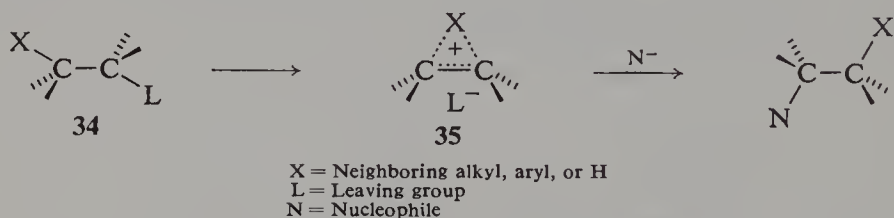


The increase in F_{eq} values with solvent changes is probably the result of a decrease in solvent nucleophilicity with a consequent decrease in k_2/k_{-1} or of an increase in solvent ionizing power which allows formation of ion pairs that are less tight.

There have also been two reports of ^{18}O equilibration studies on unactivated, nonrearranging, tertiary aliphatic derivatives [85, 87]. The first actual use of the ^{18}O method, by Doering, Streitwieser, and Friedman [85], utilized the acid phthalate of 2,5-dimethyl-2-hexanol. Unfortunately, this work has never been published. No scrambling of labeled oxygen upon solvolysis was found. Goering and Briody [87] also failed to detect oxygen scrambling in the solvolysis of carbonyl-labeled *t*-butyl *p*-nitrobenzoate. These results contrast with those of the simple secondary derivatives **32** and **33**, which gave detectable scrambling upon return. It is possible that ion pairs may be formed but that the return is not competitive with further reaction to give product. This interpretation is consistent with the observation of Goering and Chang [80] (see above) that k_{eq}/k_t is smaller for an activated tertiary derivative than for an activated secondary derivative.

3.3. Wagner-Meerwein Rearrangements

Many alkyl derivatives solvolyze with participation by neighboring alkyl [1a, 86, 92, 93] aryl [94], or hydrogen [1a, 86, 95] (**34** \rightarrow **35**) to give rearranged products. Bridged species **35** can be transition states or intermediates, and such rearrangements can be loosely classified as Wagner-Meerwein rearrangements.

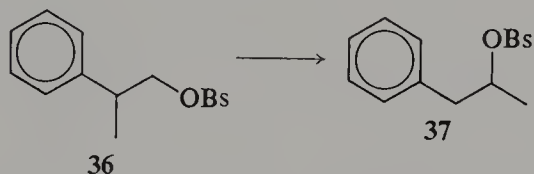
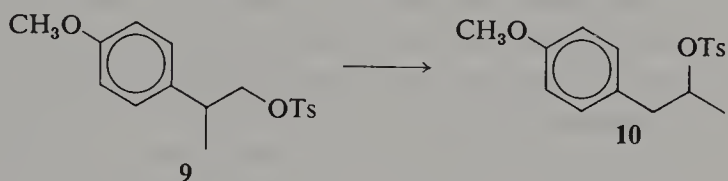


The majority of Winstein's pioneering research on special salt effects utilized compounds which gave bridged cations (**35**). It was therefore only logical that the ^{18}O scrambling technique be applied to these systems in which ion pairing was already known to be important.

The first ^{18}O study with bridged cations from **9** and **36** was carried out by Denney and Goldstein [88]. Winstein had determined that **9** exhibits a special salt effect [17] but that **36** undergoes acetolysis with only normal salt effects [16]. These results were interpreted as evidence for the formation of both intimate and solvent-separated ion pairs from **9** and intimate ion pairs only from **36** [16, 17]. In acetic acid these two substrates also give return to the secondary derivatives **10** and **37** [16]. There is no return to primary substrate.

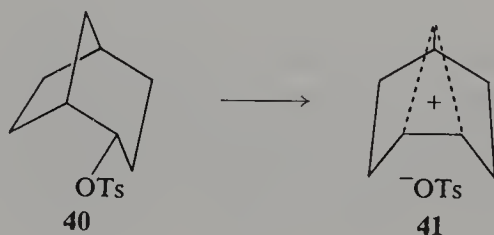
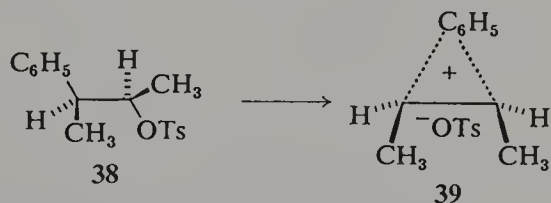
Denney and Goldstein rearranged **9** to **10** and **36** to **37** and determined the extent of scrambling of ether- ^{18}O in the ester group. Approximately 25% of the ^{18}O was scrambled in the **37** formed from **36**, while 18% scrambling

was observed when **37** itself was subjected to these conditions. Therefore the oxygens of the sulfonate ester do not become equivalent in the intimate or tight ion pair. On the other hand, the rearrangement of **9** to **10** or the partial solvolysis of **10** gives recovered **10** with completely equilibrated ^{18}O . The solvolyses of **9** and **10** therefore appear to be passing through an intermediate which is more dissociated than that from the phenyl derivatives **36** and **37**. This result is consistent with the observation of a special salt effect for the



anisyl derivative but not for the phenyl derivative. Since the more reactive **10** gives complete equilibration of ^{18}O , it is impossible to determine whether the rearrangement of primary **9** to secondary **10** proceeds with partial or complete equilibration. This is unfortunate since the comparison of the anisyl and phenyl tight ion pairs would be instructive.

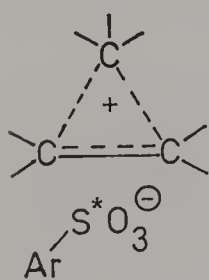
Goering and Thies [89] have studied ^{18}O scrambling in the solvolyses of **38** and **40**. Both compounds can give achiral ion pairs, and ionization to the bridged species (**39** and **41**) can be measured by k_a . Both k_{eq} and k_{rac} (where



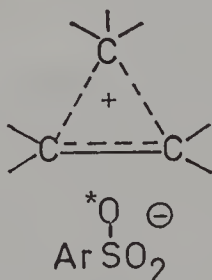
$k_{\text{rac}} = k_{\alpha} - k_t$) were found to be greater than k_t , and k_{rac} was observed to be twice as large as k_{eq} for both substrates in buffered acetic acid. Therefore at least 50% of the ion pair return occurs without oxygen equilibration.

Since both **38** and **40** solvolyze with normal salt effects only [37, 90], it had been concluded before these ^{18}O studies were undertaken that external return was not involved. Furthermore, Goering and Jones [91] showed that there was negligible exchange when **38** was solvolyzed in the presence of ^{14}C -labeled sodium *p*-toluenesulfonate. However, Goering and Thies [89a] observed that solvolysis of **40** in the presence of LiClO_4 caused, in addition to the expected decrease in total ion pair return [as measured by $100k_{\text{rac}}/(k_{\text{rac}} + k_t)$], a decrease in the ratio of $k_{\text{eq}}/k_{\text{rac}}$ from 0.47 to 0.39. This decrease in the amount of equilibration associated with return is due to the elimination of some return from a species which would give completely equilibrated substrate. In other words, two achiral ion pairs are again indicated, one of which does not contain equivalent oxygens and another in which the oxygens are equivalent. The latter species is considered to be captured by LiClO_4 , thus increasing k_t and decreasing k_{eq} relative to k_{α} . These results, which indicate return from two different ion pairs in the absence of special salt effects, suggest the existence of more than one intimate ion pair.

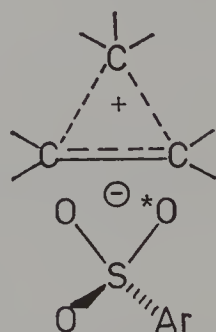
As mentioned previously, $k_{\text{eq}}/k_{\text{rac}} \simeq 0.5$ for the acetolysis of **38** and **40**. There are only two circumstances in which two achiral arenesulfonate ion pairs can give such a result: a 1:1 combination of **42** and **43** or a 1:2 combination of **43** and **44**. Obviously, no single achiral species can give $k_{\text{eq}}/k_{\text{rac}} = 0.5$.

**42**

$$k_{\text{eq}}/k_{\text{rac}} = 1$$

**43**

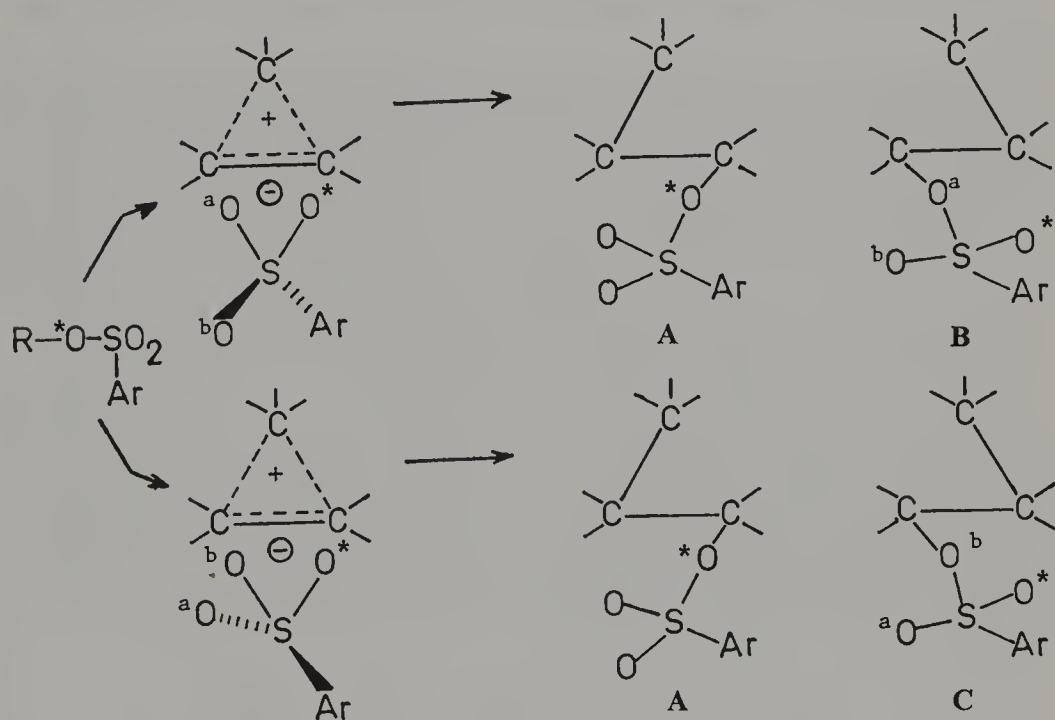
$$k_{\text{eq}}/k_{\text{rac}} = 0$$

**44**

$$k_{\text{eq}}/k_{\text{rac}} = 0.75$$

The $k_{\text{eq}}/k_{\text{rac}}$ value of 0.75 for **44** can be understood by reference to Scheme VIII where A, B, and C are formed in the ratio 2:1:1. Since complete scrambling would have given a ratio of 1:1:1, only 75% of the product mixture from **44** represents complete scrambling. The remaining 25% (A) is not scrambled at all.

A similar problem was encountered in allylic systems, where the possibilities were differentiated by separation of both enantiomers of recovered racemic substrate from the solvolysis of optically pure ester. If different amounts of ^{18}O equilibration are found for the (+) and (−) isomers, the 43–44 combination will be implicated. Goering and Thies [89b] performed this task for the acetolysis of **38** and found that ^{18}O scrambling is the same for return to either carbon. Thus it is the 42–43 combination that is occurring. Internal return to the original carbon results in approximately 50% oxygen equilibration. This result is important in interpreting results of the ^{18}O scrambling of alkyl arenesulfonates which do not rearrange (see above). If the intimate ion pairs from **32**, **33**, and **38** behave similarly, then the small degree of ^{18}O scrambling observed for **32** and **33** (Table 21) indicates that little internal return is occurring.



Scheme VIII

B \equiv C

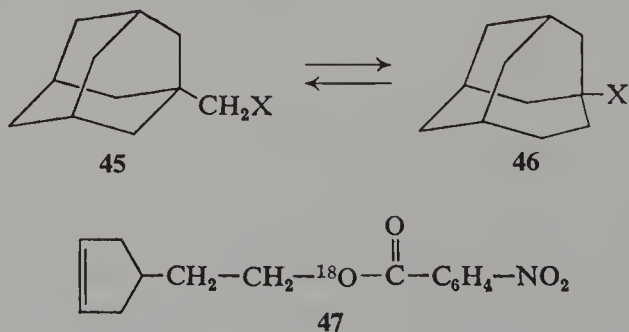
Both studies by Goering and Thies [89] present evidence for the intermediacy of two ion pairs from **38**, where no special salt effect is observed. Unlike **38**, threo-3-*p*-anisyl-2-butyl tosylate exhibits a special salt effect with added LiClO_4 [22]. Goering and Jones [91] have now dissected ion pair return into internal and external components. While $(k_{\text{eq}}/k_{\text{rac}})_{\text{ext}}$ is approximately equal to unity, $(k_{\text{eq}}/k_{\text{rac}})_{\text{iht}}$ is found to be about $\frac{1}{2}$. Acetolysis in the presence of ^{14}C -labeled sodium *p*-toluene-sulfonate showed that ion pair return is accompanied by some exchange, and that this exchange was

not eliminated by added LiClO_4 . These results imply either that LiClO_4 does not completely suppress external ion pair return or that there is a type of internal ion pair which allows exchange. Similarly, in the solvolysis of **38**, **42** appears to be the species giving ^{18}O equilibration, which is diverted by LiClO_4 . These results do not necessarily refute the theory of the origin of special salt effects [19], since more than one internal as well as an external ion pair may be involved. The special salt effect will be observed only if external ion pair return from a solvent-separated ion pair to an intimate ion pair is prevented by added salt.

To this point we have been discussing solvolyses that probably give bridged intermediates. The discussion that follows is concerned with cases such as neopentyl in which participation by a C-alkyl bond may occur in the rate-determining step (see ref. 92a, 93, 96–99 for contrasting views), although the occurrence of a bridged *intermediate* in the parent system is highly unlikely.*

Nordlander and Kelly [101] studied the solvolysis of ^{18}O -labeled neopentyl tosylate and found no scrambling of ^{18}O in recovered starting material. These results could be explained in three ways: (1) no primary ion pair is formed (i.e., migration and ionization are concerted); (2) an ion pair is formed and return occurs without scrambling (consistent with the prediction of Goering and Linsay [68] for unstable ion pairs); (3) the neopentyl ion pair is formed but return does not complete with rearrangement (consistent with the interpretation given by Shiner [99] and supported by Schubert [93]; Section 4.1).

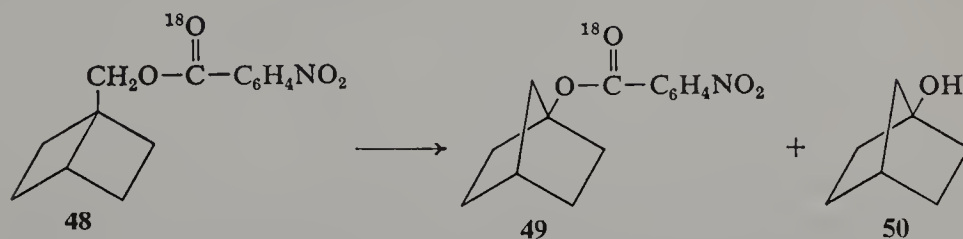
The mechanism of solvolysis of neopentyl derivatives is a controversial subject [92a, 96–101] which we will not enter into here; it is unfortunate that the ^{18}O scrambling technique cannot aid in the decision as to which of the three possibilities is correct. On the other hand, acetolysis of 1-adamantylcarbinyl *p*-nitrobenzenesulfonate (**45**, $\text{X} = \text{OSO}_2\text{C}_6\text{H}_4\text{NO}_2$) shows a special salt effect [100]. Since there is other evidence for bridging or near bridging in this system [97], an ^{18}O investigation would be of interest.



* However, bridged and classical carbocation intermediates must be much closer in energy in the 1-adamantylcarbinyl-3-homoadamantyl (**45** and **46**) system [96, 97, 100].

Bartlett and his co-workers [102] observed no ^{18}O scrambling in recovered starting substrate during the rearrangement in acetic acid of labeled **47** to *exo*-2-norbornyl acetate. The three possible explanations for the neopentyl solvolysis also apply here.

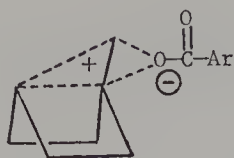
Dauben and Chitwood [103] have studied the fate of carbonyl- ^{18}O in the solvolysis of **48** in 60% acetone. For such strained neopentyl derivatives



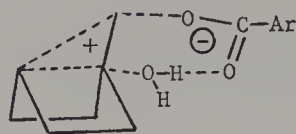
ionization and migration are expected to be concerted and the unrearranged ion pair stage should be bypassed [98, 103, 104]. Thus no ^{18}O equilibration would be expected from the solvolysis of **48**, and none was observed in return product, **49**. The large amount (81%) of rearranged ester **49** formed is also consistent with this interpretation. Compound **48** does not react in cyclohexane at 117° ; therefore the rearrangement in aqueous acetone at the same temperature is probably polar and heterolytic.

The production of 19% of 1-norbornanol (**50**) is especially noteworthy in view of the tightness of the **48** \rightarrow **49** process. Compound **50** does not arise from the solvolysis of **49**, which is stable to the reaction conditions. Neither does it come from bicyclo[2.2.0]hexane-1-methanol, which is also stable. By carrying out the solvolysis in acetone containing ^{18}O -enriched water it was determined that all of the oxygen in **50** comes from the solvent. There are several possible explanations for this result [103]. One possibility is that two ion pairs are formed (just as in the case of **38**), the first of which (**43**-like) gives no scrambling of ^{18}O and returns to give **49**, whereas the second (which might have equivalent oxygens but does not undergo return) gives rise to the 1-norbornanol (**50**). However, it must be remembered that there appears to be a relationship between stability of the resulting ion pair and the amount of ^{18}O scrambling (Section 3.2). In this case, the ion pair, if it exists at all, will certainly not be very stable and the formation of a **42**-like intermediate appears unlikely. For similar reasons, attack by water on an ion pair as in **51** seems an unattractive explanation. Perhaps the interposition of water, concomitant with rearrangement **52**, results in the formation of **50** [103]. The similarity between this explanation and the mechanism for the formation of solvolysis product with retained configuration by collapse of a solvent-separated ion (Section 3.2) [48] should be noted.

In any event, as discussed for the neopentyl case, the failure to observe ^{18}O scrambling does not unambiguously eliminate the possibility of ion pair formation.

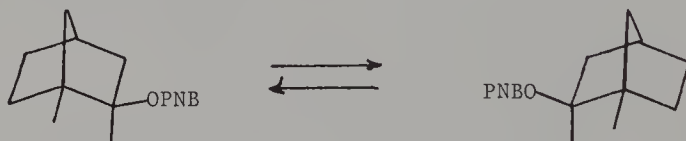


51



52

Goering and Humski studied racemization [55b] and ^{18}O equilibration [105] of **53** and estimated that return results in an upper limit of 20% oxygen equilibration. Although $k_{\text{eq}}/k_{\text{rac}}$ in 90% acetone is 0.5, ionization does not always give a symmetrical cation, for substitution products are still optically active. Since not all the ion pairs formed are achiral, an independent method for estimating total return is not available, and the calculated amount of equilibration is of necessity an approximation.



53

The result with **53** is of interest because of its consistency with the apparent relationship between the stability of the ion pair intermediates and the amount of ^{18}O equilibration associated with their return [68]. For example, complete equilibration is apparently achieved in the stable benzhydryl ion pairs (Section 3.1), partial to complete equilibration is found in allylic systems (Section 3.2), while only partial or even in one case (**48**) no equilibration results from solvolysis of rearranging aliphatic substrates in which one can be certain that ionization to a relatively unstable species has occurred.

Goering and Closson [106] have examined the transannular rearrangement of **54** to **55** in aqueous acetone, of interest because of the relatively long distance that the anion must migrate. Only 33% of the carbonyl- ^{18}O in **54** was incorporated in the ether-oxygen of product **55**; this pronounced specificity indicates that considerable bonding between cation and anion is maintained during isomerization.

The behavior on solvolysis of unactivated, nonrearranging primary, secondary, and tertiary derivatives poses a difficult problem for interpretation.

Recovered unrearranged esters from partial primary solvolyses (neopentyl [101] and **47** [102]) have not revealed any ^{18}O scrambling; the same is true for simple tertiary systems, but the available studies have not been published in full [85, 87]. A careful investigation has shown *some* oxygen equilibration in two secondary substrates, **32** and **33** [56]. How is one to interpret this result? One school of thought holds that ion pairs from such uncrowded



systems form and return many times—perhaps even thousands of times—before reaction with solvent takes place [4, 93, 99]. If this is true, then virtually every act of ionization-recombination must occur without oxygen equilibration; the behavior of **48** supports this viewpoint.* On the other hand, most rearranging aliphatic substrates (**9** [88], **36** [88], **38** [89], **53** [105], and **54** [106]) show appreciable ^{18}O equilibration. Similar amounts of equilibration were observed in the rearranged and in the nonrearranged return product from **38** [89b]. The extents of equilibration in **37** also were comparable, whether **37** was obtained by rearrangement from **36** or by recovery after partial solvolysis [88].

Although it is clear that the rate of ionization should exceed the rate of equilibration in **32** and **33** [56], one wonders whether this rate ratio is really large enough in view of the small extent of scrambling observed [56] to support the hypotheses of the ion pair school [4, 93, 99]. Unfortunately, a definitive solution to this problem is not yet available. An ion pair so tight as to prevent oxygen equilibration should behave very much like covalent substrate; the distinction is difficult to establish experimentally.

4. MISCELLANEOUS METHODS FOR THE DETECTION OF ION PAIRING

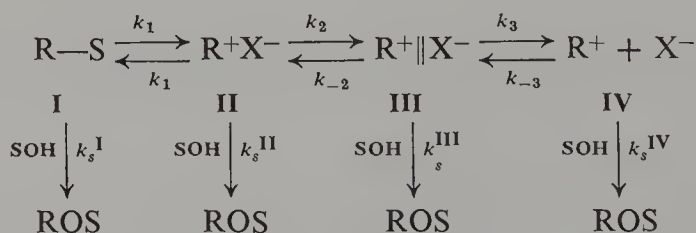
4.1. Secondary Deuterium Isotope Effects

It has been recognized for some time that secondary deuterium isotope effects—changes in rate produced by isotopic substitution of C—H bonds which are not being broken in the transition state—are dependent on the

* Because of the ion pair stability-oxygen equilibration relationship, one might expect more ^{18}O -label scrambling in tosylate than in *p*-nitrobenzoate ion pairs. This may help to explain the lack of equilibration found in going from **48** to **49**.

extent of nucleophilic involvement of the solvent during solvolysis [86, 107]. S_N2 reactions show negligible α - and β -deuterium isotope effects ($k_H/k_D \simeq 1.0$), while maximum values are observed for limiting reactions in which there is no nucleophilic assistance to ionization. Shiner and his co-workers [107–115] and Murr and Donnelly [116] have now developed a more detailed picture for the origin of isotope effects which considers the influence of ion pairing. Deuterium isotope effects in solvolysis reactions have recently been reviewed comprehensively by Shiner [107] and by Sunko and Borčić [117]. Consequently, this subject will be presented only in outline here, but from a critical perspective.

Secondary isotope effects originate from changes in vibrational force constants (CH_3 versus CD_3) in going from ground to transition states. The magnitude of α -deuterium effects is dependent on temperature, the nature of the leaving group, the solvent, and variations in the substrate structure. The effect of different leaving groups is primarily the result of force constant differences at the position of substitution in the ground state. β -Deuterium isotope effects are influenced similarly, with the exception that changes in leaving group are unimportant. For a given *mechanism* (temperature and leaving group constant), Shiner regards substrate structural variations to be of negligible importance for S_N1 processes and only to vary in a minor way for S_N2 reactions.* Consequently, the magnitude of the secondary deuterium isotope effects is a very sensitive indication of mechanism. In fact, Shiner regards this to be “probably the most powerful *single* tool available for the investigation of the mechanism of any reactions in this class” [107]. Although we concede the importance of secondary deuterium isotope effect data, we do not share Shiner’s value judgment, since more than one mechanistic influence determines the magnitude of an isotope effect. Both ion pairing and nucleophilic solvent attachment will reduce k_H/k_D ; there is no way to distinguish between these alternatives without recourse to independent techniques.



Scheme II

Shiner discusses secondary isotope effects in the context of Winstein’s [19] ion pair mechanism (Scheme II). According to Shiner, maximum α -deuterium

* This assumption has been questioned recently [118b].

Table 22 Some Illustrative α -Deuterium Isotope Effects in Solvolysis Reactions^a

Substrate	Solvent ^b	Mechanistic ^c Assignment	k_H/k_D ^d at 25°
2-Adamantyl tosylate	70 % T, 97 % T, 50 % E	k_2	1.23 ^e
3-Pentyn-2-yl tosylate	70 % T	k_2	1.26 ^f
3-Pentyn-2-yl bromide	70 % T	k_2	1.123 ^f
3-Pentyn-2-yl iodide	70 % T	k_2	1.089 ^f
1-Phenylethyl chloride	50 % E, 80 % E	k_2	1.15
5,5,5-Trifluoro-3-pentyn- 2-yl brosylate	50 % E	k_s^I	1.050
2-Propyl brosylate	TFA	k_2	1.22 ^g
	97 % T	k_s^{II}	1.152
	50 % T	k_1	1.122
	90 % E	k_s^I, k_1	1.083
3,3-Dimethyl-2-butyl brosylate	70, 97 % T	k_1	1.15
Benzyl brosylate	97 % T		1.173
	95 % E		1.053
Ethyl tosylate	H ₂ O	k_s^I	1.020
Methyl tosylate	H ₂ O	k_s^I	0.984

^a Data from ref. 107.^b The percentage refers to the organic component of aqueous mixtures; E = ethanol, T = trifluoroethanol; TFA = trifluoroacetic acid.^c The assignments (made by Shiner [107]) refer to the rate-limiting step according to Scheme II.^d The effect per deuterium atom is reported.^e Ref. 115; cf. ref. 118a.^f Ref. 114.^g Ref. 122.

isotope effects are observed when k_2 (intimate ion pair dissociation) is rate limiting [107]. Examples are provided by the first few entries in Table 22. Since *equilibrium* α -D isotope effects of 1.29 have been observed (for benzhydrol \rightleftharpoons benzhydryl cation), even higher k_H/k_D values are theoretically possible (e.g., if k_3 were rate limiting), but these have not been realized in practice [119].

Lower values, about three-quarters of the maximum observed values for a given leaving group, are expected by Shiner when any of the following steps are rate limiting: nucleophilic attack on carbonium ion (k_s^{IV}), nucleophilic attack on intimate ion pair (k_s^{II}), or intimate ion pair formation from covalent substrate (k_1) (Table 22) [107].

When k_s^I is rate determining (the classical S_N2 reaction), α -secondary deuterium isotope effects are near unity but depend somewhat on leaving group and on structure (methyl versus primary versus secondary; Table 22).

The magnitude of the α -deuterium isotope effect in isopropyl derivatives is representative of the many compounds which are highly dependent on the solvent, and $k_{\text{H}}/k_{\text{D}}$ varies from 1.08 in 90% ethanol to 1.22 in trifluoroacetic acid (Table 22). These values are, however, always well within the extremes of Table 22 for secondary arenesulfonates represented by 3-pentyn-2-yl tosylate ($k_{\text{H}}/k_{\text{D}} = 1.23$) and 5,5,5-trifluoro-3-pentyl-2-yl brosylate ($k_{\text{H}}/k_{\text{D}} = 1.05$). Shiner's interpretation is illuminating: "Thus, one of the classical examples of borderline solvolyses seems to be borderline in a bewildering number of ways! As many as four different steps, k_1 , k_2 , k_s^{I} , or k_s^{II} can be made the dominant rate-controlling influence depending on the choice of solvent. It is not surprising that because of this variety, it is difficult to find conditions which effectively isolate one mechanism to the exclusion of others. Rather the change appears to be much more continuous with a mixture of mechanisms being the rule rather than the exception" [107].

This illustrates the limitation of the method. In the absence of other evidence, the observation of an α -deuterium isotope effect of intermediate magnitude ($1.22 > k_{\text{H}}/k_{\text{D}} > 1.0$ for sulfonates) does not provide definitive mechanistic information since either nucleophilic solvent involvement or ion pairing phenomena or both may be responsible. Furthermore, Shiner's model, complicated as it is, suffers from the additional problem that the solvent may be involved nucleophilically in intimate (k_1) or solvent-separated (k_2) ion pair formation [120]. A recent mathematical analysis of isotope effects by Vogel results in a model of the ion pair with just such a rearside partially bound solvent molecule [121].

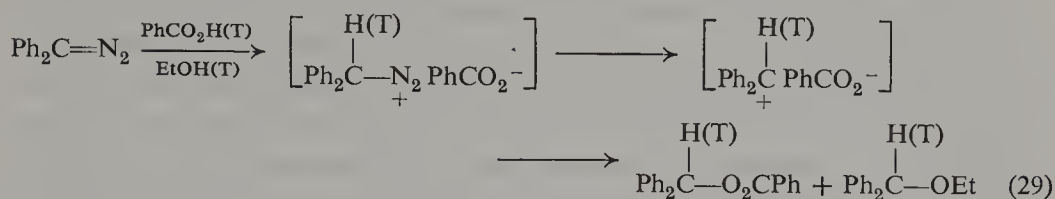
All that can be said with certainty is that nucleophilic solvent assistance would appear definitely to be implicated in the rate-limiting step or steps if an observed α -deuterium solvolysis isotope effect is significantly less than three-quarters of the maximum value for a given leaving group. Unfortunately, rather large α - $k_{\text{H}}/k_{\text{D}}$ values do not necessarily rule out significant nucleophilic solvent involvement since the interrelationship may not be linear [117, 118]. As limiting behavior is approached, relatively large changes in the nucleophilic solvent participation may be producing very small differences in the magnitude of α -D isotope effects [118].

Murr and Donnelly [116] have pointed out that there will be an isotope effect on partitioning of ion pair intermediates; for example, the isotope effects on k_{-1} and k_2 involving an intimate ion pair (II, Scheme II) will be different. This partitioning isotope effect (PIE) (Eq. 28) was determined

$$\text{PIE} = \frac{(k_{-1}^{\text{T or D}}/k_{-1}^{\text{H}})}{(k_2^{\text{T or D}}/k_2^{\text{H}})} \quad (28)$$

experimentally by treating diphenyldiazomethane with partially O-tritiated benzoic acid-ethanol and determining the specific activities of the benzhydryl

benzoate and benzhydryl ether products (Eq. 29). The key assumption here,



supported by earlier conclusions [76, 77], is that the ion pair (or ion pairs) generated via Eq. 29 is the same as that generated from benzhydryl benzoate during solvolysis.

For this system, the PIE was substantial, 1.16 at 25° (the isotope effect on solvolysis rate for the same conditions was estimated to be 1.30).

In general, Murr and Donnelly [116] evaluated approximate PIE's in the following way. For solvolysis giving product from solvent-separated ion pairs (III), the maximum isotope effect possible would be observed when $k_{-1} \gg k_2$ (i.e., k_2 is rate limiting), while the minimum value of $k_1^{\text{H}}/k_1^{\text{D or T}}$ would be observed when $k_2 \gg k_{-1}$ and $k_s^{\text{III}} \gg k_{-2}$ (i.e., k_1 is rate limiting). Maximum isotope effects for each leaving group [107, 114, 115, 118] were combined with experimental minimum isotope effect values for reactions thought to have k_1 rate limiting in order to estimate PIE's according to Eq. 30.

$$\left(\frac{k_t^{\text{H}}}{k_t^{\text{D or T}}} \right)_{\text{max}} = \text{PIE} \left(\frac{k_1^{\text{H}}}{k_1^{\text{D or T}}} \right) \quad (30)$$

This treatment provides a more detailed analysis of observed secondary solvolytic isotope effects by dissecting them into component contributions. Unfortunately the approach suffers at present from the general lack of independently determined PIE data. Moreover, it requires specific mechanistic assumptions even within the framework of Scheme II; alternatives to Scheme II such as those involving nucleophilic assistance in intimate or solvent-separated ion pair formation are not considered.

A possible method of intimate ion pair formation other than solvolysis has been explored by Shiner's group: protonic acid additions to olefins [111, 112] (discussed in detail in Section 5.3). *p*-Bromobenzenesulfonic acid in trifluoroacetic acid reacts with propene to give 2-propyl brosylate exclusively, whereas under the same conditions *t*-butylethylene gives only rearranged trifluoroacetate (unrearranged pinacolyl brosylate would have been detectable). It was suggested that both of these reactions gave the same intimate ion pairs that would be obtained from solvolysis, but internal return (k_{-1}) of the 2-propyl brosylate ion pair was very rapid relative to other processes (e.g., k_2). In contrast, the pinacolyl brosylate ion pair did not undergo internal return; methyl migration occurred exclusively, and only tertiary trifluoroacetate resulted.

Trifluoroacetolysis of pinacolyl brosylate is 2800 times faster than 2-propyl brosylate.* According to Shiner, Fisher, and Dowd [112], this pinacolyl rate enhancement is *not* due to methyl participation in the ion pair formation step (k_1)—the traditional explanation—but is the consequence of the prevention of internal return (k_{-1}) by methyl migration subsequent to *rate-controlling* intimate ion pair formation (k_1). Thus the disparity in rates is due not to an enhancement in the rate of pinacolyl solvolysis, but rather to a retardation in the overall rate of 2-propyl brosylate solvolysis caused by internal return.

α -, β -, and γ -Deuterium isotope effects are presented in support of this interpretation [115]. For pinacolyl brosylate all these effects are essentially solvent independent, but k_H/k_D for 2-propyl brosylate-2-*D* varies from 1.083 (90% ethanol) to 1.22 (trifluoroacetic acid). The latter value corresponds to the maximum observable, and in Shiner's view indicates rate-limiting dissociation of intimate ion pairs (k_2). Values less than 1.22, found in all other solvents, are considered to indicate a greater degree of nucleophilic attachment (either of solvent or of leaving group) in the rate-limiting transition state. The α -deuterium isotope effect for pinacolyl brosylate, on the other hand, was 1.15–1.16 in three solvents of varying nucleophilicity. The hindered nature of the pinacolyl system would seem to preclude backside solvent participation, so that this lack of solvent dependence is not surprising. The magnitude of the isotope effect, about three-quarters of the maximum (cf. the value of 1.23 observed for 2-adamantyl tresylate, a hindered but nonrearranging system [115, 118]), is consistent with Shiner's mechanism, k_1 being rate limiting.

However, there is another explanation for the reduction of the isotope effect to 1.15–1.16: methyl participation *during* ionization. The presence of a neighboring group at the rear would be expected to reduce the magnitude of α -deuterium isotope effects just as external nucleophiles would. Table 23 provides examples taken from Sunko and Borčić's review [117].

Shiner, Fisher, and Dowd [112] claim that the observation of very small γ - d_9 isotope effects (1.003–1.011) preclude the possibility of methyl migration in the rate-determining step. Pertinent work by Schubert et al. [93, 124] is cited in support of this claim. The pinacol rearrangement of ϕ -CHOH—C(OH)(CH₃)(CD₃) was shown by Schubert and LeFevre [124] to prefer CH₃ over CD₃ ionization by 1.23; also, correspondence of rate and product data showed the coincidence of rate- and product-controlling steps. Schubert and Henson [93] failed to observe significant *kinetic* deuterium isotope effects in the trifluoroacetolysis of γ - d_3 , γ - d_6 , and γ - d_9 neopentyl 2,4-dinitrobenzenesulfonates, but they did observe that CH₃ groups migrated with a preference of

* This difference is now found to be about a power of ten smaller (see below) [119b].

1.22–1.31 over CD_3 groups. They concluded that the migration step occurred after the rate-controlling step k_1 , thus adopting the interpretation that Shiner advanced for the pinacolyl system.

However, the evidence used to rule out concerted migration-ionization in both pinacolyl and neopentyl systems is far from unambiguous. As Table 24 shows, nonmigrating γ -deuterium isotope effects are inverse. This has been attributed by Shiner to the normal isotopic inductive effect, deuterium being more electron releasing than hydrogen. Shiner further calls attention to the large magnitude of the inverse isotope effect of the n -propyl and isobutyl substrates in Table 24, despite the fact that these reactions should proceed by an $\text{S}_{\text{N}}2$ mechanism with less positive charge development on carbon in the transition state than would be expected in $\text{S}_{\text{N}}1$ processes.

Were neopentyl and pinacolyl arenesulfonates solvolyzing by the Shiner-Schubert mechanism [rate limiting formation (k_1) of nonrearranged ion pairs], then *large inverse* γ - d_9 isotope effects would have been expected, contrary to observation. Thus the observed absence of an appreciable kinetic γ -isotope effect actually is strong evidence *against* the proposed mechanism. The observed values are consistent with concerted migration-ionization if the regular ($k_{\text{CH}_3}/k_{\text{CD}_3} \sim 1.2$) isotope effects on the migrating methyl group are compensated by inverse ($k_{\text{CH}_3}/k_{\text{CD}_3} \sim 0.90\text{--}0.95$) effects produced by isotopic substitution on the methyl groups remaining behind.* The question of whether or not secondary or primary ion pairs are formed during solvolysis without assistance from either solvent or neighboring group is not, in our view, answered definitively (see Section 5).

Recent work suggests another interpretation of the solvolytic behavior of pinacolyl tosylate [118b]. The pinacolyl/isopropyl trifluoroacetolysis rate ratio was found to be less than 200 (contrary to the larger value reported by Shiner's group [112]). This rate enhancement was indicated to be due only to inductive/hyperconjugative effects since $\log k$ (pinacolyl) obeyed the same σ^* correlation exhibited by isopropyl and other secondary tosylates without neighboring groups [118b]. On this basis, there is no evidence for methyl participation in pinacolyl and no need to invoke high k_{-1}/k_2 ratios for isopropyl.

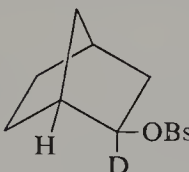
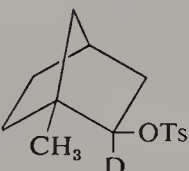
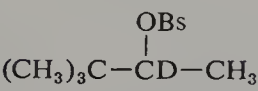
β -Deuterium isotope effects have also been used as mechanistic criteria, but their magnitude appears to be more variable, depending to a significant extent on substrate structure and conformation. Readers are referred to the reviews by Shiner [107] and by Sunko and Borčić [117] for detailed discussion.

* Schubert considers this possibility and argues that "the deuterium in the nonmigrating group would lie β to a developing cationic center" ($k_{\text{H}}/k_{\text{D}}^\beta > 1$). However, the reorganization at the migrating origin in the transition state of a participating system is known to be relatively minor [125]. Entries in Table 24 show that inverse γ -deuterium isotope effects are actually observed in systems undergoing concerted migration.

Table 23 α -Deuterium Isotope Effects in Participating Systems^a

Type of Participation	Compound	Conditions ^b	k_H/k_D per D
n		96% E 40.5°	1.00
n		96% E 40.5°	1.08
σ		Various	1.13–1.21
σ		60% aqueous diglyme 40°	1.10
π		HCO ₂ H 25° HOAc 50°	1.113 1.15
π		HCO ₂ H 25° HOAc 75°	1.102 1.18
π		HCO ₂ H 25° HOAc 93.9°	1.105 1.03
π		HOAc	1.07
π		96% E 50°	1.13
π		HOAc 30°	1.13

Table 23 (continued)

Type of Participation	Compound	Conditions ^b	k_H/k_D per D
σ		HOAc 25.15°	1.21
σ		HOAc 20.1°	1.23
$\sigma(?)$		97% T, 25° 70% T, 25° 50% E, 25°	1.153 1.152 1.159

^a Ref. 117.^b The percentages refer to the organic component of aqueous mixtures; E = ethanol, T = trifluoroethanol.

Two examples suffice here. Both deal with tertiary substrates, where, obviously, the observation of α -D effects is not possible. Frisone and Thornton [126] have found that k_H/k_D for *t*-butyl chloride-*d*₉ does not vary significantly in six solvents of the same ionizing power but differing nucleophilicity and electrophilicity. This was felt to indicate that the transition state was ion pair-like with little interaction between solvent and substrate. β -Deuterium isotope effect data and other criteria have been used also to establish that an apparent S_N2 reaction at a tertiary center in fact involves rate-limiting nucleophilic attack on an ion pair rather than on covalent substrate [127].

4.2. Interconversion of Substrates Through a Common Ion-Paired Intermediate

Although ¹⁸O scrambling studies provide one of the best methods for detection of ion pair return, such studies are not easily carried out. Several workers have utilized an alternative approach which relies on the interconversion of isomeric neutral substrates through a common ion pair. The application of this technique to the allylic isomers, α -methyl- γ -phenyl- (23)

Table 24 γ -Deuterium Isotope Effects^a

Substrate	Conditions	Total k_H/k_D	Mechanistic Observations
$CD_3CH_2CH_2Br$	H_2O , 80°	0.921	S_N2
$CD_3CH_2CH_2OMs$	H_2O , 60°	0.943	S_N2
3,3,4,4- d_4 -Cyclopentyl brosylate	HOAc, 50°	0.95	Solvated ion pair S_N2
$CD_3CH_2CCl(CH_3)_2$	80% EtOH, 25°	0.975	S_N1
$(CD_3)_2CH-CH_2Br$	H_2O , 95°	0.958	S_N2 or H participates
$(CD_3)_2CH-CH_2OMs$	H_2O , 90°	0.968	S_N2 or H participates
$\phi_2C(OH)C(OH)(CD_3)_2$ [124]	50% H_2SO_4 , 25°	1.18 ^b (0.97) ^c (1.20) ^d	Methyl participates?
$(CD_3)_2CHCH(OTs)CH_3$	HOAc	1.00	H participates
$(CD_3)_3CCH(OBs)CH_3$	97% CF_3CH_2OH , 25°	1.011	Methyl participates?
	50% EtOH, 25°	1.003	
$(CD_3)_3CCH_2OSO_2(C_6H_5)(NO_2)_2$	97.3% CF_3COOH 0.17 M CF_3COONa	1.02 ± 0.04	Methyl participates

^a Taken from ref. 107 unless otherwise indicated.^b Total effect, i.e., the ratio of the rate of the completely nondeuterated compound to that of the deuterated derivative shown.^c k_H/k_D of nonmigrating methyl in $\phi_2C(OH)C(OH)CD_3CH_3$.^d k_H/k_D of migrating methyl in $\phi_2C(OH)C(OH)CD_3CH_3$.

and α -phenyl- γ -methylpropenyl (22) *p*-nitrobenzoate by Sneen and Rosenberg [58] and by Goering and Linsay [68] was discussed in Section 3.1. The fraction of intimate ion pair return (1-*F*) for this and several other systems are presented in Table 25.

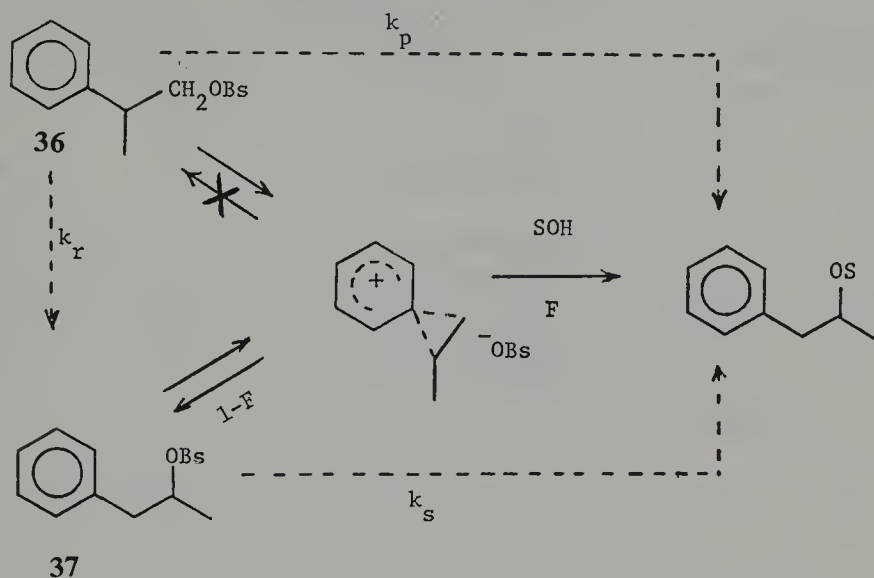
The results for 2-phenyl-1-propyl tosylate (36) (Scheme IX), studied by Diaz and Winstein [129] illustrate the method.

If the primary compound 36 is solvolyzed, the observed rate will be given by Eq. 31:

$$k_{\text{obsd}} = k_p F_p + k_s (1 - F_p) \quad (31)$$

where k_{obsd} is the instantaneous rate constant and F_p is the mole fraction of substrate present as 36 at any time [50, 129]. A steadily increasing rate constant will be observed if return to 37 is occurring, since 37 is much more reactive than 36. The changing rate constant k_{obsd} can be obtained either graphically (from the tangent of the rate curve) or more accurately by a complicated iterative procedure [50]. The rate constant for product formation from 36, k_p , can be obtained by extrapolating the instantaneous rate constant

to time zero, while k_s is simply the rate constant for solvolysis of **37**. Solution of Eq. 31 then yields values for F_p at different times.



Scheme IX. Ion Pair Return in the 2-phenyl-1-propyl tosylate system. The dashed arrows do not denote a mechanistic pathway but refer to overall rates.

The concentration of **36** at any time is given by $([36]_{t=0} - [\text{Product}]_t)F_p$, or $(a - x)F_p$; this concentration should decrease at a rate given by $(k_r + k_p)$: Solution of Eq. 32 using values of F_p from Eq. 31 gives $(k_r + k_p)$.

$$\ln \frac{a}{(a - x)F_p} = (k_r + k_p)t \quad (32)$$

Since k_p measures the amount of ion pair that goes to product and k_r measures the amount of ion pair that returns to **36** (no **36** is formed upon return), F is given by $k_p/(k_r + k_p)$.

When an achiral ion pair interconnects two enantiomers, F can be evaluated by measuring both the polarimetric (k_a) and the titrimetric (k_t) rate constants. Examples include the *exo*-2-norbornyl, *threo*-3-aryl-2-butyl and *trans*-2-aryl-cyclopentyl systems (Table 25).

Scheme X, involving the competition between discrete anchimerically assisted (k_Δ) and solvent assisted (k_s) pathways, governs these cases [19, 94, 133–136]. As Eqs. 32 and 33 define k_a and k_t , respectively, it follows that F is given by Eq. 34 [138]:

$$k_a = k_\Delta + k_s \quad (32)$$

$$k_t = Fk_\Delta + k_s \quad (33)$$

$$F = \frac{k_t - k_s}{k_a - k_s} \quad (34)$$

Table 25 Ion Pair Return Measured by Rearrangement

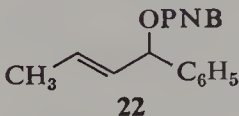
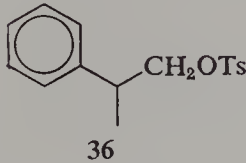
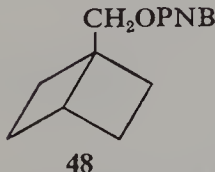
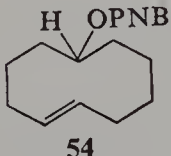

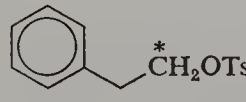
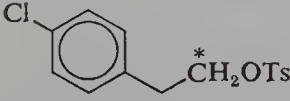
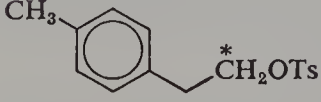
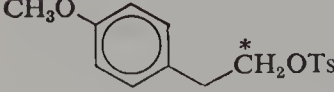
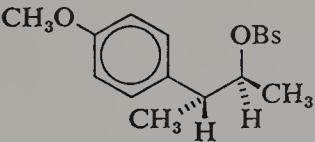
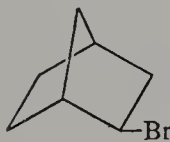
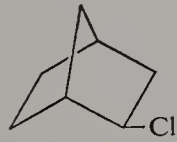
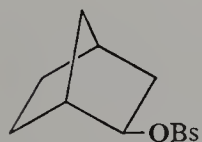
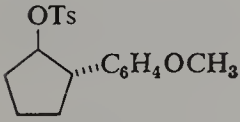
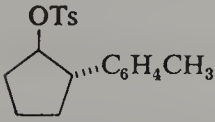
Compound	Solvent (Temp)	(1-F) ^a	Ref.
 22	CH ₃ OH (35°) 60% Dioxane (25°)	0.27 0.39	58 58, 128
 36	Ethanol (50°)	~0	129
	80% Ethanol (75°)	~0	48
	CH ₃ CO ₂ H (75°)	0.82	129
	HCO ₂ H (50°)	0.0	129
	CF ₃ CO ₂ H (25°)	0.91	129
 48	60% Acetone (117°)	0.81	103
 54	90% Acetone (118°)	0.18	106
	80% Acetone (118°)	0.15	106
 	75% Acetone (75°)	0.38	132
 	CF ₃ CO ₂ H (75°)	0.58	130
	CH ₃ CO ₂ H (90°)	0.62	131
	HCO ₂ H (74°)	0.09	137
	HCO ₂ H/NaOTs (74°)	0.15	137
 	CH ₃ CO ₂ H (90°)	0.62	131
 	CH ₃ CO ₂ H (90°)	0.65	131
 	CH ₃ CO ₂ H (75°, 90°)	0.60, 0.62	49, 130, 131

Table 25 (continued)

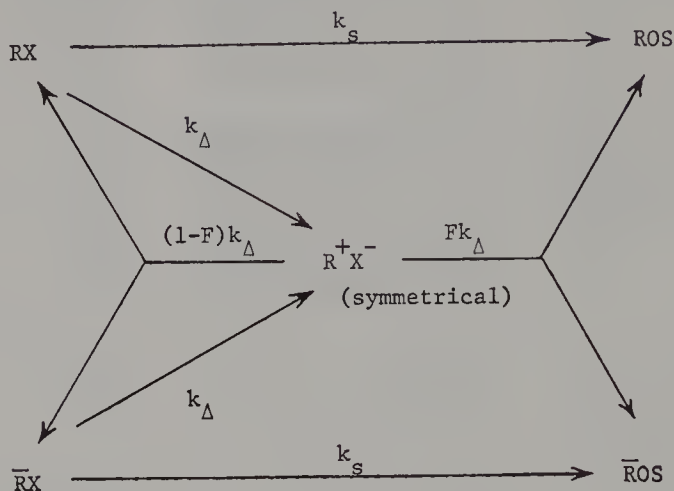
Compound	Solvent (Temp)	(1-F) ^a	Ref.
	75% AcOH-25% HCO ₂ H	0.09 ^b	19
	AcOH	0.76 ^b	19, 133
	50% AcOH-50% Ac ₂ O	0.44 ^b	19, 133
	EtOH	0.23 ^b	19
	10% HCO ₂ H-90% Dioxane	0.94 ^b	19
	<i>n</i> -C ₇ H ₁₅ CO ₂ H	0.86 ^b	19
	Ac ₂ O	0.76 ^b	19, 133
	10% AcOH-90% C ₆ H ₆	0.94 ^b	19
	Acetone	0.88 ^b	19
	12.5% AcOH-87.5% Dioxane	0.95 ^b	19
	HOAc	0.96 ^b	19
	HCO ₂ H	0.80 ^b	19
	HOAc	0.91 ^b	134
	HCO ₂ H	0.75 ^b	134
	HOAc	0.71 ^b	135
	EtOH	0.66 ^b	135
	75% Acetone-25% H ₂ O	0.29 ^b	135
	HOAc (50°)	0.72 ^{b,c}	136
	HOAc (50°)	0.71 ^{b,c}	136

^a F is the fraction of intimate ion pair which yields solvolysis product, and 1-F is the fraction which returns to neutral substrate.

^b Calculated from polarimetric/titrimetric rate ratios: $k_a/k_t = 1/F$.

^c Corrected for a k_s component (see text).

Only when the solvent-assisted pathway k_s contributes negligibly does Eq. 34 reduce to $F = k_t/k_\alpha$. An example is afforded by the 2-*exo*-norbornyl solvolyses. Precise methods are now available for evaluating the component terms of Eq. 33 for phenonium ion systems, and hence Eq. 34 can be evaluated if the necessary values of k_α are known.



Scheme X

One entirely similar approach, first employed by Jenny and Winstein [49], can be applied to achiral systems like β -arylethyl which can give rise to symmetrical ion pair intermediates. In these cases, ^{14}C or D-label scrambling in recovered starting material must be measured as a function of time; label scrambling in the product must be determined, and it is desirable to measure this also as a function of time since there is some variation [131]. For this case,



Scheme X applies and the rate of ^{14}C scrambling (k_{14}) in recovered tosylate is defined by Eq. 35:

$$k_{14} = (1 - F)k_\Delta = k_\Delta - Fk_\Delta \quad (35)$$

Since only the aryl-assisted pathway leads to label scrambling, Eqs 36 and 37 provide the necessary additional data for evaluation of F or $1 - F$ [49, 131]. (Note that for the purposes of these equations, complete scrambling is defined as 50% label rearrangement.)

$$\frac{k_\Delta}{k_s} = \frac{\% \text{ label rearrangement in product (time} = \infty)}{50 - \% \text{ label rearrangement in product (time} = \infty)} \quad (36)$$

$$\frac{Fk_\Delta}{k_s} = \frac{\% \text{ label rearrangement in product (time} = 0)}{50 - \% \text{ label rearrangement in product (time} = 0)} \quad (37)$$

The value of $1 - F$ varies with substrate structure, leaving group, and solvent (Table 25). However, for a given β -arylalkyl system, $1 - F$ does not vary much with changes in the aryl group. There is always less intimate ion pair return in formic acid and in alcohols or aqueous alcohols than in acetic and trifluoroacetic acids.

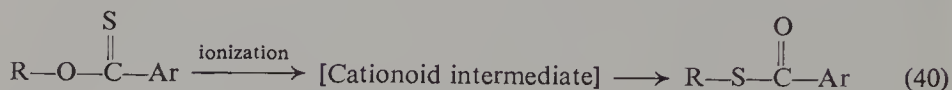
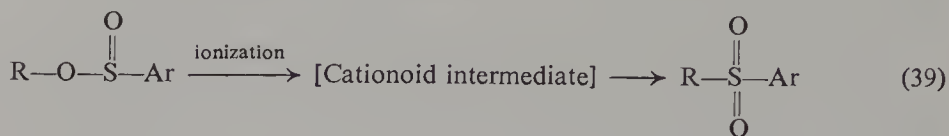
The results in the latter solvent are pertinent when it is recalled that Shiner postulates that ion pair return for isopropyl brosylate in trifluoroacetic acid may be many thousands of times faster than conversion to product. The ratio of ion pair return to product formation $[(1 - F)/F]$ for 2-phenylethyl tosylate in trifluoroacetic acid is only 1.4 and the value for **36** is 10; these are among the highest values in Table 25. Thus there is no direct support for Shiner's extreme values. It must be conceded, however, that "hidden return" cannot be ruled out. Following Winstein [19], intimate ion pairs in rearranging systems have traditionally been formulated as having *bridged* structures, and for the 2-norbornyl, 2-arylethyl, and 3-aryl-2-butyl systems, such structures would be symmetrical. If this is actually the case, then there exists no experimental support for Shiner's implications that $1 - F$ values can closely approach unity. However, there may be another kind of "intimate" intimate ion pair which retains the essential structural features of the starting material but has a lengthened bond to the leaving group, $C^{\delta+} \cdots X^{\delta-}$. Return from this type of ion pair would not involve any rearrangement, racemization, ^{14}C scrambling, or even ^{18}O scrambling in the leaving group and hence would be "hidden." Such an ion pair is obviously difficult to differentiate from covalent starting material. Although this kind of hypothetical "intimate" intimate ion pair has, in effect, been postulated by several groups of workers recently [47, 111, 112, 136, 139], there is, as yet, no unambiguous experimental evidence for the existence of such species. This matter is discussed in more detail in Section 6.

4.3. Polydentate Leaving Groups

One of the most elegant methods for the detection of return to neutral substrate after ionization involves the labeling of one oxygen of a benzoate or sulfonate ester and determination of scrambling resulting during reaction (Section 3). An alternative but similar method employs a polydentate leaving group (i.e., one with different kinds of atoms which may become attached to the cationic portion).^{*} Three reactions which have been utilized for this purpose are shown in Eqs. 38–40. The cationoid intermediate in each case

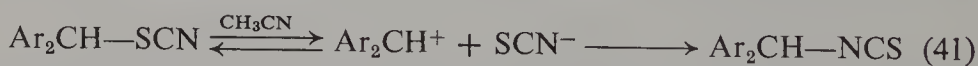
^{*} Strictly speaking, of course, a labeled benzoate or arenesulfonate anion is a polydentate leaving group.

appears to be a tight ion pair; further dissociation may also be involved in some instances.



The isomerization of thiocyanates to isothiocyanates (Eq. 38) is the most studied of these polydentate rearrangements [140, 141], with research groups led by Fava [140, 142–146, 148–150] and Spurlock [141, 151–158] being the primary contributors. The first systematic mechanistic study by Illiceto, Fava, Mazzucato, and Rossetto [142] showed that the isomerization of benzhydryl thiocyanate in inert (nonhydroxylic) solvents (1) is cleanly first order, (2) is accelerated by increasing solvent polarity, and (3) exhibits salt effects and ρ values similar to those for solvolysis of benzhydryl derivatives. These results are consistent with an ionization-recombination mechanism for isomerization (Eq. 38).

Information regarding the nature of the cationoid intermediate was derived from isomerization of 4,4'-dimethylbenzhydryl thiocyanate in the presence of $^{35}\text{SCN}^-$ [143]. Although a small amount of $\text{R}-^{35}\text{SCN}$ and $\text{R}-\text{NC}^{35}\text{S}$ was formed during isomerization, the amount was far less than that expected on the basis of either dissociated ion (Eq. 41) or solvent-separated ion pair (Eq. 42) pathways. However, the fact that some incorporation of



^{35}S -label occurred indicates that a small portion ($\approx 5\%$) of the reaction in acetonitrile does proceed through a species in which the leaving group exchanges with added $^{35}\text{SCN}^-$. However, since most of the isomerization proceeds through a polar intermediate which does not “mix” with added common ion, an intimate ion pair must be the major product-producing intermediate. The observation that chiral *p*-chlorobenzhydryl thiocyanate isomerizes with partial net retention of configuration in a variety of aprotic solvents is also consistent with reaction via an intimate ion pair [144, 145].

The identity of the intermediate involved in ^{35}S exchange was determined by studying the isomerization of 4,4'-dimethylbenzhydryl thiocyanate during

solvolysis in 95 % aqueous acetone in the presence of added $^{35}\text{SCN}^-$ (Eqs. 43) [146]:



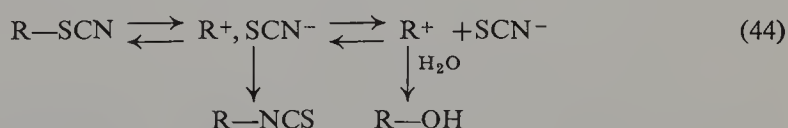
The rate of solvolysis was observed to *decrease* with added common ion, while the rate of exchange *increased* as shown in Table 26. Interestingly, the

Table 26 Rates of Solvolysis (k_{solv}), and ^{35}S Isotopic Exchange (k_{ex}) and Isomerization (k_{isom}) of 4,'4-Dimethylbenzhydryl Thiocyanate in 95 % Acetone^a

$10^2[\text{NaSCN}]$	10^5k_{solv}	10^5k_{ex}	$10^5(k_{\text{solv}} + k_{\text{ex}})$	10^5k_{isom}
0	5.60	—	5.60	8.60
0.21	4.68	1.01	5.69	8.30
0.50	3.23	2.08	5.31	7.27
1.1	2.68	2.88	5.56	7.44
2.0	1.68	3.53	5.21	6.67
4.0	0.97	4.65	5.62	6.40

^a Taken from ref. 140, p. 80, and ref. 145.

sum of $k_{\text{solv}} + k_{\text{ex}}$ was nearly constant and was equal to the rate of solvolysis in the absence of SCN^- . These data indicate that both exchange and solvolysis proceed through the same intermediate. Since common ion rate depression is generally attributed to a decrease in the rate of product formation via free carbonium ions (Section 2.1), the intermediate giving exchange and isomerization must be a free carbonium ion (Eq. 41) rather than a solvent-separated ion pair (Eq. 42). The rate of the isomerization reaction was only slightly decreased by added common ion and was probably occurring largely via the intimate ion pair. Therefore in 95 % aqueous acetone such benzhydryl thiocyanates react as shown in Eq. 44:



For benzhydryl derivatives, from 2 to 8.5 % of the intimate ion pairs appear to undergo dissociation in acetonitrile [143, 145, 146]. The S attack is about five to eight times faster than N attack [145] with cationoid species generated from solvolysis or deamination [147].

In addition, a bimolecular exchange mechanism appears to operate with *p*-nitrobenzhydryl [148] and benzyl [149] thiocyanates; second-order kinetics are observed with SCN^- in CH_3CN . Rate-limiting displacement on intimate ion pair could be responsible, but attack on covalent substrate seems more likely.

Fava and his co-workers [150] have also studied the solvolysis, isomerization, and exchange of *p*-chlorobenzhydryl thiocyanate in 80% aqueous acetone; the results again indicate nucleophilic attack. There is a mass law effect on the solvolysis rate (curve C, Fig. 5), but unlike the case of 4,4'-dimethylbenzhydryl thiocyanate in 95% acetone, the increase in exchange (curve B) more than makes up for the decrease in solvolysis rate. These results are interpreted to indicate that isotopic exchange occurs by two different pathways: (1) return from free carbonium ion and (2) direct displacement either on neutral substrate or on intimate ion pair. The rate of exchange via free carbonium ion should be given by the solvolysis rate in the absence of added common ion minus the depressed solvolysis rate:

$$k_{\text{ex}}(\text{via } \text{R}^+) = k_s^0 - k_s \quad (45)$$

If this term is subtracted from the total exchange rate, a straight line is obtained (curve D, Fig. 5) which passes through the origin and represents the bimolecular exchange pathway.

The initial substitution rate of *p*-chlorobenzhydryl thiocyanate increased linearly with added NaN_3 [150] and was considerably faster than the isomerization rate. Since the ionization rate cannot be much greater than the isomerization rate [143, 145, 146], it then seems necessary to conclude that attack by N_3^- (and SCN^-) takes place by direct displacement on neutral substrate. This appears to provide one of the few pieces of direct evidence for such a process.

However, it is disquieting to note that the addition of NaN_3 *does not suppress* the racemization of substrate [150]. Goering (Section 3.2) observed

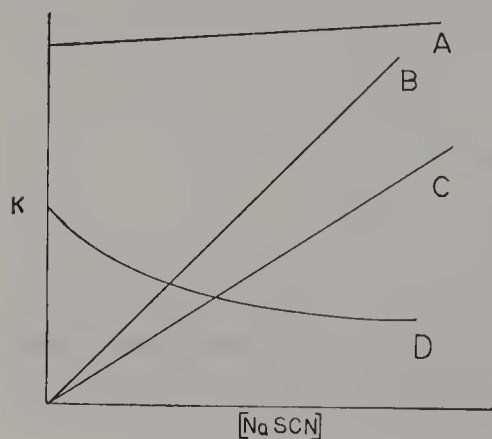
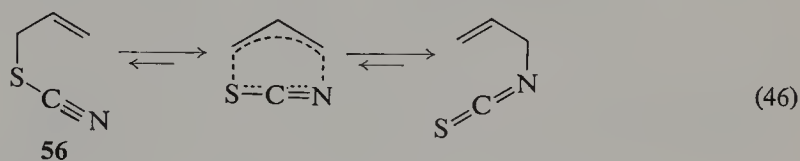


Figure 5. Initial first-order rates of solvolysis, isomerization, and exchange of *p*-chlorobenzhydryl thiocyanate in 80% aqueous acetone [150]. A, k_{isom} (Eq. 43b); B, k_{ex} (Eq. 43c); C, k_{solv} (Eq. 43a); D, $k_{\text{ex}} - (k_s^0 - k_s)$, bimolecular exchange.

that added NaN_3 essentially eliminates racemization, but not oxygen scrambling, of *p*-chlorobenzhydryl *p*-nitrobenzoate in 80% acetone [73]. This was assumed to mean that N_3^- was attacking a solvent-separated ion pair (and thus eliminating external ion pair return and racemization), but that N_3^- was not eliminating the internal return with retention from the tight ion pair which gives ^{18}O scrambling. A similar interpretation of the thiocyanate studies would suggest that racemization, as well as isomerization, can occur at the intimate ion pair stage.

Allylic thiocyanates isomerize with greater ease than corresponding benzylic systems due to the availability of the concerted, electrocyclic mechanism, Eq. 46 [140]. An ion pair mechanism is ruled out by the insensitivity of such



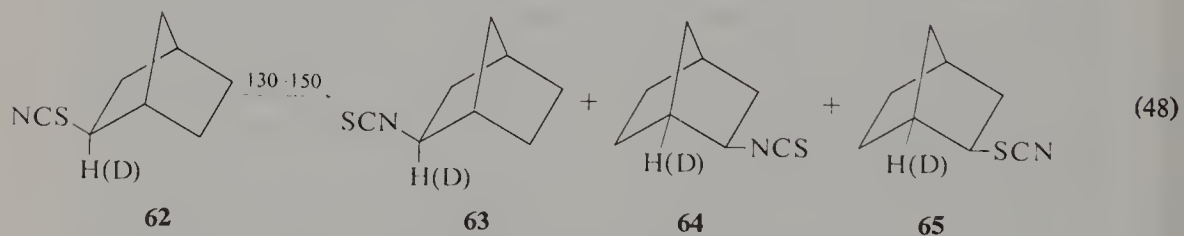
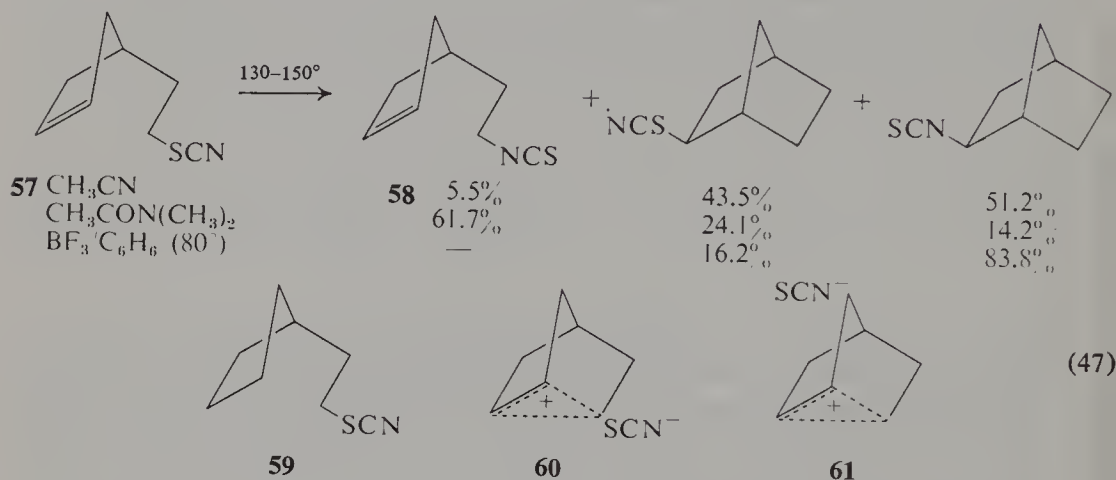
allylic rearrangements to changes in structure or in reaction medium. In aqueous solvents practically no solvolysis takes place during rearrangement.

Allyl thiocyanate isomerizations are also remarkable in being among the few in which conversion to isothiocyanate is not complete: 8% of **56** is present at equilibrium in CH_3CN [140]. Isothiocyanate is a very poor leaving group, and alkyl isothiocyanates ($\text{R}-\text{N}=\text{C}=\text{S}$) are generally thermally stable when an ionic or ion pair mechanism is the only decomposition pathway available. As expected, isothiocyanates which can give rise to a particularly stable carbonium ion do react. Thus 2% of benzhydryl thiocyanate is present at equilibrium [140]. Furfuryl thiocyanate is present to a remarkably high extent (10–20%, depending on solvent) at equilibrium with furfuryl isothiocyanate; the high solvent dependence of rate demonstrates the ionic nature of this interconversion [153].

Spurlock's group has studied the isomerization of a number of alkyl thiocyanates which give rise to nonclassical carbonium ion intermediates in aprotic solvents [141, 151, 152, 154–158]. Although the general behavior (e.g., relative rates [157, 158]) of these thiocyanate isomerizations parallels that found for the solvolysis of the analogous tosylates or chlorides, some interesting contrasts reveal details of the behavior of intimate ion pairs.

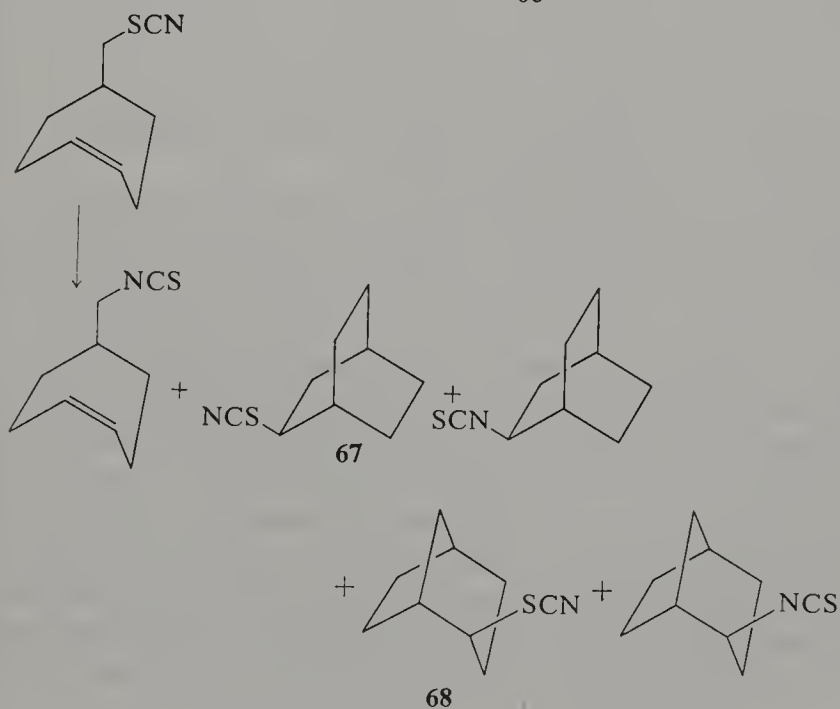
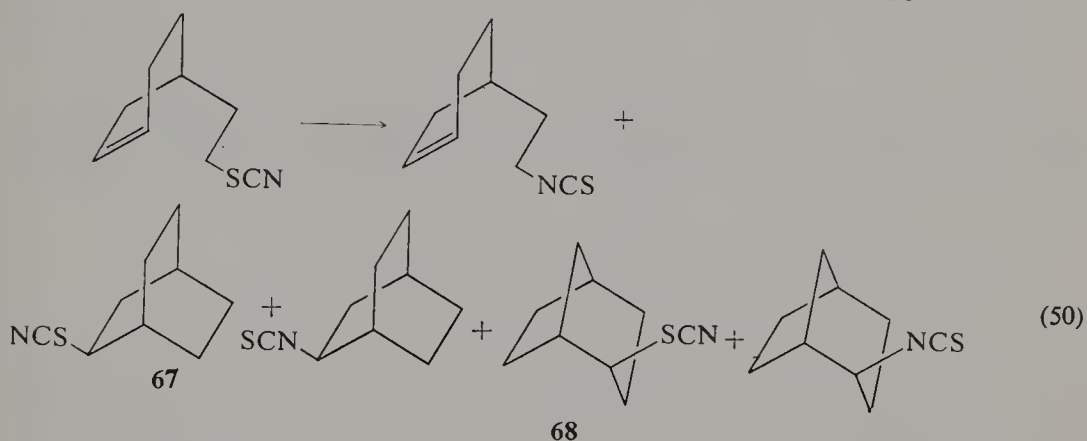
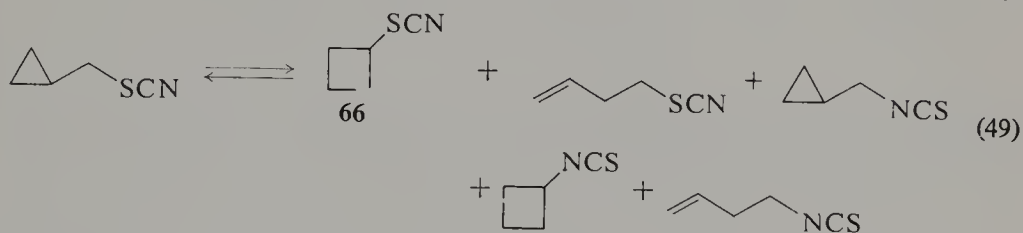
The alkyl thiocyanate isomerizations show all the characteristics of ionic processes: first-order kinetics, strong dependence of rate on solvent ionizing power, Lewis acid catalysis, and structural effects on reactivity. The absence of a LiClO_4 special salt effect [151, 152], the relatively slow incorporation of $^{35}\text{SCN}^-$ into the product, [154], and other lines of evidence suggest that isomerization occurs mostly at the intimate ion pair stage.

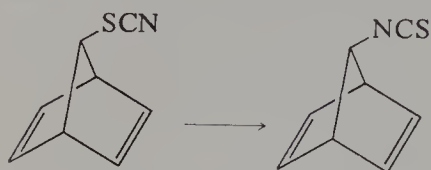
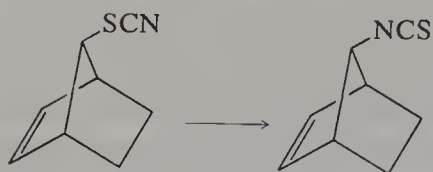
The product distributions are kinetically controlled but are often remarkably sensitive to the ionizing power of the solvent, the presence of KSCN, and sometimes even the presence of KClO_4 . They are also affected by the presence of Lewis acids and even the mode of entry (e.g., whether via σ or π route) to a carbocationic system. This behavior is convincingly interpreted as being due to the rapid collapse of intimate ion pairs before migration of the anion to an alternative site can take place. The norbornyl system (Eqs. 47 and 48) affords a good illustration [152, 154].



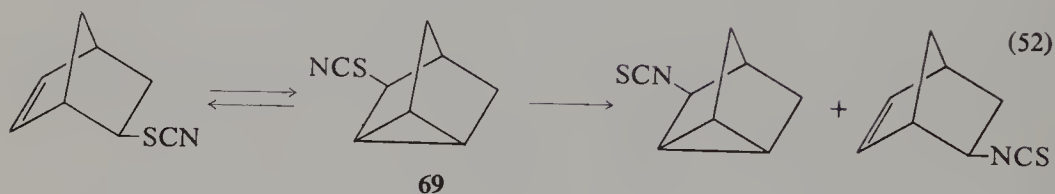
The reaction of **57** is remarkable in giving uncyclized, but rearranged product, **58**. The participation of the double bond in the reaction of **57** was demonstrated by the inertness of the saturated analog **59** under the same conditions. The π route ion pair, **60**, evidently reacts at C_6 , the only example of such attack available. Spurlock suggests that **60** may be isomeric with the ion pair **61** generated by the sigma route because of the relative locations of the leaving groups in the respective ground states, **57** and **62**. Ion pair **60**, but not **61**, might collapse to **58**; **58** is not found among the products of **62**. The use of ionizing solvents or the addition of BF_3 increases the lifetime of the ionic intermediates from **57** and favors norbornyl (cyclized) products.

2-*exo*-Norbornyl thiocyanate (**62**) gave only 2-*exo*-norbornyl products, and deuterium labeling permitted a closer study of this reaction [154]. In the reaction of **62** isothiocyanates **63** and **64** were formed in equal amounts, and no 6,2- or 3,2-hydride shifts were observed. Optically active **62** was rapidly racemized ($k_a/k_{\text{isom}} = 2.85$) during the reaction (giving **65**) and the isothiocyanate formed was racemic (i.e., consisted of equal amounts of **63** and **64**).

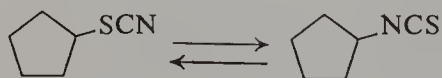




(51)



(52)



(53)

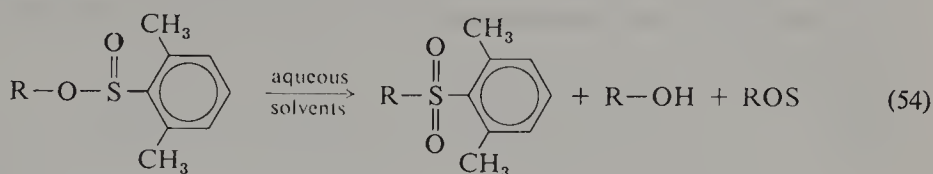
It was concluded that "no evidence was found which was inconsistent with a symmetrical bridged norbornyl cation" [141].

Equations 49 [151, 158], 50 [155], 51 [156], 52 [157], and 53 [158] summarize other reactions studied by Spurlock's group. In addition, the thiocyanate isomerization products **48–51** were studied independently. The results afford additional evidence for the intermediacy of isomeric intimate ion pairs, since the product ratios again appear to be significantly influenced by the position of the counterion with respect to the carbon framework.

The rearrangement of sulfinates to sulfones (Eq. 39) has also been extensively investigated and, as in the case of thiocyanates, it appears that intimate ion pairs provide a major pathway for isomerization [159–163]. Again, however, some dissociation to a more ionized species takes place.

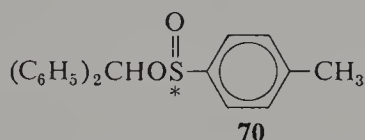
That the isomerization of alkylsulfinates to sulfones is an ionization process was shown by the sensitivity of the reactions to solvent polarity and carbonium ion stability [159, 160]. Darwish and McLaren [159] investigated

the nature of the cationoid intermediate by adding common (sulfinate) ion to several isomerization reactions (*t*-butyl, α -phenylethyl, benzhydryl) which gave sulfone as well as solvolysis product (Eq. 54). Since the added common

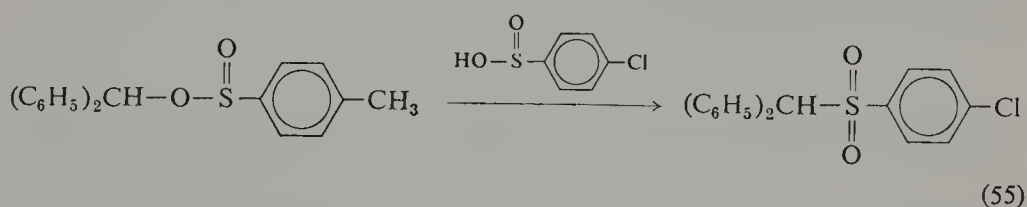


ion generally had no effect on the ratio of sulfone to solvolysis product, it appears that most of the sulfone is not formed from any dissociated species which is under competitive attack by ArSO_2^- and solvent. This interpretation is also consistent with the observation that solvolysis of the corresponding alkyl chlorides or bromides in the presence of ArSO_2^- gives no sulfone formation.

Fava and his co-workers [161] have shown that there is return from the first formed ion pair to neutral substrate by demonstrating that $k_a/k_{\text{isom}} = 2.6$ for optically active **70**. Even in acetic acid, sulfone is the major product, and very



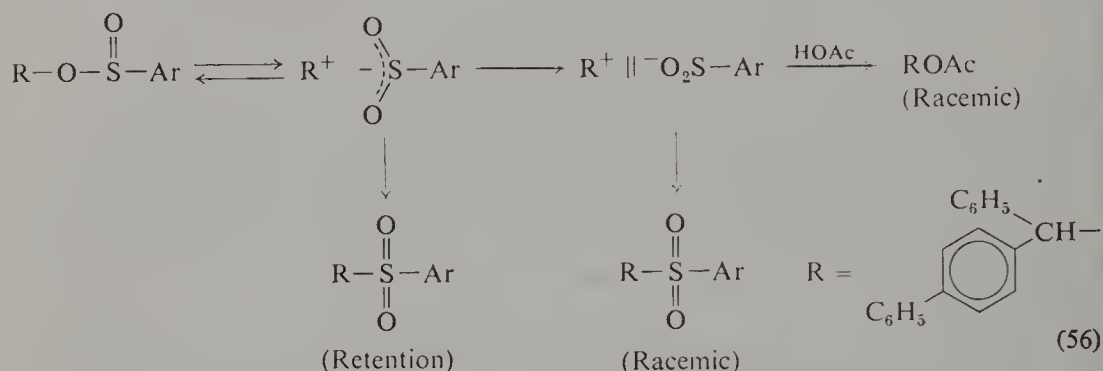
little acetate forms. Similar results were obtained by Darwish and McLaren for optically active α -phenylethyl and α -(*p*-methoxyphenyl)ethyl 2,6-dimethylbenzenesulfinate [162]. The observations of Wragg, McFadyen, and Stevens [160], who showed that there is some exchange of counterion (Eq. 55), and of Darwish and Preston [163], who demonstrated that a significant



proportion of the intermediate in the reaction of trityl 2-methylbenzenesulfinate could be trapped by azide ion, indicate that solvent-separated ion pairs or dissociated ions can also play a role in these reactions (at least with substrates which could give rise to relatively stable carbonium ions).

A much more detailed understanding of this mechanism results from the recent work of Fava and his associates [164], who examined the acetolysis of optically active (asymmetric sulfur and carbon) *p*-phenylbenzhydryl *p*-toluenesulfinate. They found: (1) the starting substrate undergoes epimerization at sulfur (oxygen scrambling) with complete retention of configuration

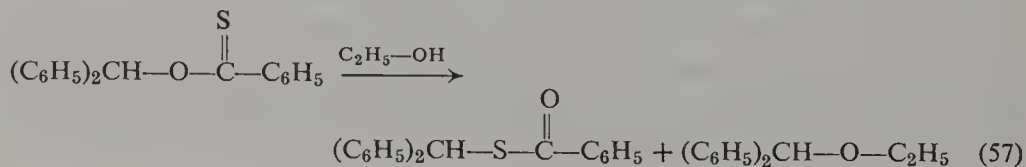
at carbon; (2) optically active sulfone is formed in 33% optical purity, presumably with overall retention; (3) a small amount (*ca.* 20%) of racemic acetate is formed; and (4) added labeled sulfinate anion is not incorporated into the sulfone or into the unreacted ester. These results are best interpreted in terms of Eq. 56.



Sulfone formation from the intimate ion pair must take place with retention of configuration. The observed formation of racemic sulfone shows that there must be formation of a more dissociated species which does not return to the intimate ion pair, but which gives racemic sulfone and acetate. The failure to observe external anion incorporation shows only that there is no return from the solvent-separated ion pair as indicated by the nonracemization of starting material.

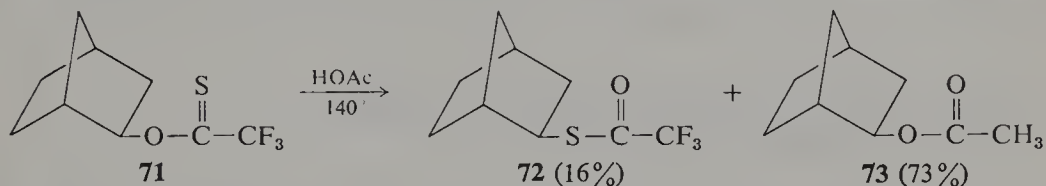
In summary, then, it appears that sulfone can form from both solvent-separated ion pairs and intimate ion pairs, but the solvolysis product forms via the solvent-separated ion pair exclusively. Return from the intimate ion pair is especially facile; however, external return was observed in only a few of the systems investigated.

The isomerization of thionbenzoates ($\text{R}-\text{O}-\overset{\text{S}}{\parallel}{\text{C}}-\text{C}_6\text{H}_5$) to thiolbenzoates ($\text{R}-\overset{\text{O}}{\parallel}{\text{S}}-\text{C}-\text{C}_6\text{H}_5$), although not as extensively studied as the previous two examples, appears to proceed through an intimate ion pair [165]. The reaction gives a ρ^+ of -3.6 , consistent with an ionic process. Reaction in ethanol (Eq. 57) results in the formation of some ether in addition to the major

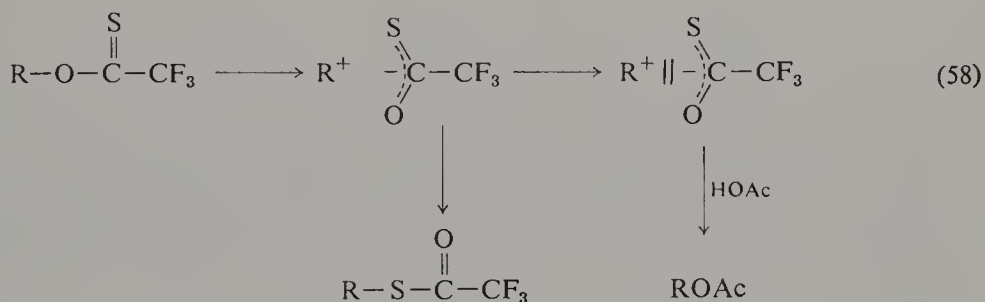


product, thiolbenzoate. If *p*-methoxythionbenzoate salt is added to reaction 57, no exchange is observed, and isomerization via the intimate ion pair is therefore indicated.

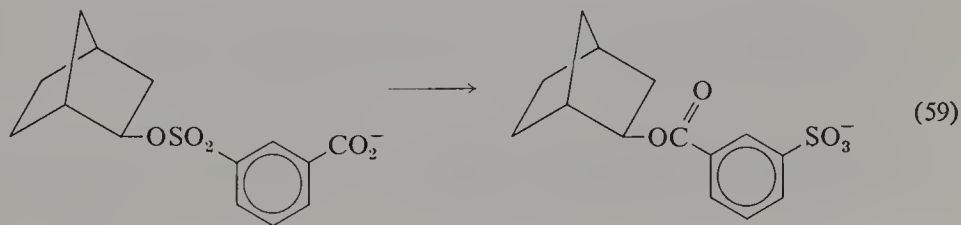
Smith and Petrovich [165b] examined the isomerization of thionbenzoate **71**. As with the analogous thiocyanate [154], the experiment was performed in an effort to determine the importance of ion pair return in the norbornyl system and to minimize competition from hydride shifts. Reaction of **71-2-d**



gave **72** with deuterium equally distributed between C-1 and C-2, thus confirming the absence of hydride shift and demonstrating the formation of a symmetrical (or rapidly equilibrating) intermediate. Acetolysis of optically active **71** gave $k_a = k_t$, therefore there is no ion pair return to **71**. Addition of LiClO_4 resulted in the exclusive formation of solvolysis product **73**, indicating that under these conditions external ion pair return is prevented and the product (derived entirely from attack by solvent) results only from solvent-separated ion pairs. The failure to observe exchange of added sulfinate ion [165a] suggests that there is little external return (to either neutral substrate or intimate ion pair), even in the absence of LiClO_4 ; together these data indicate that isomerization and solvolysis take place via different intermediates (Eq. 58):



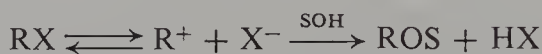
A fourth type of polydentate leaving group was also utilized to study the *exo*-2-norbornyl system by Corey and his co-workers [166] (Eq. 59):



In this case the two nucleophilic centers of the leaving group are *meta* substituents on a benzene ring. Consequently, while the carboxyl group cannot interact with the cationic center before ionization, it was anticipated that ion pair return would give the more stable carboxylate ester. When optically active starting material was rearranged in either *t*-butyl alcohol or aqueous tetrahydrofuran, the product was completely racemic within experimental error. These results again were interpreted [166] to indicate the formation of symmetrical intermediates in the ionization *exo*-2-norbornyl derivatives.

5. ION PAIRS IN THE SOLVOLYSIS OF PRIMARY AND SECONDARY DERIVATIVES

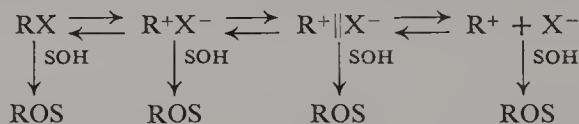
The mechanisms of solvolysis reactions originally were discussed in terms of Schemes XI and XII [6]. These were later expanded and combined to give Scheme XIII, which includes ion pairs as well as the carbonium ion [19].



Scheme XI. Representation of the unimolecular mechanism for solvolysis with direct ionization to a dissociated carbonium ion.



Scheme XII. Representation of the bimolecular mechanism for solvolysis.



Scheme XIII. Combined unimolecular and bimolecular mechanism (including ion pairs).

The reaction represented by Scheme XII has been termed the bimolecular mechanism, S_N2 , and direct displacement. Scheme XI represents a two-stage reaction where the first step (formation of an unstable carbonium ion intermediate) is rate limiting. This has been termed unimolecular, limiting, and S_N1 .

Ingold proposed six criteria that may be used for the mechanistic assignment of nucleophilic substitution reactions [7]:

1. The kinetic form of the substitution reaction.
2. The effect on rate of structural changes in the substrate.
3. The effect on rate of changes in the nucleophile.
4. The effects on rate and products of changes in solvent.
5. Salt effects on rates and products.
6. The stereochemistry of the reaction.

Extensions and modifications of these criteria have subsequently been used by a variety of workers, and Table 27 presents a summary of predictions and observations.

For a large number of solvolysis reactions the assignment of mechanism to either Scheme XI or Scheme XII was formerly thought by most chemists to be rather straightforward. Consider, for example, the solvolysis of primary or methyl derivatives in highly nucleophilic (e.g., aqueous) media. These derivatives should show little or no steric hindrance to nucleophilic attack by solvent, and they would certainly not give very stable carbonium ions. One is led directly to the conclusion that such reactions should proceed via the mechanism of Scheme XII, and this conclusion has been almost universally accepted. Similarly, the solvolysis of tertiary alkyl derivatives has long been considered to proceed via the mechanism depicted in Scheme XI; such substrates should suffer the maximum steric interference with the direct displacement of Scheme XII, yet the tertiary carbonium ion would be comparatively stable. Table 27 shows that such simple compounds as ethyl bromide and *t*-butyl bromide are easily classified in terms of Schemes XI and XII on the basis of the various mechanistic criteria.

The problems related to assignment of mechanism in solvolysis reactions have generally involved not primary and tertiary derivatives, but simple secondary analogs.* As might be expected for compounds which are intermediate in degree of substitution at the reaction center, the chemical behavior of secondary derivatives is found by most criteria to be intermediate between that of primary and tertiary substrates. Table 27 illustrates this for the case of 2-propyl bromide.

This intermediate behavior of simple secondary compounds has generally been rationalized by one of two possibilities:

1. The processes of Scheme XI and Scheme XII are occurring simultaneously and competitively, and the measured properties are a weighted average of the properties of the two mechanisms [86, 168, 169].

2. A single mechanism is operating which is "borderline" between Schemes XI and XII; the measured properties resulting from this simple mechanism would also be intermediate between the properties of the extremes [27, 86].

The transition state and consequently the reaction rate of Scheme XI is characterized by the breaking of the bond between carbon and the leaving group; this is followed at some later time by bond making (between carbon and the entering nucleophile). In contrast, the mechanism of Scheme XII

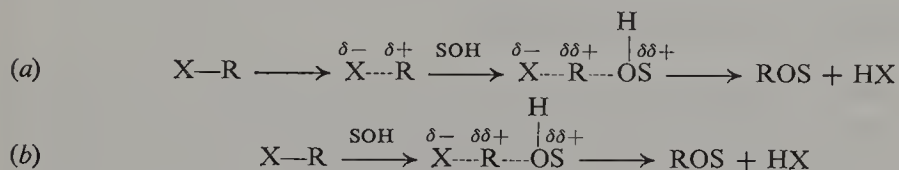
* We are using the term "simple secondary derivatives" to designate those compounds that would not yield resonance-stabilized carbonium ions and do not undergo neighboring group participation.

Table 27 Criteria for the Assignment of Mechanism of Solvolysis^a

Criterion	Scheme XI (S _N 1)	Scheme XII (S _N 2)	<i>t</i> -BuBr	2-PrBr	EtBr
Kinetic form	First order ^b	Pseudo-first order	First order ^c	Pseudo-first order	Pseudo-first order
Common ion effect	Yes (for free C ⁺ but not for ion pair)	No	Small ^d	No	No
Nonnucleophilic salt effect	Small rate increase	Very small	Small ^c	Small	—
Effect of added ⁱ nucleophile	Small (salt) effect on rate, no rate-product correlation	Large rate effect; second-order kinetics; rate-product correlation	Small rate effects ($\beta = 2$); No rate-product correlation	$[\beta \approx 10^3]$ (rate-product correlation)	$[\beta \approx 10^3]$ (rate-product correlation)
Stereochemical outcome	Ideally 50% inversion, 50% retention	100% inversion	(Slight net retention) ^e	(Nearly 100% inv.) ^e	(100% inv.) ^e
<i>m</i> Value ^f	1.0	<0.5	0.94	0.43	0.34
$[k_{\text{EtOH}}/k_{\text{HOAc}}]_{\text{Y}}^f$ (aqueous ethanol)	~ 1	$\gg 1$	3	40	80 ^h
OTs/Br ^{f,g}	$> 10^3$	~ 10	> 4000	40	10

^a Aqueous solvents.^b Small deviations from first order caused by common ion effect [6, 7].^c Small second-order components have been attributed to bimolecular elimination [44].^d See ref. 167.^e Based on similar cpds.^f Data from ref. 23.^g 80% ethanol; this criterion may be complicated by steric effects involving the leaving group; see footnote 20 of ref. 23.^h $[k_{\text{EtOH}}/k_{\text{HCO}_2\text{H}}]_{\text{Y}}$.ⁱ Where $k = k^0(1 + \beta[\text{NaN}_3])$; see ref. 46.

is characterized by simultaneous bond breaking and bond making; these influence the properties of the transition state and thus the reaction rate approximately to the same extent. In the case of a borderline mechanism the process of bond making and breaking would be neither simultaneous and equal (Scheme XII) nor completely separated in time (Scheme XI). Possibilities for such a merged mechanism are presented in Scheme XIV.



Scheme XIV. Representations of the borderline mechanism of solvolysis: (a) with some bond breaking preceding bond making; and (b) with bond breaking and bond making occurring simultaneously but to different extents.

Note that there are different ways in which the borderline mechanism could operate. In Scheme XIVa the disparity between bond making and bond breaking is one of time; substantial weakening of the bond to the leaving group has taken place before formation of a bond to the incoming nucleophile has begun. Scheme XIVb illustrates a possibility in which the two processes begin simultaneously but take place at different rates. Consequently bond breaking in the transition state is greater than bond making, even though both began at the same time. For either Scheme XIVa or XIVb, the transition state (and thus the reaction rate) will be influenced by both bond forming and bond breaking, although the effect of the latter will be greater.

The differences between Schemes XIVa and XIVb are subtle but significant. In Scheme XIVa the solvent plays no initial role (other than electrostatic solvation). Only at a subsequent stage, after substantial charge separation has already developed, does the formation of a covalent bond between the reaction center and a solvent molecule begin. In contrast, the solvent molecule in Scheme XIVb is involved in bond formation from the very beginning of the reaction, and only the greater rate of bond breaking to the leaving group results in a transition state having increased positive charge at the central carbon atom.

Further inspection of Scheme XIVa leads to the observation that since solvent can only attack a species which has a finite lifetime, this solvent attack must take place on an intermediate which has some degree of charge separation between the reaction center and the leaving group. This might be a vibrationally (thermally) excited molecule in which the stretching of the C—X bond results in charge separation; the resulting dipole could certainly provide a driving force for attack by solvent. Such a species having both charge separation and a finite lifetime might be better described as an ion pair; in this case Scheme XIVa blends into Scheme XIII, which includes other

possibilities as well. Similarly, the distinction between Scheme XIVb and Scheme XII is merely one of degree; both schemes involve solvent attack on neutral substrates but lead to different charge distributions in their transition states. Thus the difference between proposals for the detailed mechanism of borderline solvolysis may be largely one of semantics.

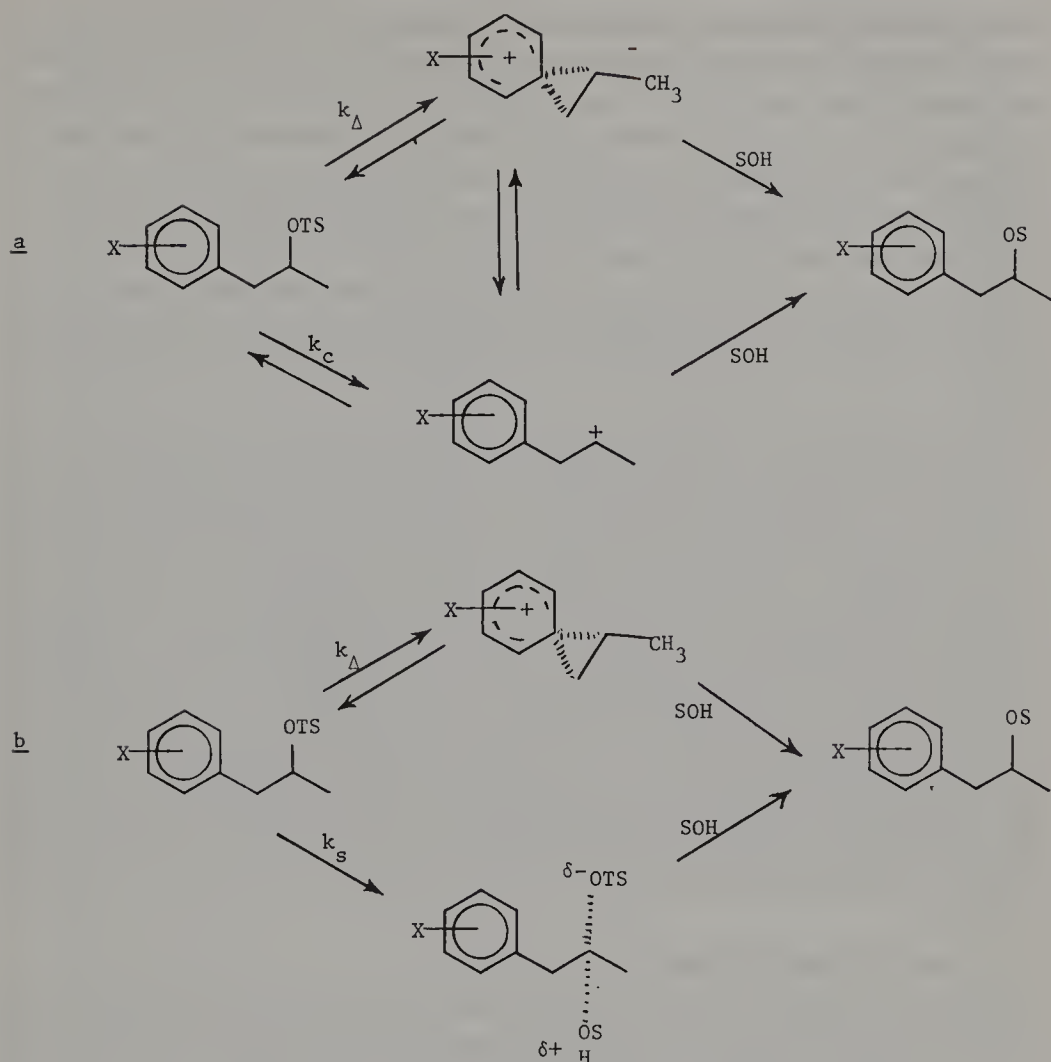
5.1. Competitive S_N1 and S_N2 Reactions

Do borderline substrates (e.g., simple secondary derivatives) solvolyze by two different mechanisms (Schemes XI and XII) operating simultaneously and competitively? If not and only a single "merged" mechanism is operative, does this correspond to Scheme XIVa or XIVb? In other words, do the processes of bond breaking and bond formation differ in time of occurrence (i.e., Scheme XIVa) or in rate of occurrence (i.e., Scheme XIVb)?

The first of these questions has been the subject of debate for many years and free carbonium ions were routinely discussed as intermediates in the solvolysis of primary [170] and secondary [6] derivatives. Even in the presence of substantial recent evidence [4, 23, 46–48, 120, 123, 171–184] to the contrary, the intermediacy of free carbonium ions in the solvolysis of simple secondary [168], primary [6], and even methyl [185] derivatives continues to be suggested. The answer to the question of competing S_N1 and S_N2 processes in the solvolysis of simple secondary derivatives hinges on the presence or absence of free secondary carbonium ions in these reactions.

Beginning in 1969 a series of papers [172–178] from Princeton afforded conclusive evidence against formation of free secondary carbonium ions during solvolysis. For example, the acetolysis and formolysis of a series of 1-aryl-2-propyl tosylates (Scheme XV) were studied. A Hammett treatment of the solvolysis rates indicated that the reactions proceeded via two competing pathways, the "normal" process k_s and participation by the neighboring aryl group k_A . The observation of a rate-product correlation indicated that the two pathways were *discrete* (i.e., no crossover between the pathways occurred). Since only small activation energies would be expected for interconversion of the free carbonium ions and the bridged ions of Scheme XVa, crossover would be anticipated. The absence of crossover indicates the absence of free carbonium ions and that the solvolysis of these derivatives proceeds as in Scheme XVb. Departure of the leaving group is strongly assisted either by neighboring group k_A or by solvent k_s , and the highly encumbered transition states or intermediates involved cannot interconvert.

Since the early 1960s there have been indications in the literature that free carbonium ions are not formed in the solvolysis of simple secondary derivatives. For example, Streitweiser and co-workers [82, 186] studied the acetolysis of 2-octyl tosylate, and Sneen and co-workers [179–181] investigated the



Scheme XV. Mechanistic possibilities for solvolysis of 1-aryl-2-propyl tosylates. (a) With competing phenonium and carbonium ion formation which should lead to crossover. (b) With two discrete pathways characterized by strong nucleophilic assistance from either solvent or neighboring aryl group.

solvolysis of the corresponding methanesulfonate in aqueous solvents. Both groups found that although there were side reactions (addition to olefins, racemization of starting sulfonate, and racemization of product acetate) that resulted in the formation of racemic product, the actual solvolysis reactions proceeded with 100% inversion of configuration. Clearly the intervention of free carbonium ions would be expected to result in at least partial retention. Nonetheless, Streitweiser and Walsh concluded that the acetolyses of secondary alkyl sulfonates are essentially limiting [82].

Peterson and his co-workers [187] compared the solvolyses of halo-substituted 2-alkyl tosylates in acetic, formic, and trifluoroacetic acids; in

acetic acid they observed a smaller rate dependence on the inductive effects of the halogen substituents, less rearrangement, and less neighboring group assistance. They interpreted these results to "indicate that acetolyses of secondary tosylates, far from being limiting, show marked S_N2 character." Further work by Peterson [188, 189] and others [84, 95, 118, 121, 122, 190] with the very nonnucleophilic trifluoroacetic acid has emphasized the nucleophilic character of the other carboxylic acid solvents.

Recent careful investigations by two groups of the acetolysis of conformationally mobile cyclohexyl substrates have revealed that substitution product formed without rearrangement is exclusively of the inverted configuration [84].

Considerable further evidence against the intervention of free carbonium ions in the solvolyses of simple secondary derivatives has been obtained from comparisons of solvolytic behavior of 2-propyl and 2-adamantyl derivatives [23, 115, 118, 123, 171], from studies of oxygen exchange in labeled alkyl tosylates [56], and from studies of the effects of added nucleophiles on solvolysis reactions [4, 46–48, 120, 179–184]. The available evidence suggests strongly that the borderline mechanism for solvolysis of secondary derivatives does not involve competitive S_N1 and S_N2 reactions, and is best represented by Scheme XIVa or XIVb. Unfortunately this does not resolve the problem completely since considerable latitude is still possible. As was discussed earlier, Scheme XIVa might refer to an ion pair mechanism, while Scheme XIVb might be regarded as only a minor perturbation of an S_N2 reaction.

5.2. The Ion Pair Mechanism

Sneen and co-workers [47, 179–184] have undertaken an extensive investigation of the solvolysis of 2-octyl arenesulfonates in aqueous dioxane in the presence of sodium azide, and they have interpreted their results in terms of an ion pair mechanism. Sneen and Larsen [4] further extended this interpretation by suggesting "that all reactions of nucleophilic substitution at a saturated carbon atom proceed via an ion-pair mechanism." Because the implications of this suggestion are very far-reaching, and since the possible generality of the ion pair mechanism has generated considerable interest [99, 111, 168, 169, 192] among chemists, a thorough discussion of the work of Sneen and his collaborators is necessary.

In their early work on the solvolysis of 2-octyl derivatives Weiner and Sneen [179–183] made several important experimental observations which were interpreted in terms of ion pair intermediates:

1. When optically active 2-octyl brosylate was solvolyzed in 75% aqueous dioxane, the stereochemistry of the 2-octanol product was influenced by the addition of sodium azide [179, 181, 182].

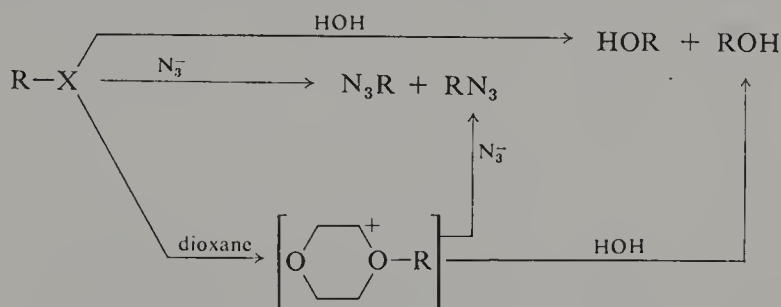
2. Racemization of unreacted 2-octyl brosylate in 75% dioxane takes place as evidenced by the ratio of polarimetric and titrimetric rate constants [180, 181].

3. An exchange reaction was observed between 2-octyl brosylate and added lithium tosylate.

4. Although significant amounts of 2-octyl azide are formed when 2-octyl mesylate is solvolysed in 25% aqueous dioxane, "the rate of reaction is unaffected by added sodium azide" [180, 181].

The influence of sodium azide on the stereochemistry of the *hydrolysis* reaction was indicative of the existence of an intermediate in the reaction. In the absence of azide ion, inverted 2-octanol was formed in an optical purity of 77%, but in the presence of 0.03 *M* sodium azide the alcohol was formed with 100% inversion [179, 181]. Clearly sodium azide intercepted some intermediate which otherwise would have yielded 2-octanol of retained configuration. However, the formation of 2-octanol with retained configuration was observed only for mixed solvent systems where one component was "inert," and Weiner and Sneen [179, 181, 183] concluded that the obligatory intermediate was not an ion pair but an oxonium ion as depicted in Scheme XVI. According to this scheme the retained 2-octanol is a consequence of two successive displacement reactions (the first by dioxane and the second by water), both of which proceed entirely with inversion of configuration. In agreement with Scheme XVI, the yield of alcohol with retained configuration decreases as the concentration of dioxane in the mixed solvent system is decreased [179, 181].*

The second key observation of Weiner and Sneen concerned the racemization of 2-octyl brosylate in 75% dioxane; although the rotation of recovered



Scheme XVI. Retention of configuration for 2-octyl solvolyses in aqueous dioxane as a consequence of a double displacement reaction.

* The problem of oxonium ion intermediates is ignored in the subsequent papers of Sneen and Larsen, which treat the solvolysis of 2-octyl mesylate in 25 and 30% dioxane. The resulting errors are probably small since solvolysis in 25% dioxane gives 2-octanol with an optical purity of 94.5%. The oxonium ion pathway thus represents only about 3% of the total reaction in the absence of salt effects.

unreacted 2-octyl brosylate was not measured, its racemization was deduced indirectly [180, 181]. The ratio of polarimetric to titrimetric rate constants, k_a/k_t , was found to be greater than unity and to increase in the presence of added salts. An interpretation in terms of ion pairs is not entirely consistent with available data on salt effects. From the available experimental [37, 49, 50] and theoretical [6, 7] data, salt effects on the titrimetric rate constant should be greater than on the polarimetric rate constant, and the k_a/k_t ratio would have been expected to *decrease* in the presence of added salts.*

Weiner and Snee [180, 181] reported several k_a/k_t ratios for 2-octyl brosylate in 75% dioxane as being greater than unity. Unfortunately error limits were not given in each instance. The rate constants in the absence of added salt [180, 181] were virtually identical within experimental error: $k_a = 24.7 \pm 0.6$, and $k_t = 23.8 \pm 0.2$. The largest ratio ($k_a/k_t = 1.17$) was reported for solvolysis in the presence of 0.006 M sodium azide, and Weiner and Snee concluded that "a mechanism must exist for racemization of starting material, competitive with the product-forming reactions" [181]. This interpretation was neither necessary nor consistent with their other data. The authors reported [179, 181] that under the same conditions (0.006 M NaN_3 /75% dioxane) inverted 2-octanol was formed with an optical purity of 100%. Clearly, the racemization of 2-octyl brosylate *did not* take place at a rate comparable to that of product formation.† The origin of values of k_a/k_t greater than unity is obscure; but racemization of 2-octyl brosylate via an ion pair intermediate does not provide a satisfactory explanation.

The third significant observation made by Weiner and Snee [180, 181] was that of an anion exchange reaction. Again, this was not observed directly by isolation. When 2-octyl brosylate was solvolyzed in 75% dioxane in the presence of lithium tosylate, only 95.8% of the theoretical amount of acid had been liberated after 8 half-lives; the titer further increased to 99% of theoretical at the end of 12.5 half-lives. This was interpreted as a result of anion exchange resulting in formation of the 2-octyl tosylate which was about three times less reactive. Accepting Weiner and Snee's argument that the small differences are significant, the evidence for ion pair intermediates is still not compelling. Winstein's acetolysis studies [13] indicated that exchange reactions at an ion pair stage were generally associated with substrates corresponding to carbonium ions of considerably greater stability. Consequently it is difficult to rule out the possibility that the exchange reaction occurred by attack of tosylate anion on neutral substrate. The nucleophilicity of tosylate anion may not be great, but neither is the amount of exchange.

* See Section 2.3 for a discussion of salt effect on various rate constants.

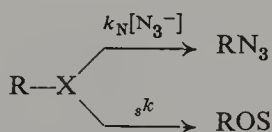
† In 80% acetone the addition of LiClO_4 was found to both increase the k_a/k_t ratio and decrease the optical purity of the 2-octanol [179]. However, this might simply reflect a greater salt effect for the oxonium ion pathway (Scheme XVI) leading to retained product.

To summarize, the results of 2-octyl mesylate solvolyses in 75% dioxane afford no compelling evidence for the intermediacy of ion pairs. As later stated by Snee and Larsen [47], "Clearly, the reaction exhibits the defining characteristics of an S_N2 reaction, bimolecular kinetics, and inversion of configuration."

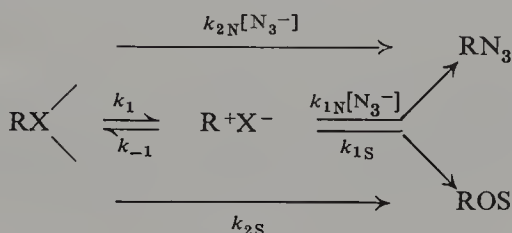
Perhaps the most significant observation made by Weiner and Snee was that although significant amounts of 2-octyl azide are formed in the reaction of 2-octyl mesylate in 25% dioxane, "the rate of reaction is unaffected by added sodium azide" [180, 181]. Snee and Larsen [47, 184] later studied a wider concentration range of sodium azide, and "a small dependence of rate on azide concentration was noted" [193]. The formation of 2-octyl azide at a rate "nearly independent of the concentration of sodium azide" [47] was considered strong evidence for ion pair intermediates.

The choice of terms such as unaffected [180, 181] and small dependence [193] was unfortunate, since the effect of sodium azide on the reaction rate is substantial. For example, 0.237 *M* sodium azide produces a rate increase of over a factor of 2 for 2-octyl mesylate in 25% dioxane [184]. This ambiguity may tend to obscure the significance of the kinetic data, since a "small" or zero dependence on azide ion concentration is not necessary for the implication of an intermediate. Actually, *any rate enhancement smaller than that calculated for an S_N2 reaction (on the basis of product data) would be indicative of an intermediate* in the reaction.

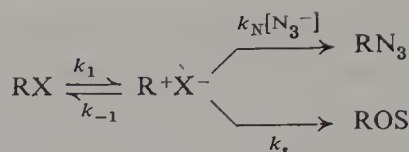
Snee and Larsen [47, 184] carried out an extensive study of the effect of sodium azide on the solvolysis of 2-octyl mesylate in 25 and 30% dioxane, and they developed alternative mathematical treatments of their data. Three different kinetic models were considered in detail: S_N2 (Scheme XVII), simultaneous S_N1 and S_N2 (Scheme XVIII), and the ion pair mechanism (Scheme XIX). The S_N1 mechanism was considered as a limiting form of the ion pair mechanism (Scheme XIX, where $k_{-1}/k_2 = 0$).



Scheme XVII. Model for competitive S_N2 reactions.



Scheme XVIII. Model for simultaneous S_N1 and S_N2 reactions.



Scheme XIX. Model for the ion pair mechanism.

For each of the possible mechanisms both rates and products should vary as a function of added azide ion, and the model predicts a certain relationship between rates and products. To assess the validity of a given kinetic model it is necessary to determine experimentally whether there exists a *rate-product correlation*. Each model also predicts a certain dependence on azide ion concentration for both the product distribution and the observed rate constant. For any of these mechanisms the observed titrimetric rate constant (k_{obs}) must equal the sum of the rate constants for the solvolysis reaction (k_{solv}) and the rate constant for alkyl formation (k_{azide}), as shown in Eq. 60:

$$k_{\text{obs}} = k_{\text{solv}} + k_{\text{azide}} \quad (60)$$

Since the quantity of each product formed must be related to its rate of formation according to Eq. 61,

$$\frac{k_{\text{azide}}}{k_{\text{solv}}} = \frac{\% \text{RN}_3}{\% \text{ROH}} \quad (61)$$

division of each term in Eq. 60 by k_{solv} gives Eq. 62:

$$\frac{k_{\text{obs}}}{k_{\text{solv}}} = 1 + \frac{k_{\text{azide}}}{k_{\text{solv}}} \quad (62)$$

and substitution with Eq. 61 then gives Eq. 63, the *general expression for a rate-product correlation*

$$k_{\text{obs}} = \left(1 + \frac{\% \text{RN}_3}{\% \text{ROH}} \right) k_{\text{solv}} \quad (63)$$

The difficulty in applying the rate-product correlation lies in the determination of k_{solv} . This rate constant cannot arbitrarily be considered to be independent of the sodium azide concentration, and its dependence on $[\text{NaN}_3]$ must be either estimated or measured.

In the case of competitive $\text{S}_{\text{N}}2$ reactions (Scheme 17) the two pathways are totally independent, and the solvolysis reaction is dependent upon azide ion concentration only to the extent of a normal salt effect as seen in Eq. 64:

$$k_{\text{solv}} = k_s = k_s^0(1 + b_s[\text{N}_3^-]) \quad (64)$$

Consequently the rate-product correlation expected for Scheme XVII (competitive S_N2 reactions) is given by Eq. 65, the *rate-product correlation for S_N2 model*:

$$k_{\text{obs}} = \left(1 + \frac{\% \text{RN}_3}{\% \text{ROH}}\right) k_s^0 (1 + b_s [\text{N}_3^-]) \quad (65)$$

Since k_{azide} is given by Eq. 66,

$$k_{\text{azide}} = k_N [\text{N}_3^-] \quad (66)$$

the dependence of the product ratio on azide concentration (according to Eq. 61) is given by Eq. 67:

$$\frac{\% \text{RN}_3}{\% \text{ROH}} = \frac{k_N}{k_s} [\text{N}_3^-] \quad (67)$$

For the case of simultaneous S_N1 and S_N2 reactions (Scheme XVIII) the expression for k_{solv} is quite complex since there is an explicit dependence on azide ion concentration in addition to the influence of salt effects. However, this mechanism appears implausible on the basis of the results of Schleyer and Lancelot for the 1-aryl-2-propyl system [172-178]. In addition Sneen and Larsen [47] showed that only in the case that $k_{1S}/k_{1N} = k_{2N}/k_{2S}$ would a plot of RN_3/ROS versus azide concentration be linear. Since selectivity ratios for the two different species should be quite different [46, 120, 195, 196] and the RN_3/ROS plot was in fact linear, Scheme XVIII does not appear to be a likely mechanism.

For the case of the ion pair mechanism (Scheme XIX) the rate of formation of solvolysis product is given by Eq. 68:

$$k_{\text{solv}} [\text{RX}] = k_s [\text{R}^+ \text{X}^-] \quad (68)$$

Application of the steady state approximation leads to Eq. 69:

$$[\text{R}^+ \text{X}^-] = \frac{k_1 [\text{RX}]}{k_{-1} + k_s + k_N [\text{N}_3^-]} \quad (69)$$

which gives the concentration of the ion pair $\text{R}^+ \text{X}^-$, and substitution into Eq. 68 gives a solution of k_{solv} as in Eq. 70:

$$k_{\text{solv}} = \frac{k_1 k_s}{k_{-1} + k_s + k_N [\text{N}_3^-]} \quad (70)$$

Since Eq. 70 still contains several terms which cannot be directly measured, it must be further modified. Multiplying both the numerator and denominator of Eq. 70 by the term $(k_{-1} + k_s)$ leads to Eq. 71:

$$k_{\text{solv}} = \left(\frac{k_1 k_s}{k_{-1} + k_s} \right) \left(\frac{k_{-1} + k_s}{k_{-1} + k_s + k_N [\text{N}_3^-]} \right) \quad (71)$$

and division of each rate constant in the second term by k_s leads to Eq. 72:

$$k_{\text{solv}} = \left(\frac{k_1 k_s}{k_{-1} + k_s} \right) \left(\frac{k_{-1}/k_s + 1}{k_{-1}/k_s + 1 + (k_N/k_s)[N_3^-]} \right) \quad (72)$$

Since the products in Scheme XIX are formed by competing displacement reactions on the same intermediate, the product ratio is again described by Eq. 67. By defining $x \equiv k_{-1}/k_s$ and using Eq. 67 to substitute the product ratio, Eq. 73 is obtained:

$$k_{\text{solv}} = \left(\frac{k_1 k_s}{k_{-1} + k_s} \right) \left(\frac{x + 1}{x + 1 + (\%RN_3/\%ROH)} \right) \quad (73)$$

Inspection of Eq. 70 reveals that the first term of Eq. 73 corresponds to the rate constant for solvolysis in the absence of nucleophilic displacement by azide ion. Sneen and Larsen [47] labeled this term k_{NA} :

$$k_{NA} \equiv \frac{k_1 k_s}{k_{-1} + k_s} \quad (74)$$

The rate constant k_{NA} cannot be assumed to be independent of salt effects, but when there is no added salt in the reaction mixture k_{NA} is identical with the observed rate constant k_{obs}^0 . Consequently Sneen and Larsen [47] *estimated* the magnitude of the sodium azide salt effects by *assuming* them to be the same as those measured for solvolysis of 2-octyl mesylate in the presence of non-nucleophilic salts, LiClO_4 , NaNO_3 , and NaBr .*

With the approximation

$$k_{NA} = k_{\text{obs}}^0(1 + b_{NA}[N_3^-]) \quad (75)$$

it is possible to calculate k_{solv} , since substitution of Eqs. 74 and 75 into Eq. 73 gives

$$k_{\text{solv}} = k_{\text{obs}}^0(1 + b[N_3^-]) \left(\frac{x + 1}{x + 1 + (\%RN_3/\%ROH)} \right) \quad (76)$$

* It is doubtful that these salts really are nonnucleophilic. Swain and Scott [197] proposed a relative scale of anion nucleophilicities in water using methyl bromide as the standard substrate:

$$\log(k/k^0) = sn$$

where k and k^0 are the rate constants for reaction with some nucleophilic anion and water, respectively, s is the substrate parameter (defined as unity for methyl bromide), and n is the nucleophilicity parameter for the anion in question. On the basis of n constants, bromide ($n = 3.9$) is as nucleophilic as azide ion ($n = 4.0$), and nitrate ($n = 1.0$) [198] is significantly more nucleophilic than water ($n \equiv 0.0$). Furthermore, the hydrogen bonding ability of ClO_4^- (an indication of its nucleophilicity) in CH_2Cl_2 is appreciable [199]; one wonders whether ClO_4^- is truly as nonnucleophilic as has long been assumed without definitive proof. Although ClO_4^- may be less nucleophilic than water, water is very nucleophilic solvent.

Substitution of this expression for k_{solV} into Eq. 63 provides the *rate-product correlation for the ion pair mechanism* of Scheme XIX:*

$$k_{\text{obs}} = \left(1 + \frac{\% \text{RN}_3}{\% \text{ROH}}\right) k_{\text{obs}}^0 (1 + b_{\text{NA}}[\text{N}_3]) \left(\frac{x + 1}{x + 1 + (\% \text{RN}_3 / \% \text{ROH})}\right) \quad (77)$$

To evaluate the relative merits of the ion pair mechanism (Scheme XIX) and the $\text{S}_{\text{N}}2$ mechanism (Scheme XVII), Sneen and Larsen [47, 184] studied the solvolysis of 2-octyl mesylate in 25 and 30% dioxane in the presence of "nonnucleophilic" salts such as lithium perchlorate and determined the salt effects on the solvolysis reaction. For both systems values of $b \approx 1$ were calculated [47]. To determine the validity of the rate-product correlation for the ion pair mechanism it was also necessary to estimate a value for the term x . Since $x \equiv k_{-1}/k_s$, this term represents the magnitude of internal return, but it is experimentally inaccessible. Consequently Sneen and Larsen [47] treated it as an adjustable parameter and utilized the value that afforded the best fit between rate and product data with Eq. 77a.

Table 28 presents a tabulation of the data for solvolysis of 2-octyl mesylate in 25 and 30% dioxane. The first three columns present the experimental data, and subsequent columns list the values of the titrimetric rate constants which are predicted by the products according to either Eq. 65 or Eq. 77. Comparison of the third column (k_{obs}) with the fourth, fifth, and sixth columns provides a measure of the quality of the rate-product correlation. Note that this rate-product correlation will be poor *either* if the given mechanism is incorrect *or* if the assumptions used to evaluate Eq. 65 or 77 are not valid. On the other hand, a good correlation between rates and products indicates either that both the mechanism and the assumptions are valid or possibly that both are incorrect and the agreement is fortuitous. Consequently the observation of a good rate-product correlation does not provide absolute evidence for a given mechanism, nor does a poor correlation necessarily rule out a given mechanism. To evaluate the significance of a rate-product correlation it is also necessary to evaluate all assumptions used in the calculations.

* Sneen and Larsen [47, 184] used a different derivation; they also expressed Eq. 77 in a slightly different form:

$$\frac{k_{\text{obs}}}{k_{\text{NA}}} = \frac{(x + 1)(1 + m[\text{N}_3^-])}{x + 1 + m[\text{N}_3^-]} \quad (77a)$$

where $m = k_{\text{N}}/k_s$. A value of m was obtained from a graphical solution of Eq. 67, and the term $m[\text{N}_3^-]$ replaces the product ratio $\% \text{RN}_3 / \% \text{ROH}$ of Eq. 77. Rather than testing the rate product correlation directly for each experimental point, Sneen and Larsen [47, 184] in effect used "corrected" values of the product ratios. The rate-product correlation was then illustrated in two ways: (1) a graphical comparison of values of $k_{\text{obs}}/k_{\text{NA}}$ calculated using Eq. 75 with those values determined from product data; and (2) a tabulation of values of k_{obs} with the predicted rate constants calculated from product data with Eq. 77a.

Table 28 Rate-Product Correlation for the Solvolysis of 2-Octyl Mesylate in 25 and 30 % Dioxane in the Presence of Sodium Azide: A Comparison of the Observed Rate Constants with the Rate Constants Predicted from Product Data^a

$[\text{NaN}_3]^b$	$\frac{\% \text{RN}_3^b}{\% \text{ROH}}$	k_{obs}^b	$k_{\text{ion pair}}^{c,d}$	$k_{\text{S}_{\text{N}}2}$ (Positive ^{e,f} Salt Effect)	$k_{\text{S}_{\text{N}}2}$ (Negative ^{e,g} Salt Effect)
25 % Dioxane					
0.000	0.00	2.21 ± 0.08	—	—	—
0.0758	0.58	3.18 ± 0.12	3.23	3.79	3.29
0.113	0.79	3.76 ± 0.07	3.60	4.44	3.65
0.156	1.09	4.34 ± 0.17	4.08	5.39	4.17
0.237	2.04	5.18 ± 0.22	5.28	8.45	5.96
30 % Dioxane					
0.000	0.00	1.74 ± 0.04	—	—	—
0.0543	0.62	2.43 ± 0.08	2.54	2.98	2.66
0.0571	0.65	2.26 ± 0.11	2.58	3.04	2.71
0.0979	1.10	2.67 ± 0.14	3.09	4.03	3.32
0.152	1.22	3.65 ± 0.14	3.34	4.46	3.25
0.199	1.78	3.73 ± 0.12	3.91	5.84	3.86
0.258	2.26	4.71 ± 0.08	4.42	7.20	4.19
0.311	2.94	4.91 ± 0.15	4.97	9.06	4.72

^a Rate constants are all in $\text{sec}^{-1} \times 10^4$.^b Ref. 47.^c Calculated from the product ratios using Eq. 77.^d Using $b = 1.08$ and $x = 2.40$ for 25 % dioxane; $b = 1.04$ and $x = 2.59$ for 30 % dioxane [47].^e Calculated from the product ratios using Eq. 65.^f Using $b = 1.08$ for 25 % dioxane and $b = 1.04$ for 30 % dioxane [47].^g Using $b = -0.3$ for 25 % dioxane and $b = -1.0$ for 30 % dioxane [120].

The fourth and fifth columns of Table 28 present the predicted rate constants for the ion pair and $\text{S}_{\text{N}}2$ mechanisms using the assumptions made by Sneen and Larsen [47]. Clearly much better agreement is found for the ion pair mechanism. Whereas the values of $k_{\text{ion pair}}$ are in fairly good agreement in every instance, the values for $k_{\text{S}_{\text{N}}2}$ are always too large and differ from the observed values by as much as a factor of 2 at high sodium azide concentration.

On the basis of the assumptions made by Sneen and Larsen [47], the solvolysis of 2-octyl mesylate in 25 and 30 % dioxane appears to be better described by the ion pair mechanism (Scheme XIX) than by competitive $\text{S}_{\text{N}}2$ reactions (Scheme XVII). However, other alternatives are possible. For example, since salt effects are not independent of the nature of the added

salt (cf. Tables 10 and 11), it is likely that the effects measured for such salts as lithium perchlorate are not identical to the salt effects produced by sodium azide. If one assumes that sodium azide produces a *negative salt effect* on k_{soliv} , evaluation of the rate-product correlation for competitive $\text{S}_{\text{N}}2$ reactions using Eq. 65 leads to the set of numbers in the last column of Table 28. In contrast to the fifth column ($k_{\text{S}_{\text{N}}2}$, positive salt effect) the assumption of a negative salt effect (last column) results in a reasonably good agreement between observed and predicted rate constants.

Table 29 presents an analysis of the errors calculated for the rate-product

Table 29 Summary of Errors in the Rate-Product Correlations for the Solvolysis of 2-Octyl Mesylate in Aqueous Dioxane^a

Error	k_{obs}^d	$k_{\text{ion pair}}^b$	$k_{\text{S}_{\text{N}}2}$ (Positive Salt Effect) ^b	$k_{\text{S}_{\text{N}}2}$ (Negative Salt Effect) ^b
25% Dioxane				
Men deviation ^c	0.13	0.13	1.40	0.29
Mean percent deviation (%)	3.5	3	30	6
Standard deviation ^c	0.16	0.17	2.20	0.47
30% Dioxane				
Mean deviation ^c	0.0	0.25	1.61	0.37
Mean percent error (%)	3.5	8	40	12
Standard deviation ^c	0.12	0.28	2.28	0.41

^a Using the data of Table 28.

^b Difference between observed and predicted values of the titrimetric rate constant.

^c Units are $\text{sec}^{-1} \times 10^{-4}$.

^d Experimental error reported by Sneen and Larsen [47].

correlations for each of the assumed mechanisms, based on the differences between the observed titrimetric rate constants (k_{obs}) and the predicted values calculated using Eq. 65 or Eq. 77. This table shows that the best rate-product correlation is found for the ion pair mechanism and the worst correlation is found for the $\text{S}_{\text{N}}2$ mechanism, assuming a positive salt effect. However, when a negative salt effect is assumed for the solvolysis reaction, the $\text{S}_{\text{N}}2$ mechanism gives a greatly improved correlation. The errors for the latter are about 50%

greater than for the ion pair mechanism with 30% dioxane (seven points) and about twice as large with 25% dioxane (four points).

Analysis of Tables 28 and 29 does not permit a clear-cut choice between the ion pair and S_N2 (negative salt effect) mechanisms. Although the rate-product correlation of the ion pair mechanism is slightly better, the differences are small. When the errors reported [47] for k_{obs} are considered, it becomes apparent that none of the mechanisms gives an entirely satisfactory rate-product correlation. Inspection of the calculated rate constants for the ion pair mechanism in Table 28 reveals that only two points for 25% dioxane and a single point for 30% dioxane fall within the experimental error limits of k_{obs} . Sneen has also studied the solvolysis of several α -arylethyl [220] and allylic substrates [64–66], and again for these systems (which are more likely than 2-octyl mesylate to give rise to ion pairs) the agreement between calculated and observed rate constants is not always entirely satisfactory.

Since consideration of the results of the rate-product correlations alone does not allow a decision to be made regarding the mechanism of solvolysis of 2-octyl brosylate in 25 and 30% aqueous dioxane, it is clearly necessary to evaluate the assumptions used in the correlations. In particular, why do neither of the mechanisms give rise to a rate-product correlation which accurately predicts the observed rate constants within experimental error?

In their analysis of the ion pair mechanism Sneen and Larsen [47] made several assumptions: They assumed that there was no salt effect on x (i.e., on k_{-1}/k_s). However, k_{-1} denotes return of ion pair to neutral starting material, which involves destruction of charge, and k_s denotes displacement by water, which results in increased charge separation (by formation of $ROH_2^+ + ^-OMs$). Such a ratio of rate constants would be expected to show a negative salt effect (cf. Table 13); the magnitude of this salt effect, however, is experimentally inaccessible. The assumption that x is a constant probably does not affect the rate-product correlation to a great extent, but it may contribute to the observed discrepancies.

Sneen and Larsen [47] estimated the magnitude of sodium azide salt effects by studying the effects of other salts. This procedure may have introduced errors in three ways:

1. Since salt effects are highly dependent on the nature of the salt (cf. Tables 10 and 11), the salt effect for sodium azide is probably not the same as that for the other salts studied.
2. As discussed earlier (Section 2.3), it is likely that Eq. 5 [34] does not afford the best description of salt effects in aqueous media.
3. The standard salts used by Sneen were not nonnucleophilic.

The final assumption which was implicitly made by Sneen and Larsen [47] is that there were no complications resulting from the oxonium ion pathway

(Scheme XVI) [179, 181, 183]. However, this pathway shows quite a different rate-product correlation [179, 180, 183]. Nevertheless, the errors introduced by ignoring the oxonium ions should not be great; this pathway constitutes but a small part of the overall reaction.

In the analysis for the competitive S_N2 reactions [120], several assumptions are also implicit. As in the case of the ion pair mechanism, salt effects were treated according to Eq. 5 [34], and the effects of the oxonium ion pathway (Scheme XVI) were not considered. However, these assumptions affect the accuracy of the rate-product correlation only to a minor extent.*

The critical assumption with regard to competitive S_N2 reactions is that of a negative salt effect. Table 11 illustrates that although they are not generally expected in solvolysis reactions, negative salt effects are possible. The expectation that added salt should enhance a solvolysis rate is based on considerations of the effect of ionic strength on the activity coefficient of the *transition state* [7]. However, the effect of ionic strength on the activity coefficient of the *ground state* (i.e., neutral substrate) has generally been ignored [240a].

Frost and Pearson [202] discuss a very pertinent case. In the hydrolysis of γ -butyrolactone addition of sodium chloride produces a rate enhancement; in contrast, addition of sodium perchlorate results in a decreased rate. These rate effects appear to be a consequence of changes in the activity coefficient of the ground state organic substrate; with sodium chloride an increase in ionic strength results in an increased activity coefficient, but with sodium perchlorate the activity coefficient is decreased. Other salts also show differing effects on the activity coefficient of the γ -butyrolactone: addition of sodium sulfate, sodium chloride, potassium chloride, barium chloride, or sodium bromide cause an increase in the activity coefficient, whereas sodium iodide, sodium perchlorate, and potassium iodide have the opposite effect. Clearly, the salt effects produced by sodium perchlorate and sodium bromide cannot provide a good measure of *either the magnitude or the sign* of the salt effects produced by other salts.

Sneen and Robbins have criticized our earlier [120] use of this example as irrelevant because the butyrolactone reaction "is acid catalyzed and therefore of a charge type fundamentally different from that of hydrolysis of 2-octyl mesylate" [200]. However, the differences in the sign and magnitude of the various salt effects in the hydrolysis of γ -butyrolactone are largely a result of changes in the activity coefficient of the *ground state* of the organic substrate. These changes are apparently greater than the changes in the activity coefficient of the transition state.

* When the data of Weiner and Sneen [179, 181, 183] are used to correct for reaction via the oxonium ion pathway, and salt effects are treated according to the logarithmic relationship of Eq. 4 [7], the mean deviation of the rate constants calculated for solvolysis of 2-octyl mesylate in 30% dioxane according to Scheme XVII decreases only from 0.37 to 0.33.

Qualitatively, the observation of negative salt effects for reactions of organic substrates in highly aqueous media should not be entirely unexpected. In highly aqueous solvent systems organic substrates are relatively insoluble. Consequently, activity effects (e.g., dimerization or aggregation) on the neutral molecules should be relatively likely. The result of these effects on the ground state molecules would be a decrease in the rate of reaction (and consequently of the observed rate constants) *but with no alteration of the product distribution*. It is precisely in this manner in which the observed behavior of 2-octyl mesylate differs from that expected for a simple (no salt effects) S_N2 reaction.*

Although it may be reasonable to expect negative salt effects in the solvolyses of 2-octyl mesylate in 25 and 30% dioxane, it is not possible on the basis of currently available information to assess the validity of this assumption. Both the ion pair mechanism and competitive S_N2 reactions appear plausible; neither possibility, however, agrees with the experimental data within the reported [47] experimental error.† Consequently it would seem that Sneen and Larsen's conclusion [4] that "the operation of this [ion pair] mechanism was demonstrated unequivocally" is not justified by the available data on the solvolysis of 2-octyl mesylate in aqueous dioxane. Additional data must be obtained before it will be possible to assess the validity of Sneen and Larsen's suggestion [4] "that all reactions of nucleophilic substitution at a saturated carbon atom proceed via an ion-pair mechanism."

Several other criticisms of Sneen's ion pair hypothesis have been published, but in each case the criticism is not entirely valid. Kurz and Harris [192] argue against the generality of the ion pair mechanism on the basis of nucleophilic displacement reactions on haloacetic acids. However, these authors considered the ion pairs to have a full positive charge on carbon. It is likely that ion pairs, especially the tight ion pairs depicted by Sneen, have a considerable degree of bonding character between the carbon atom and the gegenion; thus the assumption of a full positive charge on carbon may not be valid (see footnote 8 of ref.23).

Gregory, Kohnstam, Paddon-Row, and Queen [168] have also criticized the ion pair mechanism for the solvolysis of 2-octyl mesylate in aqueous dioxane. These authors argue in favor of simultaneous S_N2 and S_N1 pathways (as in Scheme XVIII, but with $k_{-1} = 0$), and they obtained a reasonable rate-product correlation. However, their analysis required a selectivity

* This general conclusion is supported by Grunwald and Effio, who state, "Some of Sneen's kinetic evidence in favor of ion pair intermediates . . . is distorted by salt-induced medium effects" [240b].

† The reported [47] experimental errors presumably represent the mean deviation between different determinations of the rate constant. This may simply not afford an accurate measure of the true experimental errors.

ratio β (k_{1N}/k_{1S} in Scheme XVIII, where k_{1S} is a pseudo-first-order rate constant) for the presumed carbonium ion of approximately unity. Our own work [120] (which was not available to these authors) demonstrates that a selectivity of ~ 0.02 would have been expected had the reaction proceeded via a cationoid pathway. Taken together with other evidence against the intermediacy of carbonium ions in the solvolysis of simple secondary derivatives [4, 47, 172–184, 200] (e.g., the observation of 100% inverted solvolysis product), this argues strongly against the likelihood of simultaneous S_N1 and S_N2 reactions in the solvolysis of 2-octyl mesylate.*

In an appendix to a recent article Sneen and Robbins [200] discuss these criticisms at length. They concede that the data can be accommodated by the assumption of a negative salt effect, but they question whether such negative salt effects are to be expected or are likely to be of the required magnitude. Data in Table 11 indicate that values of $b = -1$ are indeed possible. Although Sneen and Robbins provide a long list of substrates exhibiting only positive salt effects, none of these is pertinent since either (1) the substrates are expected to give rather stable allylic, benzylic, or tertiary carbonium ions and not to react by S_N2 processes; or (2) the effects observed pertain to highly nucleophilic salts such as NaN_3 . What is needed is an assessment of salt effects for S_N2 substrates (e.g., primary derivatives) in 25 and 30% dioxane using the least nucleophilic salts available (e.g., LiClO_4).

Abraham [201b] has estimated the free energy differences between neutral substrate and intimate ion pair for methyl, ethyl, isopropyl, and *t*-butyl bromide hydrolysis reactions. His calculations utilize available thermodynamic data for these systems together with extrapolated thermodynamic data from model systems, and Abraham suggests that the inherent error in these calculations is about ± 5 kcal/mol. The results are summarized in Table 30.

Abraham concludes that since the calculated ΔG_1^0 values for methyl and ethyl bromides are substantially larger than the observed free energies of activation, it is highly unlikely that such derivatives can undergo nucleophilic substitution by the ion pair mechanism. He also concludes that “the

* Gregory, Kohnstam, Queen, and Reid [169] have recently argued in favor of competitive S_N1 and S_N2 pathways in the solvolysis of benzyl halides in aqueous acetone. However, their rejection of Sneen's hypothesis is based on tenuous assumptions. These authors considered only the extremes of the ion pair scheme ($x \gg 1$ and $x \ll 1$, corresponding to either S_N2 or S_N1). Further, they apparently assume that if a substrate *solvolyzes* by one mechanism it must also react with much stronger nucleophiles by the *same* mechanism; this assumption is not justified. Their argument that the maximum rate increase (for a substrate reacting via the ion pair scheme) produced by added nucleophile should correspond to the lithium perchlorate salt effect is similarly unjustified. This would be true only for a substrate which *always* reacted via a carbonium ion, whereas the case under consideration was reaction at the stage of an ion pair.

Table 30 Calculated and Observed Free Energy Differences For Intimate Ion Pair Formation in the Hydrolysis of Alkyl Bromides [201b]

Free Energy Difference ^a	CH ₃ Br	CH ₃ CH ₂ Br	(CH ₃) ₂ CHBr	(CH ₃) ₃ CBr
ΔG_1^0	66	43	28	12
$\Delta G_{\text{obs}}^\ddagger$	26	26	25	18

^a ΔG_1^0 is the calculated free energy difference between neutral substrate and intimate ion pair; $\Delta G_{\text{obs}}^\ddagger$ is the observed free energy of activation for the hydrolysis reaction.

ion pair mechanism is slightly unfavorable for S_N reactions of simple secondary halides, though for other secondary substrates the reverse might hold" [201b].

Gregoriou [201c] has recently criticized Sneen's [47] analysis of the 2-octyl system on the basis that Sneen used the *concentration* rather than the *activity* of sodium azide. While it is clear that the two quantities are not expected to be identical and in fact are not even linearly related [201c], Gregoriou's criticism is unjustified. As we pointed out earlier [120], the relationship between activity and concentration of azide ion is treated *implicitly* in the rate-product correlation used by Sneen.

The rate-product correlation for the ion pair mechanism is given by Eq. 77, and it will be noted that there is only a single term (the salt effect on k_{obs}^0) denoting azide concentration (or activity). As Gregoriou himself observes [201c], it is probably more appropriate to use concentration here, since salt effects were evaluated from salt concentrations according to Eq. 5. (The use of azide *activities* to estimate salt effects does not lead to a significant change in any event.) The confusion apparently stems from Sneen's use of Eq. 77a in which there are several terms denoting azide *concentration*. However the values of *m* were determined from product data, and the correction for activity is *implicit* in these values.

Sneen and his co-workers have expanded their investigations to include a number of reactions in addition to solvolysis of 2-octyl mesylate. Sneen and Robbins [202] studied the reaction of α -phenylethyl bromide with sodium ethoxide in ethanol and found that the results did not appear to be consistent with competitive solvolysis and bimolecular attack on neutral substrate according to Eq. 78:

$$k_{\text{obs}} = k_1 + k_2[\text{NaOEt}] \quad (78)$$

Although one would expect that the second-order rate constant should remain nearly constant (neglecting salt effects), Sneen and Robbins found that values of k_2 calculated from Eq. 78 decreased by a factor of 2 on increasing the sodium ethoxide concentration from 0.1 to 0.5 M. Consequently, these

authors concluded that both elimination and substitution product were derived from attack on an initially formed ion pair. Analysis of the data according to the ion pair scheme satisfactorily accounted for the dependence of rate on sodium ethoxide concentration.

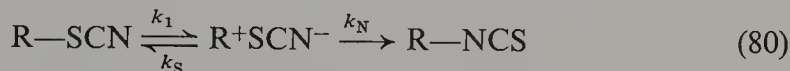
More recently this analysis has been questioned by McLennan [203a], who took into account the fact that the degree of dissociation of sodium ethoxide should also be a function of concentration. Consequently, the decrease in values of k_2 are argued to be a result of a greater degree of association of sodium ethoxide at higher base concentrations. McLennan carried out the reactions at constant ionic strength (using sodium perchlorate, which has a common cation) and argued that the degree of dissociation of sodium ethoxide was thus held constant. Under these conditions the values of k_2 calculated according to Eq. 78 remain essentially unchanged. Moreover, McLennan found that Sneed's ion pair scheme [202] did not accommodate his experimental data.

Fava and his co-workers [203b] had earlier used a similar approach in analyzing the reaction of substituted benzhydryl thiocyanates with thiocyanate ion. They carried out their reactions at constant ionic strength and their results indicated both unimolecular and bimolecular components as described by Eq. 79:

$$k_{\text{obs}} = k_1 + k_2[\text{NaSCN}] \quad (79)$$

Since elimination is not possible in this system, the data suggest that two pathways for substitution are operating simultaneously. Fava concluded that the bimolecular pathway involves attack at the stage of neutral substrate on the basis of two lines of evidence: substituent effects and kinetic data. In contrast to the unimolecular portion of the reaction ($\rho = -4.5$), the bimolecular portion shows a very small dependence on the nature of substituents on the aromatic ring. Since the isomerization reaction ($\text{R}-\text{SCN} \rightarrow \text{R}-\text{NCS}$) exhibits a ρ value of -3.4 and apparently proceeds via the intimate ion pair (see Section 4.3), the authors concluded that the bimolecular reaction takes place at the stage of neutral substrate.

Fava and co-workers [203b] also attempted to show that the pseudo-first-order rate constant $k_2[\text{NaSCN}]$ could be larger than the rate constant for ionization to intimate ion pair; this would demonstrate that ionization could not have preceded bimolecular displacement. For isomerization according to Eq. 80,



the observed rate constant k_{isom} is described by Eq. 81:

$$k_{\text{isom}} = \frac{k_1 k_N}{k_S + k_N} \quad (81)$$

which can be rearranged to Eq. 82:

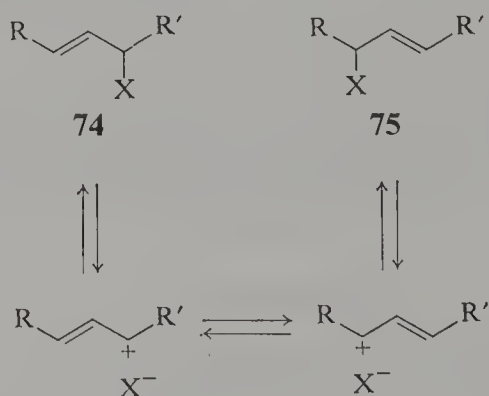
$$k_1 = k_{\text{isom}} \left(1 + \frac{k_S}{k_N} \right) \quad (82)$$

The authors then evaluated k_S/k_N by determining the distribution of radioactive products when labeled thiocyanate ion was used as a nucleophile. In several instances the pseudo-first-order rate constant for bimolecular exchange ($k_2[\text{NaSCN}]$) was shown to exceed the rate constant for ionization according to Eq. 82. Again it was concluded that the bimolecular displacement takes place at the stage of neutral substrate.

One major flaw in the latter argument lies in the assumption that the measured values of k_S/k_N using labeled NaSCN accurately reflect the corresponding ratio in return from intimate ion pair. In fact, while added NaSCN must react according to the intrinsic nucleophilicities of the sulfur and nitrogen ends of the thiocyanate ion, return from intimate ion pair may be quite different. The intimate ion pair may still possess a strong interaction between carbon and sulfur, and the true value of k_S/k_N for Eqs. 80 and 82 may be very much larger than the values calculated using added labeled NaSCN. Consequently, the claim for observing values of $k_2[\text{NaSCN}]$ which are larger than the rate constant for ionization may not be valid. Nevertheless, the data on substituent effects do suggest that nucleophilic attack can precede ion pair formation.

Sneen and co-workers have also studied the solvolytic behavior of several allylic substrates [64–66]. Reactions in the presence of added nucleophiles again were interpreted in terms of ion pair intermediates; moreover, the data indicated the involvement of isomeric allylically related ion pairs (Scheme XX).

For example, the solvolysis of optically active α,γ -dimethylallyl chloride (74 or 75, $R = R' = \text{CH}_3$, $X = \text{Cl}$) in the presence of azide or thiocyanate



Scheme XX. Formation of isomeric allylically related ion pairs. (Subsequent product-forming steps are not shown).

ion gave optically inactive solvolysis product but afforded azide or thiocyanate product which was still optically active [64]. Sneen and Bradley [64] suggested that the reactive nucleophiles could attack at the stage of the chiral intimate ion pairs while the less nucleophilic solvent attacked at the stage of a solvent-separated ion pair.

5.3. Implications of the Ion Pair Mechanism

If the mechanism of solvolysis of simple secondary derivatives cannot be decided on the basis of presently available data, then new experimental information must be generated. Certain implications of the ion pair mechanism suggest lines of possible research that might resolve some of the ambiguities. For example, the work of Weiner and Sneen [180–183] and Sneen and Larsen [4, 47, 184] shows that the solvolysis of 2-octyl derivatives can be interpreted as showing greater “S_N1-character” as the fraction of dioxane in the solvent is decreased from 75 to 25 or 30%. On this basis, the solvent system that might most clearly afford evidence for ion pair intermediates is *pure water*; water would also eliminate some of the difficulties associated with mixed solvents. The problems associated with solubility and negative salt effects might be enhanced; however, in a one-component solvent the activity effects could be measured and appropriate corrections could be made.

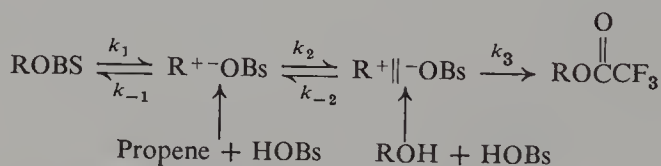
A second possibility for further investigation is suggested by the interpretation of neighboring group participation implied by the ion pair mechanism [4, 99, 204]. If nucleophilic attack is preceded by ionization, then the rate enhancements may be a consequence of a greater rate of *rearrangement*, rather than a greater rate of *formation* of the intermediate. In other words, the rate enhancement would ultimately derive from a *decrease* in internal return from the ion pair. Since internal return is measured relative to solvolysis, the term $x(k_{-1}/k_s)$ for the ion pair mechanism of Scheme XIX) provides such a measure. In addition, the value of x would place a clear and definite limit ($x + 1$) on the possible magnitude of any rate enhancement caused by neighboring group participation. Thus if one could find a system which is a good model for 2-octyl mesylate (yet contains a neighboring group), the maximum rate acceleration possible for solvolysis in 25 or 30% dioxane would be less than a factor of 4. Such experiments may be possible, but it is always difficult to find a “good” model for any compound; in addition, attachment of a neighboring group such as aryl to the 2-octyl skeleton might render it insoluble in 25 or 30% dioxane.*

An alternative method for measuring the amount of internal return (i.e., determining the value of x) would utilize the oxygen scrambling technique

* A good model in prospect would appear to be $\text{CH}_3\text{O}(\text{CH}_2)_3\text{CH}(\text{OBs})\text{CH}_3$ (Table 23) (F. L. Schadt, private communications).

developed by Goering (see Section 3). Nowever, this approach gives a result in apparent conflict with the conclusion of Sneen and co-workers. Although Diaz, Lazdins, and Winstein [56] found that equilibration of the oxygens of ^{18}O -labeled 2-octyl brosylate did take place, the extent of equilibration was quite small. If such equilibration affords a good estimate of ion pair return [68], the results in methanol indicate a value of x (i.e., $k_{\text{equilibration}}/k_{\text{solvolysis}}$) of 0.01. Yet according to Sneen's results [47] in aqueous dioxane the expected value would be two powers of 10 greater if the ion pair mechanism were operative. Consequently, although the equilibration of the ^{18}O label provides strong evidence for some ion pair formation, it does not lend support to the theory that all solvolysis product is derived from attack on these ion pairs. However, the solvents used were not the same, and it is likely that the ^{18}O method misses much internal return, since the labeled oxygen may recombine preferentially (see Section 3.3).

Shiner and co-workers [111, 112] have utilized olefin additions as a potential alternative route for the generation of intimate ion pairs. As solvents they utilized trifluoroacetic acid (TFA); on the basis of studies of neighboring group participation the trifluoroacetolysis of secondary arenesulfonates appears to be limiting with regard to nucleophilic solvent assistance [129, 187–189]. Their experiments with propene and with *t*-butylethylene are summarized in Table 31. Noteworthy is the exclusive formation of 2-propyl brosylate rather than 2-propyl trifluoroacetate with propene and *p*-bromobenzenesulfonic acid (HOBs) in TFA; 2-propanol gave only the trifluoroacetate under the same conditions. This was interpreted [111] according to Scheme XXI with propene giving intimate and 2-propanol giving solvent-separated ion pairs. If this interpretation is correct, then intimate ion pair collapse (k_{-1}) can be much more rapid than ion pair dissociation (k_2).

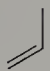
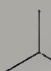

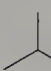
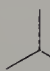
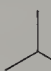
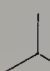
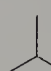

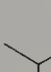






Scheme XXI. Shiner's interpretation of the reactions of propene and 2-propanol with *p*-bromobenzenesulfonic acid in trifluoroacetic acid [111].

The significance of this interpretation is very important, since no other method available has been capable of revealing such "hidden return" [111]. The ^{18}O scrambling of labeled sulfonate and carboxylate esters (Section 3) provides only minimum estimates in nonrearranging systems, since there may be a strong preference for reformation of the original C—O bond (i.e., little or no ^{18}O equilibration).

t-Butylethylene (77), in contrast to propene, reacts with *p*-bromobenzene-sulfonic acid in TFA to give only trifluoroacetate product, which, moreover,

Table 31 Reactions of Isopropyl and Pinacolyl Derivatives in Trifluoroacetic Acid^a

Reaction			$t_{1/2}$
 + BzOH	$\xrightarrow{\text{TFA } 25^\circ}$	 OBz	< 1 min
 + TFA	$\xrightarrow{\text{TFA } 25^\circ}$	 OTFA	300 min
 OBz	$\xrightarrow{\text{TFA } 25^\circ}$	 OTFA	182 min
 OH + BzOH	$\xrightarrow{\text{TFA } 25^\circ}$	 OTFA	10 min
 + BzOH	$\xrightarrow{\text{TFA } 12^\circ}$	 OTFA	< 20sec
 + TFA	$\xrightarrow{\text{TFA } 25^\circ}$	 OTFA + Small amounts of unrearranged ester	≈ 30 min
 OBz	$\xrightarrow{\text{TFA}}$	 OTFA	3.9 sec (25°); ≈ 16 sec (12°) ^b

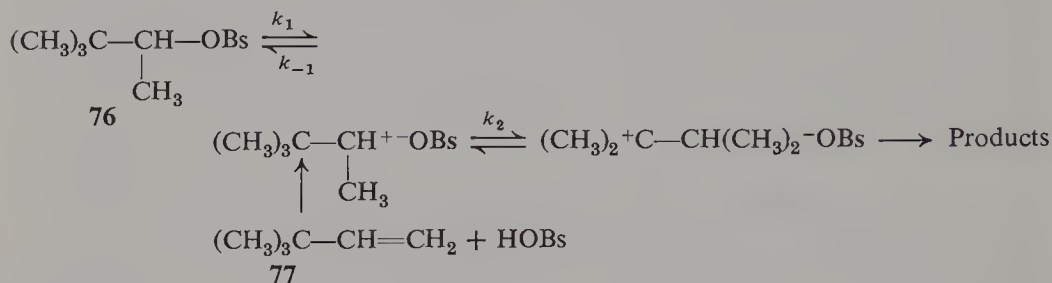
^a Ref. 111, 112.

^b Ref. 118b reports substantially lower reactivity.

is completely rearranged. The failure to observe brosylate product (detectable under those conditions) was interpreted (Scheme XXII) to mean that internal return (k_{-1}) to **76** does not compete with further reactions (k_2). The difference relative to the behavior of propene was ascribed to rapid methyl migration in the k_2 step leading to a rearranged tertiary ion pair from which return would not be observed.

In TFA, pinacolyl brosylate (**76**) solvolyzes 2800 times faster than isopropyl brosylate, a difference which, following traditional arguments, would be ascribed to methyl participation during ionization. Alternatively, the rates of intimate ion pair formation from 2-propyl and from pinacolyl brosylate may not be very different, but the isopropyl ion pair mostly returns to starting

material while the pinacolyl ion pair gives mostly solvolysis products. According to this view [111, 112], it is not participation in the initial bond ionization which is responsible for the observed pinacolyl/2-propyl rate ratio, but rather participation in the further reaction of an initially formed, unrearranged ion pair. Traditionally, participation has been considered to occur during the rate-limiting step; if Shiner's suggestion [111, 112] is correct, participation can occur *after* the rate-limiting step but still result in rate enhancement relative to a nonrearranging reference substrate.



Scheme XXII. Shiner's interpretation of the reaction of *t*-butylethylene with *p*-bromobenzenesulfonic acid in trifluoroacetic acid [112].

α -, β -, and γ -Deuterium isotope effects are cited by Shiner, Fisher, and Dowd [112] in support of this explanation, but their interpretation of the isotope effects is not free from criticism (see Section 4.1). In the more nucleophilic solvents, 2-propyl brosylate is considered to have substantial $\text{S}_{\text{N}}2$ character and not to be retarded by ion pair return. Thus in 90% ethanol the 2-propyl derivative actually reacts three times more rapidly than **76**. However, the solvolysis data are also consistent with the more traditional explanation of rate-limiting methyl participation for **76**, and the results are in fact entirely analogous to those obtained in the study of the relative reactivities of 2-propyl and 2-adamantyl tosylates [123] (where the latter is a nonrearranging substrate).

Shiner and his co-workers did not discuss the alternative possibility that the formation of 2-propyl trifluoroacetate in the reaction of 2-propanol with *p*-bromobenzenesulfonic acid in TFA [111] was not due to a substitution at carbon but was merely the result of an acid-catalyzed esterification of the alcohol with trifluoroacetic acid. Subsequent work [205] suggests that in fact this is the pathway for trifluoroacetate formation. Consequently, although an ion pair mechanism may be operating in part, the evidence by Shiner to postulate Scheme XXI was not valid. A recent paper [118b] casts further doubt on Shiner's interpretation.

If the solvolyses of secondary and primary derivatives are assumed to take place via initial ion pair formation without assistance from either solvent or

neighboring group, then it is possible to compare the magnitude of ion pair return estimated by several different procedures:

1. Using Snee's mathematical model, where $k_{-1}/k_2 \equiv x$.
2. Using equilibration data for ^{18}O -labeled substrates (or using isomerization data for substrates having polydentate leaving groups) where $k_{-1}/k_2 = k_{\text{eq}}/k_{\text{solvolysis}}$.
3. Using Shiner's explanation of anchimeric assistance, where $k_{-1}/k_2 = (\text{rate enhancement} - 1)$.
4. Using rearrangement of starting material where $k_{-1}/k_2 = (1 - F)/F = k_{\text{eq}}/k_t$.

TABLE 32 Estimation of Internal Return for Secondary and Primary Derivatives by Different Methods Assuming Initial Unassisted Ion Pair Formation

Substrate	Solvent	k_{-1}/k_2	Method	Ref.
2-Octyl mesylate	25% Dioxane	2.3	1	4
	30% Dioxane	2.6	1	4
2-Octyl tosylate	MeOH	0.01	2	56
	AcOH	0.07	2	56
	HCO ₂ H	0.09	2	56
	TFA	0.25	2	56
	HOAc	0.04	2	56
	HCO ₂ H	0.03	2	56
	TFA	0.08	2	56
	HOAc	34	3	206
	TFA	10 ³	3	211
	HOAc	3.0	4	19
	EtOH	0.3	4	19
	TFA	10 ³	3	190
β -Phenylethyl tosylate	TFA	1.4	4	130

Inspection of Table 32 reveals two clear discrepancies among the various methods. In contrast to the other three criteria, the ^{18}O equilibration studies (method 2) of unactivated secondary derivatives gives values of k_{-1}/k_2 which are lower by one to two orders of magnitude. This is perhaps a consequence of internal return with bond formation to the *same* oxygen atom; alternatively, it may indicate that some of the assumptions on which the method is based are erroneous.

The second discrepancy occurs for the amount of ion pair return estimated from rate enhancement: The entries for this method give values of k_{-1}/k_2 which are substantially larger (by several powers of 10) than the other methods. The validity of this criterion has been questioned [118b].

Other possible methods that can help elucidate the mechanism of solvolysis

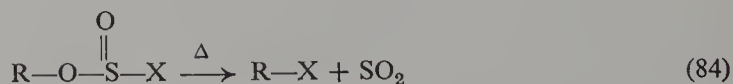
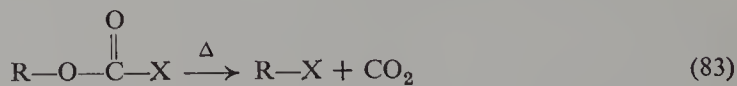
of simple secondary derivatives will certainly be found. Considerable progress in research on this question has already been achieved, and we are now concerned with some of the more subtle details. Certainly our description of the k_s process [23, 123, 171–178] and Snee's description of the ion pair mechanism [4, 47, 200] differ only in minor detail. Both descriptions emphasize the absence of carbonium ions and the large dependence of rate on nucleophilic attack by solvent or added nucleophile. The relatively subtle difference between the two descriptions can be put in terms of Scheme XIV: does bond formation between the nucleophile and carbon begin *simultaneously with* or *subsequent to* initiation of the bond-breaking process between carbon and the leaving group? Are nucleophilically solvated ion pairs the real intermediates involved? These questions remain to be answered.

6. MISCELLANEOUS METHODS FOR THE GENERATION OF ION PAIRS

The purpose of this section is to present several alternative routes for the generation of ion pairs and free carbonium ions other than the usual solvolysis reactions of alkyl halides and esters. The coverage is necessarily brief since most of the topics considered constitute major areas of organic chemistry (e.g., diazonium ion decomposition and acid addition to olefins). In each of the subsections we attempt to give a concise discussion of the mechanism and type of intermediate generated by the reaction in question along with leading references to more extensive reviews.

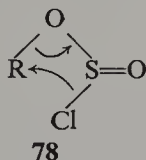
6.1. Thermal Decomposition of Alkyl Formates, Sulfinates, and Related Compounds

Alkyl formates and sulfinates can be thermally decomposed to yield CO_2 or SO_2 and a new alkyl derivative which usually has retained configuration:

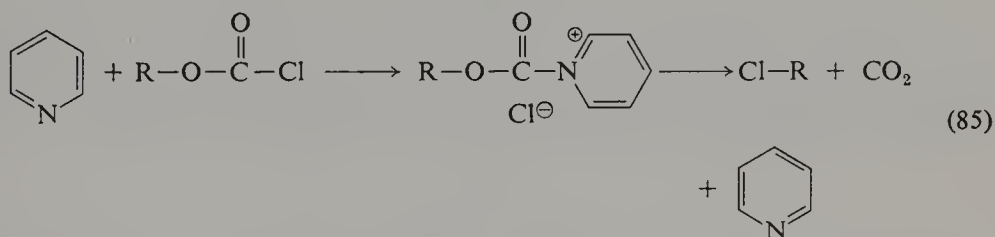


where $\text{X} = -\text{Cl}$, $-\text{SR}'$, and $-\text{OR}'$. These decompositions are known collectively as S_{Ni} reactions since they are nucleophilic substitutions by an "internal" nucleophile attached to the leaving group. Originally all were interpreted as proceeding by a cyclic mechanism as shown in 78 for a chlorosulfinate [207]. This mechanism accounts for the observed retention of

configuration but not for the high dependency of decomposition rates on solvent polarity and substrate structure. Thus more recent interpretations are based on rate-determining formation of ion pairs which in most cases collapse with retention of configuration. There is evidence for the involvement of both intimate and solvent-separated ion pairs.



The presence of bases such as pyridine during the decomposition of chloroformates or chlorosulfonates has been shown to result in inversion of configuration [208, 209], presumably through displacement of chloride by the base followed by nucleophilic attack by chloride:



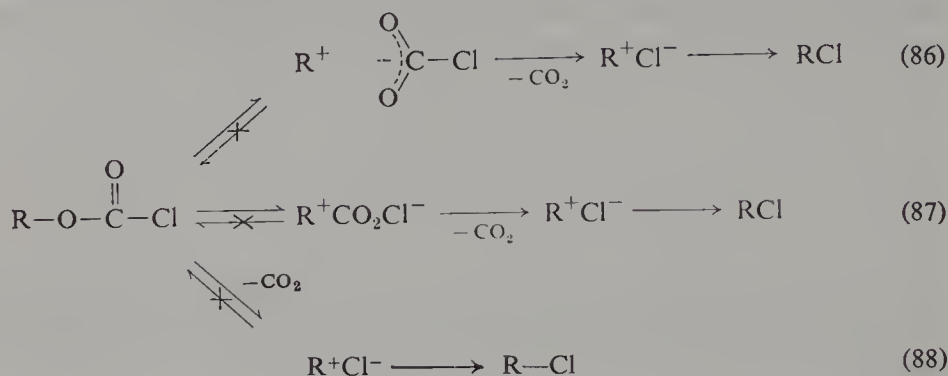
Moreover, formates and sulfonates react differently in nucleophilic and in nonnucleophilic solvents [210]. The present discussion, however, is concerned only with decomposition of neat substrate or decomposition in nonnucleophilic solvents.

6.1.1. Chloroformate and Carbonate Decomposition

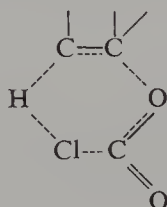
The decomposition of chloroformates has been extensively studied, and the following experimental features are observed: (1) product is formed with predominant retention of configuration [208, 211, 212]; (2) decomposition rates increase with increasing ionizing power of the solvent and with increasing carbonium ion stability [211, 212]; and (3) carbonyl ^{18}O does not equilibrate with ether oxygen in the starting substrate (α -phenylethyl) during decomposition [214]. The following mechanisms (p. 352) are consistent with these facts.

Primary chloroformates decompose slowly; for example, Olivier and Young [212] report a rate of 10^{-7} sec^{-1} for ethyl chloroformate in methylene chloride at 75° . This relative inertness and the observation of cyclic concerted decompositions in the gas phase [215] indicate that primary chloroformates, unlike the more highly substituted derivatives, may not decompose by alkyl-oxygen heterolysis [212]. To test this possibility, Clinch and Hudson [216] studied the neat decomposition of several primary alkyl chloroformates, and

they observed extensive rearrangement and elimination (for example, *n*-butyl chloroformate gives 7% *n*-butyl chloride, 27% *s*-butyl chloride, 44% 1-butene, and 22% 2-butene). The formation of large amounts of 1-alkene



suggests that elimination by a cyclic-concerted mechanism (79) may be occurring, although elimination might also occur at the stage of an ion pair. Alkyl-oxygen heterolysis is also indicated by the occurrence of rearrangement, and it must be concluded that any cyclic-concerted processes are competitive with heterolytic processes for primary alkyl chloroformates.

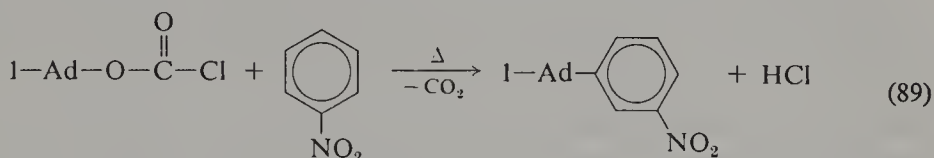


79

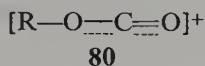
Kevill and his co-workers [213, 217, 218] have attempted to determine which of the potential heterolysis mechanisms (Eqs. 86–88) best describes chloroformate decomposition by comparing the entropies of activation for 1-adamantyl chloroformate decompositions in various solvents with those for model ionization processes (the solvolysis of 1-adamantyl halides and esters). Thus it could be reasoned that mechanisms 87 and 88 would result in more positive ΔS^\ddagger than mechanism 86. Their early results [217] showed more positive entropies for the chloroformate decompositions; however, recent experiments [218] have shown that ΔS^\ddagger for the model solvolysis reactions (all of which presumably proceed by rate-determining ionization) can vary over a wide range as a function of changes in leaving group only. Thus comparison of entropies of activation does not appear to offer a viable mechanistic probe for these reactions. Similar studies have been conducted by Buncel and Millington [220].

Kevill and Weitz [213] have suggested that some dissociation to a free carbonium ion can result upon chloroformate decomposition. This

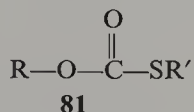
interpretation is based on the formation of hydrochloric acid and aromatic substitution product upon decomposition of 1-adamantyl chloroformate in nitrobenzene (Eq. 89). This dissociation process can potentially account for the racemization found in other chloroformate decompositions [208, 212].



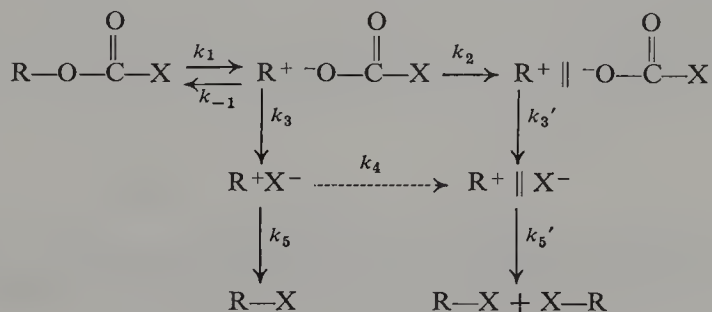
Carbonyl-chlorine heterolysis to give the acylium ion, **80**, has been shown to be important for chloroformate decomposition in cases in which highly unstable carbonium ion fragments would be formed by alkyl-oxygen cleavage (e.g., phenyl chloroformate) [219]. This process does not appear to be involved in the more typical reactions of chloroformates.



Kice and his co-workers [221–223] have studied the decomposition of a series of thiocarbonates, **81**. These decompositions should be very similar

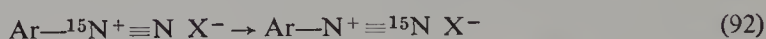
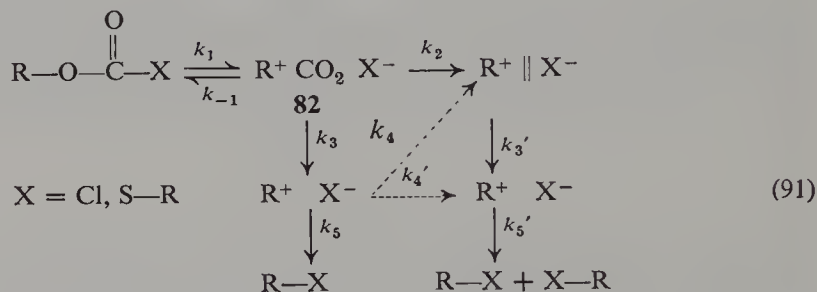


to those of chloroformates; moreover, the nucleophilicity of the internal nucleophile ($-\text{SR}'$) can be varied in the thiocarbonate system. These decompositions are also accelerated by polar solvents and increasing stability of the carbonium ion fragments. However, significant differences in behavior relative to the chloroformates were observed: (1) starting substrate racemized during the decomposition ($k_{\text{rac}} > k_{\text{decomp}}$) [222]; (2) carbonyl ^{18}O is scrambled to ether ^{18}O ($k_{\text{equil}} > k_{\text{decomp}}$) [223], and the product thioethers are completely racemic [223]. Observations 1 and 2 require that the decomposition of thiocarbonates involve a reversible step which is faster than the loss of CO_2 . To account for the fact that thiocarbonates give racemized products whereas chloroformates do not, the following generalized mechanism was proposed [223]:

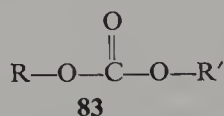


Chloroformates were suggested to decompose via intimate ion pairs and thiocarbonates were suggested to decompose via solvent-separated ion pairs. This argument is based on the expected greater stability of Cl^- relative to $\text{Cl}-\text{CO}_2^-$ than of RS^- relative to $\text{RS}-\text{CO}_2^-$. Thus the major fate of intimate ion pair derived from chloroformate is loss of carbon dioxide to give a new intimate ion pair. In contrast, the intimate ion pair formed from a thiocarbonate and can undergo further dissociation to solvent-separated ion pair. This suggestion of decreased importance of the process designated by k_3 is in agreement with the observation of internal return in thiocarbonate decompositions.

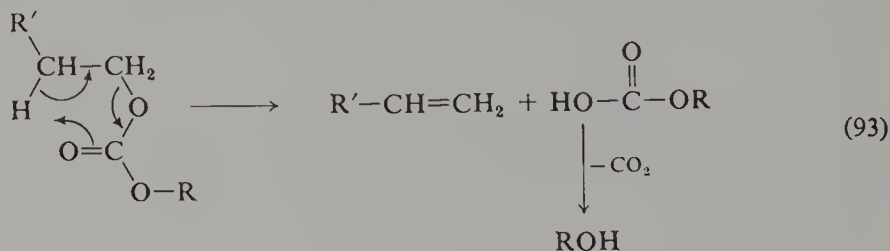
Although Kice and co-workers favor the sequential cleavage of alkyl-oxygen and carbonyl-X bonds, they suggest that simultaneous cleavage is also a possibility (Eq. 91). The recombination of a species such as **82** presents a novel reaction type which to our knowledge has been considered only once previously, in this case for the recombination of a diazonium species (Eq. 92) [224].



Carbonate (**83**) decompositions have also been studied [225, 226]. For

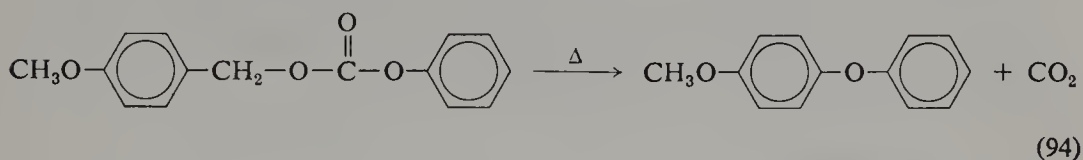


those cases in which both R and R' are simple alkyl groups (e.g., propyl or butyl groups), only elimination is observed (e.g., Eq. 93) [226]. However,



if R is an aralkyl group and R' is an aryl group (e.g., *p*-methoxybenzyl phenyl carbonate), heterolytic cleavage does occur (Eq. 94). Evidence for this

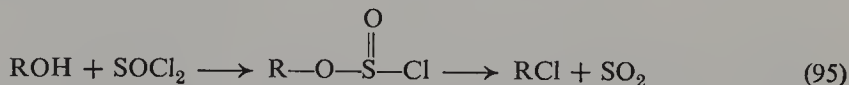
mechanism of decomposition comes from the observation of a rate dependence on polarity of the solvent and stability of the carbonium ion fragment. However, the available data for this system are not sufficient to distinguish



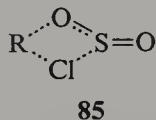
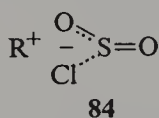
between the potential mechanisms of decomposition, represented by Eqs. 86, 87, 88, 90, and 91.

6.1.2. Chlorosulfinate Decompositions

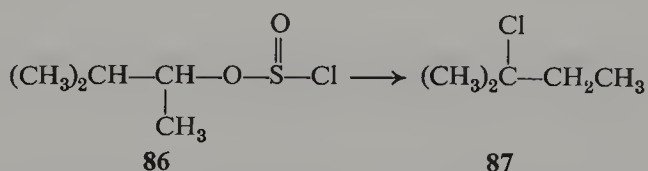
The preparation of alkyl chlorides from alcohols with predominant retention of configuration has classically been performed by reaction with SOCl_2 (Eq. 95). This reaction is known [227] to proceed via an alkyl chlorosulfinate which decompose by an $\text{S}_{\text{N}}\text{i}$ mechanism to the alkyl chloride.



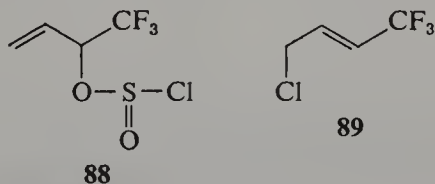
In view of the large response of reaction rates to solvent polarity and carbonium ion stability, the mechanism for decomposition of simple alkyl chlorosulfonates appears to be ionic (84) rather than concerted (85) [228, 229].



The formation of 87 from 86 also is consistent with an ionic process [230].



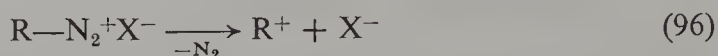
One problem associated with the study of chlorosulfonates has been their instability [212]. Pegolotti and Young [231] utilized an alkyl chlorosulfonate containing an electron-withdrawing trifluoromethyl group (88) in order to obtain a less reactive substrate which could be isolated. This molecule gives



the rearranged product (**89**) only, and shows a very low response to solvent polarity. Thus it appears that a concerted-cyclic process can compete with ionization when the carbonium ion fragment is relatively unstable. However, it should be noted that the conversion of **88** to **89** corresponds to a six-membered ring transition state in contrast to the four-center process (**85**) originally proposed for chlorosulfinate decompositions.

6.2. Diazonium Ions

The decompositions of alkyl diazonium ions have frequently been interpreted as proceeding via free carbonium ions [232, 233]:



There is evidence in favor of this interpretation. For example, the products from diazonium reactions almost always involve more rearrangement and racemization than those derived from solvolysis. Moreover, certain reaction types such as cyclopropane formation, 1,3-hydride shifts, and fragmentation (which are unusual for solvolytic processes) are frequently observed for diazonium ion decomposition and for other processes thought to generate free carbonium ions (see Tables 33 to 35) [232, 233].

Recent work in this area has shown that the differences between solvolytic and deamination processes may not be a consequence of the formation of free carbonium ions upon deamination but may result from several other factors. In this section we present some of the experiments that indicate that deamination cannot be assumed to yield free carbonium ions but actually proceeds by the same spectrum of mechanisms (Scheme II) as does the solvolysis process. Some inherent differences between solvolysis and deamination are also considered.

Table 33 A Comparison of Products from Deamination, Solvolysis, and Some "Free-Cation" Methods for the *n*-Propyl System^{a, b}

Product ^c	Solvolysis	Deamination	Deoxidation	Anodic Oxidation
CH ₃ CH=CH ₂	100	90	90	65
Cyclopropane	—	10	10	35
CH ₃ CH ₂ CH ₂ OS OS	97	42	78	34
CH ₃ CHCH ₃	3	58	22	66

^a Taken from a compilation in ref. 233, p. 633.

^b Elimination and substitution products presented on the basis of 100% for each process.

^c —OS designates product derived from reaction with a hydroxylic solvent, SOH.

Table 34 A Comparison of Product Stereochemistry for Solvolysis and Deamination




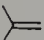
R—OBs or R—NH ₂ R =	Solvolysis	Deamination
CH ₃ CH ₂ CH ₂ CHD—	100 % inversion ^a (HCOOH)	85 % inversion ^b (CH ₃ COOH)
$\begin{array}{c} \\ \text{CH}_3\text{CH}_2\text{CHCH}_3 \end{array}$	—	64 % inversion ^c (CH ₃ COOH)
$\begin{array}{c} \\ \text{C}_6\text{H}_{13}\text{CHCH}_3 \end{array}$	100 % inversion ^d (several solvents)	—

^a A. Streitwieser, Jr., *J. Am. Chem. Soc.*, **77**, 1117 (1955).^b A. Streitwieser, Jr., and W. D. Schaeffer, *J. Am. Chem. Soc.*, **79**, 2888 (1957).^c K. B. Wiberg, Ph.D Dissertation, Columbia University, New York, 1950.^d Refs. 179, 180, and 186.

Nucleophilic and neighboring group attack can be important in deamination. For example, the predominant inversion of stereochemistry shown for deamination reactions in Table 34 is most simply explained by nucleophilic assistance of solvent to the departure of nitrogen.

Evidence for aryl participation in loss of N₂ comes from Snyder's [234] stereochemical and product study of the deamination of **90** in acetic acid. Snyder found that this reaction gave product with overall retention of stereochemistry and that the percent retention was almost exactly twice the percent rearrangement of ¹⁴C. These results were taken as evidence for competition between solvent-assisted (*k_s*) and anchimerically assisted (*k_Δ*) pathways. A

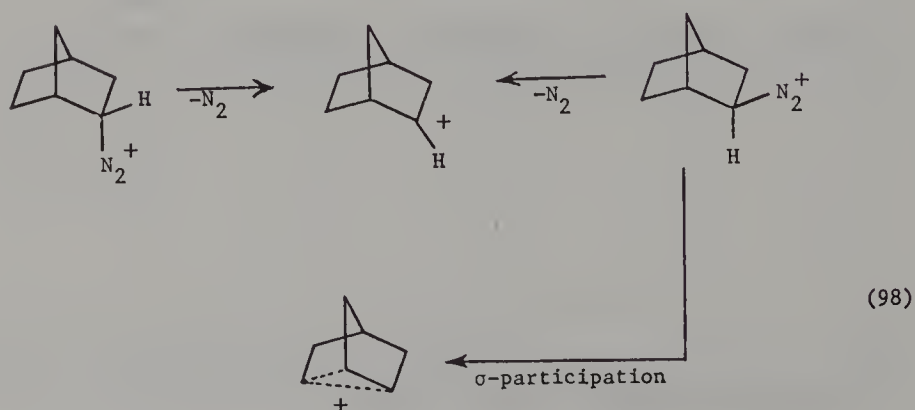
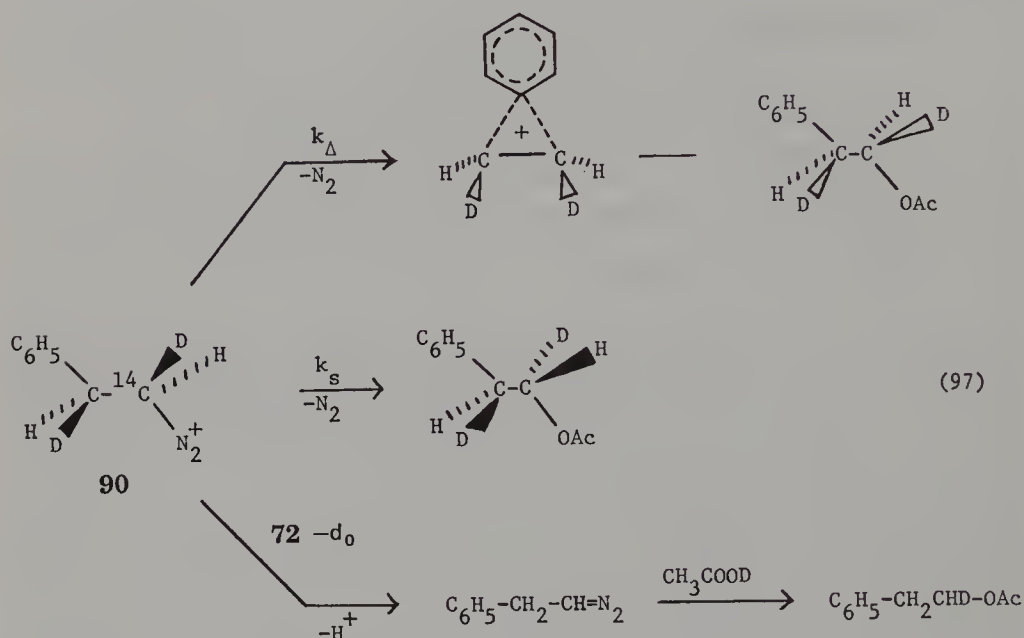
Table 35 Types of Olefin Formed from Solvolysis Compared to Those Formed from "Free-Cation Methods" for the *sec*-Butyl System^a

Olefin	Solvolysis	Deamination	Deoxidation	Anodic Oxidation
	10	25	46	49
	47	56	34	36
	43	19	20	15
	—	2	—	0

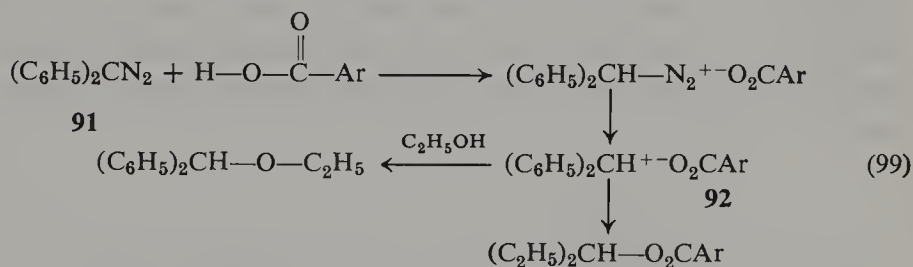
^a Taken from a compilation in ref. 233, p. 635.

third pathway (elimination-addition) was found to be the source of 6% of the products (Eq. 97).

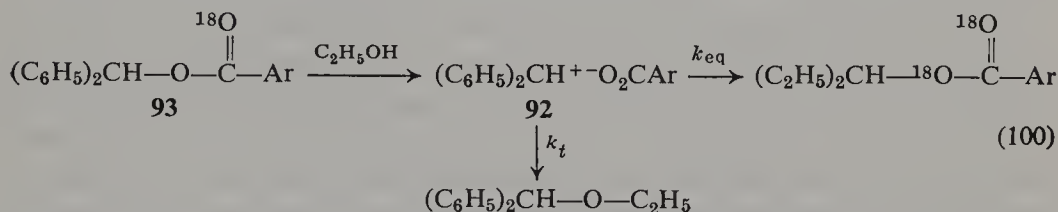
Study of the deamination of isomeric *exo*- and *endo*-norbornyl amines and *cis*- and *trans*-4-*t*-butylcyclohexyl amines has shown that the isomeric reactants give different product compositions [235–237]. If free cations were the result of N_2 loss, identical product compositions should be obtained from the isomeric amines. These results could be a consequence of neighboring group assistance (Eq. 98) or nucleophilic solvent assistance.



Alternatively, differences in solvation might be responsible for the differences in products. Diaz and Winstein [77] have provided evidence for the formation of ion pairs upon loss of N₂ from a diazonium ion by comparing the addition of acid to the diazo compound, **91**, with solvolysis of the corresponding ¹⁸O-labeled ester, **93**. Benzhydryl benzoates have been shown (see Section 3.2) to yield intimate and solvent-separated ion pairs upon solvolysis.



The relative amounts of ion pair return in reactions 99 and 100 can be determined by comparing the ratio of ester/(ester + ether for reaction 99



with the ratio of $k_{\text{eq}}/(k_{\text{eq}} + k_t)$ for reaction 100. These data are presented in Table 36, and there is fair agreement between the two measures of return (note the temperature extrapolations). Furthermore, White and Elliger [76] have derived evidence indicating that ^{18}O equilibration is not complete for the k_{eq} process Eq. 100 (see, however, p. 293). If this were the case, the estimates of return for solvolysis (Table 36) would be low and the amounts of

Table 36 Percent Return for Reactions 99 and 100

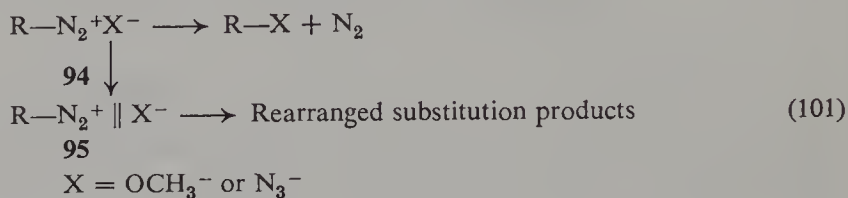
Reaction	Percent Return ^a	<i>T</i> (°C)	Ref.
93-OBz ^b + Ethanol	0.47	100	77
91 + Benzoic acid	0.558 ^c	100 ^c	77
93-OPNB ^b + 90% Acetone	0.745	118.6	70 ^b
91 + <i>p</i> -Nitrobenzoic acid	0.822 ^c	118.6 ^c	77
91 + Benzoic acid	0.609	25	77
91 + Benzoic acid	0.63	25	76

^a Percent return = $k_{eq}/(k_{eq} + k_t)$ for solvolysis and ester/(ester + ether (or alcohol)) for deamination.

^b —OBz, benzoate; —OPNB, *p*-nitrobenzoate.^c Extrapolated from lower temperature.

return for solvolytic and deamination processes would agree more closely. Thus these experiments indicate the formation of a common ion pair or spectrum of ion pairs for both deamination and solvolysis, and they present a strong argument against the formation of free carbonium ions for the deamination reaction.

Kirmse and Rinkler [238] have argued that different types of ion pair may occur and be of importance for the diazonium ion before loss of N_2 . Thus the tight ion pairs, **94**, were suggested to react without rearrangement, whereas the solvent-separated ion pairs, **95**, were suggested to give rearrangement (Eq. 101):



It is probable that similar cationoid species from solvolysis and deamination will react differently. There are several considerations leading to this conclusion. First, the decomposition of diazonium ions has a very low energy of activation and is exothermic. Thus the energy barrier to the various pathways open to the carbonium ion (or ion pair) may be compressed relative to those for a solvolytically generated carbonium ion. This factor has led to the description of carbonium ions generated from deamination as "hot" carbonium ions [232, 233]. Because of this compression subtle factors in the ground state can have a major effect on the product distribution. For example, several deaminations have been interpreted as being controlled by the conformational preferences of the ground state [239].

The solvolysis reaction is an endothermic process in which solvent plays the very important role of aiding charge development and separation, and it usually is assumed that a solvolytic intermediate is in equilibrium with its surroundings [240]. In contrast, the intermediate from exothermic

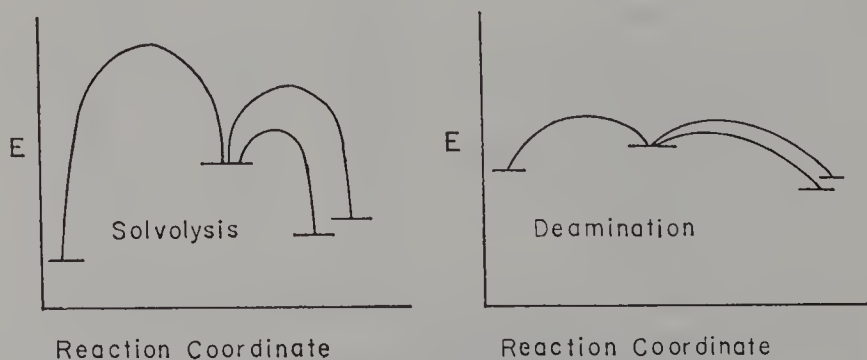


Figure 6. A comparison of potential energy diagrams for solvolysis and deamination.

deamination is probably formed with little aid from solvent, and is certainly formed much more rapidly than comparable solvolytic intermediates, as reflected by estimates of $k_{\text{deam}}/k_{\text{solv}} \simeq 10^{12}$ [77, 241]. It is thus possible that the intermediate from deamination may be formed too rapidly to be in equilibrium with its surroundings. As suggested by Keating and Skell [233], "the cation is born in a solvent cavity aligned not to the newborn cation but to the charge as it existed before birth." The deaminative positive species can then undergo unusual (for solvolysis reactions) reactions before solvent relaxation occurs. In this sense deamination may produce a "free" carbonium ion to the extent that the intermediate is less encumbered by solvent than a solvolytic intermediate.

The foregoing discussion has not been comprehensive; however, it is our opinion that the experiments discussed demonstrate that deaminations of alkyl amines (or similar processes which proceed via diazonium intermediates) do not always give free carbonium ions but proceed by a similar spectrum of mechanisms as do solvolysis reactions.

6.3. Acid Addition to Olefins

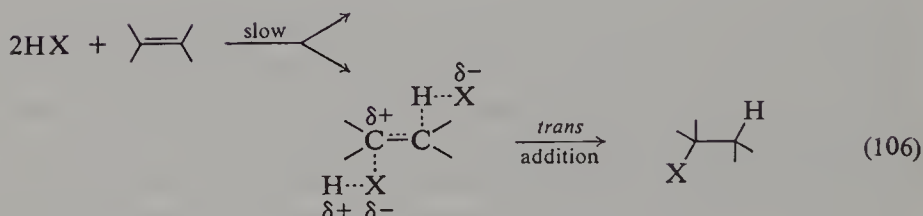
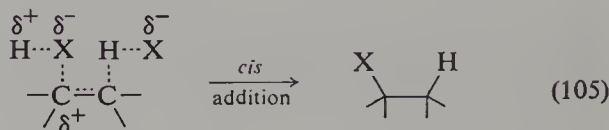
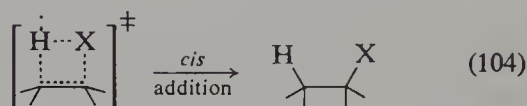
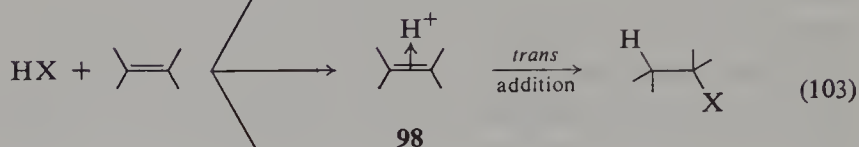
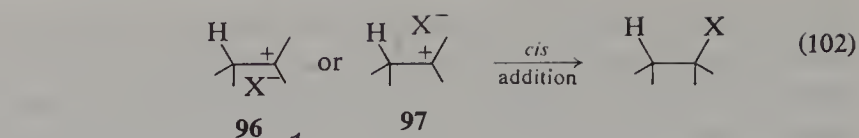
The addition of Bronsted acids to olefins has long been known to proceed in many instances through cationic intermediates [242, 243]. Thus it is not surprising that these additions frequently are used to generate intermediates for comparison with those from solvolysis reactions [99, 111, 244–246]. We have previously discussed in detail the experiments of Shiner [99, 111] in which acid addition to olefins is used to generate cationic intermediates for comparison with solvolytic intermediates. Therefore the present discussion is limited to pointing out the complexity of these addition reactions and the dangers inherent in assuming that identical intermediates are generated from solvolysis and addition reactions.

There are several recognized mechanistic possibilities by which acid addition to olefins may proceed, as shown at top of following page.

Equations 102–104 represent the $\text{Ad}_{\text{E}2}$ (addition, electrophilic, second order) mechanisms; Eqs. 105 and 106 give the $\text{Ad}_{\text{E}3}$ mechanisms.

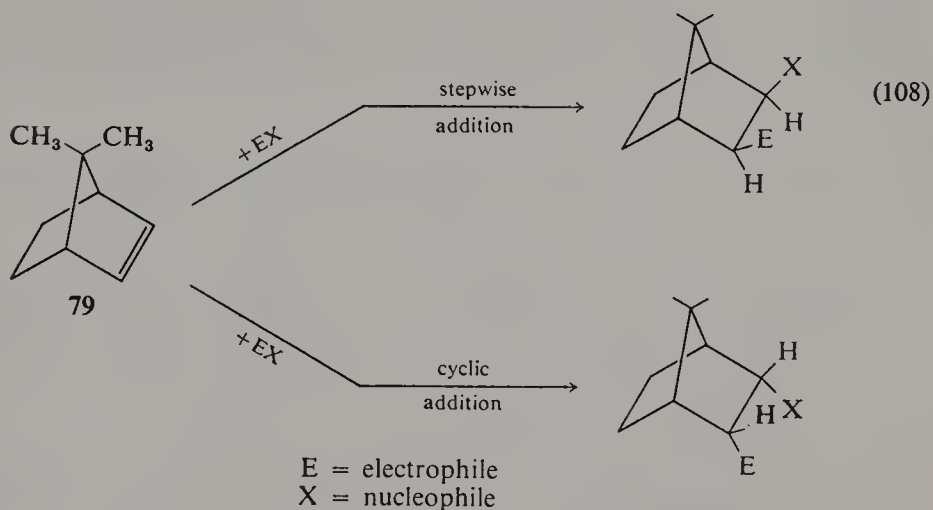
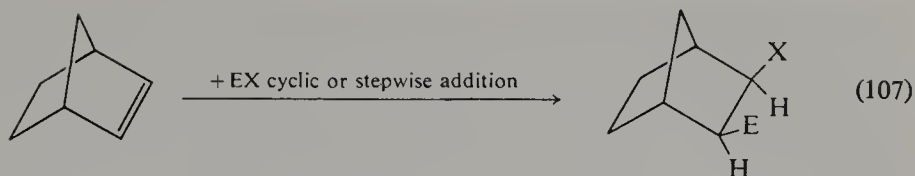
It appears that most additions to olefins proceed via mechanism 102 to give intermediate tight ion pair [247]. This mechanism accounts for the observation of predominant *cis* addition in solvents of low ionizing power and predominant *trans* addition in highly ionizing solvents.

There has been some controversy regarding the importance of π complexes (98) in addition reactions [242, 243, 247], and it is difficult at this time to estimate the relative energies of species 96 and 98. Recent experiments have shown that the barrier to 1,2-hydride shifts (presumably by way of a species



similar to **98**) in simple alkyl carbonium ions is quite low (~ 5 kcal/mole) [248]; thus **96** and **98** must have similar energies.

Cyclic molecular addition (Eq. 104) does not apply to HCl additions in diethyl ether or methylene chloride according to Brown and his co-workers [246b, 246c]. This conclusion resulted from observations of the effect of the 7,7-dimethyl groups in **99** on addition stereochemistry. Addition to norbornene (Eq. 107 by both stepwise and cyclic mechanisms yields *cis*, *exo* product stereochemistry, since addition from the *endo* side appears to be sterically hindered. Stepwise addition continues apparently unperturbed with **99** to give *exo*, *cis* stereochemistry (Eq. 108); however, the cyclic additions, having a sterically demanding transition state, are slowed greatly by the 7,7-dimethyl groups in **99** and result in formation of the *endo* product. The addition of HCl to both norbornene and 7,7-dimethylnorbornene (**99**) yields *exo*, *cis* stereochemistry and is thus concluded to occur by a stepwise mechanism.



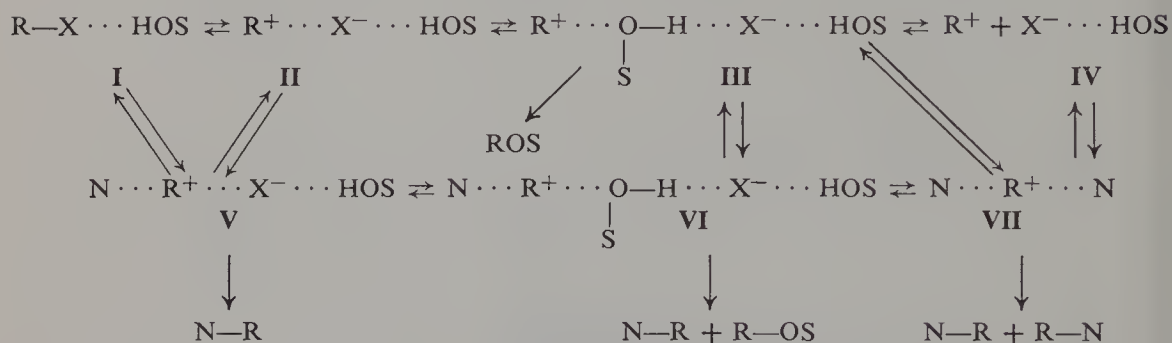
The $\text{Ad}_{\text{E}}3$ mechanisms, Eqs. 105 and 106, have been observed in several instances [243] and should be considered before assigning a mechanism to an addition reaction. However, it seems that in most instances addition to olefins proceeds via the ion pair mechanism (Eq. 102) [243].

The preceding discussion is intended to show that the addition of acids to olefins can proceed by several pathways and may or may not give intermediates similar to those from solvolysis reactions. It is also necessary to consider the possibility that similar intermediates generated by different processes may react differently. As discussed above, the rate at which an intermediate is formed may have an effect on its subsequent reactions as a consequence of the finite time required for solvent reorganization. It has also been shown that two ion pairs may differ only in the relative positioning of the counterions [249] (Section 4.3); these considerations are clearly important when attempts are made to generate the same species by different routes.

7. SOME OBSERVATIONS ON THE DETAILED MECHANISM OF SOLVOLYSIS

The mechanistic possibilities for solvolysis are many. The traditional Winstein solvolysis scheme (Scheme II) [19] can be elaborated to show more explicitly the role of nucleophile and solvent. This results in a complicated

diagram (Scheme XXIII) which accommodates most of the possibilities. The basis Winstein intermediates, I–IV, have been modified to show electrostatic solvation of the leaving group, and Winstein's more recent formulation [56] has been followed to show the solvent-separated ion pair **III** with the solvent playing a dual role, solvating both the anion (by hydrogen bonding) and the cation. In effect, the solvent molecule shown solvating the anionic portion of the intimate ion pair, **II**, has inserted itself between the two fragments to give **III**.



Scheme XXIII. N = either HOS or added nucleophile.

Species **V**, **VI**, and **VII** indicate the possibility of stable intermediates with solvation at the backside. These species are also possible transition states for direct displacements on I–IV. Whether **V**, **VI**, and **VII** are intermediates or transition states may depend on the substrate structure, the nature of the nucleophile, and the reaction conditions.

Intermediate **III** provides a simple rationalization for the several cases of *retention* of configuration which have been observed, including the solvolysis of 7-norbornyl arenesulfonates [250–251], and the phenolysis of α -phenethyl chloride [252, 253]. If the structure of **III** is such that nucleophilic attack from the rear is inhibited (i.e., **VI** does not form) and the rate of conversion to the “free” cation **IV** (or to the symmetrically solvated **VII**) is slow, then simple collapse would convert **III** to ROS with retention of configuration. This seems preferable to Okamoto's formulation [252, 253] of this retention process as collapse of a 4-center intermediate.

The role of nucleophile (or solvent acting as nucleophile is emphasized in Scheme XXIII. Direct displacement on **I** via **V** as transition state represents the classical S_N2 reaction.* Alternatively, **V** may be formed via **II**, as Snee has suggested [47]. Moreover, if ion pair intermediates are involved in the

* In Winstein's solvolysis scheme [19] such direct attack on covalent substrate is not explicitly indicated as a possibility.

solvolysis of simple secondary and primary substrates [4, 47, 99, 111, 113], it may be that V and not II is the structure of the first intermediate.*

The solvent-separated ion pair may be nucleophilically solvated (VI) or nucleophilically unsolvated (III). Additionally, there is some evidence for the existence of solvent-separated ion pairs which have two insulating solvent molecules [196]. An interesting possibility is shown: VI can, in principle, collapse in two nonequivalent ways. If a nucleophile other than solvent is present, the substitution product, N—R, should be inverted, but the solvolysis product, ROS, may have appreciable retention of configuration. Goering and Hopf [74] have performed an experiment in which optically active *p*-methylbenzhydryl *p*-nitrobenzoate was solvolyzed in 90% acetone in presence of sodium azide, conditions for which evidence showed that solvent-separated ion pairs intervened. The *solvolysis* product had net *retention* of configuration, but the *azide* product (which was also optically active) was assigned the *inverted* configuration.

Symmetrically solvated (VII) or totally nucleophilically unsolvated (IV) species would give completely racemic product, a stereochemical result seldom observed in solvolysis. A major problem remaining in the study of solvolysis reactions is the delineation of all of these mechanistic alternatives. Even Scheme XXIII may not include all possibilities. Evidence in the literature suggests the possibility of a third type of ion pair in addition to the two types (II and III) discussed by Winstein [19]. Several systems (e.g., 3-phenyl-2-butyl tosylate) solvolyze with $k_a/k_t > 1$ but do not show a special salt effect [37]. If Winstein's explanation of the special salt effect is accepted, this means that there is no return from the solvent-separated ion pair, and the disparity between polarimetric and titrimetric rates is a consequence of return from a bridged intimate ion pair. Note that the work of Schleyer and Lancelot [172–176, 178] (see especially ref. 178), which ruled out rapidly equilibrating carbonium ions, also precludes rapidly equilibrating ion pairs as the basis for the unusual kinetic and stereochemical behavior of these systems. Thus the species which reacts either by k_{Δ} or k_s (i.e., competitive nucleophilic participation by solvent and by neighboring aryl group) cannot be Winstein's intimate ion pair, since this intermediate is *already bridged*. This would indicate that the nucleophilic participation by solvent or aryl group takes place either at the stage of *neutral substrate* or at the stage of a *third ion pair* which is "less ionized" than Winstein's intimate ion pair (II). This ion

* Koskikallio [198] has suggested that methyl perchlorate hydrolyzes by the sequence



His data are consistent with such a mechanism but do not require it. His expansion of Snee's ion pair scheme [4, 47] is not well justified, and in any event the data appear to be entirely consistent with reaction by an S_N2 pathway.

pair might be considered as a structure intermediate between **I** and **II** in Scheme XXIII; alternatively, it might be represented by species **V**. Although no definitive evidence is available regarding the existence of such an "intimate" intimate ion pair, such a species has in effect been postulated recently by several groups of workers [47, 111, 112, 136, 139] (see Section 4.2).

REFERENCES

1. For short historical surveys of the development of carbonium ion chemistry, see (a) D. Bethel and V. Gold, *Carbonium Ions, An Introduction*, Academic Press, New York, 1967, pp. 6-11; and (b) C. D. Nenitzescu, in *Carbonium Ions*, Vol. I, G. Olah and P. v. R. Schleyer (eds.), Wiley, New York, 1968.
2. L. P. Hammett, *Physical Organic Chemistry*, McGraw-Hill, New York, 1940, p. 52.
3. For a brief review and complete bibliography of Winstein's work, see P. D. Bartlett, *J. Am. Chem. Soc.*, **94**, 2161 (1972).
4. R. A. Sneen and J. W. Larsen, *J. Am. Chem. Soc.*, **91**, 6031 (1969); R. A. Sneen, *Accts. Chem. Res.*, **6**, 46 (1973).
5. F. G. Bordwell, *Accts. Chem. Res.*, **3**, 281 (1970).
6. C. K. Ingold, *Structure and Mechanism in Organic Chemistry*, 2nd ed., Cornell University Press, Ithaca, N.Y., 1969.
7. L. C. Bateman, M. G. Church, E. D. Hughes, C. K. Ingold, and N. A. Taher, *J. Chem. Soc.*, **1940**, 979.
8. L. C. Bateman, E. D. Hughes, and C. K. Ingold, *J. Chem. Soc.*, **1940**, 974.
9. O. T. Benfey, E. D. Hughes, and C. K. Ingold, *J. Chem. Soc.*, **1952**, 2488.
10. B. Bensley and G. Kohnstam, *J. Chem. Soc.*, **1955**, 3408.
11. G. Kohnstam and B. Shillaker, *J. Chem. Soc.*, **1959**, 1915.
12. E. D. Hughes, *J. Chem. Soc.*, **1935**, 255.
13. S. Winstein, E. Clippinger, A. H. Fainberg, R. Heck, and G. C. Robinson, *J. Am. Chem. Soc.*, **78**, 328 (1956).
14. P. B. D. De La Mare, D. M. Hall, and E. Maugher, *Rec. Trav. Chim. Pays-Bas*, **87**, 1394 (1968).
15. W. G. Young, S. Winstein, and H. L. Goering, *J. Am. Chem. Soc.*, **73**, 1958 (1951).
16. S. Winstein and K. C. Schreiber, *J. Am. Chem. Soc.*, **74**, 2171 (1952).
17. S. Winstein, E. Clippinger, A. H. Fainberg, and G. C. Robinson, *Chem. Ind.*, **1954**, 664.
18. S. Winstein, E. Clippinger, A. H. Fainberg, and G. C. Robinson, *J. Am. Chem. Soc.*, **76**, 2597 (1954).
19. S. Winstein, B. Appel, R. Baker, and A. Diaz, *Chem. Soc. (London), Spec. Pub.*, **19**, 109 (1965).
20. S. Winstein and K. C. Schreiber, *J. Am. Chem. Soc.*, **74**, 2165 (1952).
21. E. Grunwald, *Anal. Chem.*, **26**, 1696 (1954).
22. S. Winstein and G. C. Robinson, *J. Am. Chem. Soc.*, **80**, 169 (1958).

23. J. L. Fry, C. J. Lancelot, L. K. M. Lam, J. M. Harris, R. C. Bingham, D. J. Raber, R. E. Hall, and P. v. R. Schleyer, *J. Am. Chem. Soc.*, **92**, 2538 (1970).
24. E. Grunwald, A. Heller, and F. S. Klein, *J. Chem. Soc.*, **1957**, 2604.
25. H. L. Goering and J. F. Levy, *J. Am. Chem. Soc.*, **86**, 120 (1964).
26. S. Winstein, A. Ledwith, and M. Hojo, *Tetrahedron Lett.*, **1961**, 341.
27. S. Winstein, E. Grunwald, and H. W. Jones, *J. Am. Chem. Soc.*, **73**, 2700 (1951).
28. E. Grunwald and S. Winstein, *J. Am. Chem. Soc.*, **70**, 846 (1948).
29. A. H. Fainberg and S. Winstein, *J. Am. Chem. Soc.*, **78**, 2770 (1956).
30. L. C. Bateman, E. D. Hughes, and C. K. Ingold, *J. Chem. Soc.*, **1940**, 960.
31. M. G. Church, E. D. Hughes, and C. K. Ingold, *J. Chem. Soc.*, **1940**, 966.
32. M. G. Church, E. D. Hughes, C. K. Ingold, and N. Taher, *J. Chem. Soc.*, **1940**, 971.
33. E. D. Hughes and C. K. Ingold, *J. Chem. Soc.*, **1935**, 252.
34. A. H. Fainberg and S. Winstein, *J. Am. Chem. Soc.*, **78**, 2763 (1956).
35. E. F. Duynstee, E. Grunwald, and M. L. Kaplan, *J. Am. Chem. Soc.*, **82**, 5654 (1960).
36. S. Winstein, P. E. Klinedienst, and G. C. Robinson, *J. Am. Chem. Soc.*, **83**, 885 (1961).
37. A. H. Fainberg and S. Winstein, *J. Am. Chem. Soc.*, **78**, 2780 (1956).
38. S. Winstein, S. Smith, and D. Darwish, *J. Am. Chem. Soc.*, **81**, 5511 (1959).
39. S. Winstein, E. C. Friedrich, and S. Smith, *J. Am. Chem. Soc.*, **86**, 305 (1964).
40. A. Ledwith, M. Hojo, and S. Winstein, *Proc. Chem. Soc.*, **1961**, 241.
41. A. H. Fainberg and S. Winstein, *J. Am. Chem. Soc.*, **78**, 2767 (1956).
42. A. H. Fainberg, G. C. Robinson, and S. Winstein, *J. Am. Chem. Soc.*, **78**, 2777 (1956).
43. S. Winstein and E. Clippinger, *J. Am. Chem. Soc.*, **78**, 2784 (1956).
44. S. Winstein, S. Smith, and D. Darwish, *Tetrahedron Lett. No. 16*, **1959**, 24.
45. S. Winstein, M. Hojo, and S. Smith, *Tetrahedron Lett. No. 22*, **1960**, 12.
46. J. M. Harris, D. J. Raber, R. E. Hall, and P. v. R. Schleyer, *J. Am. Chem. Soc.*, **92**, 5729 (1970).
47. R. A. Sneen and J. W. Larsen, *J. Am. Chem. Soc.*, **91**, 362 (1969).
48. D. J. Raber, J. M. Harris, and P. v. R. Schleyer, *J. Am. Chem. Soc.*, **93**, 4829 (1971).
49. E. F. Jenny and S. Winstein, *Helv. Chim. Acta*, **41**, 807 (1958).
50. S. Winstein and A. H. Fainberg, *J. Am. Chem. Soc.*, **80**, 459 (1958).
51. S. Winstein, R. Baker, and S. Smith, *J. Am. Chem. Soc.*, **86**, 2072 (1964).
52. S. Winstein and J. Sonnenberg, *J. Am. Chem. Soc.*, **83**, 3235 (1961).
53. W. P. Giddings and R. F. Bucholz, *J. Am. Chem. Soc.*, **86**, 1261 (1964).
54. S. Winstein, P. E. Klinedienst, Jr., and E. Clippinger, *J. Am. Chem. Soc.*, **83**, 4986 (1961).
55. (a) R. P. Anderson, Ph.D. Thesis, University of Wisconsin, Madison, 1966; (b) H. L. Goering and K. Humski, *J. Am. Chem. Soc.*, **90**, 6213 (1968); (c) H. L. Goering and A. C. Olson, *J. Am. Chem. Soc.*, **75**, 5853 (1953).
56. A. F. Diaz, I. Lazdins, and S. Winstein, *J. Am. Chem. Soc.*, **90**, 1904 (1968).
57. H. L. Goering and E. F. Silversmith, *J. Am. Chem. Soc.*, **77**, 5172, 6249 (1955).
58. R. A. Sneen and A. M. Rosenberg, *J. Am. Chem. Soc.*, **83**, 895, 900 (1961).
59. D. B. Denney and D. G. Denney, *J. Am. Chem. Soc.*, **79**, 4806 (1957).

60. (a) H. L. Goering, M. M. Pombo, and K. D. McMichael, *J. Am. Chem. Soc.*, **85**, 965 (1963); (b) H. L. Goering and M. M. Pombo, *J. Am. Chem. Soc.*, **82**, 2515 (1960).
61. H. L. Goering and J. T. Doi, *J. Am. Chem. Soc.*, **82**, 5850 (1960).
62. H. L. Goering, J. T. Doi, and K. D. McMichael, *J. Am. Chem. Soc.*, **86**, 1951 (1964).
63. P. v. R. Schleyer, J. L. Fry, L. K. M. Lam, and C. J. Lancelot, *J. Am. Chem. Soc.*, **92**, 2542 (1970).
64. R. A. Sneen and W. A. Bradley, *J. Am. Chem. Soc.*, **94**, 6975 (1972).
65. R. A. Sneen and P. S. Kay, *J. Am. Chem. Soc.*, **94**, 6983 (1972).
66. R. A. Sneen and J. V. Carter, *J. Am. Chem. Soc.*, **94**, 6990 (1972).
67. Cf. W. von E. Doering and W. R. Roth, *Tetrahedron*, **18**, 67 (1962).
68. H. L. Goering and E. C. Linsay, *J. Am. Chem. Soc.*, **91**, 7435 (1969).
69. H. L. Goering, G. S. Koerner, and E. C. Linsay, *J. Am. Chem. Soc.*, **93**, 1230 (1971).
70. (a) H. L. Goering and J. F. Levy, *Tetrahedron Lett.*, **1961**, 644; (b) H. L. Goering and J. F. Levy, *J. Am. Chem. Soc.*, **84**, 3853 (1962).
71. (a) S. Winstein and J. S. Gall, *Tetrahedron Lett.*, **1960**, 31; (b) S. Winstein, J. S. Gall, M. Hojo, and S. Smith, *J. Am. Chem. Soc.*, **82**, 1010 (1960).
72. H. L. Goering, R. G. Briody, and J. F. Levy, *J. Am. Chem. Soc.*, **85**, 3059 (1963).
73. H. L. Goering and J. F. Levy, *J. Am. Chem. Soc.*, **86**, 120 (1964).
74. H. L. Goering and H. Hopf, *J. Am. Chem. Soc.*, **93**, 1224 (1971).
75. H. L. Goering, R. G. Briody, and G. Sandrock, *J. Am. Chem. Soc.*, **92**, 7401 (1970).
76. E. H. White and C. A. Elliger, *J. Am. Chem. Soc.*, **89**, 165 (1967).
77. A. F. Diaz and S. Winstein, *J. Am. Chem. Soc.*, **88**, 1318 (1966).
78. K. E. Rubenstein, Ph.D. Thesis, University of Wisconsin, Madison, 1967.
79. G. Sandrock and H. L. Goering, Unpublished work cited in ref. 68.
80. H. L. Goering and S. Chang, *Tetrahedron Lett.*, **1965**, 3607.
81. H. L. Goering and G. Sandrock (Unpublished work cited in ref. 80) observed 53% racemization of α -anisylethyl-OPNB in 90% acetone at 80°.
82. A. Streitwieser, Jr., and T. D. Walsh, *J. Am. Chem. Soc.*, **87**, 3686 (1965).
83. S. Winstein and N. J. Holness, *J. Am. Chem. Soc.*, **77**, 5562 (1955).
84. (a) J. E. Nordlander and T. J. McCrary, Jr., *J. Am. Chem. Soc.*, **94**, 5133 (1972); (b) J. B. Lambert, G. J. Putz, and C. E. Mixan, *J. Am. Chem. Soc.*, **94**, 5132 (1972).
85. W. v. E. Doering, A. Streitwieser, Jr., and L. Friedman, Unpublished work cited in ref. 86.
86. A. Streitwieser, Jr., *Chem. Revs.*, **56**, 663 (1956); *Solvolytic Displacement Reactions*, McGraw-Hill, New York, 1962.
87. H. L. Goering and R. Briody, Unpublished results cited in ref. 70b.
88. D. B. Denney and B. Goldstein, *J. Am. Chem. Soc.*, **79**, 4948 (1957).
89. (a) H. L. Goering and R. W. Thies, *J. Am. Chem. Soc.*, **90**, 2967 (1968); (b) H. L. Goering and R. W. Thies, *J. Am. Chem. Soc.*, **90**, 2968 (1968).
90. H. L. Goering and G. N. Fickes, *J. Am. Chem. Soc.*, **90**, 2848 (1968).
91. B. E. Jones, Ph.D. Thesis, University of Wisconsin, Madison, 1971.
92. (a) Y. Pocker, in P. de Mayo (Ed.), *Molecular Rearrangements*, Vol. 1, Interscience, New York, 1963, p. 1; (b) J. A. Berson, *ibid.*, p. 111.

93. W. M. Schubert and W. L. Henson, *J. Am. Chem. Soc.*, **93**, 6299 (1971).
94. C. J. Lancelot, D. J. Cram, and P. v. R. Schleyer, in G. A. Olah and P. v. R. Schleyer (Eds.), *Carbonium Ions*, Vol. III, Wiley-Interscience, New York, 1972, Chap. 27, p. 1347.
95. I. L. Reich, A. Diaz, and S. Winstein, *J. Am. Chem. Soc.*, **91**, 5635 (1969).
96. J. E. Nordlander, S. P. Jindal, P. v. R. Schleyer, R. C. Fort, Jr., J. J. Harper, and R. D. Nicholas, *J. Am. Chem. Soc.*, **88**, 4475 (1966). However, later results force modification of the conclusions in this paper; see ref. 97.
97. S. H. Liggero, R. Sustmann, and P. v. R. Schleyer, *J. Am. Chem. Soc.*, **91**, 4571 (1969).
98. W. G. Dauben, J. L. Chitwood, and K. V. Scherer, Jr., *J. Am. Chem. Soc.*, **90**, 1014 (1968); W. G. Dauben and J. L. Chitwood, *J. Am. Chem. Soc.*, **92**, 1624 (1970).
99. V. J. Shiner, Jr., R. D. Fisher, and W. Dowd, *J. Am. Chem. Soc.*, **91**, 7748 (1969).
100. J. J. Harper, Ph.D. Thesis, Princeton University, Princeton, N.J., 1968; *Diss. Abst.*, **29**, 2808-B (1969).
101. J. E. Nordlander and W. J. Kelly, *J. Org. Chem.*, **32**, 4122 (1967).
102. P. D. Bartlett, S. Bank, R. J. Crawford, and G. H. Schmid, *J. Am. Chem. Soc.*, **87**, 1288 (1965).
103. W. G. Dauben and J. L. Chitwood, *J. Org. Chem.*, **34**, 726 (1969).
104. K. B. Wiberg and B. R. Lowry, *J. Am. Chem. Soc.*, **85**, 3188 (1963).
105. H. L. Goering and K. Humski, unpublished work cited in ref. 68.
106. H. L. Goering and W. D. Closson, *J. Am. Chem. Soc.*, **83**, 3511 (1961).
107. V. J. Shiner, Jr., in *Isotope Effects in Chemical Reactions*, ACS Monograph 167, C. J. Collins and N. S. Bowman (Eds.), Van Nostrand-Reinhold, New York, 1970, p. 90 ff.
108. V. J. Shiner, Jr., W. E. Buddenbaum, B. L. Murr, and G. Lamaty, *J. Am. Chem. Soc.*, **90**, 418 (1968).
109. V. J. Shiner, Jr., M. W. Rapp, E. A. Halevi, and M. Wolfsberg, *J. Am. Chem. Soc.*, **90**, 7171 (1968).
110. V. J. Shiner, Jr., W. Dowd, R. D. Fisher, S. R. Hartshorn, M. A. Kessick, L. Milakofsky, and M. W. Rapp, *J. Am. Chem. Soc.*, **91**, 4838 (1969).
111. V. J. Shiner, Jr., and W. Dowd, *J. Am. Chem. Soc.*, **91**, 6528 (1969).
112. V. J. Shiner, Jr., R. D. Fisher, and W. Dowd, *J. Am. Chem. Soc.*, **91**, 7748 (1969).
113. V. J. Shiner, Jr., M. W. Rapp, and H. R. Pinnick, Jr., *J. Am. Chem. Soc.*, **92**, 232 (1970).
114. V. J. Shiner, Jr., and W. Dowd, *J. Am. Chem. Soc.*, **93**, 1029 (1971).
115. V. J. Shiner, Jr., and R. D. Fisher, *J. Am. Chem. Soc.*, **93**, 2553 (1971).
116. B. L. Murr and M. F. Donnelly, *J. Am. Chem. Soc.*, **92**, 6686 (1970).
117. D. E. Sunko and S. Borčić, in *Isotope Effects in Chemical Reactions*, ACS Monograph 167, C. J. Collins and N. S. Bowman (eds.), Van Nostrand-Reinhold, New York, 1970, p. 160 ff.
118. (a) J. M. Harris, R. E. Hall, and P. v. R. Schleyer, *J. Am. Chem. Soc.*, **93**, 2551 (1971); (b) T. W. Bentley, S. H. Liggero, M. A. Imhoff, and P. v. R. Schleyer, *J. Am. Chem. Soc.*, **96**, 1970 (1974).
119. R. Stewart, A. L. Gatzke, M. Mocek, and K. Yates, *Chem. Ind. (London)*, **1959**, 331.

120. D. J. Raber, J. M. Harris, R. E. Hall, and P. v. R. Schleyer, *J. Am. Chem. Soc.*, **93**, 4821 (1971).
121. P. C. Vogel, *J. Am. Chem. Soc.*, **95**, 2045 (1973).
122. G. A. Dafforn and A. Streitwieser, Jr., *Tetrahedron Lett.*, **1970**, 3159.
123. P. v. R. Schleyer, J. L. Fry, L. K. M. Lam, and C. J. Lancelot, *J. Am. Chem. Soc.*, **92**, 2542 (1970).
124. W. M. Schubert and P. H. Le Fevre, *J. Am. Chem. Soc.*, **91**, 7746 (1969); **94**, 1639 (1972).
125. P. v. R. Schleyer, P. J. Stang, and D. J. Raber, *J. Am. Chem. Soc.*, **92**, 4725 (1970).
126. G. J. Frisone and E. R. Thornton, *J. Am. Chem. Soc.*, **90**, 1211 (1968).
127. F. G. Bordwell and T. G. Mecca, *J. Am. Chem. Soc.*, **94**, 2119 (1972).
128. R. A. Sneen, *J. Am. Chem. Soc.*, **82**, 4261 (1960).
129. A. F. Diaz and S. Winstein, *J. Am. Chem. Soc.*, **91**, 4300 (1969).
130. I. L. Reich, A. F. Diaz, and S. Winstein, *J. Am. Chem. Soc.*, **94**, 2256 (1972).
131. J. L. Coke, F. E. McFarlane, M. C. Mourning, and M. G. Jones, *J. Am. Chem. Soc.*, **91**, 1154 (1969); M. G. Jones and J. L. Coke, *J. Am. Chem. Soc.*, **91**, 4284 (1969).
132. S. Winstein, G. Valkanas, and C. F. Wilcox, Jr., *J. Am. Chem. Soc.*, **94**, 2286 (1972).
133. S. Winstein, R. Baker, and S. Smith, *J. Am. Chem. Soc.*, **86**, 2072 (1964).
134. J. P. Hardy, A. Ceccon, A. F. Diaz, and S. Winstein, *J. Am. Chem. Soc.*, **94**, 1356 (1972).
135. S. Winstein and D. Trifan, *J. Am. Chem. Soc.*, **74**, 1154 (1952).
136. C. J. Kim and H. C. Brown, *J. Am. Chem. Soc.*, **94**, 5051 (1972).
137. J. W. Clayton and C. C. Lee, *Can. J. Chem.*, **39**, 1510 (1961).
138. C. C. Lee and L. Noszkó, *Can. J. Chem.*, **44**, 2481 (1966).
139. J. A. Cramer and J. G. Jewett, *J. Am. Chem. Soc.*, **94**, 1377 (1972).
140. Review: A. Fava, *The Chemistry of Organic Sulfur Compounds*, Vol. II, N. Kharasch and C. Meyers (Eds.), Pergamon Press, London, 1966, p. 73.
141. Review: L. A. Spurlock and T. E. Parks, *Mechanisms of Reactions of Sulfur Compounds*, **3**, 161 (1968).
142. A. Iliceto, A. Fava, U. Mazzucato, and O. Rossetto, *J. Am. Chem. Soc.*, **83**, 2729 (1961). Also see P. A. S. Smith and D. W. Emerson, *J. Am. Chem. Soc.*, **82**, 3076 (1960).
143. A. Fava, A. Iliceto, A. Ceccon, and P. Koch, *J. Am. Chem. Soc.*, **87**, 1045 (1965).
144. U. Tonellato, O. Rossetto, and A. Fava, *J. Org. Chem.*, **34**, 4032 (1969).
145. A. Fava, U. Tonellato, and L. Congiu, *Tetrahedron Lett.*, **1965**, 1657.
146. A. Ceccon, A. Fava, and I. Papa, *J. Am. Chem. Soc.*, **91**, 5547 (1969); *Chim. Ind. (Milan)*, **51**, 53 (1969); cf. A. Ceccon and I. Papa, *J. Chem. Soc.*, (B), **1969**, 703.
147. (a) L. G. Cannel, Ph.D. Thesis, Pennsylvania State University, University Park, 1956; (b) L. G. Cannel and R. W. Taft, *Abstracts, 129th Meeting Am. Chem. Soc.*, Dallas, Tex., April 1956, p. 46N; (c) E. S. Lewis and J. E. Cooper, *J. Am. Chem. Soc.*, **84**, 3847 (1962).
148. A. Fava, A. Iliceto, and A. Ceccon, *Tetrahedron Lett.*, **1963**, 685.
149. A. Fava, A. Iliceto, and S. Bresadola, *J. Am. Chem. Soc.*, **87**, 4791 (1965).
150. A. Fava, U. Tonellato, L. Congiu, and M. Cavazza, Personal communication.
151. L. A. Spurlock and P. E. Newallis, *Tetrahedron Lett.*, **1966**, 303.

152. L. A. Spurlock and W. G. Cox, *J. Am. Chem. Soc.*, **91**, 2961 (1969).
153. L. A. Spurlock and R. G. Fayter, *J. Org. Chem.*, **34**, 4035 (1969).
154. L. A. Spurlock and T. E. Parks, *J. Am. Chem. Soc.*, **92**, 1279 (1970).
155. L. A. Spurlock and R. J. Schultz, *J. Am. Chem. Soc.*, **92**, 6302 (1970).
156. L. A. Spurlock and Y. Mikuriya, *J. Org. Chem.*, **36**, 1549 (1971).
157. L. A. Spurlock and W. G. Cox, *J. Am. Chem. Soc.*, **93**, 146 (1971).
158. L. A. Spurlock, R. K. Porter, and W. G. Cox, *J. Org. Chem.*, **37**, 1162 (1972).
159. D. Darwish and R. McLaren, *Tetrahedron Lett.*, **1962**, 1231.
160. A. H. Wragg, J. S. McFadyen, and T. S. Stevens, *J. Chem. Soc.*, **1958**, 3603.
161. E. Ciuffarin, M. Isola, and A. Fava, *J. Am. Chem. Soc.*, **90**, 3594 (1968).
162. D. Darwish and R. A. McLaren, *Abstracts, 148th Nat. Meeting Am. Chem. Soc.*, Chicago, Ill., Sept. 1964, p. 44S.
163. D. Darwish and E. A. Preston, *Tetrahedron Lett.*, **1964**, 113.
164. M. Isoza, E. Cluffarin, and A. Fava, Personal communication.
165. (a) S. G. Smith, *Tetrahedron Lett.*, **1962**, 979; (b) S. G. Smith and J. P. Petrovich, *J. Org. Chem.*, **30**, 2882 (1965).
166. E. J. Corey, J. Casanova, Jr., P. A. Vatakencherry, and R. Winter, *J. Am. Chem. Soc.*, **85**, 169 (1963).
167. C. A. Bunton and B. Nayak, *J. Chem. Soc.*, **1959**, 3854.
168. B. J. Gregory, G. Kohnstam, M. Paddon-Row, and A. Queen, *Chem. Commun.*, **1970**, 1032.
169. B. J. Gregory, G. Kohnstam, A. Queen, and D. J. Reid, *Chem. Commun.*, **1971**, 797.
170. A. Streitwieser, Jr., and W. D. Schaeffer, *J. Am. Chem. Soc.*, **79**, 6233 (1957).
171. J. L. Fry, J. M. Harris, R. C. Bingham, and P. v. R. Schleyer, *J. Am. Chem. Soc.*, **92**, 2540 (1970).
172. C. J. Lancelot and P. v. R. Schleyer, *J. Am. Chem. Soc.*, **91**, 4291 (1969).
173. C. J. Lancelot, J. J. Harper, and P. v. R. Schleyer, *J. Am. Chem. Soc.*, **91**, 4294 (1969).
174. C. J. Lancelot and P. v. R. Schleyer, *J. Am. Chem. Soc.*, **91**, 4296 (1969).
175. P. v. R. Schleyer and C. J. Lancelot, *J. Am. Chem. Soc.*, **91**, 4297 (1969).
176. J. M. Harris, F. L. Schadt, P. v. R. Schleyer, and C. J. Lancelot, *J. Am. Chem. Soc.*, **91**, 7508 (1969).
177. S. H. Liggero, J. J. Harper, P. v. R. Schleyer, A. P. Krapcho, and D. E. Horn, *J. Am. Chem. Soc.*, **92**, 3789 (1970).
178. H. C. Brown, C. J. Kim, C. J. Lancelot, and P. v. R. Schleyer, *J. Am. Chem. Soc.*, **92**, 5244 (1970).
179. H. Weiner and R. A. Sneen, *J. Am. Chem. Soc.*, **87**, 287 (1965).
180. H. Weiner and R. A. Sneen, *J. Am. Chem. Soc.*, **87**, 292 (1965).
181. H. Weiner and R. A. Sneen, *Tetrahedron Lett.* **1963**, 1309.
182. H. Weiner and R. A. Sneen, *J. Am. Chem. Soc.*, **84**, 3599 (1962).
183. H. Weiner and R. A. Sneen, *J. Am. Chem. Soc.*, **85**, 2181 (1963).
184. R. A. Sneen and J. W. Larsen, *J. Am. Chem. Soc.*, **88**, 2593 (1966).
185. J. Koskikallio, *Acta Chem. Scand.*, **23**, 1477 (1969).
186. A. Streitwieser, Jr., T. D. Walsh, and J. R. Wolfe, Jr., *J. Am. Chem. Soc.*, **87**, 3682 (1965).

187. P. E. Peterson, R. J. Bopp, D. M. Chevli, E. L. Curran, D. E. Dillard, and R. J. Kamat, *J. Am. Chem. Soc.*, **89**, 5902 (1967).
188. P. E. Peterson and J. F. Coffey, *J. Am. Chem. Soc.*, **93**, 5208 (1971).
189. P. E. Peterson and R. J. Kamat, *J. Am. Chem. Soc.*, **91**, 4521 (1969).
190. J. E. Nordlander and W. G. Deadman, *J. Am. Chem. Soc.*, **90**, 1590 (1968).
191. W. G. Dauben and J. L. Chitwood, *J. Am. Chem. Soc.*, **90**, 6876 (1968).
192. J. L. Kurz and J. C. Harris, *J. Am. Chem. Soc.*, **92**, 4117 (1970).
193. See footnote 11 of Ref. 47.
194. R. A. Sneen, J. V. Carter, and P. S. Kay, *J. Am. Chem. Soc.*, **88**, 2594 (1966).
195. C. D. Ritchie, *J. Am. Chem. Soc.*, **93**, 7324 (1971).
196. C. D. Ritchie, *Accts. Chem. Res.*, **5**, 348 (1972).
197. C. G. Swain and C. B. Scott, *J. Am. Chem. Soc.*, **75**, 141 (1953).
198. J. Koskikallio, *Acta Chem. Scand.*, **26**, 1201 (1972).
199. R. P. Taylor and I. D. Kuntz, Jr., *J. Am. Chem. Soc.*, **94**, 7963 (1972).
200. R. A. Sneen and H. M. Robbins, *J. Am. Chem. Soc.*, **94**, 7868 (1972).
201. (a) A. A. Frost and R. G. Pearson, *Kinetics and Mechanism*, 2nd ed., Wiley, New York, 1961, pp. 152, 153; (b) M. H. Abraham, *Chem. Commun.*, **1973**, 51; (c) G. A. Gregoriou, *Tetrahedron Lett.*, **1974**, 233.
202. R. A. Sneen and H. M. Robbins, *J. Am. Chem. Soc.*, **91**, 3100 (1969).
203. (a) D. J. McLennan, *J. Chem. Soc., Perkin Trans. II*, **1972**, 1577; (b) A. Ceccon, I. Papa, and A. Fava, *J. Am. Chem. Soc.*, **88**, 4643 (1966).
204. Professor R. A. Sneen, Private communication.
205. Professor V. J. Shiner, Jr., Private communication.
206. (a) S. Winstein, B. K. Morse, E. Grunwald, K. C. Schreiber, and J. Corse, *J. Am. Chem. Soc.*, **74**, 1113 (1952); (b) S. Winstein, M. Brown, K. C. Schreiber, and A. H. Schlesinger, *J. Am. Chem. Soc.*, **74**, 1140 (1952).
207. E. D. Hughes, C. K. Ingold, and I. C. Whitfield, *Nature*, **147**, 206 (1941).
208. M. B. Harford, J. Kenyon, and H. Phillips, *J. Chem. Soc.*, **1933**, 179.
209. J. Kenyon, H. Phillips, F. Martin, and H. Taylor, *J. Chem. Soc.*, **1931**, 382.
210. D. M. McKinnon and A. Queen, *Can. J. Chem.*, **50**, 1401 (1972).
211. K. B. Wiberg and T. M. Shryne, *J. Am. Chem. Soc.*, **77**, 2774 (1955).
212. K. L. Olivier and W. G. Young, *J. Am. Chem. Soc.*, **81**, 5811 (1959).
213. D. N. Kevill and F. L. Weitz, *J. Am. Chem. Soc.*, **90**, 6416 (1968).
214. J. L. Kice and G. C. Hanson, *Tetrahedron Lett.*, **1970**, 2927.
215. E. S. Lewis and W. C. Herndon, *J. Am. Chem. Soc.*, **83**, 1961 (1961).
216. P. W. Clinch and H. R. Hudson, *J. Chem. Soc. (B)* **1971**, 747.
217. D. N. Kevill and F. L. Weitz, *Tetrahedron Lett.*, **1971**, 707.
218. D. N. Kevill, K. C. Kolwyck, D. M. Shold, and C.-B. Kim, Unpublished results.
219. P. Beak, R. J. Trancik, J. B. Mooberry, and P. Y. Johnson, *J. Am. Chem. Soc.*, **88**, 4288 (1966); M. Green and R. F. Hudson, *J. Chem. Soc.*, **1962**, 1076, and references cited therein.
220. E. Buncl and J. P. Millington, *Can. J. Chem.*, **43**, 556 (1965).

221. J. L. Kice, R. A. Bartsch, M. A. Dankleff, and S. L. Schwartz, *J. Am. Chem. Soc.*, **87**, 1734 (1965).
222. J. L. Kice and M. A. Dankleff, *Tetrahedron Lett.*, **1966**, 1783.
223. J. L. Kice, R. L. Scriven, E. Koubek, and M. Barnes, *J. Am. Chem. Soc.*, **92**, 5608 (1970).
224. E. S. Lewis and R. E. Holliday, *J. Am. Chem. Soc.*, **91**, 426 (1969).
225. J. M. Prokipak and T. H. Breckles, *Can. J. Chem.*, **50**, 1770 (1972).
226. D. B. Bigley and C. M. Wren, *J. Chem. Soc.*, PII, **1972**, 2359.
227. E. S. Lewis and C. E. Boozer, *J. Am. Chem. Soc.*, **74**, 308 (1952).
228. W. A. Cowdry, E. D. Hughes, C. K. Ingold, S. Masterman, and A. D. Scott, *J. Chem. Soc.*, **1937**, 1252.
229. D. J. Cram, *J. Am. Chem. Soc.*, **75**, 332 (1953).
230. C. C. Lee, J. W. Clayton, D. G. Lee, and A. J. Finlayson, *Tetrahedron*, **18**, 1395 (1962).
231. J. A. Pegolotti and W. G. Young, *J. Am. Chem. Soc.*, **83**, 3251 (1961).
232. L. Friedman, in *Carbonium Ions*, Vol. II, G. A. Olah and P. v. R. Schleyer (Eds.), Wiley-Interscience, New York, 1970, Chap. 16.
233. J. T. Keating and P. S. Skell, in *Carbonium Ions*, Vol. II, G. A. Olah and P. v. R. Schleyer (Eds.), Wiley-Interscience, New York, 1970, Chap. 15.
234. E. I. Snyder, *J. Am. Chem. Soc.*, **91**, 5118 (1969).
235. J. A. Berson and A. Remanick, *J. Am. Chem. Soc.*, **86**, 1749 (1964).
236. E. J. Corey, J. Casanova, P. A. Vatakencherry, and R. Winter, *J. Am. Chem. Soc.*, **85**, 169 (1963).
237. E. L. Eliel, N. L. Allinger, S. J. Angyal, and G. A. Morrison, *Conformational Analysis*, Interscience, New York, 1965, pp. 89, 241.
238. W. Kirmse and H. A. Rinkler, *Sitzberg. Ges. Defoerder. Ges. Naturw. Marburg*, **83/88**, 547 (1961/1962); ref. 233, p. 614.
239. (a) D. J. Cram and J. E. McCarty, *J. Am. Chem. Soc.*, **79**, 2866 (1957); (b) E. L. Eliel, N. L. Allinger, S. J. Angyal, and G. A. Morrison, *Conformational Analysis*, Interscience, New York, 1965, pp. 300–305; (c) B. M. Benjamin and C. J. Collins, *J. Am. Chem. Soc.*, **83**, 3662 (1961).
240. (a) A. J. Parker, *Chem. Rev.*, **69**, 1 (1969); (b) E. Grunwald and A. Effio, *J. Am. Chem. Soc.*, **96**, 423 (1974).
241. D. Y. Curtin and M. Wilhelm, *Helv. Chim. Acta*, **40**, 2129 (1957).
242. P. B. D. de la Mare and R. Bolton, *Electrophilic Additions to Unsaturated Systems*, Elsevier, London, 1966.
243. R. C. Fahey, in *Topics in Stereochemistry*, Vol. 3, E. L. Eliel and N. L. Allinger (Eds.), Interscience, New York, 1968, p. 237.
244. P. v. R. Schleyer, *J. Am. Chem. Soc.*, **89**, 3901 (1967).
245. (a) P. E. Peterson, R. J. Bopp, D. M. Chevli, E. L. Curran, D. E. Dillard, and R. J. Kamat, *J. Am. Chem. Soc.*, **89**, 5902 (1967); (b) P. E. Peterson, C. Casey, E. V. P. Tao, A. Agtarap, and G. Thompson, *J. Am. Chem. Soc.*, **87**, 5163 (1965).
246. (a) H. C. Brown, J. H. Kawakami, and K.-T. Liu, *J. Am. Chem. Soc.*, **92**, 5536 (1970); (b) H. C. Brown and J. H. Kawakami, *J. Am. Chem. Soc.*, **92**, 201 (1970); (c) H. C. Brown and K.-T. Liu, *J. Am. Chem. Soc.*, **89**, 3900 (1967).

374 Ions and Ion Pairs in Solvolysis Reactions

- 247. M. J. S. Dewar and R. C. Fahey, *Angew. Chem. Int. Ed. Engl.*, **3**, 245 (1964).
- 248. P. Ausloos, R. E. Rebbert, L. W. Sieck, and T. O. Tiernan, *J. Am. Chem. Soc.* **94**, 8939 (1972), and references cited therein.
- 249. E. L. Allred and S. Winstein, *J. Am. Chem. Soc.* **89**, 4012 (1967).
- 250. F. B. Miles, *J. Am. Chem. Soc.*, **89**, 2488 (1967); **90**, 1265 (1968).
- 251. (a) P. G. Gassman and J. M. Hornback, *J. Am. Chem. Soc.*, **89**, 2487 (1967); (b) P. G. Gassman, J. M. Hornback, and J. L. Marshall, *J. Am. Chem. Soc.*, **90**, 6238 (1968).
- 252. K. Okamoto, K. Komatsu, and H. Shingu, *Bull. Chem. Soc., Jap.*, **40**, 1677 (1967).
- 253. K. Okamoto, T. Kinoshita, and H. Shingu, *Bull. Chem. Soc., Jap.*, **43**, 1545 (1970).

Ions and Ion Pairs in Ionic Polymerization

MICHAEL SZWARC

*Department of Chemistry,
State University College of Environmental
Science and Forestry,
Syracuse, New York*

1. Introduction	376
2. Anionic Propagation in Living Polymer Systems; Ion Pairs or Free Ions	376
3. Anionic Polymerization Initiated by Living Polymers; Free Ions and Various Ion Pairs	382
4. Tight and Loose Ion Pairs in Anionic Polymerization	386
5. The Effect of Complexing Agents on the Rate of Propagation of Anionic Polymerization	391
6. Intramolecularly Solvated Ion Pairs	396
7. The Transition State of Anionic Polymerization	399
8. Stereospecific Polymerization of Vinyl and Vinylidene Monomers	401
9. Effect of Ionic Structure on Molecular Weight Distribution	409
10. Role of Triple Ions in Ionic Polymerization	410
11. Polymerization Initiated by Lithium Salts of Living Polymers in Hydrocarbon Media	414
12. Stereospecificity of Diene Polymerization	416
13. Anionic Copolymerization	418
14. Effect of Structure on k_- and k_{\pm}	423
15. Anionic Polymerization Involving Activated Monomer	424
16. Cationic Polymerization of Vinyl and Vinylidene Monomers	427
17. Cationic Polymerization Initiated by Ionizing Radiation	428
18. Cationic Polymerization of Cyclic Ethers and Some Related Monomers	431
19. Ion Pairs versus Covalent Bond	437
References	441
	375

1. INTRODUCTION

Ionic polymerization, as implied by this term, involves ionic species. In most ionically polymerizing systems it is the active end group of a growing polymer that bears a charge, positive in cationic polyaddition and negative in anionic polymerization. In some systems the monomer acquires a charge prior to its addition to the electrically neutral end of a polymer, polymerization of pyrrolidone being an example. In either case, the charge of an active species has to be balanced by some proper counterion to ensure the electrical neutrality of the reacting medium.

The presence of anions and cations in ionically polymerizing systems is the cause of the complexity shown by such reactions. The growth may be propagated by free ions, by a variety of ion pairs, or by still higher aggregates. In principle, all these species contribute to the reaction, albeit each exhibits a different reactivity, and their relative abundance is determined by the pertinent ionic association and dissociation equilibria. The interplay between these equilibria and the reactivities of the individual species is responsible for the changes in the rate and character of the overall polymerization resulting from variation of temperature, the nature of the solvent, or from dilution.

Although several elementary reactions—initiation, propagation, termination, and chain transfer—are involved in addition polymerization, this discussion will be restricted to the propagation step; initiation and termination will be mentioned only occasionally. It is convenient to treat this subject under the following headings: anionic polymerization, cationic polymerization, coordination polymerization, activated monomer polymerization, and some unusual polymerizations.

2. ANIONIC PROPAGATION IN LIVING POLYMER SYSTEMS; ION PAIRS OR FREE IONS

Studies of anionic polymerization shed much light on the role of ions and ion pairs in chemical reactions; in fact, anionic living polymers provided us with a most useful tool for elucidation of these problems [1]. Polymerization initiated by living polymers is exceptionally simple. In such a system termination is excluded by a proper choice of experimental conditions. Moreover, living polymer may be prepared prior to kinetic experiments and thus the initiation step also may be eliminated. Hence on the addition of a monomer to a solution of living polymers only the propagation takes place.

In a homopropagation the reaction converts growing n -mers into $n + 1$ -mers without modifying the nature of the active end groups. Therefore in a

living polymer system the concentration of active end groups remains constant during the course of the reaction, provided that the preparation of living polymers was accomplished before the contemplated investigation. Hence the rate of consumption of monomer M is governed by first-order kinetics:

$$\frac{-d[M]}{dt} = \text{const}[M]$$

Denoting the total concentration of living polymers by [LP], the *const* acquires the form

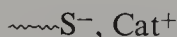
$$\text{const} = k_{\text{ap}}[\text{LP}]$$

where k_{ap} , the apparent *bimolecular* rate constant, is determined by the nature of species of which the living polymer is constituted and by their relative abundance. As remarked previously, the anionic end groups may be present in the form of free ions, tight or loose ion pairs, triple ions, and still higher aggregates. Denoting by $\gamma_1, \gamma_2, \dots$, their respective mole fractions in the system investigated, and by k_1, k_2, \dots , their characteristic rate constants, we find

$$k_{\text{ap}} = \gamma_1 k_1 + \gamma_2 k_2 + \dots + \gamma_n k_n$$

The mole fraction of species i is determined by the conditions prevailing in the polymerizing system—by temperature, pressure, type of solvent, concentration of the reagents, and so on. The simplest situation is encountered in a system composed of one species only, and then k_{ap} represents the propagation rate constant of that species.

Anionic polymerization of styrene in dioxane exemplifies such a situation [2, 3]. Living polystyrene salts in dioxane form tight ion pairs,



where $\sim\sim\sim\text{S}^-$ denotes a growing polystyryl carbanion. The low dielectric constant of that solvent prevents any detectable dissociation of the pairs into free ions, and indeed no conductance has ever been observed in those solutions. On the other hand, the relatively high capacity of dioxane to solvate the pairs (externally) prevents their association into quadrupoles or higher associates. Accordingly, the observed bimolecular rate constant k_{ap} is not affected by dilution, as demonstrated by the data collected in Table 1.

The preceding statement calls for clarification. The sodium polystyryls prepared and studied by Allen et al. [2], Bhattacharyya et al. [3], Dainton et al. [5], and others [26, 133] possessed two active carbanion end-groups in each chain. Therefore the association, if any, could be intramolecular and not intermolecular so that its degree would not be affected by dilution. To refute this objection two samples of living polystyryl sodium were prepared

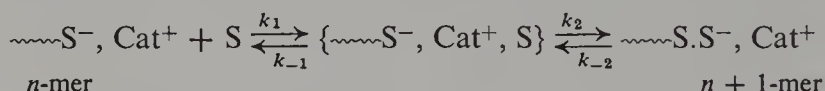
Table 1 Polymerization of the Sodium Salt of Living Polystyrene in Dioxane at 25°C [3]

$[\text{LP}] \times 10^3$ (M)	$[\text{Styrene}]_0 \times 10^3$ (M)	Percent Conversion	$k_p = k_{\pm} (M^{-1} \text{sec}^{-1})$
0.50	7.5	28-68	3.2
3.02	63.5	15-55	3.4
4.95	89.5	20-73	3.4
9.4	93.8	44-89	3.3
12.0	41.6	76-97	3.8

Note: The kinetics was studied by the capillary-flow technique [4].

[3]; in the first, each polymer molecule was endowed with one growing end, whereas in the other each polymer possessed two active end groups. Both kinds of polymer were found to be equally reactive in dioxane, thus confirming the lack of any association of living sodium polystyrene end groups in this ether.

As shown by the data collected in Table 2, the rate of propagation of living polystyrene salts in dioxane depends on the nature of the counterion, the reactivity of $\sim\text{S}^-$, Cat^+ pairs *increasing* with *increasing* size of the cation. This observation shed light on the structure of the transition state of this polyaddition. Propagation, like any other bimolecular solution reaction, can be dissected into a sequence of two or more elementary steps:

**Table 2** The Effect of Counterion on the Rate of Homopropagation of Living Polystyrene in Dioxane at 25°C

Counterion	$k_p = k_{\pm} (M^{-1} \text{sec}^{-1})$		
	[3] ^a	[2] ^b	[5] ^b
Li ⁺	0.9	—	—
Na ⁺	3.4	3-5	6.5
K ⁺	20	—	28
Rb ⁺	21.5	—	34
Cs ⁺	24.5	—	15

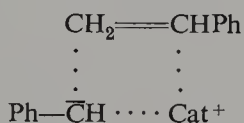
Note: Reinvestigation of this reaction by the more reliable spectrophotometric technique [4] seems to be desirable.

^a Capillary-flow technique.

^b Dilatometry.

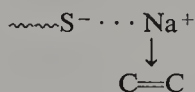
The first step represents the fast, diffusion-controlled formation of an encounter complex, a species lasting probably for about 10^{-10} sec. The second step represents the development of a new C—C covalent bond—virtually an irreversible event. The stationary state treatment of this addition then gives $k_{\pm} = k_2 k_1 / (k_{-1} + k_2)$, and the low value of k_{\pm} implies the inequality $k_{-1} \gg k_2$. Hence $k_{\pm} = k_2 K_1$ where K_1 is the equilibrium constant of the formation of the encounter complex. Does K_1 increase or decrease as the cation varies from Li^+ to Cs^+ ? It is plausible to assume that the monomer in the encounter complex displaces a molecule of solvent from the solvation shell of the $\sim\text{S}^-$, Cat^+ ion pair. Therefore the formation of the encounter complex alters only slightly the entropy of the system (see, e.g., ref. 6 where a similar problem is discussed). The heat of formation of the encounter complex, ΔH_c , is given by the difference of the interaction energies $\sim\text{S}^-$, $\text{Cat}^+ \cdots$ dioxane and $\sim\text{S}^-$, $\text{Cat}^+ \cdots \text{S}$, and since both terms decrease as the cation varies from Li^+ to Na^+ , K^+ , \dots , their difference most likely decreases too.

The interaction of the cation with the molecule of styrene is probably weaker than that with dioxane, and then ΔH_c is positive. Accordingly, a slight increase of K_1 is expected as Li^+ is substituted by Na^+ , K^+ , \dots . However, it is the second step that is crucial for this reaction. The $\text{C} \cdots \text{Cat}^+$ distance in a tight pair is too small to permit the formation of a four-membered transition state ring without stretching of the $\bar{\text{C}}-\text{Cat}^+$ bond:

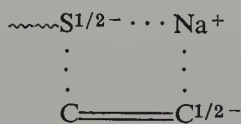


The required energy of stretching of the $\sim\text{S}^- \cdots \text{Cat}^+$ bond decreases, and probably steeply, as Li^+ is replaced by the successively larger cations. Therefore as the size of the cation increases, the value of k_{\pm} is expected to increase too, in agreement with the observations.

The temperature dependence of the polystyrene propagation in dioxane was determined only for the $\sim\text{S}^-$, Na^+ system [2]. The activation energy was found to be 9 ± 3 kcal/mole, resulting in a low frequency factor of about $10^7 M^{-1} \text{ sec}^{-1}$. The negative entropy of activation may be indicative of increasing dipole in the transition state; and the structure



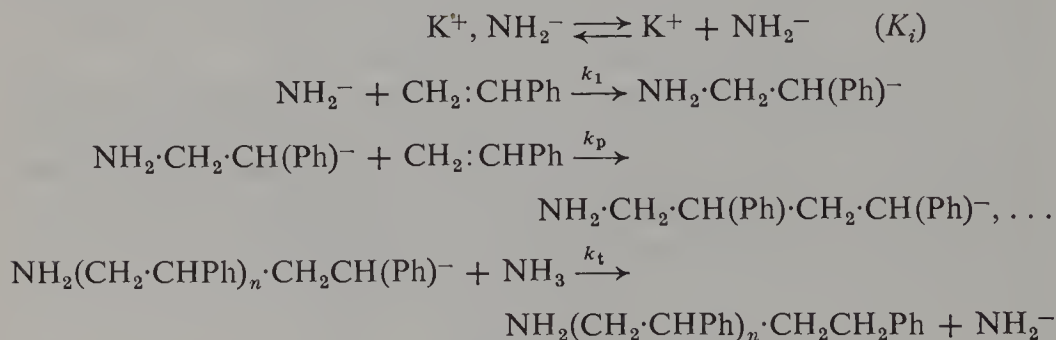
involving a stretched $\text{S}^- \cdots \text{Na}^+$ bond might represent the transition state even better than



In the latter the negative charge is delocalized, hence the degree of solvation should be reduced and therefore the entropy of activation should be positive. It would be interesting to obtain similar data for the other salts of living polystyrene.

A word of caution should be added. For no apparent reasons an irreversible transformation of living polystyrene often occurs in dioxane. This is manifested by the change of the absorption spectrum of the solution. The 340-nm absorption peak, characteristic for the $\sim\text{S}^-$ carbanions, fades and a new broad peak appears in the 500-nm region. A similar phenomenon has been observed, although less frequently in aged THF solutions of living polystyrene. The chemical changes occurring in the latter system have been investigated and are well understood now [7]. The destruction of living polymers on aging has been observed by many investigators; for example, such reactions have been described, but unfortunately not unraveled, by Schulz and his co-workers [8]. The spectral changes observed in living poly-4-vinylpyridine [139] were attributed to the same sequence of events as those elucidated by Spach, Levy, and Szwarc [7]. In view of these reports the spectrum of the polymerizing solution should be carefully checked before and after completion of each kinetic run, and whenever spectral changes are observed the kinetic results are doubtful.

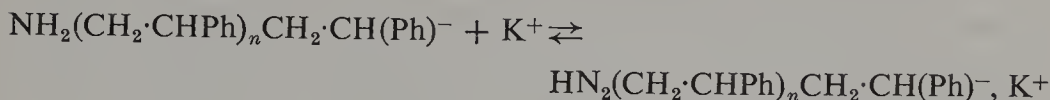
Anionic polymerization of styrene initiated in liquid ammonia by potassium amide probably provides an example of a polymerization propagated solely by free carbanions. This reaction was investigated thoroughly by Higginson and Wooding [9], who found the overall rate of propagation proportional to $[\text{styrene}]^2$ and $[\text{K}^+, \text{NH}_2^-]^{1/2}$, the latter remaining constant in each run. They therefore proposed, the following mechanism of polymerization:



Further evidence supporting this scheme was provided by the following observations:

1. Addition of other potassium salts retarded the reaction, presumably by depressing the dissociation of $\text{K}^+, \text{NH}_2^-$ ion pairs. The retardation could

not be due to the reaction



producing inert, nonpropagating ion pairs, because the rate of polymerization would not have been proportional to the square of styrene concentration.

2. Each polymeric molecule possessed one NH_2 group—strong evidence for the suggested initiation—and the lack of unsaturation in the polymer confirmed the proposed termination and argued against chain transfer to the monomer.

3. Number average molecular weight of the polymer was proportional to the concentration of styrene and independent of the concentration of potassium amide.

It should be stressed that the equilibrium concentration of K^+ and NH_2^- ions is not affected by the polymerization, because the initiation coupled with the termination leave the concentration of the NH_2^- ions unperturbed. However, had the growing polymers been associated with K^+ ions forming ion pairs, the polymerization would disturb the equilibrium $\text{K}^+, \text{NH}_2^- \rightleftharpoons \text{K}^+ + \text{NH}_2^-$, and distort the dependence of the reaction rate on $[\text{K}^+, \text{NH}_2^-]^{1/2}$. Is it reasonable to expect only a slight dissociation of $\text{K}^+, \text{NH}_2^-$ ion pairs but a virtual absence of $\sim\text{S}^-$, K^+ ion pairs? It is probable that the concentration of $\sim\text{S}^-$ ions is much lower than that of NH_2^- ions since the initiation, as will be demonstrated later, is slow. Moreover, the delocalization of the negative charge in the $-\text{CH(Ph)}^-$ ion greatly increases the dissociation of $-\text{CH(Ph)}^-$, K^+ ion pairs when compared with $\text{K}^+, \text{NH}_2^-$.

Higginson and Wooding also determined the temperature dependence of DP_n of the resulting polymer at constant concentration of the monomer. This leads to the difference of activation energies of the propagation E_p and the termination E_t :

$$E_p - E_t = -4 \pm 1 \text{ kcal/mole}$$

The temperature dependence of the overall rate of polymerization was found to be $9 \pm 2 \text{ kcal/mole}$, that is

$$E_1 + E_p - E_t + \frac{1}{2}\Delta H_i = 9 \pm 2 \text{ kcal/mole}$$

where ΔH_i denotes the heat of dissociation of the $\text{K}^+, \text{NH}_2^-$ ion pairs. Its value was determined independently to be $0 \pm 2 \text{ kcal/mole}$. Hence the activation energy of initiation $E_1 = 13 \pm 4 \text{ kcal/mole}$, indicating that the initiation is slow.

Are there any other systems involving entirely free anions as the propagating species? No definite answer can be offered at this time. Anionic polymerization initiated by ionizing radiation must be propagated by free anions

for the reasons given in the discussion concerned with γ -ray initiated cationic polymerization. It is probably that the polymerization of acrylonitrile initiated by γ -rays at -78°C [10] is an example of such a reaction, but a more thorough investigation is needed to confirm this mechanism. A more promising example is provided by the γ -ray-initiated polymerization of bulk nitroethylene [11]. This reaction is retarded by HBr—a strong indication of its anionic character. From the degree of retardation it was possible to deduce the absolute rate constant of its propagation, $k_- = 10^7 \text{ M}^{-1} \text{ sec}^{-1}$ [11]. The high value of the propagation constant provides further evidence for free anions acting as the propagating species.

3. ANIONIC POLYMERIZATION INITIATED BY LIVING POLYMERS; FREE IONS AND VARIOUS ION PAIRS

In most of the investigated systems free ions and ion pairs are simultaneously present in the polymerizing solution and both contribute to the reaction. Polymerization of styrene initiated by the salts of living polystyrene in tetrahydrofuran (THF) is a good example illustrating the characteristic features of such reactions.

Living salts of polystyrene were prepared in THF and the concentration of the growing carbanions was determined spectrophotometrically before the polymerization ensued, as well as in its course. The polymerization ensued when monomer was added to the solution of living polymers, and the progress of the reaction was monitored spectrophotometrically by recording the optical density of the solution at 291.5 nm where the absorption spectrum of the monomer has a shoulder. The details of the technique are described in the original papers [15, 17] as well as in Chapter IV of ref. 4.

Polymerization is found to be first order in styrene:

$$\frac{-d[S]}{dt} = k_u[S]$$

but the pseudo-first-order constant, k_u , is not proportional to the concentration of living polystyrene, as would be expected for a simple bimolecular reaction,



but the apparent bimolecular rate constant, $k_{ap} = k_u/[\text{LP}]$, is found to be a linear function of $1/[\text{LP}]^{1/2}$ [15, 16].* This relation applies for the Li^+ , Na^+ ,

* The experimental technique adopted by Schulz and his co-workers [16] is more complex than the spectrophotometric technique. Its details are given in refs. 16 and 17a, and its critical evaluation is presented in Ref. 4, pp. 188–197.

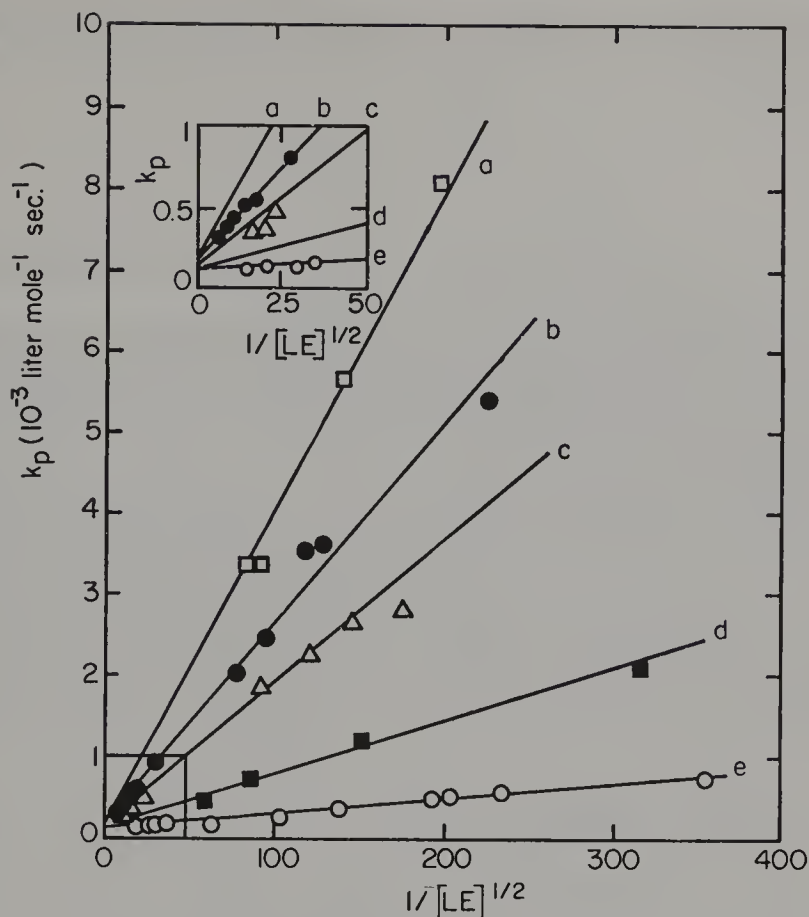


Figure 1. The apparent bimolecular rate constant of living polystyrene polymerization in THF, k_{ap} , as a function of $1/[LP]^{1/2}$. The results are given for the lithium, sodium, potassium, rubidium, and cesium salts.

K^+ , Rb^+ , and Cs^+ salts of polystyryl carbanions, as seen in Fig. 1. Apparently the $\sim S^-$, Cat^+ ion pairs are partially dissociated in THF and the free $\sim S^-$ carbanions are much more reactive than the ion pairs. Denoting by γ the mole fraction of free ions and by k_- and k_{\pm} the genuine bimolecular rate constants of propagation of the free $\sim S^-$ ions and of the $\sim S^-$, Cat^+ ion pairs, we find

$$k_{ap} = (1 - \gamma)k_{\pm} + \gamma k_-$$

In view of the equilibrium



the mole fraction γ is given by the equation

$$\frac{\gamma^2[LP]}{(1 - \gamma)} = K_{diss}$$

Under the experimental conditions maintained in these studies $\gamma \ll 1$; hence the approximation $\gamma^2[\text{LP}] = K_{\text{diss}}$ is valid, thus leading to the linear relation

$$k_{\text{ap}} = k_{\pm} + \frac{(k_- - k_{\pm})K_{\text{diss}}^{1/2}}{[\text{LP}]^{1/2}}$$

depicted in Fig. 1. Hence the intercepts provide the values of k_{\pm} while the slopes give the composite constant $(k_- - k_{\pm})K_{\text{diss}}^{1/2}$.

The propagation constant of the free $\sim\text{S}^-$ ions can be calculated provided K_{diss} is determined by the conductometric or some other technique. This was done [15] and the pertinent results, presented in Table 3, led to the value of k_- of about $65,000 \text{ M}^{-1} \text{ sec}^{-1}$ at 25°C .

The participation of the highly reactive free $\sim\text{S}^-$ ions in the polymerization of living polystyrene is confirmed by the retarding effects of salts sharing a common cation with the living polymers. For example, the addition of sodium tetraphenylboride to living polystyryl sodium greatly retards the polymerization because the dissociation of $\sim\text{S}^-$, Na^+ pairs is repressed. Denoting by $[\text{Na}^+]$ the concentration of the *free* sodium ions (derived mainly

Table 3 Dissociation Constants of $\sim\text{S}^-$, M^+ Ion Pairs in THF at 25°C

$\sim\text{S}^-, \text{M}^+ \rightleftharpoons \sim\text{S}^- + \text{M}^+; \quad K_{\text{diss}}$		
Counterion	$K_{\text{diss}} \times 10^7 (M)$	
	Conductance	Kinetics
Li^+ (one active end)	1.9 ^a	2.2 ^a
Na^+ (one active end)	1.5 ^b (extrap.)	
Na^+ (two active ends)	1.5, ^a 1.5, ^b 1.5 ^c	1.5, ^a 0.8 ^d
K^+ (two active ends)	0.7 ^a	0.8 ^a
Rb^+ (two active ends)	—	0.11 ^a
Cs^+ (one active end)	0.028 ^a	0.021 ^a
Cs^+ (two active ends)	0.165 ^{a,e}	0.0046 ^{a,e}

^a Ref. 15.

^b Ref. 17.

^c Ref. 18.

^d Ref. 16; this result was disputed. See refs. 19 and 22 and the reply in refs. 8 and 20.

^e It will be explained later why the values of the *apparent* K_{diss} of cesium salt of living polystyrene diverge when dissociation constant of the polymers possessing two active end groups is determined from the conductance and the kinetic results.

from the dissociation of the boride), we find

$$\gamma = \frac{K_{\text{diss}}}{[\text{Na}^+]} \quad ?$$

and hence

$$k_{\text{ap}} = k_{\pm} + \frac{(k_- - k_{\pm})K_{\text{diss}}}{[\text{Na}^+]}$$

Thus k_{ap} is a linear function of $1/[\text{Na}^+]$, and the experiments fully confirmed this relation [15]. The slope of the corresponding line gives $(k_- - k_{\pm})K_{\text{diss}}$, and therefore K_{diss} may be calculated from the kinetic data by combining the value of $(k_- - k_{\pm})K_{\text{diss}}$ with that of $(k_- - k_{\pm})K_{\text{diss}}^{1/2}$, the latter being given by the slopes of the lines in Fig. 1. The pertinent values derived by this approach also are listed in Table 3, and the agreement with those obtained from the conductance studies is most gratifying.

The simultaneous participation of free ions and ion pairs in anionic polymerization is observed for many monomer systems and in a variety of ethereal solvents. Most of the kinetic data have been obtained for styrene and its derivatives, for dienes, vinyl pyridines, and for some acrylates and methacrylates. A comprehensive review of the work performed up to 1968 is presented in Chapters 7 and 8 of ref. 4, and the most recent data have been collected in tabular form by Hirohara and Ise [21]. Examination of the published results shows that the values of k_- and k_{\pm} pertaining to the same system but reported by different investigators disagree often by as much as a factor of 2 or 3. This is not surprising. Living polymers are sensitive to various impurities and affected by aging. In addition, the experimental techniques are difficult and much care is needed in performing kinetic studies. Nevertheless, the broad general patterns emerge clearly in spite of these uncertainties. It is unquestionable that the reactivities of free carbanions are only slightly affected by the nature of ethereal solvents. For example, the propagation rate constants of the free ions of living polystyrene at 25°C do not deviate from their average value of $60,000 \text{ M}^{-1} \text{ sec}^{-1}$ by more than a factor of 2, whatever the solvent. In contrast, the propagation rate constants of ion pairs vary by more than three orders of magnitude, depending on solvent and counterions. This is clearly manifested by the data collected in Table 4.

The temperature dependence of the propagation constants of the free ions of living polymers was determined for several systems [8, 17, 22–24]. It seems that the reaction behaves conventionally: its rate increases with rising temperature and the Arrhenius plots are linear. For the sodium living polystyrene in THF the activation energy $E_- = 5\text{--}6 \text{ kcal/mole}$ [17, 22], the frequency factor being $10^8\text{--}10^9 \text{ M}^{-1} \text{ sec}^{-1}$. Recent extension of these studies to other solvent systems [68, 134, 135, 137] seems to indicate that a single Arrhenius

Table 4 Propagation by Living Polystyrene Salts in Various Solvents at 25°C

Solvent	k_{\pm} (liter mole ⁻¹ sec ⁻¹)					Ref.
	Li ⁺	Na ⁺	K ⁺	Rb ⁺	Cs ⁺	
Living Polystyrene						
Cyclohexane			7.7	22.5	19	88
Benzene			47	24	18	25
Dioxane	0.9	3.4	20	21.5	24.6	3
		6.5	28	34	15	5
Oxepan		14				68
Tetrahydropyran	<5	<5; 14	28	83	53	24, 26
	10; 19.5	13; 17	61; 30	40	64	69
		10				23, 27
2-Me-tetrahydrofuran	57	11	7.5		22	26
	25	23	17		23	89
Dimethoxyethane		3600			150	22
Living Poly- α -Methylstyrene Salts						
Dioxane		0.02	0.1	0.06		5, 24
Tetrahydropyran	2.6	0.047	0.25	0.35	0.26	24
Tetrahydrofuran		0.04				28

line may accommodate, within the experimental uncertainties, all the data obtained in THF, DME, THP, 3MeTHF, oxepane, and hexamethylphosphorotriamide (HMPA). Such findings reconfirm the original contention [4] that the reactivity of free anions are only slightly affected by the nature of ethereal solvents. The propagation of the free ions of living α -methylstyrene also seems to be unaffected by solvent, its activation energy being higher than that of living polystyrene, about 7.2 kcal/mole, indicating a steric strain in the transition state. The frequency factor is again about $10^8 M^{-1} \text{ sec}^{-1}$ [5, 24]. The k_+ and k_- for methylmethacrylate polymerization in THF at -75°C have been reported recently [150].

4. TIGHT AND LOOSE ION PAIRS IN ANIONIC POLYMERIZATION

Although cations are present in solutions of *free* anionic living polymers, their presence does not affect the course of polymerization because the oppositely charged ions are far apart from each other. The situation is different for ion pairs. Here the growing anion is chaperoned by a cation and therefore the nature of the anion must be reflected in the reactivity of the ion pair. Inspection of Table 4 confirms this expectation; for example, the

reactivity of living polystyryl salts in dioxane increases along the series $\text{Li}^+ < \text{Na}^+ < \text{K}^+ < \text{Rb}^+ < \text{Cs}^+$. Moreover, whereas the nature of an ethereal solvent affects only slightly the reactivity of the free polystyryl anions, the reactivities of ion pairs are strongly influenced by the nature of the medium. For example, the sodium polystyryl pair is 1000 times more reactive in dimethoxyethane (DME) than in dioxane, the respective k_{\pm} 's being about $4 \text{ M}^{-1} \text{ sec}^{-1}$ in dioxane, more than 10 in tetrahydropyran (THP), 80 or more in tetrahydrofuran (THF), and 3600 in dimethoxyethane.

The gradation of the reactivities of living polystyryl salts involving different cations shows some peculiar variations in its dependence on solvent. In dioxane the lithium salt is the least reactive while the cesium salt is the most rapidly polymerizing, the respective k_{\pm} 's being 0.9 and $24.6 \text{ M}^{-1} \text{ sec}^{-1}$. The order of reactivities is reversed in tetrahydrofuran, where k_{\pm} is $160 \text{ M}^{-1} \text{ sec}^{-1}$ for the $\sim\sim\sim\text{S}^-$, Li^+ but still about $25 \text{ M}^{-1} \text{ sec}^{-1}$ for the $\sim\sim\sim\text{S}^-$, Cs^+ salt. These results suggest that the structure of an ion pair may vary with the nature of the solvent and the counterion.

The spectroscopic evidence [12, 14] demonstrates that many salts of Li^+ and Na^+ form tight pairs in dioxane but loose pairs in DME. Apparently the salts of living polystyrene behave similarly. Their tight pairs have low reactivity whereas the reactivity of loose pairs seems to be very high. The spectroscopic data also lead to the conclusion that the cesium salts tend to form tight pairs in many solvents, whereas the sodium salts exist under such conditions, at least partially, in the loose form.

Studies of conductivity of sodium and cesium salts of living polystyrene confirmed these observations; the dissociation constant of $\sim\sim\sim\text{S}^-$, Na^+ in THF is relatively high at 25°C , $K_{\text{diss}} = 1.5 \times 10^{-7} \text{ M}$, but for the cesium salt its value is about 50 times smaller. Moreover, as the temperature of the solution is lowered to -80°C , K_{diss} increases steeply for the former salt but only slightly for the latter. These relations are seen in the van't Hoff plots shown in Fig. 2. The dissociation of these ion pairs into free ions is therefore exothermic, $-\Delta H_D$ being 9 kcal/mole for $\sim\sim\sim\text{S}^-$, Na^+ but less than 2 kcal/mole for $\sim\sim\sim\text{S}^-$, Cs^+ [17]. It seems therefore that in THF at ambient temperatures both salts exist mainly in the form of tight pairs; however, on dissociation the sodium, but not the cesium ion, gains substantially in its degree of solvation. This makes the dissociation of $\sim\sim\sim\text{S}^-$, Na^+ much more exothermic than that of $\sim\sim\sim\text{S}^-$, Cs^+ , a conclusion that gains credibility from mobility studies [29]. Indeed, the Stokes radius of the small Na^+ ion in THF is *larger* than that of the intrinsically large Cs^+ ion dissolved in the same ether.

The formation of a solvated ion is a prerequisite for the existence of loose, solvent-separated pairs. Hence it is plausible that some $\sim\sim\sim\text{S}^-$, Na^+ pairs, but not $\sim\sim\sim\text{S}^-$, Cs^+ , form loose pairs in THF, their proportion increasing with decreasing temperature.

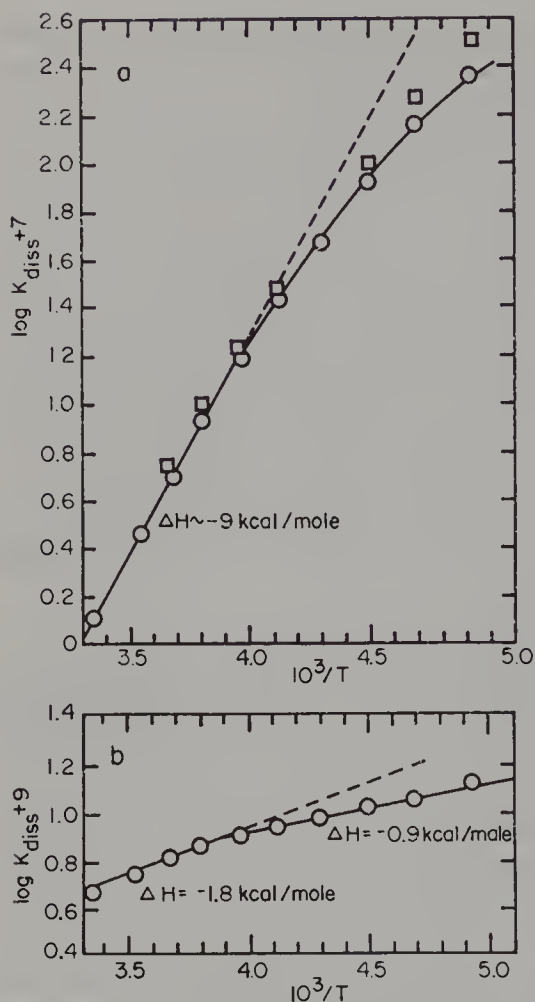
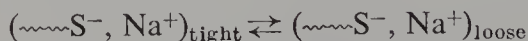


Figure 2. van't Hoff plot for the dissociation of $\sim\text{S}^-$, Na^+ and $\sim\text{S}^-$, Cs^+ ion pairs in THF.

These speculations provided the impetus for the determination of the activation energy of propagation of the $\sim\text{S}^-$, Na^+ ion pairs in THF and in DME. The resulting Arrhenius lines are drawn in Fig. 3. The "negative" activation energy of propagation by the $\sim\text{S}^-$, Na^+ pairs in THF is significant. It implies that the bulk of the salt is virtually inactive in this ether, being present in the form of unreactive tight pairs, and the observed propagation results from the presence of a small fraction of highly reactive loose $\sim\text{S}^-$, Na^+ pairs. The transformation



is exothermic, and provided that the exothermicity of this reaction is higher than the activation energy of the loose pairs propagation, the rate of such reaction should increase with decreasing temperature.

After making the simplifying assumptions that the fraction of loose pairs is low and the contribution of tight pairs to the polymerization may be neglected,

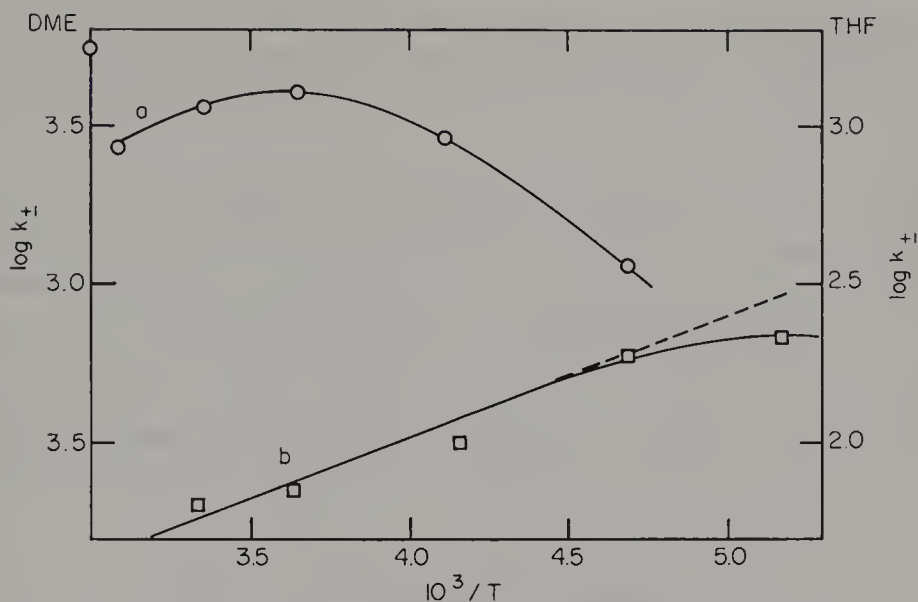


Figure 3. The Arrhenius lines describing the temperature dependence of propagation of $\sim\text{S}^-$, Na^+ ion pairs in THF and DME.

the following relation is derived for the apparent activation energy of the propagation:

$$E_{\text{ap}} = E_{\text{loose}} + \frac{\Delta H_{\text{tr}}}{(1 - K_{\text{tr}})}$$

Here E_{loose} denotes the genuine activation energy of propagation by the loose pairs, and ΔH_{tr} and K_{tr} denote the heat and the equilibrium constant, respectively, of the transformation of tight pairs into loose ones. It follows that the Arrhenius curve should reach a maximum and then decline as the temperature decreases, the maximum being attained at that temperature for which $E_{\text{ap}} = 0$:

$$E_{\text{loose}} = \frac{-\Delta H_{\text{tr}}}{1 + K_{\text{tr}}}$$

This maximum could not be reached when the reaction proceeds in THF—the fraction of the loose ion pairs is still too low, even at -80°C . However, the fraction of loose ion pairs is substantially higher in DME, as evident from the high k_{\pm} value for the propagation proceeding in that solvent, and indeed the corresponding Arrhenius line in Fig. 3 has then a maximum.

By collating all the available data it was possible to deduce the propagation constant of the loose $\sim\text{S}^-$, Na^+ pairs, namely about $30,000 \text{ M}^{-1} \text{ sec}^{-1}$ in THF and about $20,000 \text{ M}^{-1} \text{ sec}^{-1}$ in DME, both referring to 25°C . The

corresponding activation energy for the propagation in THF seems to be about 6 kcal/mole. Hence about 25% of $\sim\text{S}^-$, Na^+ pairs are in the loose form in THF at -70°C but their proportion decreases to about 0.05% at 25°C .

Let us explore these ideas still further. The transformation of the tight pairs into loose ones, like the dissociation of ion pairs into free ions, is usually exothermic—the gain in solvation energy more than counterbalances the work needed for the separation of the oppositely charged ions. Therefore at a sufficiently high temperature the polymerizing solution would contain only the tight ion pairs, the concentration of the loose pairs being then vanishingly small. Lowering of the temperature slows down the polymerization; this results from the conventional effect of the activation energy of propagation by the tight pairs. The propagation is not yet upset by the increase in the

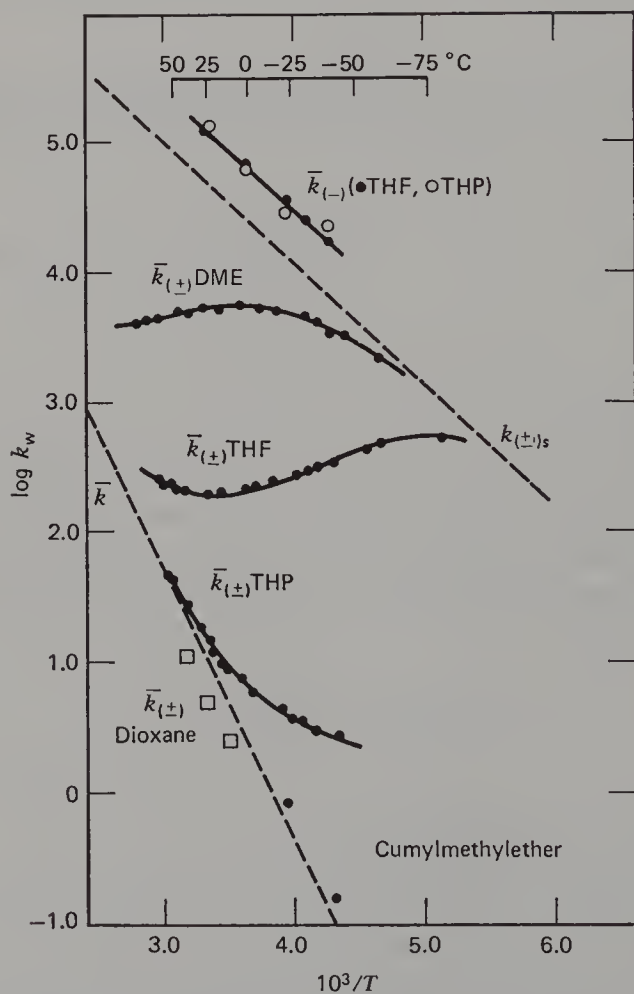


Figure 4. The temperature effect on anionic polymerization of living polystyrene in various ethereal solvents.

contribution of loose pairs because their proportion is still too low to make their contribution visible. As the temperature decreases further, the proportion of the highly reactive loose pairs becomes sufficiently large to affect the rate of the reaction. In that temperature range the Arrhenius curve would go through a minimum and thereafter would rise as $1/T$ increases, provided $E_{\text{loose}} < -\Delta H_{\text{tr}}$. On further decrease of temperature the system reaches the point where the conversion of the tight to loose pairs has progressed so far that the additional increase in the proportion of loose pairs is not sufficient to counterbalance the conventional effect of the activation energy of their propagation. The Arrhenius curve then reaches a maximum and thereafter it turns down again. Hence had the whole range of temperatures been accessible to experimentation, an S-shaped Arrhenius curve should be observed. Figure 4, constructed by Schulz et al. [8], illustrates these relations. Depending on the nature of the solvent, the equilibrium of the transformation of the tight to loose pairs is shifted in one or the other direction. Only tight pairs participate in the polymerization proceeding in dioxane or in cumyl methyl-ether—even in the lowest temperature range. In THP the contribution of the loose pairs becomes apparent at low temperatures; the loose pairs begin to dominate in the polymerization taking place in THF and their contribution becomes still greater in DME.

5. THE EFFECT OF COMPLEXING AGENTS ON THE RATE OF PROPAGATION OF ANIONIC POLYMERIZATION

In the preceding section we discussed the effect of temperature on the rate of anionic polymerization propagated by ion pairs. It has been shown that the less reactive tight ion pairs are converted into highly reactive loose pairs at low temperatures. The conversion of the tight into loose pairs also may be induced at constant temperature by the addition of some powerful cation-complexing agent. An example of such a study was provided by the work of Shinohara et al. [30, 31], their results being summarized in Fig. 5. The polymerization of the living sodium polystyrene was performed in tetrahydropyrene in the presence and in the absence of tetraglyme. The directly determined apparent bimolecular rate constants k_{ap} were plotted versus $1/[\text{LP}]^{1/2}$. Following the previous argument, the intercepts I of the resulting straight lines should yield the average propagation constant of ion pairs, while the steepness of the slopes reflects the increasing contribution of the free $\sim\text{S}^-$ ions to the polymerization. Two questions arise: How does the intercept increase on the addition of glyme? How does the slope become steeper?

In the absence of the glyme the system involves only two growing species, the $\sim\text{S}^-$, Na^+ tight ion pairs and the free $\sim\text{S}^-$ carbanions. The apparent

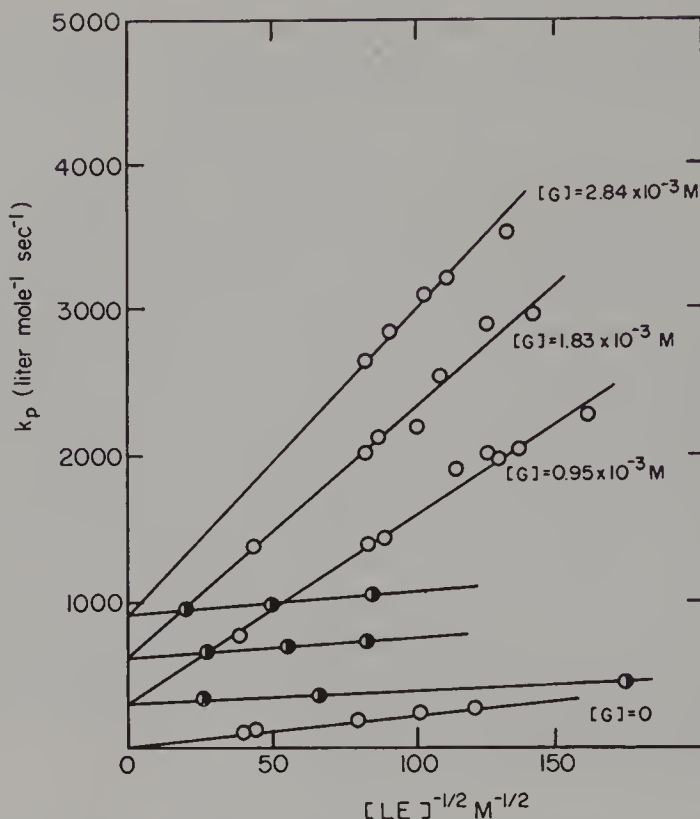
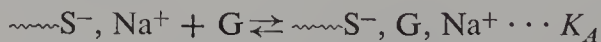


Figure 5. The effect of tetraglyme on the rate of anionic polymerization of styrene in THP. Note the increase of the slope and the intercept of the lines giving k_{\pm} as a function of $1/[LP]^{1/2}$ on increasing the concentration of glyme, $[G]$. The half-shaded points refer to experiments performed in the presence of Na^+ , BPh_4^- .

bimolecular constant k_{ap} is given then by the relation previously discussed*

$$k_{ap} = k_{\pm} + k_- K_{diss}^{1/2} / [LE]^{1/2}$$

The addition of the glyme G has a twofold effect. The glyme becomes associated with the "ordinary" $\sim\text{S}^-$, Na^+ pairs converting them partially into loose, glyme-separated pairs:



Furthermore, the glyme becomes associated with the "ordinary" free Na^+ ions converting some into Na^+ ions solvated by glyme:



* k_{\pm} is negligible when compared with k_- and hence $(k_- - k_{\pm}) \approx k_-$.

The $\sim\sim\sim\text{S}^-$, G, Na^+ pairs propagate faster than the ordinary $\sim\sim\sim\text{S}^-$, Na^+ pairs, and hence the polymerization propagated by *all* the ion pairs is accelerated on the addition of the glyme. Denoting by γ_{G} the mole fraction of the “glymated” pairs, and by $k_{\pm, \text{G}}$ and k_{\pm} the propagation constants of the “glymated” and the ordinary pairs, respectively, we find the observed intercepts I of the lines shown in Fig. 5, namely the apparent propagation constant $k_{\pm, \text{ap}}$:

$$I = k_{\pm, \text{ap}} = \gamma k_{\pm, \text{G}} + (1 - \gamma)k_{\pm}$$

Provided only a small fraction of the ordinary pairs is complexed with the glyme, we find $\gamma = K_{\text{A}}[\text{G}]$ and

$$I = k_{\pm, \text{ap}} = (k_{\pm, \text{G}} - k_{\pm})K_{\text{A}}[\text{G}] + k_{\pm}$$

that is, the intercepts of the lines in Fig. 5 should be linear with $[\text{G}]$. This is indeed the case: the plot of $k_{\pm, \text{ap}}$ versus $[\text{G}]$ yields an excellent straight line, its intercept being equal to the k_{\pm} of the ordinary $\sim\sim\sim\text{S}^-$, Na^+ pairs and the slope providing the value of $(k_{\pm, \text{G}} - k_{\pm})K_{\text{A}}$. The polymerization behaved similarly when triglyme was added instead of tetraglyme. However, the value of the slope, $(k_{\pm, \text{G}'} - k_{\pm})K'_{\text{A}}$, derived by the previously described procedure turned out to be substantially smaller. Assuming that both ion pairs, $\sim\sim\sim\text{S}^-$, tetraglyme, Na^+ and $\sim\sim\sim\text{S}^-$, triglyme, Na^+ , propagate equally fast, we find the ratio $K_{\text{A}}/K'_{\text{A}}$ to be given by the ratio of the slopes of the lines representing I as a function of $[\text{tetraglyme}]$ and $[\text{triglyme}]$, respectively. Hence the data of Shinohara et al. [30] imply that tetraglyme complexes with the $\sim\sim\sim\text{S}^-$, Na^+ pairs 40 times more powerfully than triglyme.

The complexation of the free Na^+ ions with the glyme upsets the dissociative equilibrium, $\sim\sim\sim\text{S}^-$, $\text{Na}^+ \rightleftharpoons \sim\sim\sim\text{S}^- + \text{Na}^+$, because the “ordinary” Na^+ ions are removed from the system through their association with the glyme. Thus on the addition of the glyme an increasing proportion of $\sim\sim\sim\text{S}^-$, Na^+ has to dissociate into the free $\sim\sim\sim\text{S}^-$ ions. Mathematical treatment of this problem leads then to the relation for the observed slopes σ deduced from Fig. 5:

$$\sigma = k_- K_{\text{diss}}^{1/2} (1 + K_{\text{c}}[\text{G}])^{1/2}$$

or

$$\sigma = k_- K_{\text{diss}}^{1/2} (1 + K_{\text{c}}[\text{G}]^2)^{1/2}$$

depending on whether the association of Na^+ ions with a glyme involves one or two molecules of that polyether. The symbols k_- , K_{diss} , and K_{c} used in this equation have the previously defined meanings.

For the system $\sim\sim\sim\text{S}^-$, Na^+ in THP + tetraglyme a good straight line is obtained when σ^2 is plotted versus $[\text{G}]$, demonstrating that the association of

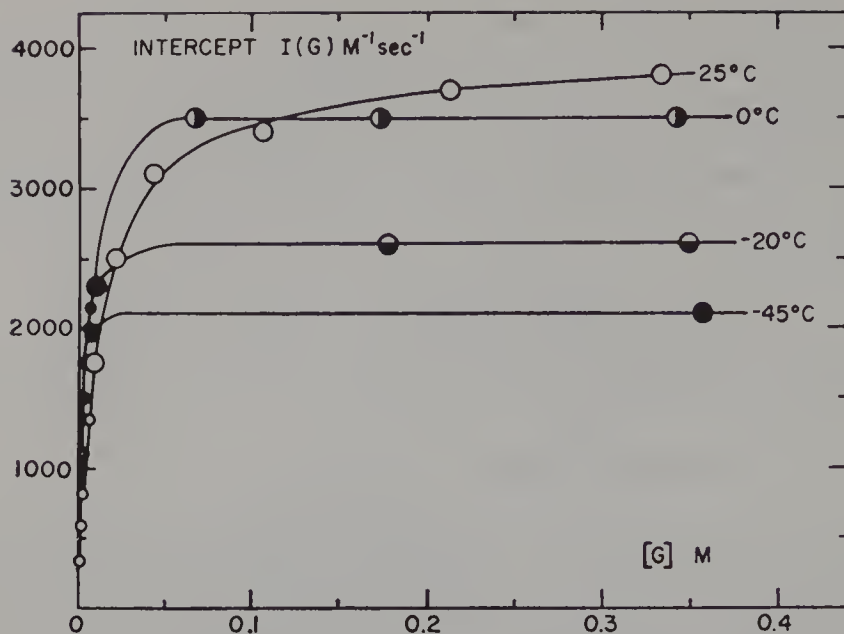


Figure 6. The average propagation constants of $\sim\sim\sim\text{S}^-, \text{Na}^+$ and $\sim\sim\sim\text{S}^-, \text{G}, \text{Na}^+$ in THP as a function of concentration of the tetraglyme. The plateaus shown in the figure give the absolute values of the propagation constant, $k_{\pm, \text{G}}$, of $\sim\sim\sim\text{S}^-, \text{G}, \text{Na}^+$ pairs at various temperatures.

the free Na^+ ions with tetraglyme involves only one molecule of the polyether. However, when triglyme is used as the complexing agent the plot of σ^2 versus $[\text{G}]^2$ is linear. Therefore under the conditions of Shinohara experiments the coordination of the free sodium ions with triglyme involves two molecules of the glyme.

The results discussed so far demonstrate that the less reactive $\sim\sim\sim\text{S}^-, \text{Na}^+$ tight pairs may be converted into the more reactive $\sim\sim\sim\text{S}^-, \text{G}, \text{Na}^+$ pairs by coordinating one molecule of the triglyme or tetraglyme. To determine the reactivity the glymated pairs and the absolute value of the association constant, K_A , experiments had to be performed at higher glyme concentrations to convert virtually all the $\sim\sim\sim\text{S}^-, \text{Na}^+$ pairs into the "glymated" pairs. The results of such experiments [31] are graphed in Figs. 6 and 7. The plateaus in Fig. 6 give the absolute values of $k_{\pm, \text{G}}$ at a series of temperatures. Alternatively, one finds that the intercepts of the plots of $k_{\pm, \text{ap}}$ versus $1/[\text{LP}]^{1/2}$, denoted by $I(\text{G})$, are related to the glyme concentration $[\text{G}]$ by the equation

$$\frac{1}{I(\text{G}) - I(0)} = \frac{1}{k_{\pm, \text{G}}} + \frac{1}{k_{\pm, \text{G}} \cdot K_A [\text{G}]}$$

Hence the linear plot of $1/\{I(\text{G}) - I(0)\}$ versus $[\text{G}]^{-1}$, presented in Fig. 7,

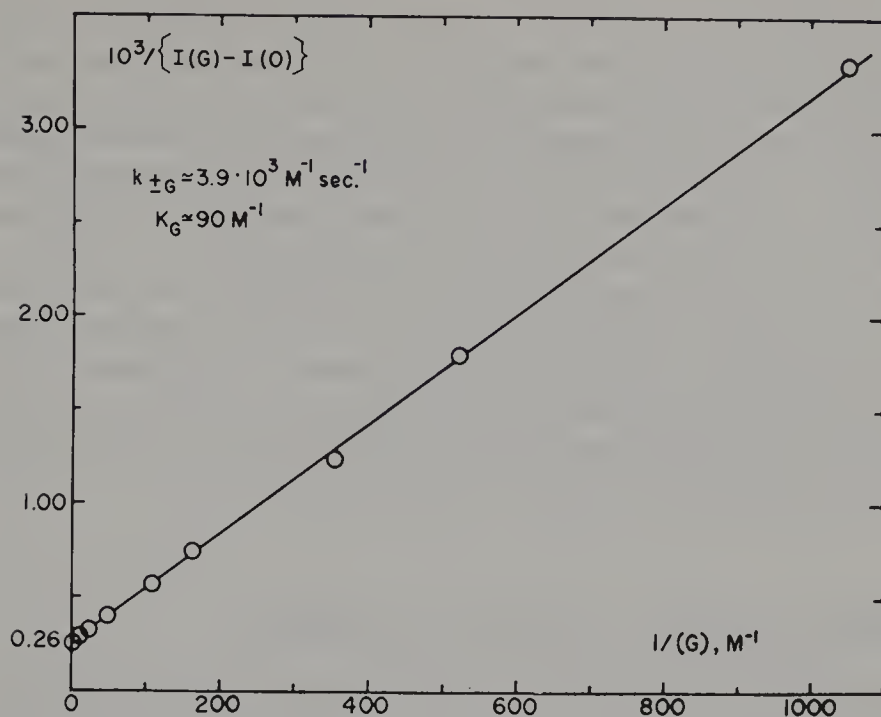
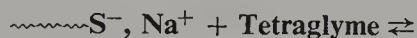


Figure 7. The plot of $1/\{I(G) - I(O)\}$ versus the reciprocal of glyme concentration $[G]$; $T = 25^\circ C$. The symbols $I(G)$ and $I(O)$ are defined in the text.

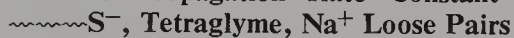
yields the values of $k_{\pm, G}$ and of K_A , the former being equal to the reciprocal of its intercept. The mere linearity of such a plot provides a strong argument favoring the proposed mechanism.

The numerical results derived from this study are given in Table 5. The exothermicity of the association is high, about 6 kcal/mole, but the activation energy of propagation is unexpectedly low, only 1.2 kcal/mole. It has been

Table 5 Equilibrium Constant K_A for the Association in THP



and the Propagation Rate Constant $k_{\pm, G}$ of



Temperature ($^\circ C$)	$K_G (M^{-1})$	$k_{\pm, G} (M^{-1} sec^{-1})$
25	90	3900
0	210	3500
-20	770	2600
-45	2000	2100

suggested [31] that the "glymated" $\sim\sim\sim\text{S}^-$, G, Na^+ ion pairs are, in fact, mixtures of two coexisting isomeric pairs, one of them being more reactive than the other. The low activation of this polymerization may be rationalized then by assuming that the proportion of the more reactive pairs increases with decreasing temperature. A closely similar situation was encountered in studies of electron-transfer processes and a tentative structure for such isomeric glymated pairs was proposed in the original paper [13].

A similar behavior was reported recently for the polymerization of living polystyrene potassium in THF in the presence of small amounts of hexamethylphosphorictriamide (HMPA). The apparent rate constants of propagation determined at -70°C increased to about $5 \times 10^3 M^{-1} \text{sec}^{-1}$ when $[\text{HMPA}] = 0.1 M$ [32]. The accelerating effect of triglyme has been reported also in the polymerization of α -methyl styrene [91].

6. INTRAMOLECULARLY SOLVATED ION PAIRS

Anionic polymerization of 2-vinyl pyridine, VP [33], and 2-vinylquinoline, VQ [34], is propagated by ion pairs of living polymers which are intramolecularly solvated by their own chain. The propagation of sodium salt of the living 2-vinyl pyridine was investigated in THF at temperatures ranging from 25 to -60°C . The plots of the directly observed bimolecular rate constants k_{ap} versus $1/[\text{LP}]^{1/2}$ are linear; however, their intercepts yield unusually high values of k_{\pm} ; for example, at 25°C $k_{\pm} = 2000 M^{-1} \text{sec}^{-1}$. The pertinent data are collected in Table 6, which includes the respective dissociation constants K_D :



Table 6 Polymerization of Sodium Ion Pair of Living Poly-2-Vinylpyridine in THF

Temperature ($^\circ\text{C}$)	$K_{\text{diss}} \times 10^9 (M^{-1})$	$k_{\pm} (M^{-1} \text{sec}^{-1})$	$k_- (M^{-1} \text{sec}^{-1})$
25	0.87 (0.8)	2100 ± 150	$100,000 \pm 30,000$
0	1.4 (1.4)	720 ± 40	$14,000 \pm 4,000$
-20	2.0 (2.2)	280 ± 40	$6,000 \pm 2,000$
-60	4.7	12 ± 25	500 ± 100

Note: The values in parentheses were reported by Sigwalt [35].

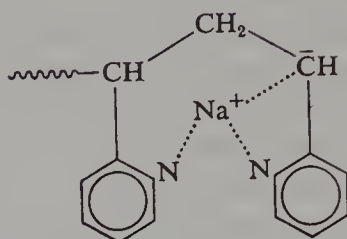
These are remarkably low; for example, in THF at 25°C, K_{diss} for $\sim\sim\sim(\text{VP})^-$, Na^+ is as low as $0.9 \times 10^{-9} M$, that is about 100 times smaller than the corresponding dissociation constant of living sodium polystyrene. The exothermicity of dissociation is also relatively low, being 2.7 kcal/mole only, as compared with about 9 kcal/mole found in the polystyrene system. Nevertheless, the negative entropy of dissociation is large, -50 eu for $\sim\sim\sim(\text{VP})^-$, Na^+ , only slightly smaller than that found for the $\sim\sim\sim\text{S}^-$, Na^+ system (-68 eu). The reliability of the conductance data is high, as demonstrated by the excellent agreement with the independently determined data of Sigwalt and his associates [35]. The usual approach leads to the rate constants k_- of propagation of the free $\sim\sim\sim(\text{VP})^-$ anions, the relevant values being included in Table 6. The activation energies of the propagation by ion pairs and by free ions are comparable, 7.7 and 7.8 kcal/mole, respectively, contrasting with the "negative activation energy" found for the sodium ion pairs of living polystyrene.

Similar results were obtained for the sodium salt of living 2-vinyl quinoline [34]. Here again the dissociation constants of $\sim\sim\sim(\text{VQ})^-$, Na^+ pairs, as well as the exothermicity of their dissociation, are low. The propagation constants of the ion pairs is high, whereas the contribution of the free ions to propagation is too low to be determined.

The similar behavior of both systems, contrasting with the behavior of living polystyrene, implies the operation of some new factor in these reactions. It seems that the ion pairs of the sodium living polyvinyl-pyridine or quinoline should be classified as loose pairs. The pyridine or quinoline moieties of the last and the penultimate units of the polymer chain act as powerful solvating agents of sodium cations, the power of their solvation being enhanced by the unavoidable vicinity of these solvating moieties to the cation. The separation of the ions increases the reactivity of the living polymers, an effect observed previously when loose ion pairs of living polystyrene were compared with the tight ones, but it does not increase their dissociation into free ions—contrasting with the behavior of the conventional loose ion pairs.

In a conventional system the fully solvated cation with its solvation shell intact is easily detached from the anion. However, if the solvation shell includes some pyridine moieties attached to the polymer chain, the detachment of the cation from the anion is hindered, and this accounts for the observed low degree of dissociation. In fact, the detached ion has to rupture its connection with the solvating pyridine (or quinoline) units to become resolvated by the free solvent molecules. Hence the negative entropy of dissociation is absolutely large, because the translational entropy is not increased by the desolvation of the pyridine moieties attached to the polymer chain, whereas the coordination of the free solvent molecules decreases the entropy of the system. The intermolecular solvation of a sodium cation in the vinylpyridine

system [36] is depicted as



As pointed out by Sigwalt [36], such a coordination is impossible in the 4-vinyl pyridine system, and indeed the degree of dissociation of $\sim\sim\sim$ 4-VP $^-$, Na $^+$ pairs is higher than that of the $\sim\sim\sim$ 2-VP $^-$, Na $^+$.

The possibility of *intramolecular* solvation in the sodium salt of a living poly-4-vinylpyridine has been raised in a recent paper by Tardi and Sigwalt [139]. They report that the dissociation constant of that salt in THF increases from about 10^{-9} *M* for polystyrene terminated only by one living polyvinylpyridine unit to 4×10^{-8} *M* when the DP of the polyvinylpyridine segment increases to 80 or 90. It is proposed that such a long chain may act as a polydentate solvating agent and thus increase the degree of dissociation. Of course, this is possible provided the solvation is *intermolecular*, that is, a Na $^+$ ion becomes solvated by a chain of a nondissociated polymer ion pair. Such a suggestion could be easily tested by investigating the effect of an added high DP *dead* poly-4-vinylpyridine on the conductance of a low DP *living* poly-4-vinylpyridine. Alternatively, *intramolecular* solvation by long chain could yield zwitter ions and these may contribute to the *AC conductance* by virtue of their large, in-phase component of their dipole moment. Again this suggestion may be tested experimentally. However, some side reactions, which according to Sigwalt mar the polymerization [35, 139], could cloud the reliability of such conductance studies.

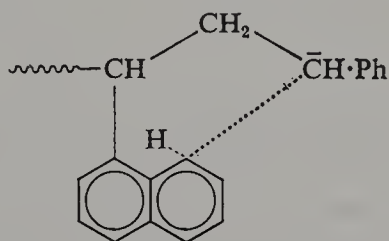
The coordination of the counterion with the moieties forming a part of the last or penultimate unit of the chain favors stereospecific polymerization (see p. 402). It is interesting therefore to note that the polymerization of the magnesium salt of the living poly-2-vinyl pyridine, but not of the 4-vinyl pyridine, yields an isotactic polymer [37].

The intramolecular solvation accounts for another interesting observation. Again, in contrast with the living polystyrene system, the reactivity of sodium pairs of the living polyvinyl pyridine is not affected by the nature of the ethereal solvent. Actually it seems to be even higher in dioxane (k_{\pm} about 3500 $M^{-1} \text{ sec}^{-1}$) or in tetrahydropyran (k_{\pm} about 4500 $M^{-1} \text{ sec}^{-1}$) than in tetrahydrofuran [33] (compare these data with those listed in Table 4).

The intramolecular solvation of cations may be significant in other living polymer systems involving polar units such as acrylates and methacrylates. Unfortunately, various side reactions complicate the propagation in these

polymer systems, and therefore little of the required information is available.

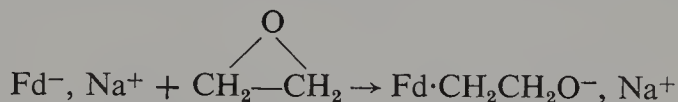
Finally, we close this section by inquiring whether living anions may be coordinated with moieties attached to the polymer chain. An interesting example of such a coordination was provided by the addition of styrene to living poly-1-vinylnaphthalene [38]. An intramolecular coordination between the living polystyryl end group and immediately preceding it the naphthyl moiety was observed:



However, the association does not take place when one or more polystyryl segments separate the anion from the naphthyl moiety. The behavior of this system has been discussed in terms of entropy of configuration and its relation to the translational entropy lost in the similar intermolecular coordination of living polystyrene with anthracene [39]—a reaction yielding dormant polymers.

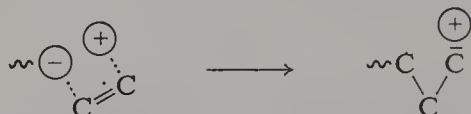
7. THE TRANSITION STATE OF ANIONIC POLYMERIZATION

The data presented so far may lead to the conclusion that the reactivity of living polymers increases as the growing end group is transformed from a tight ion pair into a loose one, and eventually into a free ion. This gradation of reactivities does not apply always. In fact, it has been shown in another chapter of this book (see p. 234) that the reverse order of reactivities is observed in the protonation of radical anions by alcohols or water. In those reactions the tight ion pairs are the most reactive, the reactivity of loose pairs is definitely smaller, and the free ions are probably the least reactive. A similar gradation of the reactivities was observed in the reaction of sodium fluoradenyl, Fd^- , Na^+ , with ethylene oxide [138]. The opening of the ring—a step corresponding to an initiation of ethylene oxide propagation,



is faster for a tight pair than for a loose one, the latter being obtained on addition of crown ethers or cryptates.

The intrinsic order of reactivities of the various ionic species in ionic polymerization cannot be established by a straightforward theoretical argument—the answers are not unequivocal. A free ion should be more reactive than an ion pair, provided the polarization of a monomer by the electric field generated by a living polymer is the most important factor determining the reactivity. However, if the addition proceeds by a push-pull mechanism such as

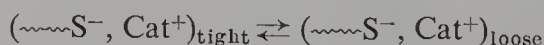


then the cation could play an important role in facilitating the process. Thus, ion pairs might be more reactive than free ions in such systems.

The push-pull mechanism is affected by the nature of the cation and its degree of solvation. In a poorly solvating medium small cations such as Li^+ may form ion pairs so tight that a substantial stretching of the $\bar{\text{C}} \cdots \text{Cat}^+$ bond is required to allow for the operation of the push-pull mechanism. The energy expended in stretching the $\bar{\text{C}} \cdots \text{Cat}^+$ bond reduces the gain arising from the cation's pull, and ultimately such an ion pair may be substantially less reactive than the free ion. Moreover, stretching of the $\bar{\text{C}} \cdots \text{Cat}^+$ bond increases the dipole of the transition state and therefore decreases its entropy, whereas the entropy of transition is positive in the reaction involving the free ions because the negative charge becomes delocalized. No stretching takes place in the addition to a loose pair, and hence such a pair should be more reactive than a tight pair; in fact, in some systems the loose pairs may be even more reactive than the free ions.

The foregoing discussion rationalizes the gradation of reactivities of the tight ion pairs of living polystyryl salts in dioxane, $\text{Li}^+ < \text{Na}^+ < \text{K}^+ < \text{Rb}^+ < \text{Cs}^+$. The degree of stretching of the $\bar{\text{C}} \cdots \text{Cat}^+$ bond decreases along this series, thus accounting for the observation. The reverse order of reactivities of $\sim\text{S}^-$, Cat^+ in THF, $\text{Li}^+ > \text{Na}^+ > \text{K}^+ > \text{Rb}^+ > \text{Cs}^+$ (see Table 4), merely reflects the increase in the fraction of loose ion pairs.

Let us consider the effect of solvent on the reactivity of loose pairs. Studies of the anionic polymerization of styrene in dioxane, tetrahydropyran, tetrahydrofuran, and dimethoxyethane could create the wrong impression that the reactivity of loose ion pairs increases with increasing capacity of the medium to solvate the cations. This conclusion is erroneous. The reported findings merely reflect the shift in the equilibrium



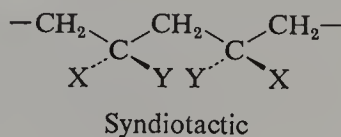
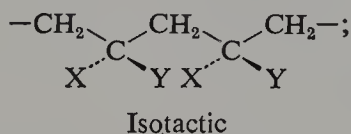
resulting from the change of solvent, and not a variation in the reactivity of a

particular kind of ion pair. Let us therefore ask a more pertinent question: How does a solvent or a solvating agent surrounding a loose ion pair affect its reactivity in a polymerization process? The answer hinges on the following problem: Does a solvent molecule in the solvation shell of the cation have to be replaced by a monomer prior to its addition to the end group of a living polymer? Apparently this is often the case because the pull of the cation is enhanced when it gets in a direct contact with the monomer. Accepting this suggestion, one may conclude that the more tenaciously the solvent molecules are attached to the cation, the more difficult becomes their replacement by monomer and therefore the lower the reactivity of the respective loose ion pair. The available data seem to confirm this conclusion: k_{\pm} of the loose $\sim\text{S}^-$, Na^+ is $20,000\text{ M}^{-1}\text{ sec}^{-1}$ in DME compared to $30,000\text{ M}^{-1}\text{ sec}^{-1}$ in THF [22]. Even more convincing are the results obtained in the presence of tetraglyme. The propagation constant of the loose $\sim\text{S}^-$, Na^+ ion pairs separated by tetraglyme is $3900\text{ M}^{-1}\text{ sec}^{-1}$ at 25°C [31], nearly 10 times less than that of the loose $\sim\text{S}^-$, Na^+ pairs separated by THF.


The previously discussed results pertaining to the polymerization of living polyvinylpyridine are now understood. The intramolecular solvation by the pyridine units attached to the polymer produces in this system loose $\sim\text{VP}^-$, Na^+ ion pairs partially solvated by the molecules of solvent. In the transition state of the polymerization the monomer replaces the latter and therefore the poorer the solvent the faster the polymerization. Indeed, the relevant k_{\pm} was found to be $2100\text{ M}^{-1}\text{ sec}^{-1}$ in THF but $4500\text{ M}^{-1}\text{ sec}^{-1}$ in tetrahydropyran [33]. This result implies that before its addition to the growing polymer the monomer replaces a solvent molecule attached to the cation, leaving intact its bonding with the pyridine moieties attached to the polymer chain. The significance of this phenomenon will become clearer when the stereospecificity of polymerization is discussed.


8. STEREOSPECIFIC POLYMERIZATION OF VINYL AND VINYLIDENE MONOMERS

The stereospecific polyaddition of vinyl or vinylidene monomers will be discussed here, leaving the discussion of the stereospecific polymerization of dienes for a later section. Polymer chains built from monomers of the $\text{CH}_2=\text{CXY}$ type with $X \neq Y$ involve two types of linkage, isotactic or syndiotactic enchainment:




In a stereospecific polymer all linkages are virtually of one type only, isotactic in isotactic polymers and syndiotactic in syndiotactic polymers. If both linkages are encountered in a chain and their distribution is somewhat random, the resulting polymer is referred to as an atactic polymer.

In a polymeric chain the  centers may be classified as being of R or S types with respect to an arbitrary center denoted as, say, an R center. The


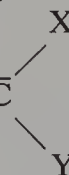
definite configuration of each  center is unaffected by any confor-

mational changes of the chain resulting from rotations around the various C—C bonds. This imposes on each center a character resembling somewhat that of an asymmetric carbon atom, and indeed it is customary to refer to such centers as being pseudo-asymmetric although not optically active.

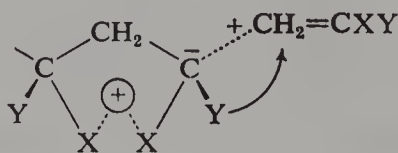
In a typical living polymer a carbanion, $-\bar{C}(XY)$, forms the last segment and its configuration remains undetermined until a subsequent monomer unit is added to the chain. The lack of a definite R or S configuration is the result

of the planarity of the  group or of the ease with which the \bar{C}

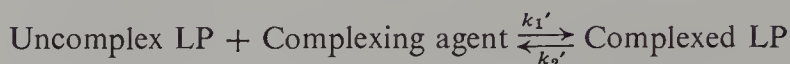
carbon atom oscillates through the plane defined by its three substituents. However, if one of the groups of the last unit, say X, and that of the penultimate unit are solvating *simultaneously* a cation, a definite correlation becomes

established between the configuration of the penultimate  and the ultimate configuration the  will acquire on the addition of a next

monomer. This is clarified by the following diagram:



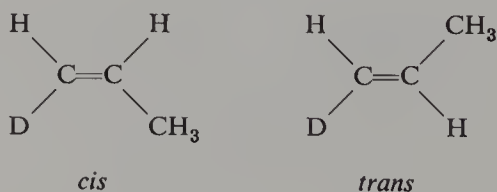
A somewhat related behavior may be visualized in a system composed entirely of living ion pairs but involving a complexing agent that modifies the stereospecificity of their growth. The respective equilibrium,



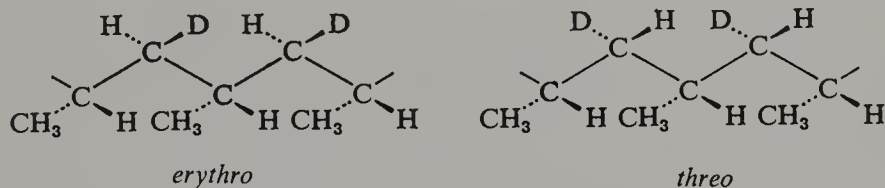
then affects the structure of the resulting polymer in a fashion similar to that discussed above. Anionic polymerizations initiated by Grignard compounds are particularly affected by the nature of solvent and additives. Extensive studies of the stereoregularities of the resulting polymers were reported by Nishioka [40], and more recently this subject was reinvestigated by Allen [41]. The additives such as ethers affect the stereoregularity and the molecular weight distribution of the product as well as the rate of polymerization. The rate increases with increasing concentration of the coordinating agent, reaches a maximum, and then decreases on its further addition. Apparently the reactive monocomplex eventually is converted into an unreactive bi-complex.

The existence of two different propagating species in anionic polymerization of methyl methacrylate is revealed by the studies of Bywater [42], who observed two absorption peaks in the UV spectrum of living polymethyl methacrylate, the relative intensities of which were solvent dependent. This implies the existence of two distinct forms of ion pair, their relative proportions depending on solvent and temperature. Another important evidence for the participation of two types of growing end in the polymerization is obtained from detailed NMR studies of polymers produced in hydrocarbon solvents in the presence of ethers. The sequences of isotactic and syndiotactic linkages are *not* given by any Markoff chain [43], a result explained only by the presence of two growing species coexisting in dynamic equilibrium. Apparently one deals with an etherated and nonetherated form of living polymer, each of them showing preference for a different type of placement.

Further insight into the mechanism of polyaddition may be obtained from studies of the modes of opening a C=C double bond. Consider for the sake of illustration *cis*- and *trans*-1-*d*₁-propene:



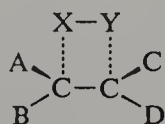
Isotactic polymerization of such monomers may produce diisotactic chains of the *erythro*- or *threo*-type:



Indeed, Natta et al. [44] observed that distinct polymers are formed from *cis*- and *trans*- d_1 -propene, each characterized by its own polarized infrared spectrum. The assignment of their configurations was achieved by Miyazawa and Ideguchi [45], who showed that the *cis*-isomer produces an *erythro*-polymer, whereas a *threo*-polymer is formed from the *trans*-olefin. These results were interpreted as evidence that *cis*-opening of a double bond occurs in the course of a polyaddition induced by the Ziegler-Natta catalyst. The same conclusion was previously reached by Natta et al. [46].

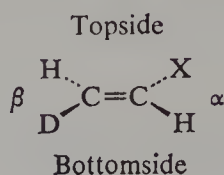
Later studies cast doubt about the *cis*-opening mechanism. Yoshino et al. [47] demonstrated that anionic polymerization of deuterated methyl acrylate initiated with lithium aluminum hydride produces diisotactic polymer and they concluded, on the basis of their NMR analyses, that this polyaddition proceeds through *trans*-addition, contrary to the previous findings. Even more surprising are the results of Schuerch et al. [48], who demonstrated that the Grignard-initiated polymerization of α -*cis*- β - d_2 -acrylate led to an isotactic polymer with respect to the α carbon, while the orientation around the β carbon results in stereoblocks. These findings call for reexamination of the concept of *cis*- and *trans*-openings.

In a polyaddition, the *cis*- and *trans*-openings have no precise meaning in terms of the structure of the transition state. The concept is unequivocal in a four-center reaction:

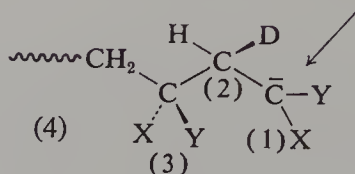


However, in a two-step process the mode of approach of the monomer to the growing polymer determines the configuration around the β carbon only (assuming the addition takes place at this position). The complete incorporation of the $\text{C}=\text{C}$ bond into a chain is accomplished only after the addition of the next monomer. The final outcome may appear then as either a *cis*- or a *trans*-opening, provided that rotation around the β - α bond is permitted.

To clarify these ideas, let us consider the addition of a monomer,



to an anion



Assume that some kind of interaction between carbons 1 and 3 forces the orientation around the last carbon to become isotactic with respect to 3 as the next monomer is added to 1. Furthermore, let us suppose that the monomer may approach the anion only from above, as indicated by the arrow, but it may reach the anion in two ways, either with its “topside” or “bottomside.” Each of these alternative approaches establishes a different well-defined configuration around the β carbon, and if one of them were isotactic with respect to carbon 4, the other would be syndiotactic. Nevertheless, either addition may lead to a desirable configuration *around the α carbon* acquired by rotating the β - α axis *after* the C(3)—C(β) bond was formed. Thus a series of monomer additions may produce the isotactic structure around α -carbons, nevertheless leaving a random configuration around β carbons.

These ideas were developed in a most interesting paper by Fowells, Schuerch, Bovey, and Hood [49] leading to the following questions:

1. Is the structure around the growing carbanion rigid or is the rotation around the β - α axis free? The rigidity of the structure *does not* preclude a rotation which occurs immediately after the addition of a monomer. Such a rotation determines the ultimately rigid structure around the last carbon atom, a structure demanded by the system for its stability. The fixed geometry of the new carbanion with respect to the preceding unit may therefore be maintained in the course of addition of the next monomer.

2. If the geometry of the carbanion is rigidly maintained, one may ask whether the approach of the monomer is restricted to one side of the carbanion or whether both sides are available for the reaction. In the former case, which is the “reactive side”?

3. Does the rotation occur in the transition state? This problem is related to question 1 above.

4. Assuming that the geometry of a carbanion is rigid and that only one of its sides is available for the reaction, we may ask whether the approaching

monomer is free to reach the carbanion with either of its sides (topside or bottomside), or whether the system favors one type of approach more than the other.

Detailed discussion of these possibilities reveals that several distinct mechanisms may yield polymers of the same structure. One should therefore ask what configuration is imposed on the product by each particular mechanism. For the sake of illustration, three types of mechanism are considered:

1. Living polyacrylate forms a contact ion pair, say with a Li^+ counterion. The Li^+ cation also is bonded to oxygen atoms of the carbonyl groups of the last and of the penultimate units. The geometry of the last unit is therefore related to the configuration of the penultimate unit. Let the approaching monomer become first bonded to the Li^+ cation by the carbonyl group attached to its α carbon. The spatial relation of thus coordinated (cation-solvating) monomer with respect to the preceding segments becomes therefore uniquely determined, and by the same token its β carbon atom has to approach the growing anion in a unique way. The new C—C bond is then formed, and thereafter the linkage between Li^+ and the formerly penultimate unit is ruptured and a linkage with the carbonyl group of the new last unit is established. The sequence of these events is depicted in Fig. 8, and such a

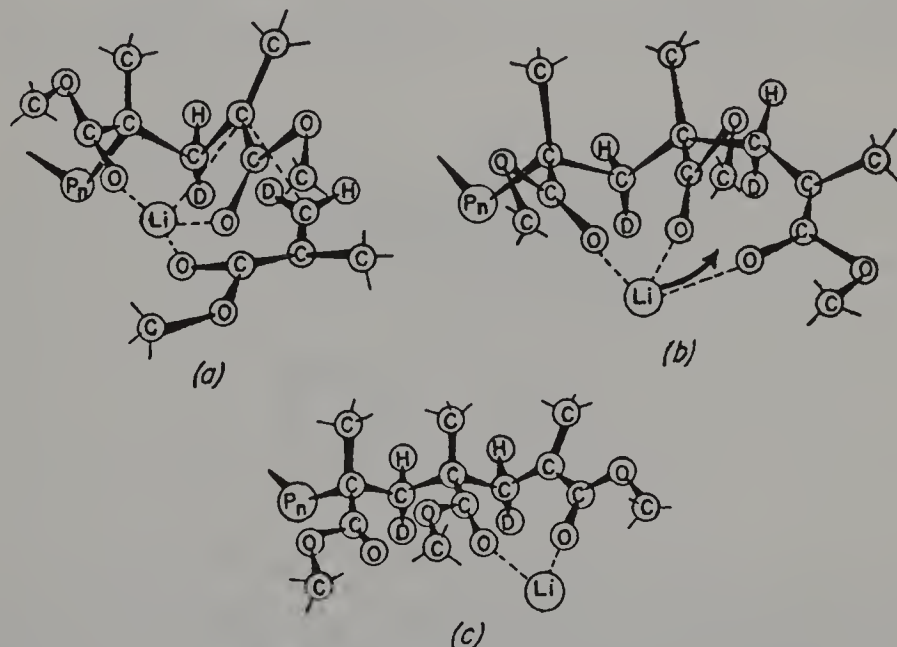


Figure 8. (a) An isotacticlike approach of the monomer to the chelated contact ion pair. (b) The new C—C bond has been formed with the methylene deuterium atom on the same side of the zigzag as the ester function. (c) The Li^+ moves up to the new anion, with concurrent rotation of the new penultimate ester group, forming the same chelated structure as in a.

mechanism ensures a unique structure around the α as well as the β atoms of the polymer. This type of addition may be represented formally as a *cis*-opening of the $C=C$ bond.

2. The Li^+ cation of the ion pair is still bonded to the two carbonyl groups as in case 1 above. However, due to the presence of some solvating agent, say tetrahydrofuran, the other coordinating sites of the Li^+ become saturated by the ether and *not available* to the approaching monomer. Nevertheless, the spatial structure around the carbanion leaves only one of its sites available for the reaction. Now the monomer reaches the carbanion only from "above" (see Fig. 9a), and it approaches the negative center preferentially with its top-side but not with its bottomside. This restriction may be imposed by steric or polar factors and the resulting configuration is shown in Fig. 9a. After

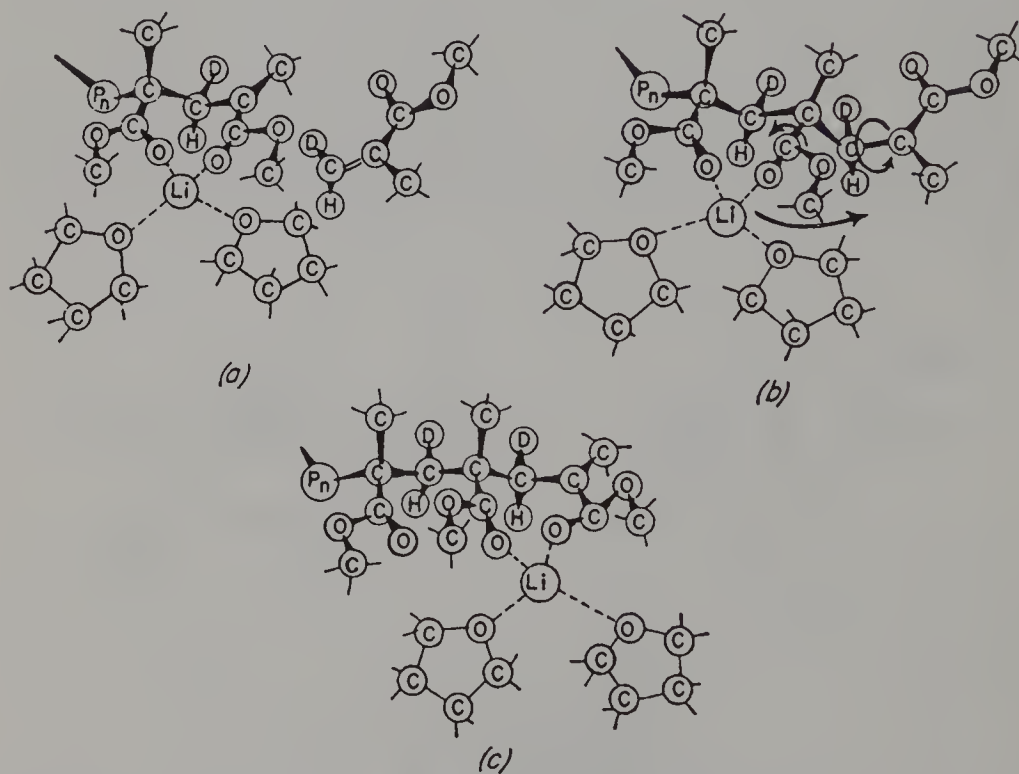


Figure 9. (a) A syndiotacticlike approach of the monomer to the peripherally solvated contact ion pair. The monomer groups are not co-ordinated with the counterion, and the nonbonded atoms interactions force the approach to be syndiotacticlike. (b) The new C—C bond has been formed. (c) The Li^+ and its peripheral solvent shell move up to the terminal unit, with the concurrent rotation of the ester function. Since the new anion resides largely on the carbonyl, there is a simultaneous rotation about the new α, β -bond to reduce charge separation. This results in an *erythro-meso* placement, the methylene deuterium atoms being on the opposite side of the zigzag from the ester groups, and the α -carbon is now in an incipient isotactic configuration.

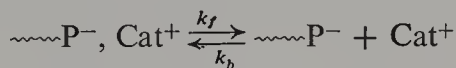
formation of the C—C bond, the rotation around the β - α axis brings the α carbon into a proper position in respect to Li^+ ; the cation becomes bonded to the carbonyl group of the newly added unit, simultaneously rupturing its link with the former penultimate unit. The resulting polymer again has well-defined configurations around α and β carbons, both being rigidly maintained along the chain. However, the addition appears now formally as a *trans*-opening of the C=C bond, as shown by the sequence of diagrams in Fig. 9a, 9b, and 9c.

3. If the restriction imposed upon the approaching monomer is lifted—if its topside and bottomside have equal chance of being added to the growing anion—then the mechanism outlined in subsection 2 still leads to stereoregularity with respect to α carbons, whereas the configurations around β carbons become random. This case has not been observed yet.

It is hoped that these examples clarify some of the problems encountered in stereoregular polymerization. It is important to realize that these ideas take cognizance of the structure of the ionic species which propagate the polymerization. They rationalize the effects of counterions, solvents, solvating additives, and so on, and show that the structure of the ion pair is of the utmost importance in determining the course of ionic polymerizations.

9. EFFECT OF IONIC STRUCTURE ON MOLECULAR WEIGHT DISTRIBUTION

In a living polymer system all the polymer molecules have an equal chance to grow and none is terminated. Hence a rapid initiation should produce polymers of Poisson molecular weight distribution (see Chapter II of ref. 4). However, if two or more ionic species participate in the growth, each propagating with a different rate, the molecular weight distribution of the polymer formed in such a system may deviate substantially from the Poisson type. For example, in a system containing ions and ion pairs propagating with the rate constants k_- and k_+ , respectively, the molecular weight distribution depends on three parameters, k_-/k_+ , k_f , and k_b , where the last two constants refer to the rates of ionic dissociation and association processes:



For $k_f = k_b = 0$ the molecular weight distribution of the resulting polymer is binodal, resulting from the superposition of two Poisson distributions, each corresponding to a different number-average molecular weight. In contrast, for k_f and k_b $[\text{Cat}^+]$ are both much greater than $k_-[\text{M}]$ and $k_+[\text{M}]$, the resulting polymer should have a molecular weight distribution closely approximating

to the Poisson type. The distribution obtained in a system composed of living and dormant polymers such as $k_- \neq 0$ and $k_{\pm} = 0$ was investigated by Szwarc and Hermans [52], and a more general case of two growing species remaining in dynamic equilibrium was examined by Coleman and Fox [50] and by Figini [51]. In such systems a careful examination of the deviation of the experimentally determined molecular weight distribution from the Poisson type permits, in principle, the determination of k_f and k_b , provided the dissociation equilibrium constant, and the ratio k_-/k_{\pm} are known. Such studies have been reported by Löhr and Schulz [53] and by Figini et al. [54]. In spite of the fine and highly sophisticated experimental techniques developed by these workers, the reliability of such a determination of k_f and k_b may be questioned, especially since other complicating features of the reaction interfere with the outcome. The problem becomes even more complex when three or more growing species participate in the propagation.

10. ROLE OF TRIPLE IONS IN IONIC POLYMERIZATION

Ion pairs may associate with free ions into new charged species referred to as triple ions [55]:



or



This association becomes significant at high salt concentration. The triple ions are charged and therefore some counterions have to be present to maintain the electrical neutrality of the solution. In the special case of $K_- = K_+$ the negative and positive triple ions neutralize each other and their formation does not affect the ratio of the free A^- and B^+ ions. However, in the more general case, when $K_- \neq K_+$, the formation of triple ions affects substantially the concentration of the free ions. For example, in a system for which $K_+ \gg K_- \approx 0$ the B^+ ions are removed, being transformed into B^+, A^-, B^+ triple ions, and consequently the concentration of the free A^- ions has to increase greatly. This is necessitated by the condition of the electrical neutrality of the solution coupled with the requirement of the equilibrium $A^-, B^+ \rightleftharpoons A^- + B^+$. The formation of B^+, A^-, B^+ ions also may be represented by the equation



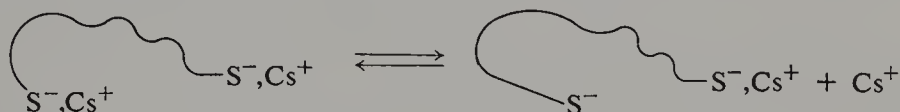
which clearly indicates that the degree of this ionization becomes independent of the concentration of salt when $B^+ \ll A^-$.

The significance of triple-ion formation becomes evident in anionic polymerization whenever the free $\sim\sim\sim P^-$ ions are much more reactive than either

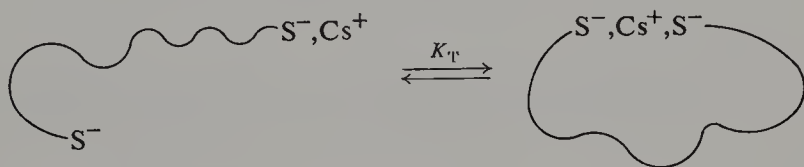
the $\sim\sim\sim\text{P}^-$, Cat^+ ion pairs or the triple ions, whether of the type $\sim\sim\sim\text{P}^-$, Cat^+ , P^- or $\sim\sim\sim\text{P}^-$, $(\text{Cat}^+)_2$. In such systems the formation of triple ions *decreases* the reactivity of living polymers if $K_- \gg K_+$, whereas the formation of triple ions *increases* the reactivity of living polymers when $K_+ \gg K_-$. In either case, the effect of triple ions becomes more pronounced as the concentration of living polymers increases. In systems containing other salts in addition to living polymers the problem of reactivity becomes even more complex because mixed triple ions as well as homotriple ions can be formed.

An interesting observation was reported by Bhattacharyya et al. [56]. In the course of studies of the reactivity of cesium salt of living polystyrene in THF they determined the dissociation constant of the salt by the conductance method and by the kinetic approach (see p. 384). Both methods led to concordant results when the polymer contained only one growing end group per chain. However, the examination of low molecular weight polymers endowed with *two* growing groups per chain led to the values of the dissociation constant which were much too high when deduced from the conductance data, but much too low when the calculation was based on the reactivity data. These puzzling results were explained by invoking participation of the intramolecular triple ions.

Ionic dissociation of one end group of the cesium salt of a polymer endowed with two carbanion end groups yields an anion which, by necessity, remains in the vicinity of an ion pair even in the most dilute solution:



Hence an intramolecular triple-ion formation takes place:



the degree of cyclization being *independent* of the concentration of the half-dissociated polymers. The removal of $\sim\sim\sim\text{S}^-$ ions upsets the equilibrium between $\sim\sim\sim\text{S}^-$, Cs^+ ion pairs and the $\sim\sim\sim\text{S}^-$ and Cs^+ free ions. Consequently, the ion pairs dissociate and thus $[\text{Cs}^+] > [\sim\sim\sim\text{S}^-]$. Since the association increases the total concentration of ions, it biases the conductance data and creates an error in the conventional calculation leading to a too high dissociation constant of ion pairs. On the other hand, because the most reactive $\sim\sim\sim\text{S}^-$ ions are partially removed from the system, its reactivity

decreases and the conventional calculation based on kinetic data lead then to an erroneous, too low value of the dissociation constant.

Proper mathematical treatment of the system, presented by Bhattacharyya et al. [56], gives the value of K_T and of the propagation rate constant of triple ions. Obviously, K_T depends on the length of the chain and decreases with its increase. This conclusion has been confirmed by experiments.

Triple ions were assumed to be the cause of another anomaly reported by Ise and his students [57]. They examined the kinetics of anionic polymerization of the lithium salt of living polystyrene in a binary mixtures of benzene and dimethoxyethane. The reaction behaved conventionally when the solvent was rich in DME (50% or more); the overall propagation constant, k_p , increased with dilution—the usual effect resulting from the increased dissociation of ion pairs into the highly reactive free ions. However, in solvents richer in benzene (40 or 30% of DME) the observed propagation constant *decreased* with dilution. This effect in conjunction with the conductance measurements led Ise et al. to the conclusion that highly reactive triple ions $(\sim\sim\sim S^-)_2 Li^+$ are formed in such solvent systems.

This writer questions that conclusion. According to Ise his data conform to a linear relation between k_p and $1/[LP]^{1/2}$ as well as $[LP]^{1/2}$ (Figs. 2 and 4 of ref. 57.). Since both relations cannot be simultaneously valid, it seems that the reliability of the experiments is not sufficient to draw any quantitative conclusions. Moreover, it appears that the triple ions $\sim\sim\sim S^-(Li^+)_2$ should be more easily formed than $(\sim\sim\sim S^-)_2 Li^+$, contrary to the opinion of Ise et al. Further difficulties arise from a possible reaction of living polymers with DME yielding lithium alkoxide. The latter is known to affect the polymerization and its presence may lead to artifacts.

It appears that mixed solvents often provide mixed blessings. In studies of solvent effects the use of a series of pure solvents, differing systematically in some critical property may provide more reliable information than a series of mixtures of two solvents.

Triple ions were assumed to contribute to the propagation involving sodium salt of living poly-2-vinylpyridine in THF [140]. By postulating the formation of Na^+ , $(\sim\sim\sim VP^-)$, Na^+ triple ions only* the following relations are obtained:

$$[\sim\sim\sim VP^-] = \{K_{diss}[IP](1 + k_A[IP])\}^{1/2}$$

and

$$[Na^+, (\sim\sim\sim VP^-), Na^+] = \frac{K_{diss}K_A[IP]^2}{\{K_{diss}[IP](1 + K_A[IP])\}^{1/2}},$$

* Only the *intramolecular* triple ions $\overset{\curvearrowright}{S^-}, Cs^+, S^-$ are formed in the system $Cs^+, -S\sim\sim\sim S^-$, Cs^+ in THF [56]. The preferable formation of these *negative* triple ions is the result of the vicinity effect which does not operate in the $\sim\sim\sim(VP^-), Na^+$ system.

where [IP] denotes the equilibrium concentration of the $\sim\sim\sim(\text{VP}^-)$, Na^+ ion pairs. The dissociation, $\sim\sim\sim(\text{VP}^-)$, $\text{Na}^+ \rightleftharpoons \sim\sim\sim(\text{VP}^-) + \text{Na}^+$, K_{diss} , and the association, $\sim\sim\sim(\text{VP}^-)$, $\text{Na}^+ + \text{Na}^+ \rightleftharpoons \text{Na}^+$, $(\sim\sim\sim\text{VP}^-)$, Na^+ , K_A , maintain the equilibrium concentration of the free ions and triple ions. Denoting by k_- , k_{\pm} , and $k_{+, -, +}$ the propagation constants of the free ions, ion pairs, and triple ions, respectively, one finds the observed propagation constant, k_p , to be

$$k_p = k_{\pm} + (k_- - k_{\pm}) \left(\frac{K_{\text{diss}}}{[\text{LP}]} \right)^{1/2} (1 + K_A[\text{LP}])^{1/2} + (k_{+, -, +} - k_{\pm}) K_{\text{diss}}^{1/2} K_A^{1/2} / \left(1 + \frac{1}{K_A[\text{LP}]} \right)^{1/2}$$

provided that the fraction of living polymers, LP, forming any ions is small. At high dilution, when $K_A[\text{LP}] \ll 1$, this equation is reduced to the conventional one,

$$k_p = k_{\pm} + (k_- + k_{\pm}) \left(\frac{K_{\text{diss}}}{[\text{LP}]} \right)^{1/2},$$

but k_p tends to a constant value of

$$\lim k_p = k_{\pm} + (k_- + k_{+, -, +} - 2k_{\pm}) (K_{\text{diss}} K_A)^{1/2}$$

as the concentration of living polymers increases, that is, for $K_A[\text{LP}] \gg 1$. Hence, if the latter inequality is fulfilled in the investigated concentration range, the plot of k_p versus $1/[\text{LP}]^{1/2}$ would be flat.

As mentioned earlier (p. 396) the k_p versus $[\text{LP}]^{-1/2}$ plots obtained for the sodium salts of living poly-2-vinylpyridine [33] or poly-2-vinylquinoline [34] in THF are unusually flat, an observation confirmed by Sigwalt et al. [140]. Therefore, the treatment outlined above seems to offer an alternative to the interpretation invoking the *intramolecular* solvated ion pairs (p. 397). This interesting approach needs a closer examination.

To account for the experimental observations in terms of triple-ion formation a value of at least 10^5 M^{-1} has to be attributed to K_A at 25°C . Accepting the value of about 10^{-9} M for K_{diss} [33, 35] we find $\lim k_p - k_{\pm} = (k_- + k_{+, -, +} - 2k_{\pm}) (K_{\text{diss}} K_A)^{1/2}$ to be $\sim 1000 \text{ M}^{-1} \text{ sec}^{-1}$ for $K_A = 10^5 \text{ M}$ provided $k_- = 100,000 \text{ M}^{-1} \text{ sec}^{-1}$ as derived from the *conventional* treatment of the data [33]. Let it be stressed that the high value of the $\lim k_p$ does not result directly from the presence of triple ions but from the increase in the fraction of the *free* ions caused by the triple-ion formation. The propagation constant of triple ions is not known and it is probably smaller than k_{\pm} .

The equivalent conductance, Λ , is given by

$$\Lambda = \left(\frac{K_{\text{diss}}}{[\text{LP}]} \right)^{1/2} \left\{ (1 + K_A[\text{LP}])^{1/2} \Lambda_0^- + \frac{K_A[\text{LP}] \Lambda_0^{+-+} + \Lambda_0^+}{(1 - K_A[\text{LP}])^{1/2}} \right\}$$

where Λ_0^- , Λ_0^{+-+} , and Λ_0^+ denote the contributions to the limiting conductance of $\sim\sim\sim\text{VP}^-$, Na^+ , $\sim\sim\sim\text{VP}^-$, Na^+ , and Na^+ , respectively, provided that all the ions form only a small fraction of ion pairs. This equation acquires a standard form when $K_A[\text{LP}] \ll 1$, and Λ approaches a constant value of $(K_{\text{diss}}K_A)^{1/2}(\Lambda_0^- + \Lambda_0^{+-+})$ as $K_A[\text{LP}] \gg 1$.

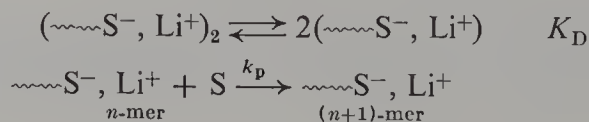
Examination of the data reveals that the large value of k_{\pm} , well in excess of $1500 \text{ M}^{-1} \text{ sec}^{-1}$, is undisputable and the large observed k_p cannot be accounted for either by the reactivity of the triple ions or of the free $\sim\sim\sim\text{VP}^-$ anions. In fact, the triple ions contribute only a little to k_p at low concentration of living polymers ($< 10^{-5} \text{ M}$). Finally, k_p is greater for the polymerization proceeding in dioxane than for the reaction taking place in THF [33]. Since the low dielectric constant of dioxane prevents the formation of any ions in that solvent, the high values of k_{\pm} are undeniable and the great reactivity of $\sim\sim\sim 2\text{-VP}^-$, Na^+ ion pairs must be attributed to the *intramolecularly* solvated loose ion pairs.

Nevertheless, triple ions seem to be formed in the system $\sim\sim\sim 2\text{-VP}^-$, Na^+ —THF at higher concentrations of living polymers. The pronounced curvature of the Fuoss plots, reported by Fisher [33a], verifies the formation of these ions and accepting Sigwalt's approach, K_A may be calculated from the reported data: $K_A = 3 \times 10^4$ at 25°C .

In conclusion, triple ions, Na^+ , $(\sim\sim\sim 2\text{-VP}^-)$, Na^+ are probably formed in the system $\sim\sim\sim 2\text{-VP}^-$, Na^+ —THF, but their influence on the polymerization is minor at higher dilutions. The high reactivity of $\sim\sim\sim (2\text{-VP}^-)$, Na^+ ion pairs must be attributed to the *intramolecular* solvation of the Na^+ ions, although the k_{\pm} values may be by 20 or 30% smaller than reported by Fisher and Szwarc [33]. Studies of the conductance of Na^+ , BPh_4^- in the presence of $\sim\sim\sim 2\text{-VP}^-$, Na^+ provide the best way to verify Sigwalt's proposal and to determine the value of the association constant K_A .

11. POLYMERIZATION INITIATED BY LITHIUM SALTS OF LIVING POLYMERS IN HYDROCARBON MEDIA

In hydrocarbon solvents the lithium salts of living polymers are aggregated into dimers or even higher associates. The first evidence of dimerization of lithium polystyryl in benzene was provided by the kinetic studies of its polymerization. The early work of Worsfold and Bywater [58] clearly demonstrated that the rate of propagation is proportional to the square root of the total concentration of $\sim\sim\sim\text{S}^-$, Li^+ . This result was accounted for by the following mechanism:



leading to the kinetic expression $-d[S]/dt = k_p K_D^{1/2} [\text{~~~~S}^-, \text{Li}^+_{\text{total}}]^{1/2} [S]$. This relation was confirmed by other workers, whose results were thoroughly reviewed by Bywater [59] and later by Hsieh and Glaze [60]. The derived kinetic expression applies only to polymerization proceeding *after* complete consumption of the initiator (BuLi). In its presence the initiation and propagation proceed simultaneously and this complicates the observed kinetics. Moreover, butyl lithium forms with living polymers mixed associates, and these are inert and do not contribute to the propagation.

The physical evidence for the dimerization of living lithium polystyryls is provided by comparison of their molecular weight with that of a "killed" polymer, the polymer produced from living species by protonation, for example,



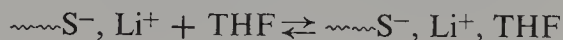
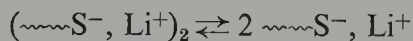
Examination of viscosities [61] or light scattering [62] of the solutions of both polymers confirmed the dimeric nature of the living end groups of lithium polystyrene in benzene and in cyclohexane.

Kinetic studies of isoprene polymerization by the living lithium polyisoprenyl were reported by several research groups. They demonstrated that the degree of association of that polymer in hydrocarbon solvents is 4 [59]—a result confirmed again by light scattering measurements in cyclohexane [63] and in heptane [64]. Only the monomeric lithium polystyryl seems to be reactive.

Similar studies of polymerization involving living lithium polybutadiene led to large discrepancies in the findings reported by various workers [60]. The presence of impurities such as lithium alkoxides may account for the contradictory claims revealed in the results of the same research groups reported at different times.

The low degree of dissociation of these aggregates makes it impossible to determine their equilibrium constant by measuring the viscosity of a living and dead polymer. The results claimed by some workers and obtained by this method are therefore meaningless. This becomes obvious when the experimental errors and the empirical assumptions are critically examined. For further discussion of this subject the reader is referred to Chapter VIII of ref. 4.

The aggregation of the lithium salt of living polystyrene in hydrocarbon solvents is destroyed when small amounts of ethers, for example, tetrahydrofuran, are added to the solution. It seems that the equilibria



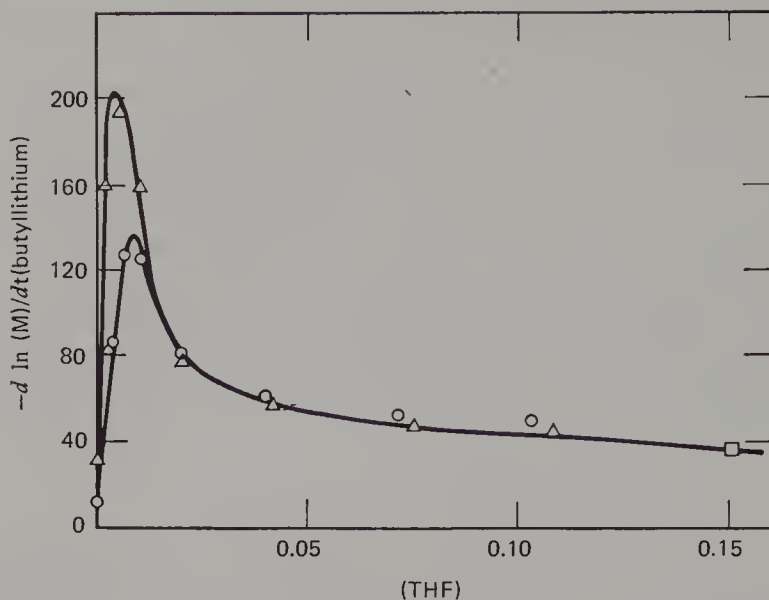


Figure 10. The effect of wide variations in the tetrahydrofuran concentration on the propagation rate at two median butyllithium concentrations: ○, $[\text{BuLi}] = 0.96 - 1.2 \times 10^{-3} M$; Δ, $[\text{BuLi}] = 1.2 - 1.8 \times 10^{-4} M$. [Reproduced by permission of the National Research Council of Canada, from *Can. J. Chem.*, **40**, 1564 (1962).]

lead to complete dissociation of the dimers. A similar behavior of alkyl-lithiums was reported by Waack and West [65]. The reactivity of the mono-etherate seems to be very high [65], but further addition of THF converts it into the much less reactive dietherate. Consequently, the rate of propagation of lithium polystyryl in benzene is greatly accelerated by the addition of small amounts of THF, although retardation is observed as the concentration of THF increases [66]. These effects are illustrated by Fig. 10.

This rather sketchy review of the behavior of the lithium salts of living polymers suffices to stress the unique properties differentiating them from living polymers of other alkali metals. The stereochemistry of their propagation, discussed in the following section, makes the lithium salts even more unusual.

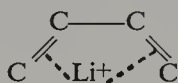
12. STEREOSPECIFICITY OF DIENE POLYMERIZATION

Several types of linkage may be formed in polymerization of dienes. For example, butadiene may be incorporated into a polymer in 1,4 or 1,2 fashion, the former enchainment may occur in a *cis* or *trans* way, and the latter may lead to isotactic or syndiotactic placements. These structures are formed by two consecutive reactions. As the diene molecule is added to the growing

center a bond is formed between the carbanion and one of the four (1, 2, 3, or 4) carbon atoms of the monomer. There is no doubt that the addition to carbon atoms 2 and 3 is all but excluded, and hence we have to inquire only which of the two centers, 1 or 4, is preferred for the first step. Of course, both centers are identical in butadiene but different in isoprene. Studies of Shima et al. [67] clearly demonstrated that the nonalkylated C=C double bond is much more reactive in anionic propagation than the alkylated one, thus the first step is uniquely determined. After the addition (to carbon atom 4), the diene is converted into an allyl derivative and the next addition, which finally determines the structure of the incorporated monomer, may take place on carbon atom 1 or 3.

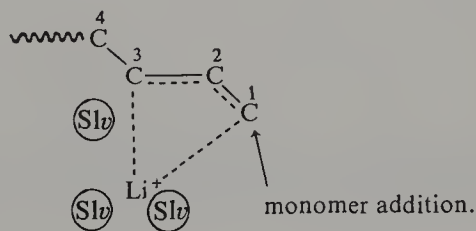
The nature of the cation and the solvent are critical in directing the addition of the next monomer to one or the other of these atoms. It seems that the larger cations, or solvated cations, make carbon 3 more reactive than 1, whereas the nonsolvated, bare lithium cation directs the addition to carbon 1. We shall not inquire how a cation directs this addition—several plausible answers may be given—but we shall proceed instead to the most intriguing question: Under what conditions does the addition to carbon atom 1 leave the incorporated monomer in a *cis* or *trans* configuration?

It is common to say that a diene may acquire a *cis* configuration by interacting with a cation, and diagrams such as



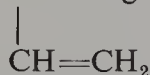
are frequently presented. However, the configuration of the monomer *prior* to its addition has no bearing on the structure of the incorporated monomer. As pointed out earlier, the latter structure is developed in the course of the *second* addition involving the allyl ion and not a *diene*.

It seems that the small, nonsolvated lithium cation polarizes strongly carbon atom 4 and attracts it to itself; thus the allyl ion *and* carbon atom 4 acquire the configuration depicted above. In the presence of a solvating agent the latter is preferred as a solvating companion of the cation, and the resulting crowding developed around the Li⁺ makes the configuration



more plausible. Thus a *cis* configuration is produced in the addition to the former ion pair but a *trans* structure results from the addition taking place to the solvated ion pair. Although the mechanism proposed here oversimplifies the problem, it describes more correctly the basic conditions required for the stereospecific diene polymerization than the hypothesis based on the monomer coordination.

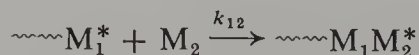
The complexity of the stereospecific polymerization of dienes is further emphasized by the results of recent NMR studies [141–143]. Living lithiated polymers were prepared from per-deuterated monomers, but the last unit, bearing the negative charge, was derived from an ordinary, proton-containing diene. On the basis of their proton NMR spectrum it was concluded that the C—Li linkages are better described as σ -bonds, $\sim\text{CH}_2\cdot\text{CH}=\text{CH}-\text{CH}_2-\text{Li}$, than as the delocalized π structures. Further addition of the per-deuterated butadiene converts this terminal units into “in-chain” units and allows to determine again their structure. Surprisingly, they contain much of the $-\text{CH}_2-\text{CH}-$ segments. Similar results were obtained by studies of model



compounds [144, 145]. Two questions are raised by these findings: Does the addition form one structure that isomerizes rapidly into another? The addition of monomer may compete then with the isomerization. Alternatively, NMR provides information about the structure of an aggregate whereas the propagation involves a monomeric living polymer. Are they structurally different? It is hoped that future research will provide the answers to these questions.

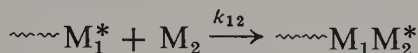
13. ANIONIC COPOLYMERIZATION

The availability of living polymers simplifies enormously studies of the kinetics of copolymerization. It is not necessary to perform the tedious and time-consuming analysis of the composition of the copolymers as a function of the feed composition which, after all, gives us only the ratios of the copropagation constants referred to as $r_1 = k_{11}/k_{12}$ and $r_2 = k_{22}/k_{21}$. The pertinent constants can be obtained directly, as has been pointed out by Bhattacharyya et al. [70], by studying the kinetics of the addition of monomer M_2 to a living polymer terminated by monomer M_1 :

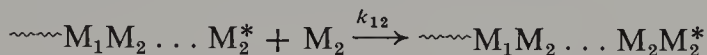


The progress of such a reaction can be followed by two techniques, either by measuring $-d[\text{M}_2]/dt$ at a predetermined concentration of the living polymers, or by observing spectrophotometrically the disappearance of the

living $\sim\sim\sim M_1^*$ end groups, preferably in the presence of a large excess of monomer M_2 . The first approach requires extrapolation of the results to zero time, because as the reaction



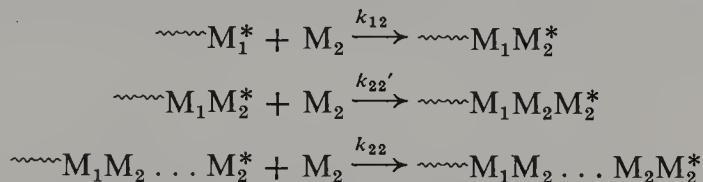
progresses it is followed by the homopolymerization of $\sim\sim\sim M_2^*$:



Therefore

$$-\frac{d[M_2]}{dt} = \{\gamma_1 k_{12} + (1 - \gamma_1) k_{22}\} [LP]_{\text{tot}} [M_2]$$

where γ_1 denotes the fraction of the original $\sim\sim\sim M_1^*$ polymers still present at time t , and $[LP]_{\text{tot}} = [LP]_0$ is the total concentration of all the living polymers. The necessity of extrapolation to zero time, although in a sense a drawback, may be taken to our advantage, because it permits studies of penultimate effects, provided they are sufficiently large. Consider the system



Its kinetics is given by three differential equations:

$$\begin{aligned} -\frac{d[M_2]}{dt} &= \{k_{12}\gamma_1 + k_{22}'\gamma_2 + k_{22}(1 - \gamma_1 - \gamma_2)\} [LP]_{\text{tot}} [M_2] \\ -\frac{d\gamma_1}{dt} &= k_{12}\gamma_1 [M_2] \\ -\frac{d\gamma_2}{dt} &= \{k_{22}\gamma_2 - k_{12}\gamma_1\} [M_2] \end{aligned}$$

At an early time of the reaction $1 - \gamma_1 - \gamma_2 \ll 1$, and the term $k_{22}(1 - \gamma_1 - \gamma_2)$ can be neglected. Under these conditions and at low percentage of conversion of M_2 into polymer,

$$\gamma_1 \approx \exp\{-k_{12}[M_2]_0 t\} \approx 1 - k_{12}[M_2]_0 t$$

and

$$\frac{d[M_2]}{dt} = k_{12}\{1 + (k_{22}' - k_{12})[M_2]t\} [LP]_{\text{tot}} [M_2]$$

or

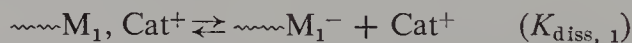
$$\frac{[M_2]}{t} = \{k_{12} + \frac{1}{2}k_{12}(k_{22}' - k_{12})[M_2]_0 t\} [LP]_{\text{tot}} [M_2]_0$$

Hence the initial slope of the plot of $[M_2]/t$ versus t provides a value from which k'_{22} may be calculated. Of course the slope is positive for $k'_{22} > k_{12}$ and negative for $k'_{22} < k_{12}$. An example of such a study was provided by the work of Lee et al. [71], although the results, viewed from our present knowledge of the subject, are questionable.

If $k_{22} \gg k'_{22}$, the value of k'_{22} may be determined easily by utilizing the stirred flow reactor technique, provided k_{22} is known from studies of homopolymerization of M_2 .

A dramatic effect of the penultimate unit was discovered by Bhasteter et al. [38], who studied the addition of styrene to living poly-1-vinyl-naphthalene. The formation of an intramolecular complex, discussed previously, reduces k'_{22} to about $2 M^{-1} \text{ sec}^{-1}$ while k_{22} is about $600 M^{-1} \text{ sec}^{-1}$ under those conditions. The difficulties of solving the three simultaneous differential equations are circumvented by using the algebraic balance equations.

The simplicity of the copolymerization step becomes complicated in systems involving more than one growing species. Consider the addition of monomer M_2 to a living polymer composed of $\sim\sim M_1^-$, Cat^+ ion pairs and the free $\sim\sim M_1^-$ ion. Initially the ionic equilibrium is determined by a single dissociation-association reaction,



However, as the reaction proceeds another equilibrium has to be maintained simultaneously with the previous one:



The rate of M_2 addition is given now by

$$-\frac{d[M_2]}{dt} = \{\gamma_1[\alpha_1 k_{12-} + (1 - \alpha_1)k_{12\pm}] + (1 - \gamma_1)[\alpha_2 k_{22-} + (1 - \alpha_2)k_{22\pm}]\}[\text{LP}]_{\text{tot}}[M_2]$$

The symbols α_1 and α_2 denote the fractions of dissociation into free ions of living polymers terminated by $-M_1^-$ and $-M_2^-$ units, respectively, their mole fractions being denoted by γ_1 and γ_2 , and the other symbols have the usual meaning. Extrapolation to zero time gives the average k_{12} equal to $\alpha_1 k_{12-} + (1 - \alpha_1)k_{12\pm}$, which increases with time if $K_{\text{diss}, 1} > K_{\text{diss}, 2}$ and decreases for $K_{\text{diss}, 1} < K_{\text{diss}, 2}$, provided that $k_{12-} > k_{12\pm}$.

The situation becomes even more complex when both monomers copolymerize simultaneously. The ratio of living polymers LP_1 and LP_2 is determined then by the conventional condition of stationary state:

$$\gamma_1\{\alpha_1 k_{12-} + (1 - \alpha_1)k_{12\pm}\}[M_2] = \gamma_2\{\alpha_2 k_{21-} + (1 - \alpha_2)k_{21\pm}\}[M_1]$$

where α_1 and α_2 are functions of $K_{\text{diss}, 1}$, $K_{\text{diss}, 2}$, and $[\text{LP}]_{\text{tot}}$ as well as of $[\text{M}_1]$ and $[\text{M}_2]$. In such a system the reactivity ratios r_1 and r_2 cease to be constant and depend on the total concentration of living polymers as well as on the ratio $[\text{M}_1]/[\text{M}_2]$.

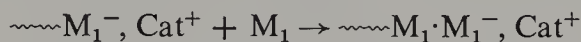
Let us consider one more example of copolymerization. It is highly speculative and may never be encountered in a real system; nevertheless, it is interesting and therefore worth considering. Assume that monomer M_2 easily forms a complex with cations of ion pairs, whether $\sim\text{M}_1^-, \text{Cat}^+$ or $\sim\text{M}_2^-, \text{Cat}^+$. Moreover, the complexation constant is sufficiently high to allow, under the conditions of the copolymerization, a virtually quantitative conversion of all the ion pairs into $\sim\text{M}_1^-, \text{Cat}^+, \text{M}_2$ or $\sim\text{M}_2^-, \text{Cat}^+, \text{M}_2$ complexes, respectively. Let us assume also that the reactions



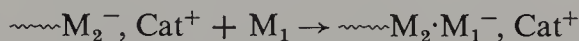
and



are relatively slow, whereas the reactions of the non-complexed living polymers



and



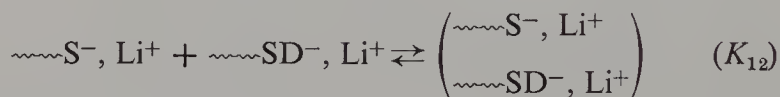
are relatively fast.

In view of the high degree of complexation of the living polymers with M_2 , the fraction of the noncomplexed polymers participating in the addition of M_1 is negligible and hence M_2 , but virtually no M_1 , polymerizes, albeit this reaction is relatively slow. However, as the concentration of M_2 decreases the proportion of the noncomplexed polymers increases and the polymerization of M_1 speeds up.

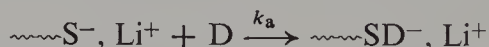
According to Korotkov [73] this situation is responsible for the peculiar behavior of the styrene-butadiene system in hydrocarbon solvents polymerizing anionically with lithium counterions. This reaction starts slowly and consumes butadiene, but after exhaustion of the butadiene supply it speeds up and styrene is then consumed. The styrene-isoprene system behaves similarly [74], and Bawn, who confirmed these observations, remarked that the onset of the fast polymerization of styrene coincides with a change of color of the polymerizing mixture, indicating the conversion of isoprenyllithium into styryllithium ([75]; see also [76]). Although these ideas are interesting, the behavior of the styrene-butadiene system arises from different reasons. Under conditions of those experiments k_{12} —the conversion of $\sim\text{S}^-, \text{Li}^+$ into $\sim\text{BD}^-, \text{Li}^+$ —is exceedingly fast and $k_{22}(\text{BD} \rightarrow \text{BD})$ is still much greater than $k_{21}(\text{BD} \rightarrow \text{S})$. Therefore, although $k_{11}(\text{S} \rightarrow \text{S})$ is greater than k_{22} ,

the reaction first consumes butadiene slowly, and only after exhaustion of this monomer does it start to consume styrene rapidly. An explanation based on these principles was presented by Kuntz [77]; however, the reaction is complicated further by the dimerization of living polymers into inactive dimers. A treatment that takes cognizance of the dimerization has been developed [78], and it accounts quantitatively for the observed kinetics.*

An interesting kinetic situation complicated by the formation of inactive polymer dimers, was unraveled by Laita and Szwarc [79]. The addition of 1,1-diphenylethylene to lithium polystyrene in benzene involves only the cross-over step, k_{12} , since 1,1-diphenylethylene does not homopolymerize. The reaction was followed spectrophotometrically by observing the disappearance of the 334-nm peak characteristic of living lithium polystyrene. In the presence of a large excess of 1,1-diphenylethylene the addition has a pseudo-first-order character with respect to $(\sim\text{S}^-, \text{Li}^+)_2$, but although the pseudo-first-order rate constant was proportional to $[1,1\text{-diphenylethylene}] = [\text{D}]$ as would be expected, it was found to be inversely proportional to the square root of $[(\sim\text{S}^-, \text{Li}^+)_2]_0$ —the *initial concentration of lithium polystyrene*. This peculiarity was accounted for by the following mechanism:



The above equilibria are assumed to be maintained all the time, whereas the reaction is attributed to the relatively slow rate-determining step



In view of the high degree of association, the concentration of the unassociated polymers is negligible compared to the concentration of the dimeric associates and hence

$$[(\sim\text{S}^-, \text{Li}^+)_2] + \left[\left(\begin{array}{c} \sim\text{S}^-, \text{Li}^+ \\ \sim\text{SD}^-, \text{Li}^+ \end{array} \right) \right] + [(\sim\text{SD}^-, \text{Li}^+)_2] = [\text{LP}]_0$$

By algebraic manipulation one finds then that

$$K_1 + K_{12}\alpha = f(K_1 + 2K_{12}\alpha + K_2\alpha^2)$$

* The absence of complexation of butadiene with living lithium polybutadiene was demonstrated by observing the NMR spectrum of ordinary, proton-containing butadiene added to an excess of perdeutero living lithium polybutadiene [141].

where

$$\alpha = \frac{[\sim\text{S}^-, \text{Li}^+]}{[\sim\text{SD}^-, \text{Li}^+]}$$

and

$$f = \frac{[\sim\text{S}^-, \text{Li}^+ \text{ in whatever form}]_t}{[\text{LP}]_0} = \frac{(\text{opt. density at } 334)_t}{(\text{opt. density at } 334)_0}$$

It is assumed here that the absorbance of $\sim\text{S}^-, \text{Li}^+$ is not affected by its state of aggregation, whether dimeric or mixed with $\sim\text{SD}^-, \text{Li}^+$. It follows that

$$\frac{df}{dt} = \frac{k_a[\text{D}]_0/[\text{LP}]_0^{1/2}}{(K_1 + 2K_{12}\alpha + K_2\alpha^2)^{1/2}}$$

This expression is simplified if $K_{12}^2 = K_1K_2$, that is, when the equilibrium constant of the mixed dimerization is equal to the geometrical average of the equilibrium constants of the homodimerizations. The denominator then is reduced to $K_1^{1/2} + K_2^{1/2}\alpha$ and the previous relation between f and α is reduced to

$$f = \frac{K_1^{1/2}}{K_1^{1/2} + K_2^{1/2}\alpha}$$

Therefore

$$-\frac{df}{dt} = \left\{ \left(\frac{k_a}{K_1^{1/2}} \right) \left(\frac{[\text{D}]_0}{[\text{LP}]_0^{1/2}} \right) \right\} f$$

in concordance with the experimental observations.

14. EFFECT OF STRUCTURE ON k_- AND k_{\pm}

The effect of structure is revealed best by comparing the copolymerization rate constants k_{1j} of a living polymer (1) with a series of monomers (j), or by comparing the copolymerization rate constants k_{k1} of a series of living polymers (k) with a monomer (1).

Such a study was reported by Shima et al. [80], who investigated the addition of substituted styrenes to living sodium polystyrene in THF. The results are presented in Table 7, and Fig. 11 is a Hammett plot of $\log k_{1j}$ versus σ . The slope of the line gives the Hammett's $\rho = +5.0$. At the time when that work was published no distinction was made between k_p and k_{\pm} and k_- . However, since the free ions dominate the propagation in THF, these data represent very closely the relation of k_- with σ . Hence $\rho = +5.0$ refers to an attack of a free $\sim\text{S}^-$ ion on a substituted styrene, and its high positive value is therefore not surprising.

Table 7 Rate Constants k_{12} of Addition of Styrene Derivatives to Sodium Polystyryl in Tetrahydrofuran at 25°C [80]
 ($[\text{~~~~~S}^-, \text{Na}^+] \approx 3 \times 10^{-3} M$)

Monomer	k_{12} (liter mole ⁻¹ sec ⁻¹)	Monomer	k_{12} (liter mole ⁻¹ sec ⁻¹)
Vinylmesitylene	0.9	<i>p</i> -Vinylbiphenyl	1,660 ^j
β -Methylstyrene	18	<i>p</i> -Fluorostyrene	1,800
α -Methylstyrene	27	1,1-Diphenylethylene	2,500
<i>p</i> -Methoxystyrene	50	1-Vinylnaphthalene	8,000
<i>p</i> - <i>t</i> -Butylstyrene	110	2-Vinylnaphthalene	8,600
2,4-Dimethylstyrene	160	<i>p</i> -Chlorostyrene	23,000
<i>p</i> -Methylstyrene	180	2-Vinylpyridine	>30,000
<i>o</i> -Methylstyrene	320	4-Vinylpyridine	>30,000
Styrene	950		

A similar study involving a Ziegler-Natta type of catalyst was reported by Natta et al. [81], and the results are presented graphically in Fig. 12. The *negative* value of ρ implies that in this system the addition of the monomer to the cation of the complex is the rate-determining step.

Further studies of anionic copolymerization involving ion pairs as well as free ions would be highly desirable.

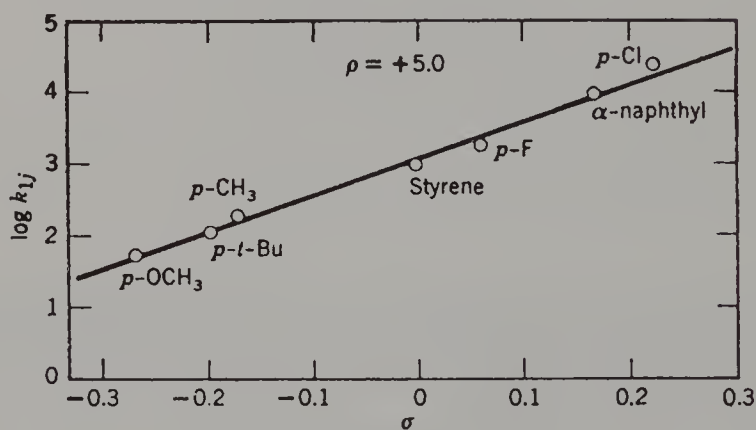


Figure 11. Hammett $\sigma - \rho$ plot for addition of *p*-substituted styrenes to living sodium polystyryl in tetrahydrofuran at 25°C (46). Note the positive ρ .

15. ANIONIC POLYMERIZATION INVOLVING ACTIVATED MONOMER

In the preceding sections we dealt with conventional anionic polymerizations involving negatively charged end groups of living polymers. Anionic

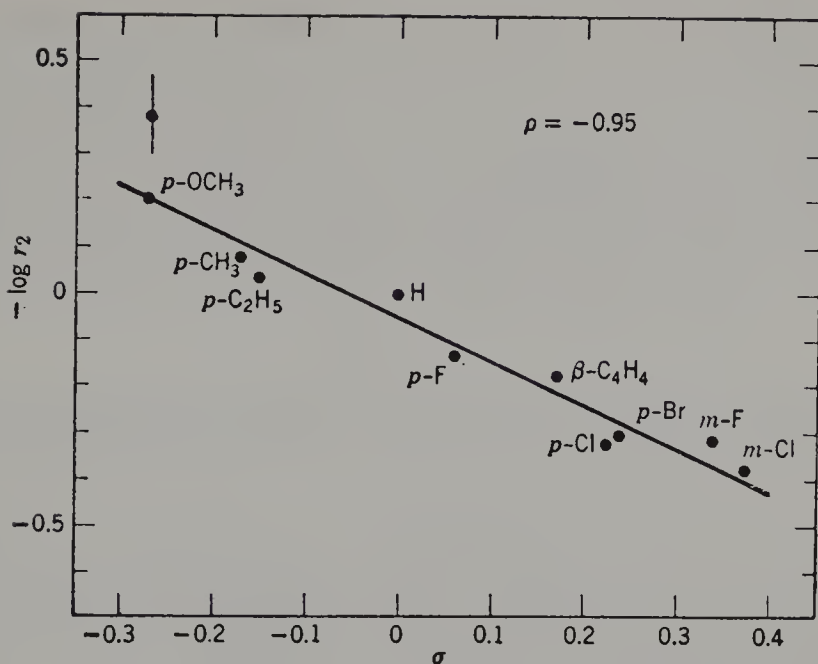
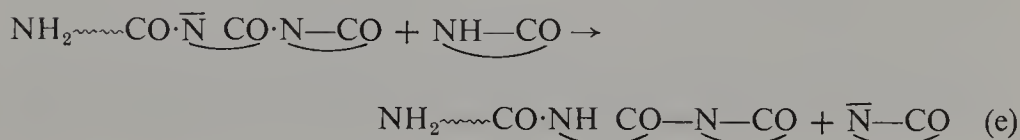
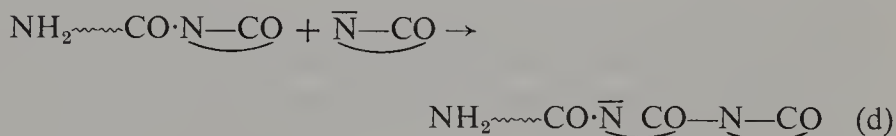
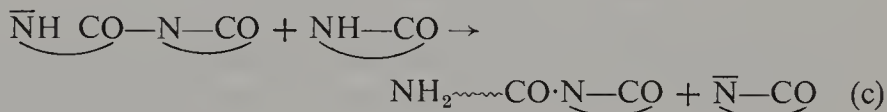
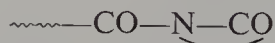


Figure 12. Hammett $\sigma - \rho$ plot for copolymerization of substituted styrenes with styrene in the polymerization initiated by Ziegler-Natta heterogeneous catalyst [49]. Note the negative ρ .

polymerizations of some cyclic monomers such as Leuchs anhydrides, pyrrolidone, and lactams require activation of the *monomer* before its addition to the chain. Polymerization of lactams may serve as an example illustrating the mechanism of such a propagation [82-84]:



Step (a) is equivalent to initiation and produces an "activated monomer" by proton abstraction from the "nonactivated monomer"; the base \bar{B} is therefore a kind of initiator. Reaction (a) may be reversible and the base need not be negatively charged, as long as it is able to abstract a proton from the monomer. Reaction (b) resembles the first step of propagation, although it differs somewhat from the subsequent propagation steps. In the subsequent propagation steps denoted by (d), the activated monomer attacks an end group of a polymer,



in which the N—CO bond is weakened by the adjacent carbonyl group and becomes therefore more reactive than the NH—CO bond of a monomer



Hence reaction (d)—the subsequent propagation—is much *faster* than reaction (b) and this accounts for the formation of high-molecular-weight polymer. Reaction (c), like reaction (e), represents the completion of the propagation cycle in which a new activated monomer is produced.

In the conventional activated monomer polymerization the propagation step (d) is much slower than the proton-transfer steps (c) and (e). The rate of the proton transfer could be determined by the NMR technique (fast exchange) using the exchange reaction



as the model process [85]; its rate is in the range of $10^5 M^{-1} \text{ sec}^{-1}$. Judging from the results of Sekiguchi [86] calculated by Barzakay et al. [87], the propagation constant of the bulk pyrrolidone polymerization is in the range of $10 M^{-1} \text{ sec}^{-1}$; however, the rate of this reaction is probably greatly affected by the nature of the counterion and solvent.

The polymerization is, on the whole, slow due to the sluggishness of reaction (b) leading to the formation of the dimers. Indeed, if the dimers are formed by this process, and a "wrong" monomer addition is avoided in the propagation, the kinetics of the overall polymerization should exhibit an auto-accelerating character because the number of growing chains would increase with time. The reaction is markedly accelerated, and its kinetics simplified, by the addition of "promoters," compounds such as $\text{CH}_3\cdot\text{CO}\ \underline{\text{N---CO}}$ or

$\text{Ph}\cdot\text{CO}\cdot\underline{\text{N---CO}}$ [82]. Such compounds are virtually identical with the dimers

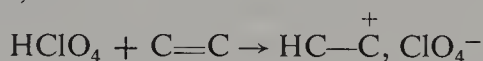
or polymers insofar as all of them involve the activated ring end group, $\text{---CO}\cdot\underline{\text{N---CO}}$, and hence they react rapidly with the activated monomer. In

their presence the number of growing chains is given by the concentration of the promoter. The reaction starts at once and does not exhibit the auto-accelerating effect.

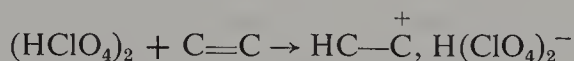
Undoubtedly, the cations, solvents, solvating agents, and so on, should play an important role in this type of polymerization. Some data pertaining to this question were reviewed in Chapter X of ref. 4 which deals extensively with the polymerization of Leuchs anhydride (NCA). More work along this line is needed for a better understanding of these problems.

16. CATIONIC POLYMERIZATION OF VINYL AND VINYLIDENE MONOMERS

In spite of the numerous and intensive studies of cationic polymerization of vinyl and vinylidene monomers initiated by Friedel-Craft's catalysts or by strong protonic acids, this field of investigation is still in a state of confusion. The mechanism of initiation is often in doubt and many details of these reactions require clarification. For example, strong protonic acids presumably initiate propagation by protonating the C=C bond; however, the nature of the protonating agent is unknown. For example, it could be either a monomeric or dimeric acid,



or



Therefore the nature of the counterions is questionable.

The nature of the propagating species needs also clarification. For example, does the reaction involve free ions, ion pairs, or still more complex aggregates as the principal propagating species? The complexity of these systems is increased further by the fact that usually only a small fraction of the initiators is utilized in the polymerization, and a variety of side reactions involving the initiator amplify these difficulties even more. Not surprisingly, very little is known about the absolute propagation constants, a subject reviewed recently by Plesch [92].

The propagation constants of the polymerization of *iso*-butyl-vinyl ether and *N*-vinyl-carbazole in methylene dichloride were determined by Bawn, Ledwith, and their associates [93, 94]. The progress of the reaction was followed calorimetrically, tropylium or trityl salts being used as initiators. The consumption of monomer obeyed first-order kinetics and the pseudo-first-order rate constant was proportional to the concentration of the initiator. These two observations led to the conclusion that the initiation is instantaneous and the termination avoided within the short time of the reaction.

Accepting these premises, we find the propagation constant $k_p = k_{\text{first order}}/C_0$, C_0 being the concentration of the initiating carbonium salt. Since the concentration of the initiator was always extremely low, it is probable that the reported $k_p \approx 10^5 M^{-1} \text{ sec}^{-1}$ refers to the growth of the free cations. However, the equilibrium, such as $P_n^+ + \text{SbCl}_6^- \rightleftharpoons P_n\text{Cl} + \text{SbCl}_5$, may somewhat reduce the actual concentration of the growing cations and lead to a too low value of k_p [146].

A promising technique, permitting the determination of momentary concentration of growing polymers, has been reported recently by Higashimura [95]. Following Saegusa's approach (see p. 433), Higashimura quenched the polymerization with bromothiophene, which supposedly adds instantaneously and quantitatively to the growing carbonium ions and provides a label determining their concentration. It remains to be seen how reliable this approach is (consult ref. 147). Such a quenching method is discussed later.

17. CATIONIC POLYMERIZATION INITIATED BY IONIZING RADIATION

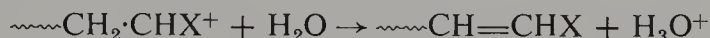
The γ -initiated cationic polymerization of highly purified hydrocarbon monomers provides the only well-documented example of a polymerization exclusively propagated by a free-ion mechanism. The irradiation of monomers by γ -rays produces positive and negative ions which annihilate each other on encounter, and therefore, as has been pointed out by this writer [89], *no stable ion pairs* can be formed in this system. Hence such an ionic polymerization has to be propagated by free ions, each chain growing until it encounters the counterion and since both ions are annihilated in such an encounter the growth is terminated. These reactions usually are performed at low temperatures and therefore the free radicals, whether formed by the annihilation processes or by some other reaction, cannot contribute significantly to the polymerization because the rate of their propagation is too low.

The theoretical treatment of such reactions requires a knowledge of the time required for the recombination of the oppositely charged ions. The primary ionization process induced by γ -rays produces electrons and positive ions in spurs. The ejected electrons are rapidly trapped by impurities such as $\text{O}_2 + e^- \rightarrow \text{O}_2^-$, or by the monomer M forming M^- radical anions. Alternatively, they may form polarons (in polar liquids) or be trapped by "bubbles"—the empty space between molecules of the irradiated liquid. Whatever their fate, the resulting negative species move more slowly than the free electrons in a gas, their diffusion coefficient is about $10^{-5} \text{ cm}^2 \text{ sec}^{-1}$ in common liquids. The diffusion of the positive ions is also relatively slow, the respective diffusion constant being again about $10^{-5} \text{ cm}^2 \text{ sec}^{-1}$. The relative slowness of the diffusion allows some of the positive ions to survive in

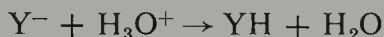
spurs for about 10^{-7} sec, and cationic polymerization may take place during this period.

Although most of the ions and electrons formed in the initial process are rapidly lost by geminate combination, a small fraction may escape and diffuse out of the original spur. It has been shown by Onsager [90] that the probability of escape is given by $\exp - (r_c/r)$ where r_c is the critical distance defined by the condition $e^2/r_c\mathcal{D} = kT$, \mathcal{D} being the dielectric constant of the medium and k the Boltzmann constant. The ions that escaped set up a steady concentration of free ions whose mean lifetime may be greater than 10^{-3} sec at conventional dose rates. These ions may produce polymers of extremely high molecular weight, provided the chain transfer is negligible.

The rate of ionic polymerization should be of one-half order with respect to the dose rate, provided the combination of the oppositely charged ions results in termination. However, earlier studies of this reaction, performed with conventionally purified monomers, showed that propagation is proportional to the *first power* of the dose rate [113]. It is significant that the reported rates became higher as the purification procedures were improved, implying that the termination results from a reaction of the growing free ions with some impurity whose concentration remained constant in the polymerizing system in spite of the continuous polymerization. This observation suggests that the termination proceeds through a process regenerating the terminating impurities. Traces of water seem to be the most plausible impurity responsible for this phenomenon, and indeed the following sequence of reactions could account for the observations:

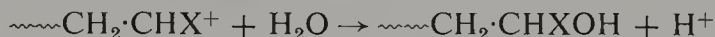


Since the system contains some negative ions that balance the charge of the positive growing polymers, the resulting H_3O^+ ions eventually react with them. Denoting the negative ions by Y^- we may expect the following reaction:



The proposed termination therefore leads to the annihilation of a growing positive ion and of its negative counterion. Thus a trace of water acts as a true catalyst of termination, being regenerated at the end of the cycle.

It is interesting to speculate why the alternative reaction leading to an alcohol does not occur in the termination. Such a reaction would lead to self-purging of the system, that is, to removal of the last traces of water, contrary to the observations. In fact, this reaction does take place when the concentration of water is sufficiently high. The reason is simple. The reaction



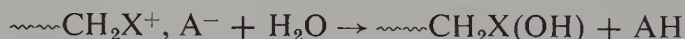
is impossible, because the formation of a bare proton requires too much energy. Therefore the two reagents may form a complex, $\sim\text{CH}_2\text{CHX}^+$,

H_2O , which eventually decomposes into an olefine and H_3O^+ , i.e. a protonic acid that cannot initiate a polymerization of olefines. However, at a sufficiently high concentration of water, a second molecule of H_2O may encounter the complex before it has a chance to decompose, and then the reaction



may take place. Restating these ideas, we conclude that a single molecule of water acts as a Brønsted base, whereas a cluster of such molecules, say $(\text{H}_2\text{O})_2$, behaves as a Brønsted acid.

The dual behavior of water is characteristic for the reactions of the *free-growing cations*. In a reaction involving ion pairs the restriction preventing the donation of the OH^- to the carbonium ion is not compulsive. In such a system the reaction



may be plausible.

Let us return to the kinetics of the γ -ray-initiated cationic polymerization. The action of ion scavengers such as water and ammonia was carefully studied by Williams and his colleagues [114, 115]. Owing to their large bond dissociation energies, H_2O and NH_3 are inert to organic free radicals, but they can act as scavengers of ions. Therefore the sensitivity of the γ -ray-induced polymerizations to traces of moisture is perhaps the best evidence for their ionic character. In the hands of Williams, the use of ammonia as a scavenger of cations allowed the determination of propagation rate constants from the kinetic data pertaining to the polymerization performed in the presence of variable amounts of scavengers [115–117].

The great sensitivity of the γ -initiated cationic polymerization to traces of moisture accounts for some peculiarity of this reaction, which led to much controversy in the past. The γ -initiated polymerization of isobutene—a monomer known to be polymerized only by cationic mechanism—was found to be markedly enhanced by incorporating a fine suspension of inorganic oxides, most notably zinc oxide [118–120], into the irradiated monomer. A similar effect was reported for the polymerization of styrene initiated by γ -rays in the presence of Aerosil [126]. These effects were attributed to the ability of the solid additive to capture the ejected electrons, affording thereby a longer lifetime to the propagating positive ions. This idea appeared to be attractive at that time and was happily accepted by many workers [121–125]. However, since these additives are effective drying agents, their action could have resulted simply from their ability to remove, or at least to reduce, the moisture content in the polymerizing medium.

The crucial experiments disproving the role of solid additives acting supposedly as electron traps or as media “stabilizing” the positive ions [127]

were reported by Kristal'nyi and Medvedev [128]. They described three series of experiments in which the polymerization of isobutene initiated by γ -rays was performed at -78°C . In the first series the pure monomer was polymerized, in the second the monomer was pretreated with the solid additive, ZnO or Al_2O_3 , and thereafter distilled off the solid and irradiated with γ -rays, whereas in the third series the monomer treated with the additives was irradiated in their presence. The rate of polymerization was virtually the same in the second and third series, although it was substantially lower in the experiments of the first series. This proved unequivocally that the additive removes the retarding impurity from the monomer, but beyond that its presence in the irradiated sample is irrelevant for the outcome of the polymerization.

The final proof of the retarding effect of moisture in the γ -ray-initiated cationic polymerization was provided by studies of polymerization of extremely pure and dry monomers. Not only were traces of water removed from the monomer, but any water adsorbed on the walls of the reactor was eliminated by a prolonged bakeout to 500°C in vacuum of all the equipment prior to the admission of the monomer [129]. The polymerization studied under such conditions was shown to be one-half order in the dose rate [131, 132], as expected for a polymerization terminated by the combination of the oppositely charged ions, and its rate was found to be higher than any rate observed in the less carefully dried systems. These results are vividly demonstrated by Fig. 13.

The absolute propagation rate constant, k_+ , of the free carbonium ions was determined from the kinetic studies involving retarding substances or, alternatively, from the combined conductivity and kinetic studies [129]. Thus the k_+ of polystyrene propagating at ambient temperature was determined to be $2.5 \times 10^8 \text{ M}^{-1} \text{ sec}^{-1}$. Similar data pertaining to other monomers are compiled in Table 8. They represent at least the lower limit of the true k_+ values; their magnitude implies, however, that they cannot be far from the ultimate values of the corresponding propagation constants of the free cations.

Do the negative ions contribute to the polymerization? This is an open question. If k_- in hydrocarbon media is the same as that found for the free ion polymerization in ethereal solvents [15], then the contribution of negative ions to the γ -initiated polymerization of styrene would amount to only 3%.

18. CATIONIC POLYMERIZATION OF CYCLIC ETHERS AND SOME RELATED MONOMERS

In contrast to the cationic polymerization of vinyl and vinylidene monomers, our knowledge of polymerization of cyclic ethers is well advanced due to

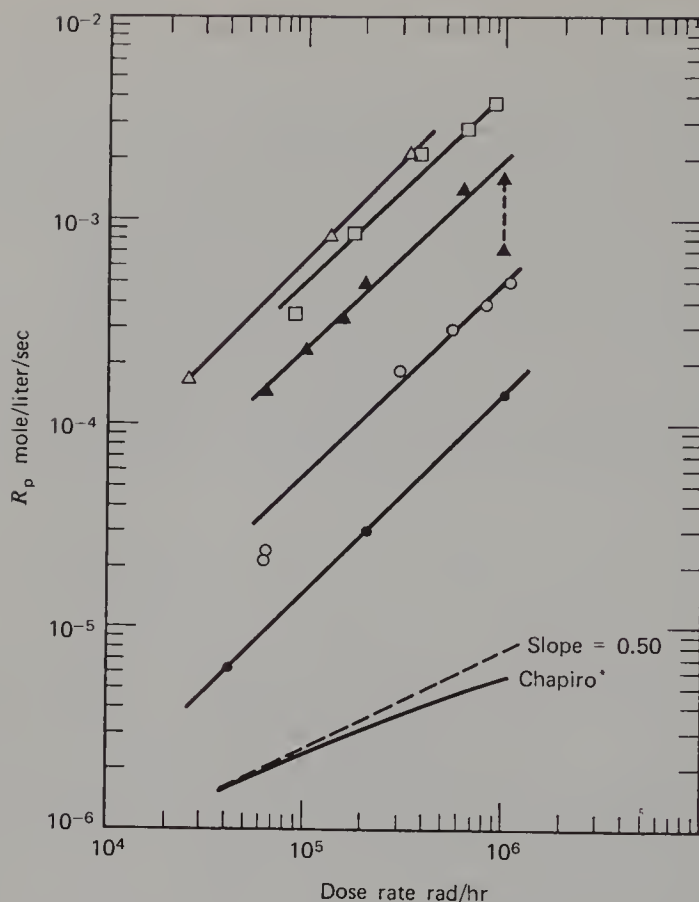


Figure 13. The rate of styrene polymerization induced by γ -rays as a function of dose rate. The lines refer to differently purified styrene—the more purified the monomer the higher the rate, that is, the higher the line.

Table 8 Propagation Constants k_+ of Free Cations (k_+ is at least the lower limit of the “true” k_+)

Monomer	Solvent	Temperature	k_+ ($M^{-1} \text{ sec}^{-1}$)	E_+ (kcal/mole)	Ref.
		(°C)			
Cyclopentadiene	Bulk	−78	6×10^8	<2	117
α -Methylstyrene	Bulk	0	3×10^6		130
Styrene	Bulk	15	3.5×10^8	~ 0	130
Vinyl-isobutyl ether	Bulk	30	3×10^5		132

the pioneering work of Saegusa, who developed the phenoxyl end-capping technique [96]. This technique permits one to determine the momentary concentration of growing oxonium ions by quenching the reaction with sodium phenolate, isolating the polymers terminated by —OPh groups, and determining spectrophotometrically the number of those end groups. The reliability of the method is based on the following facts:

1. The conversion of the propagating chain ends to phenoxyl groups is quantitative and virtually instantaneous.
2. No side reaction produces phenoxy ethers; this compound is formed exclusively with the growing oxonium ions.
3. The molar extinction coefficient of $\text{RCH}_2\text{CH}_2\text{OPh}$ group was determined and its value is independent of the nature of R.

Model compounds such as Et_3O^+ , BF_4^- were used to establish the validity of the first point. The reaction

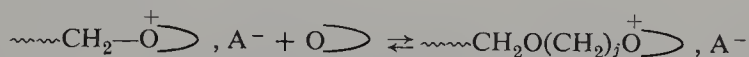


was shown to be quantitative and completed in less than 20 sec. Since the growing oxonium ion $\sim\text{CH}_2\text{O}^+$, X^- is strained, its reactivity should

be even greater than that of Et_3O^+ . The polymerizations studied by this technique are sufficiently slow and hence the capping is “instantaneous” in that time scale.

Studies of various reference reactions [96] confirmed the absence of any side reactions forming ROPh . Finally, examination of the spectra of model compounds, PhOC_2H_5 , $\text{PhO}(\text{CH}_2)_4\text{OCH}_3$, and of the capped polymers ascertained the constancy of the extinction coefficient, $\epsilon = 1.93 \times 10^3 \text{ M}^{-1} \text{ cm}^{-1}$ at $\lambda_{\text{max}} = 272 \text{ nm}$.

Propagation of polymerization of cyclic ethers is an S_N2 reaction represented by the general equation






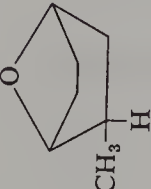
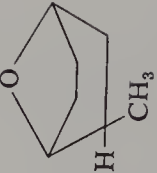


in which the oxygen center of the cyclic ether acts as a nucleophile attacking the $\alpha\text{-CH}_2$ group of the oxonium ion. The propagation may be reversible, in which case

$$-\frac{d[\text{M}]}{dt} = k_p[\text{P}^+]\{[\text{M}] - [\text{M}]_e\}$$

where $[\text{P}^+]$ denotes the momentary concentration of growing species and

Table 9 Comparison of Reactivities of Monocyclic and Bicyclic Ethers

Monomer:							
Reference:	98	98	98	100	101	100	102
Catalyst	BF_3	BF_3	BF_3	$\text{BF}_3\text{-ECH}$	$\text{BF}_3\text{-ECH}$	$\text{BF}_3\text{-ECH}$	$\text{BF}_3\text{-ECH}$
$10^3 k_p$ (1/mole·sec)							
-20°C	19	110	~(400)				
-10°C	57			1.7	0.0033	9.4	27
0°C	140			4.1	0.015		
ΔF_p^\ddagger (kcal/mole)	17	15.7		19.3	23		
ΔE_p^\ddagger (kcal/mole)	14.2	16.1		12	18	15	14
$10^{-7} A_p$ (1/mole·sec)	5300	830,000		1.1	190	4100	700
ΔF^e (kcal/mole)	21.5	17.7	14.0	2	4.9		

$[M]_e$ the equilibrium concentration of the monomer. Hence

$$\ln \frac{[M]_0 - [M]_e}{[M]_t - [M]_e} = k_p \int_0^t [P^+] dt$$

The integral is found by determining $[P^+]$ as a function of time. For all the systems investigated so far the plots of the left-hand side of the above equation versus the integral were linear, their slopes yielding the propagation constants k_p .

The results obtained by Saegusa's group are collected in Table 9. Polymerizations of oxetane [97] and of its methyl and dimethyl derivatives [98] were performed in methylene dichloride or in methyl cyclohexane. The reaction is irreversible, $[M]_e = 0$, as demonstrated by Rose [99]. Propagation is faster in methyl cyclohexane (a nonpolar solvent) than in CH_2Cl_2 (a polar solvent), indicating that the positive charge is more delocalized in the transition state than in the initial. Therefore the degree of solvation of the former state is less than that of the latter. This is an expected result for an S_N2 reaction. The rate of propagation increases on methylation of the monomer, as shown by the data collected in Table 9. The increase in the reactivity arises not from a decrease in the activation energy but from a substantial increase in the entropy of activation; in fact, the variation of the activation energy opposes the observed trend.

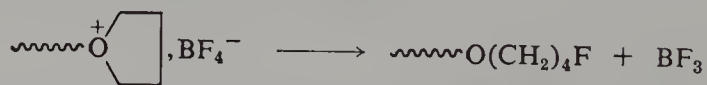
Polymerization of tetrahydrofuran is reversible, $[M]_e > 0$, a well-known fact (see, e.g., [104]). Polymerization carried out at 0°C and initiated in bulk THF by $\text{BF}_3 \cdot \text{THF}$ -ethylene chlorhydrine or by AlEt_3 , $\text{H}_2\text{O}-\text{CH}_2\text{OHCH}_2\text{Cl}$ showed a slow increase in $[P^+]$ which approached a plateau value after a few hours [96b, 105]; that is, the initiation is slow but termination is avoided. Interestingly, only a small fraction of the initiator is utilized, 19 and 1%, respectively, indicating that most of the initiator is lost in some side reactions. On the other hand, a rapid initiation followed by decay of the growing polymers is observed when the polymerization, carried again at 0°C , is initiated by $\text{SnCl}_4 \cdot \text{CH}_2\text{OHCH}_2\text{Cl}$ or $\text{EtAlCl}_2 \cdot \text{CH}_2\text{OHCH}_2\text{Cl}$. Under such conditions the reaction does not proceed to completion and only a low-molecular-weight polymer is formed.

Studies of THF polymerization initiated by Et_3O^+ , BF_4^- or Et_3O^+ , AlCl_4^- revealed the effect of counterions on the behavior of the reaction. The capping technique had to be modified for these systems since EtOPh is formed from the unutilized initiator. A method was developed by which the amount of EtOPh formed could be determined quantitatively. It was possible therefore to determine simultaneously the concentrations of the growing polymers and of the residual initiator as functions of time. The initiation by Et_3O^+ , BF_4^- is fast and it is accompanied by a slow termination; that is, $[P^+]$ rapidly reaches a maximum and then slowly decreases. In contrast, Et_3O^+ , AlCl_4^-

initiator produces rapidly decaying chains; $[P^+]$ is low and eventually it decreases slowly. In agreement with this finding only a very low-molecular-weight polymer is formed in this system.

In spite of these variations in the overall behavior of the polymerization, the propagation constant is only slightly affected by changes of the counterions or solvent. The k_p values determined at 0°C vary from 4×10^{-3} to $10 \times 10^{-3} \text{ M}^{-1} \text{ sec}^{-1}$. Apparently, only the initiation and termination are affected substantially by the nature of initiator. All these observations indicate that the propagation involves ion pairs, although some contribution of the free ions cannot be excluded. In fact, a Sangster and Worsfold [106] study of THF polymerization initiated by Et_3O^+ , BF_4^- in CH_2Cl_2 is devoted to the question of how much the free ions and the ion pairs contribute to the propagation. They concluded that $k_{\pm} = 1.4 \times 10^{-3} \text{ M}^{-1} \text{ sec}^{-1}$ and $k_- = 10 \times 10^{-3} \text{ M}^{-1} \text{ sec}^{-1}$ at about 0°C , and therefore the contribution of free ions to the propagation is marginal in view of the low dissociation constant of $5.4 \times 10^{-6} \text{ M}^{-1}$.

Investigations of Saegusa et al. also provide information about the rates of initiation and termination steps in tetrahydrofuran polymerization. Assuming unimolecular termination, for example,

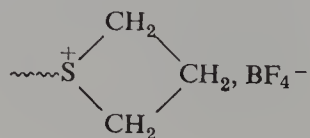


they conclude that $k_t \sim 10^{-5} \text{ sec}^{-1}$ for the BF_4^- pair and $\sim 10^{-2} \text{ sec}^{-1}$ for the AlCl_4^- pairs, indicating a much greater stability of the former than of the latter ion pairs.

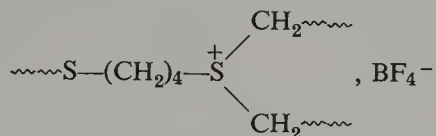
Polymerization of oxepane [101, 107], like polymerization of THF, is reversible. However, $[M]_e$ is much lower in the former reaction than in the latter. This implies that the strain is greater in the oxepane ring than in tetrahydrofuran (see Table 9); nevertheless, the propagation constant is higher for THF than for oxepane polymerization (see again Table 9).

The lack of space prevents us from discussing the polymerization of bicyclic ethers. The pertinent data characterizing their polymerization are included in Table 9 and the interested reader is referred to the original literature [100, 102] for further information on this subject.

Let us complete this section by reviewing briefly two additional systems. Polymerization of thietan was investigated by Goethals [108]. The reaction was initiated by Et_3O^+ , BF_4^- , but it stops short before the monomer is exhausted. The reactive growing sulphonium ion



interacts with a sulfur atom in a polymer chain, forming a nonreactive (not strained) sulfonium ion

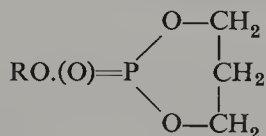


Combined kinetic and conductance study demonstrated that the initiation is virtually instantaneous and quantitative. The reaction therefore involves the propagation and termination steps only. This mechanism leads to k_p determined from the equation

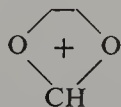
$$\frac{(\ln R)[M]}{C_0} = \ln k_p - k_t \int_0^t ([M]_0 - [M]) dt$$

Here C_0 denotes the initial concentration of the added oxonium initiator, k_p and k_t the rate constants of the propagation and termination, respectively, and $R = -d[M]/dt$.

A similar approach was adopted by Penczek [109] in his studies of *bis*-chloromethyl oxetane polymerization initiated by $(\text{iso-Bu})_3\text{Al}$, H_2O complex in chlorobenzene. This approach was used again in his studies of cationic polymerization of the six-membered cyclic esters of phosphoric acid



initiated in methylene dichloride, or in bulk, by salts of the

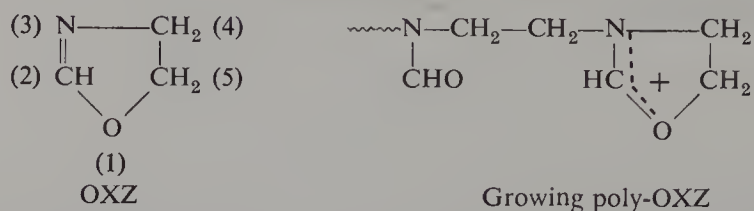


cation with PF_6^- , AsF_6^- , and SbF_6^- as the counterions [112]. Such initiators, in contrast to Ph_3C^+ , SbCl_6^- react quantitatively, yielding the propagating tetraalkoxy phosphonium cations. The reaction is reversible and an interaction with the $\text{P}=\text{O}$ groups of polymer chains results in termination.

19. ION PAIRS VERSUS COVALENT BOND

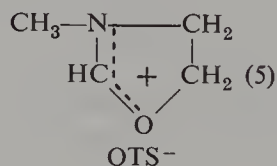
Conversion of a covalent bond into a reactive ion pair presents an interesting and intriguing problem. Studies of cationic polymerization of 2-oxazoline

(OXZ) provide an example illustrating such a possibility [111]:

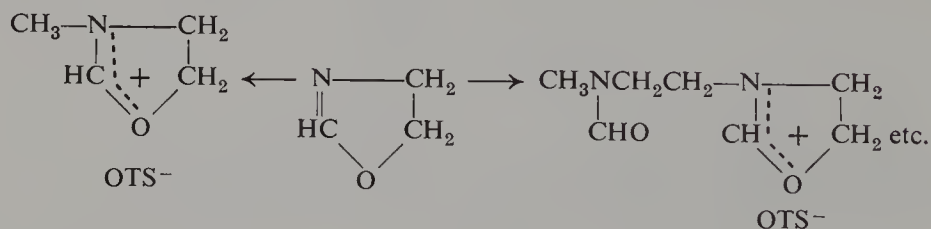


This monomer has been polymerized in aprotic solvents with Lewis acids such as BF_3OEt_2 or SbF_5 as initiators [110]. The formyl groups then may be hydrolyzed easily by alkali and thus a linear and crystalline poly-ethylene imide may be produced.

The mechanism of this polymerization initiated by methyl tosylate resembles the polymerization of cyclic ethers. Transfer of Me^+ from the tosylate to the monomer forms the cyclic cation:

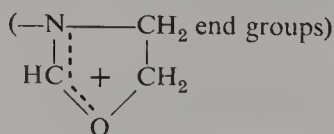


Thereafter the nucleophilic attack of the N center of a monomer on carbon 5 of the cation leads to the propagation



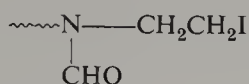
in which the C(5)—O bond is opened and the positive charge transferred to the newly added OXZ ring.

Kinetic studies of this reaction taking place in CD_3N were accomplished by the NMR technique. The NMR spectrum of the polymerizing mixture permits simultaneous determination of the momentary concentration of the remaining initiator (MeOTs), monomer (OXZ), and growing polymer



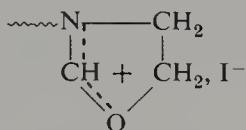
In fact, the NMR spectrum proves that the OXZ cations are the end groups of growing polymers. However, when the reaction was initiated by MeI

the growing end of the polymer was shown to have the structure



involving the covalent C—I bond.

The experimental findings demonstrated that the reaction initiated by the tosylate is propagated by the rate-determining S_N2 attack of the monomer on the cyclic cation end group. The pertinent kinetic data are collected in Table 10. In contrast, the reaction initiated by methyl iodide seems to proceed through a transition state involving $\text{CH}_2^+ \cdots \text{I}^-$ polarized bond, like Menschutkin reaction, the polarization of the CH_2-I bond being retained in the initially formed ion pair which collapses into the final covalently bonded product. In agreement with this interpretation, the propagation of the cyclic cation-tosylate ion pair requires a high activation energy and results in a high A factor, since in the transition state of this S_N2 reaction the charge is delocalized and therefore the degree of solvation is reduced (see Table 10). Propagation of the methyl iodide-initiated polymerization requires in contrast low activation energy and low A factor because the conversion of the covalent CH_2-I into $\text{CH}_2^+ \cdots \text{I}^-$ ion pair greatly increases the degree of solvation of the transition state reducing, however, the activation energy by the gain in solvation energy. Tosylate is a weak nucleophile, hence the ion pair does not collapse, whereas I^- is a strong nucleophile and therefore the intermediate ion pair



rapidly collapses into

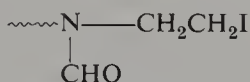


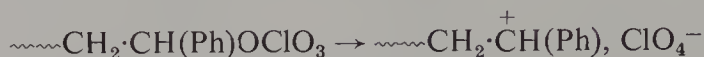
Table 10 Activation Parameters of OXZ Polymerization in CD_3CN^a

Initiator	MeOTs	MeI	$\text{Et}_3\text{N} + \text{EtI}$ in PhNO_2 (40°)
k_p (40°)	19×10^{-4}	0.18×10^{-4}	4.8×10^{-4}
ΔE^\ddagger	25	13.5	11.6
A	7.5×10^{14}	5.0×10^4	7.9×10^4

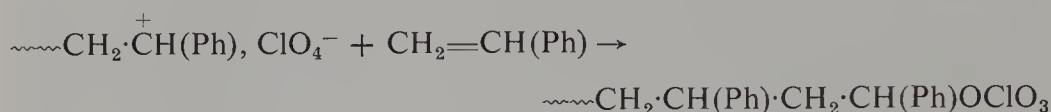
^a Polymerization conditions; $[\text{OXZ}]_0 = 3.33 \text{ mol/l.}$, initiator = 0.667 mol/l.

Ion-pairs and the isomeric, covalently bonded esters participate also in the cationic polymerization of cyclic ethers [148, 149]. In this writer's opinion, these ideas may apply after some modification to the cationic polymerization of styrene initiated by perchloric acid. A concise review of the characteristic

features of this reaction was presented recently by Plesch [92]. Apparently the proposed pseudo-cationic polymerization of the ester proceeds through the rate-determining step



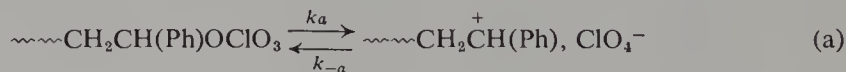
yielding a transient ion pair which in the presence of monomer collapses rapidly, simultaneously with a monomer addition



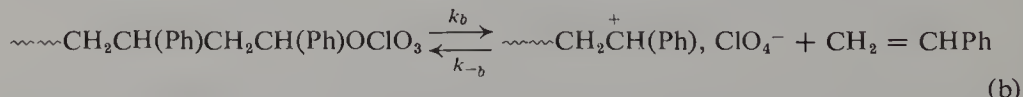
It is implied that, in accord with the principle of microscopic reversibility, the stretching of the $\text{CH}(\text{Ph})\text{—OCIO}_3$ bond may lead to depropagation with the formation of the transient ion pair. However, this system is *not in equilibrium in respect to the depropagation* when the concentration of the monomer exceeds its equilibrium concentration of about $10^{-6} M$ at ambient temperature.* Hence the concentration of the free $\sim\text{CH}_2\cdot\overset{+}{\text{CH}}(\text{Ph})$ ions is also lower during the polymerization than it would be after completion of this reaction. This explains the sudden increase of the conductance observed at the end of polymerization and the onset of the side reactions producing the colored phenyl-indenyl cations that contribute even more to the conductance than the polystyryl salt. It may be advisable to investigate the perchloric acid-initiated polymerization of α -methyl styrene, since the equilibrium concentration of this monomer is substantially greater (about $2 M$ at 25°C) than that of styrene.

It is hoped that this review illuminates and clarifies some problems associated with the nature and the behavior of ionic species in ionic polymerization. He is grateful to the National Science Foundation for their continuous financial support of the work of his group.

* Two reactions are assumed to proceed simultaneously



and



However, the equilibrium concentration of ion pairs is maintained only when the monomer concentration is equal to its equilibrium concentration in respect to polymer. At higher monomer concentration the concentration of ion pairs falls below its equilibrium concentration as determined by (a). The deviation is large when $k_{-b}[\text{CH}_2 = \text{CHPh}] \gg k_{-a}$. The decrease in the concentration of ion pairs decreases the concentration of free ions.

REFERENCES

1. M. Szwarc, *Science*, **170**, 23 (1970).
2. (a) G. Allen, G. Gee, and C. Stretch, *J. Polymer Sci.*, **48**, 189 (1960); (b) C. Stretch and G. Allen, *Polymer*, **2**, 151 (1961).
3. D. N. Bhattacharyya, J. Smid, and M. Szwarc, *J. Phys. Chem.*, **69**, 624 (1965).
4. M. Szwarc, in *Carbanions, Living Polymers and Electron-Transfer Processes*, Wiley New York, 1968, Chap. IV.
5. F. S. Dainton, G. C. East, G. A. Harpell, N. R. Hurworth, K. J. Ivin, R. T. LaFlair, R. H. Pallen, and K. M. Hui, *Makromol. Chem.*, **89**, 257 (1965); F. S. Dainton, K. M. Hui, and K. J. Ivin; *Europ. Polymer J.*, **5**, 382 (1969).
6. L. Lee, R. Adams, J. Jagur-Grodzinski, and M. Szwarc, *J. Am. Chem. Soc.*, **93**, 4149 (1971).
7. G. Spach, M. Levy, and M. Szwarc, *J. Chem. Soc. (London)*, **1962**, 355.
8. G. V. Schulz, L. L. Böhm, M. Chmelir, G. Löhr, and B. J. Schmitt, *IUPAC International Symposium on Macromolecule Chemistry*, Budapest, 1969, p. 233; *Advances Pol. Sci.* **9**, 1 (1972).
9. W. C. E. Higginson and N. S. Wooding, *J. Chem. Soc. (London)*, **1952**, 760; see also M. G. Evans, W. C. E. Higginson, and N. S. Wooding, *Rec. Trav. Chim.*, **68**, 1069 (1949).
10. H. Sobue and Y. Tabata, *J. Polymer Sci.*, **43**, 459 (1960).
11. H. Yamaoka, F. Williams, and K. Hayashi, *Trans. Faraday Soc.*, **63**, 376 (1967).
12. M. Szwarc, Ed., *Ions and Ion Pairs in Organic Reactions*, Vol. One, Interscience, New York, 1972.
13. K. Hofelmann, J. Jagur-Grodzinski, and M. Szwarc; *J. Am. Chem. Soc.*, **91**, 4645 (1969).
14. M. Szwarc, *Acc. Chem. Res.* **2**, 87 (1969).
15. D. N. Bhattacharyya, C. L. Lee, J. Smid, and M. Szwarc, *Polymer*, **5**, 54 (1964); *J. Phys. Chem.*, **69**, 612 (1965).
16. H. Hostalka and G. V. Schulz, *Z. Phys. Chem. (Frankfurt)*, **45**, 286 (1965).
17. T. Shimomura, K. J. Tölle, J. Smid, and M. Szwarc, *J. Am. Chem. Soc.*, **89**, 976 (1967)
- 17a. C. Geacintov, J. Smid, and M. Szwarc, *J. Am. Chem. Soc.*, **84**, 2508 (1962).
18. D. J. Worsfold and S. Bywater, *J. Chem. Soc. (London)*, **1960**, 5234.
19. K. J. Tölle, J. Smid, and M. Szwarc, *J. Polymer Sci. B*, **3**, 1037 (1965).
20. H. Hostalka and G. V. Schulz, *J. Polymer Sci. B*, **3**, 1043 (1965).
21. H. Hirohara and N. Ise, *J. Polymer Sci. Part D*, **6**, 295 (1972).
22. T. Shimomura, J. Smid, and M. Szwarc, *J. Am. Chem. Soc.*, **89**, 5743 (1967).
23. L. Böhm, W. K. R. Barnikol, and G. V. Schulz, *Makromol. Chem.*, **110**, 222 (1967).
24. F. S. Dainton, G. A. Harpell, and K. J. Ivin, *Eur. Polymer J.*, **5**, 395 (1969).
25. J. E. L. Roovers and S. Bywater, *Trans. Faraday Soc.*, **62**, 701 (1966).
26. M. van Beylen, M. Fisher, J. Smid, and M. Szwarc, *Macromolec.*, **2**, 575 (1969).
27. W. K. R. Barnikol and G. V. Schulz, *Makromolek. Chem.*, **68**, 211 (1963); **86**, 298 (1965).

442 Ions and Ion Pairs in Ionic Polymerization

28. D. J. Worsfold and S. Bywater, *Can. J. Chem.*, **36**, 1141 (1958).
29. C. Carvajal, K. J. Tölle, J. Smid, and M. Szwarc, *J. Am. Chem. Soc.*, **87**, 5548 (1965).
30. M. Shinohara, J. Smid, and M. Szwarc, *J. Am. Chem. Soc.*, **90**, 2175 (1968).
31. M. Shinohara, J. Smid, and M. Szwarc, *Chem. Comm. (London)*, **1969**, 1232.
32. B. Levesse, E. Franta, and P. Rempp, *Makromolek. Chem.*, **142**, 111 (1971).
33. M. Fisher and M. Szwarc, *Macromolec.*, **3**, 23 (1970).
- 33a. M. Fisher, PhD Thesis, Syracuse, N.Y. (1972).
34. A. Rigo, M. Szwarc, and G. Sackmann, *Macromolec.*, **4**, 622 (1971).
35. M. Tardi and P. Sigwalt, *Europ. Pol. J.*, **8**, 151 (1972).
36. M. Tardi, D. Rougé, and P. Sigwalt, *Eur. Polymer J.*, **3**, 85 (1967).
37. G. Natta, G. Mazzanti, P. Longi, and G. Dall'Asta, *J. Polymer Sci.*, **51**, 487 (1961).
38. F. Bahsteter, J. Smid, and M. Szwarc, *J. Am. Chem. Soc.*, **85**, 3903 (1963).
39. S. N. Khanna, M. Levy, and M. Szwarc, *Trans. Faraday Soc.*, **58**, 747 (1962).
40. A. Nishioka, H. Watanabe, K. Abe, and Y. Sono, *J. Polymer Sci.*, **48**, 241 (1960).
41. P. E. M. Allen and A. G. Moody, *Makromolek. Chem.*, **81**, 234 (1965); **83**, 220 (1965).
42. (a) S. Bywater, P. E. Black, and D. M. Wiles, *Can. J. Chem.*, **44**, 695 (1966); (b) D. M. Wiles and S. Bywater, *J. Polymer Sci. B*, **2**, 1175 (1964).
43. B. D. Coleman and T. G. Fox, *J. Chem. Phys.*, **38**, 1065 (1963); *J. Polymer Sci. A*, **1**, 3183 (1963).
44. (a) G. Natta, M. Farina, and M. Peraldo, *Atti Accad. Nazl. Lincei*, **25**, 424 (1958); (b) M. Peraldo and M. Farina, *Chim. Ind. (Milan)*, **42**, 1349 (1960).
45. T. Miyazawa and Y. Ideguchi, *J. Polymer Sci. B*, **1**, 389 (1963).
46. G. Natta, M. Farina, and M. Peraldo, *Chim. Ind. (Milan)*, **42**, 255 (1960).
47. (a) T. Yoshino, J. Komiyama, and M. Shinomiya, *J. Am. Chem. Soc.*, **86**, 4482 (1964); (b) T. Yoshino, M. Shinomiya, and J. Komiyama, *J. Am. Chem. Soc.*, **87**, 387 (1965).
48. C. Schuerch, W. Fowells, A. Yamada, F. A. Bovey, F. P. Hood, and E. W. Anderson, *J. Am. Chem. Soc.*, **86**, 4481 (1964).
49. W. Fowells, C. Schuerch, F. A. Bovey, and F. P. Hood, *J. Am. Chem. Soc.*, **89**, 1396 (1967).
50. (a) B. D. Coleman and T. G. Fox, *J. Chem. Phys.*, **38**, 1065 (1963); (b) B. D. Coleman, T. G. Fox, and M. Reinmöller, *J. Polymer Sci. B*, **4**, 1029 (1966); see also (c) B. D. Coleman and T. G. Fox, *J. Am. Chem. Soc.*, **85**, 1241 (1963); *J. Polymer Sci. C*, **4**, 345 (1963).
51. R. V. Figini, *Makromol. Chem.*, **71**, 193 (1964).
52. M. Szwarc and J. J. Hermans, *J. Polymer Sci. B*, **2**, 815 (1964).
53. G. Löhr and G. V. Schulz, *Makromolek. Chem.*, **77**, 240 (1964).
54. R. V. Figini, H. Hostalka, K. Harm, G. Löhr, and H. V. Schulz, *Z. Phys. Chem. (Frankfurt)*, **45**, 269 (1965).
55. R. M. Fuoss and C. A. Kraus, *J. Am. Chem. Soc.*, **55**, 2387 (1933).
56. D. N. Bhattacharyya, J. Smid, and M. Szwarc, *J. Am. Chem. Soc.*, **86**, 5024 (1964).
57. N. Ise, H. Hirohara, T. Makino, K. Takaya, and M. Nakayama, *J. Phys. Chem.*, **74**, 606 (1970).
58. D. J. Worsfold and S. Bywater, *Can. J. Chem.*, **38**, 1891 (1960).
59. S. Bywater, *Adv. Polymer Sci.*, **4**, 66 (1965).

60. H. L. Hsieh and W. H. Glaze, *Rubber Chem. Tech.*, **43**, 22 (1970).
61. M. Morton, E. E. Bostich, and R. Livigni, *Rubber and Plastic Age*, **42**, 397 (1961).
62. A. F. Johnson and D. J. Worsfold, *J. Polymer Sci. A*, **3**, 449 (1965).
63. D. J. Worsfold and S. Bywater, *Can. J. Chem.*, **42**, 2884 (1964).
64. H. Sinn, C. Lundbard, and O. T. Onsager, *Macromolec. Chem.*, **79**, 222 (1964).
65. R. Waack and P. West, *J. Organomet. Chem.*, **5**, 188 (1966).
66. D. J. Worsfold and S. Bywater, *Can. J. Chem.*, **40**, 1564 (1962).
67. M. Shima, J. Smid, and M. Szwarc, *J. Polymer Sci., B*, **2** (Polymer Lett.), 735 (1964).
68. G. Löhr and S. Bywater, *Can. J. Chem.*, **48**, 2031 (1970).
69. A. Parry, J. E. L. Roovers, and S. Bywater, *Macromolec.*, **3**, 355 (1970).
70. D. N. Bhattacharyya, C. L. Lee, J. Smid, and M. Szwarc, *J. Am. Chem. Soc.*, **85**, 533 (1963).
71. C. L. Lee, J. Smid, and M. Szwarc, *Trans. Faraday Soc.*, **59**, 1192 (1963).
72. C. L. Lee, J. Smid, and M. Szwarc, *J. Am. Chem. Soc.*, **85**, 912 (1963).
73. (a) G. V. Rakova and A. A. Korotkov, *Dokl. Acad. Nauk SSSR*, **119**, 892 (1958);
(b) A. A. Korotkov and N. N. Chesyokova, *Vysokomolek. Soedin*, **2**, 365 (1960);
(c) A. A. Korthov and G. V. Rakova, *Vysokomolek. Soedin*, **3**, 1482 (1961).
74. Y. L. Spirin, D. K. Polyakov, A. R. Gantmakher, and S. S. Medvedev, *J. Polymer Sci. A*, **2**, 4231 (1961).
75. C. E. H. Bawn, *Rubber Plastic Age*, **42**, 267 (1961).
76. D. J. Worsfold, *J. Polymer Sci. A1*, **5**, 2783 (1967).
77. I. Kuntz, *J. Polymer Sci.*, **54**, 569 (1961).
78. K. F. O'Driscoll and I. Kuntz, *J. Polymer Sci.*, **61**, 19 (1962).
79. Z. Laita and M. Szwarc, *Makromolec.*, **2**, 412 (1969).
80. M. Shima, D. N. Bhattacharyya, J. Smid, and M. Szwarc, *J. Am. Chem. Soc.*, **85**, 1306 (1963).
81. G. Natta, F. Danusso, and D. Sianesi, *Makromolek. Chem.*, **30**, 238 (1959).
82. O. Wichterle, J. Sebenda, and J. Kralicek, *Fortschr. Hochpolymer Forsch.*, **2**, 578 (1961).
83. G. Champetier and H. Sekiguchi, *J. Polymer Sci.*, **48**, 309 (1960).
84. R. Graf, G. Lohaus, K. Börner, E. Schmidt, and H. Bestian, *Angew. Chem. Int. Ed.*, **1**, 481 (1962).
85. S. Barzakay, M. Levy, and D. Vofsi, *Polymer Lett., B*, **3**, 601 (1968).
86. H. Sekiguchi, *Bull. Soc. Chim. (France)*, **1960**, 1831; *J. Polymer Sci. A*, **1**, 1627 (1963).
87. S. Barzakay, M. Levy, and D. Vofsi, *J. Polymer Sci. A1*, **4**, 2211 (1966).
88. J. E. L. Roovers and S. Bywater, *Can. J. Chem.*, **46**, 2711 (1968).
89. M. Szwarc, *Makromolek. Chem.*, **35A**, 123 (1960).
90. L. Onsager, *Phys. Rev.*, **54**, 554 (1938).
91. J. M. Ginn and K. J. Ivin, *Makromolek. Chem.*, **139**, 57 (1970).
92. P. H. Plesch, *Adv. Polymer Sci.*, **8**, 137 (1971).
93. (a) C. E. H. Bawn, C. Fitzsimmons, and A. Ledwith, *Proc. Chem. Soc.*, **1964**, 391;
(b) C. E. H. Bawn, C. Fitzsimmons, A. Ledwith, J. Penfold, D. C. Sherrington, and J. A. Weightman, *Polymer*, **12**, 119 (1971).

444 Ions and Ion Pairs in Ionic Polymerization

94. A. Ledwith, *Adv. Chem. Sci.*, **91**, 2458 (1969).
95. T. Higashimura, to be published.
96. (a) T. Saegusa and S. Matsumoto, *J. Polymer Sci. A1*, **6**, 1559 (1968); (b) T. Saegusa, S. Matsumoto, and Y. Hashimoto, *Polymer J.*, **1**, 31 (1970).
97. T. Saegusa, Y. Hashimoto, and S. Matsumoto, *Macromolec.*, **4**, 1 (1971).
98. T. Saegusa, H. Fujii, S. Kobayashi, H. Ando, and R. Kawase, *Macromolec.*, **6**, 26 (1973).
99. J. B. Rose, *J. Chem. Soc.*, **1956**, 542, 546.
100. T. Saegusa, S. Matsumoto, M. Motoi, and H. Fujii, *Macromolec.*, **5**, 233 (1972).
101. T. Saegusa, T. Shiota, S. Matsumoto, and H. Fujii, *Macromolec.*, **5**, 34 (1972).
102. T. Saegusa, S. Matsumoto, M. Motoi, and H. Fujii, *Macromolec.*, **5**, 236 (1972).
103. F. S. Dainton, T. R. E. Devlin, and P. A. Small, *Trans. Faraday Soc.*, **51**, 1710 (1955).
104. P. Dreyfuss and M. P. Dreyfuss, in *Ring-Opening Polymerization*, K. C. Frish and S. L. Reegen (Eds.), Marcel Decker, New York, 1969, Chap. 2.
105. T. Saegusa and S. Matsumoto, *Macromolec.*, **1**, 422 (1968).
106. J. M. Sangster and D. J. Worsfold, *Macromolec.*, **5**, 229 (1972).
107. T. Saegusa, T. Shiota, S. Matsumoto, and H. Fujii, *Polymer J.*, **1**, 40 (1972).
108. E. J. Goethals and W. Drijvers, *Makromolek. Chem.*, **136**, 73 (1970).
109. S. Penczek and S. Kubisa, *Makromolek. Chem.*, **130**, 186 (1969).
110. T. Saegusa, H. Ikeda, and H. Fujii, *Polymer J.*, **3**, 35 (1972).
111. T. Saegusa, H. Ikeda, and H. Fujii, *Macromolec.*, **6**, 315 (1973).
112. S. Penczek, J. Fejgin, P. Kubisa, K. Matyjaszewski, and M. Tomaszewicz, *Makromolek. Chem.*, **172**, 243 (1973).
113. (a) W. H. T. Davison, S. H. Pinner, and R. Worrall, *Chem. In. (London)*, **1957**, 1274; (b) R. Worrall and S. H. Pinner, *J. Polymer Sci.*, **34**, 229 (1959); (c) W. H. T. Davison, S. H. Pinner, and R. Worrall, *Proc. Roy. Soc. (London) A*, **252**, 187 (1959); (d) E. Collinson, F. S. Dainton, and H. A. Gillis, *J. Phys. Chem.*, **63**, 909 (1959); *J. Polymer Sci.*, **34**, 241 (1959); (e) A. Chapiro and V. Stannett, *J. Chim. Phys.*, **56**, 830 (1959).
114. T. H. Bates, J. V. F. Best, and F. Williams, *Nature*, **188**, 469 (1960); *Trans. Faraday Soc.*, **58**, 192 (1962).
115. M. A. Bouin, W. R. Busler, and T. F. Williams, *J. Am. Chem. Soc.*, **84**, 2895 (1962).
116. W. R. Busler, D. H. Martin, and F. Williams, *Disc. Faraday Soc.*, **36**, 102 (1963).
117. M. A. Bonin, W. R. Busler, and F. Williams, *J. Am. Chem. Soc.*, **87**, 199 (1965).
118. R. Worrall and A. Charlesby, *Int. J. Appl. Radiation Isotopes*, **6**, 8 (1958).
119. R. Worrall and S. H. Pinner, *J. Polymer Sci.*, **34**, 229 (1959).
120. A. Charlesby, S. H. Pinner, and R. Worrall, *Proc. Roy. Soc. (London) A*, **259**, 386 (1960).
121. E. Collinson, F. S. Dainton, and H. A. Gillis, *J. Phys. Chem.*, **63**, 909 (1959).
122. W. H. T. Davison, S. H. Pinner, and R. Worrall, *Proc. Roy. Soc. (London) A*, **252**, 187 (1959).
123. F. L. Dalton, G. Glawitch, and R. Roberts, *Polymer*, **2**, 419 (1961).
124. F. L. Dalton, *Polymer*, **6**, 1 (1965).
125. J. A. Bartlett and F. L. Dalton, *Polymer*, **7**, 107 (1966).
126. A. Charlesby and J. Morris, *Proc. Roy. Soc. (London) A*, **291**, 392 (1964).

127. A. Charlesby and J. Morris, *Proc. Roy. Soc. (London) A*, **273**, 387 (1963).
128. E. V. Krystal'nyi and S. S. Medvedev, *Vysokomolek. Soedin*, **7**, 1373 (1965); *Polymer Sci., USSR*, **7**, 1523 (1966).
129. D. J. Metz, *Adv. Chem. Series*, **66**, 170 (1967).
130. (a) K. Ueno, F. Williams, K. Hayashi, and S. Okamura, *Trans. Faraday Soc.*, **63**, 1478 (1967); (b) F. Williams, K. Hayashi, K. Ueno, K. Hayashi, and S. Okamura, *Trans. Faraday Soc.*, **63**, 1501 (1967).
131. D. J. Metz, R. C. Potter, C. L. Johnson, and R. H. Bretton, *J. Polymer Sci.*, **4**, 419, 2295 (1966).
132. S. Okamura, N. Kanoh, and T. Higashimura, *Makromolek. Chem.*, **56**, 65 (1962).
133. (a) W. K. R. Barnikol and G. V. Schulz, *Makromolek. Chem.*, **68**, 211 (1963). (b) J. Komiyama, L. L. Böhm, and G. V. Schultz, *Makromolek. Chem.*, **148**, 297 (1971).
134. L. L. Böhm and G. V. Schultz, *Makromolek. Chem.*, **153**, 5 (1972).
135. B. J. Schmitt and G. V. Schultz, *Makromolek. Chem.*, **142**, 325 (1971).
136. L. L. Böhm and G. V. Schultz, *Europ. Pol. J.*, in press (1974).
137. J. M. Alvarino, M. Chmelir, B. J. Schmitt, and G. V. Schultz, *J. Pol. Sci. C* **41**, 275 (1973).
138. C. J. Chang, R. F. Kiesel and T. E. Hogen-Esch, *J. Am. Chem. Soc.*, **95**, 8446 (1973).
139. M. Tardi and P. Sigwalt, *Europ. Pol. J.*, **9**, 1369 (1973).
140. D. Honnore, J. C. Favier, M. Fontanille, and P. Sigwalt, *Europ. Pol. J.*, (1974).
141. M. Morton, R. D. Sanderson, and R. Sakata, *Macromolec.*, **6**, 181 (1973).
142. M. Morton, R. D. Sanderson, R. Sakata, and L. A. Falvo, *Macromolec.*, **6**, 186 (1973).
143. M. Morton and L. A. Falvo, *Macromolec.*, **6**, 190 (1973).
144. S. Bywater, D. J. Worsfold, and G. Hollingsworth; *Macromolec.*, **5**, 389 (1972).
145. S. Brownstein, S. Bywater, and D. J. Worsfold, *Macromolec.*, **6**, 715 (1973).
146. O. Nuyken and P. H. Plesch, *Chem. Ind.* p. 379 (1973).
147. P. H. Plesch; *Makromolek. Chem.*, in press (1974).
148. S. Kobayashi, H. Danda, and T. Saegusa, *Bull. Chem. Soc. Japan*, **46**, 3214, 3220 (1973).
149. K. Matyjaszewski, P. Kubisa, and S. Penczek, International Symposium on Cationic Polymerisation, Rouen, France, Sept. 1973. See also K. Matyjaszewski and S. Penczek, I.U.P.A.C. Meeting, Madrid, Sept. 1974, reporting a direct observation of the special salt effect in the propagation of cationic polymerisation of THF:
150. (a) G. Löhr and G. V. Schulz, *Makromolek. Chem.*, **172**, 137 (1973). (b) G. Löhr, A. H. E. Müller, V. Wartzlhan, and G. V. Schulz, *Makromolek. Chem.*, **175**, 497 (1974).

5

Electric Permittivity, Dipole Moments, and Structure in Solutions of Ions and Ion Pairs

ERNEST GRUNWALD, STEFAN HIGHSMITH, and TING-PO I

*Department of Chemistry,
Brandeis University,
Waltham, Massachusetts*

1. Introduction	448
1.1. Conventions Concerning Dipole Vectors	448
2. Electric Dipole Moments of Ion Pairs in Nonpolar and Slightly Polar Media	449
2.1. Theory of Static Permittivity	449
2.2. Mutual Polarization of the Ions	452
2.3. Hydrogen-Bonded Ion Pairs	461
2.4. Association and Molecular Complex Formation	469
3. Dielectric Relaxation of Ion Pairs	480
3.1. Theory of Dielectric Relaxation	480
3.2. Quaternary and Tertiary Ammonium Salts	485
3.3. Ion Pairs and Zwitterions in Aqueous Solutions	490
4. Permittivity and Dielectric Relaxation of Solutions of Free Ions	495
4.1. Complications for Conducting Solutions	496
4.2. Aqueous Solutions	498
4.3. Ions in Nonaqueous Solvents	509
Appendix	512
References	515
	447

1. INTRODUCTION

The dielectric constant, or *electric permittivity** of electrolytic solutions is a useful property for learning about the molecular structure, dynamics, and solvation of ions and ion pairs. The static permittivity yields electric dipole moments of ion pairs and gives information about their self-association and interaction with complexing agents. The dipole moments in turn elucidate the topological and electronic structures of the ion pairs, including the mutual polarization of the ions and the degree of “tightness” of the ion pair.

The dispersion of the permittivity as a function of frequency gives information about the kinetics of dielectric relaxation and allows evaluation of the corresponding relaxation times. For ion pairs, these relaxation times give insight into molecular rotation, microscopic motions of the ions relative to each other, and, in some cases, into chemical exchange [6, 134, 135, 151]. For free ions, detailed analysis of the permittivity as a function of frequency can elucidate the structure of the ionic solvation shells and the effect of the ions on the “structure” of the solvent.

Because of the volume of experimental results that we wish to review, we shall forgo any detailed discussion of experimental methods. The interested reader is referred to the excellent reviews by Vaughan [147] and Smyth [141]. The experimental methods are currently in a state of flux because recent improvements in the field of time-domain reflectometry, combined with Fourier transformation, promise to revolutionize the collection of data points at high frequencies [144].

Although the theory of dielectrics has been an area of chemical physics where many brilliant contributions have been made, it should be realized that the theoretical models and the resulting mathematics are only good approximations rather than rigorous descriptions of reality, and they are still the subject of intensive research [151]. Thus dipole moments for ion pairs and relaxation times for electrolytic solutions are subject to some uncertainty, but this is no cause for anxiety because the effects to be interpreted are in most cases much larger than the uncertainties.

1.1. Conventions Concerning Dipole Vectors

Considerable confusion exists because there are two conventions in current use for representing dipole vectors. The physicists' convention represents the

* In the older literature the term “dielectric constant” predominates, but because this property is actually a complex function of frequency, the term “permittivity” is now preferred [142].

dipole moment as an *arrow pointing from the center of negative charge to the center of positive charge*. Organic chemists use the opposite convention. The physicists' convention is compatible with vector equations of electromagnetism for computing forces, torques, and other dynamical quantities. Although we are chemists ourselves, we feel that we should yield to the physicists' convention, for the sake of uniformity, and shall use it throughout this chapter.

2. ELECTRIC DIPOLE MOMENTS OF ION PAIRS IN NONPOLAR AND SLIGHTLY POLAR MEDIA

In discussing permittivity data, it is convenient to consider first data that have been obtained in media of low conductivity, because a high conductivity greatly complicates both the measurement and the interpretation of the results [68, 91]. We shall therefore begin by considering electrolytic solutions in nonpolar and slightly polar media, under conditions where the free ion concentrations are stoichiometrically insignificant.

2.1. Theory of Static Permittivity [24, 44, 57, 83, 140, 141]

The electric permittivity ϵ is defined by the equation $\mathbf{D} = k_\epsilon \epsilon \mathbf{E}$, where \mathbf{D} is the electric displacement, \mathbf{E} the electric field, and k_ϵ a constant depending on the system of units, chosen so that $\epsilon \equiv 1$ for empty space.* In alternating fields ϵ is a function of frequency and, since \mathbf{D} and \mathbf{E} are not necessarily in phase, ϵ is conveniently expressed as a complex variable.

Since $\mathbf{D} = k_\epsilon \mathbf{E} + 4\pi \mathbf{P}$, where \mathbf{P} is the *polarization* (defined as the electric moment induced by the field in a *unit volume* of the dielectric), an alternative definition for the permittivity is $\epsilon = 1 + 4\pi \mathbf{P}/k_\epsilon \mathbf{E}$. The polarization in turn is a vector sum of electric moments \mathbf{m}_i ascribable to individual molecules:

$$\mathbf{P} = N_0 \sum_i \bar{c}_i \mathbf{m}_i$$

where N_0 is Avogadro's number, \bar{c}_i the concentration in moles per cubic centimeter of the i th molecular species, and the summation extends over all molecular species present. The polarization therefore provides a link between the electric moments of the molecules and the experimental quantities, the permittivity and the composition.

The electric field acting on a molecule in a dielectric is different from the

* In the electrostatic system of units, $k_\epsilon = 1$; in the mks system, $\frac{k_\epsilon}{4\pi} = 8.85 \times 10^{-12}$ farad/meter.

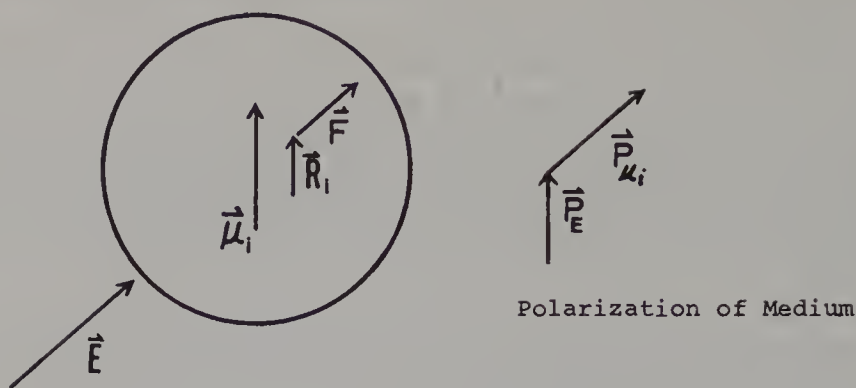


Figure 1. Model for Onsager reaction field. \mathbf{E} is the applied field, \mathbf{R} is the reaction field, and \mathbf{F} is the Lorentz field.

applied field \mathbf{E} . Debye [44] adopted the Lorenz-Lorentz field. His result, applied to a homogeneous fluid mixture, is expressed by Eq. 1, in which P_i denotes the *molar polarization* of the i th species, and \bar{c}_i its concentration in moles per cubic centimeter:

$$\frac{\epsilon - 1}{\epsilon + 2} = \sum_i \bar{c}_i P_i \quad (1)$$

According to Debye, P_i is given by Eq. 2:

$$P_i = \frac{4\pi N_0}{3} \left(\alpha_i + \frac{\mu_i^2}{3kT} \right) \quad (2)$$

where α_i denotes the molecular polarizability and μ_i the permanent molecular electric dipole moment of the given species in the gas phase.

Debye's theory is quite successful for gases and for dilute solutions in non-polar solvents. However, for polar liquids and for solutions in polar solvents, Debye's theory leads to erroneous results. Onsager [110] showed that in polar media, the internal field acting on a molecule is better expressed as a vector sum consisting of the Lorenz-Lorentz field and a *reaction field*, which he calculated. The mechanism by which the reaction field arises is as follows (Fig. 1): The dipole field produced by the given molecule polarizes the surrounding fluid. The induced polarization in turn produces a reaction field, \mathbf{R} , which polarizes the given molecule and enhances its dipole moment.

The use of Onsager's internal field leads to Eqs. 3 and 4:

$$\frac{(\epsilon - 1)(2\epsilon + 1)}{9\epsilon} = \sum_i \bar{c}_i P_i^* \quad (3)$$

$$P_i^* = \frac{4\pi N_0}{3} \left(\alpha_i^* + \frac{(\mu_i^*)^2}{3kT} \right) \quad (4)$$

Note that the molar polarization P_i^* in Onsager's theory is formally analogous to P_i in Debye's theory. However, α_i^* is an *effective* polarizability and μ_i^* is the actual dipole moment in the given medium, which includes the enhancement owing to the reaction field. Onsager's relationship between α_i^* and α_i , and between μ_i^* and μ_i , is given in Eq. 5 [24], where V_i denotes the molar volume of the i th species in cubic centimeters:

$$\frac{\alpha_i}{\alpha_i^*} = \frac{\mu_i}{\mu_i^*} = 1 - \frac{4\pi N_0 \alpha_i (2\epsilon - 2)}{3V_i(2\epsilon + 1)} \quad (5)$$

Debye's theory (Eqs. 1 and 2) and Onsager's theory (Eqs. 3–5) lead to identical dipole moments in the gas phase and to very similar results for μ_i in nonpolar solvents.

Onsager's theory becomes inaccurate for solvents that are self-associated, or for solutions in which there is molecular complexing between the solute and the solvent. For such systems, Kirkwood derived a general theory [57, 93, 95, 96] which allows for the coupling of dipoles due to molecular complexing. His result is expressed in Eqs. 6 and 7:

$$\frac{(\epsilon - 1)(\epsilon + 2)}{9\epsilon} = \sum_i \bar{c}_i P_i^\dagger \quad (6)$$

$$P_i^\dagger = \frac{4\pi N_0}{3} \left(\alpha_i + \frac{g_i (\mu_i^\dagger)^2}{3kT} \right) \quad (7)$$

Equation 6 is formally identical to Onsager's Eq. 3. The molar polarization P_i^\dagger is given by Eq. 7, in which μ_i^\dagger is the molecular dipole moment in solution, including any enhancement due to the reaction field. g_i is a *correlation factor* whose deviation from unity allows for the coupling between the orientations of the given dipole and those of surrounding dipoles. In practice, g_i will deviate substantially from unity only if such coupling is quite strong [107, 108]; ordinary dipole-dipole coupling alone is not strong enough.

The physical significance of g is as follows. According to Kirkwood's theory, for a given molecule, $g\mu^2 = \boldsymbol{\mu} \cdot \langle \boldsymbol{\mu} \rangle$, where $\boldsymbol{\mu}$ is the dipole vector of the given molecule and $\langle \boldsymbol{\mu} \rangle$ is the vector sum of that dipole plus the average dipole of the surrounding sphere of molecules (whose radius is large enough to include all dipole correlations) (see Fig. 2). In principle, g can be calculated from the angular distribution function of the molecules in the liquid [93].

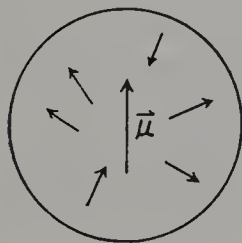


Figure 2. An instantaneous configuration of dipoles around the central dipole moment $\boldsymbol{\mu}$. $\langle \boldsymbol{\mu} \rangle$ is the vector sum of the central fixed dipole $\boldsymbol{\mu}$ plus the average resultant dipole moment of the surrounding sphere. In computing $\boldsymbol{\mu}$, one takes a time-weighted average of all instantaneous configurations.

In Eq. 7 we write g_i to indicate that the value of g is characteristic of the molecular species. Beyond that, g is also a function of composition. However, in dilute solutions, it is sufficient to assume that g_2 for the solute is constant, and that g_1 for the solvent is a linear function of \bar{c}_2 [68].

Kirkwood's theory does not give us a relationship between the moment μ_i^\dagger in solution and μ_i in the gas phase. Kirkwood suggested that μ_i^\dagger/μ_i might be calculated according to Onsager's theory (Eq. 5) by setting $\mu_i^\dagger = \mu_i^*$, or alternatively it might be given by Eq. 8, in which n denotes the refractive index of the solution:

$$\frac{\mu_i}{\mu_i^\dagger} = 1 - \frac{(n^2 - 1)(2\epsilon - 2)}{(n^2 + 2)(2\epsilon + 1)} \quad (8)$$

In practice, the difference between Eq. 5 and Eq. 8 is often small. More recent theories suggest that the correct value may lie between results given by Eqs. 5 and 8 [33].

Because Kirkwood's theory is exact and Onsager's theory is approximate, the dipole moment μ_2^* calculated by Onsager's method from data for dilute solutions is always at least somewhat approximate. μ_2^* is related to the exact value, μ_2^\dagger , given by Kirkwood's theory according to Eq. 9, in which V_1 denotes the molar volume of the solvent [68]:

$$(\mu_2^*)^2 = g_2(\mu_2^\dagger)^2 + \frac{dg_1}{d\bar{c}_2} \frac{(\mu_1^\dagger)^2}{V_1} \quad (9)$$

2.2. Mutual Polarization of the Ions [18, 23, 69, 129]

Probably the most familiar driving force for the formation of ion pairs is the coulombic attraction of the opposite ionic charges. Indeed, in many theories of ionic association, Coulomb forces are the only forces that are considered. In this section we wish to show, however, that the mutual polarization of the interacting charges is very important and contributes as much as 10–30 kcal/mole to the binding energy of typical ion pairs. To isolate the effect of mutual polarization, we shall consider ion pairs, in which at least one of the ions has a chemically stable, inert electron configuration.

2.2.1. Alkali Halide Ion Pairs in the Gas Phase

Accurate electric dipole moments and interionic distances are known for nearly all alkali halide ion pairs in the gas phase. These values are summarized in Table 1. The distances r are deduced from rotational spectra in the microwave region [17, 66], and the dipole moments are based mostly on molecular beam electric resonance and the Stark effect [25, 50, 79, 80]. Also listed in the table are interionic distances in alkali halide crystals [111]. In all cases

Table 1 Structure of Alkali Halide Ion Pairs

Salt	$r(\text{\AA})$ Gas Phase ^a	$\mu(\text{D})$ Gas Phase ^b	$er(\text{D})$ Gas Phase	$r(\text{\AA})$ Crystal ^c	$r(\text{\AA})$ (calc, Eq. 25)	$-W_\alpha$ (kcal/mole)
LiF	1.56	6.30	7.49	2.01	1.66	21.0
LiCl	2.02	7.12	9.70	2.57	2.19	24.5
LiBr	2.17	7.27	10.42	2.75	2.37	25.3
LiI	2.39	7.43	11.48	3.02	2.63	26.0
NaF	1.93	8.16	9.27	2.31	2.02	13.1
NaCl	2.36	9.00	11.34	2.81	2.50	16.6
NaBr	2.50	9.12	12.01	2.98	2.66	17.9
NaI	2.71	9.24	13.02	3.23	2.89	19.2
KF	2.17	8.6	10.42	2.66	2.26	15.3
KCl	2.67	10.27	12.82	3.14	2.80	14.0
KBr	2.82	10.41	13.54	3.29	2.96	15.0
KI	3.05	8.55(?)	14.65	3.53	2.95(?)	22.3(?)
RbF	2.27	8.55	10.90	2.82	2.34	17.0
RbCl	2.79	10.51	13.40	3.28	2.91	14.1
RbBr	2.94	—	—	3.43	—	—
RbI	3.18	—	—	3.66	—	—
CsF	2.35	7.88	11.29	3.01	2.41	22.0
CsCl	2.91	10.40	13.98	3.45	3.02	15.6
CsBr	3.07	—	—	3.60	—	—
CsI	3.32	—	—	3.82	—	—

^a Refs. 17, 66.^b Refs. 17, 50, 66, 79, 80.^c Ref. 111.

r in the gas phase is substantially smaller than r in the crystal. Moreover, the experimental dipole moments μ are substantially smaller than the product, er , expected for a pair of unit charges separated at the gas-phase distance.

The difference between μ and er can be ascribed to the mutual polarization of the ions. The electric field due to the cation produces an induced moment \mathbf{m}_- , and that due to the anion produces an induced moment \mathbf{m}_+ . As shown in Fig. 3, these moments oppose the moment er due to the charges, so that the resultant moment μ is smaller than er . A detailed analysis of bonding in alkali halide molecules, including the effect of short-range repulsion, was made by Rittner [129] in 1951 and provides a fairly satisfactory explanation of both the observed interionic distances and dipole moments. For the present purpose, however, it is sufficient to use a much simpler model described by Böttcher [23].

In Böttcher's model each ion is treated as an isotropically polarizable point charge. Let e denote the unit charge (4.803×10^{-10} esu), α_+ , α_- the

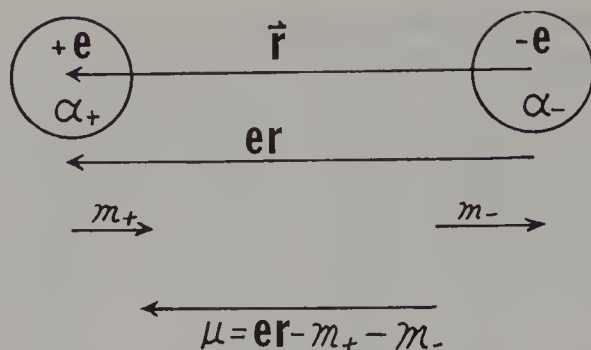


Figure 3. Vector diagram of electric moments for a pair of polarizable point charges.

ionic polarizabilities, and r the distance between the ionic centers. Assuming a permittivity of unity, the field produced by the cation (due to the charge $+e$ and the moment m_+ induced by the anion) at the position of the anion is given by

$$E_- = \frac{e}{r^2} + \frac{2m_+}{r^3}$$

The induced moment m_- , which is equal to $\alpha_- E_-$, is therefore given by Eq. 10a; similarly, m_+ is given by Eq. 10b:

$$m_- = \alpha_- \left(\frac{e}{r^2} + \frac{2m_+}{r^3} \right) \quad (10a)$$

$$m_+ = \alpha_+ \left(\frac{e}{r^2} + \frac{2m_-}{r^3} \right) \quad (10b)$$

On solving for m_+ and m_- , and subtracting from er , we obtain Eq. 11 for the dipole moment of the polarized ion pair:

$$\mu = er \left(1 - \frac{r^3(\alpha_+ + \alpha_-) + 4\alpha_+\alpha_-}{r^6 - 4\alpha_+\alpha_-} \right) \quad (11)$$

To show the approximate validity of this model, we have calculated r for each ion pair, using the experimental dipole moment and ionic polarizabilities listed in Table 2. The results are shown in the sixth column of Table 1. With one exception, the values obtained for r are intermediate between experimental values obtained in the gas phase and in the crystal, and are closer to the gas-phase value. It would seem that the Böttcher model is a valid first approximation.

Table 2 Ionic Polarizabilities Based on Ionic Refractions at Na-D (5893 Å)^a

Ion	10 ²⁴ α (cm ³)	Ion	10 ²⁴ α (cm ³)
Li ⁺	0.00 ^b	F ⁻	0.94
Na ⁺	0.25	Cl ⁻	3.40
K ⁺	1.05	Br ⁻	4.86
Rb ⁺	1.58	I ⁻	7.46
Cs ⁺	2.64	ClO ₄ ⁻	5.9
<i>n</i> -Bu ₄ N ⁺	32.5	Picrate ⁻	16.0
<i>i</i> -Am ₄ N ⁺	38.0	Benzoate ⁻	12.8
<i>n</i> -Bu ₃ NH ⁺	25.2	(C ₆ H ₅) ₃ BOH ⁻	31.9
		Acetate ⁻	4.6

^a Based on data reported by K. Fajans and G. Joos, *Z. Physik.*, **23**, 1 (1924); K. Bauge and J. W. Smith, *J. Chem. Soc.*, 1964, 4244; N. Bauer and K. Fajans, in *Physical Methods of Organic Chemistry*, A. Weissberger (Ed.), Interscience, New York, (1946) Chap. 20.

^b Reference ion; the actual value of α for Li⁺ will be less than that for He, or less than 0.20 × 10⁻²⁴ cm³.

If this be granted, then we may use the same model to estimate the interaction energy W per ion pair. The relevant equation, according to Böttcher [23], is

$$W = -\frac{e^2}{r} - \left[\frac{r^3(\alpha_+ + \alpha_-) + 4\alpha_+\alpha_-}{(r^6 - 4\alpha_+\alpha_-)} \right] \frac{e^2}{2r}$$

$$= W_e + W_\alpha \quad (12)$$

The first term, $W_e = -e^2/r$, is the familiar Coulomb energy of a pair of charges. The second term, W_α , is the additional energy due to the mutual polarization of the ions.

On using values of r calculated from Eq. 11 and converting to kilocalories per mole, we obtain the results given in the final column of Table 1. The values of W_α are well in excess of 10% of Coulomb energy, ranging from -13 to -26 kcal/mole, and are clearly important. We conclude that any theory of ion pair structure must include the mutual polarization of the ions, even in first approximation.

2.2.2. Tetraalkylammonium Salts in Benzene

Electric dipole moments of tetraalkylammonium salts in benzene were first reported by Hooper and Kraus in 1934 [85]. Although the ion pair dipole moments were only semiquantitative, owing to complications due to the

formation of higher ion pair aggregates, the values obtained seemed to be in the range 15–20 D. This pioneering work was repeated and improved by Geddes and Kraus [61], whose results (published in 1936) are still regarded as accurate to 1–2 D. In the more recent past, the effect of mutual polarization on the dipole moment of organic ion pairs was first treated by Davies and Williams [42] in 1960. In an admirable study published in 1964, Bauge and Smith [18] reported dipole moments for a series of quaternary ammonium ion pairs and accounted for mutual polarization by applying Böttcher's model.

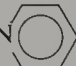
A critical summary of available dipole moments for tetraalkylammonium ion pairs in benzene is given in Table 3. Interionic distances ($r_+ + r_-$) in the ion pairs were estimated as follows. For $n\text{-Bu}_4\text{N}^+$, an effective radius of 3.1 Å was adopted on the basis of NMR studies of a contact ion pair [97]. Slightly larger radii were chosen for the structurally similar $i\text{-Am}_4\text{N}^+$ (3.2 Å) and $(\text{C}_6\text{H}_5)_3\text{BOH}^-$ (3.3 Å) ions. Other radii were taken from a recent review [143], except that the radius of $\text{ClCH}_2\text{CO}_2^-$ was assumed equal to that of CH_3CO_2^- .

The upper part of the table lists results for ion pairs formed from free ions with centric, or approximately centric, charge distributions. On applying Böttcher's model [23] (Eqs. 10–12), we find that the dipole moments lead to calculated distances r that are very close to the interionic distances ($r_+ + r_-$). The polarization energy W_α ranges from –9 to –18 kcal/mole, being again very substantial. Considering both Tables 1 and 3, it appears that the Böttcher

Table 3 Structure of Tetraalkylammonium Ion Pairs in Benzene Solution^a

Salt	μ (D)	μ_- (D)	$r_+ + r_-$ (Å)	$e(r_+ + r_-) - \mu_-$ (D)	$r(\text{Å})$ (calc, Eq. 28)	$-W_\alpha$ (kcal/mole)
$n\text{-Bu}_4\text{NBr}^b$	12.2	0.0	4.9 ₀	23.6	4.69	16.2
$n\text{-Bu}_4\text{NI}^b$	12.7	0.0	5.1 ₄	24.7	4.86	15.6
$n\text{-Bu}_4\text{NClO}_4^b$	17.2	0.0	5.4 ₆	26.2	5.21	10.0
$n\text{-Bu}_4\text{N}(\text{C}_6\text{H}_5)_3\text{BOH}^c$	19.7	0.0	6.4	30.8	6.29	9.2
$n\text{-Bu}_4\text{NAc}^c$	11.2	0.0	4.72	22.7	4.57	17.7
$n\text{-Bu}_4\text{NAc}^c$	11.2	2.0	4.72	20.7	4.87	17.1
$n\text{-Bu}_4\text{N}(\alpha\text{-ClAc})^b$	14.8	3.0	4.7	20	5.49	11.8
$n\text{-Bu}_4\text{NBz}^b$	12.1	4.0	4.8	19	5.58	14.5
Cetylpyridinium Bz ^b	7.5	4.0	—	—	5.44	21.0
$n\text{-Bu}_4\text{N}^+\text{Pi}^-$	15.3	4.0	5.92	24.4	5.94	11.5
$i\text{-Am}_4\text{N}^+\text{Pi}^-$	18.3	4.0	6.0	25	6.51	8.6

^a Dipole moments calculated using the Debye equation: Ac = acetate; $\alpha\text{-ClAc} = \text{ClCH}_2\text{CO}_2^-$

Bz = benzoate; pi = picrate; cetylpyridinium = $\text{C}_{12}\text{H}_{25}^+\text{N}$ .

^b Ref. 18.

^c Ref. 61.

model will reproduce dipole moments for a gratifyingly wide range of polarizabilities and interionic distances.

For the ion pairs listed in the lower part of Table 3, the anions do not have a centric charge distribution. In this case, Böttcher's model would treat the anion as a polarizable point charge ($-e$, α_-) superimposed on a permanent point dipole (μ_-). Unfortunately, the mathematics becomes complicated except when all dipoles (er , μ_- , m_+ , and m) are parallel. In that case, m_+ and m_- are given by Eqs. 13, which, except for the inclusion of μ_- , are analogous to Eq. 10:

$$m_+ = \alpha_+ \left[\frac{2(\mu_- + m_-)}{r^3} + \frac{e}{r^2} \right] \quad (13a)$$

$$m_- = \alpha_- \left[\frac{2m_+}{r^3} + \frac{e}{r^2} \right] \quad (13b)$$

Note that in Eq. 13a μ_- is reckoned as positive if the direction of the dipole is parallel to that of m_- , or opposite to that of er (see Fig. 3). The resultant dipole moment μ of the ion pair is therefore given by Eq. 14:

$$\mu = er - \mu_- - m_+ - m_- \quad (14)$$

Using methods described by Böttcher [23], we find that the electrostatic interaction energy is given by Eq. 15:

$$W = -\frac{e^2}{r} - \frac{e}{r^2} (m_+ + m_- + \mu_-) - \frac{2m_+(m_- + \mu_-)}{r^3} + \frac{m_+^2}{2\alpha_+} + \frac{m_-^2}{2\alpha_-} \quad (15)$$

For a nonpolarizable ion pair, the corresponding interaction energy is given by Eq. 16:

$$W_{\text{nonpolarizable}} = -\frac{e^2}{r} - \frac{e\mu_-}{r^2} \quad (16)$$

W_α is then defined as $W - W_{\text{nonpolarizable}}$.

In calculating r and W_α according to Eqs. 13–16, we used values for μ_- suggested by Bauge and Smith [18]. However, it should be realized that these values as well as the assumed parallelism of the electric moments are crude approximations. Results are listed in Table 3. The values obtained for W_α are again quite substantial. To assess the effect of possible error in the chosen value for μ_- , we calculated r and W_α for Bu_4NAc on the assumption that $\mu_- = 0.0$ D, as well as $\mu_- = 2.0$ D. Although the values obtained for r differ by 0.3 \AA , as shown in Table 3, the values obtained for W_α are quite similar. There seems little doubt that the mutual polarization of the ions in an ion pair is energetically important.

2.2.3. Effective Permittivity

According to Coulomb's law, the electric field at a given point is inversely proportional to the permittivity of the medium. In applying the Böttcher model to ion pairs, it was assumed that the effective permittivity is unity. If this assumption were incorrect, we would expect the effective permittivity to increase with the permittivity of the solvent in bulk. We would therefore expect less mutual polarization of the ions in solvents of higher permittivity [63], and because the mutual polarization reduces the dipole moment, we would expect an increase in the dipole moment. This increase in the dipole moment would be above and beyond the normal increase produced in any molecule by the Onsager reaction field.

Relevant data for tetraalkylammonium salts are summarized in Table 4.

Table 4 Effect of Solvent Permittivity on the Dipole Moments of Ion Pairs

Electrolyte	Solvent	Temperature	Permittivity	μ^g
Bu ₄ N ⁺ Pi ^{-a}	Benzene	25°	2.269	15.7
	Dioxane	25°	2.222	16.3
	Toluene	25°	2.369	14.3
	25 mole% DCB			
	in C ₆ H ₅ ^h	25°	4.167	13.8
	50 mole% DCB			
	in C ₆ H ₆ ^h	25°	5.995	16.8
	C ₆ H ₅ Cl	25°	5.621	14.4
	C ₆ H ₅ Br	25°	5.374	14.3
Bu ₄ N ⁺ Br ^b	C ₆ H ₅ Cl	25°	5.621	13.5
	C ₆ H ₅ Br	25°	5.374	11.9
	Benzene	25°	2.269	19.7
Bu ₄ N ⁺ B(C ₆ H ₅) ₃ OH ^c	Benzene	25°	2.269	19.7
Bu ₄ N ⁺ B(C ₆ H ₅) ₄ ^d	C ₆ H ₅ Cl	25°	5.621	17.3
<i>i</i> -Am ₄ N ⁺ NO ₃ ^e	C ₆ H ₅ Cl	-34.6	6.90	14.4
	C ₆ H ₅ Cl	25°	5.62	13.9
	C ₆ H ₅ Cl	59.5°	5.07	14.2
	HAc	25°	6.27	14.5
	C ₆ H ₅ Cl	25°	5.62	13.8
<i>i</i> -Am ₄ N ⁺ I ^e	HAc	25°	6.27	16.3
	C ₆ H ₅ Cl	25°	5.62	13.8
LiCl ^f	Gas phase		1.00	7.12
	Octanoic acid	25°	2.48	6.78
	Acetic acid	25°	6.27	ca. 9

^a Refs. 63, 128.

^b Ref. 63.

^c Table 3.

^d Ref. 63.

^e Refs. 68, 69.

^f Table 1 and unpublished results by Ting-Po I and M. R. Crampton.

^g Calculations are based on Onsager's theory.

^h DCB = ortho-dichlorobenzene.

In each case the ion pair dipole moment μ was calculated by Onsager's theory and is corrected for the effect of the reaction field. It will be seen that for tetraalkylammonium ion pairs in aprotic solvents, μ shows no correlation whatever with permittivity over a threefold change in permittivity [63, 69]. Indeed, those variations that are observed are within the combined errors of measurement and theory. For *i*-Am₄N NO₃ and *i*-Am₄NI, the change from chlorobenzene to the strongly self-associated solvent acetic acid seems to have only a small effect on μ [69]. For lithium chloride, the dipole moment in octanoic acid is essentially the same as in the gas phase [87], but the dipole moment in acetic acid is significantly higher, presumably due to solvation of the solute and changes in the self-association of the solvent.

Molecular models show that tetraalkylammonium ions have an "open" structure, consisting of a central core and four alkyl "limbs" projecting at tetrahedral directions into the solvent. The fact that the dipole moments of the ion pairs formed from such ions show no medium effect beyond the normal increase due to their reaction fields shows that the cation and anion polarize each other at intimate contact, as envisaged by the model of a contact ion pair.

2.2.4. Ions with Delocalized Electron Distributions

If either or both ions forming the ion pair have delocalized electron distributions, the interaction energy W_α due to mutual polarization should be even greater than one would expect from Böttcher's model. By treating the induced charge distributions as point dipoles, Böttcher's model assumes that the induced displacements of charge in the polarized ions are small compared to the distance between the ionic centers. However, when charge is displaced by a resonance mechanism, this assumption is no longer valid [70]. Instead of treating the induced charge distribution as a point dipole, it then becomes more realistic to treat it as a pair or set of equal and opposite monopoles.

For example, the 9-fluorene anion (17) can be represented as a resonance hybrid in which the charge is partly delocalized from position 9 to positions 1, 3, 6, 8 and bridge positions *a* and *b*, as shown in Fig. 4a.



Because of this resonance, the anion is easily polarized, but the polarizability is very anisotropic. Electric charge is displaced easily only among those ring positions that are involved in the resonance. Figure 4b shows the probable charge distribution in an intimate ion pair, and Fig. 4c shows the corresponding charge displacements. Note that negative charge moves specifically

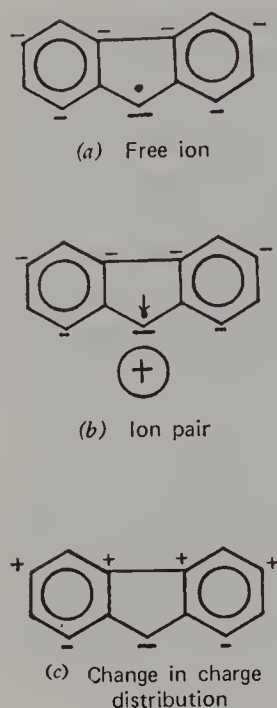


Figure 4. Resonance and polarizability in the 9-fluorene anion. Filled circle denotes center of negative charge. (a) Free ion. (b) Ion pair. (c) Change in charge distribution.

from positions 3, 6, *a*, and *b* largely to position 9, but probably also to positions 1 and 8. Although the change in charge distribution may be regarded as an induced dipole, it is more appropriate to regard it as a set of induced charges. One reason for this is that the distance between the induced charges is of the same order of magnitude as the diameter of the molecule. Thus the *center* of charge, whose position determines r in Coulomb's law, is significantly displaced toward the cation, with a resultant important increase in the magnitude of the Coulomb energy e^2/r .

In conclusion, to predict the structure of an ion pair from the known structure of the free ions, one must consider whether the electron distribution in at least one of the free ions can be polarized by a resonance mechanism. If not, the ionic centers of charge will be relatively immobile and the structure of the ion pair will be dictated largely by the ionic contours, so as to bring the centers of charge to the closest possible approach. If such polarization can occur, there will be specific sites in the resonance-stabilized ions at which the polarizability is particularly high. The positions of these polarizable sites can be predicted from the resonance structures. As the ion pair is formed, the counterion will attach itself to one of these highly polarizable sites, pulling the center of ionic charge toward it. Because of the movement of electric charge toward the given site, the interaction will resemble a chemical bond. The originally delocalized charge distribution becomes more localized, with

resulting manifestations in spectroscopic and other physical properties, many of which have been described in Volume One of this book.

2.3. Hydrogen-Bonded Ion Pairs

When a hydrogen-bonded complex composed of a Brønsted acid and base of sufficient strengths is present in solution, there is essentially complete proton transfer leading to a hydrogen-bonded ion pair [43]. The existence of such ion pairs is demonstrated by the large electric dipole moments of such complexes, observed in solvents of low permittivity in which dissociation to free ions is negligible. Typical data are listed in Table 5. Although proton transfer is in some cases not quite complete, the dipole moments are of comparable magnitude to those of typical ion pairs, as listed in Tables 1 and 3. In this section we shall consider the structure of hydrogen-bonded ion pairs

Table 5 Hydrogen-Bonded Ion Pairs from the Reaction of Acids with Bases^a

Cation	Anion	$\mu(\text{D})$	$[\text{pK}_a + \text{pK}_B]^c$	Solvent
Et_3NH^+	Pi^-	11.7	3.75	Benzene
	$\text{Cl}_3\text{CCO}_2^-$	9.6	3.98	Dioxane
	$\text{HCl}_2\text{CCO}_2^-$	7.8	4.61	Dioxane
	$\text{H}_2\text{ClCCO}_2^-$	7.2	6.32	Dioxane
	$2,6\text{-diBr-4-NO}_2\text{C}_6\text{H}_2\text{O}^-$	12.7	6.74	Trichloroethylene
	$2,6\text{-diBr-4-NO}_2\text{C}_6\text{H}_2\text{O}^-$	11.8	6.74	Toluene
	$2,4\text{-diNO}_2\text{-C}_6\text{H}_4\text{O}^-$	11.3	7.44	Benzene
	CH_3CO_2^-	4.0 ^b	8.10	Dioxane
	$\text{C}_6\text{Cl}_5\text{O}^-$	10.6	8.17	Trichloroethylene
	$\text{C}_6\text{Cl}_5\text{O}^-$	9.6	8.17	Toluene
	$2,5\text{-diNO}_2\text{C}_6\text{H}_3\text{O}^-$	9.1	8.57	Benzene
	$2,4,6\text{-triCl-C}_6\text{H}_2\text{O}^-$	8.9	9.32	Trichloroethylene
	$2,6\text{-diCl-C}_6\text{H}_3\text{O}^-$	12.0	10.14	Benzene
Bu_3NH^+	Br^-	8.5	—	Benzene
	I^-	8.1	—	Benzene
	I^-	7.7	—	Xylene
	Pi^-	11.9	4.47	Benzene
Bu_2NH_2^+	Pi^-	11.4	4.47	Xylene
	Pi^-	11.5	6.75	Benzene
$i\text{-Am}_3\text{NH}^+$	Pi^-	11.9	—	Benzene
Bz_3NH^+	Pi^-	12.0	—	Benzene
PyH^+	Pi^-	10.4	9.19	Dioxane
$\text{C}_6\text{H}_5\text{NH}_3^+$	Pi^-	7.0	9.78	Dioxane

^a Refs. 18, 42, 89, 101, 127, 146.

^b This value is surprisingly small and merits further investigation.

^c pK_a of the acid HA and pK_B of the base B, both measured in water. Values listed in this column were taken from the cited references.

and of their conjugate acid-base complexes on the basis of electric dipole moments.

2.3.1. Dipole Moment due to Hydrogen-Bond Formation

There has been for many years a strong interest in evaluating the change in electron density resulting from the formation of a hydrogen bond. Comparison of the electric dipole moment of a hydrogen-bonded complex with the sum of its constituents should give such information. Most theoreticians agree that hydrogen-bonded formation (shown symbolically in Eq. 18) is



attended by some shift of electron density from the lone-pair orbital of :B in a direction toward A, while the equilibrium position of the proton moves slightly away from A. For example, Ratajczak [125] envisions charge transfer of the type described by Mulliken, in which the electron density from :B enters a low-lying vacant molecular orbital of A—H. Thus in theory the additional dipole moment \mathbf{m}_H resulting from the formation of the hydrogen bond is a vector pointing from the hydrogen-bond donor toward the hydrogen-bond acceptor, most likely parallel to the A—H \cdots B hydrogen-bond axis, as shown in Fig. 5a. In a hydrogen-bonded ion pair, the direction of \mathbf{m}_H would therefore oppose that of the larger vector, \mathbf{er} , due to the ionic charges (Fig. 5b).

For hydrogen-bonded complexes of the type A—H \cdots B, formed from weak acids and weak bases, recent evidence indicates that \mathbf{m}_H is fairly small, probably no greater than 0.5 D [89, 126, 127, 146]. We now wish to show that for hydrogen-bonded ion pairs of the type $^+\text{C—H} \cdots \text{D}^-$, \mathbf{m}_H is similarly small. In particular, we shall analyze the dipole moments of tri-*n*-butylammonium bromide and iodide, whose ion pair structures are well defined.

It is convenient to write $\mu = \mu_B + \mathbf{m}_H$, where μ_B is the dipole moment

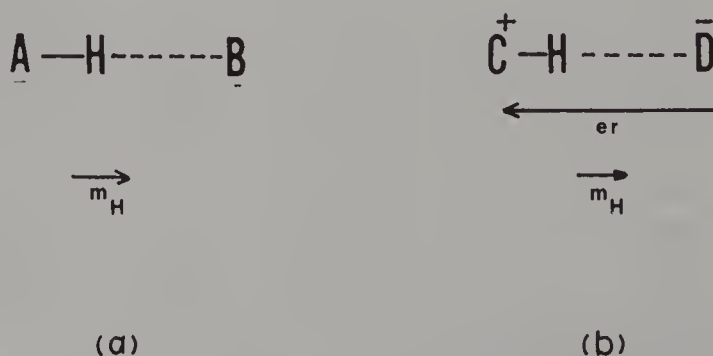


Figure 5. Direction of the additional dipole moment, \mathbf{m}_H , due to hydrogen-bond formation. (a) Hydrogen-bond donor (A—H) and acceptor (B) are uncharged molecules. (b) Hydrogen-bond donor (C—H^+) and acceptor (D^-) are ions.

as estimated from Böttcher's model [23] and m_H is the dipole moment due to hydrogen-bond formation, a negative quantity. The dipole moment μ_B can be calculated with an accuracy of about 1 D⁻; we used an analog of Eqs. 13 and 14 [18] in which μ_- (for Br⁻ and I⁻) is zero and μ_+ (for *n*-Bu₃NH⁺) = 0.85 D. The distance r between the ionic centers of charge was assumed equal to r_{crystal} , the corresponding hydrogen-bonded distance in ammonium and alkylammonium halides. For different salts there is some variability in r_{crystal} , as shown in Table 6. Since m_H is a negative quantity, we expect μ_B to be

Table 6 Analysis of Dipole Moments of tri-*n*-Butylammonium Bromide and Iodide

Ion Pair	r_{crystal} (Å) ^a	$\mu(\text{obs})$ (D)	r^b	μ_+^c	μ_B^d
<i>n</i> -Bu ₃ NHBr	3.31–3.43	8.50	3.43	0.85	7.75
<i>n</i> -Bu ₃ NHI	3.5–3.64	8.09	3.64	0.85	7.64

^a Hydrogen-bonded N–X distances in solid ammonium and alkylammonium halides, as determined by X-ray diffraction. (R. W. G. Wyckoff, *Crystal Structures*, Vol. 5, 2nd ed., Interscience, New York, 1966.)

^b Value assumed in the calculation of the dipole moment.

^c Dipole moment of *n*-Bu₃NH⁺.

^d Same method of calculation as shown in Eqs. 13–14.

greater than the experimental value of μ . In fact, μ_B turned out to be smaller than μ . Even when we used the largest available crystallographic value for r , the difference between μ and μ_B was about 0.5 D. (see the last column of Table 6). Allowing that the error in the comparison of μ and μ_B may be as high 1 D, and that m_H is negative, we conclude that $0 > m_H > -0.5$ D. This order of magnitude is fully consistent with the measured values for hydrogen-bonded complexes formed from uncharged weak acids and bases.

2.3.2. Dipole Moment and Proton Transfer

There is considerable interest in the dipole moments of acid-base complexes A—H····B as the acid strength of A—H is allowed to increase. If the acid A—H is strong enough, then the complex is of course a hydrogen-bonded ion pair, A⁻····H—B⁺. Two possibilities have been discussed for acids of intermediate strength: a tautomeric equilibrium involving two discrete species, as in Eq. 19; or a single hydrogen-bonded species of continuously increasing ion pair character.



Experimentally one measures the dipole moment μ_c of the acid-base complex and evaluates an interaction moment $\delta\mu$, defined in Eq. 20,

$$\delta\mu = \mu_c - \mu_a - \mu_b \quad (20)$$

where μ_a and μ_b denote the dipole vectors for the free acid and free base. It is assumed that the vector $\delta\mu$ points from A to B and is directed parallel to the A—H·····B hydrogen-bond axis. The magnitude of $\delta\mu$ provides an approximate measure of hydrogen-bond polarity.

We shall consider mainly the concordant results of recent studies in two independent laboratories [89, 127]. In these studies a single base triethylamine was allowed to interact with a series of substituted phenols of widely varying strength in solvents of low permittivity. This system is attractive because presumably the geometry of the hydrogen bond is unaffected by the changes in phenol substituents. The results obtained for $\delta\mu$ may be summarized as follows (see Fig. 6): In any given solvent, the plot of $\delta\mu$ versus pK_a has a characteristic sigmoid shape; for any given acid-base complex, $\delta\mu$ increases with solvent polarity.

The sigmoid shape of the relationship of $\delta\mu$ versus pK_a is characteristic of an equilibrium involving two discrete species, according to Eq. 19, but it cannot be explained readily in terms of a single hydrogen-bonded species of continuously increasing ion pair character. Thus the dipole moment studies are consistent with existing evidence from IR and UV visible spectra which indicate the presence of two discrete species in equilibrium and a double-well potential minimum [10, 14, 20, 30, 71, 86].

If the existence of two discrete species be accepted, then the value of μ_c can be used to estimate the equilibrium constant. Unfortunately this cannot be done with thermodynamic rigor but requires the making of extrathermodynamic assumptions. Our calculation will be along the lines suggested by Jadzyn and Malecki [89] but will eliminate several unnecessary approximations.

Let P_0 and P_{\pm} denote the molar polarizations of A—H·····B and A[−]·····HB⁺, respectively, and let μ_0 and μ_{\pm} denote the corresponding dipole moments. Let x be the fraction of A—H·····B in the equilibrium mixture, and $K = x/(1 - x)$. Let P_c be the experimental polarization per mole of hydrogen-bonded complex, which will be a weighted average of P_0 and P_{\pm} :

$$P_c = xP_0 + (1 - x)P_{\pm} \quad (21)$$

We may assume, (without much error) that the molecular polarizabilities and molar volumes of A—H·····B and A[−]·····H—B⁺ are equal. It then follows (from either Eqs. 21 and 2 or Eqs. 4 and 5) that μ_c is related to x according to

$$\mu_c^2 = x\mu_0^2 + (1 - x)\mu_{\pm}^2 \quad (22)$$

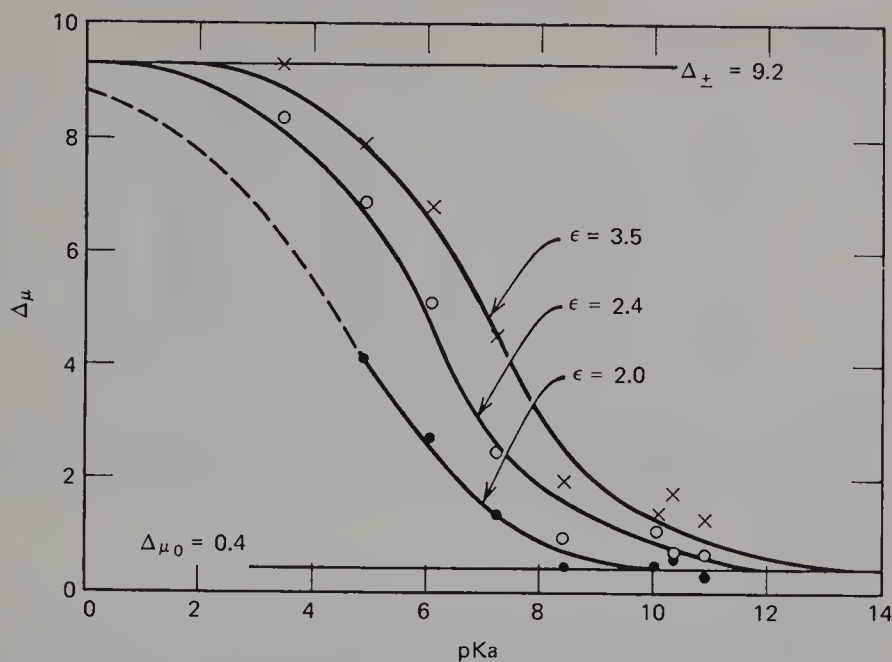


Figure 6. Interaction dipole moment versus pK_a (in water) for acid-base complexes of substituted phenols with triethylamine in cyclohexane ($\epsilon = 2.0$), toluene ($\epsilon = 2.4$), and trichloroethylene ($\epsilon = 3.5$). Data from ref. 89.

Thus if μ_0 and μ_{\pm} can be evaluated independently, x (and hence K) can be derived from the experimental value of μ_c .

To evaluate μ_0 and μ_{\pm} , we write the vector equations

$$\mu_0 = \mu_a + \mu_b + \delta\mu_0 \quad (23a)$$

$$\mu_{\pm} = \mu_a + \mu_b + \delta\mu_{\pm} \quad (23b)$$

where $\delta\mu_0$ and $\delta\mu_{\pm}$ denote the interaction dipole moments of the discrete species. We then note that the plots of $\delta\mu$ versus pK_a (Fig. 6) appear to approach well-defined asymptotes, which are independent of the solvent and the acid. It therefore seems reasonable to assume that for *any* acid in the series, $\delta\mu_0$ is given by the lower asymptote, 0.4 D, and $\delta\mu_{\pm}$ is given by the upper asymptote, 9.2 D.

Experimental dipole moments μ_c and equilibrium constants derived from them by the preceding method are summarized in Table 7. It is gratifying to note that the values of K increase with the strength (pK_a) of the acid and with the permittivity of the solvent. Indeed, plots of $\log K$ versus pK_a are approximately straight lines with slopes of about 0.4 for each solvent [89, 127].

To interpret the increase of K with solvent polarity, Jadzyn and Malecki [89] used the model of equilibrium between two nonpolarizable dipoles in a

Table 7 Analysis of Dipole Moments for Substituted Phenol-Triethylamine Complexes According to Eq. 33^a

Substituted Phenol ^b	pK _a (in water)	μ_0 (D) ^c	μ_{\pm} (D) ^c	Cyclohexane		Toluene		Cl ₂ C=CHCl	
				μ_c (D)	K^d	μ_c (D)	K^d	μ_c (D)	K^d
<i>m</i> -NO ₂	8.35	5.05	13.75	5.1	—	5.6	0.037	6.6	0.124
<i>p</i> -NO ₂	7.15	5.90	13.84	6.7	0.069	7.6	0.172	9.45	0.533
2,4,6-Cl ₃	6.0	2.61	11.35	4.9	0.164	7.2	0.585	8.9	1.46
Cl ₅	4.82	3.20	11.96	6.9	0.392	9.6	1.61	10.6	3.33
2,6-Br ₂ -4-NO ₂	3.39	4.20	12.71	—	—	11.8	5.45	12.7	—

^a Data of ref. 89.^b Dipole moments of uncomplexed phenols: *m*-NO₂, 3.92; *p*-NO₂, 5.06; 2,4,6-Cl₃, 1.50; Cl₅, 2.05; 2,6-Br₂-4-NO₂, 3.17; Et₃N, μ_b = 0.78 D. For direction of dipole vectors, see ref. 86.^c Equation 23.^d Based on Eq. 21-22.

dielectric continuum [23]. For a mole of spheres of uniform radius b , and dipole moment μ , the standard free energy of transfer from the gas phase to a liquid medium of permittivity ϵ is given by Eq. 24, in which N_0 is Avogadro's number:

$$G_{\epsilon} - G_g = -N_0 \frac{\mu^2}{b^3} \frac{\epsilon - 1}{2\epsilon + 1} \quad (24)$$

Jadzyn and Malecki assumed that A—H·····B and A[−]·····HB⁺ have the same radius b , and that this radius may be estimated from the molar volume V according to $4\pi N_0 b^3/3 = V$. Thus for the equilibrium shown in Eq. 19, they obtained

$$\Delta G^0 = \Delta G_g^0 - \frac{4\pi N_0^2 (\epsilon - 1)}{3V(2\epsilon + 1)} (\mu_{\pm}^2 - \mu_0^2) \quad (25)$$

The physical significance of this equation is seen in Fig. 7. In the example chosen, ΔG_g^0 is positive, that is, the more polar ion pair A[−]·····H—B⁺ is less stable than A—H·····B in the gas phase. However, this relationship changes with increasing $(\epsilon - 1)/(2\epsilon + 1)$, because the stabilization of the highly polar ion pair is proportional to μ_{\pm}^2 , whereas that of the nonionic complex is proportional to the much smaller quantity μ_0^2 . The semiquantitative agreement between predictions based on Eq. 25 and equilibrium constants listed in Table 7 is illustrated in Fig. 8. The experimental slopes are roughly one-half the predicted slopes.

In our view, the importance of Eq. 25 lies not so much in its quantitative success at reproducing data (which is limited) as in the qualitative relationships it predicts. As ϵ becomes large without limit, $(\epsilon - 1)/(2\epsilon + 1)$ approaches a limiting value of 0.5. Thus if $\epsilon > 15$, $(\epsilon - 1)/(2\epsilon + 1)$ is already

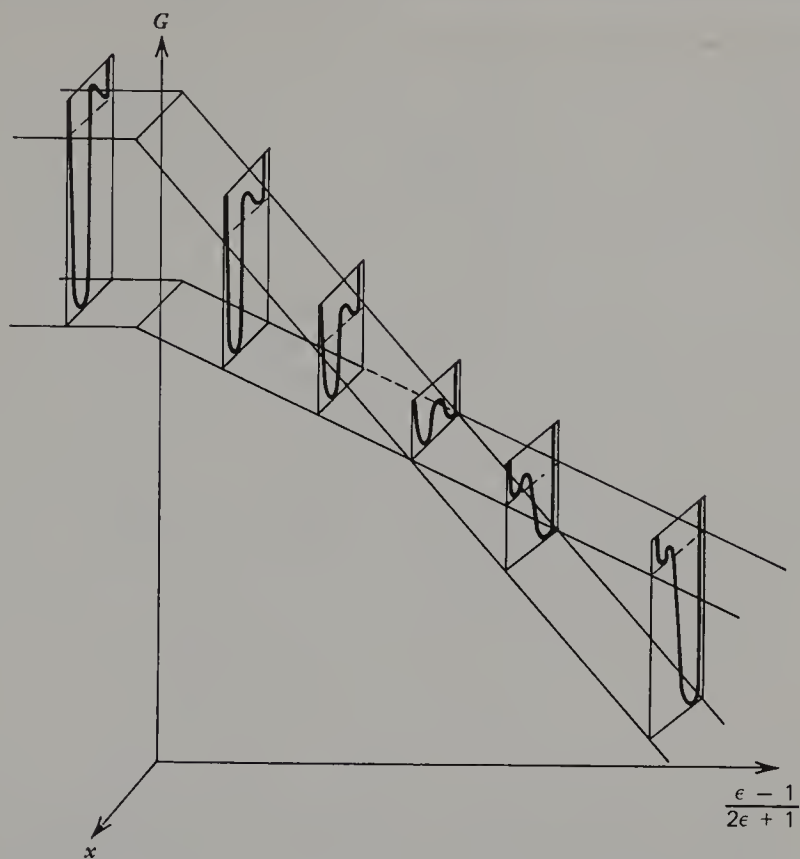


Figure 7. Free energy of $A-H \cdots B$ and $A^- \cdots HB^+$ as a function of $(\epsilon - 1)/(2\epsilon + 1)$ according to Eq. 25. The x -axis denotes the position of the proton and points in the direction from atom B to atom A. Reprinted with permission from ref. 89.

within 10% of its limiting value, and K should therefore be relatively insensitive to the permittivity. This predicted lack of sensitivity of K to the solvent has in fact been noted for proton transfer within hydrogen-bonded complexes [67].

In conclusion, dipole moments of acid-base complexes yield a clear insight into the mechanism of proton transfer and lead to equilibrium constants of at least semiquantitative accuracy.

2.3.3. Ultrafast Proton Transfer. Time-Averaging of Fluctuating Dipole Moments

The electric dipole moment of a molecule is always a rapidly fluctuating function of time. The instantaneous dipole moment will vary due to the motions of electrons and polar modes of vibration, due to conformational changes and Walden inversion of polar centers, and due to intramolecular reactions such as proton transfer within a hydrogen-bonded acid-base complex.

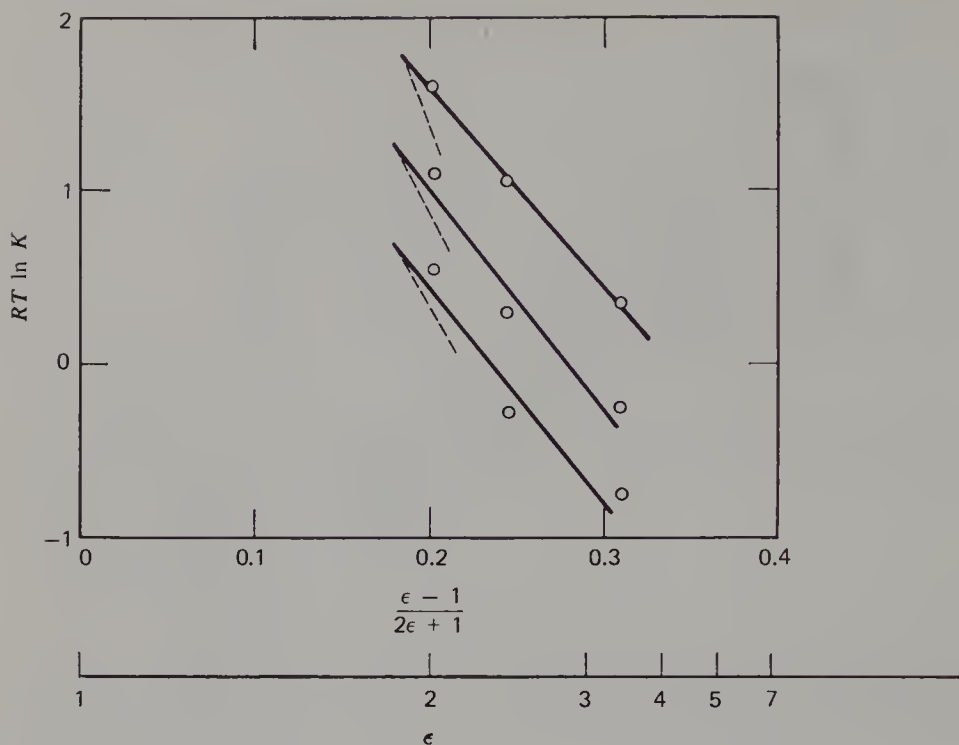


Figure 8. Plots of $-RT \ln K$ for proton transfer to triethylamine versus $(\epsilon - 1)/(2\epsilon + 1)$. The slopes predicted according to Eq. 25 are indicated as dashed lines. Acid: top, *p*-nitrophenol ($V = 236$ ml); middle, 2,4,6-trichlorophenol ($V = 280$ ml); bottom, pentachlorophenol ($V = 290$ ml). Some of the molar volumes (V) of the acid-base complexes were estimated from constitutive parameters.

Electric dipole moments derived from the static permittivity are time-averaged dipole moments in which the time average is taken over a period τ called the *dielectric relaxation time*. On the macroscopic scale, dielectric relaxation is the process in which dipoles partly oriented by an electric field relax to random orientations after the field is turned off. In first approximation, the rate of change of the electric polarization P toward its equilibrium value P_e in the given field follows first-order kinetics:

$$\frac{dP}{dt} = \frac{P_e - P}{\tau} \quad (26)$$

Note that $1/\tau$ is the analog of a first-order rate constant. For the regular small molecules in liquids of ordinary viscosity, τ is usually in the range 10^{-10} – 10^{-12} sec.

If the rate constant for an intramolecular process is high compared to $1/\tau$, then the measured dipole vector is the *mean* of the instantaneous dipole vectors. If it is small compared to $1/\tau$, then the measured (scalar) dipole

moment is the root mean square (rms) dipole moment. For instance, the measured dipole moment for the benzene molecule is zero even though on the time scale of electronic motions (10^{-15} sec) the benzene molecule is highly polar. However, the dipole vectors change rapidly, and their mean value throughout the period τ is zero. On the other hand, the measured dipole moment for the ammonia molecule is 1.5 D in spite of the well-known Walden inversion about nitrogen.

The physical basis for the change in the average dipole moment, as the rate constant for an intramolecular process passes through $1/\tau$, will be derived in the Appendix. The phenomenon is of interest in connection with hydrogen-bonded acid-base complexes because there is much evidence that proton transfer according to Eq. 19 is ultrafast, the rate constant for proton exchange being one or two orders of magnitude greater than that for dielectric relaxation [67]. If this evidence is valid, then the treatment of the data described in the preceding section will have to be modified. Equation 22, it will be noted, expresses μ_c as a rms dipole moment, with μ_0^2 and μ_{\pm}^2 being weighted according to the respective mole fractions x and $(1 - x)$. The treatment therefore implies that proton transfer is slow compared to $1/\tau$.

If proton transfer were in fact fast compared to $1/\tau$, the data would have to be treated in a different way. In particular, the dipole vector μ_c of the acid-base complex would be given by Eq. 27 instead of Eq. 22. The molar free energy G_c of the complex would be expressed by Eq. 28, in which a single term proportional to μ_c^2 accounts for the dipole solvation; and the condition that thermodynamic equilibrium exists would be expressed by Eq. 29. Research is currently in progress in the authors' laboratory to test this hypothesis.

For fast exchange:

$$\mu_c = x\mu_0 + (1 - x)\mu_{\pm} \quad (27)$$

$$G_c = xG_0 + (1 - x)G_{\pm} + RT [x \ln x + (1 - x) \ln (1 - x)] - \frac{4\pi N_0^2(\epsilon - 1)\mu_c^2}{3V(2\epsilon + 1)} \quad (28)$$

$$(\partial G_c / \partial x)_{T, \epsilon} = 0 \quad (29)$$

2.4. Association and Molecular Complex Formation

It has been emphasized throughout preceding chapters of this treatise that ion pairs associate—with other ion pairs, or polar ligands, or solvent molecules—to form complexes in which the mutual interaction of the ions is quite different from that in the original ion pairs. For example, there is spectroscopic evidence for lithium fluorenone that complexation of the lithium ion with agents such as glymes or crown ethers converts the originally tight

ion pair into a loose pair in which the polarization of the electron distribution of fluorenone ion is reduced [138, 139]. We may expect that a change in electron distribution such as this will have a marked effect on the electric dipole moment.

In view of the insights that can be gained, it is perhaps surprising that the effects of association and molecular complex formation on the dipole moment have received so little attention in previous research on ion pairs. In the following discussion we shall examine the available information, including recent results obtained in our own laboratory.

2.4.1. Dielectric Measurement of Association Constants

The concentrations at which the association of ion pairs is studied experimentally are low enough so that the change in permittivity, or dielectric increment $\Delta\epsilon$, for each species is proportional to its concentration. This fact is expressed by Eq. 30, in which ϵ_0 is the permittivity of the pure solvent, S_i is the molar dielectric increment, and c_i is the molar concentration (per liter) for the i th species. The summation $\sum S_i c_i$ extends over all solutes:

$$\Delta\epsilon = \epsilon - \epsilon_0 = \sum S_i c_i \quad (30)$$

According to Eq. 30, the relationship of $\Delta\epsilon$ to molar concentrations is mathematically analogous to that of the optical density per centimeter, which is given by the familiar relation $A/l = \sum \epsilon_i c_i$. The measurement of an association constant by means of the dielectric increment is therefore identical in principle to that by means of light absorption, which has been thoroughly discussed [19, 130].

For example, let the stoichiometry of the association process be that shown in Eq. 31:



let c_A and c_B denote formal (i.e., total) concentrations, and let $[A]$, $[B]$, and $[C]$ denote molar concentrations. On writing $\Delta\epsilon = S_A[A] + S_B[B] + S_C[C]$ and applying the conditions of mass balance, we then obtain

$$\delta\Delta\epsilon = \Delta\epsilon - S_A c_A - S_B c_B = (S_C - S_A - S_B)[C] \quad (32)$$

which defines an experimental quantity $\delta\Delta\epsilon$ that is directly proportional to $[C]$. The required values of S_A and S_B are obtained from measurements on the separate solutes. Measurements of $\delta\Delta\epsilon$ for a number of (c_A, c_B) pairs then enables us to deduce K and $S_C - S_A - S_B$ by suitable statistical methods [22, 74, 149].

The relationship of the molar dielectric increment S_i to the dipole moment μ_i of the given species depends on the theory used for interpreting the dielectric data [39, 68, 73, 81]. If Debye's Eq. 1 is used, it can be shown that S_i is related to the molar polarizations P_i , P_s and the molar volumes V_i , V_s of the

solute i and solvent s :

$$S_i = \frac{(\epsilon_0 + 2)^2}{3000} \left(P_i + \frac{V_i P_s}{V_s} \right) \quad (33)$$

The denominator here is 3000 rather than 3 because c_i is expressed in moles per liter rather than moles per cubic centimeter. The polarizations P_i and P_s are expressed by Eq. (2). For complex formation according to Eq. 31 it is reasonable to assume that $\alpha_C = \alpha_A + \alpha_B$ and that $V_C = V_A + V_B$. The experimental parameter $S_C - S_A - S_B$ is therefore given by

$$S_C - S_A - S_B = \frac{4\pi N_0(\epsilon_0 + 2)^2}{27,000kT} (\mu_C^2 - \mu_A^2 - \mu_B^2) \quad (34)$$

Expressions for S_i when the Onsager or Kirkwood equations are used have been given elsewhere [39, 68]. If the Onsager equation is applied to complex formation according to Eq. 31, it is reasonable to assume that $\alpha_C^* = \alpha_A^* + \alpha_B^*$ and that $V_C = V_A + V_B$. On that basis, the experimental parameter $S_C - S_A - S_B$ is given by Eq. 35:

$$S_C - S_A - S_B = \frac{4\pi N_0}{9000kTA} (\mu_C^2 - \mu_A^2 - \mu_B^2) \quad (35a)$$

$$A = \frac{2\epsilon_0^2 + 1}{9\epsilon_0^2} - \frac{12\varphi_0\{[(\epsilon_0 - 1)(\epsilon_0 + 2)/9\epsilon_0] - \varphi_0/2h_0\}}{h_0(2\epsilon_0 + 1)^2} \quad (35b)$$

$$h_0 = 1 - \frac{2\varphi_0(\epsilon_0 - 1)}{2\epsilon_0 + 1} \quad (35c)$$

in which φ_0 denotes the specific refraction of the solvent: $\varphi_0 = (n_0^2 - 1)/(n_0^2 + 2)$. It is clear from Eqs. 34 and 35 that, in order to evaluate μ_C , it is necessary that μ_A and μ_B be available from independent measurements.

Error analysis of the fitted parameters follows the same principles as in the case of spectrophotometric data. The determination of either K or μ_C will be much more accurate if the other parameter is already known from other sources. When both parameters must be determined simultaneously, the accuracy will improve if $S_C - S_A - S_B$ is substantially different from zero. Indeed, when $S_C = S_A + S_B$, $\delta\Delta\epsilon \equiv 0$ and complex formation will have no effect on the permittivity. The condition that $S_C = S_A + S_B$ is realized when $\mu_C^2 = \mu_A^2 + \mu_B^2$. Thus if μ_C is simply the vector sum of μ_A and μ_B , complex formation becomes undetectable when μ_A and μ_B are mutually perpendicular [101].

2.4.2. Ion Pair Dimers

Available data for the dipole moments and formation constants of ion pair dimers are listed in Table 8. The accuracy of the dipole moments is about

Table 8 Dipole Moments and Association Constants for the Formation of Ion Pair Complexes

Reactants		Complex			K (M^{-1})
A	μ_A (D)	B	μ_B (D)	C	
Bu_4NI^a	12.7	Bu_4NI	12.7	Dimer	1,560
Bu_4NBr^a	12.2	Bu_4NBr	12.2	Dimer	2,960
$Bu_4NClO_4^a$	17.2	Bu_4NClO_4	17.2	Dimer	7,760
$i-Am_4NSCN^a$	15.4	$i-Am_4NSCN$	15.4	Dimer	510
$Bu_4N(\alpha-ClAc)^a$	14.8	$Bu_4N(\alpha-ClAc)$	14.8	Dimer	2,660
Bu_4NBz^a	12.1	Bu_4NBz	12.1	Dimer	1,510
$Pr_2NH_2Pi^b$	11.5	Pr_2NH_2Pi	11.5	Dimer	120
$Bu_2NH_2Pi^b$	11.5	Bu_2NH_2Pi	11.5	Dimer	190
Bu_4NBr^c	12.2	CH_3OH	1.70	Composition un- known; 1,1 complex assumed	—
$LiCl^d$	6.78	$LiCl$	6.78	Dimer	183
$LiCl^d$	6.78	p -Nitrophenol	6.40	No interaction	—
$LiCl^d$	6.78	Crown-5	4.00	1,1-complex	6,000
$LiCl^d$	6.78	Crown-6	1.37	No interaction	—
$KOTs^d$	4.81	Crown-5	4.00	1,1-complex	13,000
$KOTs^d$	4.81	Crown-6	1.37	1,1-complex	50,000

^a Ref. 18.^b Ref. 101.^c Ref. 128.^d Ref. 87.

1 D. The ion pair dimers may be divided into two groups on the basis of their dipole moments: nonpolar dimers and polar dimers.

Before discussing the structures of the dimers in detail, we wish to consider the interaction energy of two dipoles [23]. For definiteness, consider the interaction of two dipoles, m_1 and m_2 , separated by a distance s in a medium of unit permittivity. The interaction energy W then varies from a maximum of $+2m_1m_2/s^3$ to a minimum of $-2m_1m_2/s^3$, depending on the relative directions

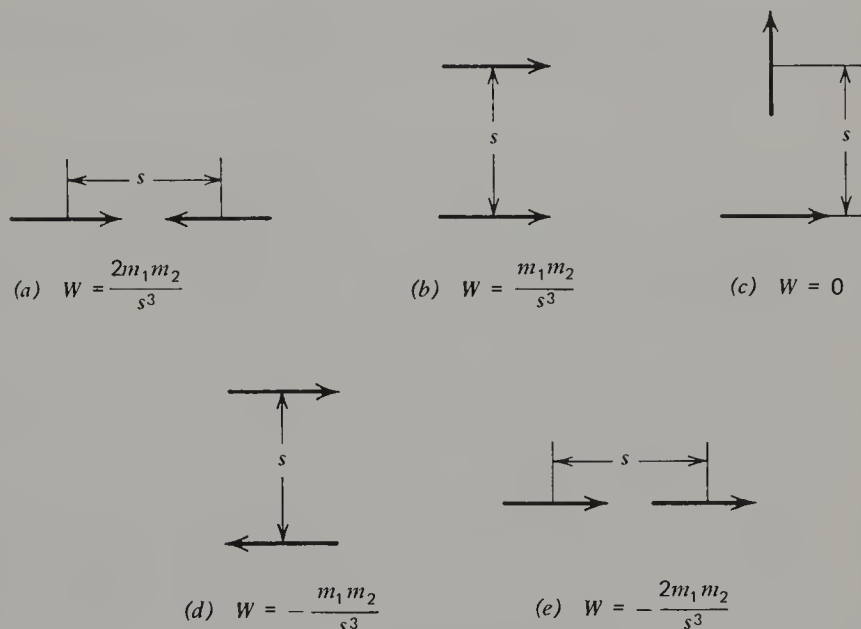


Figure 9. Interaction energies for pairs of dipoles.

of the vectors m_1 , m_2 , and s . Thus the interaction energies for various parallel, perpendicular, or antiparallel arrangements are presented in Fig. 9. Only two types of arrangement lead to stabilization: If the dipoles are opposed, the ion pairs sit side-by-side (e.g., Fig. 9d); if the dipoles point in the same direction, the ion pairs are arranged head-to-tail (e.g., Fig. 9e).

Since the interaction energy varies as the inverse third power of the distance between the dipoles, the *shape* of the *ion pairs* will tend to dictate the most stable configuration of the dimer. As Fuoss has pointed out [58], in most ion pairs the dipole vector is perpendicular to a short axis in the molecule, and the most stable dimer then has a side-by-side configuration. As seen in Fig. 10, two types of side-by-side configuration must be distinguished. In Fig. 10a the dipoles are antiparallel and $\mu = 0$; the ionic charge centers are at the corners of a parallelogram. In Fig. 10b the dipoles are obliquely opposed and μ is not zero, but μ is less than μ_{IP} , the dipole moment of the ion pair monomer; the ionic charge centers are usually not coplanar. In Fig. 10c μ_{IP} is

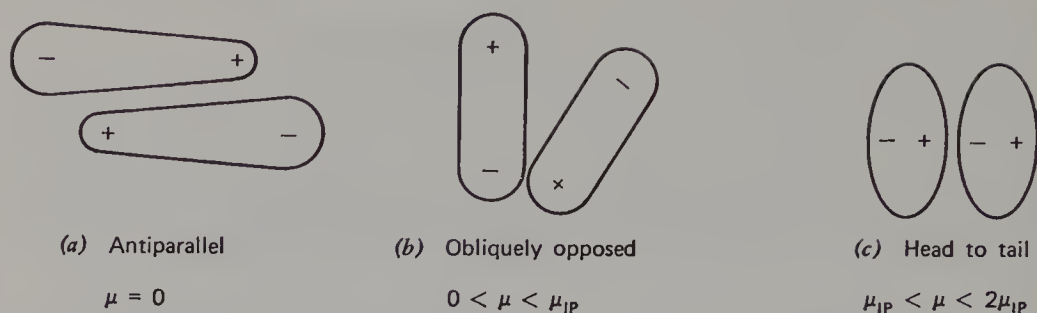


Figure 10. Dipole moment and configuration of ion pair dimers. μ_{IP} is the dipole moment of the ion pair monomer.

pointing along a short axis of the molecule, and the head-to-tail configuration is favored. In this case μ for the dimer will be between μ_{IP} and $2\mu_{IP}$.

As seen in Table 8, the dimer of LiCl has zero dipole moment and therefore an antiparallel side-by-side configuration. The structures of the tetra-*n*-butylammonium salts are more complicated because the Bu_4N^+ ion is not spherical. A reasonable model is to regard the ion as consisting of a central sphere from which four flexible limbs stick out in tetrahedral directions. In the ion pair the anion probably sits on a "threefold axis," that is, in the cavity formed by three limbs, so that the ionic centers of charge are at closest approach. Figure 11 is stylized representation of such ion pairs and possible dimers. In the antiparallel configuration, the directions of the tetraalkyl limbs resemble those of the carbon bonds in a somewhat twisted version of ethylene. Molecular models indicate that such a structure is sterically permitted because the alkyl groups are flexible.

In the other dimer shown in Fig. 11, the dipoles are obliquely opposed so that μ for the dimer is nonzero but less than μ_{IP} . According to the data in Table 8, head-to-tail configurations in which $\mu > \mu_{IP}$ have not yet been observed.

In the light of this discussion, the dimers of tetraalkylammonium iodide, bromide, perchlorate, and thiocyanate have antiparallel configurations, whereas those of benzoate and α -chloroacetate have obliquely opposed configurations. For the latter dimers we believe that in one of the anions the two carboxylate oxygens become virtually equivalent by interacting with two cations at closest approach; in the other anion the two oxygen-cation distances are nonequivalent.

The dimers of dipropyl- and dibutylammonium picrate are also polar, with dipole moments whose magnitudes indicate obliquely opposed configurations. In the case of the dimers of other secondary ammonium salts (in which the anions can accept two hydrogen bonds) there is spectroscopic [43] and kinetic [38] evidence for cyclic hydrogen-bonded structures. It is not clear whether

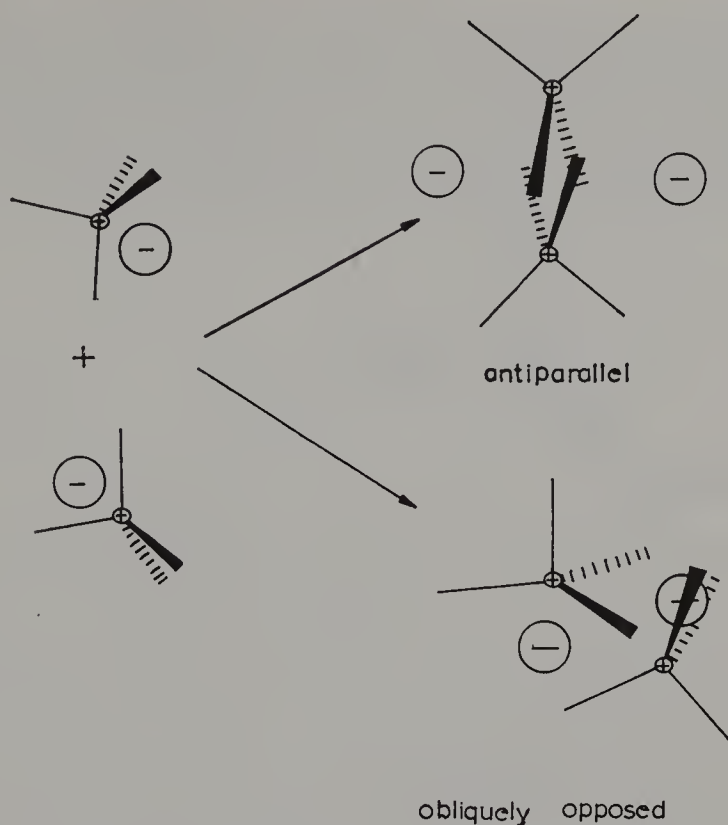


Figure 11. Stylized representation of tetraalkylammonium halide ion pairs and their dimers. The alkyl "limbs" are flexible.

the present dimers will have cyclic hydrogen-bonded structures; if they do, such structures must be nonplanar. The ion pair dimers of long-chain alkylammonium salts also appear to be polar [99].

2.4.3. Molecular Complexes of Ion Pairs

From the point of view of structural chemistry, the measurement of dipole moments for complexes of ion pairs with ligands has two interrelated objectives: to determine the geometry of the complex, and to evaluate any change in electron distribution upon complexation. For the latter purpose it is convenient to define an interaction dipole vector $\delta\mu$ according to Eq. 36,

$$\delta\mu = \mu_C - \mu_{IP} - \mu_L \quad (36)$$

where μ_C , μ_{IP} , and μ_L are the dipole vectors of the complex, ion pair, and ligand, respectively.

The earliest work on the dipole moment of a complex is that of Richardson and Stern [128], who measured the effect of methanol on the molar polarization of tetrabutylammonium bromide in benzene. Their results clearly show

that methanol interacts with the Bu_4NBr ion pairs, because the formation of ion pair dimers is largely suppressed. We have interpreted their data on the assumption that a 1,1-complex is formed in which the methanol molecule is hydrogen-bonded to the bromide ion. The result of the vector analysis is seen in Fig. 12a. It has been assumed in this analysis that $\delta\mu = 0$.

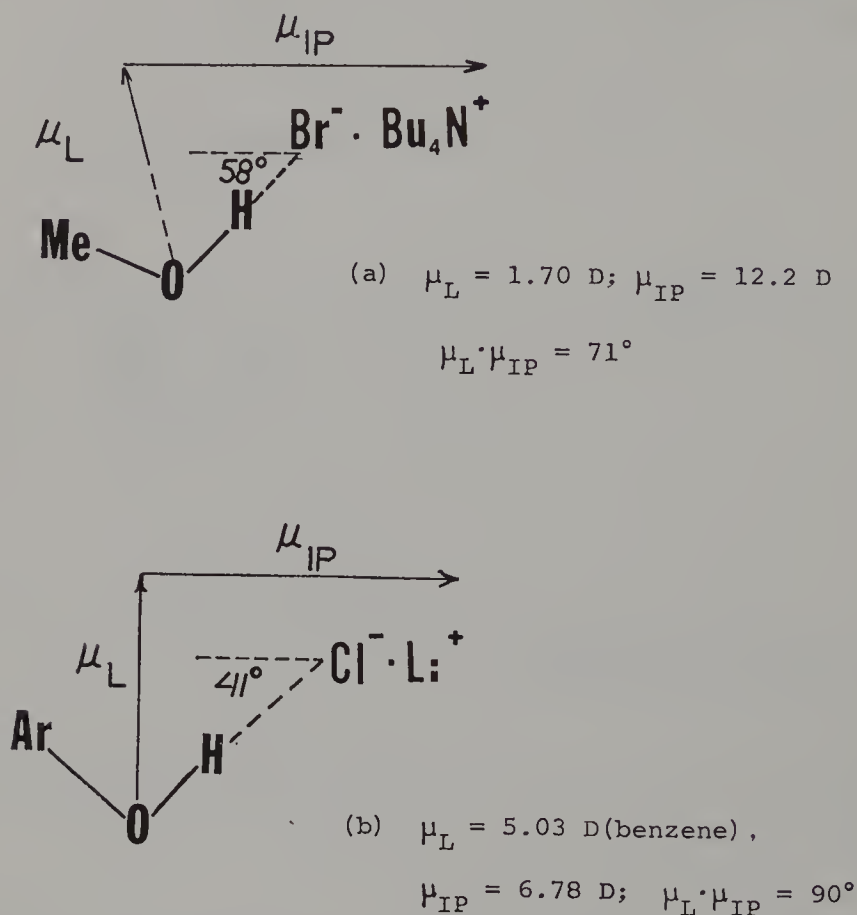
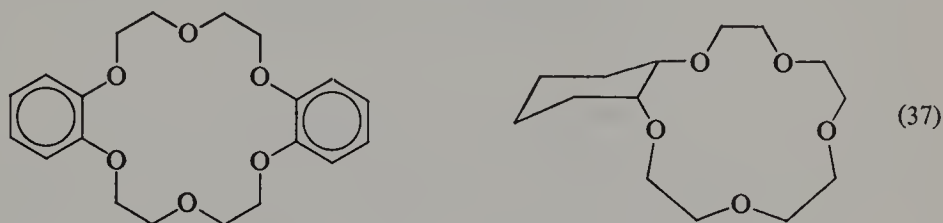


Figure 12. Molecular geometry of two ion pair complexes in which the ligand is hydrogen bonded to the anion, as determined by analysis of dipole moments. Rotation of MeOH and ArOH about an axis defined by μ_{IP} is permitted.

Preliminary work in our own laboratory suggests a very similar structure for the complex of *p*-nitrophenol with lithium chloride. For solutions containing both substances as dilute solutes in octanoic acid, $\delta\Delta\epsilon$ (Eq. 32) is practically zero. This means either that hydrogen-bonded complexes are not formed, or (if they are formed and $\delta\mu \approx 0$) that the *p*-nitrophenol dipole will be perpendicular to the LiCl dipole, as in Fig. 12b. Even though the existence of such complexes has not been proved yet, we regard it as probable. The marked tendency of *p*-nitrophenol toward hydrogen-bond formation in

this medium is indicated by the high value of its apparent dipole moment (6.40 D); in benzene, the dipole moment of *p*-nitrophenol is 5.06 D [89, 103].

To study the effect of complex-formation to the cation in an ion pair, we have obtained data for the association between LiCl or potassium *p*-toluenesulfonate (KTs) and two crown ethers, dibenzo-18-crown-6 and cyclohexyl-15-crown-5, whose structural formulas are presented in Eq. 37.*



In solvents of high permittivity, crown-6 is a good ligand for potassium ion and crown-5 is a good ligand for both potassium ion and lithium ion [31, 54, 55, 88, 112, 113, 115].

Our own measurements were made in octanoic acid, whose low permittivity ($\epsilon = 2.48$) indicates that this acid exists predominantly in the form of non-polar hydrogen-bonded dimers. It turns out that $\delta\Delta\epsilon$ for complex formation is large, and the complexes have a 1,1-stoichiometry. The association constants (Table 8) are of a plausible magnitude† and follows trends similar to those observed for the free ions [31, 54, 88, 112, 113]. The dipole moments of the complexes are high, and it becomes of interest to ask whether there has been a change from tight to loose ion pairs. To answer this question, we shall calculate $\delta\mu$ (Eq. 36) and see whether there has been a “loosening” or reduction in the mutual polarization of the ions.

Since Eq. 36 is a vector equation, we must first establish the vectors μ_C , μ_L , and μ_{IP} . Beginning with μ_{IP} , for lithium chloride the dipole is parallel with the LiCl bond axis. For KOTs, two plausible structures may be proposed. Figure 13a is an unsymmetrical structure, with the cation interacting strongly with only one of the three oxygen atoms. The structure in Fig. 13b is more symmetrical, with the cation interacting equally with all three oxygen atoms.

Of the two structures in Fig. 13, only the lower is consistent with the experimental dipole moment of 4.81 D in the ion pair. Following the previous analysis, we shall represent μ_{IP} as the sum of a vector μ_- assignable to the

* It is not known at this writing whether the crown-5 ether is the 1,2-*cis*- or 1,2-*trans*-cyclohexane isomer. The experimental dipole moment could be consistent with either isomer. For definiteness in the following discussion, we shall assume the *cis*-structure.

† The association constant for the complex between KTs and crown-6 has been confirmed spectrophotometrically.

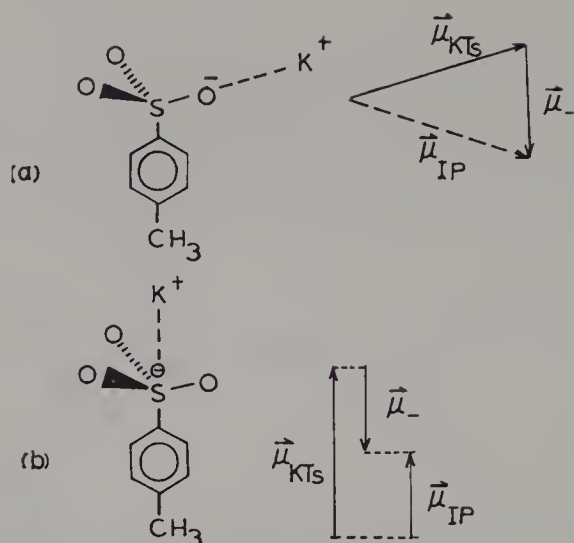


Figure 13. Plausible structures and the corresponding dipole-moment diagrams for potassium *p*-toluenesulfonate ion pairs.

p-toluenesulfonate anion, and a vector μ_{K+Ts^-} due to the ionic charges and their mutual polarization. The value of μ_- may be estimated with good accuracy from the experimental dipole moment of *p*-toluenesulfonyl chloride, 5.04 D [103], and a small correction (0.5 D, added vectorially) to account for the electronegativity difference between oxygen and chlorine. The result is $\mu_- = 5.2$ D. Structure *a* may then be ruled out because the vector equation, $\mu_{IP} = \mu_- + \mu_{K+Ts^-}$, has no solution. The minimum possible value for μ_{IP} is 4.90 D when $\mu_{K+Ts^-} = 1.75$ D. Even if we allow errors of 0.2 D in the measurement of μ_{IP} and estimation of μ_- , the maximum value for μ_{K+Ts^-} cannot exceed 2.5 D. In view of data for the potassium halides listed in Table 1, such a value is totally implausible. On the other hand, if we assume structure *b*, μ_- and μ_{K+Ts^-} are antiparallel, and μ_{K+Ts^-} is evaluated as 10.0 D. This result is fully consistent with values for the potassium halides.

Molecular models suggest that the *cis*-isomer of crown-5 has a fairly rigid 15-membered ring structure, with four C—O—C dipoles pointing "down" with respect to the plane of the ring, and the fifth dipole lying roughly in the plane of the ring. Adopting 1.3 D for each C—O—C dipole (this is the experimental value for diethyl ether), this model is consistent with the experimental dipole moment of 4.00 D. On complexing with a cation, the conformation of the C—O—C dipoles could change somewhat. However, the molecular models indicate that major changes are unlikely due to the incursion of considerable strain in the cyclohexane ring. It seems reasonable, therefore, to let $\mu_L = 4.0$ D. The direction of μ_L would be roughly collinear with μ_{IP} for both LiCl and KTs.

Molecular models suggest that crown-6 has several stable conformations



(a) CROWN-6, nonpolar conformation



(b) CROWN-6, polar conformation

Figure 14. Some conformations of crown-6 ether. Conformation (b) is favorable for complex formation.

of comparable free energy. These stable conformations represent a favorable compromise between minimizing the repulsion of the nonbonded electrons on different oxygen atoms and minimizing the repulsion among nonbonded hydrogen atoms and angle strain. To reduce the repulsion among nonbonded atoms, the C—O—C bond dipoles must point in different directions for nearby oxygen atoms, so that the dipole moment for the entire molecule will tend to be small. Thus Fig. 14a shows a nonpolar conformation whose free energy should be low. Other stable conformations suggested by the molecular models should be slightly polar. The experimental dipole moment of 1.37 D is consistent with this view.

Because the C—O—C dipoles in the stable crown-6 conformations point different directions, the stable conformations are not particularly good ligands. However, there is a polar conformation (Fig. 14b) in which all the C—O—C dipoles point toward a common focus. This conformation is particularly favorable for complex formation to cations, since the six oxygen atoms form a cavity in which a cation can sit without steric interference by the rest of the molecule. The size of this cavity matches that of the potassium ion [31, 54, 55, 88], which accounts for high association constants for it and potassium ion. We estimate that the dipole moment of this polar conformation is about 4.0–4.6 D. It seems reasonable therefore to let $\mu_L = 4.3 \pm 0.3$ D, with a direction that is collinear with μ_{IP} .

On the basis of this analysis and values of μ_C listed in Table 8, we calculate $\delta\mu$ as follows:

LiCl · crown-5	$\delta\mu = 9.97 - 6.78 - 4.00 = -0.81$ D
KTs · crown-5	$\delta\mu = 8.92 - 4.81 - 4.00 = 0.11$ D
KTs · crown-6	$\delta\mu = 8.27 - 4.81 - 4.3 = -0.8$ D

Thus we find that $\delta\mu$ is either close to zero or slightly negative.

At first sight, a negative value of $\delta\mu$ may suggest a reduced distance between the ionic centers of charge. However, this analysis overlooks the effect of the considerable polarizability of the crown ligand. In applying Böttcher's model to interpret these results, we consider the cation with its associated ligand as a single polarizable point charge superposed on the dipole moment of the ligand, with the polarizability being the sum of the polarizabilities of the cation and the ligand [87]. On this basis we find that the cation-anion distance is actually stretched by a few tenths of an Ångstrom unit in $\text{LiCl} \cdot \text{crown-5}$ and $\text{KTs} \cdot \text{crown-6}$, and that it is perhaps slightly stretched in $\text{KTs} \cdot \text{crown-5}$ [87]. This conclusion is consistent with bond distances in *solid* $\text{RbNCS} \cdot \text{crown-6}$ and $\text{NaBr} \cdot \text{crown-6}$, as revealed by X-ray crystallography [145a]. It is also consistent with spectroscopic evidence summarized by Smid [138, 139] which indicates a "loosening" of the mutual polarization of the ions in fluorenone ion pairs upon complex formation to the cation.

3. DIELECTRIC RELAXATION OF ION PAIRS

By measuring the permittivity as a function of frequency one can derive dielectric relaxation times. Such experiments give further insight into molecular structure and complement the information derived from the measurement of static permittivities. In particular, one can learn about the mechanism and energetics of dipole reorientation, whether it involves rotation of the ion pair as a rigid unit, or whether the point of contact between the ions shifts. In some cases one can determine the degree of flexibility of polar part structures and the rates of internal rotations. By deducing the hydrodynamic radius, one can hope to detect the existence of solvent-solute complexes. If the experiment reveals several discrete relaxation times or a distribution of relaxation times, one can learn about heterogeneity on the microscopic level, either of the solute itself or of its solvent cage, and in favorable cases determine the rates of exchange.

3.1. Theory of Dielectric Relaxation

Although the basic theory of dielectric relaxation is well established, the description of the relaxation process in terms of molecular motions is intricate and continues to be a subject of deep concern [6, 35, 64, 151]. In this section we shall give a brief summary of those facets of the theory that are useful for the following discussion.

3.1.1. Debye's Theory of Dielectric Relaxation

When an alternating electric field $E(t)$ is applied to a dielectric, the polarization P is also a function of time. Debye assumed that there is a single relaxation time τ and that the relaxation behavior is described by a first-order

differential equation:

$$\tau \frac{d\mathbf{P}}{dt} + \mathbf{P} = \frac{k_\epsilon(\epsilon_s - \epsilon_\infty)\mathbf{E}}{4\pi} \quad (38)$$

According to Eq. 38, there is a time lag between \mathbf{P} and \mathbf{E} , depending on the frequency f (in herz) or ω (in radians; $\omega = 2\pi f$) of the alternating field. Since $\epsilon = 1 + 4\pi\mathbf{P}/k_\epsilon\mathbf{E}$, Eq. 38 can be solved to obtain the permittivity ϵ^* as a function of ω :

$$\epsilon^* = \epsilon' - j\epsilon'' = \epsilon_\infty + \frac{\epsilon_s - \epsilon_\infty}{1 + j\omega\tau} \quad (39)$$

Because of the phase-lag between \mathbf{P} and \mathbf{E} , ϵ^* is a complex variable; ϵ' is the component in-phase with \mathbf{E} , and ϵ'' is the component that is 90° out of phase. The minus sign implies that \mathbf{P} lags behind \mathbf{E} . ϵ_s is the static permittivity, which up to now has been denoted simply by ϵ , ϵ_∞ is the "high-frequency" permittivity, that is, the limit reached by the permittivity when the frequency of \mathbf{E} is so high that the torque acting on the dipoles cannot overcome the molecular inertia.

The components ϵ' and ϵ'' are obtained as a function of frequency by rationalizing Eq. 39:

$$\epsilon' = \epsilon_\infty + \frac{\epsilon_s - \epsilon_\infty}{1 + \omega^2\tau^2} \quad (40a)$$

$$\epsilon'' = \frac{(\epsilon_s - \epsilon_\infty)\omega\tau}{1 + \omega^2\tau^2} \quad (40b)$$

In Fig. 15 ϵ' and ϵ'' are shown as functions of $\log \omega$ for $\tau = 10^{-10}$ sec. In this example, $\epsilon_s = 10$ and $\epsilon_\infty = 2$. Note that ϵ' decreases with increasing frequency; at half-decade the frequency ω^* equals $1/\tau$. The out-of-phase component ϵ'' approaches zero at both low and high frequencies and goes through a maximum, at which $\epsilon'' = (\epsilon_s - \epsilon_\infty)/2$, at the same frequency ω^* at which ω equals $1/\tau$.

Cole and Cole [36] have shown that when ϵ'' is plotted versus ϵ' , that is, when ω is eliminated between Eqs. 40a and 40b, the result is a semicircle, as seen in Fig. 16. Each point on the semicircle corresponds to a specific frequency; as ω increases, motion along the semicircle is from right to left. At the point over the center, $\omega = 1/\tau$.

3.1.2. Polar Solutes in Nonpolar Solvents

A common experimental arrangement is to measure the dielectric relaxation of a polar substance in dilute solution in a nonpolar solvent. In this case we may assume that the dielectric constant ϵ_0 and the molar polarization P_S

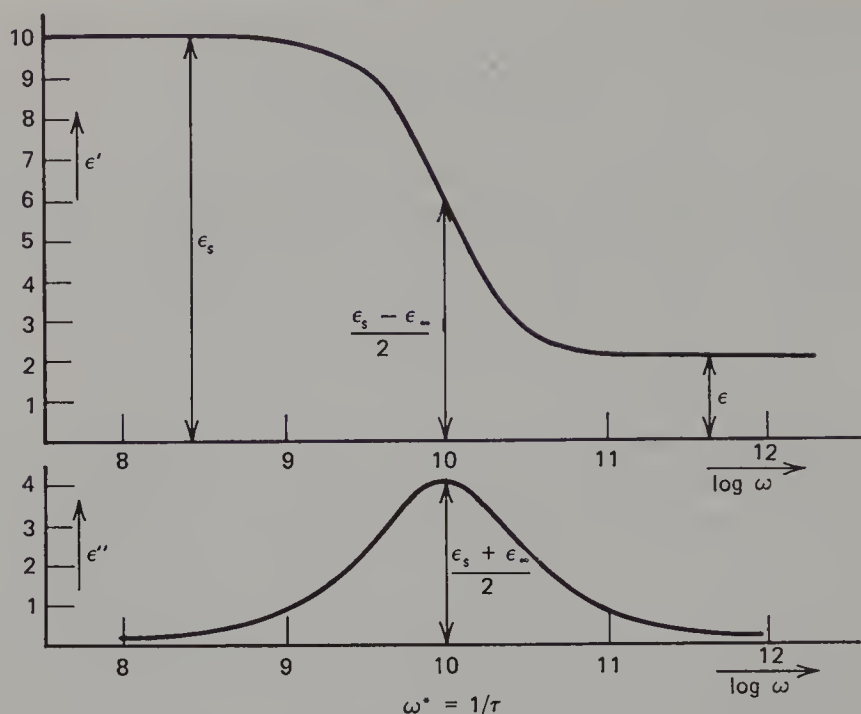


Figure 15. Graph of Eq. 40. $\epsilon_s = 10$, $\epsilon_\infty = 2$, $\tau = 1 \times 10^{-10}$ sec.

of the solvent are independent of frequency. Thus $(\epsilon_s - \epsilon_\infty)$ in Eq. 39 becomes $\Delta\epsilon_s - \Delta\epsilon_\infty$. On letting c_2 denote the molar concentration and τ_2 the dielectric relaxation time of the solute, and on writing $\Delta\epsilon_s = S_{2,s}c_2$ and $\Delta\epsilon_\infty = S_{2,\infty}c_2$ (cf. Eq. 30), Eq. 39 becomes

$$\epsilon^* = \epsilon_\infty + \frac{(S_{2,s} - S_{2,\infty})c_2}{1 + j\omega\tau_2} \quad (41)$$

Since the solvent is nonpolar, Debye's theory may be used. Thus $(S_{2,s} - S_{2,\infty})$ may be evaluated by use of Eq. 33 with $(P_{2,s} - P_{2,\infty}) = 4\pi N_0\mu_2^2/9kT$ and $(P_{S,s} - P_{S,\infty}) = 0$. This leads to the useful result

$$\epsilon^* = \epsilon_\infty + \frac{(\epsilon_0 + 2)^2 4\pi N_0\mu_2^2 c_2}{27,000kT(1 + j\omega\tau_2)} \quad (42)$$

On comparing Eq. 42 with Eq. 39, we find an exact mathematical analogy, with τ_2 taking the place of τ . The magnitude of the relaxation step, that is, the value of $\epsilon_s - \epsilon_\infty$, is proportional to $\mu_2^2 c_2$. Thus nonpolar solutes do not give dielectric relaxation.

If the solution contains a number of independent polar species, each having a characteristic relaxation time τ_i , then Eq. 42 may be written in the general form

$$\epsilon^* = \epsilon_\infty + \frac{4\pi N_0(\epsilon_0 + 2)^2}{27,000kT} \sum_i \frac{\mu_i^2 c_i}{1 + j\omega\tau_i} \quad (43)$$

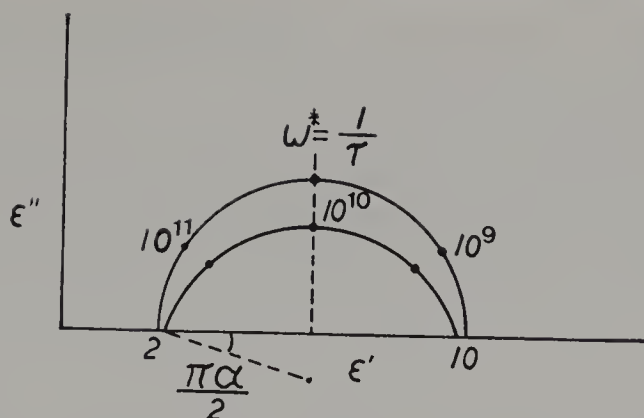


Figure 16. Cole-Cole plots of ϵ'' versus ϵ' for $\epsilon_s = 10$, $\epsilon_\infty = 2$, and $\tau = 1 \times 10^{-10}$ sec. Solid semicircle, for relaxation with a single relaxation time according to Eq. 39. Lower arc, for a distribution of relaxation times according to Eq. 44.

In this context, molecular species are “independent” if the rate of any inter-conversion among them is slow compared to the dielectric relaxation rates. According to Eq. 43, the total relaxation is the sum of independent relaxation steps, with the magnitude of each step being proportional to $\mu_i^2 c_i$ for the respective solute species. It should be noted that since ϵ^* is a complex variable, the summation indicated in Eq. 43 is in effect a vector summation.

For solutions in *polar* solvents, the relaxation due to dilute solutes is often masked by the dominant relaxation of the solvent. However, in some cases the relaxation times of solvent and solute are far enough apart so that the independent relaxation steps can be resolved. In such cases Eq. 41 may be applied, provided that suitable values are chosen for ϵ_s and ϵ_∞ . However, the molar dielectric increments S must be calculated according to Onsager’s or Kirkwood’s theory.

3.1.3. Distribution of Relaxation Times

Although the theory involving a single relaxation time (Eq. 39) fits many data quite well, most plots of ϵ' and ϵ'' versus $\log \omega$ tend to be broader than predicted by Eqs. 40. Cole and Cole [36] found that in such cases the empirical equation 44 often reproduces the facts:

$$\epsilon^* = \epsilon_\infty + \frac{\epsilon_s - \epsilon_\infty}{1 + (j\omega\tau_0)^{1-\alpha}} \quad (44)$$

A plot of ϵ' and ϵ'' according to Eq. 44 is a circular arc, as in Fig. 16, whose center lies below the ϵ' -axis. The frequency ω of the point on the arc over the

center is equal to $1/\tau$. The parameter α may be evaluated by constructing the angle shown in Fig. 16.* In most cases in which Eq. 44 fits the data, α is less than 0.2; values in excess of 0.5 are rare.

Cole and Cole pointed out that Eq. 44 implies not a single, uniform relaxation time τ , but a continuous distribution of relaxation times about a most probable value τ_0 . This distribution is plotted as a function of $\log(\tau/\tau_0)$ in Fig. 17. The distribution function is symmetrical and somewhat sharper than a

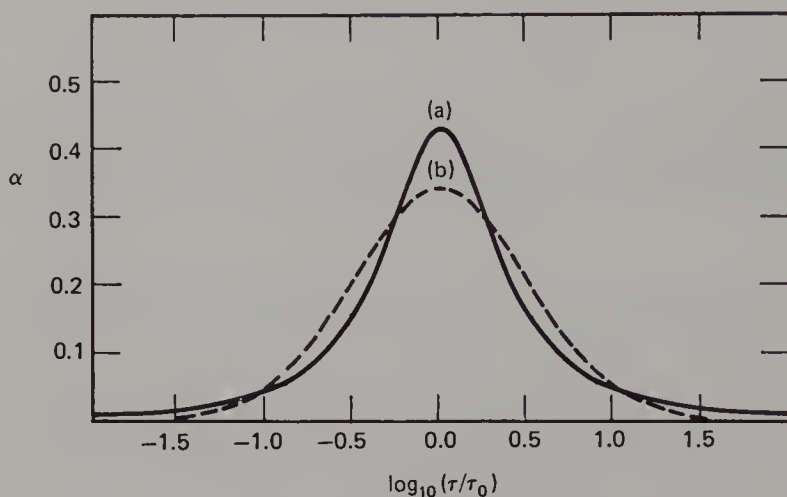


Figure 17. Distribution of dielectric relaxation times. Solid curve, distribution corresponding to Eq. 44 with $\alpha = 0.23$. Dashed curve, a corresponding Gaussian distribution. (Reproduced with permission from ref. 36.)

corresponding Gaussian distribution. Nevertheless, the distribution in actual cases tends to be fairly broad. The half-width is roughly 3% of τ_0 for each 0.01 unit of α . Thus in the typical case $\alpha = 0.10$, relaxation times differing from τ_0 by $\pm 30\%$ are still roughly half as probable as those very close to τ_0 .

In theory, a continuous distribution of relaxation times rather than a single relaxation time will arise if either the solute molecule or the solvent cage in which the relaxation takes place has a spectrum of probable configurations. For the various configurations to give a range of relaxation times, their rates of interconversion must be not fast compared to the differences in the dielectric relaxation rates [120]. A continuous (but not symmetrical) distribution of relaxation times owing to a wide spectrum of probable molecular configurations is found in the dielectric relaxation of many polar polymers [60].

* Böttcher [24] has used the symbol h instead of α , presumably to avoid possible confusion with the polarizability, which is also commonly denoted by α . However, Böttcher's symbol has not gained wide acceptance.

3.1.4. Microscopic Relaxation Times

Debye [44] pointed out that owing to the interaction of the polar molecule and the surrounding medium, the relaxation time τ of the macroscopic polarization is probably different from the microscopic relaxation time τ_μ of the polar molecule. The precise nature of this difference has been the subject of much controversy. However, the Powles-Glarum relation (45), which was derived for unassociated polar molecules, has been sustained by recent theoretical and experimental investigations [64, 82, 121, 104].

$$\tau_\mu = \frac{2\epsilon_s + \epsilon_\infty}{3\epsilon_s} \quad (45)$$

According to Eq. 45, the difference between τ_μ and τ is relatively small: τ_μ/τ ranges from unity in nonpolar media to $\frac{2}{3}$ in highly polar media.

To estimate τ_μ , Debye adopted the model of a sphere undergoing rotational Brownian motion in a viscous continuum. His result is stated in Eq. 46

$$\tau_\mu = \frac{4\pi\eta a^3}{kT} \quad (46)$$

in which η denotes the coefficient of viscosity and a the radius of the sphere.

On introducing Onsager's approximation that $4\pi N_0 a^3 = 3V$, where V is the molar volume of the polar substance, we obtain the convenient result

$$\tau_\mu = \frac{3V\eta}{N_0 kT} \quad (47)$$

This simple theory predicts values for τ_μ that are of the same order of magnitude as the experimental relaxation times τ . Indeed, in some cases the agreement becomes semiquantitative. For instance, for the ion pairs of triisomylammonium picrate ($V = 360 \text{ cm}^3$) at 292°K in benzene ($\eta = 6.49 \times 10^{-3}$ poise), τ_μ is predicted to be 2.9×10^{-10} sec; the experimental value for τ at 0.03 M concentration is 2.3×10^{-10} sec [28].

Substantial deviations from Eq. 47, when they occur, have been blamed variously on the failure of Eq. 45 or on the failure of the bulk viscosity η or molar volume V to describe the corresponding hydrodynamic variables on the microscopic scale. However, when the molar volume of the solute is at least three times that of the solvent, substantial deviations are not expected, and when they nevertheless occur, the mechanism of molecular rotation assumed for the dielectric relaxation becomes suspect.

3.2. Quaternary and Tertiary Ammonium Salts

Since typical dielectric relaxation times for ion pairs are on the order of 10^{-10} sec, the frequency range in which dielectric relaxation is best studied is

about 0.1–20 GHz, that is, in the upper range of radiofrequencies and at microwave frequencies. However, the necessary technology for making such measurements is of relatively recent origin. The early microwave equipment, vintage 1950, was cumbersome and expensive, and one needed a roomfull of equipment for each frequency. The pioneering work of Kraus and co-workers [136, 137], reported in 1947, was still done at radiofrequencies and therefore necessarily preliminary. Nevertheless, the results correctly established the order-of-magnitude of ion pair relaxation times and showed that ion pairs behave in dipole relaxation much like ordinary polar molecules.

In the more recent past, the dielectric relaxation of ion pairs has been studied with modern apparatus, in nonpolar and slightly polar solvents, mainly in the laboratories of Davies and Cavell. Results obtained in these laboratories are mutually consistent and the dielectric relaxation times are precise to 10% or better.

3.2.1. *Effect of Electrolyte Concentration and Solvent*

It is known—from static permittivities (Table 8) and colligative properties, for example—that ion pairs associate in nonpolar solvents to form dimers and higher ion pair aggregates. One would therefore expect the dielectric relaxation to be correspondingly complex. In fact, the dielectric relaxation times of electrolytes in such solvents as benzene and tetrahydrofuran increase consistently with concentration.

The relaxation conforms to the simple Debye model (Eq. 39) only if the electrolyte consists largely of ion pairs, that is, if the aggregation number \bar{n} (based on colligative properties) is essentially unity. As \bar{n} increases with increasing concentration, the molecular complexity of the electrolyte is reflected by a distribution of relaxation times. The data are usually reproduced by the Cole-Cole Eq. 44, and the distribution parameter α tends to increase with increasing concentration.

Typical data for the effect of concentration on relaxation times in benzene are presented in Table 9. Triisomylammonium picrate is relatively weakly associated and the α values are correspondingly small. Tetrabutylammonium thiocyanate is strongly associated, and although it is possible to fit the data to Eq. 44 with a single value of τ_0 and concentration-dependent values of α , the values of α are so large that the assumed model of a single molecular species with a broad distribution of relaxation times is suspect [42]. Indeed, judging by the high values of \bar{n} for these solutions, the model is almost certainly inappropriate.

When \bar{n} is not too large ($n < 2$), the parameter τ_0 in Eq. 44 measures essentially the relaxation time of the ion pair monomers. To show this, consider Eq. 43. Since the relaxation amplitude for the i th solute species is proportional to $\mu_i^2 c_i$, the weighted average relaxation time for all species

Table 9 Effect of Electrolyte Concentration on Dielectric Relaxation in Benzene

Concentration (F)	\bar{n}	η/η_0	ϵ_s	$10^{12}\tau_0$ (sec)	α (Eq. 54)	$10^{12}\tau_0\eta_0/\eta$	$10^{12}\tau_\mu\eta_0/\eta$
Triisoamylammonium Picrate (19°C)							
0.0299	1.18	1.02	2.78 ^b	230	0.00	226	212
0.0830	1.45	1.06	3.78	243	0.00	229	199
0.2697	2.10	1.33	7.66	503	0.10	378	289
0.5394	2.57	2.03	14.8	888	0.05	437	314
Tetrabutylammonium Thiocyanate (19°C)							
0.0103	4.2	1.005	2.33 ^b	410	0.35	—	—
0.0165	(5)	1.012	2.37	410	0.57	—	—
0.0197	(6)	—	2.39	410	0.61	—	—

^a Dielectric data and relative viscosities η/η_0 from refs. 40 and 42. Mean aggregation numbers \bar{n} from ref. 43.

^b ϵ_s for benzene is 2.275. Apparent mean dipole moment, i -Am₃NHPI, 12.1 D; Bu₄NSCN, 6.5 D.

may be defined according to

$$\langle\tau\rangle = \frac{\sum_i (\tau_i \mu_i^2 c_i)}{\sum_i (\mu_i^2 c_i)} \quad (48)$$

This average is weighted heavily in favor of the ion pair monomer, because the monomer has a high dipole moment, whereas stable ion pair aggregates tend to be relatively nonpolar.

In interpreting the data for i -Am₃NPI in Table 9, we shall identify τ_0 with $\langle\tau\rangle$ and thus, in first approximation, regard τ_0 as measuring the relaxation of the ion pair monomer. As the concentration increases from 0.03 to 0.54 F, τ_0 increases by a factor of nearly 4. However, much of this increase could be due to the increased viscosity (Eq. 47): the function $\tau_0\eta_0/\eta$ varies less than a factor of 2. Moreover, as the concentration increases the static permittivity ϵ_s of the solutions increases markedly. Thus Eq. 45 predicts that the ratio τ_μ/τ_0 of the microscopic to the measured relaxation time will decrease with increasing concentration. Accordingly, on computing the function $[\tau\eta_0(2\epsilon_s + \epsilon_\infty)/3\epsilon_s\eta]$ (called $\tau_\mu\eta_0/\eta$ in Table 9), the effect of concentration is again cut in half.

Very similar results have been reported for the effect of concentration on the dielectric relaxation of n -Bu₃NHPI in benzene [29]. In this case, data have been obtained over a substantial temperature range. The activation energy for dielectric relaxation was found to be 3.5 ± 0.5 kcal, independent of the concentration.

Table 10 Dielectric Relaxation of 0.2 *M* Electrolytes in Various Solvents at 25°C^a

Solvent	$10^3\eta_0$ (Poise)	ϵ_0	$\tau \times 10^{12}$ (sec)		
			Bu ₃ NHPh	Bu ₃ NHI	Bu ₄ NBr
<i>m</i> -Xylene	8.09	2.57	(286) ^b	—	—
Cl ₃ CCH ₃	7.95	7.53	422	—	—
ClCH ₂ CH ₂ Cl	7.82	10.36	344	204	—
C ₆ H ₆	6.49	2.28	364(223) ^b	—	—
CHCl ₃	5.41	4.81	320	218	—
Cl ₂ CHCH ₃	5.05	10.3	260	161	235
Tetrahydrofuran	4.60	7.58	262	—	—
3-Pentanone	4.42	16.6	—	163	163
CH ₂ Cl ₂	4.16	8.93	212	—	—
Acetone	3.04	20.7	—	86	80

^a Data from refs. 26, 27, 28, 42.^b Concentration is 0.021–0.025 *M*. Temperature is 20° for *m*-xylene.

Available data for the effect of the solvent on dielectric relaxation times in 0.2-F solutions are listed in Table 10. For reasons similar to those discussed above, we regard these relaxation times as measuring essentially the relaxation of the ion pair monomers. Moreover, because of the high concentration of electrolyte, the static permittivity of the *solutions* is high enough, even when the solvent is benzene, so that τ_μ/τ according to Eq. 45 varies by less than 10%.

In the light of these statements, the relaxation times in Table 10 provide a direct measure of the microscopic relaxation times of the given ion pairs. Thus it is clear that these relaxation times show a strong correlation with the solvent viscosity η_0 but no discernible correlation with the solvent permittivity. Moreover, the solvent effects on τ for the quaternary ammonium salt, Bu₄NBr, are very similar to those for the tertiary salt, Bu₃NHI, suggesting that the relaxation mechanisms are also similar. Although acetone is the least viscous of the solvents used, the relaxation times in this medium strike us as anomalously low. If an anomaly really exists, it might be caused by the presence of a substantial fraction (on the order of several percent, judging by the conductivity) of free ions.

3.2.2. Mechanisms of Dielectric Relaxation

The dielectric relaxation time is a measure of the rate of change of the macroscopic polarization. In the case of ion pairs, the polarization can relax by rotation of the entire ion pair as a rigid unit, or by a rotation of polar part-structures about intramolecular bonds or about the interionic point of

contact, or by a shifting of this point of contact. In addition, the polarization may relax as a result of chemical exchange such as an interconversion of intimate and solvent-separated ion pairs, if the rate of exchange is sufficiently fast and if the dielectric relaxation times and/or dipole vectors of the exchanging species are different.

In the case of tertiary and quaternary ammonium salts, the symmetry and chemical properties of the ions may allow some of these mechanisms to be ruled out a priori. In tertiary ammonium ion pairs, the cation and anion are joined by a hydrogen bond which fixes their point of contact. In such ion pairs, if the dipole vectors of the cation and anion are directed along the line connecting the ionic charge centers, rotation of the ions about this line will not relax the polarization. In the present case, the ion pairs of *i*-Am₃NH⁺Py⁻, *n*-Bu₃NH⁺Py⁻, and *n*-Bu₃NH⁺I⁻ have symmetrical structures of this type. The most plausible relaxation mechanism for these ion pairs is rotation as a rigid unit. That this is indeed the probable relaxation mechanism is indicated by the correspondence of the observed relaxation times with predictions based on Eq. 47, and especially by their strong correlation with the viscosity.

Although the data for the symmetrical ion pairs can give no information about the speed of rotation about ⁺N—H ··· X⁻ hydrogen-bond axis, the data listed in Table 11 suggest that this rotation is in fact faster than that of molecular rotation. For the symmetrical ion pairs of *i*-Am₃NH⁺Py⁻ and *n*-Bu₃NH⁺Py⁻, the ratio τ/V of the observed relaxation time to the molar volume in benzene has the uniform value of 0.64, whereas for the unsymmetrical pyridinium trichloroacetate τ/V is only 0.33. One is tempted to speculate that for the latter, dielectric relaxation is enhanced by rotation about the hydrogen-bond axis (Fig. 18*a*). In that case there are really two relaxation times, one for rotation of the entire ion pair and a second, shorter one for rotation about the hydrogen-bond axis. Experimentally, the two modes of relaxation are not resolved and the reported relaxation time is an appropriate average.

For quaternary ammonium ion pairs, dielectric relaxation can occur by a mechanism in which the point of contact between the ion shifts. This process might be called *potential-well hopping* because it requires an activation energy. For example, in the ion pairs of *n*-Bu₄N⁺Br⁻, the bromide ion probably sits in a cavity formed by three alkyl groups, so that the ionic centers of

Table 11 Dielectric Relaxation of Electrolytes in Benzene^a

Solute	μ	c	\bar{n}	$\tau \times 10^{12}$ (sec)	$10^{12}\tau/v$
<i>n</i> -Bu ₃ NH ⁺ Py ⁻	11.9	0.025	1.15	223(25°)	0.64
<i>i</i> -Am ₃ NH ⁺ Py ⁻	11.9	0.030	1.17	230(19°)	0.64
PyH ⁺ O ₂ CCl ₃ ⁻	7.8	0.036	—	62(25°)	0.33

^a Dielectric data of refs. 29, 40, 41. Mean aggregation numbers \bar{n} from ref. 43.

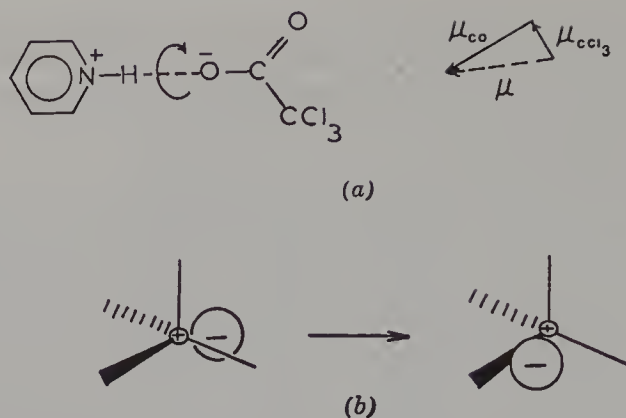


Figure 18. Possible dielectric relaxation mechanisms for ion pairs. (a) Rotation about the axis joining the ionic charges. (b) Potential well hopping.

charge are at closest approach. In potential-well hopping (Fig. 18b), the bromide ion hops to one of the other three cavities. A familiar example of potential-well hopping in an ion pair is Ford and Cram's "conducted tour mechanism" for base-catalyzed deuterium migration in the fluorene system [51] (see also Chapter 2). However, because of the marked similarity of the solvent effects on τ for Bu_4NBr and Bu_3NHI , we conclude that potential-well hopping is not a significant mechanism of dielectric relaxation in this case.

3.3. Ion Pairs and Zwitterions in Aqueous Solutions

As is well known, electrolytes tend to dissociate to free ions in solvents of high permittivity. However, dissociation is not complete except at high dilutions, especially if the valence type of the electrolyte is higher than one-to-one. Thus for 1-F aqueous solutions of several divalent metal sulfates, it has been possible to detect dielectric dispersion that may be reasonably attributed to the relaxation of ion pairs. Although there is no similar evidence for univalent ion pairs, there is fortunately a large body of information about the dielectric properties of zwitterions, especially of amino acids and their derivatives. These data along with those for the metal sulfates show that the mechanisms of dielectric relaxation of molecules with paired ionic charges in aqueous solutions are qualitatively similar to those of ion pairs in nonpolar solvents.

3.3.1. Divalent Metal Sulfates

In an important contribution, Pottel [119] has measured the complex permittivity of 1-F aqueous solutions of CuSO_4 , NiSO_4 , MnSO_4 , BeSO_4 and

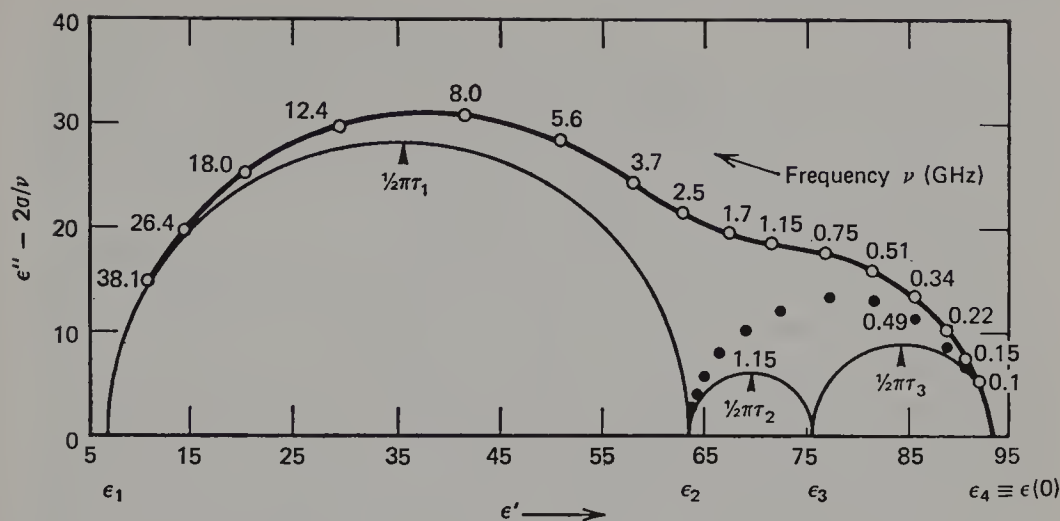


Figure 19. Dielectric dispersion for 1-F aqueous beryllium sulfate. In each semicircle, the frequency increases from zero on the right to infinity on the left. The frequencies along the semicircle therefore do not correspond to the indicated frequencies along the experimental skew-shaped arc. $\tau_2 = 1.38 \times 10^{-10}$ sec.; $\tau_3 = 3.2 \times 10^{-10}$ sec. (Reproduced with permission from ref. 119)

CdSO_4 at enough frequencies so that the fine-structure of the dielectric dispersion curves can be resolved. Typical data for BeSO_4 are reproduced in Fig. 19. The measured curve (open circles) clearly shows evidence for more than one relaxation process. Preliminary analysis separates out a semicircle with a relaxation time of the characteristic magnitude for the solvent water molecules, and an apparently circular arc (solid circles) whose shape can easily be fitted to a Cole-Cole relation for a continuous distribution of relaxation times (Eq. 44 and Fig. 16). However, Pottel showed that this "arc" can be successfully resolved into two semicircles corresponding to two discrete relaxation processes.

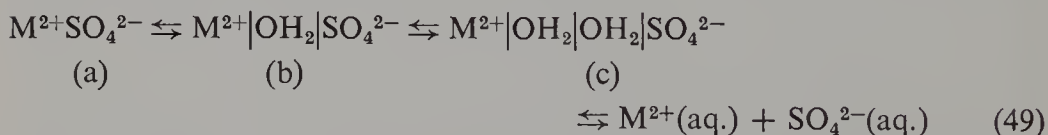
Pottel's analysis brings into focus the general problem of distinguishing between continuous and discrete distributions of dielectric relaxation times. The Debye equation for a single relaxation process (Eq. 39) involves three parameters: ϵ_s , ϵ_∞ , and τ . When the fit of Eq. 39 is inadequate, the Cole-Cole Eq. 44 introduces a fourth parameter, α . In theory, Eq. 44 describes a particular distribution of relaxation times, an example of which was shown in Fig. 17, but in fact the equation will give adequate fit for a wide variety of distributions or, better, of deviations from the single relaxation model.

In the case of Pottel's work for metal sulfates, it is only the large number of experimental frequencies that allows him to decide that two discrete relaxation processes are more probable than a continuous distribution. All in all, the analysis into three circular arcs seen in Fig. 19 involves seven parameters.

As Pottel has pointed out, the interpretation of the relaxation processes is not clear-cut. Since the solutions contain a high concentration of free ions in equilibrium with the ion pairs, one or even two of the relaxation processes could somehow involve the free ions and their ionic atmospheres, but Pottel showed that this proposal is relatively improbable. He therefore ascribed the relaxation processes to ion pairs.

In principle there are two ways in which the metal sulfate ion pairs could produce two dielectric relaxation times: there might be two kinds of ion pair with different properties, or there might be two processes in which different dipole vectors in a single species relax independently. (If there were two parallel mechanisms for relaxing a single dipole vector in a single species, one would observe a single relaxation step with $1/\tau = 1/\tau_1 + 1/\tau_2$.) However, for metal sulfate ion pairs the second possibility can be ruled out because the ions have central distributions with zero dipole moments. Moreover, if the ion pairs were complexed to water molecules, it is unlikely that rotation of the relatively small water dipoles, if independent, could be detected experimentally.

Thus Pottel was able to conclude that the aqueous metal sulfate solutions contain two different kinds of ion pair. Actually he discussed his results in terms of *three* ion pair species as well as free ions (Eq. 49), referring to evidence from ultrasonic relaxation [7-9, 47]:



However, Pottel concluded from the ultrasonic results that the concentration of the intimate ion pair species *a* would be too low to give an observable dielectric relaxation step. He built molecular models of the solvent-separated species *b* and *c* and showed that molecules of the given molecular shape and charge separation relaxing as rigid units could give rise to dielectric relaxation times and amplitudes of the observed magnitude.

In our view, the importance of Pottel's work lies not so much in defining the structures of the ion pairs (which it does only in crude approximation), but in providing independent evidence that there are two discrete ion pair species. We believe that the structures indicated in Eq. 49 are open to question and suggest those presented in Fig. 20 instead. In proposing these structures, we assume that the metal ion has six octahedral binding sites.

The structure of the intimate ion pair *a* is consistent with that of potassium *p*-toluenesulfonate. The solvent-bridged intimate ion pair *b* retains considerable charge-charge interaction energy and has a strain-free cyclic hydrogen-bonded structure in which only two water molecules become immobilized. In the solvent-separated or next-nearest-neighbor structure *c* the sulfate ion

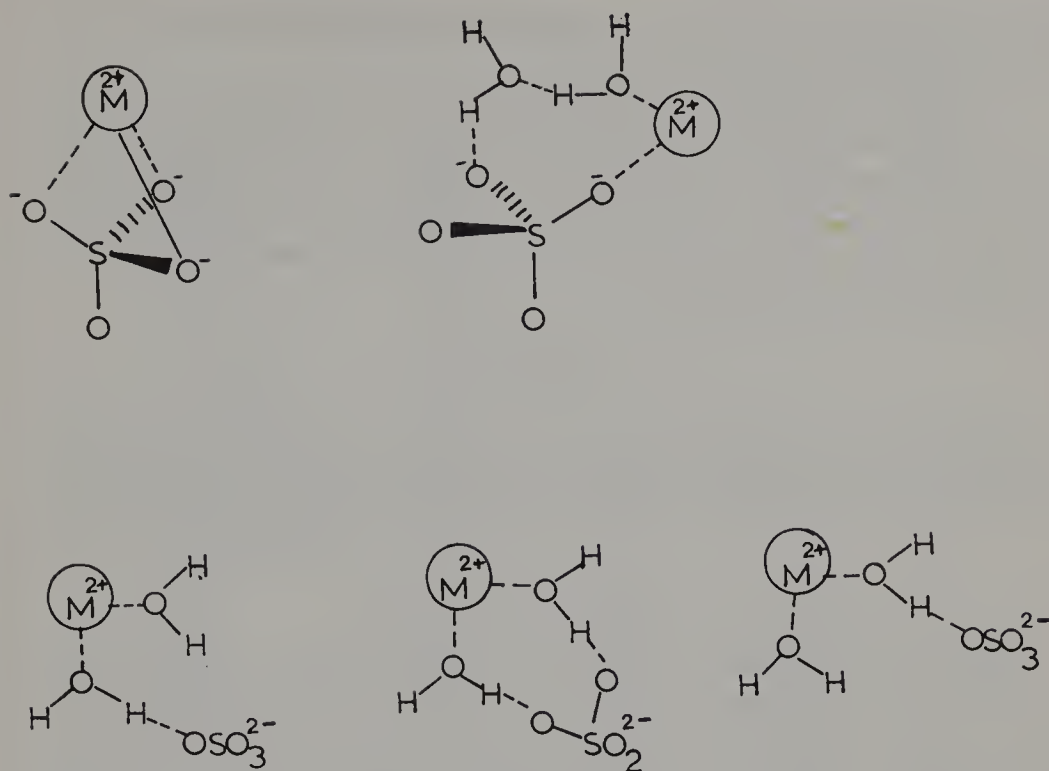


Figure 20. Models for metal sulfate ion pairs.

could be hydrogen-bonded to one water molecule or form a strain-free cyclic structure involving two octahedral water molecules. According to the molecular models, the ionic charges are still in fairly close proximity. We do not know whether the open structure or the cyclic bifunctional structure is more stable, but it is clear that potential-well hopping, in which the sulfate ion hops to an adjacent chemically equivalent site, should be a very rapid process.

3.3.2. Zwitterions

Zwitterions are an especially interesting class of molecules for dielectric studies. Their dipole moments are larger than those for any nonionic molecule; indeed, the dipole moments provided the most unequivocal proof of the zwitterionic structure.

Being insoluble in nonpolar solvents, zwitterions have been studied mostly in aqueous solutions. Dielectric studies in water offer special experimental difficulties due to the relatively high conductance of even the pure solvent. In the classic work done before the advent of microwave methods, these

difficulties were overcome by use of fairly concentrated solutions and careful control experiments [46].

In addition to the experimental difficulties there are theoretical problems in the interpretation of the data. Since water is a hydrogen-bonded liquid, the use of Kirkwood's theory in the form of Eqs. 6 and 7 would seem appropriate. However, the required correlation factors are not easily predicted and therefore Onsager's theory (Eqs. 3–5) was in fact used. In view of Eq. 9, this is tantamount to assuming that

$$g_2 - 1 + \frac{dg_1}{dc_2} \frac{\mu_1^2}{\mu_2^2 V_1} \ll 1$$

Because of the experimental and theoretical uncertainties, Onsager's equations may be simplified, without introducing significant additional error, so that the dipole moments of highly polar solutes in water at 25° are given by

$$\mu = 3.30S^{1/2} \quad (50)$$

where S denotes the molar dielectric increment [94].

Selected data for dipole moments and available data for relaxation times of zwitterions are listed in Table 12. The dipole moments are as great or greater than those of typical ion pairs. If one writes $\mu = e\mathbf{r}$ and interprets \mathbf{r} as being approximately the distance between the charged centers, one obtains values for the amino acids that are consistent with distances inferred from molecular models. Especially instructive are the dipole moments of the glycine oligopeptides, $(\text{gly})_n$. As shown in Table 12, μ/\sqrt{n} is quite constant for $n > 2$. Since the charged centers in these molecules are at the ends of the molecular chains, the constancy of μ/\sqrt{n} clearly indicates that the chains have randomly coiled conformations [145]. Of course, assuming that μ is proportional to the distance between the charged centers is an approximation which neglects induced polarization and the dipole moments of peptide and other polar groups, which are substantial. We venture the opinion that further investigation of the dipole moments of amino acids and oligopeptides will be rewarding.

The dielectric relaxation times for glycine, α - and β -alanine, and for the dipeptides of glycine and α -alanine were measured by modern microwave techniques [1–3]. The relaxation times for the amino acids are short, in terms of Debye's model for dipole rotation of rigid molecules (Eq. 47). This fact suggests either an anomalously low microscopic viscosity, that is, solvent-disordering by the zwitterions, or enhancement of relaxation by intramolecular rotation. It is relevant in this connection that the data suggest a distribution of relaxation times with $\alpha \approx 0.05$.

That intramolecular motion may facilitate dielectric relaxation is further shown by the data for the glycine- α -alanine dipeptides. There is a correlation

Table 12 Dielectric Properties of Zwitterions in Aqueous Solution^a

Substrate	μ (D)	Temperature (°C)	$10^{12}\tau$ (sec)	μ/\sqrt{n}
Glycine	15.7	20	72	15.7
α -Alanine	17.0	20	93	—
β -Alanine	19.4	20	86	—
α -Aminobutyric acid	17.7	—	—	—
<i>L</i> -Glutamic acid	18.8	—	—	—
<i>L</i> -Arginine	27.1	—	—	—
<i>o</i> -Benzbetaine	18.0	—	—	—
<i>m</i> -Benzbetaine	25.3	—	—	—
<i>p</i> -Benzbetaine	29.8	—	—	—
Glycine betaine	16.6	—	—	—
β -Alanine	19.4	—	—	—
β -Aminobutyric acid	24.6	—	—	—
δ -Aminobutyric acid	27.5	—	—	—
gly-gly	27.8	20	147	19.7
ala-gly	28.6	20	190	—
gly-ala	29.2	20	169	—
ala-ala	25.0	20	215	—
leu-gly	—	25	180	—
leu-ala	—	25	246	—
(gly) ₃	37.2	20	181	21.5
(gly) ₄	42.6	25	247	21.3
(gly) ₅	49.5	25	366	22.1
(gly) ₆	52.0	—	—	21.2

^a Data from refs. 1, 2, 3, 37, 46.

between the relaxation time and the nature of the *N*-terminal amino acid (e.g., *ala* in *ala*-gly) such that the shorter relaxation time corresponds to the more flexible linkage. The observed differences in relaxation times can be predicted qualitatively by means of Ramachandran's "allowed" angles of rotation for N—C _{α} and C _{α} —CO bonds [123].

The relaxation times for the glycine oligopeptides were reported in 1941, before the advent of microwave instrumentation, and are based on permittivities measured at high radiofrequencies [37]. If there is, in fact, a distribution of relaxation times, the values obtained for τ under these conditions will be weighted in favor of the slowest times. The actual values are nearly proportional to *n*, the oligomer number, and therefore to the molar volume, suggesting rotation of the entire molecule.

4. PERMITTIVITY AND DIELECTRIC RELAXATION OF SOLUTIONS OF FREE IONS

We have seen that permittivity measurements on electrolytic solutions of low conductivity provide direct and decisive information about the molecular

aggregation, structure, and modes of dipole rotation of the ion pairs. By comparison, permittivity measurements on solutions of high conductivity, in which the electrolyte is largely dissociated to free ions, by themselves are relatively uninformative. However, if the data are fortified with a good theory of solvent and solution structure, they acquire great vitality and provide explicit insights into the structure and dynamics of the ionic solvation shells.

4.1. Complications for Conducting Solutions

For electrolytic solutions of low conductivity, it is sufficient to represent the measuring cell as a capacitance C (due to the dielectric) in parallel combination with a small conductance G , as indicated in Fig. 21a. However, for

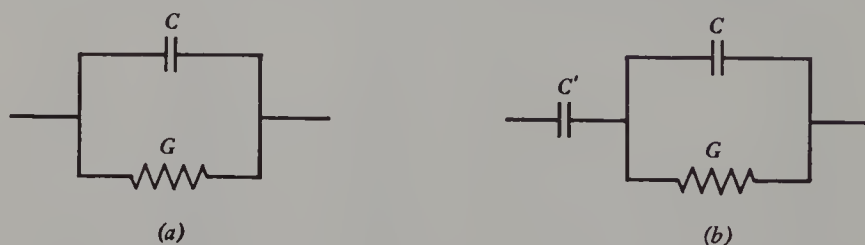


Figure 21. Electrical model of a conductive dielectric: (a) without double layers; (b) with purely capacitive double layers.

solutions of higher conductivity, the electrical double layer at the electrode surfaces can no longer be ignored. A simple and often adequate model then is a pure capacitance C' , to represent the double layer, in series combination with the dielectric (Fig. 21b). According to this model, the effect of the double layer on the measured capacitance and conductance varies as $1/\omega^2$ [69, 90], so that at sufficiently high frequencies—usually radiofrequencies and higher—the effect is negligible.* Under such conditions, the measured ac admittance Y , which for the assumed electrical model (Fig. 21a) is equal to $G + j\omega C$, is that of the dielectric.

To obtain a quantity that is independent of the dimensions of the measuring cell, one next calculates the admittance $y = Yl/A$, which is a characteristic property of the dielectric. The *cell constant* l/A is the ratio of the current path-length to the cross-sectional area. The admittance is a complex variable, a function of frequency, and it can be shown that y is equal to the ratio J/E of current density to electric field.

To avoid confusion between experimental and theoretical quantities, we

* Methods for evaluating and correcting for the effect of the electrical double layer at audiofrequencies have been described [90, 92, 148].

shall represent the admittance (an experimental quantity) in complex notation as $y^* = y' + j\omega y''$. The symbols y' and y'' denote the respective components of y^* that are in phase ($y' = Gl/A$) and 90° out of phase ($y'' = Cl/A$) with the voltage. The theoretical quantities are the ionic conductivity σ due to the moving ions, and the displacement current due to the changing polarization of the dielectric. The total current density \mathbf{J} is therefore given by

$$\mathbf{J} = \sigma \mathbf{E} + \frac{k_\epsilon \epsilon}{4\pi} \frac{d\mathbf{E}}{dt} \quad (51)$$

where \mathbf{E} denotes the alternating electric field. On writing $\mathbf{E} = E_0 \exp(j\omega t)$, taking the derivative, substituting in Eq. 51, and rearranging, we obtain a theoretical expression for the admittance:

$$\frac{\mathbf{J}}{\mathbf{E}} = y^* = \sigma + \frac{j\omega k_\epsilon \epsilon}{4\pi} \quad (52)$$

In Eq. 52 the permittivity is a complex variable: $\epsilon^* = \epsilon' - j\epsilon''$, as described previously (Eq. 39). The conductivity is likewise a complex variable: $\sigma^* = \sigma' + j\sigma''$, because the ionic current may not be in phase with the alternating voltage. On introducing these quantities as complex variables in Eq. 52, we obtain Eq. 53a, which is in a convenient form for comparison with the experimental quantities y' and y'' :

$$y^* = \left(\sigma' + \frac{\omega k_\epsilon \epsilon''}{4\pi} \right) + j\omega \left(\frac{k_\epsilon \epsilon'}{4\pi} + \frac{\sigma''}{\omega} \right) \quad (53a)$$

$$y^* = y' + j\omega y'' \quad (53b)$$

The complications arising from a high ionic conductivity are now obvious: We measure two quantities, y' and y'' ; but the theoretical equation involves four unknowns, σ' , σ'' , ϵ' , ϵ'' , of which the last two are to be evaluated. To obtain a mathematical solution, it is therefore necessary to make approximate assumptions concerning σ' and σ'' . The usual assumptions are that σ' is essentially equal to the low-frequency conductivity σ_s , which is measured at audiofrequencies, and that σ''/ω is negligible relative to $k_\epsilon \epsilon'/4\pi$.

Let us briefly analyze the validity of these assumptions. According to current thinking, the conductivity of an ionic species is a sum of three terms, each with a characteristic relaxation time [24a, 59, 153, 154]. A complete equation has not yet been derived, and the final result is likely to be fairly complicated. However, the essence of the phenomenon is reproduced by the approximate Eq. 54. According to this equation

$$\sigma^* = \frac{\sigma_1}{1 + j\omega\tau_1} - \frac{\sigma_2}{1 + j\omega\tau_2} - \frac{\sigma_3}{1 + j\omega\tau_3} \quad (54)$$

the intrinsic conductivity of an ionic species, $\sigma_1/(1 + j\omega\tau_1)$, is reduced by two retarding forces: the drag of the ionic atmosphere $[\sigma_2/(1 + j\omega\tau_2)]$ and the drag of the solvent polarization $[\sigma_3/(1 + j\omega\tau_3)]$ acting on the moving ions. The relaxation time τ_1 results from the inertia of the ions and should be on the order of 10^{-12} – 10^{-13} sec. In the usual experiments at microwave frequencies this relaxation is unimportant, $\omega\tau_1 \ll 1$.

The relaxation time τ_2 is that of the ionic atmosphere and can be evaluated according to the theory of Debye and Falkenhagen [45]. The result is that $\tau_2 = 8.85 \times 10^{-14} \epsilon_0/\sigma_s$, where ϵ_0 denotes the solvent permittivity and σ_s the low-frequency conductivity. For 1-F electrolytes in water, $\tau_2 \approx 10^{-10}$ sec; that is, relaxation occurs between about 0.1 and 10 GHz.

The relaxation time τ_3 is that of the ion-induced polarization of the solvent. In first approximation τ_3 should be similar to the dielectric relaxation time of the solvent, but in fact τ_3 appears to be 10–100 times greater [8], $\tau_3 \approx 10^{-9}$ – 10^{-10} sec.

The relative amplitudes $\sigma_1/\sigma_2/\sigma_3$ of the three relaxation terms for univalent ions in water are typically 5/1/1 in 1-F solution.

Based on these considerations, calculation shows that the neglecting of σ'/ω relative to $k_\epsilon\epsilon'/4\pi$ in the expression for y'' is probably justified at the usual experimental frequencies of 0.6–40 GHz (see Eqs. 53). On the other hand, the assumption that $\sigma' = \sigma_s$ probably leads to significant error because σ' is greater than σ_s and increasing with frequency by something like 20–40% in the experimental range. Thus the assumption that $\sigma' = \sigma_s$ will lead to an overestimate of ϵ'' , as was pointed out by Hasted and Roderick [75]. Of course, in measurements of the admittance of fused salts, both y' and y'' represent essentially the components of the conductivity [4].

4.2. Aqueous Solutions

The dielectric properties of aqueous solutions of electrolytes have been of interest for many decades. However, concordant results could be obtained only after the development of microwave measuring techniques.

For all electrolytic solutions, the parameter ϵ_s derived from the microwave data, which represents the static permittivity, is less than ϵ_0 , the static permittivity of pure water. Within experimental error, the relationship is linear up to at least 1 – F concentration of the electrolyte:

$$\epsilon_s - \epsilon_0 = S_\epsilon c \quad (55)$$

The molar dielectric increment S_ϵ thus is a negative quantity; $-S_\epsilon$ is often called the *molar dielectric decrement*.

The *magnitude* of S_ϵ for aqueous electrolytes generally decreases with increasing temperature. Selected results are listed in Tables 13 and 14. Table 13

Table 13 Effect of Electrolytes on the Dielectric Properties of Water at 25°

Solute	S_ϵ (M ⁻¹)	$S_\tau \times 10^{12}$ (sec M ⁻¹)
LiCl ^{a, b}	-12.8, -15.6	-0.34, -0.40
LiBr ^a	-13.3	-0.57
LiI ^a	-14.3	-0.81
LiNO ₃ ^g	-16.4	-0.4
NaF ^{a, b}	-8.9, -10.1	-0.09, -0.3
NaCl ^{a, c, f}	-11.0, -15.8	-0.60, -1.0
NaBr ^{a, b}	-11.6, -16.3	-0.80, -1.1
NaI ^{a, b}	-12.8, -16.5	-1.05, -1.4
Na propionate ^e	-11.4	+1.5
KF ^{a, b}	-8.4, -11.8	-0.21, -0.4
KCl ^{a, b}	-9.4, -12.8	-0.65, -1.0
KBr ^a	-10.1	-0.84
KI ^a	-10.5	-1.0
RbF ^a	-7.5	-0.24
RbCl ^{a, b}	-8.6, -12.5	-0.66, -0.8
RbBr ^a	-8.8	-0.82
RbI ^a	-9.8	-0.98
CsF ^a	-7.1	-0.04
CsCl ^a	-7.6	-0.50
CsBr ^a	-8.0	-0.60
CsI ^a	-8.4	-0.75
MgCl ₂ ^c	-37.0 (10°)	-5.09 (10°)
BaCl ₂ ^c	-26.4 (10°)	-4.8 (10°)
MnCl ₂ ^d	-19.4	-1.08
CoCl ₂ ^d	-20.8	-0.32
NiCl ₂ ^d	-23.1	-1.0
CuCl ₂ ^d	-17.8	-0.26
LaCl ₃ ^c	-48 (3°)	-10.7 (3°)
HCl ^c	-27.2 (10°)	-3.7 (10°)
NH ₄ Cl ^b	-13.2	-0.8
EtNH ₃ Cl ^b	-11.0	+1.1
Et ₂ NH ₂ Cl ^b	-18.8	+0.7
Et ₄ NCl ^b	-21.6	+1.6
<i>n</i> -PrNH ₃ Cl ^b	-14.1	+0.8
Guanidine·HCl ^b	-14.4	+0.4
Me ₄ NBr ^e	-15.4	+1.4
Me ₄ NI ^b	-18.1	+1.0
H ₂ SO ₄ ^c	-40 (10°)	—
MnSO ₄ ^d	-17.4	-0.37
NiSO ₄ ^d	-18.3	-0.90
CoSO ₄ ^d	-17.7	-0.53
CuSO ₄ ^d	-19.1	-0.26

^a Ref. 62.

^b Ref. 72.

^c Ref. 75.

^d Ref. 124.

^e Ref. 78.

^f Additional concordant data in refs. 72, 78, and 98.

^g Ref. 16.

Table 14 Effect of Temperature on Dielectric Properties of Aqueous Solutions

Solute	Temperature (°C)	$S_\epsilon (M^{-1})$	$10^{12} S_\tau (\text{sec } M^{-1})$
NaBr ^a	10	-15.5	-2.6
	20	-16.1	-1.2
	30	-13.7	-0.6
	40	-11.7	-0.1
	50	-12.7	+0.2
	60	-9.6	+0.6
<i>n</i> -PrNH ₃ Cl ^a	10	-13.0	+0.8
	20	-13.9	+1.1
	30	-12.5	+1.1
	40	-12.1	+1.3
	50	-12.2	+1.3
	60	-10.2	+1.3
BaCl ₂ ^b	3	-27.6	-6.8
	10	-26.4	-4.8
	25	-20.8	—
	40	-20.0	—

^a Ref. 78.^b Ref. 75.

also compares data from different laboratories; the discrepancies are tolerably small and due partly to differences in the nature of the assumed relaxation function, especially whether or not there is a distribution of relaxation times.

The dielectric relaxation time τ refers to the relaxation of water molecules. The effects of different electrolytes on τ are highly specific: some cause τ to decrease below the value τ_w for pure water others cause τ to increase. At concentrations up to 1 M , the variation of τ with concentration is nearly linear:

$$\tau - \tau_w = S_\tau c \quad (56)$$

The slopes S_τ are either positive or negative, and their algebraic values tend to increase with increasing temperature. Selected results are included in Tables 13 and 14.

The study of dielectric relaxation times has been extended to very high concentrations of electrolyte [76, 77] at which the water molecules may be said to exist in the coordination spheres of the ions. It is found that regardless of the sign of S_τ at low concentrations of the given electrolyte, τ always increases with concentration at sufficiently high concentrations [76].

In the early studies at microwave frequencies, the data were insufficient to prove a distribution of relaxation times, but later work established that a distribution really exists. The Cole-Cole parameter α for pure water has a

constant value of 0.012 ± 0.007 throughout the temperature range 0–75°C [65]. When electrolyte is present, α increases consistently with the concentration [76].

4.2.1. Interpretation of Results

In interpreting the dielectric data, the aim is to establish the structure and dynamics of the ionic solvation shells. Unfortunately, the chain of reasoning which leads from observation to logical conclusion is very long, and many links in the chain require the making of plausible assumptions or approximations.

The effect of making a series of assumptions is to reduce greatly the probability that the final result will have quantitative significance. The situation here is analogous to the familiar problem of overall yield in a multistep synthesis. Even when each step proceeds with a 90% yield, the overall yield after n consecutive steps is only $(0.9)^n$. Similarly, let us say that a well-designed theoretical model has a 90% chance of giving quantitative agreement with reality. The use of 10 such models in series will then reduce the probability for quantitative success of the final result to $(0.9)^{10}$, or 35%. Thus even though each of the models in the series *by itself* is very good, the odds are two-to-one against the final result's being *quantitatively* useful: The usefulness is more likely to be qualitative, even though the results are stated in the language of precise numbers. Accordingly, in the following discussion we shall stress qualitative conclusions, without getting involved in mathematical details.

In interpreting the dielectric data for aqueous electrolytes, two different approaches have been tried. One stresses the effect of the added electrolyte on the hydrogen-bonded structure of the water molecules; the other stresses the formation of discrete solvation complexes.

4.2.2. Approaches that Emphasize the Water Structure

According to Bernal and Fowler [21], the structure of liquid water is best described as a broken-down ice structure. When ice melts, some hydrogen bonds break and the tetrahedral orientations of the remaining hydrogen bonds become distorted. Haggis, Hasted, and Buchanan [72], in a classic paper, applied this model to predict the dielectric properties of liquid water. They assumed a dynamic equilibrium in which individual water molecules can form 0, 1, 2, 3, or 4 hydrogen bonds, and they calculated the relative concentrations of these species from thermal data. On combining these concentrations with appropriate Kirkwood g factors, they were able to reproduce the static permittivity of water over a wide temperature range.

The experimental relaxation times could be reproduced equally well with a consistent model. The virtual absence of a spread in relaxation times suggests that of the five stepwise hydrogen-bonded water species, only one is

responsible for the relaxation process. However, the value obtained for ϵ_∞ is abnormally high ($\epsilon_\infty = 4.2$ whereas n^2 is only 1.8), which indicates that there is another relaxation process at frequencies well above those of the experimental microwave range. This additional relaxation was ascribed to water molecules with 0 and 1 hydrogen bonds, because rapid dipole rotation is possible for such molecules, without constraint by hydrogen bonding, about at least one axis. It was noted further that molecules with 3 and 4 hydrogen bonds cannot rotate without hydrogen-bond breaking, but that two-bonded molecules with one donor and one acceptor bond can rotate relatively freely. Assuming that the rate-determining step for dipole rotation is the conversion of water molecules with three hydrogen bonds to rotationally active molecules with two hydrogen bonds, Haggis, Hasted, and Buchanan [72] were able to reproduce the experimental relaxation times with good precision.

More recently, theoretical calculations have indicated that cyclic hydrogen-bonded water structures [76] might be exceptionally stable. Hasted [76] has tested these predictions against the dielectric data for liquid water, but the fit is not nearly as good as that of the preceding model.

In discussions of water structure in electrolytic solutions, the basic concept is that there is a conflict between the structural requirements of the ionic solvation shells and those of bulk water. The electric fields produced by the ions will favor solvation shells in which the water dipoles are oriented radially, as in Fig. 22a. On the other hand, the structure of the surrounding bulk water will favor tetrahedral orientations, such as those in Figs. 22b and 22c, which are more compatible with surrounding hydrogen-bonding sites. In view of this conflict of favored orientations, Frank and Wen [52] stress the existence of a disordered water layer between the hydration shell and the bulk solvent. The simple model suggested by them is shown in Fig. 23. Region A represents the ordered solvation shell, and region C the bulk solvent.

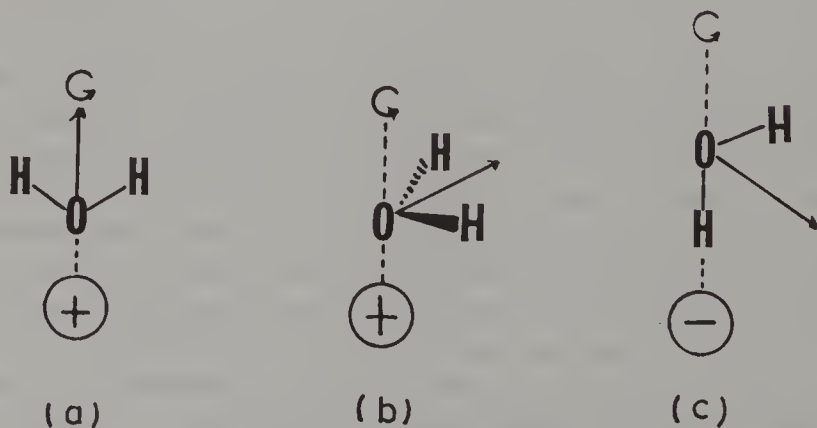


Figure 22. Models of ionic hydration.

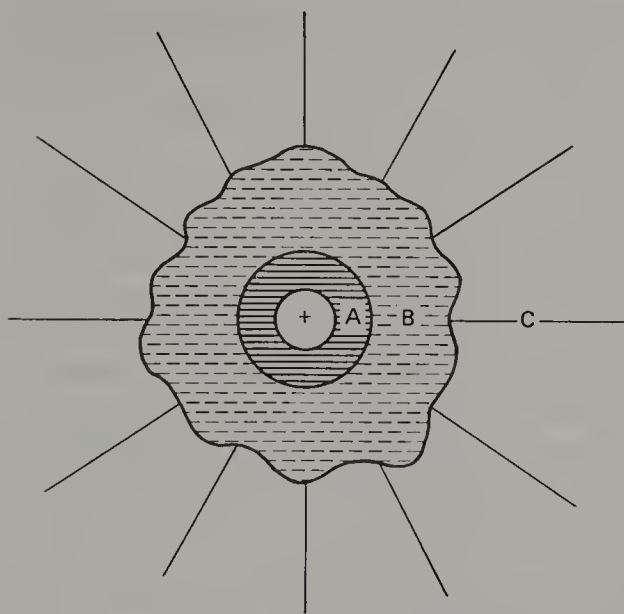


Figure 23. A simple model for the structure modifications produced by a small ion. A, region of immobilization of water molecules; B, region of structure breaking; C, structurally "normal" water. (Reproduced with permission from ref. 52.)

Region B is a disordered transition layer, nominally outside the solvation shell and thus part of the overall solvent medium. The relative importance of the three regions depends on the specific ion and on the temperature. With increasing temperature the water structure in C gradually becomes less ordered and the difference between B and C becomes less distinct. For strongly orienting ions (with a high charge/radius ratio), the ordered layer A is extensive and its effect may become dominant over that of the disordered layer B. The opposite relationship of A relative to B is expected for weakly orienting ions; indeed, an ordered solvation shell A may not even exist.

According to the scaled-particle theory of liquid solution, it is necessary to consider yet another water-structural effect [116, 117]. When a solute is introduced into a solvent medium, work is required to create a cavity of the appropriate size. In the scaled-particle theory this work is calculated by the methods of statistical mechanics [131], treating the solute molecule as a "hard sphere," a sphere with an impenetrable surface which exerts no attractive force. The work varies with the size of the cavity and depends on specific properties of the solvent, particularly on the heat of vaporization and the coefficient of thermal expansion [116]. As is well known, the latter is very anomalous for water, and as a result the work of cavity formation is also anomalous [117]. The nature of the anomaly is such that the effect, on the thermodynamic properties, of introducing a hard sphere into liquid water is

equivalent to that of promoting ordered water structure. This “structure-promoting” effect should be dominant whenever the attractive interaction of the solute with the solvent is relatively small. Probable examples are large ions such as organic ions with long alkyl chains.

When the dielectric relaxation times of electrolytic solutions are examined in light of these concepts, it becomes highly significant that τ normally decreases when salt is added to water at 25°, except for certain salts with organic ions (Table 13). As the temperature is raised, the slope S_τ becomes less negative and in some cases even positive (Table 14). These observations suggest that the change in τ is determined largely by the extensiveness of the disordered region B (Fig. 23) and the difference in “order” between regions B and C, while molecules in the solvation shells A have relatively little effect. Presumably the molecules in region B have shorter relaxation times than those in C, owing to the less ordered structures of their environments. In terms of the model of Haggis, Hasted, and Buchanan [72], it may be that the rate of formation of water molecules with two hydrogen bonds is increased. However, the usual increase of the Cole-Cole α -parameter suggests that other modes of relaxation are present as well.

With increasing temperature, the difference of relaxation times between regions B and C diminishes, so that S_τ becomes less negative. The eventual change in sign of S_τ at sufficiently high temperatures can be explained in two ways: Either the molecules in shell A begin to contribute noticeably to the relaxation process, lengthening the average relaxation time or the “hard-sphere effect” becomes important. In the latter case one would predict from scaled-particle theory that S_τ goes through a maximum.

For organic ions, the positive values of S_τ indicate that the hard-sphere effect is dominant even at room temperature.

4.2.3. *Restricted Dipole Rotation in the Solvation Shells*

Because of the intense electric fields experienced by water molecules near an ion, it has long been supposed that the rotational freedom of water dipoles in the ionic solvation shells is severely restricted by electrical saturation effects [44]. If the restriction were complete, then the ion with its solvation shell would behave like a nonpolar solute, and the static permittivity of the electrolytic solution would be less than that of the pure solvent.

In support of this view, the addition of electrolyte to water always results in a decreased permittivity. The slopes S_ϵ may be used to estimate the numbers of water molecules whose dipole rotation has been effectively quenched. The calculation is simplest if one assumes that the solvent outside the ionic solvation shells has the normal permittivity ϵ_0 of pure water. This assumption is basic to the theory of discrete solvation complexes, to be discussed in the next section, and has also been adopted as a reasonable approximation in the

Table 15 Restricted Dipole Rotation of Water Molecules in the Solvation Shells of Aqueous Electrolytes at 25° ^a

Solute	Z^b	Solute	Z^b
LiCl	5.5	MgCl ₂	14
LiBr	5.5	BaCl ₂	9
LiI	5.4	MnCl ₂	14
		CoCl ₂	16
NaF	4.3	NiCl ₂	18
NaCl	4.5	CuCl ₂	12
NaBr	4.5	LaCl ₃	16
NaI	4.5	HCl	11
Na propionate	4 ± 1	NH ₄ Cl	4
		EtNH ₃ Cl	1 ± 1
KF	3.6	Et ₂ NH ₂ Cl	3 ± 2
KCl	3.1	Et ₄ NCl	1 ± 2
KBr	3.1	<i>n</i> -PrNH ₃ Cl	1 ± 1
KI	2.8	Guanidine·HCl	3 ± 1
		Me ₄ NBr	2 ± 2
RbF	2.7	Me ₄ NI	1 ± 2
RbCl	2.4		
RbBr	2.2		
RbI	2.0		
CsF	2.1		
CsCl	1.6		
CsBr	1.4		
CsI	0.9		

^a Data for alkali halides, ref. 62. Data for transition-metal chlorides, ref. 124. Others from ref. 72.

^b Number of moles of water whose dipole rotation is quenched by one formula weight of electrolyte.

theory of Haggis, Hasted, and Buchanan [72] which attempts to allow for water structure.

Table 15 lists values of the number of moles of water, Z , whose dipole rotation is quenched by one formula weight of electrolyte. All values were calculated by a consistent method and should be comparable. However, Z is only an *effective* number; for instance, two molecules whose rotation is half-quenched would be counted as one molecule quenched.

The calculation of Z may be outlined briefly as follows. Let f denote the fractional volume of the solution in which dipole rotation is effectively quenched. Regard each ion with its "frozen" solvation shell as a sphere of permittivity ϵ_∞ , and regard the solution as a suspension of such spheres in a solvent medium of permittivity ϵ_0 . Then if $\epsilon_0 \gg \epsilon_\infty$, f is related to the decrease

in static permittivity according to Eq. 57 [72, 62]:

$$f = (\epsilon_0 - \epsilon_s) \frac{2}{3(\epsilon_0 - \epsilon_\infty)} = - \frac{2S_\epsilon c}{3(\epsilon_0 - \epsilon_\infty)} \quad (57)$$

The fraction f in turn is related to Z through Eq. 58, in which ρ denotes density and M denotes molecular weight:

$$Zc = (\text{total solvent}) - (\text{"free" solvent}) \quad (\text{mole l}^{-1}) \quad (58a)$$

$$= \frac{1000\rho - M_2c}{M_1} - \frac{1000(1 - f)}{V_1} \quad (58b)$$

On expressing ρ in terms of the apparent molar volume of the solute, solving for f , and substituting in Eq. 57, we arrive at a relationship between S_ϵ and Z :

$$-S_\epsilon = \frac{3(\epsilon_0 - \epsilon_\infty)}{2000} (ZV_1 + V_2^{\text{app}}) \quad (59)$$

On examination of the values listed in Table 15, a number of generalizations may be made:

1. Z is much more sensitive to the nature of the cation than to that of the anion.
2. For inorganic salts with the same anion, Z decreases with decreasing charge/radius ratio of the cation.
3. For halide salts with the same cation, Z is nearly the same for Cl^- , Br^- , and I^- , and about one unit greater for F^- .
4. For salts with organic cations, the generalization that $Z = 1 \pm 1$ would fit all data.

If the basic assumption that the permittivity outside the ionic solvation shells remains equal to ϵ_0 can be accepted, then some conclusions may be justified. The pattern of results 1–3 above suggests that water dipoles lose much more rotational freedom in the solvation shells of inorganic cations than of halide ions. A solvation-shell structure like that suggested in Fig. 22a thus seems probable for the inorganic cations, at least for those with a high charge-radius ratio. On the other hand, water dipoles around halide ions and around organic cations remain relatively lively, with relaxation times comparable to those in the bulk solvent. For the halide ions, a solvation-shell structure like that shown in Fig. 22c seems plausible.

4.2.4. Approaches Involving Discrete Solvation Complexes

The model of Fig. 23, which shows three layers of water molecules around each ion, has so many built-in adjustable features that there is little hope of

pinning down the properties of the solvation shells quantitatively. To a chemist wishing to express microscopic structure in terms of precise numbers, this is a frustrating situation. Much research has therefore been done in the search for simpler models that might adequately reproduce reality.

The most obvious simplification is to eliminate the disordered layer B from the model of Fig. 23. The result is an ionic solvation complex bordering directly onto a medium whose properties are those of the pure solvent in bulk. In such a model there are three kinds of water molecule: those in the cationic solvation shells, those in the anionic solvation shells, and those in the bulk solvent.

Giese, Kaatz, and Pottel [62] have applied this simple model to dielectric relaxation. To strengthen the credibility of any conclusions that might be reached, they compared their results for dielectric relaxation with Engel and Hertz' results for nuclear magnetic relaxation [49], and they attempted a logical synthesis of the two kinds of evidence.

A brief digression to discuss nuclear magnetic relaxation may be useful. The rotational relaxation time that can be deduced from NMR data for aqueous solutions is that for rotation of the water molecules about their twofold axes, but the procedure for doing this involves microscopic assumptions. Experimentally one measures the longitudinal or T_1 relaxation time of the water protons in the solution. This relaxation is due to magnetic field fluctuations experienced by the water protons, and the measurement of T_1 leads directly to the *magnetic correlation time* τ_c [118]. The physical meaning of τ_c may be described as follows: Suppose that at $t = 0$ the magnetic field at a given proton deviates from its time-averaged value. Then τ_c is the mean time (based on many observations) for this deviation to decay to $1/e$ of its initial value.

Magnetic field fluctuations arise from the magnetism and physical motion of nearby protons. If the physical motion consists of independent translational and rotational degrees of freedom, then $1/\tau_c$ is simply the *sum* of independent translational and rotational terms.* The translational term can be estimated with useful accuracy if the self-diffusion coefficient of water in the solution is known. The rotational term is then calculated by difference [49, 118]. The rotational term leads directly to the relaxation time T for the rotation of water molecules about their twofold axes.

Proceeding in this manner, Engel and Hertz [49] evaluated T for a variety of aqueous solutions. In interpreting the results, they used the model of discrete solvation complexes and assumed that exchange of water molecules between the ionic solvation shells and bulk water is so fast that T is simply the average

* It is almost certain that translational and rotational motions of water molecules in liquid water are not strictly independent.

value for all water molecules.* Let x_+ , T_+ ; x_- , T_- ; and $(1 - x_+ - x_-)$, T_0 denote the mole fraction and relaxation time, respectively, of the water molecules in cationic solvation shells, anionic solvation shells, and bulk solvent. The average value of T is then given by

$$T = x_+T_+ + x_-T_- + (1 - x_+ - x_-)T_0 \quad (60)$$

Precise evaluation of T_+ and T_- on this basis requires a sensible way of separating the contributions from the two ions, and prior knowledge of ionic hydration numbers. However, in spite of the lack of this information, Engel and Hertz [49] were able to conclude that T_+ and T_- are of comparable magnitude to T_0 . In particular, this conclusion seemed justified for all alkali ions, from Li^+ to Cs^+ , and for all halide ions, from F^- to I^- .

Returning to the dielectric data, by applying the model of discrete solvation complexes to the static permittivity, it was concluded in Section 4.23 that the rotation of water dipoles becomes partly or largely quenched in the solvation shells of alkali cations, and a solvation-shell structure like that in Fig. 22a seemed probable. On the other hand, water dipoles around halide ions remain rotationally mobile, and a solvation-shell structure like that shown in Fig. 22c was suggested. The dielectric and NMR data are therefore consistent in indicating that water molecules in the solvation shells of halide ions retain a high rotational mobility, comparable to that in bulk water. For water molecules in the solvation shells of alkali cations a discrepancy seems to exist, but this discrepancy could be apparent rather than real. As shown in Fig. 22a, rotation about the twofold axis (the relaxation time for which is measured by T_+) could remain quite free even when dipole rotation is quenched [62].

Comparison of dielectric and NMR-rotational relaxation times provides a more stringent test of consistency because the agreement must be quantitative. Giese, Kaatze, and Pottel [62] addressed themselves to this problem. To obtain precise numbers, they separated cationic and anionic contributions to T in Eq. 60 by assuming that $T_{\text{K}^+} = T_{\text{Cl}^-}$ and calculating ionic hydration numbers from ion size, following the method of Hertz and co-workers [48]. Thus they inferred the following values for T_+/T_0 and T_-/T_0 : Li^+ , 2.5; Na^+ , 1.5; K^+ , 0.9; F^- , 2.6; Cl^- , 0.9; Br^- , 0.8; I^- , 0.4. Arguing that for the halide ions, T_-/T_0 should be equal to the corresponding ratio τ_-/τ_0 of *dielectric* relaxation times, they analyzed the experimental values of S_r (Table 13) and

* Actually this is not a drastic assumption because one needs to assume only that the characteristic time λ for exchange is short compared to $1/T_1$ for each subspecies [48]. In the case of water molecules and discrete solvation complexes, this implies that $T_+, T_- \ll 10^{-11}/\lambda$. The sharpness of the water proton resonance signals in aqueous salt solutions indicates that $\lambda < 10^{-4}$ sec. Hence Eq. 60 will apply if T_+ and T_- are shorter than 10^{-7} sec.

showed that the given values of T_-/T_0 can reproduce the changes in S_r for halide salts as the halide ion varies from F^- to I^- .

For the alkali cations, a similar identification of T_+/T_0 with τ_+/τ_0 must be rejected because it would not be consistent with the conclusion that dipole rotation in the cationic solvation shells becomes quenched. On the other hand, if one assumes that $\tau_+/\tau_0 = 0$, it becomes impossible to account for the negative sign, let alone the actual value, of S_r . Noting that the use of Eq. 60 already implies rapid exchange of water molecules, Giese, Kaatze, and Pottel [62] resolved this dilemma by pointing out that rapid exchange of water molecules between the cationic solvation shells and bulk solvent would reduce the dielectric relaxation time since water polarization becomes quenched by the intense electrical fields when water molecules enter the cationic solvation shells. Given this additional mechanism for dielectric relaxation, it becomes possible to deduce the mean lifetimes λ of the water molecules in the cationic solvation shells. The results, expressed as λ/τ_0 , are 3.1 for Li^+ , 1.3 for Na^+ and 0.8 for K^+ , in almost quantitative agreement with the values of T_+/T_0 inferred from the NMR data [62]. The absolute values of λ are quite short; on introducing $\tau_0 = 8.1 \times 10^{-12}$ sec, we find that the longest value of λ , for the lithium ion, is 2.5×10^{-11} sec.

Equality of λ and T_+ for alkali cations, if real, would suggest that the corresponding processes are directly coupled. For example, a water molecule in the hydration shell might be able to rotate about its twofold axis only if a second water molecule simultaneously departs from the hydration shell.

In spite of their internal consistency, conclusions based on the model of discrete solvation complexes probably ought to be treated with reservation. For one thing, the value of 2.5×10^{-11} sec obtained for λ of a water molecule in the hydration shell of lithium ion seems suspiciously small when compared with λ values of 0.01–0.001 sec for Be^{2+} , 10^{-5} sec for Mg^{2+} , and >0.02 sec for Al^{3+} . The latter values are based on direct measurements of λ at 25° , or on extrapolation to 25° of direct measurements at lower temperatures [13, 53, 102]. Perhaps more revealing is the comparison of aqueous with nonaqueous solutions of ions, which places water squarely into a family of solvents whose hydrogen-bonded structure is sensitive to the presence of ions also outside the ionic solvation shells.

4.3. Ions in Nonaqueous Solvents

Dielectric data for solutions of electrolytes in nonaqueous solvents of high permittivity are relatively scarce. This is regrettable, because such data can greatly broaden our perspective beyond the aquocentric view afforded in the preceding section. Selected and typical results are listed in Table 16. Further

Table 16 Dielectric Data for Electrolytes in Nonaqueous Solvents at 25°^a

Solvent	S_0	g	τ_0 (psec)	Salt	S_ϵ	$10^{12}S_r$	$d\alpha/dc^b$	S_ϵ/ϵ_0V_1
HOH	78.4	2.68	8.3	LiNO ₃	-16.4	-0.4	0	-0.012
MeOH	32.4	2.94	53	LiCl	-27	-17	+	-0.020
				NaI	-27	-30	+	-0.020
				LiCl	-10(?) ^c	-32	+	-0.0070(?)
EtOH	24.4	3.04	160	NaI	-38	-320	+	-0.026
				LiNO ₃	-194	-32	+	-0.018
HCONHCH ₃	182	4.31	123	LiNO ₃	-26	+1.0	0	-0.0060
HCONH ₂	109.5	2.22	37	LiNO ₃	-5.0	+2.4	+++	-0.0017
HCON(CH ₃) ₂	37.4	1.11	11	LiNO ₃	-11.6	+5.2	++	-0.0034
(CH ₃) ₂ SO	47.3	1.19	20	LiNO ₃	-19.4	+16	+++	-0.0038
[(CH ₃) ₂ N] ₃ PO	29.6	1.96	80	LiNO ₃				

^a Based on data in refs. 16 and 75.^b Change in Cole-Cole parameter per formal electrolyte.^c This result seems anomalous. We suspect that there is considerable ion pair formation.

relevant results have been reported by Badiali, Barthel, Hasted, Sastry, and their co-workers [12, 15, 75, 132].

The solvents listed in Table 16 span a variety of chemical types: hydroxylic solvents, hydrogen-bonding amides, and the dipolar aprotic solvents dimethylformamide, dimethylsulfoxide, and hexamethylphosphoramide. Their static permittivities range from 182 to 24. Their Kirkwood g factors range from 4.3 to close to unity. With the possible exception of LiCl in ethanol, the added electrolytes appear to be largely dissociated to free ions.

The effects of the electrolytes are measured in Table 16 by the molar dielectric increment S_ϵ (Eq. 55), the molar change in relaxation time S_r (Eq. 56), and the change $d\alpha/dc$ in the Cole-Cole parameter. Values of S_ϵ are consistently negative; values of S_r are negative in some solvents and positive in others; and $d\alpha/dc$ varies qualitatively from zero (to indicate "no change") to +++ (to indicate a marked broadening of the distribution function).

Before discussing the effects of the electrolytes, it is worthwhile to correct S_ϵ for differences in solvent properties. To do this, we recall the model of discrete solvation complexes, which led to Eq. 59 for S_ϵ . According to this model, the dipole-rotational quenching number Z will remain closely proportional to $S_\epsilon/(\epsilon_0V_1)$, as the solvent is changed, the approximations being that $(\epsilon_0 - \epsilon_s) \approx \epsilon_0$ and that $(ZV_1 + V_2^{\text{app}}) \approx ZV_1$. Thus if we simply divide S_ϵ by ϵ_0V_1 , we correct for specific solvent properties and arrive at a useful index for Z . This index should remain useful even if we abandon the specific model that led to Eq. 59. Accordingly, values of $S_\epsilon/(\epsilon_0V_1)$ are included in Table 16.

According to the values of S_r , $d\alpha/dc$, and $S_\epsilon/(\epsilon_0V_1)$ listed in Table 16, there is a striking difference between hydrogen-bonding solvents, on the one hand,

and dipolar aprotic solvents, on the other. Judging by the limited data available, electrolytes in dipolar aprotic solvents cause a substantial lengthening of the mean dielectric relaxation time, together with a marked, and even enormous, broadening of the distribution function, and relatively small magnitudes of $S_e/(\epsilon_0 V_1)$. By contrast, electrolytes in hydrogen-bonding solvents typically cause a shortening of the mean dielectric relaxation times, together with little or no broadening of the distribution function and relatively large magnitudes of $S_e/(\epsilon_0 V_1)$.

Although it would be foolish to make sweeping generalizations with such a limited sample, the data *are* quite suggestive. In the dipolar aprotic solvents, the behavior of the ions is essentially that to be expected if discrete solvation complexes were formed, as indicated particularly by the spreading-out of the relaxation times. If this be granted, then we may infer from the rather small magnitudes of $S_e/(\epsilon_0 V_1)$ and the positive values of S_r that dipole rotation in the ionic solvation shells is not really quenched but only somewhat constrained, so that the molecules in the solvation shells remain able to rotate, but with a longer relaxation time.

The dipolar aprotic solvents are effective at solvating cations but not anions. It is therefore tempting to ascribe the different behavior in the hydrogen-bonding solvents to additional anion solvation. However, this theory must be ruled out; one would hardly expect a reduction, and little spreading-out, of the dielectric relaxation time. Instead, the trends of the data suggest "structure-breaking" in the bulk solvent. The high g factors of the pure hydrogen-bonding solvents indicate the existence of hydrogen-bonded chains or aggregates in which the molecular dipoles reinforce each other. When the permittivity is lowered by the addition of an electrolyte, the medium becomes less able to tolerate high dipole moments and the equilibrium among the various hydrogen-bonded solvent species shifts toward shorter, less polar chains and cyclic aggregates. Thus one might envisage the formation of cyclic hydrogen-bonded structures in the alcohols and of nonpolar head-to-head dimers in the amides. Be that as it may, the initial lowering of the permittivity due to the added electrolyte induces further lowering of the permittivity due to a shift of "structure" toward less polar species in the bulk solvent. Inasmuch as such species tend to have lower molecular weights, the average relaxation time of the solvent molecules is reduced.

Judging by the magnitudes of the observed values of S_e and S_r , these "structure-breaking" effects in the bulk solvent are clearly more important than the "normal" effects (seen in dipolar aprotic solvents) that are associated with the solvation of the ions. If this be granted, then the typical "sharpness" of the distribution of relaxation times in hydrogen-bonding solvents suggests that the processes of hydrogen-bond formation and breaking are very fast—distinctly faster than those of dielectric relaxation. In this sense, the term

“flickering clusters” introduced by Frank and Wen [52] to describe the behavior of aggregates of water molecules may be quite apt for hydrogen-bonded solvents in general.

APPENDIX. THEORY OF MOLAR POLARIZATION FOR FLUCTUATING DIPOLE MOMENT

It was pointed out in Section 2.33 that for molecules with fluctuating dipole moments, the observed polarization depends on the relative magnitudes of the dielectric relaxation time τ and the rate constant for the process which causes the dipole fluctuations. Because we have not seen a published derivation of the equations governing this phenomenon, we shall derive these equations at this time, within the framework of Debye’s theory [44].

For definiteness, consider a polar solute at concentration \bar{c}_2 in a nonpolar solvent such as benzene. Assume that the solute is actually an equilibrium mixture of two rapidly interconverting subspecies, A and B, whose dipole moments are μ_A and μ_B . Let x be the mole fraction of A in the solute ($x = [A]/([A] + [B])$), and let λ_A and λ_B denote the mean lifetimes of the subspecies:



Let the dielectric relaxation times assignable to the subspecies be τ_A and τ_B , respectively. If the interconversion is a much slower process than the dielectric relaxation, that is if $\lambda_A^{-1} + \lambda_B^{-1}$ is small compared to $\tau_A^{-1} + \tau_B^{-1}$, then the two subspecies will act as discrete dipoles and make additive contributions to the molar polarization P_2 of the solute component (Eq. 62). The formal “solute component” comprises the two interconverting subspecies:

$$P_2 = xP_A + (1-x)P_B \quad (62)$$

On applying Debye’s Eq. 2 and letting $\alpha_2 = \alpha_A = \alpha_B$ we obtain Eq. 63 for the measured dipole moment μ of the formal solute (cf. Eq. 22):

$$\mu^2 = x\mu_A^2 + (1-x)\mu_B^2 \quad (\text{for slow exchange}) \quad (63)$$

On the other hand, if the interconversion is a much faster process than the dielectric relaxation, then the two subspecies will no longer act as discrete dipoles, and we measure an average dipole moment μ , (cf. Eq. 27):

$$\mu = x\mu_A + (1-x)\mu_B \quad (\text{for fast exchange}) \quad (64)$$

In deriving Eqs. 63 and 64, it will be helpful to consult Figs. 24 and 25. According to Debye, the mean polarization per molecule $\langle m \rangle = \mu \langle \cos \theta \rangle$,

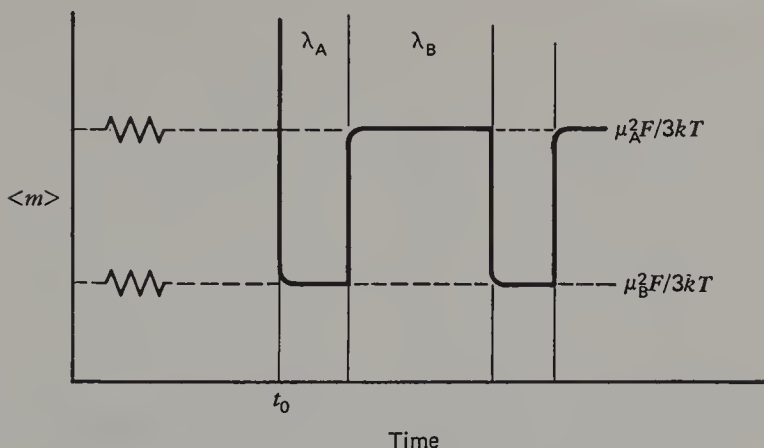


Figure 24. Average behavior of $\langle m \rangle$ as a function of time when chemical exchange is slow compared to dielectric relaxation.

where θ is the angle between the direction of the electric field and the dipole axis. If there are no dipole fluctuations, $\langle \cos \theta \rangle$ approaches an equilibrium value equal to $\mu F / 3kT$, where F is the Lorentz-Lorentz internal field. In a steady applied field, the approach of $\langle \cos \theta \rangle$ to the equilibrium value $\mu F / 3kT$ will follow first-order kinetics with relaxation τ :

$$\frac{d\langle \cos \theta \rangle}{dt} = \frac{(\mu F / 3kT) - \langle \cos \theta \rangle}{\tau} \quad (65)$$

When there is slow exchange between two subspecies A and B (with dipole moments μ_A and μ_B), the *average* behavior of $\langle m \rangle$ per molecule during one cycle is shown in Fig. 24. Since the dielectric relaxation times τ_A and τ_B are short compared to λ_A and λ_B , $\langle m \rangle$ is essentially a step-function of time. To obtain the average value of $\langle m \rangle$, it will be sufficient to consider one cycle, as follows:

$$\begin{aligned} \langle \bar{m} \rangle &\equiv \frac{\mu^2 F}{3kT} = \frac{\int_{t_0}^{t_0 + \lambda_A + \lambda_B} \langle m \rangle dt}{\int_{t_0}^{t_0 + \lambda_A + \lambda_B} dt} \\ &= \frac{(\lambda_A \mu_A^2 + \lambda_B \mu_B^2) F}{(\lambda_A + \lambda_B) 3kT} = \frac{[x \mu_A^2 + (1 - x) \mu_B^2] F}{3kT} \end{aligned} \quad (66)$$

It is obvious on inspection that Eq. 66 reduces to Eq. 63.

When there is fast exchange between the two subspecies, the *average* behavior of $\langle m \rangle$ and $\langle \cos \theta \rangle$ is shown in Fig. 25. When a steady state is reached, $\langle \cos \theta \rangle$ shows only small fluctuations about its average value, $\overline{\langle \cos \theta \rangle}$, because

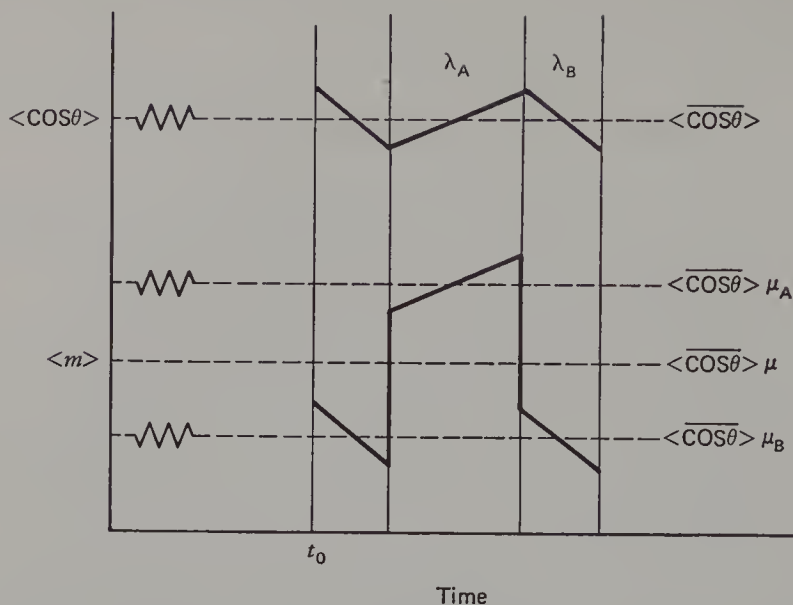


Figure 25. Average behavior of $\langle \cos \theta \rangle$ (upper graph) and $\langle m \rangle$ (lower graph) as a function of time when chemical exchange is fast compared to dielectric relaxation.

the dielectric relaxation is so much slower than the fluctuation of the dipole moment. To calculate the average value of $\langle \cos \theta \rangle$ in the steady state, we introduce the condition stated in 67, which assures that $\langle \cos \theta \rangle$ remains constant:

$$\int_{t_0}^{t_0+\lambda_A} \frac{d\langle \cos \theta \rangle}{dt} dt + \int_{t_0+\lambda_A}^{t_0+\lambda_A+\lambda_B} \frac{d\langle \cos \theta \rangle}{dt} dt = 0 \quad (67)$$

Since $\lambda_A, \lambda_B \ll \tau_A, \tau_B$, we introduce for $d\langle \cos \theta \rangle/dt$ the average value during each half-cycle, according to Eq. 65. The result, after integration, is

$$\frac{\lambda_A}{\tau_A} \left(\frac{\mu_A F}{3kT} - \overline{\langle \cos \theta \rangle} \right) + \frac{\lambda_B}{\tau_B} \left(\frac{\mu_B F}{3kT} - \overline{\langle \cos \theta \rangle} \right) = 0 \quad (68)$$

Solving for $\overline{\langle \cos \theta \rangle}$, we then obtain

$$\overline{\langle \cos \theta \rangle} \left(\frac{\lambda_A}{\tau_A} + \frac{\lambda_B}{\tau_B} \right) = \frac{F}{3kT} \left(\frac{\mu_A \lambda_A}{\tau_A} + \frac{\mu_B \lambda_B}{\tau_B} \right) \quad (69)$$

Because the exchange is fast compared to dielectric relaxation, it is reasonable to suppose that the solvent environment for the two subspecies is practically the same. Writing $\tau = 4\pi\eta a^3/kT$ and assuming that the molecular radius a is the same for A and B, we conclude that $\tau_A = \tau_B = \tau$. Eliminating τ from Eq. 69 we then obtain the simple result

$$\overline{\langle \cos \theta \rangle} = \frac{F}{3kT} (x\mu_A + [1 - x]\mu_B) \quad (70)$$

Using the same method as before (Eq. 66), we then evaluate the average value of $\langle \bar{m} \rangle$:

$$\langle \bar{m} \rangle = \frac{\mu^2 F}{3kT} = \frac{F}{3kT} (x\mu_A + [1 - x]\mu_B)^2 \quad (71)$$

It is obvious on inspection that Eq. 71 reduces to Eq. 64.

ACKNOWLEDGMENT

It is a pleasure to thank the National Science Foundation and the National Institutes of Health for postdoctoral fellowships to T-P. I. and S. H., respectively, during the period in which this chapter was written.

REFERENCES

1. N. W. Aaron and E. H. Grant, *Trans. Faraday Soc.*, **52**, 85 (1962).
2. N. W. Aaron and E. H. Grant, *Trans. Faraday Soc.*, **63**, 2177 (1967).
3. N. W. Aaron and E. H. Grant, *Br. J. Appl. Phys.*, **18**, 957 (1967).
4. J. H. Ambrus, C. T. Moynihan, and P. B. Macedo, *J. Phys. Chem.*, **76**, 3287 (1972).
5. J. E. Anderson, *Ber. Bunsenges. Phys. Chem.*, **75**, 294 (1971).
6. J. E. Anderson and R. Ullman, *J. Chem. Phys.*, **47**, 2178 (1967).
7. G. Atkinson and S. K. Kor, *J. Phys. Chem.*, **71**, 673 (1967).
8. G. Atkinson and Y. Mori, *J. Phys. Chem.*, **71**, 3523 (1967).
9. G. Atkinson, *Kem. Kozlem.*, **33**, 113 (1970).
10. H. Baba, A. Matsuyuma, and N. Kokubun, *J. Chem. Phys.*, **41**, 895 (1962).
11. J. P. Badiali, H. Cachet, and J. C. Lestrade, *J. Chim. Phys.*, **64**, 1350 (1967).
12. J. P. Badiali, H. Cachet, and J. C. Lestrade, *Electrochim. Acta*, **16**, 731 (1971).
13. H. W. Baldwin and H. Taube, *J. Chem. Phys.*, **33**, 206 (1960).
14. G. M. Barrow, *J. Am. Chem. Soc.*, **78**, 5802 (1956).
15. J. Barthel, F. Schmithals, and H. Behret, *Z. Physik Chem., Neue Folge*, **71**, 115 (1970).
16. J. Barthel, H. Behret, and F. Schmithals, *Ber. Bunsenges. Phys. Chem.*, **75**, 305 (1971).
17. R. K. Bauer and H. Lew, *Can. J. Phys.*, **41**, 1461 (1963).
18. K. Bauge and J. W. Smith, *J. Chem. Soc.*, **1964**, 4244.
19. M. T. Beck, *Chemistry of Complex Equilibria*, Van Nostrand-Reinhold, New York, 1970.
20. C. L. Bell and G. M. Barrow, *J. Chem. Phys.*, **31**, 1158 (1959).
21. J. D. Bernal and R. H. Fowler, *J. Chem. Phys.*, **1**, 515 (1933).
22. P. R. Bevington, *Data Reduction and Error Analysis for the Physical Sciences*, McGraw-Hill, New York, 1969.

23. C. F. J. Böttcher, *Theory of Electric Polarization*, Elsevier, Amsterdam, 1952, Chap. 5.
24. C. F. J. Böttcher, *Theory of Electric Polarization*, Elsevier, Amsterdam, 1952, Chap. 10.
- 24a. R. H. Boyd, *J. Chem. Phys.*, **35**, 1281 (1961).
25. F. W. Breivogel, Jr., A. J. Hebert, and K. Street, Jr., *J. Chem. Phys.*, **42**, 1555 (1965).
26. E. A. S. Cavell, *Trans. Faraday Soc.*, **61**, 1578 (1965).
27. E. A. S. Cavell and P. C. Knight, *Trans. Faraday Soc.*, **68**, 765 (1972).
28. E. A. S. Cavell, P. C. Knight, and M. A. Sheikh, *Trans. Faraday Soc.*, **67**, 2225 (1971).
29. E. A. S. Cavell and M. A. Sheikh, *Trans. Faraday Soc.*, **69**, 315 (1973).
30. G. W. Ceska and E. Grunwald, *J. Am. Chem. Soc.*, **89**, 1371 (1967).
31. J. J. Christensen, J. O. Hill, and R. M. Izatt, *Science*, **174**, 459 (1971).
32. E. J. Cohn and J. T. Edsall, *Amino Acids, Peptides and Proteins*, Reinhold, New York, 1943, Chap. 6.
33. R. H. Cole, *J. Chem. Phys.*, **27**, 33 (1957).
34. R. H. Cole, "Theories of Dielectric Polarization and Relaxation" in *Progress in Dielectrics*, Vol. 3, Wiley and Sons, New York 1961, pp. 47-100.
35. R. H. Cole, *J. Chem. Phys.*, **42**, 637 (1965).
36. R. H. Cole and K. S. Cole, *J. Chem. Phys.*, **9**, 341 (1949).
37. W. P. Connors and C. P. Smyth, *J. Am. Chem. Soc.*, **64**, 1870 (1942).
38. M. R. Crampton and E. Grunwald, *J. Am. Chem. Soc.*, **93**, 2987 (1971).
39. C. W. N. Cumper and P. G. Langley, *Trans. Faraday Soc.*, **65**, 35 (1971).
40. M. Davies and G. Johansson, *Acta Chem. Scand.*, **18**, 1171 (1964).
41. M. Davies and L. Sobczyk, *J. Chem. Soc. A*, **1962**, 3000.
42. M. Davies and G. Williams, *Trans. Faraday Soc.*, **56**, 1619 (1960).
43. M. M. Davis, *Acid-Base Behavior in Aprotic Organic Solvents*, National Bureau of Standards Monograph 105, Washington, D. C., 1968.
44. P. Debye, *Polar Molecules*, Dover, New York, 1929.
45. P. Debye and H. Falkenhagen, *Physik. Z.* **29**, 401 (1928); H. Falkenhagen, *Electrolytes*, Clarendon Press, Oxford, 1934.
46. J. T. Edsall and J. Wyman, *Biophysical Chemistry*, Vol. I, Academic Press, New York, 1958, Chap. 6.
47. M. Eigen and K. Tamm, *Ber. Bunsenges. Phys. Chem.*, **66**, 107 (1962).
48. L. Endom, H. G. Hertz, B. Thül, and M. D. Zeidler, *Ber. Bunsenges. Phys. Chem.*, **71**, 1008 (1967).
49. G. Engel and H. G. Hertz, *Ber. Bunsenges. Phys. Chem.*, **72**, 808 (1968).
50. B. P. Fabricand, R. O. Carlson, C. A. Lee, and I. I. Rabi, *Phys. Rev.*, **91**, 1403 (1953).
51. W. T. Ford and D. J. Cram, *J. Am. Chem. Soc.*, **90**, 2606 (1968).
52. H. S. Frank and W.-Y. Wen, *Disc. Faraday Soc.*, **24**, 133 (1957).
53. A. Fratiello, R. E. Lee, V. M. Nishida, and R. E. Schuster, *J. Chem. Phys.*, **48**, 3705 (1968).
54. H. K. Frensdorff, *J. Am. Chem. Soc.*, **93**, 600 (1971).

55. H. K. Frensdorff, *J. Am. Chem. Soc.*, **93**, 4684 (1971).
56. H. Fröhlich, *Trans. Faraday Soc.*, **44**, 238 (1948).
57. H. Fröhlich, *Theory of Dielectrics*, Oxford, 1949.
58. R. M. Fuoss, *J. Am. Chem. Soc.*, **56**, 1027, 1031 (1934).
59. R. M. Fuoss, *Proc. Nat. Acad. Sci., U.S.*, **45**, 807 (1959).
60. R. M. Fuoss and J. G. Kirkwood, *J. Am. Chem. Soc.*, **63**, 385 (1941).
61. J. A. Geddes and C. A. Kraus, *Trans. Faraday Soc.*, **32**, 585 (1936).
62. K. Giese, U. Kaatze, and R. Pottel, *J. Phys. Chem.*, **74**, 3718 (1970).
63. W. R. Gilkerson and K. K. Srivastava, *J. Phys. Chem.*, **64**, 1485 (1960).
64. S. H. Glarum, *J. Chem. Phys.*, **33**, 1371 (1960).
65. E. H. Grant and R. Shack, *Br. J. Appl. Phys.*, **18**, 1807 (1967); E. H. Grant, *J. Phys. Chem.*, **73**, 4386 (1969).
66. G. W. Green and H. Lew, *Can. J. Phys.*, **38**, 482 (1960).
67. E. Grunwald, *Prog. Phys. Org. Chem.*, **3**, 317 (1965).
68. E. Grunwald and A. Effio, *J. Solution Chem.*, **2**, 373 (1973).
69. E. Grunwald and A. Effio, *J. Solution Chem.*, **2**, 393 (1973).
70. E. Grunwald and E. Price, *J. Am. Chem. Soc.*, **86**, 4517 (1964).
71. G. V. Gussakova, G. S. Denissov, and A. L. Smolyansky, *Organic Reactivity*, **9**, 1141 (1972).
72. G. H. Haggis, J. B. Hasted, and T. J. Buchanan, *J. Chem. Phys.*, **20**, 1452 (1952).
73. F. Halverstadt and W. D. Kumler, *J. Am. Chem. Soc.*, **64**, 2988 (1942).
74. W. C. Hamilton, *Statistics in Physical Science, Estimation, Hypothesis Testing and Least Squares*, Ronald Press, New York, 1964.
75. J. B. Nasted and G. W. Roderick, *J. Chem. Phys.*, **29**, 17 (1958).
76. J. B. Hasted, in *A Specialist Periodical Report: Dielectric and Related Molecular Processes*, Vol. 1, The Chemical Society, Burlington House, London, 1972, p. 121.
77. F. E. Harris and C. T. O'Konski, *J. Phys. Chem.*, **61**, 310 (1957).
78. J. B. Hasted and S. H. M. El Sabeh, *Trans. Faraday Soc.*, **49**, 1003 (1957).
79. A. J. Hebert, F. W. Breivogel, Jr., and K. Street, Jr., *J. Chem. Phys.*, **41**, 2368 (1964).
80. A. J. Hebert, F. J. Lovas, C. A. Melendres, C. D. Hollowell, T. L. Story, Jr., and K. Street, Jr., *J. Chem. Phys.*, **48**, 2824 (1968).
81. I. G. Hedestrand, *Z. Physik. Chem.*, **2B**, 428 (1929).
82. N. E. Hill, *Proc. Phys. Soc.*, **72**, 1532 (1958).
83. N. E. Hill, W. E. Vaughan, A. H. Price, and M. Davies, *Dielectric Properties and Molecular Behaviour*, Van Nostrand-Reinhold, London, 1969.
84. C. D. Hollowell, A. J. Hebert, and K. Street, Jr., *J. Chem. Phys.*, **41**, 3540 (1964).
85. G. S. Hooper and C. A. Kraus, *J. Am. Chem. Soc.*, **56**, 2265 (1934).
86. R. A. Hudson, R. M. Scott, and S. M. Vinogradov, *Spectrochim. Acta*, **26**, 337 (1970).
87. Ting-Po I and E. Grunwald, Unpublished results.
88. R. M. Izatt, J. H. Rytting, D. P. Nelson, B. L. Haymore, and J. J. Christensen, *Science*, **164**, 443 (1969); *J. Am. Chem. Soc.*, **93**, 1619 (1971).

89. J. Jadzyn and J. Malecki, *Acta Phys. Polonica*, **A41**, 599 (1972).
90. C. F. Johnson and R. H. Cde, *J. Am. Chem. Soc.*, **73**, 4536 (1951).
91. R. L. Kay and K. S. Pribadi, *Rev. Sci. Instrum.*, **40**, 726 (1969).
92. R. L. Kay, G. A. Vidulich, and K. S. Pribadi, *J. Phys. Chem.*, **73**, 445 (1969).
93. J. G. Kirkwood, *J. Chem. Phys.*, **7**, 911 (1939).
94. J. G. Kirkwood, in *Proteins, Amino Acids and Peptides*, E. J. Cohn and J. T. Edsall (Eds.), Reinhold, New York, 1943, Chap. 12.
95. J. G. Kirkwood, *Trans. Faraday Soc.*, **A42**, 7 (1946).
96. J. G. Kirkwood, *Ann. N.Y. Acad. Sci.*, **40**, 315 (1940).
97. G. N. LaMar, *J. Chem. Phys.*, **43**, 235 (1965).
98. J. A. Lane and J. A. Saxton, *Proc. Roy. Soc. London*, **A214**, 531 (1952).
99. O. Levy, G. Markovits, and A. S. Kertes, *J. Phys. Chem.*, **75**, 542 (1971).
100. Z. Luz and S. Meiboom, *J. Chem. Phys.*, **40**, 2686 (1964), Eq. 16.
101. A. A. Maryott, *J. Res. Nat. Bur. Stands*, **41**, 1 (1948).
102. N. A. Matwiyoff and H. Taube, *J. Am. Chem. Soc.*, **90**, 2796 (1968).
103. A. L. McClellan, *Tables of Experimental Dipole Moments*, Freeman, San Francisco, 1963.
104. R. C. Miller and C. P. Smyth, *J. Am. Chem. Soc.*, **79**, 3310 (1957).
105. C. T. Moynihan, R. D. Bressel, and C. A. Angell, *J. Chem. Phys.*, **55**, 4414 (1971).
106. G. Oster, *J. Am. Chem. Soc.*, **66**, 948 (1944).
107. G. Oster, *J. Am. Chem. Soc.*, **68**, 2036 (1946).
108. G. Oster and J. G. Kirkwood, *J. Chem. Phys.*, **11**, 175 (1943).
109. G. Oster, D. Price, L. G. Joyner, and J. G. Kirkwood, *J. Am. Chem. Soc.*, **66**, 946 (1944).
110. L. Onsager, *J. Am. Chem. Soc.*, **58**, 1486 (1936).
111. L. Pauling, *The Nature of the Chemical Bond*, Cornell University Press, Ithaca, N.Y., 1944, Chap. 10.
112. C. J. Pedersen, *J. Am. Chem. Soc.*, **89**, 7017 (1967).
113. C. J. Pedersen, *Fed. Proc.*, **27**, 1305 (1968).
114. C. J. Pedersen, *J. Am. Chem. Soc.*, **92**, 391 (1970).
115. C. J. Pedersen and H. K. Frensdorff, *Angew. Chem. Int. Ed.*, **11**, 16 (1972).
116. R. A. Pierotti, *J. Phys. Chem.*, **67**, 1840 (1963).
117. R. A. Pierotti, *J. Phys. Chem.*, **69**, 281 (1965).
118. J. A. Pople, W. G. Schneider, and H. J. Bernstein, *High-Resolution Nuclear Magnetic Resonance*, McGraw-Hill, New York, 1959.
119. R. Pottel, *Ber. Bunsenges. Phys. Chem.*, **69**, 363 (1965).
120. R. Pottel, *Ber. Bunsenges. Phys. Chem.*, **75**, 286 (1971).
121. J. G. Powles, *J. Chem. Phys.*, **21**, 633 (1953).
122. K. S. Pribadi and R. L. Kay, *Rev. Sci. Instrum.*, **40**, 726 (1969).
123. R. N. Ramachandran, *J. Molec. Biol.*, **7**, 95 (1963).
124. P. S. Krishna Mohana Rao and D. Premaswarup, *Trans. Faraday Soc.*, **66**, 1974 (1970).
125. H. Ratajczak, *J. Phys. Chem.*, **76**, 3000 (1972).

126. H. Ratajczak and W. J. Orville-Thomas, *J. Chem. Phys.*, **58**, 911 (1973).
127. H. Ratajczak and L. Sobczyk, *J. Chem. Phys.*, **50**, 556 (1969).
128. E. A. Richardson and K. H. Stern, *J. Am. Chem. Soc.*, **82**, 1296 (1960).
129. E. S. Rittner, *J. Chem. Phys.*, **19**, 1030 (1951).
130. F. J. C. Rossotti and H. Rossotti, *The Determination of Stability Constants*, McGraw-Hill, New York, 1961.
131. H. Reiss and D. M. Tully-Smith, *J. Chem. Phys.*, **55**, 1674 (1971), and the preceding references cited therein.
132. P. S. Sastry and D. Premaswarup, *J. Ind. Pure Appl. Phys.*, **11**, 253 (1970).
133. G. Scatchard, *J. Chem. Phys.*, **9**, 34 (1941).
134. G. Schwarz, *J. Phys. Chem.*, **71**, 4021 (1967).
135. G. Schwarz, *Rev. Modern Phys.*, **40**, 206 (1968).
136. A. H. Sharbaugh, Jr., C. Schmelzer, H. C. Eckstrom, and C. A. Kraus, *J. Chem. Phys.*, **15**, 47 (1947).
137. A. H. Sharbaugh, Jr., H. C. Eckstrom, and C. H. Kraus, *J. Chem. Phys.*, **15**, 54 (1947).
138. J. Smid, in *Ions and Ion Pairs in Organic Reactions*, Vol. One, M. Szwarc (Ed.), Wiley-Interscience, New York, 1972, Chap. 3.
139. J. Smid, *Angew. Chem. Int. Ed.*, **11**, 112 (1972).
140. J. W. Smith, *Electric Dipole Moments*, Butterworths, London, 1955.
141. C. P. Smyth, *Dielectric Behavior and Structure*, McGraw-Hill, New York, 1965.
142. C. P. Smyth, in *Symposium on Molecular Relaxation Processes*, The Chemical Society, London, 1965, Special Publication No. 20, p. 12.
143. K. H. Stern and E. S. Amis, *Chem. Rev.*, **59**, 1 (1959).
144. A. Suggett, in *A Specialist Periodical Report: Dielectric and Related Molecular Processes*, Vol. 1, The Chemical Society, Burlington House, London, 1972, p. 100.
145. C. Tanford, *The Physical Chemistry of Macromolecules*, Wiley, New York, 1967, p. 124.
- 145a. D. Bright and Mary R. Thuter, *J. Chem. Soc (B)*, **1970**, 1544; M. A. Bush and Mary R. Truter, *J. Chem. Soc (B)*, **1971**, 1440.
146. H. Tsubomora, *Bull. Chem. Soc. Japan*, **31**, 435 (1958).
147. W. E. Vaughan, Chap. 2 in ref. 83.
148. G. A. Vidulich, D. F. Evans, and R. L. Ray, *J. Phys. Chem.*, **71**, 656 (1967).
149. D. J. Wilde, *Optimum Seeking Methods*, Prentice-Hall, Englewood Cliffs, N.J., 1964.
150. G. Williams, *Adv. Mol. Relaxation Processes*, **1**, 409 (1970).
151. G. Williams, *Chem. Revs.*, **72**, 55 (1972).
152. J. Wyman, Jr., *Chem. Rev.*, **19**, 213 (1936).
153. R. Zwanzig, *J. Chem. Phys.*, **38**, 1603 (1963).
154. R. Zwanzig, *J. Chem. Phys.*, **52**, 3625 (1970).

Author Index

Numbers in parenthesis are the reference numbers found on the pages preceding them. A complete list of references is given at the end of each chapter.

- Aalbersberg, W.I., 39, 40, 43 (162)
Aaron, N.W., 494, 495 (1-3)
Abe, K., 404 (40)
Abley, P., 101 (273)
Abraham, M.H., 341, 342 (201)
Acrivios, J.V., 128 (105)
Adam, F.C., 62, 65, 67 (208)
Adams, G.E., 125 (128)
Adams, R.F., 56 (191), 60 (196), 66, 67 (216)
Adams, R.N., 70 (222, 223), 85 (254)
Agtarap, A., 361 (245)
Ahrens, M.L., 184 (75)
Aial, S., 90 (351)
Alder, B.J., 130, 135 (313)
Allen, A.O., 119 (75, 112)
Allen, G., 377, 379 (2)
Allen, J.D., 196 (93)
Allen, P.E.M., 404 (41)
Allendoerfer, R.D., 104 (356)
Allinger, N.L., 358 (237), 360 (239)
Allred, E.L., 363 (249)
Almy, J., 208 (121, 122, 124), 217 (121, 122), 219 (124), 220 (122, 124)
Alvarino, J.M., 385 (137)
Ambrus, J.H., 498 (4)
Amphlet, C.B., 58 (207)
Anbar, L.M., 125 (130)
Anderson, E.W., 405 (48)
Anderson, J.E., 448, 480 (6)
Anderson, R.P., 279, 281, 282 (55)
Ando, H., 434, 435 (98)
Angelo, B., 129 (91)
Angyal, N.L., 358 (237), 360 (239)
Appel, B., 253, 254, 256, 281, 285, 286, 294, 298, 307, 309, 311, 322, 363-365 (19)
Appenrodt, J., 94 (261)
Applequist, D.E., 172 (44)
Arai, S., 61 (201), 87 (241, 243), 88 (243), 125 (300), 222 (144, 145), 223 (145, 147), 224 (147)
Arnett, E.M., 156 (14), 157 (23), 158 (24)
Aten, A.C., 39, 40 (164)
Atherton, N.M., 60 (196), 62, 63 (204)
Atkinson, G., 492 (7-9), 498 (8)
Ausloos, P., 362 (248)
Baba, H., 464 (10)
Badding, V.G., 156 (12)
Badiali, J.P., 510 (12)
Bahsteter, F., 399, 420 (38)
Bailey, T.L., 22 (50)
Baker, R., 253, 254, 256 (19), 273 (51), 281, 285, 286, 294, 298 (19), 307, 309 (19, 133), 311, 322, 363-365 (19)

- Bakulina, I.N., 22 (49)
 Baldwin, H.W., 509 (13)
 Bank, S., 221 (141), 237, 239
 (141, 158), 240 (141), 295,
 297 (102)
 Barabas, J.T., 112 (338)
 Bard, A.J., 85 (253)
 Bar-Eli, K., 129 (107), 132
 (107, 319), 133 (319), 134
 (107), 135 (107)
 Barnes, M., 353 (223)
 Barnett, B.L., 135 (362)
 Barnikol, W.K.R., 377 (133),
 385 (23)
 Barrow, G.M., 464 (14, 20)
 Barrow, R.F., 16 (33)
 Barthel, J., 499 (16), 510
 (15, 16)
 Bartlett, J.A., 430 (125)
 Bartlett, P.D., 248 (3), 257
 (102), 295 (102)
 Barton, F.E., 112 (338)
 Bartsch, R.A., 353 (221)
 Barzakay, S., 426 (85, 87)
 Basolo, F., 3 (10)
 Bateman, L.C., 249 (7, 8), 251,
 252 (7), 257 (7, 8, 30), 259,
 260, 261, 265, 266, 269, 270,
 322, 324, 330, 339 (7)
 Bates, D.R., 9, 18 (21)
 Bates, R.G., 156 (17)
 Bates, T.H., 430 (114)
 Bauer, R.K., 452, 453, 459 (17)
 Bauge, K., 452, 456, 457, 461,
 463, 470 (18)
 Bauld, N.L., 107 (290)
 Bawn, C.E.H., 421 (75), 427 (93)
 Baxendale, J.H., 120 (80), 125
 (128), 127 (367)
 Beak, P., 353 (219)
 Beauchamp, J.L., 45 (346)
 Beck, M.T., 470 (19)
 Becker, E., 130, 135 (313)
 Becker, R.S., 25 (56), 26 (55,
 57), 31 (56), 111 (55)
 Behret, H., 499 (16), 510 (15,
 16)
 Bell, C.L., 464 (20)
 Bell, R.P., 152, 181 (1), 195
 (90) 196 (89)
 Belousova, M.I., 52, 54 (185)
 Benfey, O.T., 250, 266, 275 (9)
 Benjamin, B.M., 360 (239)
 Bennett, J.E., 94 (265)
 Bensley, G., 25 (11)
 Bent, H.E., 33 (143)
 Bentley, T.W., 298, 300-303,
 328, 347-349 (118)
 Bergman, I., 40, 43 (156)
 Bernal, I., 103 (281)
 Bernal, J.D., 501 (21)
 Bernstein, H.J., 507 (118)
 Berry, M.G., 127, 138 (134)
 Berry, R.S., 21 (39)
 Berson, J.A., 358 (235)
 Best, J.V.F., 430 (114)
 Bestian, H., 425 (84)
 Bethel, D., 248, 290 (1)
 Bevinton, P.R., 470 (22)
 Beylen, M. Van, 377 (26)
 Bhattacharyya, D.N., 201-203
 (103), 377, 378 (3), 382 (15),
 384 (15), 386 (3), 411, 412
 (56), 418 (70), 423, 424 (80),
 431 (15)
 Bigeleisen, J., 137 (328), 196
 (92)
 Bigley, D.B., 354 (226)
 Bingham, R.C., 254, 256, 324
 (23), 326, 328, 350 (23, 171)
 Binks, J.H., 43 (179)
 Black, P.E., 404 (41)
 Blackledge, J., 32, 91 (139)
 Blades, H., 123 (118)
 Blandamer, M.J., 127 (132)
 Blume, R.J., 128 (100)
 Boag, J.W., 125 (128)
 Bockrath, B., 112 (342), 131
 (314), 221 (141), 236 (168),
 237, 239 (141, 158)
 Boeckner, C., 16, 17 (31)
 Boer, E. de, 33 (146), 39, 40,
 43 (162), 91 (146), 92 (259)
 Böhm, L.L., 377 (133), 380 (8),
 384 (8), 385 (8, 23, 134), 391 (8)
 Bohme, D.K., 27 (61)
 Bolton, R., 361 (242)
 Boozer, C.E., 355 (227)
 Bopp, R.J., 327, 346 (187),
 361 (245)

- Borčić, S., 298, 300, 302, 303, 305 (117)
- Bordwell, F.G., 187 (78, 79, 83), 188 (78), 196, 199 (94), 249 (5), 305 (127)
- Born, M., 155 (7)
- Börner, K., 425 (84)
- Boschi, R., 29 (348, 349)
- Bostich, E.E., 415 (61)
- Böttcher, C.F.J., 449, 451 (24), 452, 453, 455-457, 463, 466, 473 (23), 484 (24)
- Bovey, F.A., 405 (48), 406, 425 (49)
- Bovin, M.A., 430 (115, 117), 432 (117)
- Bowden, K., 171, 174, 175 (51)
- Boyd, R.H., 497 (249)
- Boyle, W.J., 187 (79, 83), 196, 199 (94)
- Boyle, W.J. Jr., 187 (79), 188 (78)
- Bradley, W.A., 338, 344, 345 (64)
- Brandon, J.R., 87 (244), 223 (147), 224 (147, 148), 225, 226, 237 (148)
- Branscomb, L.M., 9 (19-23), 18 (21)
- Brauman, J.I., 163, 169, 171 (27), 205 (133), 206 (133, 136, 137)
- Breckles, T.H., 354 (225)
- Breivogel, F.W., Jr., 452 (25, 79), 453 (79)
- Bresadola, S., 312, 314 (149)
- Bretton, R.A., 431 (131)
- Briggs, J.P., 155, 156 (37)
- Briody, R.G., 285 (72), 286, 287, 288 (75), 289 (72), 290, 297 (87)
- Britt, A.D., 85 (251)
- Brogli, F., 29 (350)
- Brokaw, M.L., 189, 190, 200 (49)
- Bromskill, M.J., 125 (124), 127 (368)
- Brønsted, J.N., 180 (72, 73)
- Browall, K.W., 136 (326)
- Brown, H.C., 307, 309, 311 (136), 326, 333, 341, 350, 361, 362 (246), 365 (178), 366 (136)
- Brown, M.S., 107 (290)
- Bruce, C.R., 85 (249)
- Bruning, W.H., 67 (217), 85 (252, 255), 86 (255)
- Bryson, J.A., 206 (137)
- Buchanan, T.J., 499, 501, 502, 504-506 (72)
- Bucholz, R.F., 273 (53)
- Buck, W.L., 122 (83)
- Buddenbaum, W.E., 298 (108)
- Buncel, E., 338, 352 (220)
- Bunton, C.A., 324 (167)
- Burch, D.S., 9 (22)
- Burhop, E.H.S., 3 (8)
- Burley, J.W., 56 (229)
- Burwell, R.L., 169 (40)
- Buschow, K.H.J., 92 (260)
- Busler, W.R., 430 (115-117), 432 (117)
- Büthker, C., 39, 40 (164)
- Bydin, Yu. F., 17 (35)
- Bywater, S., 384 (18), 385 (68), 404 (42), 414 (58), 415 (59, 63, 66), 418 (144, 145)
- Cachet, H., 510 (12)
- Cafasso, F., 129 (88)
- Caldwell, R.A., 167 (31), 192 (129), 199, 206 (31)
- Caluwe, P., 79, 82 (239)
- Calvin, M., 22 (44)
- Cannel, L.G., 313 (147)
- Careri, G., 118 (71)
- Carlson, R.O., 452, 453 (50)
- Carraway, R., 60, 62, 63, 68 (199)
- Carter, J.V., 158 (24), 338, 344 (66)
- Carvajal, C., 64 (214), 387 (29)
- Carvell, E.A.S., 485 (28), 487 (29), 488 (26-28), 489 (29)
- Casanova, J., Jr., 321, 322 (166), 358 (236)
- Casey, C., 361 (245)
- Catterall, R., 129, 132-134 (316)
- Cavazza, M., 312, 314 (150)

- Cde, R.H., 496 (90)
 Ceccon, A., 307, 309 (134),
 312 (143, 146, 148), 313
 (143, 146), 314 (143, 146,
 148), 343 (203)
 Ceraso, J.M., 135 (362), 221,
 234, 235, 238-240 (142)
 Ceska, G.W., 464 (30)
 Chadha, S.C., 110 (298)
 Champetier, G., 425 (83)
 Chan, L.L., 55 (189), 177 (61),
 201, 202, 237 (104)
 Chang, C.J., 159, 160 (52),
 163 (28), 164, 165 (52), 166,
 169 (28), 171 (52, 53, 101),
 174, 177 (53), 189, 190 (50),
 191 (50, 101), 192 (28, 101),
 200, 201 (50), 399 (138)
 Chang, P., 32, 36, 46, 62-64
 (149)
 Chang, R., 60 (198, 200), 65
 (198)
 Chang, S., 288, 290 (80)
 Chapiro, A., 429 (113)
 Charlesby, A., 430 (118, 120,
 126, 127)
 Chaudhuri, J., 37 (148, 151),
 40 (152, 153), 43 (152), 50
 (148)
 Chaykovsky, M., 206 (138)
 Chen, A., 172 (46)
 Chen, E., 3 (6), 5 (14), 23
 (54), 25 (54, 56), 31 (56)
 Chen, K.S., 68 (310)
 Chesnyokova, N.N., 421 (73)
 Chevll, D.M., 327, 346 (187),
 361 (245)
 Chibrikin, V.M., 76 (233)
 Chitwood, J.L., 294 (98), 295
 (98, 103), 308 (103)
 Chivers, J., 172 (46)
 Chmelir, M., 380, 384 (8), 385
 (8, 137), 391 (8)
 Christensen, J.J., 124 (305),
 477, 479 (31, 88)
 Christophorou, L.G., 22 (52)
 Chu, K.C., 208, 216 (165)
 Chu, W.K.C., 189, 190, 200 (49)
 Chupka, W.A., 3 (2)
 Church, M.G., 249, 251, 252 (7),
 257 (7, 31, 32), 259, 260,
 261, 265, 266, 269, 270, 322,
 324, 330, 339 (7)
 Ciuffarin, E., 163 (26, 27),
 169 (27), 171 (26, 27), 318
 (161), 319 (161, 164)
 Claesson, S., 56 (230), 87
 (299), 88 (226), 99 (272), 134
 (226, 229), 138 (226, 272,
 299), 153 (5), 177 (62)
 Clare, B.W., 157, 158 (10)
 Clayton, J.W., 308 (137), 355
 (230)
 Clinch, P.W., 351 (216)
 Clippinger, E., 252 (13), 253
 (13, 17, 18), 254 (13, 18),
 255 (13), 264 (18), 265 (43),
 271 (18, 43), 272 (18), 273
 (18, 43), 274 (13, 18, 43, 54),
 276 (13, 17, 43, 54), 277,
 278 (54), 285, 290 (17), 330
 (13)
 Closson, W.D., 296, 297, 308
 (106)
 Cockerill, A.F., 171 (51, 65),
 174, 175 (51), 179 (65)
 Coffey, J.F., 328, 346 (188)
 Cohen, M.H., 118 (72)
 Coke, J.L., 308, 310 (131)
 Cole, R.H., 452 (33), 480 (35),
 481, 483, 484 (36)
 Cole, R.S., 94 (264, 266), 99
 (266)
 Coleman, B.D., 404 (43), 410
 (50)
 Coll, K.S., 481, 483, 484 (36)
 Collins, C.J., 360 (239)
 Collinson, E., 429 (113), 430
 (121)
 Compton, R.N., 22 (52)
 Conant, J.B., 167 (33)
 Conception, J.G., 105 (358)
 Congiu, L., 312 (145, 150),
 313 (145), 314 (145, 150)
 Connelly, R.J., 117 (68)
 Connor, H.D., 51 (184), 61
 (203), 78 (237), 79 (237, 209),
 82 (209)
 Connors, W.P., 495 (37)
 Cook, D., 157, 158 (10)

- Cooper, J.W., 13 (16)
 Corey, E.J., 206 (138), 321, 322 (166), 358 (236)
 Coulson, C.A., 8 (15), 103 (283)
 Cowdry, W.A., 355 (228)
 Cox, W.G., 312 (152, 157, 158), 315 (152, 157), 316 (152), 318 (157, 158)
 Cram, D.J., 152 (2), 171, 172, 181 (2), 188, 190 (85), 198 (98), 199 (85), 208 (98, 115-126, 165), 210 (115), 211 (115, 116), 212 (117, 127), 213 (116, 117, 127), 214 (117-120, 122, 127), 216 (127, 165), 217 (118-120, 122), 218 (2, 98, 115, 123), 219 (2, 124), 220 (115, 120, 122, 124, 125), 221 (120), 290, 307 (94), 355 (229), 360 (239), 490 (51)
 Cramer, J.A., 311, 366 (139)
 Crawford, R.J., 295, 297 (102)
 Cserhegyi, A., 37, 50 (148), 98 (154)
 Cumper, C.W.N., 470 (39)
 Curran, E.L., 327, 346 (187), 361 (245)
 Curtin, D.Y., 361 (241)
 Dafforn, D.A., 299, 328 (122)
 Dainton, F.S., 129 (89), 377 (5), 385 (24), 386 (5, 24), 429 (113), 430 (121)
 Dall'Asta, G., 398 (37)
 Dalton, L.R., 124, 130, 132 (308), 430 (123-125)
 Dankleff, M.A., 353 (221, 222)
 Danusso, F., 424 (81)
 Darwish, D., 262 (38), 265, 266 (44), 318 (159, 162, 163), 319 (162, 163), 324 (44)
 Dauben, H.J., 107 (289)
 Dauben, W.G., 294 (98), 295 (98, 103), 308 (103)
 David, C.W., 21 (39)
 Davidov, A.S., 120, 121 (77)
 Davies, M., 449 (83), 456, 461, 486 (42), 487 (40, 42), 488 (42), 489 (40, 41)
 Davis, G.J., 112 (307)
 Davis, H.T., 117 (68), 119 (76)
 Davis, M.M., 461, 474, 487, 489 (43)
 Davison, W.H.T., 429 (113), 430 (122)
 Dawson, L.R., 158 (15)
 Deadman, W.G., 328 (190)
 De Backer, M.G., 124, 126 (325), 129 (115), 130 (327)
 Debye, P., 449, 450 (44), 485 (44, 45), 498 (45), 504, 512 (44)
 Deigen, M.F., 120, 121 (77)
 De La Mare, P.B.D., 252, 266 (14), 361 (242)
 De Maeyer, L., 182 (87)
 Denissov, G.S., 464 (71)
 Denney, D.B., 279 (59), 290, 297 (88)
 Denny, D.G., 279 (59)
 Dessy, R.E., 172 (46, 47)
 Dewald, R.R., 130 (309), 136 (326)
 Dewar, M.J.S., 29 (63), 361 (247)
 Diaz, A., 253, 254, 256, 281, 285, 286 (19), 290 (95), 294, 298, 307, 309, 311, 322, 328, 363, 364, 365 (19)
 Diaz, A.F., 279 (56), 288 (77), 289, 297 (56), 301 (77), 306 (129), 307 (134), 308 (129, 130), 309 (134), 328 (56), 346 (56, 129), 359 (77), 361 (77), 364 (56)
 Dieleman, J., 92 (258)
 Dietrich, B., 124 (117)
 Dietz, R., 40 (172)
 Dillard, D.E., 327, 346 (187), 361 (245)
 Dillon, R.L., 183, 185 (74)
 Dix, D.T., 129 (93)
 Djibelian, M., 32 (141)
 Dobson, G., 138 (331)
 Dodelet, J.P., 119 (110, 113)
 Doering, W. von E., 282, 284 (67), 290, 297 (85)
 Doi, J.T., 279, 281, 282 (61, 62)

- Donnelly, M.F., 298, 300, 301 (116)
- Doran, M.A., 207 (114)
- Dorfmann, L.M., 61 (201), 87 (241-244), 88 (243), 90 (351, 354, 112 (342), 125 (130, 300, 301), 131 (301, 314), 136 (325), 222 (144, 145), 223 (145, 147), 224 (147, 148), 225, 226 (148), 236 (168), 327 (148)
- Doty, P.M., 22 (43)
- Dowd, W., 294 (99), 298 (110-112, 114), 299 (114), 301 (111, 112, 114), 302, 303 (112), 311 (111, 112), 328 (111), 345 (99), 346, 347, 348 (111, 112), 361 (99), 365 (99, 111), 366 (111, 112)
- Down, J.L., 129 (94)
- Dreyfuss, M.P., 435 (104)
- Dreyfuss, P., 435 (104)
- Drijvers, W., 436 (108)
- Dukelskii, V.M., 135 (321)
- Duynstee, E.F., 260, 267 (35)
- Dye, J.L., 123 (318), 124 (115, 304, 308), 125 (304), 129 (115, 315), 130 (308, 309, 327), 132 (308, 315), 135 (304, 362), 136 (325), 221, 234, 235 (142), 238, 239 (142, 154), 240 (142)
- Dzidic, I., 155 (36)
- Eargle, D.H., 99 (352)
- East, G.C., 377, 386 (5)
- Ebinghaus, H., 135 (323)
- Eckstrom, H.C., 486 (136, 137)
- Edgell, W.F., 161, 235 (20)
- Edsall, J.T., 494, 495 (46)
- Effio, A., 360 (240), 449 (68), 452, 458 (68, 69), 459 (69), 470, 471 (68), 496 (69)
- Eigen, M., 181 (68), 182 (68, 87), 184 (68), 492 (47)
- Eliason, R., 195 (91)
- Eliel, E.L., 358 (237), 360 (239)
- Elliger, C.A., 288, 301, 359 (76)
- Ellis, S.H., 129 (93)
- Ellison, F.O., 11 (28)
- El Sabeh, S.H.M., 499, 500 (78)
- Emerson, D.W., 312 (142)
- Endom, L., 508 (48)
- Engel, G., 507, 508 (48)
- Evans, D.F., 496 (148)
- Evans, E.G., 94 (263, 265)
- Evans, J.C., 94 (263, 265)
- Evans, M.G., 380 (9)
- Eyre, J.A., 136 (325)
- Eyring, H., 58 (192)
- Fabricand, B.P., 452, 453 (50)
- Fahey, R.C., 361 (243, 247), 363 (243)
- Fainberg, A.H., 252 (13), 253 (13, 17, 18), 254 (13, 18), 255 (13), 257 (29), 258 (34), 260 (34, 37), 261 (34), 262 (34, 37) 263 (37), 264 (18, 34, 37, 41, 42), 265 (37), 267 (41), 268, 269 (50), 271 (18, 34, 41, 42, 50), 272 (18), 273 (18, 41, 42, 50), 274 (13, 18, 41, 50), 275 (50), 276 (13, 17, 50), 285, 290 (17), 306 (50), 330 (13, 37, 50), 338, 339 (34), 365 (37)
- Falkenhagen, H., 485, 498 (45)
- Falvo, L.A., 418 (142, 143)
- Fan, J.W., 39, 40 (168)
- Fano, V., 13 (16)
- Farina, M., 405 (44), 406, 424 (45)
- Farragher, A.L., 22 (46)
- Fava, A., 312 (140, 142-146, 148-150), 313 (140, 143, 145, 146), 314 (143, 145, 146, 148-150), 315 (140), 318 (161), 319 (161, 164), 343 (203)
- Favier, J.C., 412, 413 (140)
- Fayter, R.G., 312, 315 (153)
- Feld, M., 34, 36, 46, 102 (147), 229 (150)
- Fickes, G.N., 292 (90)
- Field, F.H., 3, 14 (4) 45 (345)
- Fielden, E.M., 125 (128)
- Figini, R.V., 410 (51, 54)
- Finlayson, A.J., 355 (230)

- Firestone, R.F., 90 (351)
- Fischer, H.P., 208, 217 (119, 120), 220, 221 (120)
- Fisher, M., 87, 88 (226), 131 (299), 134, 138 (226, 299), 377 (26), 396, 398, 401, 413, 414 (33)
- Fisher, R.D., 294 (99, 110, 112, 115), 299 (115), 301 (112, 115), 302 (112, 115), 303, 311 (112), 328 (115), 345 (99), 346-348 (112), 365 (99), 366 (112)
- Fitzsimmons, C., 427 (93)
- Fogel, Ya M., 135 (321, 322)
- Fontanille, M., 412, 413 (140)
- Ford, W.T., 208 (116, 117, 126), 211 (116), 212 (117, 127), 213 (116, 117, 127), 214 (117), 216 (127), 490 (51)
- Forno, A.E., 70 (224)
- Fort, R.C., Jr., 294 (96)
- Fowells, W., 405 (48), 406, 425 (49)
- Fowler, R.H., 501 (21)
- Fowles, G.W.A., 124 (95)
- Fox, J.D., 155, 190 (163)
- Fox, T.G., 404 (43), 410 (50)
- Fraenkel, G.K., 102 (279), 103 (281, 282), 104 (282)
- Frank, H.S., 502, 503, 512 (52)
- Franklin, J.L., 3 (4, 7), 14 (4)
- Franta, E., 37, 50 (148), 396 (32)
- Fратиello, A., 509 (53)
- Freeman, G.R., 117 (111), 119 (74, 109, 110, 113)
- Frenkel, G., 129 (93)
- Frensdorff, H.K., 124 (305), 477 (54, 55, 115), 479 (54, 55)
- Friedhan, L., 290, 297 (85), 356, 360 (232)
- Friedrich, E.C., 261, 262 (39)
- Friscone, G.J., 305 (126)
- Frölich, H., 449, 451 (57)
- Fry, J.L., 254, 256 (23), 281 (63), 324 (23), 326, 328 (23, 123, 171), 348 (123), 350 (23, 123, 171)
- Fujihara, M., 211, 240 (159)
- Fujii, H., 434 (98, 100-102), 435 (98), 436 (100-102, 107), 438 (110, 111)
- Funderburk, L., 196 (93)
- Fuoss, R.M., 410 (55), 473 (58), 484 (60), 497 (59)
- Galiano, F.R., 112 (337)
- Gall, J.S., 285 (71)
- Gantmakher, A.R., 421 (74)
- Garst, J.F., 94 (264, 266, 274), 95, 97 (266), 99 (266, 353), 101 (274), 102 (275), 112 (338, 340, 360)
- Garwood, D.C., 208, 219, 220 (124)
- Gassman, P.G., 364 (251)
- Gatzke, A.L., 299, 302 (119)
- Geacintov, C., 382, 384 (17)
- Geddes, J.A., 456 (61)
- Gee, G., 377, 379 (2)
- Gerson, F., 75, 76 (235)
- Geske, D.H., 70 (221)
- Giddings, W.P., 273 (53)
- Giese, K., 499, 505-509 (62)
- Gilbert, J.M., 206 (139)
- Gilkerson, W.R., 458, 459 (63)
- Gilling, L.J., 131 (311, 312), 134 (365), 138 (311, 312)
- Gillis, H.A., 429 (113), 430 (121)
- Gilman, H., 207 (113)
- Ginn, J.M., 396 (91)
- Given, T.H., 39, 43 (165)
- Glarum, S.H., 129 (108, 480, 485 (64)
- Glawitch, G., 430 (123)
- Glaze, W.H., 415 (60)
- Glocker, G., 22 (44)
- Goedde, A.O., 77 (347)
- Goering, H.L., 253, 254 (15), 256, 266 (25), 271 (15), 279 (55, 57, 60-62), 281 (60-62), 282 (60-62, 68), 283 (68), 284 (69), 285 (70, 72, 73), 286, 287 (74, 75), 288 (74, 75, 79, 80), 289 (72-74, 81), 290 (80, 87), 291 (89), 292

528 Author Index

- (89, 90), 293 (89), 296 (55, 68, 105, 106), 297 (89, 105, 106), 306 (68), 308 (106), 315 (73), 359 (70), 365 (74)
- Goethals, E.J., 436 (108)
- Gold, M., 123 (119)
- Gold, V., 248, 290 (1)
- Golden, S., 123 (120-122), 128 (120), 135 (320, 324)
- Goldstein, B., 290, 297 (88)
- Gomer, R., 116 (66, 69), 117 (69)
- Goodall, D.M., 196 (89)
- Goode, G.C., 3 (5)
- Gordy, W., 157 (22)
- Gosser, L., 208 (115, 116, 118, 125), 210 (115), 211 (115, 116), 213 (116), 217 (118), 218 (115), 220 (115, 125)
- Gottschall, W.C., 125 (126)
- Gough, T.E., 66 (215)
- Graceffa, P., 63 (212)
- Graf, R., 425 (84)
- Graham, E.W., 208 (126)
- Granger, M.R., 160 (54), 167 (31), 171, 191, 193 (54), 199, 206 (31)
- Grant, E.H., 494, 495 (1-3), 501 (65)
- Green, G.W., 452, 453 (66)
- Green, M., 353 (219)
- Gregorieu, G.A., 342 (201)
- Gregory, B.J., 323 (168, 169), 326 (168), 328 (168, 169), 340 (168)
- Grev, D.A., 222 (144)
- Griffin, R.G., 67 (217)
- Grobb, C.R., 129 (114)
- Grossweiner, L.I., 138 (331)
- Grunwald, E., 157, 158 (16), 181 (67), 183 (80-82), 254 (21), 256 (24) 257 (27, 28), 260, 267 (35), 323 (27), 340, 360 (240), 449 (68), 452, 458 (68, 69), 459 (69, 70, 87), 464 (30), 467, 469 (67), 470, 471 (68, 69), 472, 480 (87), 496 (69)
- Gussakova, G.V., 464 (71)
- Gutowsky, H.S., 82 (240)
- Guttman, C., 123, 128 (120), 135 (320)
- Guvigny, T., 129 (91)
- Häfelinger, J.R., 171, 191, 192 (101)
- Haggis, G.A., 499, 501, 502, 504-506 (72)
- Halevi, E.A., 298 (109)
- Hall, D.M., 252, 266 (14)
- Hall, R.E., 254, 256 (23), 266, 267 (46), 299 (118), 300 (118, 120), 301, 302 (118), 324 (23, 46), 326 (23, 46, 120), 328 (23, 46, 118, 120), 333 (46, 120), 336, 339, 341, 342 (120), 350 (23)
- Halpern, B., 116, 117 (69)
- Halpern, J., 3 (10), 101 (273)
- Halverstadt, F., 470 (73)
- Hamill, W.H., 90 (355), 127 (136)
- Hamilton, W.C., 470 (74)
- Hammett, L.P., 2 (248)
- Hammons, J.H., 163 (26, 27), 169 (27), 171 (26, 27), 173 (102), 176 (60)
- Hanna, B., 197 (95)
- Hansen, E.M., 124, 130, 132 (308)
- Hanson, G.C., 351 (214)
- Hardy, J.P., 307, 309 (134)
- Harford, M.B., 351, 353 (208)
- Harm, K., 410 (54)
- Harpell, G.A., 377 (5), 385 (24), 386 (5, 24)
- Harper, J.J., 294 (96, 100), 326, 333, 341, 350 (173, 177), 365 (173)
- Harriman, J.E., 71, 74, 77, 78 (234)
- Harris, F.E., 500 (77)
- Harris, J.C., 328, 340 (192)
- Harris, J.M., 254, 256 (23), 266 (46), 267 (46, 48), 287, 295 (48), 299 (118), 300 (118, 120), 301, 302 (118), 308 (48), 326 (23, 46, 48, 120, 171, 176), 328 (23, 46, 48, 118, 120, 171), 333 (46,

- 120, 176), 339 (120), 341
 (120, 176), 342 (120), 350
 (23, 171, 176), 365 (176)
- Hart, E.J., 125 (123, 125,
 126, 129)
- Harter, D.A., 87 (242)
- Hartshorn, S.R., 298 (110)
- Hashimoto, Y., 433 (96), 435
 (96, 97)
- Hasted, J.B., 499 (72, 78),
 500 (78), 501, 502, 504-506
 (72)
- Hautala, J.A., 187 (79)
- Hayano, S., 211, 240 (159)
- Hayashi, K., 382 (111), 432
 (130)
- Haymore, B.L., 477, 479 (88)
- Hebert, A.J., 452 (25, 79, 80),
 453 (79, 80)
- Heck, R., 252-255, 274, 276,
 330 (13)
- Hedestrand, I.G., 470 (81)
- Heffley, P.D., 156 (13)
- Heilbronner, E., 29 (350)
- Heller, A., 256 (24)
- Helmiak, L.S., 194 (169)
- Henson, W.L., 290, 294, 302
 (93)
- Hermans, J.J., 410 (52)
- Herndon, W.C., 351 (215)
- Hertz, H.G., 507 (49), 508
 (48, 49)
- Higashimura, T., 428 (95),
 431, 432 (132)
- Higginson, W.C.E., 380 (9)
- Hill, J.O., 124 (305), 477,
 479 (31)
- Hill, N.E., 449 (83), 485
 (82)
- Hindle, P.R., 66 (215)
- Hine, J., 223 (146)
- Hine, M., 223 (146)
- Hirohara, H., 385 (21), 412
 (57)
- Hirota, N., 60 (199), 62
 (199, 210, 211), 63, 64
 (199, 211), 68 (199, 220,
 218, 219, 310), 69 (218), 70
 (332), 107 (294)
- Hodgins, J.W., 123 (118)
- Höfelmann, K., 49, 60, 61, 64,
 65 (183), 396 (13)
- Hofmann, J.E., 198 (97)
- Hogen-Esch, T.E., 153 (4), 203
 (106), 204, 215 (4), 399 (138)
- Hoijsink, G.J., 33, 37 (146),
 39, 40 (162-164), 42 (174),
 43 (162, 163, 174-180), 91
 (146, 257), 92 (260), 138
 (329, 330)
- Hojo, M., 257 (26), 262 (40),
 266 (45), 273 (26), 276 (45),
 285 (45, 71)
- Holliday, R.E., 354 (224)
- Hollingsworth, G., 418 (145)
- Hollowell, C.D., 452, 453 (80)
- Hollyhead, W.B., 159, 160 (52),
 163 (28), 164, 165 (52), 166,
 169 (28), 171 (52), 189, 190
 (49, 50), 191 (50), 192 (28),
 200 (49, 50), 201 (50)
- Holm, C.H., 128 (101)
- Holness, N.J., 289 (83)
- Holtz, D., 199 (99)
- Holz, J.B., 60, 85 (206)
- Honnore, D., 412, 413 (140)
- Hood, F.P., 405 (48), 406,
 425 (49)
- Hooper, G.S., 455 (85)
- Hopf, H., 286-289, 365 (74)
- Horn, D.E., 326, 333, 341,
 350 (177)
- Hornback, J.M., 364 (251)
- Hostalka, H., 381 (16), 384
 (16, 20), 410 (54)
- Howe, S., 117 (70)
- Hsieh, H.L., 415 (60)
- Hudson, H.R., 351 (216)
- Hudson, J.A., 180, 199 (66)
- Hudson, R.A., 464, 466 (86)
- Hudson, R.F., 353 (219)
- Huebner, R.H., 22 (52)
- Hughes, E.D., 249 (7, 8), 250
 (9), 251 (7), 252 (7, 12),
 257 (7, 8, 30-33), 259-261
 (7), 265 (7), 266 (7, 9),
 269 (7), 270 (7, 33), 275 (9),
 322, 324, 330, 339 (7), 350
 (207), 355 (228)
- Hughes, T.R., 128 (103)

- Hui, K.M., 377, 386 (5)
 Humski, K., 279 (55), 296 (55, 105), 297 (105)
 Hunt, J.W., 125 (124), 127 (368)
 Hurley, I., 123 (122), 129, 132, 134 (316)
 Hurworth, N.R., 377, 386 (5)
 Hush, N.S., 31 (343), 32, 91 (139)
 Hutchison, C.A., 127 (87), 128 (98)
- Ideguchi, Y., 405 (45)
 Ikeda, H., 438 (110, 111)
 Illiceto, A., 312 (142, 143, 148, 149), 313 (143), 314 (143, 148, 149)
 Imhoff, M.A., 298, 300-303, 328, 347-349 (118)
 Ingold, C.K., 249 (6-8), 250 (6, 9), 251, 252 (7), 257 (7, 8, 30-33), 259, 260, 261 (7), 265 (6, 7), 266 (7, 9), 269 (6, 7), 270 (6, 7, 33), 275 (9), 322, 324 (6, 7), 326 (6), 330 (6, 7), 339 (7), 350 (207), 355 (228)
 Inu, E.C.Y., 7 (18)
 Ionov, N.I., 22 (49, 51), 135 (321)
 Isaeva, V.N., 167 (70)
 Ise, N., 385 (21), 412 (57)
 Isola, M., 318 (161), 319 (161, 164)
 Ivin, K.J., 377 (5), 385 (24), 386 (5, 24), 396 (91)
 Izatt, R.M., 124 (305), 477, 479 (31, 38)
- Jadzyn, J., 461, 462, 464-467, 477 (89)
 Jagur-Grodzinski, J., 34, 36 (147), 37 (148, 151), 40 (152, 153), 43 (152), 46 (147), 50 (148), 56 (191), 60, 61, 64, 65 (183), 98 (154), 102 (147), 110 (297, 298), 222 (143), 229 (150), 396 (13)
 James, H.M., 16 (32)
 Jencks, W.P., 155, 190 (163)
- Jenny, E.F., 268, 269, 308, 310, 330 (49)
 Jermini, C., 197 (95)
 Jewett, J.G., 311, 366 (139)
 Jindal, S.P., 294 (96)
 Johansson, G., 487, 489 (40)
 Johnson, A.F., 415 (62)
 Johnson, C.F., 496 (90)
 Johnson, C.S., 60 (198, 200, 206), 65 (198), 85 (206, 250)
 Johnson, P.Y., 353 (219)
 Jolly, W.L., 123 (119)
 Jones, B.E., 292, 293 (91)
 Jones, H.W., 257, 323 (27)
 Jones, M.G., 308, 310 (131)
 Jones, R.P., 138 (333)
 Jordan, R.W., 112 (337)
 Jortner, J., 115 (65), 118 (65, 72), 120, 121 (79), 138 (333)
 Jumper, C.F., 183 (80)
- Kaatze, U., 499, 505-509 (62)
 Kahl, D.C., 206 (136, 137)
 Kalinin, V.N., 167 (70)
 Kamat, R.J., 327 (187), 328 (189), 246 (187, 189), 361 (245)
 Kanasawa, Y., 205, 206 (133)
 Kanoh, N., 431, 432 (132)
 Kaplan, J., 122 (84)
 Kaplan, M.L., 260, 267 (35)
 Karasawa, Y., 29 (166), 47, 49, 50 (182)
 Katz, T.J., 102 (277, 278), 103 (277, 278A, 282), 104 (282), 105 (277), 107 (288)
 Kawakami, J.H., 361, 362 (246)
 Kawase, R., 434, 435 (98)
 Kay, J., 22 (46)
 Kay, P.S., 338, 344 (65)
 Kay, R.L., 449 (91), 496 (92, 148)
 Keating, J.T., 356, 357, 360, 361 (233)
 Kebarle, P., 155, 156 (37)
 Keene, J.P., 125 (128)
 Keevil, N.B., 33 (143)
 Kelly, W.J., 294, 297 (101)
 Kenyon, J., 351 (208, 209), 353 (208)

- Kertes, A.S., 475 (99)
 Kessick, M.A., 298 (110)
 Kevill, D.N., 352 (213, 217, 218)
 Khanna, S.N., 399 (39)
 Kice, J.L., 351 (214), 353 (221, 222, 223)
 Kiesel, R.F., 399 (138)
 Kim, C.-B., 352 (218)
 Kim, C.J., 307, 309 311 (136), 326, 333, 341, 350, 365 (178), 366 (136)
 Kingsbury, C.A., 198, 208, 218 (98)
 Kinoshita, T., 364 (253)
 Kirkwood, J.G., 451 (93, 95, 96), 484 (60), 494 (94)
 Kirmse, W., 360 (238)
 Kirova, A.W., 194 (86)
 Kistiakowsky, G.B., 176 (59)
 Kitching, W., 172 (46)
 Kittel, C., 3 (11), 122 (84)
 Klager, K., 102 (276)
 Klein, F.S., 256 (24)
 Klinedienst, P.E., 260, 265 (36), 274 (54), 276, 277, 278 (36, 54)
 Kloosterboer, J.G., 131 (311, 312), 134 (365), 138 (311, 312)
 Knight, P.C., 485 (28), 488 (27, 28)
 Ko, E.C.F., 157, 158 (10)
 Kobayashi, S., 434, 435 (98)
 Koch, H.F., 194, 198 (96)
 Koch, P., 312-314 (143)
 Koermer, G.S., 284 (69)
 Kohnstam, G., 251 (10, 11), 323 (168, 169), 326 (168), 328 (168, 169), 340 (168)
 Kokubun, N., 464 (10)
 Kollmeyer, W.D., 188, 190, 199 (85), 208, 218 (120)
 Kolthoff, I.M., 42 (176)
 Kolwych, K.C., 352 (218)
 Komatsu, K., 364 (252)
 Komiyama, J., 377 (133), 405 (47)
 Koopmans, T., 5, 10 (13)
 Kor, S.K., 492 (7)
 Korotkov, A.A., 421 (73)
 Koskikallio, J., 326 (185), 334 (198)
 Koslov, V.F., 135 (322)
 Kosower, E.M., 172 (48)
 Koubek, E., 353 (223)
 Koutecky, J., 42 (173)
 Kowert, B.A., 85 (253)
 Kralicek, J., 425, 426 (82)
 Krapcho, A.P., 326, 333, 341, 350 (177)
 Kraus, C.A., 121 (78), 122 (81, 82), 123 (86), 130 (86, 137), 410 (55), 455 (85), 456 (61), 486 (136, 137)
 Kreevoy, M.M., 195 (91)
 Kreilick, R., 62 (210)
 Kresge, A.J., 188 (84)
 Krishna Mohana Rao, P.S., 499, 505 (124)
 Kruger, T.L., 189, 190 (49, 50), 191 (50), 200 (49, 50), 201 (50)
 Krystal'Nyi, E.V., 431 (128)
 Ku, A.Y., 183 (81)
 Kubise, S., 437 (109)
 Kuhn, R., 160 (56)
 Kume, S., 37 (151)
 Kumler, W.D., 470 (73)
 Kuntz, I., 422 (77, 78)
 Kuntz, I.D., Jr., 334 (199)
 Kurz, J.L., 184 (162), 328, 340 (192)
 Kurz, L.C., 184 (162)
 La Flair, R.T., 377, 386 (5)
 Lagendijk, A., 109 (295)
 Lagowski, J.J., 123 (199)
 Laita, Z., 422 (79)
 Laitinen, H.A., 39, 40 (166, 167), 41 (166)
 Lam, L.K.M., 254, 256 (23), 281 (63), 324 (23), 326, 328 (23, 123), 348 (123), 350 (23, 123)
 La Mar, G.N., 456 (97)
 Lamaty, G., 298 (108)
 Lambert, J.B., 289, 328 (84)
 Lamper, J.E., 171, 179 (65)
 Lancelot, C.J., 254, 256 (23),

- 281 (63), 290, 307 (94), 324
 (23), 326 (23, 123, 172-176,
 178), 328 (23, 123), 333
 (172-175, 178), 341 (172-176,
 178), 348 (123), 350 (23, 123,
 172-176, 178), 365 (172-176,
 178)
 Landau, L., 114 (64)
 Landholm, R.A., 195 (91)
 Lane, J.A., 499 (48)
 Langford, C.H., 169 (40)
 Langley, P.G., 470 (39)
 Langworthy, W.C., 192 (128),
 198 (96), 206 (111)
 Larchevegue, M., 129 (90)
 Larsen, J.W., 248 (4), 267,
 268, 311 (47), 326, 328 (4,
 47, 184), 331 (47, 184), 333,
 334 (47), 335 (47, 184), 336-
 338 (47), 340 (4, 47), 341
 (4, 47, 184), 342 (47), 345
 (4, 47, 184), 346 (47), 350
 (4, 47), 364 (47), 365 (4,
 47), 366 (4)
 Latimer, W.M., 39 (161)
 Laughton, P.M., 167, 199,
 206 (31)
 Lawler, R.G., 192 (129)
 Lazdins, I., 279, 289, 297,
 328, 346, 364 (56)
 Le Blanc, O.H., 119 (73)
 Ledwith, A., 257 (26), 262
 (40), 273 (26), 427 (93, 94)
 Lee, C.A., 452, 453 (50)
 Lee, C.C., 307, 308 (138),
 355 (230)
 Lee, C.L., 201-203 (102), 382,
 384 (15), 418 (70), 420 (71),
 431 (15)
 Lee, D.G., 355 (230)
 Lee, L., 56 (191)
 Lee, R.E., 509 (53)
 Lee, Y., 17 (34)
 Le Fevre, P.H., 302 (124)
 Leffler, J.E., 181 (67)
 Lehn, J.M., 124 (117, 361)
 Lekner, J., 116 (66)
 Lestrade, J.C., 510 (12)
 Levin, G., 47, 49, 50 (182),
 99 (272), 109 (296), 111 (359),
 138 (272), 139 (366), 166
 (29), 229 (149), 230 (149,
 152), 231 (149), 232 (167)
 Levinthal, E.C., 129 (106)
 Levresse, B., 396 (32)
 Levy, J.F., 256, 266 (25),
 289 (72, 73), 315 (73), 359
 (70), 285 (70-73)
 Levy, M., 75-77 (236), 380 (7),
 399 (39), 426 (85, 87)
 Levy, O., 475 (99)
 Lew, H., 452, 453 (17, 66),
 459 (66)
 Lewis, E.S., 196 (93), 351
 (215), 354 (224), 355 (227)
 Lewis, G.N., 137 (328)
 Lewisk, J., 129 (94)
 Libby, W.F., 58 (193)
 Liggero, S.H., 294 (97), 298,
 300-303 (118), 326 (177), 328
 (118), 303, 341 (177), 347-
 349 (118)
 Lindberg, B.J., 12 (29)
 Lindquist, R.H., 130, 135 (313)
 Lingane, J.L., 42 (176)
 Linsay, E.C., 282, 283 (68),
 284 (69), 294, 296, 306 (68)
 Linschitz, H., 127, 138 (104)
 Lipkin, D., 112 (337), 137
 (328), 221 (140)
 Liu, K.-T., 361, 362 (246)
 Livigni, R., 415 (61)
 Lohaus, G., 425 (84)
 Lohr, G., 380, 384 (8), 385
 (8, 68), 391 (8), 410 (53, 54)
 Lok, M.T., 124, 125 (304), 135
 (304, 362)
 Long, L.D., 221, 234, 235, 238,
 239, 240 (142)
 Longi, G., 398 (37)
 Longuet-Higgins, H.C., 43 (178)
 Lovas, F.J., 452, 453 (80)
 Lovelock, J.V., 5 (14), 22 (53),
 23, 25 (54)
 Lown, J.W., 71 (271)
 Lowry, B.R., 295 (104)
 Lucasse, W.W., 121 (78)
 Ludwig, P., 70 (222), 85
 (254)
 Lundbard, C., 415 (64)

- Lundgren, B., 56 (230), 153
(5), 177 (62)
- Lux, G.A., 112 (339)
- Lynch, R., 21 (39)
- Lyons, L.E., 43 (175)
- Maass, G., 184 (75)
- Mac, Y.C., 157, 158 (10)
- McCall, D.W., 82 (240)
- McCarty, J.E., 360 (229)
- McClellan, A.L., 477, 478 (103)
- McConnell, H.E., 59 (205)
- McConnell, H.M., 71 (227), 74
(231), 103 (280, 286), 128
(101)
- McCrary, T.J., Jr., 289, 328
(84)
- McDaniel, E.N., 3 (9)
- Macedo, P.B., 498 (4)
- McEwan, W.K., 167 (37)
- McFadyen, J.S., 318, 319 (160)
- McFarlane, F.E., 308, 310 (131)
- McGregor, W.R., 124 (95)
- McKeever, L.D., 172 (45)
- Mackie, J.C., 21 (39)
- McKinnon, D.M., 351 (210)
- McLachlan, A.D., 103 (286, 287)
- McLaren, R.A., 318 (159, 162),
319 (162)
- McLennan, D.J., 343 (203A)
- McMichael, K.D., 279-282 (60,
62)
- McMillen, D.F., 205, 206 (133)
- McNinch, H.A., 207 (113)
- Mac Quarrie, R.A., 189-200 (49)
- Mahan, B., 17 (34)
- Maki, A.H., 70 (221), 71, 74,
77, 78 (234)
- Makino, T., 412 (57)
- Malecki, J., 461, 462, 464-
467, 477 (89)
- Malinoski, G.L., 67 (217)
- Manousek, O., 42 (170)
- Mao, S.W., 68 (310)
- Marcoux, L., 85 (253)
- Marcus, R.A., 58 (192)
- Marcus, R.J., 58 (192)
- Mares, F., 160, 171 (54), 179
(71), 180 (71, 66), 191, 193
(54), 194 (131), 199 (71)
- Markovits, G., 475 (99)
- Marmo, F.F., 7 (18)
- Marr, G.V., 3 (1)
- Marshall, J.H., 129 (108)
- Marshall, J.L., 364 (251)
- Martin, D.H., 430 (116)
- Martin, F., 351 (209)
- Martin, W.B., 75, 76 (235)
- Marton, L., 9 (19)
- Maruyama, K., 107 (293)
- Maryott, A.A., 461, 471, 472
(101)
- Massey, H.S.W., 3 (8), 18, 19
(37)
- Masterman, S., 355 (228)
- Matalon, S., 135 (324)
- Matheson, M.S., 125, 138 (127)
- Matsen, A., 33, 43 (169)
- Matsumoto, S., 404 (100-102),
433 (96), 435 (96, 97, 105),
436 (100-102, 107)
- Matsuyama, A., 464 (10)
- Matwiyoff, N.A., 509 (102)
- Maugher, E., 252, 266 (14)
- Mayer, J.E., 22 (40-43)
- Mazzanti, G., 398 (37)
- Mazzucato, U., 312 (142)
- Mecca, T.G., 305 (127)
- Medvedev, S.S., 421 (74), 431
(128)
- Megerle, G.H., 156, 158 (11)
- Meiboom, S., 183 (80)
- Melendres, C.A., 452, 453 (80)
- Melquist, J.L., 195 (91)
- Metz, D.J., 431 (129, 131)
- Meyer, L., 117 (68)
- Michael, A., 94 (261)
- Michael, B.D., 125 (125)
- Michejda, C.J., 85 (252)
- Michl, J., 43 (344)
- Mikuriya, Y., 312, 315, 318
(156)
- Milakofsky, L., 298 (110)
- Miles, F.B., 364 (250)
- Miller, L.S., 117 (70)
- Miller, R.C., 485 (104)
- Miller, T.A., 70 (223)
- Millington, J.P., 338, 352 (220)
- Minday, R.M., 119 (76)
- Minnich, E.R., 221, 234, 235

534 Author Index

- (142), 238, 239 (142, 154),
240 (142)
- Mitchell, E.J., 157 (23)
- Mitchell, J.J., 22 (41)
- Mixan, C.E., 289, 328 (84)
- Miyazawa, T., 405 (45)
- Mocek, M., 299, 302 (119)
- Moffitt, W.E., 103 (283)
- Mohler, F., 16, 17 (31)
- Mooberry, J.B., 353 (219)
- Moody, A.G., 404 (41)
- Moore, B., 129 (74)
- Morantz, D.J., 111 (336)
- Mori, Y., 492, 498 (8)
- Morris, G.C., 43 (175)
- Morris, J., 430 (126, 127)
- Morrison, G.A., 358 (237), 360
(239)
- Morton, M., 415 (61), 418
(141-143), 422 (141)
- Moshuk, G., 51 (184), 79, 82
(239)
- Motoi, M., 434, 436 (100, 102)
- Mottl, J., 29 (62)
- Mourning, M.C., 308, 310 (131)
- Moynihan, C.T., 498 (4)
- Mulac, W.A., 125, 138 (127)
- Munson, M.S.B., 45 (345)
- Murdoch, J.R., 163, 166, 169
(28), 171, 191 (101), 192
(28, 101)
- Murr, B.L., 298 (108, 116),
300, 301 (116)
- Murrell, J.N., 29 (348)
- Nakamura, K., 68 (310), 70
(332)
- Nakayama, T., 29 (62), 412
(57)
- Nasted, J.B., 498, 499 (75,
76), 500 (75, 76), 501, 502
(76), 510 (75)
- Natta, G., 398 (37), 405 (44,
46), 424 (46, 81)
- Nayak, B., 324 (167)
- Nebenzah, L., 169 (43)
- Nelson, D.P., 477, 479 (88)
- Nelson, N.J., 206 (136, 137)
- Nenitzescu, C.D., 248 (1)
- Netzel, T.L., 139 (366)
- Newallis, P.E., 312, 315, 318
(151)
- Nicely, V.A., 124, 129 (115)
- Nicholas, R.D., 294 (96)
- Nicholls, D., 36, 46, 62 (150),
204 (108)
- Nickols, R.E., 198 (97)
- Niemeyer, H.N., 169, 171, 179,
180 (55), 189, 190 (49), 191
(55), 200 (49)
- Nishida, V.M., 509 (53)
- Nishioka, A., 404 (40)
- Norberg, R.E., 85 (249)
- Nordberg, R., 12 (29)
- Nordlander, J.E., 289 (84),
294 (96, 101), 297 (101), 328
(84, 190)
- Normant, H., 129 (90, 91, 92)
- Normant, J., 129 (91)
- Norris, J.R., 60 (197)
- Noszkó, L., 307 (138)
- Nuyken, O., 428 (146)
- O'Brien, D.F., 172 (44)
- O'Driscoll, K.F., 422 (78)
- Ogg, R.A., 128 (102), 129 (106)
- Okamoto, K., 364 (252, 253)
- Okamura, S., 431 (132), 432
(130, 132)
- O'Konski, C.T., 500 (77)
- Olah, G., 248 (1)
- Olivier, K.L., 351, 353, 355
(212)
- Olson, A.C., 279 (55)
- Onsager, O.T., 415 (64), 450
(110)
- O'Reilly, D.E., 128 (98)
- Orville-Thomas, W.J., 462 (126)
- Ostermayer, F., 129 (114)
- Ottolenghi, M., 135 (324)
- Ovenall, D.W., 92 (262)
- Owen, E.D., 94 (263, 265)
- Owens, P.H., 189-200 (49)
- Pacifici, J.G., 102 (275)
- Paddon-Row, M., 323, 326, 328,
340 (168)
- Padgett, W.M., 163 (25)
- Page, F.M., 3 (5), 22 (5, 45-
47)

- Page, M.I., 155, 190 (162)
 Pallen, R.H., 377, 386 (5)
 Papa, I., 243 (203b), 312-314 (146)
 Parker, A.J., 157, 158 (10), 339, 360 (240)
 Parks, T.E., 312, 315 (141, 154), 316, 317 (154), 318 (141), 321 (154)
 Pastor, R.C., 127 (87)
 Paul, D.E., 221 (140)
 Pauling, L., 452, 453 (111)
 Pearson, J.M., 75, 76 (236), 77 (236, 347)
 Pearson, R.G., 3 (10), 183, 185 (74)
 Pedersen, C.J., 124 (116, 305), 219 (132), 477 (112, 113, 115)
 Pedersen, K.J., 180 (72)
 Penczek, S., 437 (109, 112)
 Penfold, J., 427 (42)
 Peover, M.E., 40 (172), 70 (224)
 Peraldo, M., 405 (44), 406, 424 (45)
 Peterson, P.E., 327 (187), 328 (188, 189), 346 (187-189), 361 (245)
 Petrov, E.S., 52, 54 (185, 186), 167 (70)
 Petrovich, J.P., 320, 321 (165)
 Phillips, H., 351 (208, 209), 353 (208)
 Piccardi, G., 26 (59)
 Pierotti, R.A., 503 (116, 117)
 Piette, L.H., 85 (254)
 Pinner, S.H., 429 (113), 430 (119, 120, 122)
 Pinnick, H.R., 298, 365 (113)
 Pitzer, K.S., 39 (161), 128 (105), 129 (104)
 Plesch, P.H., 427 (92), 428 (146, 147), 440 (92)
 Pocker, Y., 290, 294 (92)
 Podjaatmaka, A.H., 189, 190 (49, 50), 191 (50), 200 (49, 50), 201 (50)
 Podle, J.A., 31 (343), 507 (118)
 Polanyi, M., 111 (335)
 Pollak, V.L., 128 (99)
 Polyakov, D.K., 421 (74)
 Polykova, G.N., 135 (322)
 Pombo, M.M., 279, 281, 282 (60)
 Porhort, J.I., 206 (112)
 Porter, R.K., 312, 315, 318 (158)
 Pottel, R., 484 (120), 490, 491 (119), 499, 505-509 (62)
 Potter, R.C., 431 (131)
 Powell, D.G., 54 (187)
 Powles, J.G., 485 (121)
 Premaswarup, D., 499, 505 (124), 510 (132)
 Preston, E.A., 318, 319 (163)
 Pribadi, K.S., 449 (91), 496 (92)
 Price, A.H., 449 (83)
 Price, E., 157, 158 (16), 459 (70)
 Prock, A., 32 (141)
 Prokipak, J.M., 354 (225)
 Psarras, T., 172 (46)
 Putz, G.J., 289, 328 (84)
 Queen, A., 323 (168, 169), 326 (168), 328 (168, 169), 340 (168), 351 (210)
 Quinn, R.K., 123 (119)
 Rabani, J., 125, 138 (127)
 Raber, D.J., 254, 256 (23), 266 (46), 267 (46, 48), 287, 295 (48), 300 (120), 303 (125), 308 (48), 324 (23, 46), 326 (23, 46, 48, 120), 328 (46, 48, 120), 333 (46, 120), 336, 339, 341, 342 (120), 350 (23)
 Rabi, I.I., 452, 453 (50)
 Rainis, A., 92 (160), 227 (153, 156), 228 (153), 232, 234 (153, 166), 235 (156), 236, 237 (153, 156), 238 (156, 166), 239 (153, 156)
 Rakova, G.V., 421 (73)
 Ralph, E.K., 183 (82)
 Ramachandran, R.N., 495 (123)
 R  mme, G., 87, 88 (226), 131 (299), 134, 138 (226, 299)
 Rapp, M.W., 298 (109, 110, 113), 365 (113)
 Ratajczak, H., 461 (127), 462 (125-127), 464, 465 (127)
 Rebbert, R.E., 362 (248)
 Reich, I.L., 290 (95), 308 (130)

536 Author Index

- Reid, D.J., 323, 328 (169)
Reimann, C.W., 21 (39)
Reinhardt, P.W., 22 (52)
Reinmüller, M., 410 (50)
Reinmoth, W.H., 102, 103, 105 (277)
Reiss, H., 503 (131)
Relles, H.M., 208, 217, 220, 221 (120)
Remanick, A., 358 (235)
Rempp, P., 396 (32)
Rentzepis, P.M., 138 (333, 334), 139 (366)
Reppe, W., 102 (276)
Rettschnick, R.P.H., 131, 138 (311, 312)
Reuben, D.M.E., 166, 167, 169 (35), 171 (35, 53), 172 (35), 174, 177 (53)
Reuer, J.F., 200 (100)
Rewicki, D., 160 (56)
Reynold, W.L., 70 (225)
Rice, S.A., 116 (66), 117 (68)
Richards, J.T., 127 (135)
Richards, P.M., 70 (223)
Richardson, E.A., 458, 472, 475 (128)
Rickborn, B., 198, 208, 218 (98)
Rieger, P.H., 103 (281), 104 (356)
Rifi, M.R., 107 (289)
Rigo, A., 396, 397, 413 (34)
Rinkler, H.A., 360 (238)
Ritchie, C.D., 156 (9, 11, 12, 13), 157 (9), 158 (11), 169 (41, 42), 171 (42), 172 (41), 175 (58), 181 (9), 184 (76), 186, 194 (77), 204 (76), 205 (134), 230 (151), 242 (42), 333 (195, 196), 365 (196)
Rittner, E.S., 452, 453 (129)
Robbins, H.M., 339, 341 (200), 342, 343 (202)
Roberts, R., 430 (123)
Roberts, R.C., 95, 97, 98 (267)
Robertson, E.W., 16 (33)
Robinson, G.C., 252 (13), 253 (13, 17, 18), 254 (13, 18, 22), 255 (13), 256 (22), 260 (36), 263 (22), 264 (18, 42), 265 (36), 271 (18, 22, 42), 272 (18, 22), 273 (18, 22, 42), 274 (13), 276 (13, 17, 22), 277 (22, 36), 278 (36), 285, 290 (17), 293 (22), 330 (13)
Robinson, M.G., 117 (111)
Roderick, G.W., 498-500, 510 (75)
Rogers, E.H., 129 (106)
Rolla, L., 26 (59)
Romans, D., 85 (252)
Rose, J.B., 435 (99)
Rosenberg, A.M., 279, 282, 306, 308 (58)
Rossetto, O., 312 (142, 144)
Rossotti, F.J.C., 470 (130)
Rossotti, H., 470 (130)
Roth, W.R., 282, 284 (67)
Rougé, D., 398 (36)
Rubenstein, G., 123 (121)
Rubenstein, K.E., 288 (78)
Rubenstein, P.A., 189, 190, 200 (49)
Ruhoff, J.R., 176 (59)
Rynbrandt, J.D., 124, 130, 132 (308)
Rytting, J.H., 477, 479 (88)
Sackmann, G., 396, 397, 413 (34)
Saegusa, T., 433 (96), 434 (98, 100-102), 435 (96, 97, 98, 105), 436 (100-102, 107), 438 (110, 111)
Sakata, R., 418 (141, 142), 422 (141)
Salinger, R.M., 172 (46, 47)
Sanderson, R.D., 418 (141, 142), 422 (141)
Sandrock, G., 286, 287 (75), 288 (75, 79), 289 (81)
Sargent, G.D., 112 (339)
Sastry, P.S., 510 (132)
Satterthwait, A., 155, 190 (163)
Sauer, M.C., 87 (242), 125 (300)
Sauvage, J.P., 124 (117)

- Saxton, J.A., 499 (98)
 Scannon, P.J., 169, 171, 180, 191 (55)
 Scarmuzi, F., 118 (71)
 Schaad, L.J., 200 (100)
 Schadt, F.L., 326, 330, 341, 365 (176)
 Schaeffer, W.D., 326 (170)
 Scherer, K.V., Jr., 294, 295 (98)
 Schlenk, W., 94 (291)
 Schleyer, P.v.R., 248 (1), 254 (23), 256 (23), 266 (46), 267 (46, 48), 281 (63), 287 (48), 290 (94), 294 (96, 97), 295 (48), 298, 299 (118), 300 (118, 120), 301, 302 (118), 303 (118, 125), 307 (94), 308 (48), 326 (23, 46, 48, 120, 123, 171-178), 328 (23, 46, 48, 118, 120, 123, 171), 333 (46, 120, 172-178), 336 (120), 339 (120), 341 (120, 172-178), 347 (118), 348 (118, 123), 349 (118), 350 (23, 123, 171-178), 361 (244), 365 (172-176, 178)
 Schlichting, O., 102 (276)
 Schmelzer, C., 486 (136, 137)
 Schmid, G.H., 295, 297 (102)
 Schmidt, E., 425 (84)
 Schmidt, K.H., 122 (83), 125 (125)
 Schmidt, L.D., 119 (76)
 Schmidt, W., 29 (348, 349)
 Schmidt, W.F., 119 (75, 112)
 Schmithals, F., 499 (16), 510 (15, 16)
 Schmitt, B.J., 380, 384 (8), 385 (8, 135, 137), 391 (8)
 Schneider, H., 162 (69)
 Schneider, W.G., 507 (118)
 Schook, W., 60, 62, 63, 68 (199)
 Schooten, J. van, 39, 40, 43 (162, 163)
 Schreiber, K.C., 253 (16), 254 (16, 20), 263 (20), 271 (16, 20), 290 (16)
 Schreisham, A., 198 (97)
 Schubert, W.H., 290, 294 (93), 302 (93, 124)
 Schuerch, C., 405 (48), 406, 425 (49)
 Schull, H., 11 (28)
 Schultz, G.V., 377 (133), 380 (8), 382 (16), 384 (8, 16, 20), 385 (8, 23, 134, 135, 137), 391 (8), 410 (53, 54)
 Schultz, R.J., 312, 315, 318 (155)
 Schuster, R.E., 509 (53)
 Schwager, I., 51 (190), 163 (25)
 Schwartz, S.L., 353 (221)
 Schwarz, G., 448 (134, 135)
 Schweitzer, D., 127, 138 (134)
 Scott, A.D., 355 (228)
 Scott, C.B., 334 (197)
 Scott, D.A., 208, 217 (119, 120), 220, 221 (120)
 Scott, R.M., 464, 466 (86)
 Scriven, R.L., 353 (223)
 Sears, P.B., 158 (15)
 Sebenda, J., 425, 426 (82)
 Sekiguchi, H., 425 (83), 426 (86)
 Sentowski, F.J., 105 (357)
 Shack, R., 501 (65)
 Shank, N.E., 90 (354)
 Sharbaugh, A.H., Jr., 486 (136, 137)
 Shatenshtein, A.I., 52, 54 (185, 186), 167 (70), 215 (110)
 Sheikh, M.A., 485 (28), 487 (29), 488 (28), 489 (29)
 Shen, E., 232 (167)
 Sherrington, D.C., 427 (93)
 Shida, T., 90 (355)
 Shields, L., 127 (132)
 Shillaker, B., 251 (11)
 Shima, M., 417 (67), 423, 424 (80)
 Shimada, K., 61 (202, 203), 78 (237), 79 (237, 239), 82 (239)
 Shimomura, T., 113 (341), 202 (105), 203 (105, 107), 282 (17), 284, 285 (17, 22), 387 (17), 401 (22)

- Shiner, V.J., Jr., 294 (99),
298 (107-115), 299 (107, 114,
115), 300 (107), 301 (107,
111, 112, 114, 115), 302 (112,
115), 303 (107, 112), 306
(107), 311 (111, 112), 328
(111, 115), 345 (99), 346,
347 (111, 112), 348 (111, 112,
205), 361 (111), 365 (99,
111), 366 (111, 112)
- Shingu, H., 364 (252, 253)
- Shinohara, M., 391 (30, 31),
393 (30), 394, 396, 401 (31)
- Shinomiya, M., 405 (47)
- Shiota, T., 434 (101), 436
(101, 107)
- Shiusaka, K., 119 (113)
- Shold, D.M., 352 (218)
- Shryne, T.M., 351 (211)
- Sianesi, D., 424 (81)
- Sieck, L.W., 362 (248)
- Siegbahn, K., 12 (29), 13 (30)
- Siew, L.C., 107 (288)
- Sigwalt, P., 380 (139), 396,
397 (35), 398 (35, 36, 139),
412 (140), 413 (35, 140)
- Silversmith, E.F., 279 (57)
- Simmonds, P.G., 22 (53)
- Sinn, H., 415 (64)
- Skell, P.S., 356, 357, 360,
361 (233)
- Skinner, G.A., 156 (12)
- Slansky, C.M., 39 (161)
- Slater, J., 129, 132, 133 (316)
- Slates, R.V., 32, 36, 46 (142,
149), 52, 55 (188), 62, 63,
64 (149)
- Slichter, C.P., 82 (240)
- Smid, J., 55 (189), 56 (12),
64 (214), 113 (341), 153 (4),
161 (20), 177 (61), 201 (103,
104), 202 (103-105), 203
(103, 105, 106, 107), 204 (4),
215 (4), 219 (20), 235 (20),
327 (104), 377 (3, 26), 378
(3), 382 (15, 17), 384 (15,
17, 19, 22), 385 (17, 22),
386 (3), 387 (17, 29), 391
(30, 31), 393 (30), 394 (31),
396 (31), 399 (38), 401 (22,
31), 411, 412 (56), 417 (67),
418 (70), 420 (38, 71), 420,
424 (80), 470, 480 (138, 139)
- Smith, D.E., 102, 103, 105 (277)
- Smith, H.A., 176 (59)
- Smith, J.W., 449 (140), 452,
456, 457, 461, 463, 470 (18)
- Smith, P.A.S., 312 (142)
- Smith, S., 261 (39), 262 (38,
39), 265 (44), 266 (44, 45),
270 (51), 276 (45), 285 (45,
71), 307, 309 (133), 324 (44)
- Smith, S.G., 320, 321 (165)
- Smith, S.J., 9 (20, 22)
- Smolyansky, A.L., 464 (71)
- Smyth, C.P., 448 (141, 142),
449 (141), 485 (104), 495 (37)
- Sneen, R.A., 248 (4), 267, 268
(47), 279, 282 (58), 306 (58),
308 (58, 128), 311 (47), 326,
328 (4, 179-184), 329 (179,
181, 183), 330 (179, 180, 181),
331 (47, 180, 181, 184), 333,
334 (47), 335 (47, 184), 336,
337 (47), 338 (47, 64-66),
339 (170-181, 183, 200), 340
(47), 341 (47, 179-184, 200),
342 (47, 202), 343 (202), 344
(64-66), 345 (47, 64, 180-184),
346 (47), 350 (47, 200), 357
(180), 364-366 (47)
- Snyder, E.I., 357 (234)
- Snyder, L.C., 103 (287)
- Sobczyk, L., 461, 462, 464,
465 (127), 489 (41)
- Sobue, H., 382 (10)
- Solodovnikov, S.S., 76 (233)
- Sonnenberg, J., 273 (52)
- Sonnichsen, G., 189-191, 200,
201 (50)
- Sono, Y., 404 (40)
- Sorensen, S.P., 85, 86 (255)
- Sorgo, M. de, 85 (248), 167
(32)
- Spach, G., 380 (7)
- Spear, W.E., 117 (70)
- Spirin, Y.L., 421 (74)
- Spokes, G.N., 21 (39)
- Springett, B.E., 118 (72)
- Spurlock, L.A., 312, 316 (141,

- 150-152, 154-158), 317 (154),
318 (141, 151, 155-158), 321
(154)
- Srivastava, K.K., 458, 459 (63)
- Stanford, S.C., 157 (22)
- Stang, P.J., 303 (125)
- Stannett, V., 429 (113)
- Staples, T.L., 66, 67 (216),
107 (292), 167 (32)
- Steiner, B., 9 (24)
- Steiner, E.C., 206 (139)
- Stern, K.H., 458, 472, 475
(128)
- Stevens, T.S., 318, 319 (160)
- Stevenson, G.R., 105 (357,
358)
- Stewart, R., 299, 302 (119)
- Stivers, E.C., 200 (100)
- Story, T.L., Jr., 452, 453 (80)
- Straub, T.S., 195 (91)
- Strauss, H.A., 8 (15)
- Strauss, H.L., 102 (278, 279),
103, 104 (282)
- Street, K., Jr., 452 (25, 79,
'80), 453 (79, 80)
- Strehlow, H., 156 (18)
- Streitweiser, A., 51 (190),
159 (52), 160 (52, 54), 163
(25-28), 164, 165 (52), 166
(28, 35), 167 (31, 35), 169
(27, 28, 35, 43, 55), 171
(26, 27, 35, 52-55), 172 (35),
173 (103), 174 (53), 176 (60),
177 (53), 179 (55, 71), 180
(55, 66, 71), 189, 190 (49,
50), 191 (50, 54, 55, 101),
192 (28, 101, 128, 129), 193
(54, 130), 194 (96, 131), 198
(96), 199 (31, 66, 71, 99),
200 (49), 201 (50), 206 (31,
111), 289 (82), 290 (85, 86),
297 (85), 298 (86), 299 (122),
323 (86), 326 (82, 170, 186),
327 (82), 328 (122), 357
(186)
- Stretch, C., 377, 379 (2)
- Struve, W.S., 139 (366)
- Suggett, A., 448 (144)
- Sullivan, S., 32 (141)
- Sundheim, B.R., 129 (88)
- Sunko, D.E., 298, 300, 302,
303, 305 (117)
- Sustmann, R., 294 (97)
- Sutphen, C., 36, 46, 62 (150),
204 (108), 229-231 (149)
- Sutton, P.P., 22 (40)
- Suzuki, H., 211, 240 (159)
- Swain, C.G., 200 (100), 334
(197)
- Swift, E., 33 (145)
- Symons, M.C.R., 123 (317), 124
(95, 307), 127 (132), 129,
132, 133, 134 (316)
- Szwarc, M., 4 (12), 32 (140,
142, 149), 34 (147), 36 (142,
147, 149, 150), 37 (148, 151),
40 (147, 151, 153), 43 (151,
179), 46 (12, 140, 147, 149,
150), 47 (182), 49 (182, 183),
50 (148, 182), 51 (184), 52,
55 (188), 56 (12, 191, 230),
60 (183), 61 (183, 202, 203),
62 (12, 149, 150), 63 (149),
64 (149, 183, 214), 65 (183),
66 (216), 567 (216), 78 (237),
79 (237, 239), 82, 85 (239),
87, 88 (226), 92, 95, 97
(160), 98 (154, 160), 99 (272),
102 (147), 107 (292), 109
(295, 296), 110 (297, 298),
111 (359), 113 (341), 129
(12), 131 (299), 134 (226,
299), 138 (226, 272, 299),
139 (366), 152 (3, 5, 6), 156,
159 (8), 161 (3, 8, 19), 166
(29, 57), 167 (32), 177 (62),
201 (103), 202 (103, 105),
203 (103, 105, 107), 204 (108),
210 (3), 221 (3), 222 (143),
227 (153, 156), 228 (153), 229
(149, 150), 230 (149, 152),
231 (149), 232 (153, 166, 167),
234 (3, 153, 166), 235 (156),
236 (153, 156), 237 (153, 156,
157), 238 (156, 166), 239
(153, 156), 376 (1), 377 (3,
26), 378 (3, 4), 380 (7), 382
(15, 17), 384 (15, 17, 19, 22),
385 (17, 22), 386 (3, 4), 387
(12, 14, 17, 29), 391 (30, 31),

- 393 (30), 394 (31), 396 (13, 31, 33, 34), 397 (34), 398 (33), 399 (38, 39), 401 (22, 31, 33), 411, 412 (56), 413 (33, 34), 414 (33), 417 (67), 418 (70), 420 (38, 71), 422 (79), 423 (7, 80), 424 (80), 428 (89), 431 (15)
- Tabata, Y., 382 (10)
- Tabner, B.J., 43 (159), 94 (263, 265)
- Taft, R.W., 313 (147)
- Taher, N.A., 249, 251, 252 (7), 257 (7, 32), 259-261, 265, 266, 269, 270, 322, 324, 330, 339 (7)
- Takaya, K., 412 (57)
- Tamm, K., 492 (47)
- Tanford, C., 480, 494 (145)
- Tao, E.V.P., 361 (245)
- Tardi, M., 380 (139), 396, 397 (35), 398 (35, 36, 139), 413 (35)
- Taub, I.A., 87 (242)
- Taube, H., 3 (10), 509 (13, 102)
- Taylor, H., 351 (209)
- Taylor, R.L., 21 (39)
- Taylor, R.P., 334 (199)
- Tehan, F.J., 124, 125 (304), 135 (304, 362)
- Tewari, P.H., 119 (74, 109)
- Thai, A., 94 (261)
- Thies, R.W., 291-293, 297 (89)
- Thomas, I.D., 12 (29)
- Thomas, J.K., 127 (135)
- Thompson, G., 361 (245)
- Thompson, J.O., 118 (71)
- Thornton, E.R., 305 (126)
- Thül, B., 508 (48)
- Tiernan, T.O., 362 (248)
- Ting-Po, I., 459, 472, 480 (87)
- Tipping, J.W., 129, 132 (316)
- Toepel, T., 102 (276)
- Tolle, K.J., 64 (214), 113 (341), 203 (107), 382 (17), 384 (17, 19), 385 (17), 387 (17, 29)
- Tonellato, U., 312 (144, 145, 150), 313 (145), 314 (145, 150)
- Trancik, R.J., 353 (219)
- Travis, N., 16 (33)
- Tremba, E.L., 223, 224 (147)
- Trifan, D., 307, 309 (135)
- Tsubomora, H., 461, 462 (146)
- Tully-Smith, D.M., 503 (131)
- Tung, R., 26, 111 (55), 227 (153, 156), 228 (153), 232, 234 (153), 236, 237 (153, 156), 238 (156), 239 (153, 156)
- Tupizin, J.F., 194 (86)
- Turner, D.W., 3 (3), 9 (26)
- Tuttle, T.R., 63 (212), 123 (120-122), 128 (120), 129 (107), 132 (107, 319), 133 (319), 134 (107), 315 (107, 320)
- Ueda, H., 90 (355)
- Ueno, K., 432 (130)
- Ullman, R., 448, 480 (6)
- Uschold, R.E., 169, 171 (42), 175 (58), 184 (76), 186 (77), 194 (77), 204 (76), 205 (134), 206 (42)
- Uyeda, R.T., 208, 217 (121)
- Valkanias, G., 308 (132)
- Vandenheuvel, W.J.A., 22 (53)
- Van der Meij, P.H., 33 (146), 91 (146, 257)
- Van Sickle, D.E., 193 (130), 198 (96), 206 (111)
- Van Voorst, J.D.W., 131 (311, 312), 138 (311, 312, 330)
- Vatakencherry, P.A., 321, 322 (166), 358 (236)
- Vaughan, W.E., 176 (59), 448 (147), 449 (83)
- Vidulich, G.A., 496 (92, 148)
- Vier, D.T., 22 (42)
- Vincow, G., 85 (245)
- Vinogradov, S.M., 464, 466 (86)
- Vofsi, D., 425 (85, 87)
- Vogel, P.C., 300, 328 (121)
- Vos, K.D., 129, 132 (315)

- Voyerodskii, V.V., 76 (233)
 Vukm-Rovich, Z., 167 (70)
- Waack, R., 206 (112), 207 (114), 416 (65)
 Walsh, T.D., 289 (82), 326 (82, 186), 327 (82), 357 (186)
 Ward, R.L., 59, 61 (194)
 Ward, T.A., 111 (359)
 Wardman, P., 127 (367)
 Warhurst, E., 54 (187), 111 (336)
 Warneck, P., 9 (25)
 Warren, L.J., 43 (175)
 Wasserman, B., 85 (248), 167 (32)
 Watanabe, K., 7 (17, 18), 29 (62), 404 (40)
 Wawzdnek, H., 39, 40 (166, 167), 41 (167)
 Wawzonek, S., 39, 40 (168)
 Weaver, H., 59 (205)
 Weda, H., 90 (351)
 Weightman, J.A., 427 (93)
 Weijland, W.P., 33, 191 (146)
 Weiner, H., 326, 328, 329 (179-181, 183), 330 (179-181), 331 (180, 181), 339 (179-181, 183), 341 (179-183), 345 (180-183), 357 (179, 180)
 Weiss, A.W., 17 (36)
 Weissman, S.I., 59 (194, 195), 60 (195), 61 (194), 62 (208, 209), 63 (204, 209, 213), 65, 67 (208), 68 (195, 219), 84 (195), 85 (249), 221 (140)
 Weitzl, F.L., 352 (213, 217)
 Wen, W.-Y., 502, 503, 512 (52)
 Wentworth, W.E., 3 (6), 5 (14), 23, 25 (54), 26 (55, 57), 111 (55)
 West, P., 206 (112), 416 (65)
 Westheimer, F.H., 196 (88)
 Weyl, W., 123 (85)
 Wheland, G.W., 43 (177), 167 (33)
 Whiffen, D.H., 94 (262)
 White, E.H., 288, 301, 359 (76)
- Whitfield, I.C., 350 (207)
 Whittaker, R., 111 (336)
 Wiberg, K.B., 295 (104), 351 (211)
 Wichterle, O., 425, 426 (82)
 Wilcox, C.F., Jr., 308 (132)
 Wilde, D.J., 470 (149)
 Wiles, D.M., 129 (89), 404 (41)
 Wilhelm, M., 361 (241)
 Wilkinson, G., 129 (49)
 Willey, F., 208, 217 (119, 120), 220, 221 (120)
 Williams, D.J., 75, 76 (236), 77 (236, 347)
 Williams, F., 382 (11), 430 (114, 116, 117), 432 (117, 130)
 Williams, G., 448 (151), 456, 461 (42), 480 (151), 486-488 (42)
 Williams, J.M., 195 (91)
 Williams, T.F., 430 (115)
 Willigen, H., van, 105, 106 (291)
 Wilson, R., 70 (224)
 Winstein, S., 252 (13), 253 (13, 15-19), 254 (13, 15, 16, 18-20, 22), 255 (13), 256 (19, 22), 257 (26-29), 258 (34), 260 (34, 36, 37), 261 (34, 39), 262 (34, 37, 38, 40), 263 (20, 37), 264 (34, 37), 265 (37, 44), 266 (44, 45), 268 (49, 50), 269 (49, 50), 271 (15, 16, 18, 20, 22, 34, 41-43, 50), 272 (18, 22), 273 (18, 22, 26, 41-43, 50-52), 274 (13, 18, 43, 50, 54), 275 (50), 276 (13, 22, 36, 43, 50, 54), 277 (22, 36, 45), 278 (36, 54), 279 (56), 285 (17, 19, 45, 71), 286 (19), 288 (77), 289 (56, 83), 290 (16, 17, 95), 292 (37), 293 (22), 294 (19), 297 (56), 298 (19), 301 (77), 306 (50, 129), 307 (19, 133-135), 308 (49, 129, 130, 132), 309 (19, 133-135), 310 (49), 311, 322 (19), 323

- (27), 324 (44), 328 (56, 95),
330 (13, 37, 49, 50), 338,
339 (34), 346 (56, 129), 359,
361 (77), 363 (19, 249), 364
(19, 56), 365 (19, 37)
Winter, R., 321, 322 (166),
358 (236)
Wolf, R.A., 160, 171, 191,
193 (54)
Wolf, R.K., 127 (368)
Wolfe, J.R., Jr., 326, 357
(186)
Wolff, R.K., 125 (124)
Wolford, R.K., 158 (15)
Wolfsberg, M., 298 (109)
Wooding, N.S., 380 (9)
Wong, B.F., 68, 69 (218), 70
(332)
Worley, S.D., 29 (63)
Worrall, R., 429 (113), 430
(118-120, 122)
Worsfold, D.J., 384 (18), 414
(58), 415 (62, 63, 66), 418
(144, 145), 421 (76)
Wragg, A.H., 318, 319 (160)
Wren, C.M., 354 (226)
Wright, A.N., 129 (89)
Wright, C.V., 16 (33)
Wyman, J., 494, 495 (46)

Yahada, A., 405 (48)
Yakovleva, E.A., 52, 54 (186),
167 (70)
Yakushin, F.S., 167 (70)

Yamaoka, H., 382 (11)
Yamdagni, R., 155, 156 (37)
Yandle, J.R., 43 (159)
Yang, S.L., 34, 36, 46, 102
(147), 229 (150)
Yates, K., 299, 302 (119)
Yee, K.C., 187 (78, 79), 188
(78)
Yoshida, M., 107 (288)
Yoshino, T., 405 (47)
You, F.J., 125, 131 (301)
Young, L.B., 27 (61)
Young, R.N., 56 (229)
Young, W.G., 253, 254, 571
(15), 351, 353, 355 (212)

Zabolotny, E.R., 94 (266, 274),
95, 97, 99 (266), 101 (274),
102 (275)
Zakaarkin, L.I., 167 (70)
Zandberg, E. Ya, 22 (51), 135
(321)
Zandstra, P.J., 59, 60 (195),
63 (204), 68, 86 (195), 138
(329)
Zatsepina, N.N., 194 (86)
Ziedler, M.D., 508 (48)
Ziegler, G.R., 192 (129)
Zollinger, H., 197 (95)
Zoltewicz, J.A., 194 (169)
Zuman, P., 42 (170, 171)
Zwanizig, R., 497 (153, 154)
Zwolinski, B.J., 58 (192)

Subject Index

- Acenaphthalene, electron affinity in different solvents, 38
ionization potential of, 30
Acetate ions, as bases, 196
Acetic acid, pK of, in different solvents, 158
Acetophenone, electron affinities in gas phase, 26
Acetylene, acidity of, 171
ionization potential of, 28, 29
Acidity, of hydrocarbons, 170, 171
scales of, 167-172
structural factors affecting, 172-180
Acridine, ionization potential of, 30
polarimetric $\epsilon_{1/2}$, potentiometric ϵ_0 of, 41
Acrylates, anionic polymerization of, 385, 398
 α -cis- β -d₂-Acrylate, Grignard-initiated polymerization of, 405
Acrylonitrile, γ -ray initiated polymerization of, 382
Activity coefficients, use in approach to solvent basicity, 156
1-Adamantyl bromide, salt effects on solvolysis of, 267
1-Adamantyl-carbinyl p-nitrobenzene sulfonate, aceto-lysis of, 294
1-Adamantyl chloroformate, decomposition of, 352, 353
2-Adamantyl tosylate, α -D isotope effect in solvolysis of, 299
salt effect on solvolysis of, 266, 267
solvolysis of, 302, 328, 348
AdE2, mechanism for acid addition to olefins, 361, 362
AdE3, mechanism for acid addition to olefins, 361, 362, 360
Affinity spectrum, 18
Alanines, dielectric relaxation times for, 494, 495
Alcoholates, of Na and Li in association with ion pairs in ethereal solvents, 54
Alcohols, spectra of solvated electrons in, 125, 126
Alkali halide, ion pairs of, in gas phase, 452, 455
Alkali metals, equilibrium between aromatic acceptors and, 51-57
esr of free atoms of, 132-137
esr spectra in liquid ammonia, 127
heat of sublimation and ionic potential of, 51
negative ions of, 135
solubility enhancement, with crown ethers, 124
solutions of, in amines or ethers, 123, 124, 129

- Alkylarenesulfonates, common
ion rate depression and ex-
change in acetolysis of,
252, 253
normal salt effects in aceto-
lysis of, 260, 261
180-scrambling in solvolysis
of, 289, 293
special salt effects in acet-
olysis of, 271
- Alkyl bromides, hydrolysis of,
341, 342
- Alkyl chlorides, reaction with
Na naphthalenide, 112
solvolysis mass law and rate
constant, 252
- 9-Alkylfluorenes, acidities
of, 175, 176
- Alkylformates, thermal de-
composition of, 350-356
- Alkyl halides, hydrolysis of,
249, 341
ionization of, 253
medium effects on rate con-
stants for solvolysis of,
259
- Alkylsulfinate esters, iso-
merization to sulfones,
318, 319
thermal decomposition of, 350
- Alkylthiocyanates, isomeriza-
tion of, 315
- 2-Alkyltosylates (halo-substi-
tuted), solvolysis of, 327
- Allene, ionization potential
of, 28, 29
- Allylic systems, internal re-
turn in, 280
- Allylic thiocyanates, isomer-
ization of, 315
- Allyllithium, 206, 207
- Allyl *p*-nitrobenzoates, sol-
volysis of, 288
- Amines, effect of addition on
rate of polymerization of
radical anions, 224, 225
solution of alkali metals in,
123, 129, 132-135
ultraviolet irradiation of,
137
- Ammonia, basicity of, 155
dipole moment of, 469
- Ammonia (liquid), 136
alkali metal solution in, 121,
123, 128, 130
binding energy of electron in,
120
spectrum of electron in, 126,
127
- Ammoniated electrons, optical
spectrum of, 125
- Ammonium salts, dielectric re-
laxation times for, 485-490
- Anchimeric assistance, 258
- Aniline, basicity of, 155
ionization potential of, 30
- Anionic polymerization, effect
of complexing agents on
rate of propagation of,
391-396
free ions and ion pairs in,
385
initiated by Grignard com-
pounds, 404
initiated by living polymers,
382-386
involving activated monomer,
424-427
by ionizing radiation, 381,
382
of styrene, 377-381
transition state of, 399-401
- Anisole, ionization potential
of, 30
- Threo*-2-*p*-anisyl-3-butylarene-
sulfonate, normal salt ef-
fect, 263
- Threo*-3-*p*-anisyl-2-butylarene-
sulfonate, acetolysis of,
268
salt effect in ionization of,
263
- α,ℓ -*Threo*-3-*p*-anisyl-2-butyl-
tosylate, acetolysis of,
253, 255, 256, 264, 265,
268
special salt effect in aceto-
lysis of, 271-276
- Threo*-3-*p*-anisyl-2-butyltosy-
late, salt effect on

- acetolysis of, 268, 273, 293
- Trans*-2-*p*-anisylcyclopentyl-brosylate, salt effect on acetolysis of, 264, 273
- α -Anisylethylnitrobenzoates, solvolysis of, 286, 287, 288
- 2-*o*-Anisylethyltosylate, salt effect on acetolysis of, 264, 273
- 2-*p*-Anisylethyltosylate, salt effect on acetolysis of, 264, 267, 268, 269, 273, 274
- 9-(*m*-Anisyl) fluorene, acidity of, 170
- 9-(*p*-Anisyl) fluorene, acidity of, 170
- 1-*p*-Anisyl-2-propylbrosylate, salt effect on acetolysis of, 264, 274
- 1-*p*-Anisyl-2-propyltosylate, acetolysis of, 253, 265, 267, 274, 276-278
- exchange reaction with bromide salts, 278
- 2-*p*-Anisyl-1-propyltosylate, exchange reaction with bromide salts, 278
- salt effect on acetolyses of, 264, 268, 269, 273
- Anthracene, dissociation constant of Na salt of radical anion of, 36
- electron affinity in gas phase, 26
- electron exchange with its radical anion, 72
- electron transfer, with free biphenylide, 88, 89
- with free pyrenide, 88, 89
- with free *p*-terphenylide, 88
- heat of solvation of radical anion in THF, 32
- ionization potential of, 30
- potentiometric ϵ of, 40, 43
- protonation, of dianions of, 237, 238, 239
- of radical anions of, 221, 223, 224
- pyrene e-transfer system, 46, 89
- redox potential of, 93
- relative halfwave potential of, 49
- Anthracenides, kinetic data for protonation of, 233
- Arene sulfonates, acetolysis of, 258
- ionization of, 253
- Argon, mobility of electron in liquid, 119
- Aromatic aldehydes and ketones, electron affinities in gas phase, 26
- Aromatic hydrocarbons, dissociation constants of Na salts of radical anions of, 36
- electron affinities, in different solvents, 38
- in gas phase, 26, 27
- ionization potentials of, 28, 29, 30
- heats of solvation of radical anions in THF, 32
- potentiometric studies of solution electron affinities of, 33-38
- radical cations of, 85
- relative polarographic half-wave potentials of, 40
- β -Arylalkyl tosylates, LiClO₄ salt effect on ionization, solvolysis and rearrangement of, 269
- 1-Arylethanes, Brønsted α values for deprotonation of *m*-substituted, 187
- β -Arylethyl tosylates, detection of ion pairing in solvolysis of, 310
- 9-Arylfluorenes, acidity of, 179
- Arylmethanes, Brønsted relation for, 192
- 1-Arylnitroethanes, 187
- 1-Arylnitromethanes, 187, 188
- 1-Aryl-2-propyl tosylates, solvolysis of, 326, 327, 333

- Association, of radical anions with counterions, 61
- Association constants, dielectric measurement of, 470-471
- Autoionization, 3, 13
- Aza-aromatics, polarographic $\epsilon_{1/2}$, and potentiometric ϵ_0 for, 41
- Azulene, electron affinity in gas phase, 26
ionization potential of, 30
- Basicity, of liquid solvents, 155
- Benzaldehyde, electron affinity in gas phase, 26
ionization potential of, 30
- Benz(a)anthracene, electron affinity in gas phase, 26
- Benzanthracene, 1, 2, ionization potential of, 30
- Benzene, acidity of, 171
aggregation of ion pairs in, 167
electron exchange with its radical anion, 72
heat of solvation of radical anion in THF, 32
ionization potential of, 28, 29, 30
propagation by living polystyrene salts in, 386
- 1,2-Benzfluorene, acidity of, 170, 190
1H-transfer to fluorenyls, 203, 204
- 2,3-Benzfluorene, acidity of, 171, 190
- 3,4-Benzfluorene, acidity of, 170, 190
proton transfer to fluorenyls, 203
- Benzhydrylbenzoate, solvolysis of, 301, 359
- Benzhydrylchloride, rate constant of solvolysis, 252, 259
salt effect on solvolysis of, 266
- Benzhydryl-*p*-nitrobenzoates, 180
equilibration in solvolysis of, 285
180 scrambling in racemization for *p*-substituted-, 288
- Benzhydrylfulfinate, isomerization of, 319
- Benzhydrylthiocyanate, isomerization of, 312, 313
reaction of substituted-, with thiocyanate ion, 343
- Benzo-[e]-cinnoline, polarimetric $\epsilon_{1/2}$ and potentiometric ϵ_0 of, 41
- Benzoic acid, proton transfer with carbanions and methoxide ion, 186
- Benzonitrile, electron exchange with its radical anion, 73
- Benzo[c]phenanthrene, electron affinity in gas phase, 26
- Benzophenone, exchange with its ketyls, 69
- Benzo[a]pyrene, electron affinity, in different solvents, 38
in gas phase, 26
- Benzo[e]pyrene, electron affinity in gas phase, 26
- 5,6-Benzoquinoline, polarimetric $\epsilon_{1/2}$ and potentiometric ϵ_0 for, 41
- 5,6-Benzoquinoline, polarimetric $\epsilon_{1/2}$ and potentiometric ϵ_0 for, 41
- 7,8-Benzoquinoline, polarimetric $\epsilon_{1/2}$ and potentiometric ϵ_0 for, 41
- p*-Benzoquinone, electron exchange with its radical anion, 73
- p*-Benzoquinone radical anion lifetime of, in gas phase, 18
- Benzotrifluoride, ionization potential of, 30
- Benzypyrene, 1, 2 ionization potential of, 30

- Benzpyrene 3,4 ionization potential of, 30
 Benzylbrosylate, α -D isotope effect in solvolysis of, 298
 Benzyl carbanions, protonation of, 236
 Benzylchloride, reaction with Na naphthalenide, 112
 Benzyldrylbromide, salt effect on acetolysis of, 266
 9-Benzylfluorenylcesium, 177
 Benzyllithium, 206, 207
 Benzyl radical, electron affinity in gas phase, 27
 Benzyltricyanates, isotopic exchange in, 314
 Betaines, dielectric relaxation for, 495
cis-3-Bicyclo[3.1.0]hexyltosylate, special salt effect on acetolysis of, 273
trans-3-Bicyclo[3.1.0]hexyltosylate, special salt effect on acetolysis of, 273
 Biphenyl, dissociation constant of Na salt of radical anion of, 36, 37
 electron affinity in different solvents, 38
 electron exchange with its radical anion, 72
 electron transfer with sodium pyrenide, 87
 equilibrium with metallic sodium in solution, 52
 heat and entropy of dissociation of Na salt of radical anion of, 37
 ionization potential of, 30
 kinetic data for protonation of radical anion of, 223, 224
 relative halfwave potential of, 40
 1,1,3,3-bis(Bisphenylene)-propene, acid base equilibria of salts of, 165
 pK_{ion} pair of, 160
 10-Biphenyl-9,9-dimethyl-9,10-hydroanthracene acidity of, 171
p-Biphenyldiphenylmethane, acidity of, 171, 178, 190
 ^3H exchange with Li cyclohexylamide, 191
 Brønsted relation for, 192
 bis(*p*-Biphenyl) methane, acidity of, 171, 190, 191
 Brønsted relation for, 192
p-Biphenylphenylmethoxymethane, stereochemical aspects of isotope exchange, 218
 2,2'-Bipyridyl, polarimetric $\epsilon_{1/2}$ and potentiometric ϵ_0 for, 41
 4,4'-Bipyridyl, polarimetric $\epsilon_{1/2}$ and potentiometric ϵ_0 of, 41
 Born-Oppenheimer approximation, 74
 Böttcher model, for ion pairs, 453-457, 463
 Bromobenzene, ionization potential of, 30
p-Bromobenzenesulfonic acid, reaction with propene, 301
 Bromothiophene, 428
 Brønsted relation, 180-194
 Butadiene, copolymerization with styrene, 42
 1,4 and 1, 2 enchainment, 416
 polymerization by lithium polybutadiene, 415
 Butadiene and butenes, ionization potential of, 28, 29
t-Butylacetylene, acidity of, 171
p-t-Butylbenzhydrylchloride, solvolysis of, 252, 259, 266
t-Butylbromide, solvolysis of, 266, 323
t-Butylbrosylate, salt effect on acetolysis of, 265
t-Butylchloride, solvolysis mass law and rate constant, 252
n-Butylchloroformate, decomposition of, 352, 358
cis-trans-4-*t*-Butylcyclohexyltosylate, solvolysis of 180-

- labelled, 289
- sec-Butyldiazonium salts, 357
- t-Butylethylene, reaction, with propene, 301
- in THA, 346, 347, 348
- 9-t-Butylfluorene, acidity of, 171, 179
- n-Butyllithium, 207
- α -Butylnaphthalene, exchange with free naphthalenide ions, 61
- intermolecular exchange with radical anion, 78
- n-Butyl- α -naphthalenide radical anions, esr spectra of, 82
- intermolecular exchange with n-butyl- α -naphthalene, 78-85
- t-Butyl-p-nitrobenzoate, 180
- scrambling in solvolysis of, 290
- p-t-Butylstyrene, 424
- ϵ -Butylsulfinate, isomerization of, 319
- iso-Butyl-vinyl ether, propagation constant for polymerization of, 427
- γ -Butyrolactone, hydrolysis of, 339
- Carbanions, effect of cations on stereochemistry of, 218
- Carbon acids, 188
- application of Brønsted relation to, 183
- dissociation of neutral -, 153
- Carbonates, decomposition of, 351-355
- Cationic polymerization, of cyclic ethers, 431-437
- initiated by γ -irradiation, 382, 428-431
- of 2-oxazoline, 437
- of vinyl and vinylidene monomers, 427
- Cesium, solution in ethylenediamine, 130-131, 136
- Cesium cyclohexylamide, 191
- Chlorobenzene, ionization potential of, 30
- p-Chlorobenzyhydryl-p-nitrobenzoates, effect of NaN_3 on solvolysis of, 286, 287, 315
- 180 equilibration in solvolysis of, 285
- p-Chlorobenzhydryl thiocyanate, solvolysis, isomerization, and exchange of, 314
- p-Chlorobenzyl, radiochloride exchange of, 257, 267
- salt effect on solvolysis of, 266, 276, 285
- m-Chlorodinitrobenzene, electron exchange with its radical anion, 73
- Chloroformates, decomposition of, 351-355
- bis-Chloromethyl oxetane, polymerization of, 437
- 9-(m-Chlorophenyl) fluorene, acidity of, 170
- 9-(p-Chlorophenyl)fluorene, acidity of, 170
- Chlorosulfonates, decomposition of, 351, 355, 356
- Cholesterylbrosylate, acetolysis, 250, 273, 276
- Cholesteryltosylate, salt effect on acetolysis of, 265, 273, 274, 276
- Chrysene, electron affinity in different solvents, 38
- electron affinity in gas phase, 26
- ionization potential of, 30
- relative halfwave potential of, 40
- Cinnoline, ionization potential of, 29, 31
- polarimetric $\epsilon_{1/2}$ and potentiometric ϵ_0 of, 41
- Cole-Cole Parameters, 500, 504, 510
- Common ion, exchange of, 252, 253, 256
- Common ion effect rates, 249-252, 253, 277
- "Conducted Tour," mechanism for proton transfer, 212, 213, 214, 215, 217, 220

- Copolymerization, anionic, 418-423
 structural information from rate constants of, 423
 Crown ethers, 136, 399, 469, 477, 478, 479
 enhancement of racemization in proton-exchange, 219
 enhancement of solubility of alkali metals in ethers and amines, 124, 129
 retardation of protonation by, 234, 235
 Cryptates, 136, 399
 for enhancement of solubility of alkali metals in amines and ethers, 124, 129
 Cumene, acidity of, 171
 2-Cyano-9-methylfluorene, kinetic data for isotope exchange of, 213
 stereochemistry in isotope exchange, 211, 212
 4-Cyano-9-phenylfluorene, acidity of, 170
 Cycloheptatriene, disproportionation of radical anion of, 103
 Cyclohexane, effect of addition of, on rate of protonation of radical anions, 225
 ionization potential of, 28, 29
 propagation of living polystyrene salts in, 386
 Cyclohexyltosylate, salt effect on acetolysis of, 264
 Cyclooctatetraene, disproportionation of radical anion of, 102-107
 Cyclopentadiene, acidity of, 170
 ionization potential of, 28, 29
 propagation constant of free cations, 432
 Cyclopentane, ionization potential of, 28, 29
 Cyclophanes, para-, esr of radical anions of, 75, 77, 78
 Cyclopropane, ionization potential of, 27, 28
 Cyclopropylmethylcarbonyl *p*-nitrobenzoate, solvolysis of, 288
 Debye theory, 451
 Dialkylmagnesium compounds, 172
 Dialkylmercury compounds, 172
 Dianions, protonation of, 221-240
 1,5-Diazabicyclo[4.3.0]non-5-ene, stereochemical aspects of isotope exchange, 216
 Diazo coupling, 197
 Diazonium ions, decomposition of alkyl-, 356-361
 stereochemistry of decomposition product, 357
 Dibenz[a,h]anthracene, electron affinity in gas phase, 26
 Dibenz[a,j]anthracene, electron affinity in gas phase, 26
 Dibenzo-*p*-dioxin, exchange with its radical cation, 85, 86
 Di-*p*-biphenylmethane, 179
 3,5-Dichlorodinitrobenzene, electron exchange with its radical anion, 73
 Dichlorodiphenylmethane, solvolysis of, 257
 Dicyclohexyl-18-crown-6-ether, effect of addition of, on rate of protonation, 234
 Dielectric constant, 120, 155, 157, 159, 161, 162, 168, 210, 215, 257, 377, 414, 448-509
 Dielectric increment, molar, 498
 Dielectric relaxation, Debye theory of, 480-481
 distribution of relaxation times, 483, 484
 mechanisms of, 488-490
 microscopic relaxation times, 485
 of polar solutes in nonpolar solvents, 481-483
 of solution of free ions, 495-512
 time, 468

- Dienes, anionic polymerization of, 385
 stereospecificity of polymerization of, 416
- Diethylamine, as base, 187
- Diethylether, aggregation of ion pairs in, 167
 dissolution of alkali metal in, 124
 optical spectrum of electron in, 124, 126
- m*-Difluorobenzene, carbanion stabilization factor for, 180
- o*-Difluorobenzene, acidity of, 179
 carbanion stabilization factor for, 180
- p*-Difluorobenzene, carbanion stabilization factor for, 180
- Diglyme, spectrum of electron in, 126
- 9,10-Dihydroanthracene, 232
- Dihydronaphthalene, 231
- Diisotactic polymer, 405
- Dimethoxyethane, propagation by living polystyrene salts in, 386
 solutions of K and Cs in, 129
 spectrum of electron in, 126
- 2-(2,4-Dimethoxyphenyl)-ethyl-brosylate, acetolysis of, 253, 276
 salt effect on acetolysis of, 265, 273, 274
- 9-(*p*-N,N-Dimethylaminophenyl)fluorene, acidity of, 170
- 9,10-Dimethylantracene, electron transfer with pyrenide radical anion, 46, 88, 89
- p,p*-Dimethylbenzhydryl chloride, rate constant for solvolysis of, 249, 250
 solvolysis, 249, 250, 252, 259, 266
- 4,4'-Dimethylbenzhydryl thiocyanate, isomerization of, 312, 313
 solvolysis of, 313, 314
- 1,3-Dimethyl-2-butyl-brosylate, α -D isotope effect on solvolysis of, 299
- 2-(N,N-Dimethylcarboxamido)-9-methylfluorene, ¹H exchange with, 199
- 2-(N,N-Dimethylcarboxanido)-9-methylfluorene-9-d, effect of cations on stereochemistry of carbanion, 218
 kinetic data for isotope exchange of, 213, 214
 stereochemical aspects in isotope exchange, 210, 211, 212, 213, 215
 stereochemical fate of ion pairs in dissociating solvents, 220
- 3-(N,N-Dimethylcarboxamido)-9-methylfluorene-9-d, kinetic data for isotope exchange of, 213, 214
 stereochemical aspects in isotope exchange, 210, 211, 212, 215
 stereochemical fate of ion pairs in dissociating solvents, 220
- 2-(N,N-Dimethylcarboxamido)-7-nitro-9-methylfluorene-9-d, kinetic data for isotope exchange, 213
 stereochemical aspects in isotope exchange, 210, 211, 212, 215
 temperature and medium effects on racemization of, 216
- Dimethylformamide, addition of, to sodium fluorenone ketyl, 69
 basicity of, 157
 use as a polarographic solvent, 39
- 2,5-Dimethyl-2-hexanol, ¹⁸O equilibration of acid phthalate of, 290
- 7,7-Dimethylnorbornene, acid addition to, 362
- 9,9-Dimethyl-10-phenyldihydroanthracene acidity of, 178

- N,N-Dimethylphenylenediamine,
 exchange of, with radical
 cation of, 86
 2,4-Dimethylstyrene, 424
 Dimsyl ions, effect of aggre-
 gation on proton transfer,
 206
 Dinaphthylethane, dispropor-
 tionation of radical anions
 of, 108, 109
m-Dinitrobenzene, electron ex-
 change with its radical
 anion, 73
p-Dinitrobenzene, electron ex-
 change with its radical
 anion, 73
 2,4-Dinitrophenol, pK of, in
 different solvents, 158
 Dioxane, propagation by living
 polystyrene salts in, 386
 solvent in polarography, 39
 Diphenylacetylene, electron
 affinity in different sol-
 vents, 38
 relative halfwave potential
 of, 40
 1,3-Diphenylbutene, lithium
 salt of, 56
 Diphenyldiazomethane, 300
 1,3-Diphenylindene, acid-base
 equilibria of salts of,
 164, 165
 acidity of, 170
 pK_a pair of, 160
 Diphenylmethane, acidity of,
 171, 178, 188, 190, 191
 Brønsted relation for, 192
 Dipole moments, due to hydro-
 gen-bond formation, 462-463
 of ion pairs in nonpolar and
 slightly polar media, 449-
 469
 and proton transfer, 463-467
 for substituted phenol-tri-
 ethylamine complexes, 466
 time averaging of fluctuating,
 467-469
 of tri-*n*-butylammonium bro-
 mide, 463
 Di-*n*-propylamine, 210
 Dispersion forces, contribution
 to heat of protonation, 158
 effect of, on acid-base equil-
 ibria, 157
 Disproportionation, free ener-
 gy of, 91
 of radical anions, 90-108
 Dissociation constants, of ion
 pairs derived from conjuga-
 ted aromatic hydrocarbons,
 162
 of Na salts of radical anions
 in THF and DME, 36, 37
 Duroquinone, electron-exchange
 with its radical anion, 73
 Electric displacement, 449
 Electron, description of, in
 various states, 114 et seq.
 formation of "bubble" from
 quasi-free-, 117
 mobilities of, when injected
 into nonpolar liquids, 117
 scattering of, in gas phase,
 114
 Stokes treatment of mobility
 of, 118
 Electron affinity, of aromatic
 hydrocarbons in different
 solvents, 38
 correlation of, with gaseous
 electron affinities, 43, 44
 with potentiometric and po-
 larographic data, 43, 44
 dependence on molecular struc-
 ture, 27-31
 determination of, 21-27
 from electron transfer equil-
 ibria, 45
 by electron impact, 22
 from flame equilibria, 26, 27
 in gas phase, 5, 9
 by photoabsorption, 21
 by photoionization, 21
 potentiometric studies of,
 33-38
 in solution, 31-33
 by surface ionization, 22
 using electron capture de-
 tector, 22, 23

- Electron attachment, 3, 87
- Electron capture, dissociative, 111
 in the gas phase, 17-20
 by neutral molecules, 20
 by radical anion, 18, 19
- Electron ejection, by chemical reaction, 16
 for determination of solvation energies, 32
 by electron impact, 13, 14
 in gas phase, 4-16
 by ionizing radiation, 14, 15, 16
 in liquids and glasses, 137-139
 photochemical, 5, 6
 in photoelectron spectroscopy and E.S.C.A.
 thermal, 5
- Electron exchange, intramolecular, 71-85
- Electron impact, 3
 electron ejection by, 13, 14
 ionization by, 9
 technique for ionization potentials, 7, 14
- Electron mobility, 119
 in liquid, 119
- Electron transfer, 2
 apparent equilibrium constant for, 47
 equilibria between radical anions and aromatic acceptors, 45-51
 in exchange, involving free ions and ion pairs, 65
 of ketyls with parent ketones, 68
 $A + A^+ \rightarrow$ exchange, 85, 86
 in the gas phase, 3
 involving electron capture, 4
 involving electron ejection, 4
 kinetics of $A^{\cdot-} + B \xrightarrow{k} A + B^{\cdot-}$, 86-90
 to organic halides, 111-113
 oxidation in, 2
 reduction in, 2
 in rigid media, 3
 in solution, 3
 transfer from free ions, ion pairs, triple ions, 67
 from a triple ion to parent acceptor, 66
- Encounter complex, 182, 184, 198, 238, 379
- Entropy of dissociation, of Na salts of aromatic radical anions, 37
- ESCA (Electron spectroscopy for Chemical Analysis), 9, 12, 13
 of ethyltrifluoroacetate, 12
 of O_2 , 12
- ESR spectroscopy, application in exchange kinetics, 59
 demonstration of existence of triple ions by, 66
 effect of intramolecular electron-exchange, 74
 of free alkali atoms, 132-134
 for interconversion of tight and loose ion pairs, 63
 of solvated electrons, 123-130
 splitting of lines of radical anion by counterion, 62
 summary of results of, in kinetics of exchange reaction, 67
- Ethane, 1,2-di(9-carbazyl)-ethane, esr spectrum of, 77
- Ethanol, as electron trap, 127
 spectrum of electron in, 126
- Ethers, comparison of reactivities of monocyclic and bicyclic-, in polymerization, 434, 436
 solution of alkali metals in, 123, 135
- Ethylamine, 132
 Na in mixtures of ammonia and, 133
 Na in mixtures of methylamine and, 134
 optical spectrum of electron in, 124, 126
- Ethylbromide, solvolysis of, 323
- N-Ethylcarbazole, esr spectrum of radical anion of, 77

- Ethylchloroformate, decomposition of, 351
- Ethylene, ionization potential of, 28
- Ethylenediamine, 135, 136
cesium in, 130
esr of lithium and sodium in, 129
optical spectrum of electron in, 126
- Ethylene, 1, 1-diphenyl-, addition of sodiumpolystyrene, 424
addition to lithiumpolystyrene, 422
electron transfer from Na anthracenide to, 110
- Ethyleneglycol, spectrum of electron in, 126
- Ethyleneoxide, reaction with sodiumfluoradenyl, 399
- 9-Ethylfluorene, acidity of, 170
- α -Ethyl-naphthalene, exchange with free naphthalenide ions, 61
- β -Ethyl-naphthalene, exchange with free naphthalamide ions, 61
- Ethyltosylate, α -D isotope effect on solvolysis of, 299
- Exchange reactions, kinetics of, 57-86
- External ion return, 254
- External ion pair return, 254
- External return, 254, 279, 292
- Fast exchange limit, for esr spectroscopy, 60, 63, 65, 66, 85
- Feshbach resonance, 19
- Flash photolysis, 138
for optical spectroscopy of solvated electron, 124
- Fluoradene, acidity of, 170
pK ion pair of, 160
- Fluoranthene, electron affinity in different solvents, 38
- ionization potential of, 30
- Fluorene, acidity of, 170, 175, 176, 178, 190
base-catalyzed deuterium exchange of, 188, 189
exchange between methanol and tritium-labelled, 200
ionization potential of, 30
- 9-Fluorene anion, charge distribution in, 459, 460
- Fluorenes, temperature dependence of equilibria involving salts of substituted, 174, 177
- Fluorenone, electron transfer with its radical anion, 73
exchange with sodium fluorenone ketyl, 69
- Fluorinated benzenes, acidities of, 179
carbanion stabilization factors for, 180
- Fluorobenzene, ionization potential of, 30
- p*-Fluprostyrene, 424
- Franch-Condon principle, 10
- Free ions, experimental distinction from ion pairs, by esr, 62
participation in anionic polymerization, 385, 400
- Friedel-Craft's catalysts, initiation of polymerization of vinyl and vinylidene monomers, 427
- Glass electrode, technique for pK of hydrocarbon acids, 169
- Glycines, dielectric relaxation times for, 494, 495
- Halfwave potential, of aromatic hydrocarbons by polarography, 40
of aza-aromatics, 41
of substituted ethylenes, 41
- Halides, electron transfer to, 111-113
- Heat of dissociation of Na salts of aromatic radical anions, 37

- Heat of solvation, 51
 - of aromatic radical anions in THF, 32, 43
 - of lithium and sodium ion pairs, 54
- Helium, cavity formation in liquid, 121
- Hexahelicene, electron exchange with its radical anion, 72
- Hexamethylphosphorictriamide (HMPA), 135
 - propagation of living polystyrene salts in, 386, 396
 - solutions of alkali metals in, 129
 - spectrum of electron in, 126
 - suitability for potentiometric titrations, 37
- Hexamethyl-trans-stilbene, electron-exchange with its radical anion, 72
- n-Hexane, electron mobility in liquid-, 119
 - ionization potential of, 28, 29
- 9-Hexylfluorenyllithium, loose ion pairs in solutions of, 177
- Hydrated electrons, optical spectra of, 125
- 1,2-Hydride shifts, 361
- Hydrocarbon acids, acid-base equilibria of salts of conjugated aromatic-, 163
 - effect of substituents on acidity of, 175
 - ion pair acidity of strong, 159, 160
 - MSAD scale of pK of, 170, 171
- Hydrocarbons, equilibrium and kinetic acidities of some, 190
- Hydrogen bonding, effect on acidity, 156-158
 - formation of, in encounter complex, 184
 - of solvent to acid or base in proton transfer, 184
- Hydroxides, of sodium and lithium in association with ion pairs in ethers and solvents, 54
- Hydroxy acids, acidity of, 156-157
 - and nitrogen bases, 184
- Hyperfine lines, overlap of, in esr spectra, 60
- Indene, acidity of, 170, 190
 - ionization potential of, 30
- Infra-red spectroscopy, of solvated electron, 124
- Internal return, 197, 199, 200, 201, 211, 213, 254, 275, 279, 280, 282, 284, 285, 345, 346, 349
- Intramolecular rearrangement, extent of, in proton transfers in polar solvents, 220
- Inversion of configuration, in proton transfer, 207
- Iodobenzene, ionization potential of, 30
- 3-iodo-9-methylfluorene-9-d, stereochemical aspects in isotope exchange, 211
- Ion-cyclotron resonance, study of electron transfer in gas phase, 45
- Ionization, 4
 - auto-, 5
 - direct, 5
 - by electron impact, 9
 - involving predissociation, 5
 - photosensitized, 16
 - ionization of alkali vapors, 16, 17
 - surface, 22
- Ionization potential, 4
 - spectroscopic determination of, 7
 - of acetylenes, 28
 - of aliphatic hydrocarbons, 27, 28
 - of alkali metals, 51
 - of condensed aromatic hydrocarbons, with and without substituents, 30
 - dependence on molecular structure, 27-31

- determination by photoelec-
tron spectroscopy, 7, 9
- of dienes, 28
- of heterocyclic analogs and
benzene and naphthalene, 30
- of olefins, 28
- vertical, 8
- Ion pairing, methods for de-
tection of, 297-322
- Ion pair return, 254, 263, 265,
271, 272, 278, 282, 292,
294, 348
- measured by rearrangement,
308, 309
- Ion pairs, acidity of, and dis-
sociation of, 158-162
- aggregation of, 167
- in anionic polymerization,
385-400
- association and molecular
complex formation of, 469-
470
- versus covalent bond, 437-440
- detection in solvolysis by
 ^{18}O scrambling, 279
- dielectric relaxation of, 480-
490
- differentiation between types
of, 161
- dipole moments of dimers of,
471-475
- effect of temperature on na-
ture of, 63
- electric dipole moments of,
449-469
- in electron-transfer equilib-
ria, 47-49
- existence of two distinct
loose, 65
- experimental distinction, by
esr, 62
- forms of, 46, 55, 212
- hydrogen-bonded-, 461
- interconversion of tight and
loose-, 63, 65, 68
- as intermediates in acetolysis
reaction, 256
- intimate, solvent-separated,
254, 273, 276
- intramolecularly solvated,
396-399
- isomerization of i.p.o trig-
lyme, 55
- methods for generation of,
350-363
- molecular complexes of, 475
- proof of existence of, 62
- in solvolysis of primary and
secondary derivatives, 322
- stereochemical fate of, in
dissociating solvents, 220
- tight and loose, in anionic
polymerization, 386-391
- Ions, with delocalized elec-
tron, 459-461
- free, pairs, triple, etc., 3
- in nonaqueous solvents, 509-
512
- Isobutene, ionization potential
of, 28
- γ -ray initiated polymerization,
430, 431
- Isoprene, copolymerization
with styrene, 421
- polymerization by living poly-
isoprenyl, 415
- Isopropyl brosylate, ion pair
return for, in TFA, 311
- solvolysis of, 347
- Isoquinoline, ionization po-
tential of, 29, 31
- potentiometric titration of,
37
- Isotactic polymer, 401, 402
- Isothiocyanates, 312
- Isotope effects, α -deuterium-,
in participating systems,
304, 305
- in solvolysis, 299
- γ -deuterium, 306
- partitioning-, (PIE), 300
- secondary deuterium, 297-305
- Isotope exchange reactions, 211
- Ketyls, exchange with parent
ketones, 68, 69
- Kirkwood theory, 451, 452, 494
- Knight shift, 128
- Krypton mobility of electron
in liquid, 119

- Lactams, polymerization of, 425
 Leaving groups, polydentate, 311
 Leuchs anhydrides, polymerization of, 425
 Lithium, electron-photoejection from, 138
 in equilibrium with biphenyl, 54
 esr of its solution in methylamine, 129
 Lithium alkyls, relative reactivities toward triphenylmethane, 207
 Lithium anthracenide, 204
 protonation of, 227, 235, 237
 Lithium arenesulfonate, 252
 Lithium bromide, association with ion-pairs, 54
 Lithium *t*-butylacetylenide, 166
 Lithium carbazole, photoejection of electrons from, 127, 138
 Lithium cyclohexylamide, 191, 206
 thermochromism of equilibrium with triphenylmethane, 166
 Lithium fluorenyl, 166, 203
 dissociation constant in cyclohexylamine, 163
 Lithium naphthalenide, temperature effect on esr spectrum of, 92
 Lithium perchlorate, nucleophilicity of, 334
 salt effect of, on ionization of *p*-methoxyneophyl-tosylate, 262
 in solvolysis of neophyl derivatives, 258, 260, 261
 Lithium phenylacetylenide, 166
 Lithium salts, of living polymers, as initiators for polymerization, 414
 Lithium tetraphenylboride, 235
 Lithium polystyryl, dimerization of, 414, 415
 Living polymers, anionic propagation by, 376
 polymerization initiated by lithium salts of, 414, 416
 2,6-Lutidine, as base, 196
 Marcus, treatment of ionic solvation, 58, 60, 61, 75, 89, 90
 Markoff chains, 404
 Mass law constant, 251, 252
 Mass law effect, 249
 Mass spectrometry, study of electron transfer in gas phase by, 45
 Methacrylates, anionic polymerization of, 385, 398
 Methane, electron mobility in liquid-, 119
 Methanol, spectrum of electron in, 126
p-Methoxybenzylphenylcarbonate, decomposition of, 354
 2-Methoxy-1-ethanol(cellosolve), use as poorly protonating solvent in polarography, 39
p-Methoxyneophylbrosylate, salt effect on acetolysis of, 264
p-Methoxyneophyl halides, acetolysis of, 258
p-Methoxyneophyltosylate, solvolysis of, 261, 262, 264, 271
 α -(*p*-Methoxyphenyl)ethyl 2,6-dimethyl benzene sulfinat, 319
p-Methoxystyrene, 424
 Methylamine, 132, 136, 138
 esr of solution of lithium and sodium in, 129
 -glass, 127, 128
 sodium in solution of ethylamine and, 134
p-Methylaniline, as base, 210
 2-Methylantracene, Brønsted relation for, 192
 4-Methylantracene, Brønsted relation for, 192
 Trityl 2-Methylbenzenesulfinat, isomerization of, 319

- p*-Methylbenzhydrylchloride, solvolysis of, 252
- p*-Methylbenzhydryl-*p*-nitrobenzoates, solvolysis of, 286, 287, 365
- 1-Methyl-1-*d*-3-*t*-butylindene, effect of cations on carbanion stereochemistry, 218
- extent of intramolecular rearrangement of, in polar solvents, 220
- stereochemical aspects of isotope exchange, 217, 219, 220
- cis*-5-Methyl-2-cyclohexenylchloride, salt effect on acetolysis of, 265
- 4,5-Methylenephenanthrene, acidity of, 170
- 3-Methylfluoranthene, Brønsted relation for, 192
- 8-Methylfluoranthene, Brønsted relation for, 192
- Methylfluorene, kinetic data for isotope exchange of, 213
- 9-Methylfluorene, acidity of, 170, 176
- ¹H exchange with NaOMe, 201
- 3-Methylhexane, as trap for electrons, 127
- Methylolithium, 207
- Methylmethacrylate, propagating specities in anionic polymerization of, 404
- 1-Methylnaphthalene, Brønsted relation for, 192
- 2-Methylnaphthalene, Brønsted relation for, 192
- 3-Methylnaphthalene, Brønsted relation for, 192
- 4,5-Methylphenanthrene, acidity of, 190
- 9-Methylphenanthrene, Brønsted relation for, 192
- 10-Methylphenothiazine, exchange of, with radical cation of, 86
- Methylphenylacetylene, acidity of, 232
- electron transfer from sodium-biphenylide to, 110, 230, 231
- α -Methyl- γ -phenyl-*p*-nitrobenzoates, 305
- 1-Methylpyrene, Brønsted relation for, 192
- 2-Methylpyrene, Brønsted relation for, 192
- α -Methyl-trans-stilbene, disproportionation of radical anion, 102
- electron-exchange with its radical anion, 72
- 2-Methyl-trans-stilbene, electron-exchange with its radical anion, 72
- α -Methylstyrene, 424, effect of triglyme on polymerization of, 396
- perchloric acid-initiated polymerization of, 440
- propagation constant of free cations, 432
- propagation of free ions of living-, 386
- β -Methylstyrene, 424
- ortho*- and *para*-Methylstyrene, 424
- 2-Methyltetrahydrofuran, propagation, by living polystyrene salts in, 386
- spectrum of electron in, 126, 127
- Methyltosylate, as initiator in cationic polymerization, 438
- α -D isotope effect in solvolysis of, 299
- Molecular beam electric resonance, 452
- Molecular weight distribution, effect of ionic structure on, in polymers, 409-410
- Morpholine, as base, 187
- MSAD, scale of pK values, 170, 171
- Naphthaldehyde-1, electron affinity in gas phase, 26

- Naphthaldehyde-2, electron affinity in gas phase, 26
- Naphthalene, dissociation constant of sodium salt of radical anion of, 36
- effect of counterion and solvent on rate of exchange with naphthalenide salts, 62
- electron affinity in different solvents, 38
- in gas phase, 26
- electron exchange with its radical anion, 72
- equilibrium with free biphenylide radical anion, 88
- with sodiumbiphenylide, 47-51, 88
- with sodium in various solvents, 56, 57
- heat of solvation of radical anion in THF, 32
- ionization potential of, 30
- preparation of radical anions of, 221
- reaction of, with free naphthalenide ions, 60, 61
- relative halfwave potential of, 40
- triphenylene electron-transfer system, 46
- p*-Naphthaquinone, electron-exchange with its radical anion, 73
- 1,4-Naphthaquinone radical anions, lifetime of, in gas phase, 18
- Naphthylidene, polarographic $\epsilon_{1/2}$ and potentiometric ϵ_0 of, 41
- α -Naphthyl-(CH₂)_n- α -naphthyl esr spectra of, 79, 80
- intramolecular electron transfer in, 78 et seq.,
- 1-Naphthyl-1-phenylethane, electron exchange with its radical anion, 72
- Neopentane, electron mobility in liquid, 119
- Neopentyl-2,4-dinitrobenzenesulfonates, trifluoroacetolysis of, 302
- Neopentyl tosylate, ¹⁸O-scrambling in solvolysis of, 294
- Neophylhalides, acetolysis of, 258, 260, 261
- Neophyl tosylate, acetolysis of, 258, 260, 266
- Nitroalkanes, 199
- Nitrobenzene, electron-exchange with its radical anion, 72
- ionization potential of, 30
- p*-Nitrobenzhydrylthiocyanates, isotopic exchange in, 314
- p*-Nitrobenzoate esters, use of ¹⁸O in solvolysis of, 279-297
- Nitro compounds, kinetic isotope effects in reactions with bases, 196
- Nitromethane, reaction with trityl anion and 9-fluorenyl anion, 184
- 2-Nitro-9-methylfluorene, isotope-exchange of, 211-213
- p*-Nitrophenol, complex with LiCl, 476, 477
- pk of, in different solvents, 158
- p,p'*-bis-(*p*-Nitrophenyl)methane, esr spectrum of, 76-78
- NMR double resonance, application to fluorene-fluorenyl ¹H exchange, 205
- Norbornene, acid addition to, 362
- exo-2-Norbornylacetate, ¹⁸O-scrambling in solvolysis of, 295
- exo- and endo-Norbornylamines, deamination of, 358
- 7-Norbornyl arene sulfonates, solvolysis of, 364
- exo-2-Norbornylbrosylate, 311
- acetolysis of, 253, 264, 272, 276
- exo-2-Norbornylthionbenzoate, isomerization of, 321
- 2-exo-Norbornylthiocyanate, isomerization of, 317
- Nuclear paramagnetic resonance, 128

- ¹⁸⁰ scrambling technique, for solvolysis studies, 279-297, 345
 2-Octylarenesulfonates, solvolysis, 328
 2-Octylbrosylate, solvolysis of ¹⁸⁰ labelled, 289, 346
 solvolysis of optically active, 328, 330, 338
 2-Octylmesylate, solvolysis, 267, 329, 331, 334-337, 339-342, 345
 2-Octyltosylate, acetolysis of, 326
 Olefins, acid addition to, 361-363
 Onsager internal field, 450, 458
 Optical spectra, of alkali metals in amines and ether, 123, 124
 of solvated electron, 123-130
 2-Oxazoline, cationic polymerization of, 437, 438, 439
 Oxepan, polymerization of, 436
 propagation by living polystyrene salts in, 386
 Oxetane, polymerization of, 435
 Oxygen acids, pK of, in different solvents, 158

 Pentacene, ionization potential of, 30
 Pentafluorobenzene, acidity of, 179
 Pentamethylguanidine, isotope exchange of, 216
 n-Pentane, electron mobility in liquid, 119
 ionization potential of, 28, 29
 3-Pentyn-2-yl bromide, α -D isotope effect in solvolysis of, 299
 3-Pentyn-2-yl iodide, α -D isotope effect in solvolysis of, 299
 3-Pentyl-2-yl tosylate, α -D isotope effect in solvolysis of, 299, 300

 Permittivity, effective, 458-459
 effect of solvent, on dipole moments of ion pairs, 458
 electric, 448-509
 Perylene, dissociation of sodium salt of radical anion of, 36, 37
 electron affinity of, 38
 electron-transfer with tetracene, 46
 halfwave potential of, 40
 ionization potential of, 30
 redox potential of, 93
 Phenanthrene, electron affinity in gas phase, 26
 in solvents, 38
 equilibrium with biphenylide anion, 88, 89
 halfwave potential of, 40
 heat of solvation of radical anion of, 32
 ionization potential of, 30
 Phenanthrene aldehyde-9, electron affinity in gas phase, 26
 Phenanthridine, polarographic $\epsilon_{1/2}$ and potentiometric ϵ_0 for, 41
 1,10-Phenanthroline, polarographic $\epsilon_{1/2}$ and potentiometric ϵ_0 for, 41
 Phenanthroquinone, electron transfer from the dianion to, 107
 1,1,3,3-bis(4,5-Phenanthrylene)-propene, acid-base equilibria of salts of, 164, 165
 p^K ion pair of, 160
 Phenazine, polarographic $\epsilon_{1/2}$ and potentiometric ϵ_0 of, 41
 Phenol, ionization potential of, 30
 reaction with radical anions, 184
 Phenothiazine, exchange of, with radical cation of, 86
 Phenoxathiin, exchange of, with radical cation of, 86
 Phenoxazine, exchange of, with radical cation of, 86

- Phenylacetylene, acidity of, 167, 171
 ionization potential of, 30
 reaction with sodium anthracene, 232
- 1-Phenyl-1-*p*-anisyl-2-propylbrosylate, acetolysis of, 264
- threo*-2-Phenylarylsulfonate, normal salt effect, 263
- 9-Phenyl-3,4-benzfluorene, acidity of, 170, 190
- p*-Phenylbenzhydryl *p*-toluenesulfinate, acetolysis of, 319
- 2-Phenyl-2-butyl *p*-nitrobenzoate, solvolysis of, 288
- threo*-3-Phenyl-2-butyltosylate, acetolysis of, 267, 268, 272, 365
- α -Phenyl- α -*d*-butyranitrile, 217, 218
- 10-Phenyl-9,9-dimethyl-9,10-dihydroanthracene, acidity of, 171
- 10-Phenyl-9,9-dimethylhydroanthracene, acidity of, 190
- 1,12-(*o*-Phenylene)-7,12-dihydropleiadene, acidity of, 170, 190
- α -Phenylethylbromide, reaction with NaOEt, 342
- 1-Phenylethylchloride, phenolysis of, 364
 solvolysis of, 266, 299
- α -Phenylethyl *p*-nitrobenzoates, solvolysis of, 288
- α -Phenylethylsulfinate, isomerization of, 319
- 2-Phenylethyltosylate, acetolysis of, 264, 267
- 9-Phenylfluorene, acidity of, 167, 178, 179, 190, 201
 proton-exchange with NaOMe, 201
- Phenyllithium, 206, 207
- 1-Phenyl-1-methoxy ethane, stereochemical aspects of isotope exchange, 218
- α -Phenyl- γ -methyl propenyl *p*-nitrobenzoates, 306
- 1-Phenylnitroethane, proton-transfer from, 187
- 1-Phenyl-2-nitropropane, proton-transfer from, 187
- 1-Phenyl-2-propyltosylate, solvolysis of, 267
- 2-Phenyl-1-propyltosylate, solvolysis of, 267, 306, 307
- Phenyl radical, electron affinity in gas phase, 27
- 4-Phenyltoluene, acidity of, 171, 191, 192
- Photoelectron spectroscopy, 3, 9, 10, 12, 29
 of chlorobenzene, 12
 of water vapor, 11, 12
- Photoionization, gaseous, 3, 9
 in glass, 137
 mass spectroscopy, 7, 9
- Phthalazine, ionization potential of, 29, 31
 polarographic $\epsilon_{1/2}$ and potentiometric ϵ_0 of, 41
- Picene, electron affinity in gas phase, 26
- Pi-complexes, in addition reactions, 361
- Picric acid, *pK* of, in different solvents, 158
- Pinacol rearrangement, 302
- Pinacolyl brosylate, acetolysis of, 264
 trifluoroacetolysis of, 302, 347
- Pinacolyl tosylate, solvolysis of, 264, 303
- Piperazine, as base, 187
- Piperidine, as base, 187
- Plasma, collisional phenomena in gaseous, 3
- Polarizability, ionic, 455
 molecular, 450
- Polarization, molar, 449, 450, 512-515
 mutual-, of ions in an ion pair, 452-461
- Polarographic wave, 38
- Polarography, of aromatic

- hydrocarbons, 40
- $\epsilon_{1/2}$ of aza-aromatics by, 41
- determination of solution
 - electron affinities by, 38-43
 - of organic compounds, 39-43
- Plaron theory, 120, 121, 128
- Polyacrylate, living, anionic polymerization of, 407, 408, 409
- Polyarylmethanes, base catalyzed deuterium exchange of, 188, 189
- ^3H -exchange with cyclohexylamine, 193
- Polyfluorobenzenes, isotope effect in exchange with methanol, 199
- Polystyrene, living, addition of NaPh_4B to, 384
- addition of styrene to, 423, 424
- aggregation of lithium salt of, 415
- dissociation constants of salts of, 384, 397
- effect of counterion on homopropagation of, 378
- evidence for triple ions in, 411, 412
- ion pairs of, 387-391
- irreversible transformation of, 380
- polymerization, in presence of complexing agents, 391, 396
- of sodium salt of, 378
- propagation by salts of, 386
- protonation by triphenylmethane, 237
- reactivity of salts of, in dioxane, 387, 400
- Poly-1-vinylnaphthalene, addition of styrene to living, 399
- Poly-2-vinylpyridine, triple ions in propagation of polymerization of living-, 412, 413
- Poly-4-vinylpyridine, aging of, 380
- Potassium, dissociation of, in various solvents, 124
- esr spectrum in liquid ammonia, 127
- Potassium anthracenide, protonation of, 234, 237
- Potassium 2,2'-bipyridyl radical anion, exchange of electron with parent, 70
- Potassium methoxide, 189
- Potassium-naphthalene, in DME, 57
- Potentiometric studies, of solution electron affinities, 33-38
- Potentiometry, ϵ_0 of aza-aromatics by, 41, 44
- n*-Propane, ionization potential of, 28, 29
- 1-Propanol, spectrum of electron in, 126
- 2-Propanol, spectrum of electron in, 126
- Propene, ionization potential of, 28, 29
- reaction of, in TFA, 346, 347
- cis* and *trans*-1-d-propene, mechanism of polyaddition, 404, 405
- n*-Propylamine, 210
- 2-Propylbromide, solvolysis of, 323
- 2-Propylbrosylate, solvolysis of, 299, 302, 348
- n*-Propyldiazonium salts, products from decomposition of, 356, 357
- 9-*i*-Propylfluorene, acidity of, 171
- 2-Propyltosylate, solvolysis, 328, 348
- Proton affinity, 156
- of common solvents in gas phase, 154, 155
- Proton-transfer, dipole moment of, 463-467
- kinetics of, 180-240
- involving ion pairs and higher aggregates, 201-207

- isotope effects in, 195-201
 stereochemistry of, 207-221
 thermodynamics of, 153-172
 ultrafast-, 467-469
 Pulse radiolysis, of aromatic hydrocarbons in chlorinated solvents, 90
 for perturbation of an equilibrium of type $A^- + B \rightleftharpoons A + B^-$, 87
 for study of electron-transfer from radical anions to halides, 112
 for study of optical spectra of solvated electrons, 124, 125, 131
 for study of reaction of naphthalene with free naphthalenide ions, 61
 Pyrazine, polarimetric $\epsilon_{1/2}$ and potentiometric ϵ_0 for, 41
 1,4-Pyrazine, ionization potential of, 29, 31
 Pyrene, electron affinity in gas phase, 26
 in electron transfer systems, 46, 88, 89
 ionization potential of, 30
 potentiometric ϵ of, 40, 43
 1,2-Pyridazine, ionization potential of, 29, 31
 Pyridine, 42, 155, 196
 ionization potential of, 29, 30
 polarographic $\epsilon_{1/2}$ and potentiometric ϵ_0 of, 41
 Pyridinium ion, acidity of, 156
 Pyridopyrazine, polarographic $\epsilon_{1/2}$ and potentiometric ϵ_0 of, 41
 1,3-Pyrimidine, ionization potential of, 29, 31
 polarographic $\epsilon_{1/2}$ and potentiometric ϵ_0 for, 41
 Pyrrolidone, polymerization of, 425, 426
 Quinazoline, ionization potential of, 29, 31
 Quinoline, ionization potential of, 29, 31
 potentiometric titration of, 37
 polarographic $\epsilon_{1/2}$ and potentiometric ϵ_0 for, 41
 Quinoxaline, ionization potential of, 29
 polarographic $\epsilon_{1/2}$ and potentiometric ϵ_0 of, 41
 Radical anions, dissociation of, 36, 37
 electron-photoejection from, 138
 in electron-transfer with aromatics, 45-51
 protonation of, and of dianions of, 221-240, 399
 reactions initiated by disproportionation of, 108-111
 Radiochloride exchange, of p-chlorobenzhydryl chloride, 262, 285
 Redox potentials, of anthracene and perylene, 93
 Reorganization parameter, for solvent molecules, 59
 Rydberg electron, 6
 Salt effects, cation specificity of, 262
 normal, 257-271
 special, 271-279
 Scaled-particle theory, of liquid solution, 503
 Semiquinones, esr spectra of sodium salts of, 66
 Slow exchange limit, for esr line broadening, 59
 S_N1 , competitive S_N1 and S_N2 reactions, 326
 mechanism of solvolysis, 249
 S_N1 reactions, 350
 Sodium, contamination by potassium, 63
 dissolution of, 124, 133, 134
 metal with biphenyl in solvent, 52-57

- metal with naphthalene in solvent, 56, 57
- negative ion of, 136
- Sodium anthracenide, protonation of, 227, 228, 232, 237
- reaction with phenylacetylene, 232
- Sodium benzophenone, esr spectrum of, 65, 68
- Sodium biphenylide, electron-transfer to halide, 112
- equilibrium with complexing agents, 54-55
- equilibrium with naphthalene, 47-51
- reaction with methylphenylacetylene, 230
- Sodium fluoradenyl, reaction with ethylene oxide, 399
- Sodium naphthalenide, dissociation of ion-pairs of, 62, 63
- electron-transfer to halide, 112
- esr spectrum of, 64
- reaction with phenylacetylene, 232
- Sodium perylenide, disproportionation of, 239
- protonation of, 229, 230
- Sodium polystyryl, polymerization by its free ions, 201
- Sodium pyrenide, electron photoejection from 134, 138
- in electron-transfer equilibrium with biphenyl, 87
- Solvated electrons, 113-130, 138
- aggregation of, 130-137
- from alkali atoms, 123
- mobilities of, 122
- optical and esr spectra of, 123-130
- spin relaxation of, 128
- Solvation, of lithium cation, 164
- restricted dipole rotation in shell of, 504-506
- shell on ions, 3
- Solvation energy, of aromatic radical anions, 32
- of quasi-free electron, 116
- from sphere in continuum approximation, 155
- Solvolysis, mechanism of, 324, 363, 366
- Spin transfer, 74
- Spirodienyl *p*-nitrobenzene, ionization of, 262
- Stark effect, 452
- Steady state approximation, 255, 263, 333
- Stereospecific polymerization, of vinyl and vinylidene monomers, 401-409
- Stilbenes, electron affinity of, 38
- electron exchange with its radical anion, 72
- disproportionation of radical anion of, 102
- halfwave potential of, 40
- isomerization of, 111
- Stokes, treatment of electron mobility, 118
- Stop-flow technique, 108, 136, 205, 221, 226
- Styrene, anionic polymerization of, 377, 380, 382, 383
- cationic polymerization of, 432, 439
- copolymerization of, 421
- electron-transfer from sodium anthracenide to, 110
- ionization potential of, 30
- polymerization by γ -irradiation, 430
- Sulfates, complex permittivity of divalent metal-, 490-493
- Syndiotactic polymers, 401, 402
- p*-Terphenyl, electron-transfer to, 72, 88
- Tetraalkylammonium salts, dimers of, 474
- dipole moments in benzene, 455-458
- Tetra-*n*-butylammonium salts, structure of, 474, 475
- Tetrabutylammonium thiocyanate,

- dielectric relaxation time
for, 486, 487
- Tetracene, electron affinity
in different solvents, 38
electron-transfer system with
perlene, 46
ionization potential of, 30
relative halfwave potential
of, 40
- Tetracyanoethylene, electron-
exchange with its radical
anion, 72
- 1,2,3,4-Tetrafluorobenzene,
acidity of, 179
- Tetraglyme, addition of, to
sodium fluorenone ketyl in
THF, 69
to sodium naphthalenide in
THP, 49
equilibrium with sodium bi-
phenylide, 55
in living polymerization of
sodium polystyryl, 391-396,
401
spectrum of electron in, 126
- Tetrahydrofuran, polymeriza-
tion of, 435, 436
propagation, by living poly-
styrene salts in, 386
solutions of K and Cs in,
129
spectrum of electron in, 126
- Tetrahydropyran, propagation
by living polystyryl salts
in, 386
- Tetramethylammonium phenoxide,
219
- Tetramethylhydrazine, exchange
with its radical cation, 85
- Tetramethyl-*p*-phenylenediamine,
exchange with radical ca-
tion of, 85, 86
- Tetramethylsilane, electron
mobility in, 119
- Tetraphenylethylene, dispro-
portionation of radical
anion of, 94-101
electron affinity in differ-
ent solvents, 38
photoejection of electron
from dianion of, 138
potentiometric titration of
salts of radical anion of,
37
relative halfwave potential
of, 43
- Thermal decomposition, for
generation of ion-pairs,
350
- Thianthrene, salts of radical
anions of, 85
- Thietan, polymerization of,
436
- Thiocarbonates, decomposition
of, 354
- Thiocyanates, isomerization
of, 312
- Thionbenzoates, isomerization
to thiolbenzoates, 320
- Toluene, acidity of, 171, 178,
188, 192
electron exchange with, 72,
198
- p*-Toluenesulfonate esters,
equilibration of 180 in,
279-297
- p*-Toluenesulfonic acid, reac-
tion with trityl- and 9-
fluorenyl anion, 184
- p*-Tolyl-*N,N*-dimethylacetimi-
date, aminolysis of, 190
- 9(*n*-Tolyl) fluorene, acidity
of, 170
- 9-(*p*-Tolyl) fluorene, acidity
of, 170
- 1-*p*-Tolyl-2-propyltosylate,
solvolysis of, 267
- Tri-*n*-butylammonium bromide,
dipole moment of, 462, 463
- Trichloromethylpentamethyl-
benzene, acetolysis of, 273
- Triethylamine, acid-base com-
plexes of substituted phe-
nols with, 464, 465
- Triethyloxoniumtetrafluorobor-
ate, in cationic polymeri-
zation, 433, 436
- 9-Trifluoromethylfluorene,
acidity of, 194
- 9-(*m*-Trifluoromethylphenyl)

- fluorene, acidity of, 170
- 5,5,5-Trifluoro-3-pentyl-2-yl-brosylate, α -D isotope effect in solvolysis of, 299, 300
- Triglyme, equilibrium with sodium biphenylide, 55
- in living polymerization of styrene, 393, 394, 396
- spectrum of electron in, 126
- Triisoamylammonium picrate, dielectric relaxation time for, 486
- 2-(N,N,N-Trimethylammonium)-9-methyl-fluorene-9-d, effect of cation on carbanion stereochemistry, 18, 218
- stereochemical aspects in isotope exchange, 211, 216
- Triphenylene, dissociation of sodium salt of radical anion of, 36, 37
- electron affinity in gas phase, 26
- in solvents, 38
- electron-transfer with naphthalenide, 46
- halfwave potential of, 40
- ionization potential, 30
- protonation of radical anion of, 223-224
- Triphenylmethane, acidity of, 171, 178, 179, 190, 191, 192, 194
- equilibrium with lithium cyclohexylamide, 166
- metalation of, by lithium alkyls, 206, 207
- proton exchange with methoxide, 201
- proton transfer to polystyryl base, 201-203, 237
- Triphenylmethyl radicals, electron exchange with corresponding carbonium ion, 71
- Triphenylmethyl sodium dissociation of, 33
- 1,1,3-Triphenylpropene, acidity of, 171
- Triple ions, demonstration of existence of, 66
- role in ionic polymerization, 410-414
- Tri-n-propylamine, 211
- Tritium exchange, between hydrocarbons and cyclohexylamine, 191, 193
- between hydrocarbons and methoxide, 189
- tri-p-Tolylmethane, 179
- Tropylium cation, initiator for polymerization, 427
- polarographic reduction of, 42
- Tropylmethylether, potassium salt of radical anion, 107
- Ultrasonic relaxation, 492
- 1-H-Undecafluorobicyclo (2.2.1) heptane, proton transfer with, 199
- p-Vinylbiphenyl, 424
- N-Vinyl-carbazole, propagation constants of polymerization of, 427
- Vinyl lithium, 207
- Vinylmesitylene, 424
- 1-Vinyl naphthalene, 424
- 2-Vinyl naphthalene, 424
- Vinylpyridine, anionic polymerization, 385, 401
- 2-Vinylpyridine, 424
- anionic polymerization of, 396, 397, 398
- dissociation of ion pairs of living, 397
- polymerization of sodium ion pair of, 396
- 4-Vinylpyridine, 397, 398, 424
- 2-Vinylquinoline, 396, 397
- Wagner-Meerwein rearrangements, 290-297
- Walden inversion, 467, 469
- Walden's rule, 117, 130, 136
- Water, binding energy of electron in liquid, 120
- as a catalyst of termination, 429
- cavity formation in liquid, 121

- effect of electrolytes on dielectric properties of, 499, 500
- as ion scavenger, 430
- reaction with trityl and 9-fluorenylamine, 184
- restricted dipole rotation of molecules, 505
- spectrum of electron in, 126
- structure of, 501
- Winstein solvolysis scheme, 253, 254, 298, 363
- Wurster's Blue, see Tetramethyl-*p*-phenylenediamine)
- Xanthone, exchange with its ketyls, 69
- Xenon, mobility of electron in liquid-, 119
- p*-Xylene, electron-exchange with its radical anion, 72
- Zinc oxide, in polymerization of isobutene, 430, 431
- Zwitterions, ion pairs and, in aqueous solution, 490-495

11/1/74

DATE DUE

NOV 29 1974

MAY 13 1975

FEB 28 1977

OCT 03 1979

JUN 2 1982

APR 9 1985

MAY 15 1986



3 3311 00109496 2

JUL 3 1 1989

